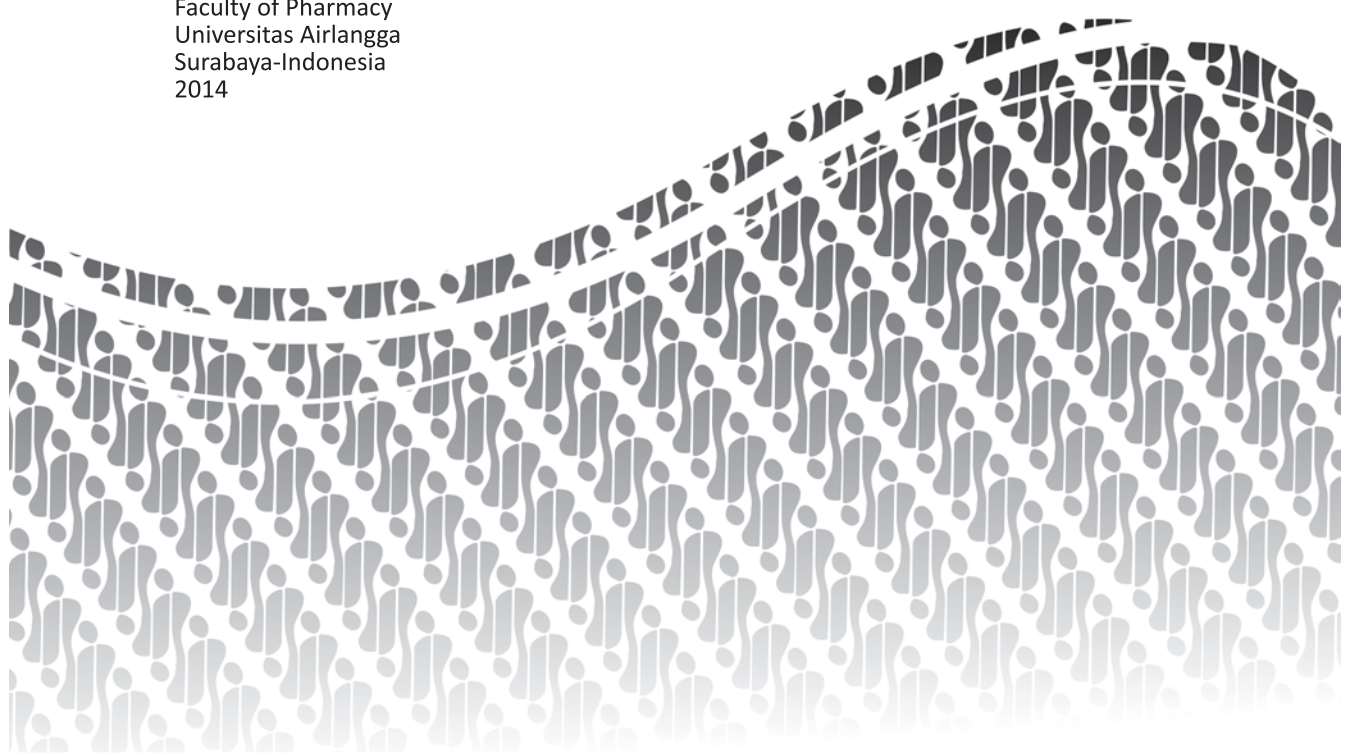


Proceeding

The 1st International Conference on Pharmaceutics & Pharmaceutical Sciences

Published and Organized by
Faculty of Pharmacy
Universitas Airlangga
Surabaya-Indonesia
2014



The 1st International Conference on Pharmaceutics & Pharmaceutical Sciences Proceedings

ISBN : 978-602-72333-0-0

(Letter of National ISBN Agency No. 4127/E.8/p/03.2015 Date 18 March 2015)

1st edition Proceeding

Published by:

Faculty of Pharmacy Universitas Airlangga
Surabaya, Indonesia

Address:

Kampus B Jl. Dharmawangsa Dalam
Surabaya 60286

Phone +62 31 5033710

Fax +62 31 5020514

Website: www.icpps2014.com or www.ff.unair.ac.id

Email: icppinfo@gmail.com

ISBN 978-602-72333-0-0



9 786027 233300

PREFACE From Chairman

It is our pleasure to present you the proceedings of The 1st International Conference on Pharmaceutics and Pharmaceutical Sciences (ICPPS) organized by The Faculty of Pharmacy Universitas Airlangga Surabaya Indonesia.

The proceeding was produced based on papers and posters presented at The 1st International Conference on Pharmaceutics and Pharmaceutical Sciences (ICPPS), held in Surabaya, Indonesia, 14-15 November 2014.

The proceeding clearly reflects broad interest, from the participants that coming from all around the world.

The papers presented were pharmaceutics and biopharmaceutics; requirements on how to evaluate molecules in discovery and their appropriateness for selection as potential candidate; their development in context of challenges and benefits, together with associated time and cost implications and also requirements to progress through pre-clinical and clinical.

In this an opportunity, I would like to express my appreciation to the editorial team of the proceeding who have been working hard to review manuscripts, and making the first edition of this proceeding be possible.

I would like also to thanks to all invited speakers and presenters who participated in The 1st International Conference on Pharmaceutics and Pharmaceutical Sciences (ICPPS) and your contribution to this proceeding.

Finally, I hope this proceeding will give contribution to the Pharmaceutics and Pharmaceutical Sciences research.

Chairman,

Dra. Esti Hendradi, MSI., Ph.D., Apt

COMMITTEE

Advisor : Dean of Faculty of Pharmacy Universitas Airlangga
Chairman : Dra. Esti Hendradi, M.Si., Ph.D, Apt.

Editor : Dr. Wouter LJ. Hinrichs (Netherlands)
Prof. Kozo Takayama (Japan)
Dr. Srinivas Mutalik (India)
Dr. Nuttakorn Baisaeng (Thailand)
Prof. Dr. Widji Soeratri, DEA (Indonesia)

Committee : Prof. Dr. Widji Soeratri, DEA, Apt.
Prof. Dr. Siswandono, MS., Apt.
Prof. Dr. Tutuk Budiati, MS., Apt.
Prof. Dr. rer.nat. Muhammad Yuwono, MS., Apt.
Drs. Hadi Poerwono, MSc., Ph.D, Apt.
Drs. Marcellino Rudyanto, MSi., Ph.D, Apt.
Drs. Bambang Widjaja, M.Si, Apt.
Drs. Sugiyartono, MS, Apt.
Dra.Tutiek Purwanti, MSi, Apt.
Dra.Tristiana Erawati, MSi, Apt.
Dra.Retno Sari, MSc, Apt.
Dra.Dewi Isadiartuti, MSi, Apt.
Dra.Noorma Rosita, MSi, Apt.
Dr. Dwi Setyawan, SSi, MSi., Apt.
Dr. Riesta Primaharinastiti, SSi, MSi, Apt.
Dewi Melani Hariyadi, SSi, M.Phil., Ph.D, Apt.
Helmy Yusuf, SSi, MSc., Ph.D, Apt.
Dr. rer. nat. Maria Lucia Ardhani Dwi Lestari, SSi,MPHarmSci., Apt.
Melanny Ika Sulistyowati, SFarm, M.Sc, Apt.
Febri Annuryanti, SFarm,M.Sc, Apt.
M. Faris Adrianto, MFarm, Apt.
Dini Retnowati, SFarm,Apt.
Abhimata P, SFarm, Apt.

TABLE of CONTENT

Preface from Chairman

Committee	ii
Table of Contents	iii
Author Index	iii

AUTHOR INDEX

COMPARISON OF SODIUM STARCH GLYCOLATE AND CROSSCARMELLOSE SODIUM AS SUPERDISINTEGRANT IN MEFENAMIC ACID FAST DISINTEGRATING TABLET Adeltrudis Adelsa D, Oktavia Eka Puspita, Amalia Ayuningtyas, Marulita Isadora	1
STUDY EXPRESSION OF HUMAN ERYTHROPOIETIN EXPRESSION IN MAMMALIAN CELL Adi Santoso, Popi Hadiwisnuwardhani, Yana Rubiana, Yulaika Romadhani, Endah Puji Septisetyani, Dyanningtyas D.P. Putri	4
ANTIOXIDANT STABILITY ASSAY OF ALPHA TOCOPHERYL ACETATE IN SOLID LIPID NANOPARTICLE SYSTEM (LIPID BASE BEESWAX AND MONOSTEARIC GLISERYL 50:50) Anggie Widhi, Noorma Rosita, Widji Soeratri	8
A BIOACTIVE <i>BOVINE HYDROXYAPATITE</i> –GELATIN IMPLANT FOR IN VITRO GENTAMICIN RELEASE Aniek Setiya Budiatin, M. Zainuddin, Junaidi Khotib, Diah Himawati	13
EFFECT OF COMPARISON SURFACTANT AND COSURFACTANT IN WATER/OIL MICROEMULSION IN RELEASE OF OVALBUMIN Microemulsion Water/Oil with Surfactant (Span 80-Tween 80) : Cosurfactant (Ethanol) =5:1, 6:1, and 7:1 Anisa Rizki Amalia, Riesta Primaharinastiti, Esti Hendradi	18
ANALYSIS OF MYCOLIC ACIDS CLEAVAGE PRODUCT OF <i>Mycobacterium tuberculosis</i> BY GAS CHROMATOGRAPHY-FLAME IONIZATION DETECTOR Asri Darmawati, Deby Kusumaningrum, Isnaeni, Muhamad Zainuddin	21
PERIPLASMIC EXPRESSION OF GENE ENCODING ANTI-EGFRvIII SINGLE-CHAIN VARIABLE FRAGMENT ANTIBODY USING PeIB LEADER SEQUENCE IN <i>ESCHERICHIA COLI</i> Kartika Sari Dewi, Debbie Sofie Retnoningrum, Catur Riani, Asrul Muhamad Fuad	24
IN VIVO ANTIMALARIAL ACTIVITY OF ETHANOL EXTRACT AND ETHYL ACETATE FRACTION OF <i>Alectryon serratus</i> LEAVES ON <i>Plasmodium berghei</i> INFECTED MICE Aty Widyawaruyanti, Uswatun Khasanah, Lidya Tumewu, Hilkatul Ilimi, Achmad Fuad Hafid, Indah S Tantular	30
PROFILE OF COMMUNITY PHARMACISTS KNOWLEDGE IN PATIENT ASSESSMENT WITH INFLUENZA SYMPTOMS AND ITS PRODUCTS Azza Faturrohmah, Arie Sulistyarini, Ana Yuda	33

SOLUBILITY AND DISSOLUTION STUDY OF KETOPROFEN – HIDROXYPROPYL- β -CYCLODEXTRIN INCLUSION COMPLEX (Prepared by Kneading Method) Bambang Widjaja, Achmad Radjaram, Arafah Zulhana	37
FORMULATION AND STABILITY TESTING OF MELOXICAM SOLID DISPERSION GEL Budipratiwi Wisudyaningsih, Inka Dewi Nur Anggaraini, Fersiya Wardani	40
EFFECT OF MENTHOL AS PENETRATION ENHANCER TO DICLOFENAC SODIUM MEMBRANE-TYPED TRANSDERMAL PATCH CHARACTERIZATION Destria Indah Sari, Esti Hendradi, Junaidi Khotib	43
PHYSICAL CHARACTERISTICS AND RELEASE STUDY OF OVALBUMIN FROM ALGINATE MICROSPHERES PREPARED BY DIFFERENT CONCENTRATION OF ALGINATE AND BaCl ₂ USING AEROSOLIZATION TECHNIQUE Dewi Melani Hariyadi, Tristiana Erawati, Sisilia Ermawahyuningtyas	46
MUCOADHESIVE TABLET OF ETHANOLIC EXTRACT OF SAMBILOTO (<i>Andrographis paniculata</i>) AS ANTIDIABETIC USING CHITOSAN Dhadhang Wahyu Kurniawan, Hening Pratiwi, and Lingga Ikaditya	50
PHYSICAL INTERACTION STUDY OF IBUPROFEN-STEARIC ACID BINARY MIXTURE Diajeng Putri Paramita, Dwi Setyawan, Dewi Isdiartuti	59
MOLECULAR MODELING AND SYNTHESIS OF 1-(3,4-Dichlorobenzoyl)-1,3-dimethylurea Dian Agung Pangaribowo, Siswandono, Bambang Tri Purwanto	63
EXPRESSION OF RECOMBINANT HUMAN GRANULOCYTE-COLONY STIMULATING FACTOR WITHIN PERIPLASMIC COMPARTMENT OF <i>Escherichia coli</i> USING PeIB LEADER PEPTIDE Dian Fitria Agustiyanti, Asrul Muhamad Fuad	66
EVALUATION OF ANTIHYPERURICEMIC ACTIVITY FROM BULBS OF BAWANG TIWAI (<i>Eleutherine palmifolia</i> (L.) Merr.) BY IN VITRO AND IN VIVO STUDIES Dian Ratih Laksmiawati, Rininta Firdaus, Yulinda, Mediana Astika	72
ANTIOXIDANT ACTIVITY OF 96% ETHANOL EXTRACT OF COMBINATION OF STRAWBERRY FRUIT (<i>Fragaria x ananassa</i> Duch.) AND STARFRUIT (<i>Averrhoa carambola</i> L.) USING ABTS FREE RADICAL SCAVENGING METHOD Diana Serlahwaty, Indira Natalia Timang	76
ENHANCEMENT OF SOLUBILITY AND DISSOLUTION ATORVASTATIN BY MICROCRYSTALLIZATION METHOD Dolih Gozali, Yoga Windu Wardhana, Ronny Tandela	79
<i>IN VITRO</i> ANTIMALARIAL ACTIVITY OF DICHLOROMETHANE SUB-FRACTION OF <i>Eucalyptus globulus</i> L. Stem AGAINST <i>Plasmodium falciparum</i> Elis Suwarni, Achmad Fuad Hafid, Aty Widnyawaruyanti	86
<i>Arcangelisia flava</i> INCREASES RATS' LEUKOCYTES BUT HAS BIPHASIC EFFECT ON RATS' LYMPHOCYTE Endah Puspitasari, Evi Umayah Ulfa, Vita Ariati, Mohammad SulthonHabibi	89

IN VITRO ANTIMALARIAL ACTIVITY OF CHLOROFORM SUBFRACTION OF SALAM BADAK LEAVES
(*Acmena acuminatissima*)

Erna Cahyaningsih, Achmad Fuad Hafid, Aty Widayawaruyanti 92

CHARACTERIZATION OF DOSAGE FORM AND PENETRATION DICLOFENAC SODIUM WITH
MICROEMULSION SYSTEM IN HPMC 4000 GEL BASE (Microemulsion W/O with ratio use of surfactant
Span 80 – Tween 80 : Cosurfactant Ethanol 96% = 6:1)

Esti Hendradi, Tutiek Purwanti, Karina Wahyu Irawati 95

CONSTRUCTION AND VALIDATION OF THE STRUCTURE-BASED VIRTUAL SCREENING PROTOCOLS
WITH PDB CODE OF 3LN1 TO DISCOVER CYCLOOXYGENASE-2 INHIBITORS

Mumpuni E, Nurrochmad A, Pranowo HD, Jenie UA, Istyastono EP 99

VALIDATED UV SPECTROPHOTOMETRIC METHOD FOR THE DETERMINATION OF ASPIRIN IN RABBIT
PLASMA : APPLICATION TO BIOAVAILABILITY STUDY OF ASPIRIN MICROCAPSULE IN RABBIT

Faizatun, Novi yantih, Teguh Iman Saputra 102

EFFECT OF COMPARISON OF SURFACTANT AND COSURFACTANT W/O MICROEMULSION OVALBUMIN
WITH SOYBEAN OIL TO PHYSICO-CHEMICAL CHARACTERIZATION (w/o Microemulsion with Surfactant
Span 80- Tween 80 : Cosurfactant Ethanol 96% = 5:1; 6:1 and 7:1)

Farida Mutiara Sari, Riesta Primaharinastiti, Esti Hendradi 105

pH INFLUENCE IN DESALTING PROCESS OF CRUDE PERTUSSIS TOXIN (PT) AND FILAMENTOUS
HEMAGGLUTININ (FHA) PURIFICATION FROM *Bordetella pertussis* BY SEPHADEX G-25 COLUMN
CHROMATOGRAPHY

Faris Adrianto, Esti Hendradi, Neni Nurainy, Isnaeni 108

SEPARATION OF COSMETIC PRESERVATIVES USING SILICA-BASED MONOLITHIC COLUMN

Febri Annuryanti, Riesta Primaharinastiti, Moch. Yuwono 111

PREPARATION AND CHARACTERIZATION OF TELMISARTAN-CITRIC ACID CO-CRYSTAL

Fikri Alatas, Hestiary Ratih, Sundani Nurono Soewandhie 114

PATIENTS' AND CAREGIVERS' LIQUID MEDICATION ADMINISTRATION ERRORS

Gusti Noorizka Veronika Achmad, Gesnita Nugraheni 117

THE POTENCY OF CANARIUM OIL (*Canarium indicum*) AS A MATERIAL FOR STRUCTURED LIPID
PRODUCTION

Hamidah Rahman, Johnner P Sitompul, Kusnandar Anggadiredja, Tutus Gusdinar 121

EFFECT OF TREHALOSE ON THERMAL PROPERTIES OF PHOSPHOLIPID-DDA AND TPGS MIXTURES

Helmy Yusuf 124

PREPARATION AND CHARACTERIZATION OF FLUKONAZOLE- β -CYCLODEXTRIN INCLUSION COMPLEXES

Hestiary Ratih, Fikri Alatas, Erin Karlina 127

ISOLATION AND IDENTIFICATION OF ANTIOXIDANT COMPOUND BY BIOPRODUCTION OF
ENDOPHYTIC FUNGI OF TURMERIC (*Curcuma longa* L.) ISOLATE CL.SMI.RF11

Hindra Rahmawati, Bustanussalam, Partomuan Simanjuntak 130

MODIFICATION PROCESS OF NATURAL CASSAVA STARCH : THE STUDY OF CHARACTERISTICS AND PHYSICAL PROPERTIES

Prasetia, Jemmy A, C.I.S. Arisanti, N.P.P.A. Dewi, G.A.R. Astuti, N.W.N Yulianingsih, I M.A.G. Wirasuta 133

DRUG USE PROFILE OF DIABETIC PATIENTS IN EAST SURABAYA PRIMARY HEALTH CARE

I Nyoman Wijaya, Azza Faturrohmah, Ana Yuda, Mufarriha, Tesa Geovani Santoso, Dina Kartika, Hikmah Prasasti N, Whanni Wido Agustin 136

GLYCINE MAX DETAM II VARIETY AS PREVENTIVE AND CURATIVE ORGAN DAMAGE DUE TO EXPOSURE TO ,LEAD (Pb)

Rika Yulia, Sylvan Septian Ressandy, Gusti Ayu Putu Puspikaryani, I Putu Agus Yulyastrawan, Dewa Ayu Kusuma Dewi 142

AN ACTIVITY TEST OF MATOA LEAVES EXTRACT AS HEART RATE FREQUENCY REDUCTION WITH ADRENALINE INDUCTION

Ika Purwidyaningrum, Elin Yulinah Sukandar, Irda Fidrianny 144

EFFORT TO REDUCE COMPRESSIBILITY OF RAMIPRIL THROUGH CRYSTAL ENGINEERING

Indra, Sundani N Soewandhi 147

IN VITRO ALPHA-GLUCOSIDASE INHIBITORY ACTIVITY OF ETHANOLIC LEAF EXTRACT AND FRACTIONS OF *Rauwolfia serpentina* (L.) Benth. ex Kurz

Julie Anne D. Bolaños, Ivan L. Lawag 150

PERIPLASMIC EXPRESSION OF GENE ENCODING ANTI-EGFRvIII SINGLE-CHAIN VARIABLE FRAGMENT ANTIBODY USING PeIB LEADER SEQUENCE IN *Escherichia coli*

Kartika Sari Dewi, Debbie Sofie Retnoningrum, Catur Riani, Asrul Muhamad Fuad 153

CHARACTERIZATION AND LD₅₀ VALUE DETERMINATION OF 1,5-bis(3'-ethoxy-4'-hydroxyphenyl)-1,4-pentadiene-3-one (EHP)

Lestari Rahayu, Septian, Esti Mumpuni 159

DEVELOPMENT OF MELOXICAM TRANSDERMAL MATRIX TYPE PATCH USING POLYVINYLPIRROLIDONE, HYDROXYPROPYL METHYLCELLULOSE, AND ETHYL CELLULOSE COMBINATION

Lidya Ameliana, Monica Iwud, Selly Rio 162

ANTIHEPATITIS C VIRUS ACTIVITY SCREENING ON *Harpullia arborea* EXTRACTS AND ISOLATED COMPOUND

Lidya Tumewu, Evhy Apryani, Mei Ria Santi, Tutik Sri Wahyuni, Adita Ayu Permanasari, Myrna Adianti, Chie Aoki, Aty Widyawaruyanti, Achmad Fuad Hafid, Maria Inge Lusida, Soetjipto, Hak Hotta..... 165

HPLC METHOD PRECISION TO ASSAY OF A-MANGOSTIN IN Mangosteen (*Garcinia mangostana* L.) FRUIT RIND EXTRACT FORMULATED IN ORAL SOLUTION

Lilie Nurhidayati, Siti Sofiah, Ros Sumarny, Kevin Caesar 168

PREPARATION AND CHARACTERIZATION OF NARINGENIN-LOADED CHITOSAN NANOPARTICLES FOR CHEMOPREVENTION

Lina Winarti, Lusia Oktora Ruma Kumala Sari 170

RELATIONSHIP OF KNOWLEDGE AND PATIENT BEHAVIOR ON SELF MEDICATION PIROXICAM (Studies of Pharmacy in Sukun District, Malang City)

Liza Pristianty, Reshtia Eriana Putri, Hidayah Rachmawati 173

EFFECT OF CHRONIC USE OF ENERGY DRINK ON KIDNEY

Mahardian Rahmadi, Zamrotul Izzah, Mareta Rindang A, Aniek Setya B, Suharjono 176

SCREENING OF SURFACE MODIFIERS TO PRODUCE STABLE NANOSUSPENSION : A GENERAL GUIDANCE

Maria Lucia Ardhani Dwi Lestari 179

DEVELOPMENT OF SIMPLE POLYPHENOL SENSOR BASED ON SODIUM META PERIODATE AND 3-METHYL-2-BENZOTHAZOLINONE HYDRAZONE FOR COFFEE SAMPLES

Moch. Amrun Hidayat, Nindya Puspitaningtyas, Agus Abdul Gani, Bambang Kuswandi 181

VALIDATION OF AN HPLC ANALYTICAL METHOD FOR DETERMINATION OF LEVOFLOXACIN IN OPHTHALMIC PREPARATIONS

Mochamad Yuwono, Riasta Primaharinastiti, Ageng Teguh Wardoyo 184

VALIDATION OF SPECTROPHOTOMETRIC METHOD FOR ESTIMATION OF EPERISONE HYDROCHLORIDE IN TABLET DOSAGE FORM

Nia Kristiningrum, Diah Yuli Pangesti 187

ANTIOSTEOPOROTIC ACTIVITY OF 96% ETHANOLIC EXTRACTS OF ABELMOSCHUS MANIHOT L.MEDIK LEAVES AND EXERCISE ON INCREASING BONE DENSITY OF FEMALE MICE'S FEMORAL TRABECULAR

Niliestria Ayu Faramitha Sholikhah 190

EFFECT OF -CYCLODEXTRIN ON SPF VALUE AND INHIBITION OF KOJIC ACIDSTYROSINASE ACTIVITY IN VANISHING CREAM BASE FORMULATION (ON SUNSCREEN PRODUCT CONTAINED OXYBENZONE)

Noorma Rosita, Diana, Diana Winarita, Tristiana Erawati, Widji Soeratri 193

ANTIMICROBIAL ACTIVITY OF LACTOBACILLI PROBIOTIC MILK AND GUAVA LEAF ETHANOLIC EXTRACT (Psidium guajava) COMBINATION AGAINST BACTERIAL CAUSE OF DIARRHEA

Nur Putri Ranti, Isaeni, Juniar Moechtar, Febri Annuryanti 197

THE INFLUENCES OF PARTICLE SIZE AND SHAPE ON ZETA POTENTIAL OF COENZYME Q10 NANOSUSPENSION

Nuttakorn Baisaeng 200

SYNTHESIS, MOLECULAR DOCKING, AND ANTITUMOR ACTIVITY OF N,N'-Dibenzoyl-N,N'-Dimethylurea AGAINST HUMAN BREAST CANCER CELL LINE (MCF-7)

Nuzul Wahyuning Diyah 203

EXPRESSION OF ANTI-EGFRVIII SINGLE CHAIN FRAGMENT ANTIBODY (SCFV) ON THE SURFACE OF PICHIA PASTORIS

Pratika Viogenta, Asrul Muhamad Fuad, Suharsono 206

SUBCLONING OF <i>csf3syn</i> (COLONY STIMULATING FACTOR-3) GENE INTO pGAPZ? AND TRANSFORMATION OF RECOMBINANT VECTOR INTO <i>PICHIA PASTORIS</i>	
Prety Ihda Arfia, Asrul Muhamad Fuad	212
THE USE OF PERICARP MANGOSTEEN (<i>Garcinia mangostana</i> L.) EXTRACT IN FORMULATION OF CREAM-TYPE O / W	
Rahmah Elfiyani, Naniek Setiadi Radjab, Mia Sagita Sofyan	218
CHITOSAN BASED PARTICULATE CARRIER OF DITERPENE LACTON OF SAMBILOTO PREPARED BY IONIC GELATION-SPRAY DRYING :EFFECT OF STIRRING RATE AND NOZZLE DIAMETER	
Retno Sari, Titin Suhartanti, Dwi Setyawan, Esti Hendradi, Widji Soeratri	222
GAS CHROMATOGRAPHY-MASS SPECTROMETRY METHOD VALIDATION FOR PESTICIDES RESIDUES ANALYSIS IN FOOD USING QuEChERS KIT	
Riesta Primaharinastiti, Setyo Prihatiningtyas, Mochammad Yuwono	225
CHARACTERIZATION OF PARACETAMOL ORALLY DISINTEGRATING TABLET USING GELATIN 1% AND 2% AS BINDER AND POLYPLASDONE XL-10 10% AS DISINTEGRANT (Prepared by Freeze Drying Method)	
Roisah Nawatila, Dwi Setyawan. Bambang Widjaja	230
ANTIOXIDANT STUDY OF COSOLVENT SOLUTION OF MANGOSTEEN (<i>Garcinia mangostana</i> L.) RIND EXTRACT IN RATS BY USING MDA PARAMETER	
Ros Sumarny, Liliek Nurhidayati, Yati Sumiyati, Fransiska Diana Santi	233
SCREENING OF SELECTED PHILIPPINE ROOT CROPS FOR β -Glucosidase INHIBITION	
Sarah Jane S. Almazora, Ivan L. Lawag	236
NIOSOME EMULGEL FORMULATION AND STABILITY TEST OF CINNAMON (<i>Cinnamomum burmanii</i> Nees & Th. Nees) Bark ETHANOLIC EXTRACT AS ANTIOXIDANT	
Sasanti Darijanto, Fidriani Irda, Widhita P.A.S	239
THEOPHYLLINE RELEASE FROM SUSTAINED RELEASE TABLET USING LACTOSA AND PVP K30 AS A CHANELLING AGENT	
Sugiyartono, Retno Sari, Agus Syamsur Rijal, TriMulyani, Agustina Maharani	242
EFFORTS TO PRODUCE 1-(BENZOYLOXY)UREA AS ANTICANCER DRUG CANDIDATE	
Suko Hardjono	245
DEVELOPMENT OF PEGylated RAPAMYCIN LITHOCHOLIC ACID MICELLE FOR CANCER THERAPY	
Aran Tapsiri, Kanokwan Jaiprasert, Rungtip Nooma, Awadsada Sukgasem, Supang Khondee	248
FEASIBILITY OF ORAL IMMUNIZATION AGAINST JAPANESE ENCEPHALITIS VIRUS USING CHITOSAN PARTICLES	
Supavadee Boontha, Worawan Boonyo, Hans E. Junginger, Tasana Pitaksuteepong, Neti Waranuch, Assadang Polnok, Narong Nitatpattana, Sutee Yoksan	251

THE INFLUENCE OF HYDROXY GROUP AT ORTHO (o) AND PARA (p) POSITIONS ON METILBENZOAT AGAINST SYNTHESIS OF HIDROKSIBENZO HIDRAZIDA DERIVATIVES Suzana, Adita R, Melanny Ika .S, Juni Ekowati, Marcellino Rudyanto, Hadi Poerwono, Tutuk Budiati	254
ANTIOXIDANT ACTIVITY TEST OF BEE PROPOLIS EXTRACT (Apis mellifera L.) USING DPPH (1,1-diphenyl-2-picrilhidrazy) FREE RADICALS SCAVENGING ACTIVITY Titiek Martati, Shahyawidya	258
CAPSULE FORMULATION and EVALUATION COMBINATION OF AQUEOUS EXTRACT OF Phaleria's (Phaleria macrocarpa (Scheff Boerf)) FRUITS and LEAVES as ANTIHIPERTENSIVE AGENT Titta H Sutarna, Sri Wahyuningsih, Julia Ratnawati, Fahrouk P, Suci Nar Vikasari, Ita Nur Anisa	260
MANUFACTURE AND CHARACTERIZATION OF SOLID DISPERSION GLIKLAZID- PVP K90 Titta H Sutarna, Fikri Alatas, Cicih Ayu Ningsih	264
ANTI-INFLAMMATORY ACTIVITY OF PARA METHOXY CINNAMIC ACID (PMCA) IN NANOEMULSION USING SOYBEAN OIL Tristiana Erawati M, Anneke Indraswari P, Nanda Ghernasih N.C, Noorma Rosita, Suwaldi Martodihardjo, Widji Soeratri	266
PHYSICAL CHARACTERISTICS AND PENETRATION OF DICLOFENAC SODIUM NIOSOMAL SYSTEM USING SPAN 20 AND SPAN 60 Tutiek Purwanti, Esti Hendradi, Noverika A. Putri, Nurtya J. Devi	271
FORMULATION AND CHARACTERISZATION OF JUICE OF LIME GEL USING CMC-Na BASE Uswatun Chasanah, Esti Hendradi, Inayah	275
HEPATOPROTECTIVE ACTIVITY OF Bidens pilosa L. IN CARBON TETRACHLORIDE INDUCED HEPATOTOXICITY IN RATS Vina Alvionita Soesilo, C.J. Soegihardjo	278
CYTOTOXIC ACTIVITY ASSAY AGAINTS HELA CELL LINES OF NOVEL ANTICANCER DRUG : N-(PHENYL CARBAMOYL) ISOBUTIRAMIDE Wimzy Rizqy Prabhata, Tri Widiandani, Siswandono	284
SIMPLE STEPS PURIFICATION OF RECOMBINANT HUMAN ERYTHROPOIETIN PRODUCED IN CHINESE HAMSTER OVARY CELL CULTURE Yana Rubiyana, Endah Puji Septisetyani, Adi Santoso	287
KINETICS STUDY COCRYSTALS KETOCONAZOLE-SUCCINIC ACID PREPARED WITH SLURRY METHOD BASED ON POWDER X-RAY DIFFRACTION (PXRD) Yuli Ainun Najih, Dwi Setyawan, Achmad Radjaram	290
CONSTRUCTION OF RECOMBINANT IMMUNOTOXIN Anti-EGFRvIII scFv::HPR FUSION PROTEIN AND INDUCIBLE EXPRESSION IN Pichia pastoris AS A TARGETED DRUG CANDIDATE Yuliawati, Asrul Muhamad Fuad	297
ALTERED PHARMACOKINETIC OF LEVOFLOXACIN BY COADMINISTRATION OF ATTAPULGITE Zamrotul Izzah, Toetik Aryani, Amalia Illiyin, Budi Suprpti	303

COMPARISON OF SODIUM STARCH GLYCOLATE AND CROSSCARMELLOSE SODIUM AS SUPERDISINTEGRANT IN MEFENAMIC ACID FAST DISINTEGRATING TABLET

Adeltrudis Adelsa D., Department of Pharmacy, Faculty of Medicine, Brawijaya University Malang, mohabbat.elcha@gmail.com, +6285855021145, **Oktavia Eka Puspita***, Department of Pharmacy, Faculty of Medicine, Brawijaya University Malang, oktaviaeka@gmail.com, **Amalia Ayuningtyas**, Department of Pharmacy, Faculty of Medicine, Brawijaya University Malang, **Marulita Isadora**, Department of Pharmacy, Faculty of Medicine, Brawijaya University Malang

INTRODUCTION

Fast disintegrating tablets (FDT) dissolve rapidly in the saliva. It is useful for those who has difficulty in swallowing, pediatrics, geriatrics, and also if there is little or no access to water. Superdisintegrant is the most important excipient in FDT. By the mechanism of wicking and swelling, water is pulled then particles swell and break up the matrix form within the tablet. Mefenamic acid is one of Non Steroidal Anti Inflammatory Drugs (NSAIDs) which mostly used for its analgesic effect. The formulation of mefenamic acid FDT is expected to give more rapid onset of action of the analgesic effect. Two swelling mechanism superdisintegrants were chosen to be analyzed. They were sodium starch glycolate (SSG) and croscarmellose sodium (CCS). The objective of this study is to compare those two superdisintegrants and find the optimal concentration.

MATERIAL & METHODS

Materials

Mefenamic acid, croscarmellose sodium, microcrystalline cellulose, sodium starch glycolate, and magnesium stearate were obtained from Kimia Farma. Mannitol and Talc were obtained from Bratachem.

Methods

THE RESEARCH WAS IN TRUS EXPERIMENTAL DESIGN. WE DESIGNED SIX FORMULAS AS FOLLOWS:

Ingredient (%)	Formulation					
	F1	F2	F3	F4	F5	F6
Mefenamic acid	50	50	50	50	50	50
Croscarmellose Sodium	0,5	2	5	-	-	-
Sodium Starch Glycolate	-	-	-	2	5	8
Mannitol	30	30	30	30	30	30
Magnesium Stearate	1	1	1	1	1	1
Talc	2	2	2	2	2	2
Microcrystalline Cellulose	Ad 100%	Ad 100%	Ad 100%	Ad 100%	Ad 100%	Ad 100%

Table 1. Formulation of Mefenamic Acid Tablets
(Total Weight of tablet = 500 mg)

Mixing of Bulk

Each of material was weighed and homogenized. Mefenamic acid, superdisintegrants (CCS or SSG) and microcrystalline cellulose were mixed for 7 minutes until homogen. Mannitol, talc and magnesium stearate were added and mixed for 2 minutes

Flow Properties

As many as 100 grams of bulk was flowed through the funnel. Angle of Repose were between 46-55 which means poor flow property. It must be agitated or vibrated. The flow property was stated good or excellent if the angle of repose more than 30. Also, the flow rate was not good because the value was below 10 grams/second.



	Angle of Repose (°)	Flow rate (g/sec)
F1	47.24 ± 0.34	4.35 ± 0.19
F2	47.24 ± 0.34	4.36 ± 0.31
F3	47.24 ± 0.34	4.35 ± 0.19
F4	47.24 ± 0.34	4.20 ± 0.05
F5	47.24 ± 0.34	4.20 ± 0.14
F6	47.24 ± 0.34	4.26 ± 0.09

Table 2. Flow Properties

Manufacturing of Mefenamic Acid Tablets

The tablets were made by direct compression method.

Evaluation of Mefenamic Acid Tablets

They were evaluated for characteristics of prepared tablets such as organoleptic, size and weigh uniformity, hardness, friability, wetting time, disintegration time, dissolution test and drug content.

RESULT

All of the tablets were white, smooth, round and flat. Those six formulas have diameter and thickness of tablet as 1.1 cm and 0.4 cm respectively. The weigh uniformity of the tablets was also fulfilled the requirement from Farmakope Indonesia. Meanwhile, the result of hardness, friability, disintegration time, swelling time, dissolution and drug content can refer to Table 3.

ANOVA One Way and HSD Tukey were performed to analyze the data and obtain the most optimum concentration of superdisintegrant. From the statistical analysis, the optimum concentration was denoted in F6 (SSG 8%).

DISCUSSION

All of the formulas have completed the requirements for weight variation and hardness. The friability value was more than 1%. It indicated that the tablets were friable. It might be due to manual direct compression had been used.

The result also pointed out the higher swelling and disintegration time for sodium starch glycolate as superdisintegrant. Crosscarmellose sodium is one of crosslinked cellulose. Its mechanism as superdisintegrant is swelling and wicking. It swells 4-8 times in less than 10 seconds. It swells in two dimensions. Meanwhile, sodium starch glycolate is one of cross-linked starch which has swelling mechanism. It swells 7-12 times in three dimensions less than 30 seconds. Based on their characteristics, it can be seen that sodium starch glycolate has higher swelling ability than crosscarmellose sodium. That is the reason why sodium starch glycolate gave faster swelling and disintegration time.

From the dissolution data, we can see that the result is below the requirements (<10%). Based on USP-NF25, the dissolution test of mefenamic acid can be approved if Q value was 75% or more in 45 minutes. The low Q value can be due to the medium. Aquadest was chosen as the medium based on Albreiki et al. 2013. Mefenamic acid soluble in alkali

	Drug content (%)	Weight variation (mg/tab)	Thickness (cm)	Friability (%)	Hardness (kg)	Swelling Time (sec)	Disintegration Time (sec)	Dissolution (%)
F1	96.09 ± 0.77	498.62 ± 3.11	0.4	2.40 ± 0.06	6.53 ± 0.54	149.4 ± 1.20	124.80 ± 4.08	2.10 ± 0.55
F2	101.85 ± 1.05	498.70 ± 3.24	0.4	2.52 ± 0.01	5.31 ± 0.44	70.2 ± 1.20	92.40 ± 4.38	5.09 ± 1.67
F3	103.71 ± 0.67	499.12 ± 2.79	0.4	2.67 ± 0.03	4.81 ± 0.49	76.2 ± 3.60	69.60 ± 2.70	9.31 ± 0.43
F4	100.7 ± 2.10	500.62 ± 3.50	0.4	2.36 ± 0.09	6.81 ± 0.44	79.00 ± 1.00	53.67 ± 1.53	4.68 ± 0.20
F5	100.5 ± 1.57	501.00 ± 4.11	0.4	2.66 ± 0.09	5.01 ± 0.46	70.67 ± 3.05	45.67 ± 1.15	5.81 ± 0.36
F6	100.9 ± 2.00	500.60 ± 0.44	0.4	2.91 ± 0.01	5.09 ± 0.39	53.33 ± 5.77	42.33 ± 2.03	6.23 ± 0.02

Table 3. Characteristics of prepared Mefenamic Acid Tablets



solution. Before measurement of the concentration, as 1 ml of dissolution samples were diluted in NaOH 0.1 M until 10 ml. According to Patil et al. 2010, mefenamic acid in aqueous dissolution medium was only soluble about 5.4%. Although, we had diluted in alkali solution, the result was similar when using aqueous only. We suggest phosphate buffer pH 7.4 or Tris buffer as alternative in dissolution media for mefenamic acid tablet.

CONCLUSION

Sodium starch glycolate is more rapid in wetting time and disintegration time than cross-carmellose sodium. It might be due to the three dimensional swelling mechanism of SSG. The optimal concentration is the formula with SSG 8%.

REFERENCES

1. Albreiki, HM, Kumar, S, Khan, SA. (2013). In Vitro Bioavailability and Pharmaceutical Evaluation of Five Brands of Mefenamic Acid Tablet Marketed in Oman. *Adv J Pharm Life Sci Res*, 1(1):1-6
2. Ansel, HC, Popovich, NG, Allen, LV, (2011). *Ansel's Pharmaceutical Dosage Forms and Drug Delivery Systems: Ninth Edition*. Lippincott Williams & Wilkins, Wolter Kluwer Business. Philadelphia
3. Bala, R, Sushil, K, Pravin, P. (2012). Polymers in Fast Disintegrating Tablet: A Review. *Asian J Pharmaceut Clin Res*, 5(2):11
4. British Pharmacopoeia Commission. (2002). *British Pharmacopoeia Volume 1 and 2*. London: The Department Health.
5. Departemen Kesehatan Republik Indonesia. 1979. *Farmakope Indonesia edisi III*. Jakarta. Dirjen Pengawasan Obat dan Makanan
6. Departemen Kesehatan Republik Indonesia. 1995. *Farmakope Indonesia edisi IV*. Jakarta. Dirjen Pengawasan Obat dan Makanan
7. Garg, A. (2013). Mouth Dissolving Tablets: A Review. *J Drug Delivery Ther*. 3(2). 207-214
8. Gupta, A, Mishra, SK, Gupta, V. et al. (2010). Recent Trends of Fast Dissolving Tablet – An Overview of Formulation Technology. *Int J Pharm Biolo Archiv*. 1(1):1-10
9. Khan, T, Nazim, S, Shaikh, S. et al. (2011). An Approach For Rapid Disintegrating Tablet: A Review. *Int J Pharm Res Dev*. 3(3):170-183.
10. Mangal, M, Thakral, S, Goswami, M, Ghai, P. (2012). Superdisintegrants: An Update Review. *Int J Pharm Pharmaceut Sci Res*. 2(2):32.
11. Rowe, CR, Sheskey, PJ, Owen, SC. (2006). *Handbook of Pharmaceutical Excipients*. USA. Pharmaceutical Press and American Pharmacists Association.
12. The United States Pharmaceutical Convention. (2006). *USP-NF25*. United States of America



STUDY EXPRESSION OF HUMAN ERYTHROPOIETIN EXPRESSION IN MAMMALIAN CELL

Adi Santoso, Research Center for Biotechnology, Indonesian Institute of Sciences Jl. Raya Bogor KM 46 Bogor, 19611, Indonesia, adi.santoso1960@gmail.com, **Popi Hadiwisnuwardhani**, **Yana Rubiana**, Research Center for Biotechnology, Indonesian Institute of Sciences Jl. Raya Bogor KM 46 Bogor, 19611, Indonesia, **Yulaika Romadhani**, **Endah Puji Septisetyani**, Research Center for Biotechnology, Indonesian Institute of Sciences Jl. Raya Bogor KM 46 Bogor, 19611, Indonesia, **Dyaningtyas D.P. Putri**, Faculty of Pharmacy, Gadjah Mada University Sekip Utara Yogyakarta, 55281, Indonesia

ABSTRACT

Recombinant human erythropoietin (EPO) is a glycoprotein with three complex type N-glycans and one O-glycan. EPO is the principle growth factor produced as a therapeutic agent for the treatment of anemia associated with severe kidney damage. EPO is composed of 165 amino acids in its mature form with an average molecular weight of 30 kDa. Sixty percent (by weight) of the molecule is the weight of the polypeptide, while the rest 40% of the weigh is the carbohydrate molecules.

Earlier study has proved that EPO with two additional N-link sugar chains showed better biological activity and longer half-life than EPO with native pattern (containing only 3 N-link sugar chains). In this study, EPO containing two additional N-link sugar chains (total 5 N-link sugar chains) was constructed. The recombinant plasmid, pcDNA3-EPO, was transfected to CHO-K1 cells. Besides study the expression of hEPO in CHO-K1 cells, we are also interested in determining the growth curve of the cells in relation to when the protein exactly expressed. How the CHO-K1 cell grow without being transfected was also studied and compared.

Keywords: erythropoietin, CHO-K1, protein expression.

INTRODUCTION

Erythropoietin (EPO) is a glycoprotein that stimulates the differentiation of late erythroid progenitor cells to mature red blood cells and as a consequence increases haemoglobin levels. EPO is approximately 30-37 kDa glycoprotein (exact molecular weight depends on degree of glycosylation) in which sixty percent of the molecule is an invariant 165 amino acid single polypeptide chain containing two disulphide bonds. The remaining 40% of the EPO mass consists of carbohydrate covalently attached at three N-linked and one O-linked sugar chain at Ser126 (Skibeli et al., 2001)

Recombinant human EPO (rHuEPO) has been known to be a stimulating agent in the treatment of anemia associated with various pathologies (i.e. cancer, HIV, chemotherapy, chronic renal insufficiency) (Egrie et al., 2001). With the patents of rhEPO and other therapeu-

tic proteins expired, the market has opened for biosimilar recombinant products from the same cell line with identical or improved pharmacokinetic properties and less immunogenic response. The production of recombinant human proteins has enabled great progress in healthcare and drug technology. With this, the availability of approved biopharmaceuticals has increased tremendously in the last several years.

Recently, the use of alternative expression systems was often mentioned. Two of well-known alternative systems for protein expression are yeast (e.g. *Pichia pastoris*) (Cereghino GPL and Cregg, 1999) and *Escherichia coli* (Fischer et al., 1999). However, for the therapeutic glycoprotein to be functional the glycosylation pattern has to be properly expressed. Thus, almost 70% of therapeutic proteins available in the market are expressed in mammalian cells.



This has enabled mammalian cells to provide the potential for stable and correctly folded recombinant proteins that have undergone all the post-translational modifications required for functionality (Mataschi et al., 2008). For this reason the demand of rhEPO protein currently met by recombinant expression in mammalian cells, especially CHO cells. In this study the growth curve and density of cells in relation to when the protein exactly expressed was examined.

MATERIALS AND METHODS

Cell Culture and Reagents

The CHO-K1 cells were obtained from Prof. Masashi Kawaichi, Nara Institute of Science and Technology (NAIST), Japan. The cells were grown in Nutrient Mixture F-12 Ham (F12) media (Sigma N6658) in the presence of 10% of fetal bovine serum (FBS, Sigma), 100U of benzylpenicillin and 100µg of streptomycin (Gibco, Invitrogen). The cell culture was grown in an incubator with the condition of 5% CO₂ and 37°C temperature.

Expression of rhEPO CHO-K1 Cells

The pcDNA 3 recombinant plasmid containing human epo gene with five N-linked carbohydrate chains was transfected into CHO-K1 cells by using Lipofectamin 2000 (Invitrogen) according to manufacturer's protocol. Stable expressing transformants were screened by using 1,000ng of G418. For single cell cloning, the cell was cultured in 96 well plate with the density of 1 cell per well. The cells were cultured untouched for 10 days. After 10 days, the cell colonies that grown from a single cell were transferred to 24 well plates. After confluencies have been reached the cell was then transferred to a bigger plate (6 well plates) and finally to 10 cm dish.

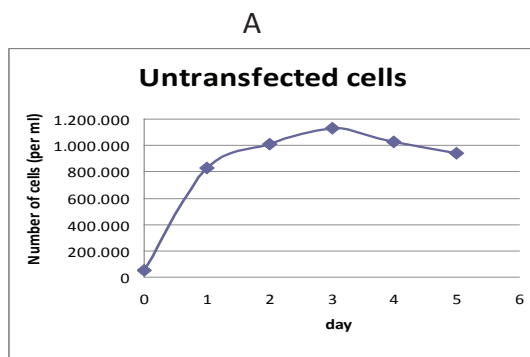
SDS-PAGE and Western Blotting

The purity of the protein analyzed by SDS/PAGE performed as previously described¹⁹ in a 12% separating gel with a 5% stacking gel us-

ing the Mini-PROTEAN-3 apparatus (Bio-Rad, Hercules, CA, USA). Following electroporation, proteins were transferred to Amersham Hybond ECL (GE Healthcare) by electroblotting. Western blots were performed using polyclonal anti human EPO antibody (Sigma, St. Louis, MO, USA) as the primary antibody and anti rabbit IgG alkaline phosphatase linked whole antibody (Promega, Madison, WI, USA) as the secondary antibody. The bands were detected by BCIP/NBT color development substrate (5-bromo-4-chloro-3-indolyl-phosphate/nitro blue tetrazolium) (Promega, Madison WI, USA).

RESULTS AND DISCUSSION

Recombinant plasmid pcDNA 3 containing human epo gene with five N-linked oligosaccharide chains was constructed. The coding sequence was fused with polyhistidine tag to enable easy and rapid purification and was placed under the control of CMV promoter. The plasmid was transfected into CHO-K1 cells using Lipofectamine 2000, and G418 resistance colonies were selected. Having pool of cells resistant to G418, the cells were then screened individually in 96 well plates. A cell clone that originated from a single cell was then transferred and continued to be screened successively in 24 and 6 well plates. Finally, the cell was cultured in 10 cm dish using the media mentioned above.





B

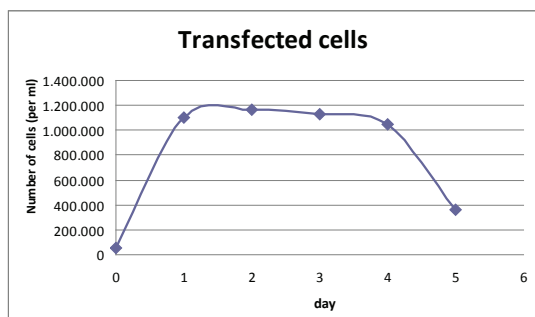


Figure 1. The growth curve of transfected and untransfected cells

One clone expressing hEPO and the CHO-K1 cell with no plasmid as negative growth curve control were used for subsequent study. The media were collected by centrifugation at 6000rpm for 5 min and the supernatant containing rHuEPO was collected while the cells were removed. Following purification, the sample was run on SDS/PAGE and detected with Western blot analysis using polyclonal anti human EPO antibody.

To find the optimum condition of rhEPO expression in CHO-K1 cells, 5×10^4 cells/ml media were cultured in 10cm in diameter dish containing 10 ml media. Before the experiment, the cell culture was passaged three times to make sure that the cells were ready for the expression study. The cells were cultured for five days and the samples were taken for protein rhEPO analysis using Western blot technique. For comparison of the growth curve between CHO-K1 with and without being transfected with plasmid, the CHO-K1 cell without transfection was cultured. The result (Fig. 1 A) show that, for transfected cells, the growth of the cell increased tremendously on day one. Right after day one, the cell density reached plateau. The density remained high until day 4 with the peak at day 2 which is about 1.16×10^6 cells/ml media. When we compared the growth curve of the transfected cells (Fig. 1 A) with Figure 2 interesting result was found. Analysis using Western blot shown that the

highest rhEPO protein expressed was at day 5. On the contrary, the highest density of the cell occurred at day 2 (Fig. 1A). Thus, the peak of cell density was not followed by the peak of protein expression. This data might show that it takes time for the cell to synthesize the protein of interest, in this case rhEPO.

Figure 1. The growth curve of transfected and untransfected cells

One clone expressing hEPO and the CHO-K1 cell with no plasmid as negative growth curve control were used for subsequent study. The media were collected by centrifugation at 6000rpm for 5 min and the supernatant containing rHuEPO was collected while the cells were removed. Following purification, the sample was run on SDS/PAGE and detected with Western blot analysis using polyclonal anti human EPO antibody.

To find the optimum condition of rhEPO expression in CHO-K1 cells, 5×10^4 cells/ml media were cultured in 10cm in diameter dish containing 10 ml media. Before the experiment, the cell culture was passaged three times to make sure that the cells were ready for the expression study. The cells were cultured for five days and the samples were taken for protein rhEPO analysis using Western blot technique. For comparison of the growth curve between CHO-K1 with and without being transfected with plasmid, the CHO-K1 cell without transfection was cultured. The result (Fig. 1 A) show that, for transfected cells, the growth of the cell increased tremendously on day one. Right after day one, the cell density reached plateau. The density remained high until day 4 with the peak at day 2 which is about 1.16×10^6 cells/ml media. When we compared the growth curve of the transfected cells (Fig. 1 A) with Figure 2 interesting result was found. Analysis using Western blot shown that the highest rhEPO protein expressed was at day 5. On the contrary, the highest density of the cell occurred at day 2 (Fig. 1A). Thus, the peak of cell density was not followed by the peak of

protein expression. This data might show that it takes time for the cell to synthesize the protein of interest, in this case rhEPO.

Day	Transfected cells /ml media	Untransfected /ml media
0	50.000	50.000
1	827.500	1.100.000
2	1.010.000	1.162.500
3	1.130.000	1.130.000
4	1.030.000	1.050.000
5	942.500	360.000

Table 1. Cell density of cultured cells

To study and compare on how transfection affect cell growth in CHO-K1, CHO-K1 cells were cultured on the same media and time. The data showed that, on day 5, the density of untransfected cells was still high (9.4×10^5 cells/ml media), while the transfected one was about 3.6×10^5 cells/ml media). On day 1, 2, 3, and 4 the density of the cells was comparable. It is very possible that overproduction of specific protein like heterologous recombinant protein production affect the growth of the cell itself.

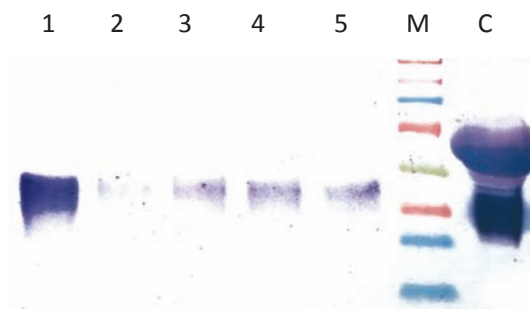


Figure 2. Western blot analysis of rhEPO protein expression. 1-5: day 1 to day 5 (molecular weight: approximately 47 kDa), M: protein marker, C: Positive control (molecular weight: approximately 30 kDa).

CONCLUSION

The data of this research showed that the connection between cell growth, cell density and peak of the interested protein being expressed was complex and not linear. As differ-

ent cell line and protein may have their own complexity, the best way of finding the right timing, cell density and cell growth to obtain the highest protein production was to perform cell growth and protein expression experiment of that specific protein.

ACKNOWLEDGEMENT

This study was supported by the National Innovation Program (SiNas), Ministry of Research and Technology (Menristek) (grant No. RD 2013-096). The authors are grateful to Prof. Masashi Kawaichi for providing CHO-K1 cells.

REFERENCES

1. Cereghino GPL and Cregg JM. (1999). Applications of yeast in biotechnology: protein production and genetic analysis, *Curr Opin Biotech*, 10(5): 422-427.
2. Egrie JC, Browne JK. (2001). Development and characterization of novel erythropoiesis stimulating protein (NESP), *Neophrol Dial Transplant*, 16(7): 3-13.
3. Fischer R, Drossard J, Emans N, Comman deur U and Hellwig S. (1999). Towards molecular farming in the future: moving from diagnostic protein and anti body production in microbes to plants, *Biotechnol. Appl. Biochem.* 30: 117-120.
4. Matasci M, Hacker DL, Baldi L and Wurm FM. (2008). Protein therapeutics recombinant therapeutic protein production in cultivated mammalian cells: current status and future prospects. In: *Drug Discov ery Today: Technologies*, 5: 37-42.
5. Skibeli V, Nissen-Lie G, and Torjesen P. (2001). Sugar profiling proves that human serum erythropoietin differs from recombinant human erythropoietin, *Blood*, 98: 3626-3634.



ANTIOXIDANT STABILITY ASSAY OF ALPHA TOCOPHERYL ACETATE IN SOLID LIPID NANOPARTICLE SYSTEM (LIPID BASE BEESWAX AND MONOSTEARIC GLISERYL 50:50)

Anggie Widhi, Pharmaceutics Department Faculty of Pharmacy Universitas Airlangga, anggiewip@gmail.com,
Noorma Rosita, Pharmaceutics Department Faculty of Pharmacy Universitas Airlangga, Widji Soeratri, Pharma-
ceutics Department Faculty of Pharmacy Universitas Airlangga

ABSTRACT

Introduction : As an antioxidant, alpha tocopheryl acetate is easily degraded by light and free radical in air. Solid Lipid Nanoparticle (SLN) is a system that can provide protection of active ingredient because of its drug entrapment ability and physical protective from UV light due to its nano-sized. The aim of this study is for investigated the ability of SLN that could increase stability of antioxidant potency from alpha tocopheryl acetate. SLN is expected to have higher stability of antioxidant potency compared with simple cream.

Methods : SLN and simple cream was made SLN was made using lipid beeswax (BW) and monostearic glyceryl (GMS) as base and Tween 80 as stabilizer. SLN was produced using high shear homogenization method and simple cream was produced using hot plate magnetic stirrer. Antioxidant potency was measured by DPPH method. Sample was radiated by UV C light as free radical initiator.

Result and Discussion : Alpha tocopheryl acetate loaded in SLN system has higher stability of antioxidant potency compared with simple cream that shown with k value as constanta of antioxidant potency degradation between time. This could be due to its physical blocker of UV light and drug entrapment properties.

Conclusion : SLN was selected as antioxidant carrier due to its ability to increase antioxidant stability of alpha tocopheryl acetate.

Keywords : antioxidant, alpha tocopheryl acetate, DPPH, stability, SLN

INTRODUCTION

Solid Lipid Nanoparticle (SLN) is a dispersion system with nano-sized particles in range 40-1000 with spherical shape (Muller, 2009). SLN has widely used in cosmetic formulation because of its advantages due to its nano-sized particle such as UV protective effect and enhance emmolient (Souto, 2008; Wissing, 2002).

Alpha tocopheryl acetate is derivate from tocopherol that commonly used as an antioxidant in cosmetic due to its properties of photo protective for skin and could decrease skin's damage of free radical (Nam, 2012; Tsai, 2012). As an antioxidant, alpha tocopheryl acetate is easily degraded by light and free radical in air. SLN is one of the system that could prevent the antioxidant degradation of alpha tocoph-

eryl acetate especially because the presence of light. It is result from SLN ability to scattering light with its nano-sized particles and produce physical UV protective effect (Golmohammadzadeh, 2012). The lipid matrix that contained in SLN also has the protective effect for active ingredient (Souto, 2008).

The aim for this study was for investigated the impact of SLN system with binary lipid beeswax and monostearic glyceryl (50:50) on antioxidant stability of alpha tocopheryl acetate compared with simple cream. Antioxidant activity is measured by DPPH method. Combination 50:50 of lipid component beeswax and monostearic glyceryl was selected due to the combination has higher physical stability and drug entrapment (Jenning, 2000; Rosita, 2013).



MATERIALS AND METHOD

Materials:

Tocopheryl acetate, DPPH (Sigma Aldrich), beeswax, monostearic glyceryl, tween 80, (PT. Bratako). Dapar component: acetic acid and sodium citrate (E. Merck), aquadest (PT. Jawis-esa).

Instrument:

Double beam UV Spectrophotometer UV-1800 Shimadzu, One Fourier Transform Infrared (FTIR) Spectrophotometer, pH meter Eutech Instruments pH 700, Differential Thermal Analyzer (DTA), DelsaTMNano C Particle Analyzer, JEOL JEM-1400 Electron Microscope, Ultra Turrax IKA® T25 Digital High Shear Homogenizer, Sentrifuge Hettich Rotofix 32, Ultrasonic LC 60h Elma, , Hot plate, UV C lamp

Preparation method of SLN

SLN formed by beeswax and monostearic glyceryl (GMS) as lipid core 50: were prepared by high shear homogenization method. 10% of tween 80 was used as surfactant and 20% of propylene glycol was used as co-surfactant. Acetic buffer pH 4.2, $\mu=0,5$ was used as aqueous phase (table 1). They were stirred at 24,000 rpm for 8 minutes, with 30 seconds intervals every two minutes, using an Ultra Turrax homogenizer T-25. The hot dispersion were cooled keep in stirring decreased speed gradually.

Ingredient	Function	Concentration
Beeswax	Lipid	10 %
Monostearic glyceryl	Lipid	
Alpha tocopheryl acetate	Active ingredient	10%
Tween 80	surfactant	10%
Propilen glycol	Co-surfactant	20%
Acetic buffer pH 4,2 , $\mu= 0,5$	Aqueous phase	Ad 100%

Table 1. Formula of SLN and simple cream tocopheryl acetate

Characterization of SLN

Measurement of Particle Size

Each sample was diluted with water before measurement. The particle sizes were analyzed by Delsa Nano Particle Size Analyzer at 25°C. Each measurement was performed in triplicates and the particle average diameter and polydispersity index (PI) was determined.

Observation of SLN morphology

The morphology of SLNs was observed by Transmission Electron Microscope (TEM). Either SLN blanks or SLN-PMCA were stained with phosphotungstic acid 2% w/v and placed on copper grids with former film for viewing at 120 kV (JEOL JEM-1400) and operated using software. The shape of SLN observed with Thermal Electron Microscope (TEM) and Drug entrapment of PMCA was measured by centrifugation method.

Measurement IC 50 Value of Alpha Tocopheryl Acetate

IC 50 value of alpha tocopheryl acetate was measured by DPPH method. The series of concentration of alpha tocopheryl acetate was prepared. 2 ml of sample in ethanol solution was centrifuged with 2 ml of DPPH solution. After 30 minutes absorbance of sample was measured by spectrophotometer in 517 nm.

Measurement of Antioxidant stability of Alpha tocopheryl acetate in SLN and simple cream

Each sample of SLN and simple cream alpha tocopheryl acetate was radiated by UV C light as free radical initiator. 1 gram of each sample was taken and diluted in ethanol and then centrifuged at 2500 rpm for 20 minutes. Supernatant was taken 2 ml and then mixed with 2 ml of DPPH. The reduction in DPPH radical was measured by spectrophotometer at 517 nm.

$$\% \text{ reduction} = \left\{ \frac{A_{\text{control}} - A_{\text{sample}}}{A_{\text{control}}} \right\} \times 100\%$$

RESULT AND DISCUSSION

SLN-alpha tocopheryl acetate had most spherical shape (fig 1,). Range of particle size, average of particle size and their Polydispersity Index (PI) can be seen in table 2.

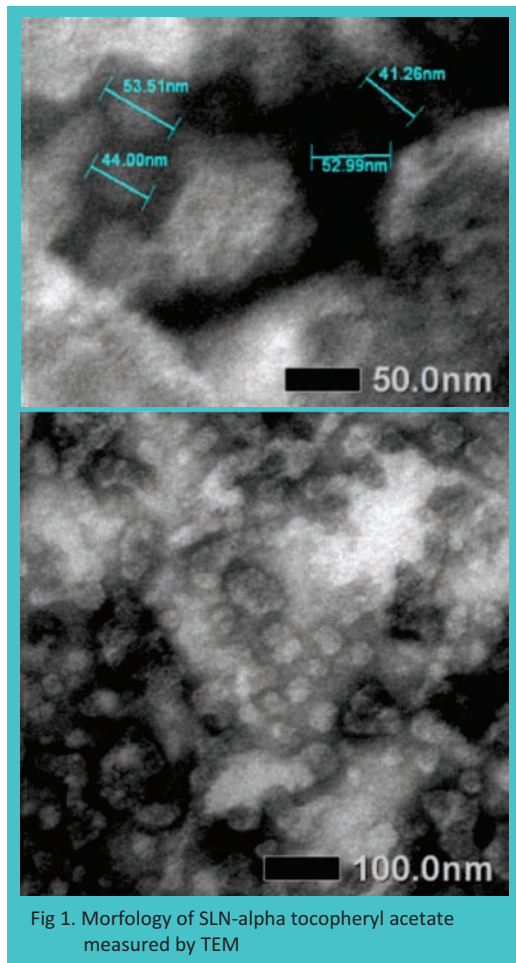


Fig 1. Morfology of SLN-alpha tocopheryl acetate measured by TEM

The existence of the particle size of SLN alpha tocopheryl acetate that are outside the range because the weakness of the manufacturing method of SLN with high shear homogenizer / high speed homogenizer which can result in the size of the microparticles in the SLN (Lason, 2011).

From table 3 it shown the IC 50 value of alpha tocopheryl acetate. The mean value of IC 50 alpha tocopheryl acetate is 2,56% ± 0,0850.

Replication	IC 50 Value (%)	Mean of IC 50 value ± SD (%)
1	2,66	
2	2,53	2,56±0,0850
3	2,50	

Table 3. IC 50 value of alpha tocopheryl acetate

The antioxidant stability of SLN and simple cream alpha tocopheryl acetate was shown in table 4 and fig.2.

System	Replication	Diameter range (nm)	Poly –dispersity Index (PI)	Diameter (nm)	Mean of Particle size ± SD (nm))
SLN alpha tocopheryl acetate	1	252,2 – 2544,9	0,345	900,7	1087,03 ± 256,28
	2	353,5 – 1764,3	0,386	981,1	
	3	338,4 – 6184,0	0,530	1379,3	
Simple cream alpha tocopheryl acetate	1	727,6 – 34129,2	0,766	2302,5	1957,9 ± 321,95
	2	414,7 – 213904,4	0,623	1664,8	
	3	417,9 – 95650,4	0,642	1906,4	

Table 2. Range of particle size, average of particle size and their Polydispersity Index (PI)

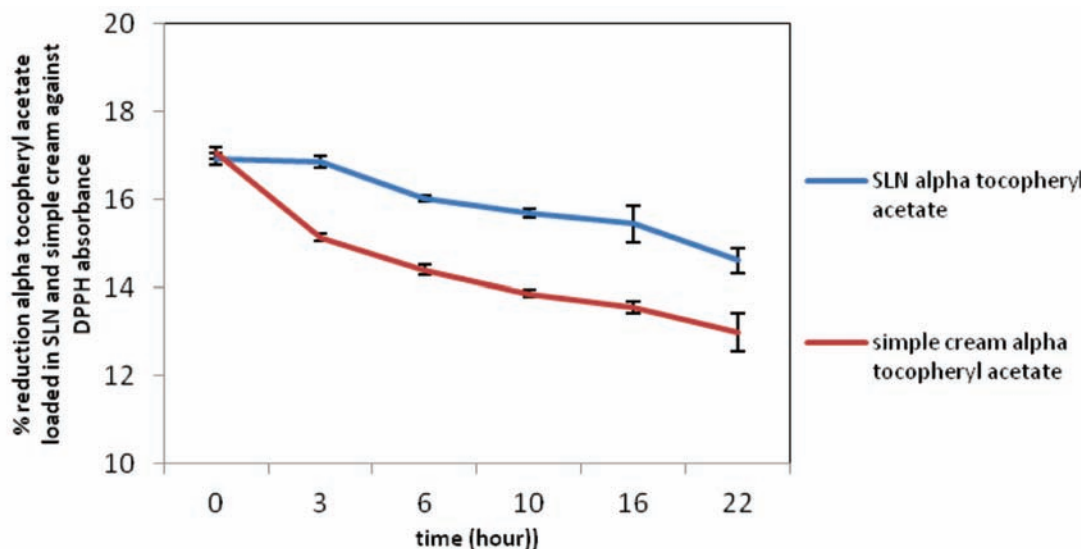


Fig. 2. Graphic % reduction alpha tocopheryl acetate loaded in SLN and simple cream against DPPH absorbance between time

System	Replication	constanta of antioxidant potency degradation between time (/hour)	Mean of constanta of antioxidant potency degradation between time \pm SD
SLN alpha tocopheryl acetate	1	0,0913	0,1030 \pm 0,0175
	2	0,0946	
	3	0,1232	
Simple cream konvensional alpha tocopheryl acetate	1	0,1714	0,1558 \pm 0,0169
	2	0,1379	
	3	0,1580	

Table 4. Constanta value of antioxidant potency degradation between time

From graphic in fig.2 it can be determined that SLN alpha tocopheryl acetate shown less sloping than simple cream alpha tocopheryl acetate. It means that decrease of antioxidant stability of alpha tocopheryl acetate loaded in SLN over the time is smaller than loaded in simple cream. This result was confirmed with constanta value of antioxidant potency degradation between time among SLN and simple cream loaded alpha tocopheryl acetate. SLN alpha tocopheryl acetate has smaller value of constanta of antioxidant potency degradation between time than simple cream alpha tocopheryl acetate. This phenomenon may occur as a result of UV blocker by SLN and drug entrapment effect of SLN that could protect active ingredient.

CONCLUSION

SLN was selected as antioxidant carrier due to its ability to increase antioxidant stability of alpha tocopheryl acetate.

REFERENCES

- Golmohammadzadeh, Shiva., Mortezaia, So-maye., Jaafari, M.R. 2012 Improved Photostability, Reduced Skin Permeation And Irritation Of Isotretinoin By Solid Lipid Nanoparticles. *Acta Pharm*, Vol 62, p.547-562
- Jenning, Volkhard., Gohla, Sven. 2000. Comparison of Wax and Glyceride Solid Lipid Nanoparticle (SLN). *International Journal of Pharmaceutics*, Vol 196, p.219-222



ICPPS 2014

Proceeding
The 1st International Conference
on Pharmaceutics & Pharmaceutical Sciences

Lason, Elwira., Ogonowski, Jan. Solid Lipid Nanoparticles – Characteristics, Application And Obtaining. 2011. CHEMIK. Vol 65, p.960-967

Muller, R.H., Hommoss, Aiman., Pardeike, Jana. 2009. Lipid Nanoparticles (SLN, NLC) In Cosmetic And Pharmaceutical Dermal Products. International Journal of Pharmaceutics, Vol 366, p.170-184

Rosita, Noorma., Soeratri, Widji. 2013. Pembuatan Dan Karakterisasi Sistem Solid Lipid Nanopartikel Asam Para Metoksisinamat (SLN-APMS) Dengan Basis: Berbagai Komposisi Beeswax dan Gliseril Monostearat. Surabaya : Universitas Airlangga

Souto, E.B., Muller, R.H. 2008. Cosmetic Features And Applications Of Lipid Nanoparticles (SLN, NLC). International Journal of Cosmetic Science, Vol 30, p.157-165

Nam, Yoong Sun., Kim, Jin-Woong., Han, Hoon Sang. 2012. Tocopheryl Acetate Nanoemulsions Stabilized With Lipid–Polymer Hybrid Emulsifiers For Effective Skin Delivery. Colloids and Surfaces B: Biointerfaces. Vol 94, p.51-57

Tsai, Feng-Jen., Wang, Yuang-Dai., Wu, Yu-Jen. 2012. Evaluation Of The Antioxidative Capability Of Commonly Used Antioxidants In Dermocosmetics By In Vivo Detection Of Protein Carbonylation In Human Stratum Corneum. Journal of Photochemistry and Photobiology B: Biology. Vol 112, p.7-15

Wissing, S.A., Muller, R.H. 2002. Solid Lipid Nanoparticles As Carrier For Sunscreens: In Vitro Release And In Vivo Skin Penetration. Journal of Controlled Release, Vol 8, p. 225-233



A BIOACTIVE BOVINE HYDROXYAPATITE–GELATIN IMPLANT FOR IN VITRO GENTAMICIN RELEASE

Aniek Setiya Budiatin, Faculty of Pharmacy Universitas Airlangga, anieksb@yahoo.co.id; **M. Zainuddin**, Faculty of Pharmacy Universitas Airlangga; **Junaedi Khotib** Faculty of Pharmacy Universitas Airlangga; **Diah Himawati**, Faculty of Science and Technology Universitas Airlangga

INTRODUCTION

The utilizing of drug delivery system (DDS) for releasing of drug locally is very important in aspect of therapy and orthopedic surgical, due to there is no guarantee it is free from microorganism infection during surgical perfectly. One of serious complications in case of open fracture and bone defect reconstruction is infection which are usually delivered by contamination of Gram positive Staphylococci (*S aureus*, *S epidermidis*) and Gram negative such as *Escherichia coli* and *Pseudomonas aeruginosa*. In osteomyelitis case, if serious complications happen such as decrease of function and sepsis should be avoid by implant as a must be choiced.¹

Penetration of drug locally is a difficult problem in the therapy of bone infection. Utilizing of antibiotic by intravena or oral way caused drug reached its target in low concentration. This is meant, dose of antibiotic used should be in high concentration to fulfill therapeutic dose in the target, but this way could cause side effect. Based on the condition, it is needed to develop biomaterial which biodegradable and osteoconductive that could take the function as drug delivery system (DDS). The beneficial of using DDS which biodegradable, bioresorption are: there is no need of re-surgical operation for taking the material off, decrease toxicity of foreign things, and the speed of drug releasing could be controlled through degradation modification.² Recently biomaterial is developed, those materials such as polimer natural collagen, gelatin, chitosan, and calcium compound (calcium phosphate, hydroxyapatite) as antibiotic delivery agent for bone infection therapy, to build protein-like composition and bone mineral.³

This study used bovine hydroxyapatite (BHA) –gelatin (GEL) as bioactive, biodegradable, and biocompatible material which take role as DDS and gentamicin as antibiotic. The beneficial of BHA-GEL are: there is no need of re-surgical operation to take it off because the biomaterial is one of bone mineral components and protein. The osteoconductivity of BHA is higher than HA synthesis. BHA-GEL pellet could deliver gentamicin (GEN) in higher concentration than MIC (minimum inhibitory concentration) that could eradicate pathogen microorganism, avoid over-dose and toxicity. Gentamicin widely used in bone infection therapy, having narrow therapy index, broad spectrum, resistant of high temperature, cause side effect of using systemic-ototoxicity, and nephrotoxic that cause GEN by its characters which well used for local application to less the side effects. To control GEN releasing from DDS, it is used cross-link agent glutaraldehyde (GA). In vitro characteristic of crosslinking BHA-GEL-GEN processed to GA could be performed; the changing of function cluster with FITR; morphology of compound surface with SEM; the changing of porosity and density and releasing of GEN from DDS.

METHODS

Material

Bovine hydroxyapatite (BHA) was accepted from RSUD Dr Soetomo Surabaya. Gelatin was purchased from Rousselot (Guangdong Chines). Acetone; glutaraldehyde, ethanol, K₂HPO₄, KH₂PO₄, NaCl, were purchased from Aldrich Chemical Co.,USA Gentamicin sulfate was purchased from Arshine Technology CO, Limited, Wanchai Chines; Gentamicin ELISA



Kit Catalog No CSB-E 12088f, Nutrient agar was purchased from E. Merck.

Implant preparation modified method2

BHA powder (20g) were mixed with 10 ml gelatin 20 % and added with gentamicin 10%. It was then mixed until looked such paste and then passed through a 1 mm mesh screen to granulate it and finally dried at 400C overnight. It was then immersed with 0.5%; 1.0% and 2.5% glutaraldehyde for 24 hr, subsequently washed with distilled water and then repeated with phosphate buffer saline and finally dried at 400C overnight.

Implants were molded into cylinder shape by compressing 100 mg of the resulting granulate in cycle dying (4 mm diameter) with force of 3 ton for 1 min, using Carver hydraulic press at room temperature. The pellet resulted was 4 mm in diameters and 3.2 mm in thickness.

Characterization

Measurement of Porosity and Density

A liquid displacement method was used to measure the porosity and density of composite of BHA-GEL-GA and BHA-GEL-GA-GEN. The density measurements provided information about pore size and distribution, permeability and composite structure. A composite of weight W was immersed in a graded cylinder containing a known of volume (V1) of water. The total volume of the water and composite was then recorded as V2. The volume difference (V2-V1) was the volume of the ceramic. The composite was removed from the water and the residual water volume was measured as V3.

Fourier Transform Infra Red (FT-IR)

In the present study, FT-IR spectroscopy (Parkin-Elmer) was used to estimate the conformational change of the structure in BHA-GEL and BHA-GEL-GEN composites cross-linked by GA.2

Scanning Electron Microscopy (SEM)

The morphology and microstructure of the

ceramic were examined using SEM (FEI type Inspect S 50 at 10 kV). The composite were cut by a razor and polished and then were gold-sputtered.4

In Vitro Release Study

Determination of Release Kinetics and Bioactivity5

The composite BHA-GEL-GA-GEN pellet was immersed in 2,0 ml of phosphate buffer saline (PBS), pH 7,4 at 370C. To determine the concentration of gentamicin release: 0,5 ml of PBS were withdrawn and replaced by fresh PBS after 3, 6, 12, 24 h and everyday until 21st and 28th. The eluted of PBS samples were frozen at -200C for microbiological assay. Control experiment using gentamicin-free composite sample was performed under the same experiment conditions and negative control, all sample were performed in triplicate. The concentration and bioactivity of the GEN release was determined using the diffusion method. Nutrient Agar plate inoculated with Staphylococcus aureus (ATCC 25923) was used to create a 106 colony- forming units/ml (CFU/ml) in 0,45% NaCl. One milliliter of S. aureus suspension was incorporated into 15 mL of Nutrient Agar medium heated at 450C. The agar was poured into a sterile glass plate and left to reach room temperature. Sixty microliters of samples were deposited in triplicate into 10-mm hole was made in the agar. Sample were located in different areas in the plates and left at room temperature for 30 min before incubation at 370C. After 24 hr of incubation, the diameters of inhibition zone were measured in triplicate and expressed as mean \pm SD as a function of time. The corresponding negative control samples (PBS) were measured using the same methodology. In addition, standard solutions of known gentamicin concentrations were prepared and tested with the same method to calculate the unknown gentamicin concentration in the samples.

RESULTS AND DISCUSSION

Implant Preparation

Result of cross-link process on BHA-GEL granule and BHA-GEL-GEN in concentration of GA 0.5%; 1.0% and 2.5%, shown that concentration of GA 0.5 % was more appropriate to be used than concentration 1.0% and 2.5%, this is shown at Figure 1. The utilizing of GA > 0.5% was just too much, it was detected by the appearance of turbidity or deposit which it came from result of reaction between GEL that released from the granule and shown excessive of GA would be reacted with GEL released from BHA-GEL granule and BHA-GEL-GEN which caused GA solution turned from clear to turbid, misty one.

Porosity and Density Analysis. Density of the pellet influenced mechanical power, permeability and the cure form of defect. Density measurement result of composite of BHA-GEL and BHA-GEL-GEN which cross-link with GA in the following way: chronologically were $0.3460 \pm 0.1584 \text{ g/cm}^3$; $0.9120 \pm 1.698 \text{ g/cm}^3$ and porosity $11.6667 \pm 3.2146\%$ and $2.6633 \pm 1.3395\%$; while for trabecular bone density, generally its number were between 0.14 to 1.10 g/cm^3 , it was meant that both sample were fulfilled density number.6

Observation result by SEM as seen in Figure 1A and Figure 1B shown that with addition of GEN and cross-linking with GA, caused change of surface morphology of BHA-GEL-GEN pellet turned to got more solid which this condition would affect porosity. SEM result figured out that the surface of pellet showing asymmetric surface and roughness, these would make cell got easier to attach and enter into it to proliferate and differentiate as also make antibiotic got easier to elute. In micrograph was also shown that GEL turned BHA to be more solid and trapped GEN particle inside and part of it attached outside (adsorbed). Adsorbed GEN would be first dissolved when got in touch with liquid that cause drug level released directly in much amount as load dose.7

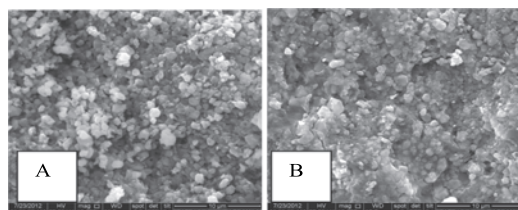


Figure 1: SEM of BHA-GA-GEL (A) and BHA-GEL-GEN (B)

Infrared Analysis

Figure 2 shows FITR spectra (Absorption vs wave-number) of composite material of BHA-GEL-GEN and BHA-GEL-GEN-GA. Specific wave-number of glutaraldehyde (GA) is 1715 cm^{-1} which shown C=O cluster of aldehyde, and after cross-linking process the wave-number was no longer seen. Because C=O cluster would turn to C=N which given wave-number range $1670\text{-}1650 \text{ cm}^{-1}$. This fact shown that GA was united with BHA-GEL and BHA-GEL-GEN formed covalent bond and turned to BHA-GEL-GA and BHA-GEL-GEN-GA. The wave-number $1400\text{-}1260$ show specific characteristic of C=O cluster of prolin GEL which it is 1337 cm^{-1} , which this is specific wave-number of collagen type 1 (Narbat et al., 2006). Wave-number of PO4- range $1090\text{-}1030\text{-}957 \text{ cm}^{-1}$ and $600\text{-}500 \text{ cm}^{-1}$, -NH2- cluster; -N=C from amida $1650\text{-}1628 \text{ cm}^{-1}$; 1540 and 1240 cm^{-1}

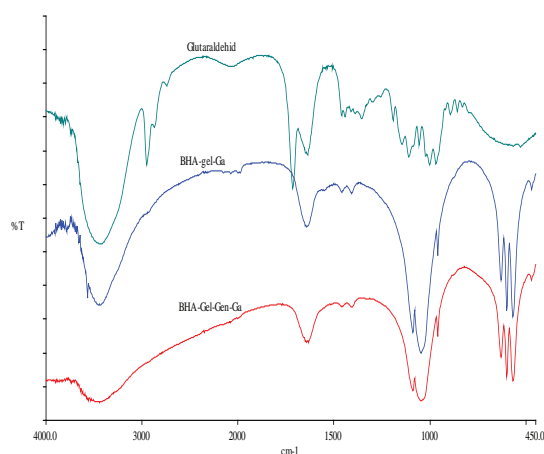


Figure 2: FTIR spectra of the materials: GA; BHA-GEL-GEN and BHA-GEL-GEN-GA



Release Profile and Biological Activity

The making of calibration curve of inhibition zone diameter and GEN concentration of some concentrations of GEN (1.25 to 40.00 ppm) was obtained equation $Y = 0.1515X + 10.313$; $R = 0.9869$, and the method taken was some standard concentrations of gentamicin flowing into a hole on media agar which contained *Staphylococcus aureus*, resulted correlation between standard concentration of gentamicin (GEN) and diameter of zone inhibition and resulted there was a linear correlation in R^2 -value = 0.9740. From the equation obtained it could be used to count sampling samples of in vitro release test during 28 days.

Figure 3 shows incubation result of releasing test sampling of GEN pellet by in-vitro, observed that inhibition zone diameters were bigger than MIC value during long periode, 28 days. It is mean that BHA-GEL-GEN-GA able to control GEN release during long periode and total releasing about 99,43%.

Result shows (Figure 4) that gentamicin (GEN) released from pellet BHA-GEL-GEN-GA in in-



Figure 3: Solution from dissolution test were determined with diffusion test with *Staphylococcus aureus* in Nutrient Agar

vitro releasing test during 28 days and than microbiologically tested gave antibacterial activity with inhibition zone diameter that bigger than MIC value of *Staphylococcus aureus*. It is expected that BHA-GEL-GEN-GA pellet could be in-vivo tested in rabbit as testing animal by making a defect/hole in the middle of its femur and than pellet is put into the hole as what performed by Meseguar- Olmo et al., (2006).

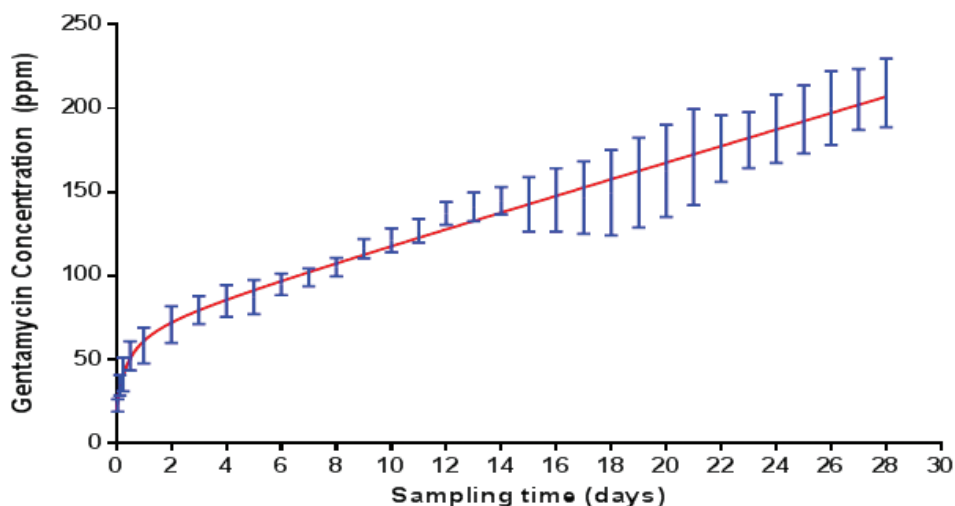


Figure 4: Concentration (ppm) vs Release time of GEN from BHA-GEL-GEN-GA implant



CONCLUSION

The characteristic of composite BHA-GEL-GEN-GA is similar bone mineral-protein phase and GEN can be released higher than MIC from GEN to inhibit *Staphylococcus aureus* for 28 days.

REFERENCES

13. Meseguer-Olmo L., Nicolas-Ros MJ., Sainz-Clavel M., et al. (2002). Biocompatibility and in vivo Gentamicin Release from Bioactive Sol-Gel Glass Implants. *Journal of Biomedical Materials Research Part A*, 61 (3): 458-465
14. Hae-Won K, Knowles JC, (2005). Hydroxyapatite and Gelatin Composite Foams Processed via Novel Freeze-drying and Crooslink for Use as Temporary Hard Tissue Scaffold. *J. Biomed Mater Res 72A*: 136-145
15. Baro M, Sanchez E, Delgado, Perera A, et al. (2002). In vitro- in vivo characterization of gentamicin bone implants. *Journal of Controlled Release* 83: 353-364
16. Virto MR, Frutos P, Torrado S., Frutos G., (2002). Gentamicin release from modified acrylic bone cements with lactose and hydroxypropylmethylcellulose. *Biomaterials* 24: 79-87
17. El-Ghannam A, Ahmed K, Omran M. (2005). Nanoporous Delivery System to Treat Osteomyelitis and Regenerate Bone: Gentamicin Release Kinetics and Bactericidal Effect. *J. Biomed Mater Res Part B: Appl Biomater* 73B: 277-284
18. Narbat, M.K., Orang F., Hashtjin M.S., and Goudarzi A. (2006). Fabrication of Porous Hydroxyapatite-Gelatin Composite Scaffolds for Bone Tissue Engineering, *Iranian Biomedical Journal* 10 (4): 215-223
19. Hillig WB, Choi S, Murtha S, et al, (2008). An Open-Pored Gelatin/Hydroxyapatite Composite as a Potential Bone Substitute, *J. Mater Sci: Mater Med* 19: 11-17



EFFECT OF COMPARISON SURFACTANT AND COSURFACTANT IN WATER/OIL MICROEMULSION IN RELEASE OF OVALBUMIN (Microemulsion Water/Oil with Surfactant (Span 80-Tween 80) : Cosurfactant (Ethanol) =5:1, 6:1, and 7:1)

Anisa Rizki Amalia, Faculty of Pharmacy, Universitas Airlangga, Surabaya, Indonesia, **Riesta Primaharinastiti**, Faculty of Pharmacy, Universitas Airlangga, Surabaya, Indonesia, **Esti Hendradi**, Faculty of Pharmacy, Universitas Airlangga, Surabaya, Indonesia esti_hendradi@yahoo.com

INTRODUCTION

Topically administering vaccines are currently being developed because of many bacterial and viral pathogens are able to enter the body through the skin¹). Topical administration has the advantage, among others, to avoid the first-pass effect in the liver metabolism, prevent degradation in the gastrointestinal tract, as well as easier to use and comfortable for the patient²). Therefore we need a system that is capable of delivering the vaccine to be able to penetrate the skin. Microemulsion is a stable colloidal dispersion system is thermodynamically and consists of phases of oil, water, surfactant, and cosurfactant which forms a clear solution with a droplet size of < 200 nm³). This system is an ideal system for use as a drug delivery has advantages because it is thermodynamically stable, ease of manufacturing process, has a low viscosity, and droplet sizes are very small so that it has a greater surface area which facilitates penetration of the active compound molecules into the membrane²). As a prototype vaccine protein, ovalbumin used as an active ingredient. Therefore ovalbumin dissolved in water, it will be made the microemulsion with the type w/o (Water in oil) where ovalbumin will be in the water phase which trapped by the oil phase. With the microemulsion type w/o active ingredient will be stable. Comparison between the surfactant and cosurfactant composition will affect the characteristics of the microemulsion system⁴). The characteristics of this system to be a factor of the release of the active ingredient. The

aim of this study was to investigate the effects of comparison surfactant (Span 80-Tween 80): cosurfactant (ethanol) = 5:1, 6:1, and 7:1 in released of ovalbumin from microemulsion water/oil (w/o) system.

METHODS

Material

Ovalbumin (Sigma-Aldrich), soybean oil food grade (PT Pan Pacific Indonesia), Tween 80 (Croda), Span 80 (Croda), ethanol (Merck), reagen Coomassie Brilliant Blue (Sigma-Aldrich), aquabidest (PT Widatra Bhakti).

Preparation

Span 80, Tween 80, soybean oil, surfactant and cosurfactant were mixed in different ratio (Table 1). In every ratio total concentration Surfactant and cosurfactant were 60%. Added aquabidest as water phase slowly to form a stable water in oil system. Then, mixed Ovalbumin into the system at high speed.

Material	Concentration (%)		
	5:1	6:1	7:1
Ovalbumin	1	1	1
Soybean oil	31	31	31
Span 80	37.38	38.45	39.25
Tween 80	12.62	12.98	13.25
Ethanol	10	8.57	7.5
Aquabidest	8	8	8

Table 1. Formula of ovalbumin in W/O microemulsion

Evaluation

Organoleptic Evaluation

Organoleptic evaluation carried out visually includes examining the color, odor, and consistency. The evaluations performed on microemulsion before and after added ovalbumin.

Evaluation Size Distribution of Droplet

Examination of the size and distribution of the microemulsion droplet size was performed with a submicron Delsa™ Nano Particle Size and Zeta Potential Dynamic Light Scattering. The evaluations performed on microemulsion before and after added ovalbumin.

In vitro release studies

The in vitro release of the diclofenac was performed using Franz diffusion Cell with selofan as a membran. All in vitro released study were performed at 100 rpm, with each medium of dissolution (aquabidestilata) was ± 21.5 mL. In every 50 μ l samples added 2.5 mL reagen Coomassie Brilliant Blue at different time intervals were analyzed for drug content using spectrophotometer Double Beam UV-VIS Recording UV 18000 (Shimadzu) at a maximum wavelength. All of the results were analyzed by statistic one way analysis of variance with degree of believed 95%.

RESULT AND DISCUSSION

Organoleptic evaluation of the microemulsion before and after added ovalbumin ovalbumin in each ratio have the same organoleptic which has a distinctive odor, clear yellow color and viscous consistency like oil.

In Figure 1 shown the result of the size and distribution of the microemulsion droplet size showed that the value \pm SD from 3 replications before added ovalbumin in formula 5:1 was 30.7 ± 4.01 nm; formula 6:1 was 27.6 ± 2.97 nm; and formula 7:1 was 27.1 ± 1.70 nm. Meanwhile, at the formula that has been added ovalbumin has a droplet size in formula 5:1 was 26.4 ± 0.94 nm; formula 6:1 was 23.8

± 0.26 nm; and formula 7:1 was 25.0 ± 1.14 nm. The statistical analysis using Independent T-Test showed that the value of Tcalculation (1,781) < Ttable (2.776) in formula 5:1, Tcalculation (2.190) < Ttable (2.776) in formula 6:1, and Tcalculation (1.804) < Ttable (2.776) in formula 7:1. It means that there was no significant difference in each formula before and after added ovalbumin.

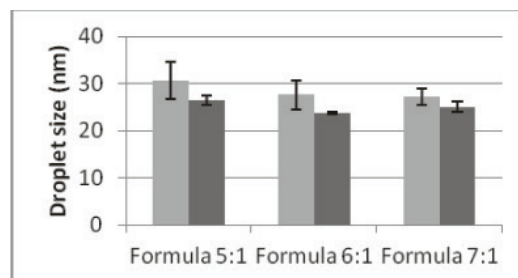


Figure 1 Histogram of the droplet size in microemulsion before and after added ovalbumin. Each column represents the mean \pm SD (n=3)

Figure 2 showed the released process of ovalbumin in system microemulsion W/O. Ovalbumin release was calculated by calculating the AUC (Area Under Curve) value of the cumulative amount of ovalbumin released per unit area per time. Figure 3 showed the AUC (Area Under Curve) of in vitro ovalbumin released study in system microemulsion W/O each formula. AUC results obtained in the formula 5:1 was 4693.46 g /cm² ± 1764.77 , formula 6:1 was 6590.04 g /cm² ± 1084.94 , and formula 7:1 was 5288.90 g /cm² ± 412.30 . The result of statistic using ANOVA one way showed that Fcalculated (1.898) < Ftable (5.14). It means that there was no significant difference minimum one pair data. Based on these results as a whole, with an increase in surfactant-cosurfactant ratio on formula ratio 5:1, 6:1 and 7:1 have not been able to provide a statistically significant difference from the results of droplet size. Therefore, the release of the results obtained did not give a significant difference.

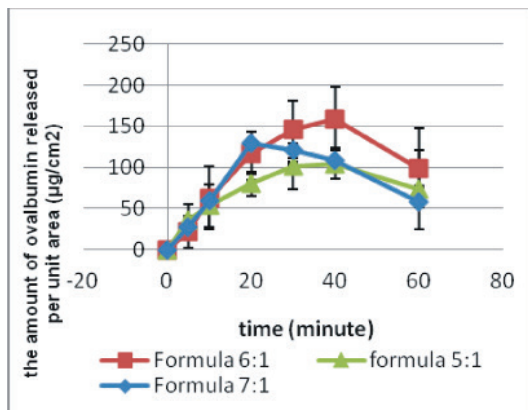


Figure 2. Profile between the amount of ovalbumin released per unit area ($\mu\text{g}/\text{cm}^2$) in a variety of formulas versus time

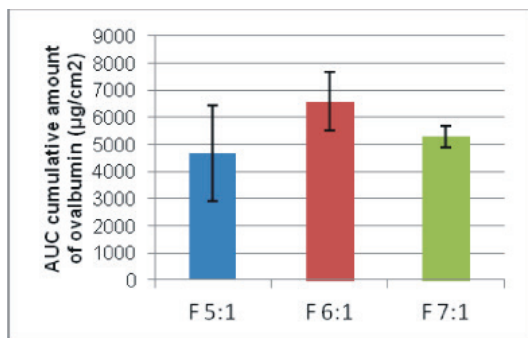


Figure 3. Histogram of AUC the cumulative amount of ovalbumin released in each formula. Each column represents the mean \pm SD ($n=3$).

CONCLUSION

The released of ovalbumin from microemulsion with the comparison of surfactant (Span 80-Tween 80): cosurfactant (ethanol) =5:1, 6:1, and 7:1) was no significant difference.

REFERENCE

1. Gupta, P. N., Singh, P., Mishra, V., Sanyog J., Dubey, P.K., and Vyas, S.P., 2003. Topical immunization : Mechanistic Insight and Novel Delivery. Indian Journal of Biotechnology vol 3, Januari 2004, pp. 9-21.
2. Kogan, A., Garti, N., 2006. Microemulsions as Transdermal Drug Delivery Vehicles. Advance in Colloid Interface Science 123-126 (2006) 369-385
3. Narang, A. S., Delmarre, D., and Gao, D., 2007. Stable Drug Encapsulation in Micelles and Microemulsions. International Journal of Pharmaceutics 345 (2007) 9–25.
4. Santos, A.C., Watkinson, A.C., Hadgraft, J., and Lane, M.E. 2008. Application of Microemulsions in Dermal and Transdermal Drug Delivery. Skin Pharmacology and Physiology 2008;21:246–259.

ANALYSIS OF MYCOLIC ACIDS CLEAVAGE PRODUCT OF MYCOBACTERIUM TUBERCULOSIS BY GAS CHROMATOGRAPHY-FLAME IONIZATION DETECTOR

Asri Darmawati, Faculty of Pharmacy Airlangga University, Surabaya, Indonesia, asridarmawati@yahoo.com, Deby Kusumaningrum, Clinical microbiology department, Dr. Soetomo Hospital, Surabaya, Indonesia, Isnaeni, Faculty of Pharmacy Airlangga University, Surabaya, Indonesia, Muhamad Zainuddin, Faculty of Pharmacy Airlangga University, Surabaya, Indonesia.

INTRODUCTION

Mycolic acids (MAs) are specific lipid fractions of the outer cell wall of Mycobacterium species. The characteristic structure of MA is not affected by culture conditions. MAs are recognized as a stable phenotypic property of Mycobacterium species (1). MAs are high-molecular weight of β -hydroxyl fatty acids with long alkyl chains at α position. Each MA molecule contains 60-90 carbon atoms with some cyclopropane ring at meromycolate chain (Figure 1). M. tuberculosis (MTB) produces alpha MA (70%), methoxy MA and keto MA (10-15) %. Different strains of MTB contained significantly different MAs components (5).

Identification of anomaly structure (or composition) of MAs can be based on MAs chromatogram profile using gas chromatography (GC). MAs can be identified as MAs methyl ester (6) or as MAs cleavage products (3, 4).

Since producing MAs methyl ester using Methanol-toluene-H₂SO₄ is time consuming (3-16 hours at 80°C) (4, 6), this study used BF₃-methanol reagent, in order to shorten production time of MAs methyl ester. Although, methanolic-BF₃ had been reported could cleave the cyclopropane ring, oxidize unsaturated of fatty acid and produce methoxy artifacts when be used in a high concentration, it has same disadvantages as other acidic reagents in low concentration (2).

The aim of this study was to obtain a specific cleavage product or MAs cleavage product profile that can be used as a marker for identification of MAs MTB strain.

MATERIALS AND METHODES

Sample

H37Rv strain MTB, INH sensitive MTB isolate and INH resistant MTB isolate. All strains were supplied from Clinical Microbiology department of Dr. Soetomo Hospital.

Reagents

Middlebrook 7H10 with OADC supplement, Trehalose dimycolate (TDM) of M. Bovis ex Sigma, Tricosanoic methyl ester (TME) ex Sigma. KOH, NaOH, HCl, Na₂SO₄ exciccatus, NaCl, BF₃14% in methanol, methanol, heptane chloroform, (all of the reagents were pro analyze grade) except for heptane was pro GC.

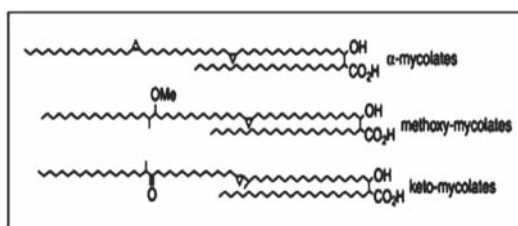


Figure 1. Mycolic acids structure (6)

Instrument

GC Agilent 6890 series, HP5 capillary column (30 m x 0,32 mm x 0,25 μ m), with Flame Ionization Detector (FID)

Sample preparation

Samples were grown on middlebrook media for 21-30 days. Biomass (+50 mg) placed in pyrex tube containing 2 ml of 25% KOH in a



mixture of methanol: water (1:1), and auto-claved for 1 hour at 121oC.

Isolation of mycolic acids of *M. tuberculosis*
1.5 ml of hydrochloric acid (1:1) was added to the pyrex tube and MAs were extracted with 3x 2 ml of CHCl₃. The collected chloroform extracts was dried in a gentle stream of N₂ gas.

Esterification of mycolic acids

1.0 ml of 0.5N methanolic-NaOH was added to the dried MAs extract in a pyrex cupped tube, and heated on the water bath for 5 minute at 95oC. The sample have been cooled to room temperature before addition of 1.0 ml 14% BF₃ in methanol and heating in water bath at 95oC for 1 hour. The obtained methyl ester MAs fragment was extracted using 3x1 ml heptane by agitation on vortex for 2 minutes. Heptane extract was separated by centrifugation at 2000 rpm for 2 minute and then transferred to another clean tube. Heptane extract was added with 2 ml saturated NaCl and agitated for 2 minute before separated to another tube. 1 g of Na₂SO₄ exsiccatus was added to heptan phase before the extract was dried by a stream of N₂ gas. The dried extract was re-dissolved in 0.30 ml heptane prior to injection in GC-FID.

RESULT AND DISCUSSION

The optimum operational conditions of GC-FID were as follow. Inlet and detector temperatures were set at 285oC, carrier gas (He) flow rate was 1 ml/minute, 2µL sample was injected by splitless technique. Column temperature was programmed as follow. It was started at 180 oC and hold for 6 minute, ram 2 oC/minute to 200 oC, maintained at 275oC for 1 minute, increased 5 oC/minute to 300 oC, and finally maintained at 300oC for 14 minute.

Esterification of MAs using methanolic-BF₃ fragmented TDM (ex. *M. bovis*) into 3 specific fragments which have t_R of 26.89, 28.51 and 30.09 minute respectively. Those specific fragments were also obtained in chromatogram of

H37Rv strain, INH resistant MTB isolate and INH sensitive MTB isolate (figure 2). Those fragments were identified (by GC-MS) as tetracosane methyl ester (C24), pentacosane methyl ester (C25) and hexacosane methyl ester (C26) (figure 2). MAs fragment of H37Rv has a different profile compared to two MAs fragment profiles of MTB isolates when using MAs fragments which have t_R of (6.22, 10.62, 11.32, 12.44 minute) and t_R of (8.45, 11.30, 12.44, 17.77, 26.82, 28.43, 28.85, 32.23 minute) (Table 1). Those MAs profiles are characteristic. MAs fragment profile of INH resistant MTB isolate distinguished from MAs fragment profile of INH sensitive MTB isolate with match factor (MF) of 8926.

t _R Code	t _R (minute)	Normalization area (%)		
		INH sensitive MTB isolate *	Strain H37Rv *	INH resistant MTB isolate **
2	8.5	3.6 ± 0.3	3.3 ± 0.9	5.3 ± 1.34
4	11.3	39.0 ± 2.3	24.7 ± 4.0	39.9 ± 9.32
5	12.5	21.3 ± 3.6	47.7 ± 5.1	28.1 ± 9.42
6	17.8	1.8 ± 0.6	1.5 ± 1.0	2.2 ± 0.66
7	26.8	8.9 ± 3.3	10.4 ± 3.6	9.3 ± 2.60
8	28.4	3.1 ± 1.2	2.8 ± 1.2	2.8 ± 1.53
9	28.9	1.6 ± 0.8	8.5 ± 5.6	1.6 ± 1.19
11	32.1	20.7 ± 1.9	1.0 ± 1.3	10.8 ± 4.59

* Average of three sample ** average of 6 sample

Table 2. Area normalization of MAs cleavage signal

CONCLUSION

This study concluded that the profile of MAs fragment of MTB strain was characteristic and can be distinguished each other. But, the profile of MAs fragment couldn't show which one of the MAs structure that had been changed .

REFERENCES

- Butler W, Guthertz LS. (2001). Mycolic Acid Analysis by High-Performance Liquid Chromatography for Identification of Mycobacterium Species. Clin. Microb. Reviews, 704-726.
- Christie, W. W. (1993). Preparation

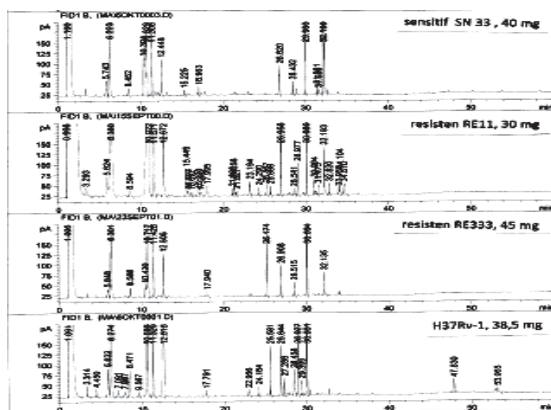


Figure 2. Chromatogram GC-FID of MAs

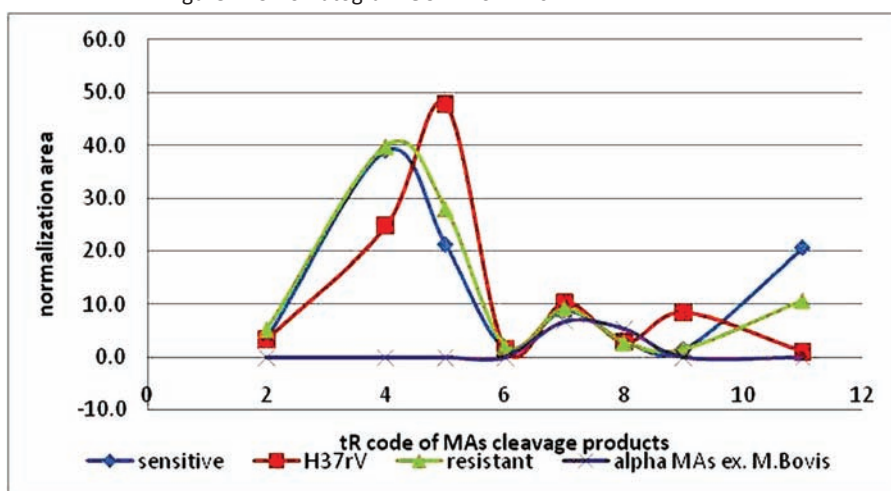


Figure 3. Mycolic acid cleavages profile

of Ester Derivatives of Fatty Acids for Chromatographic Analysis. In W. Christie, *Advances in Lipid Methodology*, 69-111.

3. Dang, N. A., Kolk, A. H., & Kuijper, S. (2013). The identification of biomarkers differentiating *M. tuberculosis* and nontuberculous mycobacteria via thermally assisted hydrolysis and methylation gas chromatography-mass spectrometry and chemometrics. *Metabolomics*, 9(9), 1274-1285.
4. Lambert, Mary A, C Wayne Moss, Vella A Silcox, and Robert C Good. (1986). *Analysis of Mycolic*

Acid Cleave Products and Cellular Fatty Acids of Myco-bacterium Species by Capillary Gas Chromatography. *J Clin. Microbiol*, 6: 731-736.

5. Verschoor, J. A., Baird, M., & Grooten, J. (2012). Towards understanding the functional diversity of cell wall mycolic acids of mycobacterium tuberculosis. *Progress in lipid research* 51, 325-339.
6. Vilcheze, C and Jacobs, William R. (2007). Isolation and Analysis of Mycobacterium tuberculosis of Mycolic acid. In *Current Protocols in Microbiology*, 10A.3.1. John Wiley & sons, 2007.



PERIPLASMIC EXPRESSION OF GENE ENCODING ANTI-EGFRvIII SINGLE-CHAIN VARIABLE FRAGMENT ANTIBODY USING PeIB LEADER SEQUENCE IN ESCHERICHIA COLI

Kartika Sari Dewi, School of Pharmacy, Bandung Institute of Technology, Jalan Ganesa 10, Bandung; Research Center of Biotechnology, Indonesian Institute of Sciences (LIPI), Cibinong Science Center, Jalan Raya Bogor Km. 46, Cibinong, Bogor; **Debbie Sofie Retnoningrum**, School of Pharmacy, Bandung Institute of Technology, Jalan Ganesa 10, Bandung; **Catur Riani**, School of Pharmacy, Bandung Institute of Technology, Jalan Ganesa 10, Bandung; **Asrul Muhamad Fuad**, Research Center of Biotechnology, Indonesian Institute of Sciences (LIPI), Cibinong Science Center, Jalan Raya Bogor Km. 46, Cibinong, Bogor,
Corresponding author: asrul.m.fuad@gmail.com.

INTRODUCTION

Many growth factors and their receptors play important roles in modulating cell division, proliferation and differentiation. Overexpression of growth factor receptors has been implicated as an important factor in the proliferation of malignancies and has also been identified as a marker of poor prognosis (Kuan et al., 2001).

Epidermal growth factor receptor variant III (EGFRvIII) is a mutant variant of EGFR that commonly overexpressed in human malignant cells. EGFRvIII has in frame deletion of exons 2-7 that encodes extracellular domain, resulting in the formation of new Glycine residue. Although EGFRvIII is unable to bind EGF or other EGFR-binding ligands, it is constitutively phosphorylated and able to activate downstream signaling cascades, which end up with cell differentiation (Pedersen et al., 2001). The possibility of disrupting this process has led to the development of novel therapeutic agents for cancer treatment (Kuan et al., 2001).

EGFRvIII is commonly found in glioblastoma multiforme and has been reported also in breast, ovarian, prostate, lung, head and neck carcinomas, but did not found in normal cells (Huang et al., 1997; Batra et al., 1995; Sok et al., 2006). Lacks of 267 amino acids from extracellular domain of EGFRvIII has resulted in the formation of a new immunogenic epitope near the amino terminus. Therefore this receptor might be used as an ideal molecular target

in immunology based cancer therapy (Gupta et al., 2010). In such kind of targeted cancer therapy, antibody fragments were frequently used as targeting moiety.

Fv fragment is the smallest unit of antibody molecule that preserves its antigen-binding properties. Thus, it can facilitate a targeted drug delivery for a treatment that requires high specificity. Single-chain variable fragment (scFv) is an antibody fragment that consists of variable regions of heavy (VH) and light chains (VL), joined together by a flexible peptide linker. Thus, it can be easily expressed in *Escherichia coli* (Ahmad et al., 2012). However, an scFv molecule has at least two disulfide bonds in its structure which are required to be correctly formed in order to preserve its antigen-binding affinity. In *E. coli* expression system, periplasmic compartment is preferably used for recombinant protein production that needs a correct protein folding and disulfide bond formation (Kipriyanov et al., 1997).

Periplasmic production of recombinant proteins provides several advantages compared to cytosolic production. For example, the authentic N-terminal amino acid sequence without the Methionine extension can be obtained after cleavage by the signal peptidase. Also, there appears to be much less protease activity in the periplasmic space than in the cytoplasm. In addition, recombinant protein purification is simpler due to fewer contaminating proteins in the periplasm (Makrides,



1996; Choi et al., 2000)

In this study, we reported the periplasmic expression of an anti-EGFRvIII scFv in *E. coli* BL21(DE3) periplasm. Prior to periplasmic expression, the DNA fragment encoding anti-EGFRvIII scFv was subcloned into pJ414 expression vector containing pelB leader sequence, which is derived from *Erwinia carotovora* (Lei et al., 1987). This leader sequence consists of 22 amino acids residues, which directs the recombinant protein production fused with this leader sequence into periplasmic compartment in gram-negative bacteria, such as *E. coli* (Choi and Lee, 2004).

MATERIALS AND METHODS

Plasmid containing DNA fragment of anti-EGFRvIII scFv (pJ201_scFv) was obtained from previous research. Expression vector containing pelB leader sequence (pJ414_pelB), *E. coli* TOP10 and BL21(DE3) are available in our laboratory. Primers used in this study were: scFv1-forward primer containing NcoI site (5'-GGC-CATGGC TCAAGTTCAATTGGTTGAGTCAGG-3'), scFv1-reverse primer containing XhoI site (5'-CGCCATGGCTCGAGT GATTAACAATGATGATG-GTGG-3'), and T7-promoter primer. All primers were purchased from IDT.

Construction of plasmid pJ414_pelB-scFv
DNA fragment encoding anti-EGFRvIII scFv was amplified from pJ201_scFv by PCR method. PCR was conducted as follows: initial denaturation at 95 °C for 1 m; 25 to 30 cycles of denaturation at 95 °C for 1 m, annealing at 60 °C for 30 s, and extension at 72 °C for 1 m, then final extension at 72 °C for 5 m. PCR products were analyzed with 1 % agarose gel electrophoresis.

Purified PCR product and pJ414_pelB expression vector were double digested using NcoI and XhoI enzymes (3 IU /1 µg product), then incubated at 37 °C for 18 h. Digested products were examined with 1% agarose gel electrophoresis, subsequently isolated from an agarose gel using Gel/PCR DNA Fragments Extrac-

tion Kit (Geneaid).

Purified scFv gene and plasmid were ligated using T4-DNA ligase (1 IU/50 ng plasmid), then transformed into *E. coli* TOP10 using transformation and stock solution (TSS) (Chung et al., 1989). Recombinant plasmids were isolated from *E. coli* transformants, then characterized by migration, restriction, and PCR analyses. It was subsequently sequenced to ensure no mutation presents within the gene sequence. Confirmed recombinant plasmid was then transformed into *E. coli* BL21(DE3).

Growth conditions for scFv expression

E. coli BL21(DE3) carrying pJ414_pelB_scFv were grown overnight in Luria Bertani medium with 100 µg/mL ampicillin (LBamp) at 37°C. This culture was diluted 1:50 with 20 mL LBamp medium, grown at 37°C in 100 mL shaking flask. When cultures reached OD600 = 0.8, IPTG was added and growth was continued at room temperature (20-23°C) for 18-20 h. Optimization of IPTG concentration was carried out by varying IPTG concentration from 0.1 to 1 mM.

Isolation of soluble periplasmic proteins

Cells were harvested by centrifugation at 5000 x g and 4°C for 15 m. Pelleted cells were resuspended with hypertonic solution consisting of 20% sucrose, 30 mM Tris-Cl, and 1 mM EDTA pH 8. After 1 h incubation on ice with occasional stirring, the spheroplasts were centrifuged at 11600 x g and 4 °C for 30 m, leaving the soluble periplasmic extract as the supernatant and spheroplasts plus the insoluble periplasmic material as the pellet (Kipriyanov et al., 1997). Supernatant containing periplasmic proteins were separated, and then analyzed by 10% SDS-PAGE.

Comparison of total proteins, soluble periplasmic and cytoplasmic proteins

As much as 100 mL culture was prepared by method previously described, induced by optimized IPTG concentration. Analysis of total proteins was done by adding 100 µL sample buffer into pellet cells from 1 mL culture. The remaining culture was pelleted, and then



soluble periplasmic and cytoplasmic proteins were isolated.

Isolation of cytoplasmic proteins was performed by freeze thaw method. Spheroplasts from periplasmic extraction were resuspended with lysis buffer consisting of 50 mM Tris-Cl, 3 mM EDTA, and 1 mM PMSF. Spheroplast suspension was subjected to five freeze-thaw cycles by freezing at -20 °C for 15 m and thawing for 15 m in room temperature. After that, thawed spheroplasts suspension was centrifuged at 11600 x g and 4 °C for 30 m, leaving the soluble cytoplasmic extract as the supernatant (Johnson and Hecht, 1994; Shrestha et al., 2012). Total proteins, soluble cytoplasmic and periplasmic proteins were then analyzed by 10% SDS-PAGE.

RESULT AND DISCUSSION

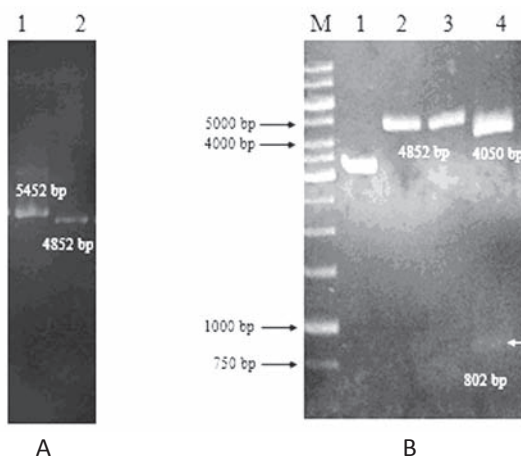
The pJ201_scFv plasmid was used as template for the scFv gene amplification, resulting in 802 bp of PCR product. The amplification product contains poly-histidine tag at the downstream of scFv sequence, and also NcoI and XhoI restriction sites to facilitate the cloning step. This DNA fragment was subcloned into NcoI and XhoI sites of pJ414_pelB vector. The recombinant plasmid obtained was named pJ414_pelB_scFv. To confirm correct recombinant plasmids, some analyses were carried out including migration, restriction, PCR and DNA sequencing.

Recombinant plasmid (4852 bp) and control plasmid (5452 bp) were run on agarose gel electrophoresis. Migration rate of recombinant plasmid would be faster than the control plasmid due to their sizes. Figure 1A showed the band of recombinant plasmid compared to control plasmid. To determine the actual size of the plasmid and insert DNA, restriction analysis was carried out. Figure 1B showed restriction of recombinant plasmid using NcoI or XhoI, which showed a single DNA band of 4852 bp. Double restriction analysis using both (NcoI and XhoI) resulting DNA bands with size of 802 and 4050 bp which corresponded to the

theoretical size of insert DNA and pJ414_pelB, respectively.

The PCR analysis was performed using T7-promoter and scFv1-reverse primers. These primers were used to determine the full-length construct of the gene within the pJ414_pelB plasmid. Thus, the PCR product would consist of T7 promoter, pelB leader sequence, scFv gene, and poly-histidine tag. Figure 1C showed a DNA band of approximately 900 bp, which corresponds to the theoretical size of desirable fragment. Based on DNA sequencing analysis (data not shown), there were no mutation in DNA encoding anti-EGFRvIII scFv gene. After all of analyses conducted, it could be concluded that the recombinant plasmid was successfully constructed.

E. coli is currently used as the host for producing antibody fragments. For disulfide-bonded proteins, good expression levels have been achieved via soluble production, secreting the proteins into the oxidizing environment of the bacterial periplasm where assembly and disulfide bond formation can occur. Periplasmic secretion is achieved by genetically fusing the leader sequence onto the N-terminus of the antibody sequence (Poplewell et al., 2005)



A

B

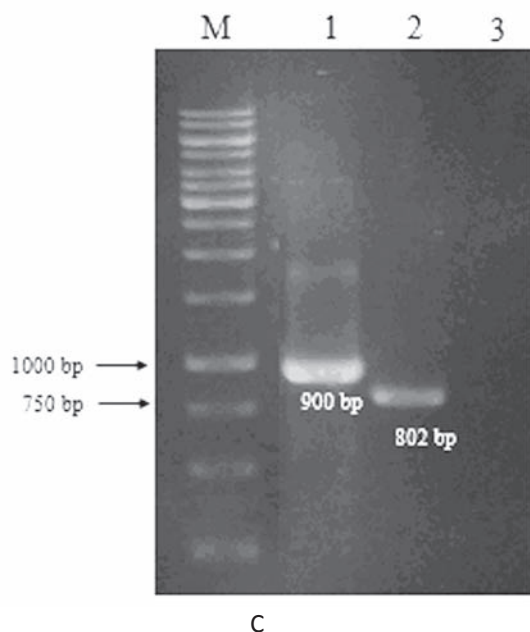


Figure 1. (A) Migration analysis of pJ414_pelB_scFv. Lane 1, comparator plasmid (5452 bp); lane 2, pJ414_pelB_scFv recombinant plasmid (4582 bp). (B) Restriction analysis of pJ414_pelB_scFv. Lane 1, pJ414_pelB_scFv uncut; lane 2, digested with NcoI restriction enzyme; lane 3, digested with XhoI restriction enzyme; lane 4, digested with NcoI and XhoI restriction enzyme. (C) PCR analysis of pJ414_pelB_scFv. Lane 1, using T7 promoter and reverse primers; lane 2, using forward and reverse primers; lane 3, negative control.

The oxidizing environment of periplasmic space, rich in proteins which are important for folding and catalyzing disulfide bond formation (PDI, DsbA and DsbC) or chaperones such as SKp (Fernandez, 2004; Bothmann and Pluckthun, 2000), is most suitable for proper folding of scFv fragment. Antibody fragments expressed in the periplasmic space have been shown to be correctly folded with excellent yield. Additionally, extraction of periplasmic-expressed proteins can easily be performed by a simple osmotic shock procedure (Tiwari et al., 2010)

The early stage in overproduction of scFv proteins was to optimize the optimal concentration of IPTG as inducer. Figure 2 lanes 3-6

showed total protein bands of induced *E. coli* culture using various IPTG concentrations. The scFv band is deduced to have approximate size of 28.76 kDa as it is shown on the SDS-PAGE analysis (Figure 2). The band size corresponds to the theoretical size of scFv proteins. Furthermore, total scFv proteins induced with 0.1 and 0.25 mM IPTG has a thicker band compared to those from 0.5 and 1 mM IPTG. However, such information was not enough to be used as a reference to determine the optimal concentration of IPTG in producing scFv proteins in periplasmic space. Therefore, analysis was continued to determine the effect of various IPTG concentration in the periplasmic protein expression.

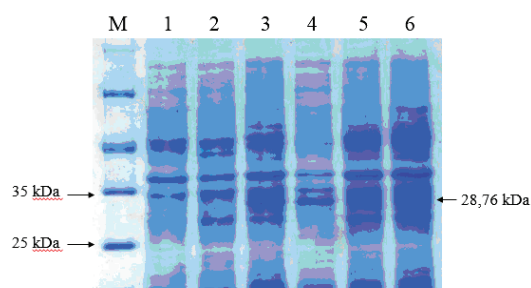


Figure 2. SDS-PAGE analysis of total proteins induced with various IPTG concentration. The scFv band is marked with an arrow (28.76 kDa). Lane 1, non transformant induced with 0.5 mM IPTG; lane 2, non induced transformant; lane 3, transformant induced with 0.1 mM IPTG; lane 4, transformant induced with 0.25 mM IPTG; lane 5, transformant induced with 0.5 mM IPTG; lane 6, transformant induced with 1 mM IPTG.

Figure 3 gives an overview of protein profiles extracted from the *E. coli* periplasm. Analysis was carried out to compare periplasmic protein profiles from induced and uninduced *E. coli* cultures. Based on the electrophoregram, it was observed that the bands of scFv protein clearly detected in periplasmic extract of transformant *E. coli* cultures induced with 0.1 and 0.25 mM IPTG. Considering these results, low concentration of IPTG was apparently optimum for periplasmic-proteins expression of this scFv.

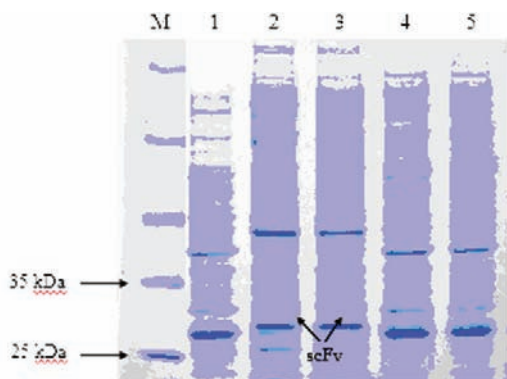


Figure 3. SDS-PAGE analysis of periplasmic proteins induced with various IPTG concentrations. The scFv bands are marked with arrows. Lane 1, non induced transformant; lane 2, transformant induced with 0.1 mM IPTG; lane 3, transformant induced with 0.25 mM IPTG; lane 4, transformant induced with 0.5 mM IPTG; lane 5, transformant induced with 1 mM IPTG

To find out the protein profiles produced using this expression system, a comparative analysis of total proteins, periplasmic proteins, and cytoplasmic proteins was carried out. Cytoplasm has a much larger space than periplasm. However, Figure 4 lanes 5 and 6 showed that the soluble scFv protein in cytoplasmic space was much less than in periplasmic space. This result indicates that the majority of scFv proteins in the cytoplasm were in the form of inclusion bodies.

ScFv protein has a disulfide bond in each VH and VL domains, but the cytoplasmic space has a reductive environment (Snyder and Champness, 2003). Therefore, disulfide bonds are unlikely be formed within the cytoplasm. Theoretically, it could be the cause of inclusion bodies formation within the cytoplasm.

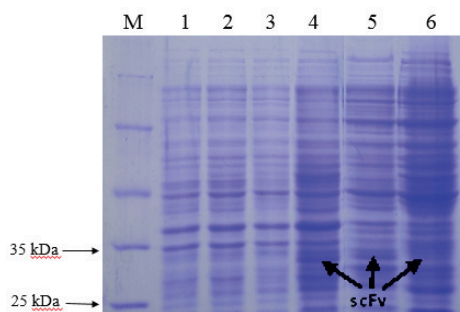


Figure 4. SDS-PAGE analysis of total proteins, soluble periplasmic and cytoplasmic proteins. The scFv band is marked with an arrow. Lane 1, total proteins of non induced non transformant; lane 2, total proteins of non transformant induced with 0.5 mM IPTG; lane 3, total proteins of non induced transformant; lane 4-6, total proteins, periplasmic and cytoplasmic proteins (respectively) of transformant cultures induced with 0.1 mM IPTG,.

All of those analyses indicates a protein band of 28.76 kDa observed in protein profiles of periplasmic and cytoplasmic of induced culture extracts which is not present in uninduced culture extracts. These results suggest that the scFv protein has been successfully expressed and found in samples of total proteins, periplasmic and cytoplasmic fractions. Thus, it can be concluded that pJ414_pelB_scFv plasmid has successfully express scFv protein in the periplasmic space using PelB leader sequence.

CONCLUSION

The pJ414_pelB_scFv plasmid has been successfully constructed and its sequence has been confirmed. Protein expression analyses have confirmed that the scFv protein has successfully been expressed in periplasmic space using pelB leader sequence and showed molecular size of approximately 28.76 kDa.

REFERENCES

Ahmad ZA, Yeap SW, Ali AM, et al. (2012). ScFv cliniantibody: principles and clinical application. Clin Dev Immunol, 2012:1-15.
Batra SK, Shobha CP, Wikstrand CJ, et al. (1995). Epidermal growth factor ligand-independent, unregulated, cell-transforming potential of a naturally occurring human mutant EGFRVIII gene. Cell Growth Differ, Oct;6:1251-1259.
Bothmann H, Pluckthun A. (2000). The periplasmic Escherichia coli peptidylprolyl cis,trans-isomerase FkpA. I. Increased functional expression of antibody fragments with and without cis-prolines. J Biol Chem, 275:17100-17105.



- Choi JH, Lee SY. (2004). Secretary and extracellular production of recombinant protein using *Escherichia coli*. *Appl Microbiol Biot*, 64:625-635.
- Fernandez LA. (2004). Prokaryotic expression of antibodies and affibodies. *Curr Opin Biotechnol*, 15:364-373.
- Gupta P, Han SY, Mitra SS, et al. (2010). Development of an EGFRvIII specific recombinant antibody. *BMC Biotechnol*, Oct;10(72):1-13.
- Huang HJS, Nagane M, Klingbeil CK, et al. (1997). The enhanced tumorigenic activity of a mutant epidermal growth factor receptor common in human cancers is mediated by threshold level of constitutive tyrosine phosphorylation and unattenuated signaling. *J Biol Activ*, 272:2927-2935.
- Johnson BH, Hecht MH. (1994). Recombinant proteins can be isolated from *E. coli* cells by repeated cycles of freezing and thawing. *BIO/TECHNOLOGY*, 12:1357-1360.
- Kipriyanov SM, Moldenhauer G, Little M. (1997). High level production of soluble single chain antibodies in small-scale *Escherichia coli* cultures. *J Immunol Methods*, 200:69-77.
- Kuan CT, Wikstrand CJ, Bigner DD. (2001). EGF mutant receptor vIII as a molecular target in cancer therapy. *Endocrine-Related Cancer*, 8:83-96.
- Lei SP, Lin HC, Wang SS, et al. (1987). Characterization of *Erwinia corotovora pelB* gene and its product pectate lyase. *J Bacteriol*, 169(9):4379-4383.
- Makrides SC. (1996). Strategies for achieving high-level expression of genes in *Escherichia coli*. *Microbiol Rev* 60:512-538.
- Pederson MW, Meltorn M, Damstrup L, Poulsen HS. (2001). The type III epidermal growth factor receptor mutation (biological significance and potential target for anti-cancer therapy). *Annals of Oncology*, 12:745-760.
- Popplewell AG, Sehdev M, Spitali M, Weir ANC. (2005). Therapeutic proteins: methods and protocols. *Methods in molecular biology*, 308:17-30.
- Shrestha P, Holland TM, Bundy BC. (2012). Streamlined extract preparation for *Escherichia coli*-based cell-free protein synthesis by sonication or bead vortex mixing. *Biotechnology, Sep*;53:163-174.
- Snyder L, Champness W. (2003). Molecular genetics of bacteria. American Society for Microbiology Press. Washington D.C.
- Sok CJ, Coppelli FM, Thomas SM, et al. (2006). Mutant epidermal growth factor receptor (EGFRvIII) contributes to head and neck cancer growth and resistance to EGFR targeting. *Clin Cancer Res*, 12(7):5064-5073.
- Tiwari A, Sankhyan A, Khanna N, Sinha S. (2010). Enhanced periplasmic expression of high affinity humanized scFv against hepatitis B surface antigen by codon optimization. *Protein Express Purif*, Jun;74:272-279.



IN VIVO ANTIMALARIAL ACTIVITY OF ETHANOL EXTRACT AND ETHYL ACETATE FRACTION OF ALECTRYON SERRATUS LEAVES ON PLASMODIUM BERGHEI INFECTED MICE

Aty Widyawaruyanti, Department of Pharmacognosy and Phytochemistry, Faculty of Pharmacy, Universitas Airlangga, Surabaya; Institute of Tropical Disease Universitas Airlangga, Surabaya, aty-w@ff.unair.ac.id; Uswatun Khasanah, Pharmacy Department, Faculty of Medicine, Universitas Brawijaya, Malang; Lidya Tumewu, Hilkatul Ilimi, Institute of Tropical Disease Universitas Airlangga, Surabaya; Achmad Fuad Hafid, Department of Pharmacognosy and Phytochemistry, Faculty of Pharmacy, Universitas Airlangga, Surabaya; Institute of Tropical Disease Universitas Airlangga, Surabaya; Indah S Tantular, Department of Parasitology, Faculty of Medicine, Universitas Airlangga, Surabaya; Institute of Tropical Disease Universitas Airlangga, Surabaya.

INTRODUCTION

Malaria was a major global public health concern due to the development of resistance by the most lethal causative species, *Plasmodium falciparum*. Natural products were potential sources of new antimalarial drugs (Bero, 2011; Nogueira, 2011). In vitro antimalarial activity screening of several Indonesian plants using HRP2 method showed that ethanol extract and ethyl acetate (EA) fraction of *Alectryon serratus* were active as an antimalarial (Widyawaruyanti, 2014). The aim of this study is to identify Thin Layer Chromatography (TLC) profile and investigate in vivo antimalarial activity of extract and fraction of *Alectryon serratus* leaves.

MATERIALS AND METHOD

Plant material and extraction

Leaves of *Alectryon serratus* was collected from Alas Purwo National Park, Banyuwangi, East Java, Indonesia, Authentication and identification of plant was carried out at the Purwodadi Botanical Garden, East Java. 1 kg of powdered material was extracted using 80% ethanol by ultrasonic assisted extraction (UaE) for two minutes, three times replication. The ethanol extract were filtered, pooled, and dried at 40°C using rotary evaporator and weighed afterwards. 100 grams of crude extract was suspended in distilled water and partitioned with dichloromethane and ethyl acetate successively, which were in turn concentrated to dryness in rotary evaporator. The crude extract and fractions were kept in air

tight containers and were stored at 4°C for use in phytochemical screening and antimalarial bioassay.

Phytochemical screening

Dried crude extract and ethyl acetate fraction (10 mg) was dilute in methanol. The phytochemical screening was performed by Thin Layer Chromatography (TLC) method to determine the content of chemical compound of extract and fraction using certain optimized mobile phase and sprayed by 10% sulphuric acid reagent.

Animals

Male mice BALB/C strain were obtained from LPPT-Universitas Gajah Mada, Yogyakarta. They were weighting between 20-30 g and maintained on standard animal pellets and water ad libitum at Animal Laboratory of Institute of Tropical Disease, Universitas Airlangga. Permission and approval for animal studies were obtained from Faculty of Veterinary Medicine, Universitas Airlangga.

Rodent malaria parasite

Rodent parasites used were *Plasmodium berghei* ANKA strain. The parasite has been maintained at Institute of Tropical Disease, Universitas Airlangga by passage in male BALB/C mice. In vivo antimalarial activity test

In vivo antimalarial activity was performed based on Peter's test (The 4-days suppressive test) (Phillipson, 1991).

Ethanol extract and ethyl acetate (EA) fraction were tested using 28 mice which divided to 7 groups. 3 groups were treated using extract at a dose of 100 mg/kgBW, 10 mg/kgBW, and 1

mg/kgBW, respectively. Meanwhile, 3 other groups were treated using EA fraction at a dose of 100 mg/kgBW, 10 mg/kgBW, and 1 mg/kgBW, respectively. One group was treated using CMC-Na 0.5% (as negative control). Each mice received 0,2 ml of diluted blood containing 5% *P. berghei* infected erythrocytes by intraperitoneal route. Treatment of extract, EA fraction and negative control was given at one day after inoculation of parasite by orally at day-0 until day-3 (four consecutive days). Thin blood smears were made every day for 7 days (day-0 until day-6) and stained using 10% giemsa dye. Percentage of parasitemia and percentage of inhibition growth of *P. berghei* were calculated using the formula in below.

Percentage of parasitemia:

$$Xe/Xk \times 100\%$$

Percentage of inhibition:

$$100\% - (Xe/Xk \times 100\%)$$

Xe: % parasitaemia growth of experimental group

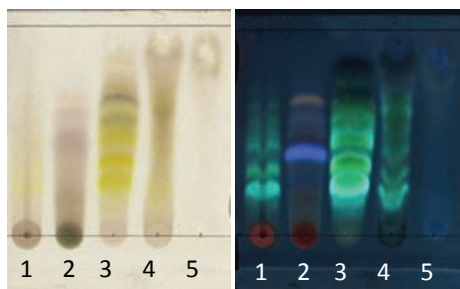
Xk: % parasitaemia growth of negative control

Data analysis

The ED50 (Effective dose) were analyzed using probit analysis (SPSS software).

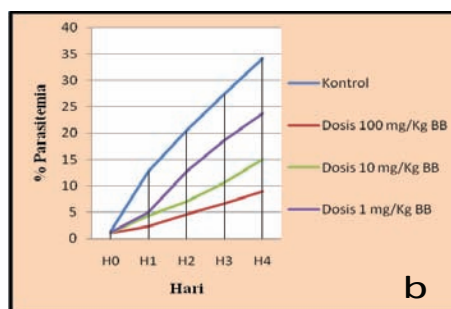
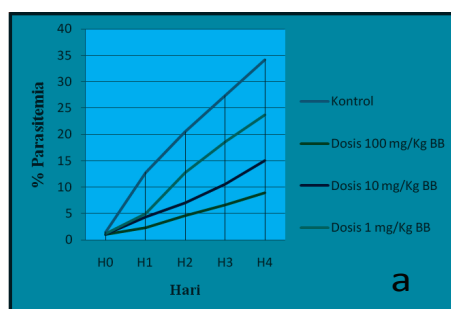
RESULTS DAN DISCUSSION

TLC profile showed that EA fraction of *A. serratus* (Picture 1, spot number 3) contained flavonoid compounds.



Picture 1. TLC Profile of extract Alectryon serratus

In vivo antimalarial assay of ethanol extract and EA fraction of *A. serratus* was done on *P. berghei* infected mice at a concentration of 100 mg/kgBW, 10 mg/kgBW and 1 mg/kgBW, respectively. The result showed that ethanol extract and EA fraction of *A. serratus* active as antimalarial agent with ED50 value of 13.82 mg/kg BW and 5.92 mg/kg BW. Flavonoid compound is considered to take effect in antimalarial activity of EA fraction from *Alectryon serratus* leaves. Further study to determine the active antimalarial compounds from *A.Serratus* leaves was needed.



Picture 2. Percentage parasitemia of ethanol extracts (a) and EA fraction (b) of *A. serratus* leaves against *P. berghei*.



Table 1. Activity of ethanol extract of *A. serratus* leaves on *P. berghei* infected mice

Dose (mg/Kg BW)	R	% Parasitemia					% Inhibition
		H0	H1	H2	H3	H4	
Negative control	1	1.50	12.2	22.67	29.87	38.50	
	2	1.44	13.0	19.89	25.60	32.43	
	3	1.55	13.1	20.05	29.40	35.78	
	4	1.38	12.9	19.50	24.71	30.18	
100	1	1.02	3.34	7.93	10.32	16.44	52.93
	2	0.90	2.70	5.20	7.48	10.32	71.25
	3	1.17	3.04	6.96	9.98	13.22	63.22
	4	1.05	2.65	5.10	7.50	10.20	72.07
10	1	1.58	5.06	9.98	14.05	17.85	50.34
	2	1.49	4.85	9.87	13.45	17.71	50.49
	3	1.59	4.98	10.60	14.21	18.10	49.60
	4	1.60	5.89	10.50	14.87	18.46	48.53
1	1	1.80	7.17	13.95	18.70	24.99	29.21
	2	1.50	6.40	13.56	17.63	25.24	27.53
	3	2.08	7.20	14.72	17.10	25.87	27.38
	4	1.98	7.28	14.21	18.85	25.67	27.69

Tabel 2. Activity of EA fraction of *A. serratus* leaves on *P. berghei* infected mice

Dose (mg/Kg BW)	R	% Parasitemia					% Inhibition
		H0	H1	H2	H3	H4	
Negative control	1	1.50	12.2	22.67	29.87	38.50	
	2	1.44	13.0	19.89	25.60	32.43	
	3	1.55	13.1	20.05	29.40	35.78	
	4	1.38	12.9	19.50	24.71	30.18	
100	1	1.09	2.31	4.42	6.20	8.24	78.17
	2	0.90	2.15	5.08	7.38	9.98	72.28
	3	1.00	2.10	4.64	6.97	8.95	75.73
	4	1.09	2.50	4.50	6.10	8.47	77.47
10	1	1.00	3.87	6.45	10.95	14.60	58.49
	2	1.10	4.05	6.37	9.89	14.34	59.58
	3	1.15	4.42	7.76	11.30	15.98	54.73
	4	1.20	4.85	7.50	10.25	15.50	56.35
1	1	1.22	5.23	12.78	18.22	23.30	32.60
	2	1.18	4.95	12.34	18.90	23.65	31.41
	3	1.20	4.80	12.10	17.86	23.10	33.15
	4	1.25	5.15	13.77	19.36	24.80	28.11

CONCLUSION

Ethanol extract and EA fraction of *A. serratus* were very active as antimalarial agent (very active if ED50 < 100 mg/kgBW based on Munoz, 2000). EA fraction had higher antimalarial activity with ED50 value of 5.92 mg/kgBW and potential to be developed as a new antimalarial drug.

ACKNOWLEDGEMENT

This study was supported by Directorate General of Higher Education DIPA BOPTN 2014, contract no 965/UN3/2014.

REFERENCE

- *. Bero, J., Quetin-Leclercq, J. 2011. Natural Products Published in 2009 from Plants Traditionally Used to Treat Malaria (Reviews). *Planta Med*, 77: 631–640.
- *. Munoz, V., Sauvain, M., Bourdy, G. et al. 2000. A search for natural bioactive compounds in Bolivia through a multidisciplinary approach: Part I. Evaluation of the antimalarial activity of plants used by the Chacobo Indians. *J. Ethnopharmacol* 69 (2): 127-137.
- *. Nogueira, C.R., Lopes, M.L.X. 2011. Antiplasmodial Natural Products (Review). *Molecules*, 16, 2146-2190; doi:10.3390/molecules16032146.
- *. Phillipson, J.D., Wright, C.W. 1991. Anti Protozoal Agent from Plant Sources. *Planta Medica* 57, hal 53-59.
- *. Widyawaruyanti, A., Devi, A.P., Fatria, N. et al. 2014. In Vitro antimalaria screening on several Indonesia Plants using HRP2 assay. *International Journal of Pharmacy and Pharmaceutical Sciences*, vol 6, issue 6.



PROFILE OF COMMUNITY PHARMACISTS KNOWLEDGE IN PATIENT ASSESSMENT WITH INFLUENZA SYMPTOMS AND ITS PRODUCTS

Azza Faturrohman, Department of Pharmacy Practice, Faculty of Pharmacy, Airlangga University Dharmawangsa Dalam Surabaya 60286, +62-31-5033710, azzaseza04@yahoo.com, **Arie Sulistyarini**, Department of Pharmacy Practice, Faculty of Pharmacy, Airlangga University Dharmawangsa Dalam Surabaya 60286, **Ana Yuda**, Department of Pharmacy Practice, Faculty of Pharmacy, Airlangga University Dharmawangsa Dalam Surabaya 60286.

INTRODUCTION

Influenza is one of the most common minor illness experienced and self-medicated by community (Sulistyarini, et al., 2010; Yuda, et al., 2011). Influenza comprises a mixture of upper respiratory tract viral infections. Although it is self limiting many people choose to buy OTC medicines for symptomatic relief. Some of the ingredients of OTC cold remedies may interact with prescribed drugs, occasionally with serious consequences. Therefore, these consequences can be avoided by carefully taking medicine history and selecting an appropriate product (Blekinsopp et al., 2009). The use of OTC medicines in the treatment of influenza is widespread and such products are heavily advertised to the public. There is little doubt that appropriate symptomatic treatment can make the patient feel better; the placebo effect also plays an important part here. The pharmacist's role is to select appropriate treatment based on the patient's symptoms (Blekinsopp et al., 2009). Through patient assessment, community pharmacist can guarantee the accuracy, safety, and rational self medication (WHO, 1998; Blekinsopp et al., 2009).

This study aims to determine the knowledge of community pharmacists in patient assessment with influenza and its products.

METHODS

Data collection

This research was conducted by cross sectional study. Questionnaire distributed to 100 community pharmacists in Surabaya. Respondents were taken by random sampling technique.

The study was conducted during the months of August to November 2010.

Instrument

The questionnaire was consisted of closed and open questions. Closed questions related to respondent demographics. Open questions ask about patient assessment (extracting information) with influenza symptoms that were asked by pharmacist and drug product for self-medication. Open questions about patient assessments were provided four columns of answers and about frequently administered drug product of influenza were provided six columns.

Data analysis

Community pharmacists as respondents were classified into two categories. Respondents who could answer correctly more than half from four columns (3 & 4 answers) about patient assessment and six columns (4,5,& 6 answers) about drug product of influenza were categorized as having good knowledge. On the other hand, respondents who could answer correctly less and half from those columns were classified as having lack of knowledge.

RESULTS AND DISCUSSIONS

A total of 47 community pharmacists willing to fill out the questionnaire (response rate = 47%). Demographics of respondents are provided in table 1, shows that the majority of respondents were women, aged up to 50 years, and the working hour per week between 31 to 50 hours.



Table 1. Characteristics of Respondents (n=47)

No	Characteristics	n(%)	Mean
1	Sex	Men	11(23.40)
		Female	36(76.60)
2	Age (years)	= 30	18(38.30)
		31-50	16(34.04)
		>50	10(21.28)
		NA	3(6.38)
3	Number of working hours in a week (hours)	<10	12(25.53)
		11-30	9(19.15)
		31-50	13(27.66)
		>50	6(12.76)
		NA	7(14.89)

NA=not available data

The total of respondents' answers can be seen from Table 2, shows that majority of community pharmacists had good knowledge (59.57%) in patient assessment with influenza symptoms. The mean of answer of respondents in this study was 2.66 with maximum point of four. It shows that respondents willing to answer of the four columns and also indicated that respondents were confidence with their knowledge.

Table 2. Number of answers of respondents about patient assessment with influenza symptoms

Number of answers	Respondents, n(%)
4	16 (34.04)
3	12 (25.53)
2	13 (27.66)
1	3 (6.38)
0	3 (6.38)
Total	47 (100)
Mean	2.66

As Table 3 shown, most of components of patient assessments that asked by community pharmacists to patient were the duration of symptoms (18.60%), present medication (17.05%), high temperature (13.95%) and previous history (13.95%). Pharmacists should develop a method of information seeking that suitable for them. There is no right and wrong here. WWHAM is one of a mnemonic frequently used, although care needs to be taken not to recite questions in rote fashion

without considering their relevance to the individual case. Good listening will glean much of the information required. The mnemonic can help to ensure all relevant information has been obtained. Developing rapport is essential to obtain good information, WHAM is abbreviation from: W – Who is the patient and what are the symptoms?, H – How long have the symptoms been present?, A – Action taken?, and M – Medication being taken? (Blekinshopp, 2009)

Table 3. Components of patient assessment with influenza symptoms

No.	Components	Respondent, n(%)
1	Duration of the symptoms	24 (18.60)
2	Present medication	22 (17.05)
3	High temperature	18 (13.95)
4	Previous history	18 (13.95)
5	Sneezing/Coughing	12 (9.30)
6	Runny/Blocked nose	9 (6.98)
7	Age	6 (4.65)
8	Child or adult	6 (4.65)
9	Generalized aches/headache	6 (4.65)
10	Dosage form	3 (2.33)
11	General symptoms	3 (2.33)
12	Sore Throat	1 (0.78)
13	Go to doctor	1 (0.78)
Total		129 (100)

The majority of pharmacists had good knowledge which answered four until six products (89.36%) in providing examples of influenza medicine products that were often administered at the their pharmacy (Table 4). In average, respondents gave 5.19 number of product, from six of products. Interestingly, there were 6.38% (3) respondents who did not complete the six columns at all. This result could be caused these respondents did this in purpose for certain reason or did not know at all influenza medicines products. If the last cause happened, it indicates that respondents who were community pharmacists did not practice at all in their pharmacies so they had lack knowledge about those products.



Table 4. Number of answers of influenza medicines products

Number of answers	Respondents, n(%)
6	35 (74.47)
5	3 (6.38)
4	4 (8.51)
3	0 (0.00)
2	1 (2.13)
1	1 (2.13)
0	3 (6.38)
Total	47 (100)
Mean	5.19

According to the respondents' answers, the most often medicine products dispensed to patients with influenza symptoms in the pharmacy for self-medication was Decolgen® (Table 5).

Tabel 5. Influenza medicines product frequently administered in pharmacies for self medication

No.	Influenza medicine products	Respondent, n(%)
1	Decolgen®	28(11.52)
2	Neozep®	22(9.05)
3	Mixagrip®, Actifed®	14(5.76)
4	Tremenza®, Demacolin®	13(5.35)
5	Decolsin®	12(4.94)
6	Ultraflu®, Sanaflu®, Bodrex flu®	9(3.70)
7	Tuzalos®	7(2.88)
8	Procold®, Hufagrip®	6(2.47)
9	Stopcold®, Paratusin®, Triaminic®, Panadol flu®, Inza®	5(2.06)
10	Intunal®, Rhinos®, Trifed®	4(1.65)
Other products were: Bisolvon Flu®, Disudrin®, Nalgestan®, Paramex®, Pimtrakol®, Rhinofed® @3(1.23%); Bodrexin Flu®, Deconal®, Decold®, Fludane®, OBH Combi®, Pimacolin® @2(0.82); Allerin®, Alpara®, Baby Cough®, Colvin®, Comtusi®, CTM®, Etaflusin®, Fludexin®, Koldex®, Lapifed®, Mextril®, OBH Tropica®, Refagan®, Termorex® @1(0.41)		

The results of this study show that medicine product of influenza that frequently administered for self-medication contains more than one active ingredient. Products containing drug combination combinations should be selected carefully in order to ensure that they are suitable for the symptoms and rational (Nathan, 2010). Pharmacists in particular can play a key role in giving advice to consumers on the proper and safe use of medicinal products intended for self-medication. Therefore, it is important to take this role into account both in their training and in practice (WHO, 2000).

CONCLUSIONS

The majority of community pharmacists had good knowledge in influenza medicine product than in patient assessment with influenza symptoms. This knowledge should be followed up by interacting directly with patients as a form of professional responsibility of the community pharmacists to ensure the accuracy, security, and rational of self-medication. Improving directly interaction with patients can increase the role of the community pharmacists and the quality of the self-medication service in the pharmacy.

Acknowledgements,

We thank to pharmacy students for their participation as surveyors and IMHERE B.2c project for funding this study.

REFERENCES

1. Blenkinsopp, A. Paxton, P. dan Blenkinsopp, J., 2009, Symptoms in the Pharmacy: A Guide to the Management of Common Illness, 9th ed, West Sussex: Blackwell Publishing Ltd.
2. FIP and WSMI, 1999, Joint Statement : Responsible Self Medication



ICPPS 2014

Proceeding
The 1st International Conference
on Pharmaceutics & Pharmaceutical Sciences

3. Nathan, A., 2010, Non-Prescription Medicines, 4th Ed., London: Pharmaceutical Press
4. Sulistyarini, A., Faturrohmah, A., dan Yuda, A., 2010, Pelayanan Swamedikasi Oleh Apoteker Di Apotek, Proceeding Kongres Ilmiah XVIII & Rapat Kerja Nasional Ikatan Apoteker Indonesia (ISFI), Jakarta: IAI
5. World Health Organization, 2000, Guide line for Regulatory Assessment of Medicinal Product for Use in Self-Medication, Geneva:WHO
6. Yuda, A., Faturrohmah, A., Sulistyarini, A., 2011, Self-Medication Profile in Surabaya, Abstract Book of the 5th Conference of Asian Association of Schools of Pharmacy (AASP), Bandung



SOLUBILITY AND DISSOLUTION STUDY OF KETOPROFEN – HIDROXYPROPYL- β -CYCLODEXTRIN INCLUSION COMPLEX

(Prepared by Kneading Method)

Bambang Widjaja, Department of Pharmaceutics – Faculty of Pharmacy Airlangga University, **Achmad Radjaram**, Department of Pharmaceutics – Faculty of Pharmacy Airlangga University, **Arafah Zulhana**, Department of Pharmaceutics – Faculty of Pharmacy Airlangga University

INTRODUCTION

Ketoprofen is a NSAID (non-steroid anti-inflammatory) that decreases inflammation, pain and fever, probably through non-selective inhibition of cyclooxygenase activity and prostaglandin synthesis (Sweetman, 2009). Use of ketoprofen is associated with two major limitations; first, rare, but serious and sometimes fatal, gastrointestinal (GI) side-effects, and second, poor water solubility due to which its dissolution in GI fluid is very low, which in turn adversely affects the bioavailability (50–60% only) (Kaur et al., 2013). Based on BCS, ketoprofen is in class II that have poor solubility but high permeability (Shohin et al., 2011).

Dissolution rate is a function from solubility in a dissolution media, then it influences in absorption of insoluble drugs (Wadke et al., 1989). Improvement of drug solubility will be increase on it absorption and bioavailability (Jayshree et al., 2012).

Complexation is one of several ways to enhance the physicochemical properties of pharmaceutical compounds. These complexes are formed when a “guest” molecule is partially or fully included inside a “host” molecule e.g., CD with no covalent bonding. When inclusion complexes formed, physicochemical parameters of guest molecule are altered and improvements in the molecule’s solubility, stability, taste, safety, bioavailability, etc., are commonly seen (Mosher & Thompson, 2007). CDs are cyclic oligosaccharides derived from starch (Brewster & Loftsson, 2007). CDs are able to form water-soluble inclusion complexes with many poorly soluble lipophilic drugs (Kurkov & Loftsson, 2013). Cyclodex-

trin have hydrophobic cavity and hydrophilic on surface. That makes be able to interaction with the most molecules then form non-covalent inclusion complexes (Brewster & Loftsson, 2007). Based on these dimensions, β -cyclodextrin will complex aromatics and heterocycles (Del Valle, 2004). β -cyclodextrin is the most commonly use. Because its relatively poor solubility, so that derivated into hydroxypropyl- β -cyclodextrin (HP β CD) with high solubility and safe (Gould & Scott, 2005).

On this study, we made ketoprofen - hydroxypropyl- β -cyclodextrin (HP β CD) inclusion complexes with kneading method. The advantage of kneading method is simple and only use small solvent (Patil, 2010). Then we did solubility and dissolution test of ketoprofen - hydroxypropyl- β -cyclodextrin (HP β CD) inclusion complexes.

MATERIALS, EQUIPMENTS AND METHODS

Materials

Ketoprofen; hydroxypropyl- β -cyclodextrin p.g.; ethanol p.a.; and aquadest

Equipments

- Spectrophotometer UV-Vis (Cary 50 Conc),
- Spectrophotometer IR (Jasco FT - IR 5300),
- DTA (Mettler Toledo FP9 TA Cell),
- Diffractometer X-ray Philips X’pert,
- Sieve with mesh no. 60 (Retsch Type ASTM),
- Shaker,
- Dissolution machine (Erweka DT 700),
- Glasses



Methods

Inclusion Complex Preparation

In equimolar of ketoprofen and hydroxypropyl- β -cyclodextrin (1:1) is prepared. Mix them until homogen. Little amount of ethanol are added into mixture until form kneaded mass (paste). Dried at 45oC oven in vacuum condition. Sieve mass with mesh 60.

Determination of Ketoprofen, Physical Mixture and Inclusion Complex Solubility

Prepare 50.0 mg or equivalent 50.0 mg ketoprofen then dissolved in buffer pH 1.2 on shaker at 37 ± 0.5 oC 50 rpm until 5 hours (saturated solubility). Observe the absorbances use spectrophotometer UV-Vis.

Dissolution test of Ketoprofen, Physical Mixture and Inclusion Complex

Dissolution test was performed using apparatus II at 37 ± 0.5 oC 75 rpm in phosphate buffer medium pH 7.4. Observe the absorbances of 3, 5, 10, 20 and 30 minutes sample use spectrophotometer UV-Vis.

RESULTS

On this study, solubility and dissolution test of ketoprofen - hydroxypropyl- β -cyclodextrin (HP β CD) inclusion complexes have done.

Sample	Solute Concentration (mg/L)
Ketoprofen	105,0 \pm 0,0
Physical mixture	850,0 \pm 0,0
Inclusion complex	943,3 \pm 5,8

Table 1. Ketoprofen, ketoprofen - hydroxypropyl- β -cyclodextrin physical mixture and inclusion complex solubility at $37 \pm 0,5$ oC

Based on dissolution test we can determine values of ED 30, slope and angle.

Replication	ED 30 (%)		
	KTP	PM	IC
1	79,2	90,2	99,6
2	81,7	88,8	97,3
3	79,2	90,2	100,3
Mean	80,0	89,7	99,1
SD	1,4	0,8	1,6
%CV	1,8	0,9	1,6

Table 2. ED 30 of ketoprofen, ketoprofen -hydroxypropyl- β -cyclodextrin physical mixture and inclusion complex

Replication	Slope		
	KTP	PM	IC
1	11,7	27,3	34,7
2	12,1	24,9	33,3
3	11,7	27,8	33,3
Mean	11,8	26,7	33,8
SD	0,2	1,6	0,8
%CV	2,0	5,8	2,4

Table 3. Slope of ketoprofen, ketoprofen - hydroxypropyl- β -cyclodextrin physical mixture and inclusion complex

Replication	Sudut Kemiringan		
	KTP	PM	IC
1	85,1	87,9	88,3
2	85,3	87,7	88,3
3	85,1	87,9	88,3
Mean	85,2	87,8	88,3
SD	0,1	0,1	0,0
%CV	0,1	0,1	0,0

Table 4. Angle of ketoprofen, ketoprofen - hydroxypropyl- β -cyclodextrin physical mixture and inclusion complex



CONCLUSION

The study can be concluded that the solubility and dissolution rate of ketoprofen was increased with ketoprofen – hydroxypropyl- β -cyclodextrin inclusion complex prepared by kneading method.

REFERENCES

1. Brewster, M. E. & Loftsson, T., 2007. Cyclodextrins as Pharmaceutical Solubilizers. *Elsevier*, pp. 645-666.
2. Del Valle, E., 2004. Cyclodextrins and Their Uses: a Review. *Process Biochemistry* 39, pp. 1033-1046.
3. Gould, S. & Scott, R. C., 2005. 2-Hydroxypropyl- β -cyclodextrin (HP- β -CD): A toxicology review. *Food and Chemical Toxicology* 43, pp. 1451-1459.
4. J.S., P., 2010. Inclusion Complex System a Novel Technique to Improve The Solubility and Bioavailability of Poorly Soluble Drugs: a Review. *International Journal of Pharmaceutical Sciences Review and Research*, pp. 29-34.
5. Jayshree, T. et al., 2012. Effect of Hydrophilic Polymer on Solubility and Dissolution of Atorvastatin Inclusion Complex. *International Journal of Pharmaceutical and Chemical Sciences*, pp. 374-385.
6. Kaur, A., Sharma, N. & S.L., H., 2013. Design and Development of Ketoprofen Pharmasomes for Oral Delivery. *Pharmacophore*, pp. 111-119.
7. Kurkov, S. V. & Loftsson, T., 2013. Review: Cyclodextrins. *International Journal of Pharmaceutics*, pp. 167-180.
8. Mosher, G. & Thompson, D. O., 2007. Complexation: Cyclodextrins. In: *Encyclopedia of Pharmaceutical Technology*, 3rd ed, vol. 1. USA: Informa Healthcare, pp. 671-696.
9. Shohin, I., Kulinich, J., Ramenskaya, G. & Vasilenko, G., 2011. Evaluation of In Vitro Equivalence for Drugs Containing BCS Class II Compound Ketoprofen. *Dissolution*, pp. 26-29.
10. Sweetman, S. C., 2009. *Martindale The Complete Drug Reference*, 36th ed. London SE1 7JN, UK: Pharmaceutical Press.
11. Vikesh, S., Rajashree, M., Ashok, A. & Fakkirappa V., M., 2009. Influence of β -Cyclodextrin Complexation on Ketoprofen Release from Matrix Formulation. *IJPDR*, pp. 195-202.
12. Wadke, D. A., Serajuddin, A. T. M. & Jacobson, H., 1989. In: *Pharmaceutical Dosage Forms: Tablets*, vol. 1, 2nd ed.. New York: Marcel Dekker, pp. 18-23, 12-18



FORMULATION AND STABILITY TESTING OF MELOXICAM SOLID DISPERSION GEL

Budipratiwi Wisudyaningsih, Pharmaceutical Department, Faculty of Pharmacy, Jember University, Indonesia, tiwiks_email@yahoo.co.id, (0331)324736; **Inka Dewi Nur Anggaraini**, Faculty of Pharmacy, Jember University, Indonesia; **Ferisyia Wardani**, Faculty of Pharmacy, Jember University, Indonesia

INTRODUCTION

Non-Steroid Anti-Inflammatory Drugs (NSAIDs) are a class of drugs most often used in the treatment given by health personnel. Meloxicam is one of NSAID drug that can be used in the treatment of arthritis, rheumatic, osteoarthritis, and other joint diseases. Meloxicam can cause GI disorders, dyspepsia, diarrhea, upper gastrointestinal tract infections, and nausea, in oral use. These side effects are reported to occur in 15-20 % of patients and mild when compared to piroxicam, diclofenac, and naproxen on long-term oral use (Aronson, 2005). Topical gel was preferred as selected dosage form to prevent unwanted effects of Meloxicam. Gel preparation can provide a good drug release, has the ability to spread good, easily removed in case of irritation of the skin, and gives a cool effect when used (Voight, 1994). The poor solubility and wettability of meloxicam leads to poor dissolution of meloxicam in topical gel (Kumar and Mishra, 2006). Pharmaceutical strategies that can be used to overcome the low solubility in Meloxicam is the development in the form of solid dispersion (Anshu and Jain, 2011).

OBJECTIVES

The objectives of this research were to generate a stable NSAID drug product using solid dispersion technique to prevent the occurrence of undesirable side effects of meloxicam, but can provide an optimal bioavailability and therapeutic effect.

METHODS

Meloxicam Solid Dispersion Preparation
Meloxicam solid dispersion systems were prepared using PVP (1:1; 1:5; 1:7) and PEG 6000 (1:1; 1:5; 1:8) and evaluated for its FTIR and DTA profile

Meloxicam Gel Preparation

Meloxicam-PVP solid dispersion gel

Formula	F1 (%)	F2 (%)	F3 (%)
Meloxicam-PVP	0,6	1,8	2,4
Carbopol	3	3	3
Triethanolamine	0,25	0,25	0,25
Propylene glycol	15	15	15
Aquadest	ad 100	Ad 100	ad 100
Total	100	100	100

Table 3. Meloxicam-PVP gel formulation

Meloxicam-PEG 6000 solid dispersion gel

Formula	F4 (%)	F5 (%)	F6 (%)
Meloxicam-PEG 6000	0,6	1,8	2,7
CMC Na	3	3	3
Triethanolamine	0,6	0,6	0,6
Propylene glycol	10	10	10
Aquadest	ad 100	ad 100	ad 100
Total	100	100	100

Table 2. Meloxicam-PEG 6000 gel formulation



Meloxicam solid dispersion gels were stored in temperature 25°C and 50°C for 1 month in order to observe its stability. Meloxicam solid dispersion in topical gel were evaluated for color, viscosity, pH, drug content, rheological properties, spreadability and in vitro drug release.

RESULTS

Meloxicam Solid Dispersion FTIR Profile

Meloxicam-PVP solid dispersion was prepared using solvent method, on the other hand meloxicam-PEG 6000 solid dispersion was prepared using fusion method. Solid dispersions were evaluated for its FTIR and DTA profile (see Figure 1, Figure 2, Figure 3 and Figure 4)

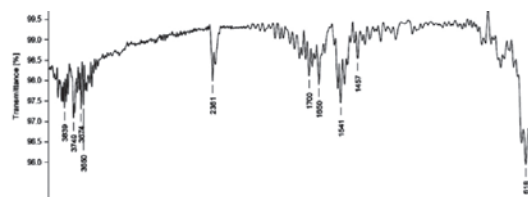


Figure 1. Meloxicam-PVP FTIR Profile

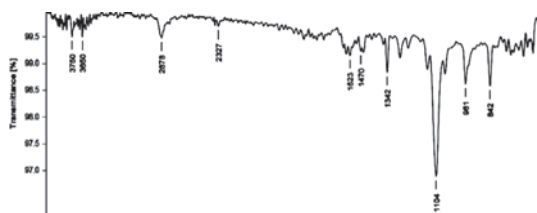


Figure 2. Meloxicam-PEG 6000 FTIR Profile

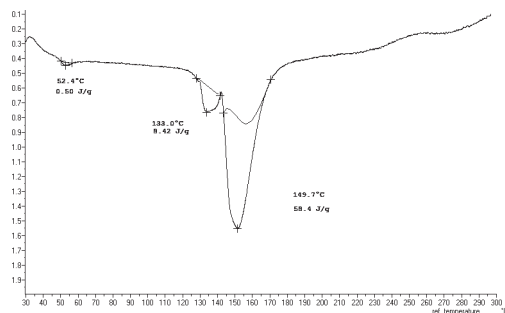


Figure 3. Meloxicam-PVP DTA Profile

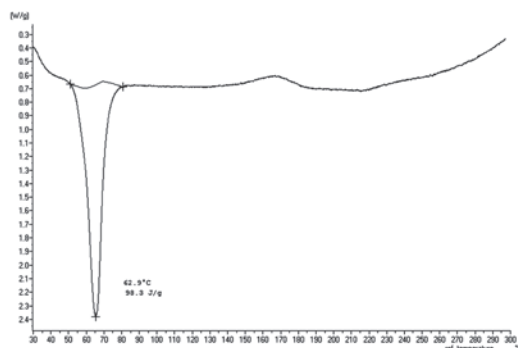


Figure 4. Meloxicam-PEG 6000 DTA Profile

Meloxicam Solid Dispersion Gel Evaluation
 Meloxicam gel were characterized for physico-chemical properties such as color, viscosity, pH, drug content, rheological properties, spreadability and in vitro drug release. The results shows that meloxicam-PVP gel have a significant when PVP composition was increased. While meloxicam-PEG 6000 show no significant respon. Meloxicam solid dispersion gel release profile show no significant respon on stability testing (see Fig. 5 and Fig. 6)

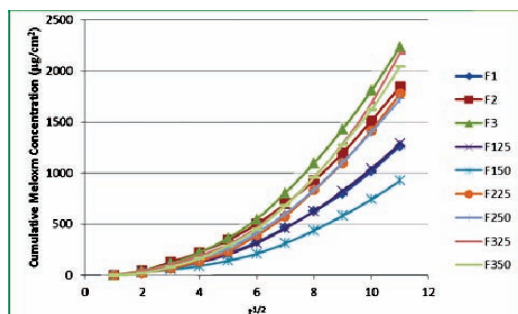


Figure 5. Meloxicam-PVP DTA Profile

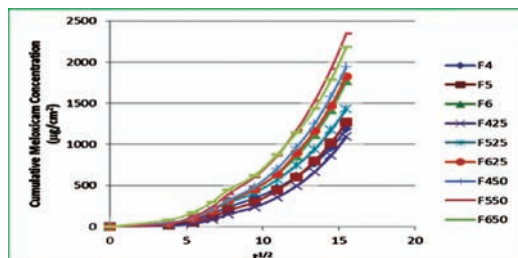


Figure 6. Meloxicam-PEG 6000 DTA Profile



CONCLUSION

The result shown that improving composition of meloxicam-PVP solid dispersion have a significant influence on the physico-chemical characteristics of the gel formulation. Increased meloxicam-PEG 6000 solid dispersion composition did not have a significant influence on the physico-chemical characteristics of the gel, but significantly increase the rate of meloxicam in vitro release. Neither physico-chemical characteristics nor meloxicam in vitro release of gel show significant changes on stability testing at a temperature of 50°C and 25°C for 30 days.

REFERENCES

1. Chen D, Endres RL, Erickson CA, et al. (2000). Epidermal immunization by a needle-free powder delivery technology: immunogenicity of influenza vaccine and protection. *Immune Nat Med*, Oct;6(10):1187-90.
2. Cox RJ, Brokstad KA, Ogra P. (2004). Influenza virus: immunity and vaccination strategies. Comparison of the immune response to inactivated and live, attenuated influenza vaccines. *Scand J Immunol*, Jan;59(1):1-15.
3. Chang LL, Shepherd D, Sun J, et al. (2005). Mechanism of protein stabilization by sugars during freeze-drying and storage: native structure preservation, specific interaction, and/or immobilization in a glassy matrix? *J Pharm Sci* Jul;94(7):1427-44.
4. Cox RJ, Hovden AO, Brokstad KA, Szyszko E, Madhun AS, Haaheim LR. (2006). The humoral immune response and protective efficacy of vaccination with inactivated split and whole influenza virus vaccines in BALB/c mice. *Vaccine*, Nov 10;24(44-46):6585-7.



EFFECT OF MENTHOL AS PENETRATION ENHANCER TO DICLOFENAC SODIUM MEMBRANE-TYPED TRANSDERMAL PATCH CHARACTERIZATION

Destria Indah Sari, Program Studi Farmasi FMIPA Unlam, Jl. A.Yani km 36 Banjarbaru, di.sari@yahoo.co.id, 085751082312; **Esti Hendradi**, Fakultas Farmasi Unair, Jl.Dharmawangsa Dalam Surabaya, esti_hendradi@yahoo.com, 081330175672; **Junaidi Khotib**, Fakultas Farmasi Unair, Jl.Dharmawangsa Dalam Surabaya, joen_70@yahoo.com, 081331840710.

INTRODUCTION

Inflammation is a non-specific immune response that occurs in reaction to any type of bodily injury. The cardinal signs of inflammation can be explained by increased blood flow, elevated cellular metabolism, vasodilatation, release of soluble mediators, extravasation of fluids and cellular influx¹.

Non-Steroidal Anti-Inflammatory Drugs (NSAIDs) are drug class which commonly used to treat inflammation. Diclofenac sodium is one of the drug class of non steroidal anti-inflammatory drugs (NSAIDs) are widely used to relieve pain and inflammation. Absorption of sodium diclofenac in oral delivery is very fast but only about 60% of which reaches the systemic circulation, this is because first-pass metabolism that occurs in the liver². Half-life of diclofenac sodium was also very brief about 2 hours and a few other side effects such as gastrointestinal disorders (ulcers in the stomach) and the reaction idionsynchratic. One way to overcome this problem, given by way of diclofenac sodium transdermal. Diclofenac sodium is not absorbed through the skin as perfect hydrophilic can be seen from log P of sodium diclofenac of 4.42,

Absorption of sodium diclofenac into the skin can be improved by the addition of enhancers such as menthol. Adding one or more excipients could change dosage form characteristics. This study was aimed to determine effect of menthol to patch characteristics when it added to diclofenac sodium membrane-typed patch.

METHODS

Material

Diclofenac sodium (Aarti Drugs Limited), alginate sodium (Sigma-Aldrich), hydroxypropil methylcellulose E-15 (ILE Pharmaceutical), propylenglycol (Bratachem), L-menthol (Bratachem), ethanol 96% (Bratachem), and aquades

Preparation of patch

Patches were made using formula in Table 1. Dose of diclofenac sodium in dosage is 100 mg/50 cm² patch. Sodium alginate were dissolve in water:ethanol (80:20) and stirred constantly to make alginate sodium 9%. Diclofenac sodium previously dissolved in same solvent and were added with alginate sodium 9%, and stirred homogenously. The mixture were poured into mold and it dried on 45°C for an hour. HPMC E-15 were dissolved in water to made 20% concentration. Propylenglycol were added and stirred constantly. Menthol were dissolved in ethanol, previously, and were added to HPMC E-15 and propylenglycol, and stirred. This mixture were poured on to alginate sodium and dried on 40°C for an hour

Table 1 Formulation of diclofenac sodium membrane-typed patch

Composition	Function	Weight (mg/12,56 cm ²)	
		FI	FII
Diclofenac sodium	Active ingredients	25,2	25,2
Alginate sodium 9%	Drug reservoir	1308,4	1308,4
HPMC E15 20%	Rate-controlling membrane	1280	1280
Propylenglycol	Plastisizer	53,3	53,3
Menthol	Enhancer	26,7	-
Weight Total		2693,6	2666,9



Organoleptic evaluation

Organoleptic evaluation were observed on patch characteristic, odor, and consistency.

Moisture content evaluation

The films were weighed and kept in a desiccator containing calcium chloride at room temperature for 24 hours. Values for the percentage of moisture content, calculated as the percentage of difference between the constant final and initial weight with respect to the initial weight.

Surface homogeneity

Surface homogeneity were observed using Scanning Electron Microscope (SEM) FEI INSPECT S50 on magnification x1000.

Stability evaluation

Stability evaluation were performed 12 weeks (1,3,6,12 weeks), regarding to change of organoleptic, moisture content, and concentration of active ingredient (diclofenac sodium).

Statistical analysis

The results were expressed as arithmetic mean ± SD. The statistical analysis was performed using Anova one-way. The data was considered significant at p>0.05.

RESULTS

Organoleptic evaluation

As menthol added, there were only odor difference on patches. Their color and elasticity remain same.



Figure 1. Diclofenac sodium membran-typed patch with and without menthol (left and right, respectively)

The results of evaluation of diclofenac sodium membrane-typed patch were summarize on Table 2.

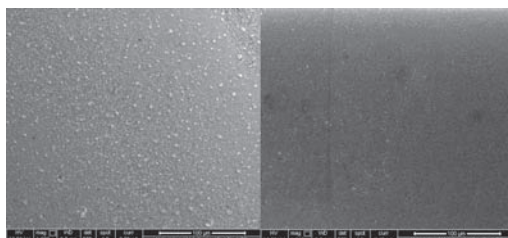


Figure 2. Scanning electron microscope photograph of diclofenac sodium membrane-typed transdermal patch with (left) and without (right) menthol on magnification x 1000.

The results of evaluation of diclofenac sodium membrane-typed patch were summarize on Table 2.

Table 2. Evaluation of diclofenac sodium membrane-typed patch

Week Observation	Type of evaluation	Formula	
		I	II
0	Organoleptic (colour, odor, consistency)	Transparent, mentholic odor, elastic	Transparent, no mentholic odor, elastic
	% Moisture content	42.84 ± 9.08	47.48 ± 2.41
	% Diclofenac sodium content	100.70 ± 0.85	102.02 ± 0.59
1	Organoleptic (colour, odor, consistency)	Transparent, mentholic odor, elastic	Transparent, no mentholic odor, elastic
	% Moisture content	29.15 ± 2.93	26.76 ± 6.37
	% Diclofenac sodium content	97.67 ± 1.55	96.68 ± 0.62
3	Organoleptic (colour, odor, consistency)	Transparent, mentholic odor, elastic	Transparent, no mentholic odor, elastic
	% Moisture content	20.83 ± 1.02	26.88 ± 2.17
	% Diclofenac sodium content	96.17 ± 4.42	95.13 ± 3.28
6	Organoleptic (colour, odor, consistency)	Transparent, no mentholic odor, elastic	Transparent, no mentholic odor, elastic
	% Moisture content	19.89 ± 0.65	21.02 ± 1.39
	% Diclofenac sodium content	97.21 ± 5.70	97.21 ± 0.71
12	Organoleptic (colour, odor, consistency)	Transparent, no mentholic odor, elastic	Transparent, no mentholic odor, elastic
	% Moisture content	22.27 ± 2.63	21.61 ± 0.39
	% Diclofenac sodium content	99.46 ± 0.62	99.03 ± 0.62



CONCLUSION

Menthol as penetration enhancer did not give difference on diclofenac sodium membrane-typed transdermal patch characterization.

ACKNOWLEDGMENT

The authors are thankful to DIKTI for financial support in the form of Post Graduate Grand Project.

REFERENCES

1. Ferrero-Miliani, L., Nielsen, O.H., Andersen, P.S., Girardin, S.E. (2006). Chronic Inflammation: importance of NOD2 and NALP3 in interleukin-1 β generation. *Clinical and Experimental Immunology*, Vol.147 : 227-235.
2. Chuasuwan, B., Binjesoh, V., Poli, J.E., Zhang, H., Amidon, G.I., Junginger, H.E., Midha, K.K., Shah, V.P., Stavchansky, S., Dreesman, J.B., Barends, D.M. (2008) Biowaiver Monographs for Immediate Release Solid Oral Dosage Forms: Diclofenac Sodium and Diclofenac Potassium. *Journal of Pharmaceutical Sciences*, Vol.98(4) : 1206-1223.



PHYSICAL CHARACTERISTICS AND RELEASE STUDY OF OVALBUMIN FROM ALGINATE MICROSPHERES PREPARED BY DIFFERENT CONCENTRATION OF ALGINATE AND BaCl₂ USING AEROSOLIZATION TECHNIQUE

Dewi Melani Hariyadi, Faculty of Pharmacy Airlangga University, Dharmawangsa Dalam Surabaya, dewi-m-h@ff.unair.ac.id, dewiffua96@yahoo.com ; **Tristiana Erawati**, Faculty of Pharmacy Airlangga University, Dharmawangsa Dalam Surabaya, era_ffua@yahoo.co.id ;

Sisilia Ermawahyuningtyas, Faculty of Pharmacy Airlangga University, Dharmawangsa Dalam Surabaya

ABSTRACT

Microsphere formulations have been widely used for oral applications. The aim of this research was to study physical characteristics and release study of ovalbumin from alginate microspheres prepared by different concentration of alginate polymer and BaCl₂. This research used concentrations of BaCl₂ of 0,5M and 0,75M and concentrations of alginate of 2,5% w/v and 3,5% w/v. Ionotropic gelation using aerosolization technique was applied in this study. All ovalbumin – loaded alginate microspheres were characterized in terms of size, morphology, protein loading, encapsulation efficiency, yield, and release profile of ovalbumin. In vitro release study was conducted in the simulated gastric fluid (HCl pH 1.2) and simulated intestinal fluid (PBS pH 7,4) at temperature 37°C. Results showed spherical and smooth microspheres were produced. In addition, smaller particle size of less than 8 μm was produced by increasing alginate and BaCl₂ concentration. A factorial design ANOVA and one way ANOVA were used for statistical analysis at a 95% confidence interval. No significant effect was shown by increasing alginate and BaCl₂ concentration on the protein loading, encapsulation efficiency, and yield. No significant differences of ovalbumin release were found when increasing concentration of BaCl₂ from 0,5M to 0,75M, however ovalbumin release decreased by increasing alginate concentration and slower release in HCl

pH 1,2 during 2 hours followed by complete release in PBS pH 7,4 after 17 hours.

Keywords: Microspheres, Ovalbumin, Sodium alginate, Aerosolisation, Release.

INTRODUCTION

Alginate microspheres have been investigated to protect antigen from acid pH and enzymatic degradation in gastrointestinal tract. The aim of this research was to investigate physical characteristics of ovalbumin-loaded alginate microspheres. Ovalbumin is egg white glycoprotein that comprises 385 aminoacids (molecular weight 43 kDa) that easily denatured at high temperature and acid pH (O'neil et al., 2001). Ovalbumin as a model antigen, could stimulate the formation of antibodies and improve immunity. Administering oral antigen is the most effective way to induce immunological tolerance to protein antigens (Mowat, 1985).

Current study applies ionotropic gelation method based on polyelectrolyte capability to form hydrogel using polymer and crosslinking agent. Aerosolization technique was used because it is a cost effective, fast, simple technique. Moreover, it does not involve organic solvent which can contribute to protein integrity (Yeo et. al., 2001). Polymer is required to coat drug or the core of active substance (Dubey et al., 2009). Sodium alginate is a biodegradable and biocompatible natural polymer, non toxic to the body, cheap and most



commonly used as polymer in the microparticles (Maria et al., 2012). Crosslinking agents are usually cations such as Pb²⁺, Cd²⁺, Zn²⁺, Cu²⁺, Co²⁺, Ca²⁺, Ba²⁺, dan Sr²⁺ (Gombotz et al., 1998). Barium ions have been extensively used as crosslinking agents because its ability to produce strong gel and high potential (Ciofani et al., 2007). In addition, Ba²⁺ resulted high biocompatibility with alginate and able to protect human cell from xenorejection following transplantation (Lanza et al., 2007).

Several factors affect the microparticles preparation such as concentration of polymer and crosslinking agents (Jin et al., 2009). Higher polymer concentration produced bigger microspheres, but more spherical in shape (Joshi et al, 2012). Crosslinking agents also influenced particle size. Lower crosslinking agents, produced fragile and amorphous microspheres, even it could not form the microspheres (Suksamra et al., 2009). Higher concentration of crosslinker produced smaller microspheres size as a result of stronger binding between them, but often resulted rough surface (Jin et al., 2009). Therefore, this research were conducted to study the potential of ovalbumin-alginate microspheres

MATERIAL AND METHODS

Alginate microsphere preparation using Iontropic Gelation – Aerosolization Method
 Preparation of alginate microsphere using

ionotropic gelation method by aerosolization techniques could be explained as follows: Alginate solution (concentration of 2.5 and 3.5%) containing 2.5% ovalbumin was sprayed into crosslinking agent BaCl₂ solution (concentration of 0.5 and 0.75M) at 40 psi and was stirred continuously for 2 hours at 1000 rpm. The microspheres were collected by centrifugation at 2500 rpm for 6 minutes, washed two times with aquadest and finally freeze dried 20 hours at -80°C. Alginate microspheres formulation were summarized in Table 1.

Table 1. Ovalbumin-alginate microspheres formulation

BaCl ₂ concentration (M)	Alginate concentration (%)	
	2.5	3.5
0.5	F1	F2
0.75	F3	F4

F1: Alginate 2.5% and BaCl₂ 0.5 M; F2: Alginate 2.5% and BaCl₂ 0.75 M

F3: Alginate 3.5% and BaCl₂ 0.5 M ; F4: Alginate 3.5% and BaCl₂ 0.75M

Morphology analysis

The morphology of microspheres were characterized by optical microscope with camera and scanning electron microscopy (SEM).

Protein Loading

Loading of ovalbumin into microspheres was analyzed following breakdown of 400 mg of microspheres suspensions in 50 mL sodium citrate solution over 12 hours at 1000 rpm at room temperature. The drug content was determined using protein quantification assay using UV spectrophotometry.

RESULTS AND DISCUSSION

The Aerosolization technique produced homogenous, small, smooth and spherical microspheres. Small particle size of less than 8 μm was produced by increasing alginate and BaCl₂ concentration (Table 2).

Table 2. Particle size of formula F1,F2.F3 and F4.

Formula	Average of particle size (μm)
F1	6.54
F2	5.22
F3	4.99
F4	3.73

using different concentration of alginate polymer and BaCl₂ crosslinker.

This smaller ovalbumin-loaded alginate microspheres were suitable for oral administration. Mishra et al (2008) that immune response after oral administration could be achieved from microspheres with 1-30 μm in size. Manjanna et al (2010) reported that by increasing concentration of Ba²⁺ formed



spherical and smaller microsphere's size. This report was in agreement with Joshi et al (2012) and Singh dan Kumar (2012).

Figure 1 shows that almost spherical morphological microspheres were produced by scanning electron microscope. Some rough surface was maybe caused by no cryoprotectant agent to protect microspheres during freeze drying was added to stabilize microspheres.

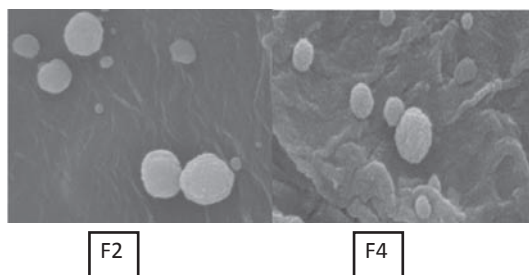


Figure 1. Scanning electron microscope of ovalbumin-loaded alginate microspheres

Encapsulation efficiency, protein loading and yield of microspheres can be seen in Table 3.

Table 3. Encapsulation efficiency, protein loading and yield of microspheres

Formula	Encapsulation Efficiency (EE) (%)	Protein Loading (%)	Yield (%)
F1	80,47 ± 9,52	66,86 ± 10,36	60,63 ± 3,06
F2	81,81 ± 10,77	65,17 ± 12,24	63,43 ± 4,98
F3	90,88 ± 7,37	61,34 ± 4,16	62,74 ± 5,96
F4	92,17 ± 5,57	53,59 ± 2,70	71,93 ± 6,73

It was observed that larger amounts of BaCl₂ (from 0.5M to 0.75M), increased encapsulation efficiency ovalbumin in alginate microspheres (from 80% to 82% in formula F1 and F2; from 90% to 92% in formula F3 to F4). An increase of encapsulation efficiency is most likely caused by larger amounts of availability of Ba²⁺ that crosslinked with carboxylates from guluronic acid in alginate indicates more ovalbumin was entrapped within alginate microspheres (Gu-

lati, et. al., 2011). This trend was also similar to an increase of alginate concentration. The more number of crosslinked alginate-BaCl₂, resulted the more ovalbumin was encapsulated (Manjanna et al, 2010). Similar studies were also confirmed that encapsulation efficiency increased by increasing concentration of polymer and crosslinking agents (Joshi et al, 2012 ; Singh dan Kumar, 2012).

In terms of yield, similar results were shown. Alginate microspheres produced using both alginate concentration (2.5 and 3.5%) using highest concentration of CaCl₂ (0.75M) indicated the highest yield of about 72% compare to formulas produced using lower concentration of BaCl₂. In the case of microspheres crosslinked using higher alginate concentration, the yield was also increased. This behaviour indicates that the more number of Ba²⁺ contact with alginate provide a gel network that able to increase yield of microspheres (Jin et.al., 2009).

There was no significant differences of all loading's formula. This may be explained by similar strength and network between carboxylates and Ba²⁺ ions produce similar amount of space for ovalbumin inside microspheres. In terms of release study, formula F2 and F4 were incubated in HCl medium for 2 hours followed by PBS buffer pH 7.4 for 1020 minutes.

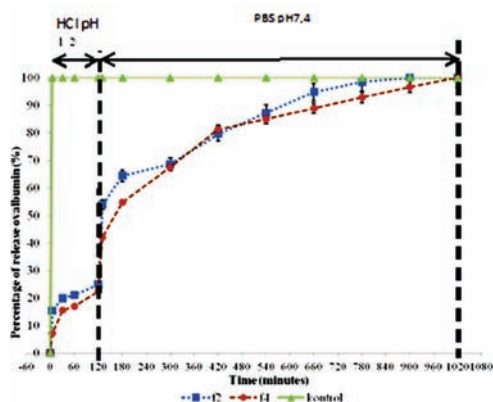




Figure 2. Profile of ovalbumin release from alginate microspheres

Results of release profile showed that ovalbumin-loaded alginate microspheres was able to protect protein from acid degradation, indicated by very small amount of ovalbumin was released during 2 hours incubation in acid pH (less than 25%) in both formulas (Figure 2). Moreover, 100% ovalbumin released from F2 microspheres in 900 minutes, whereas complete released of ovalbumin from F4 microspheres was occurred after 1020 minutes. However, the differences of ovalbumin release were not significant. It may be due to the similar swelling behaviour of alginate microspheres in pH 7.4 followed by diffusion of ovalbumin from the matrix. By increasing alginate concentration, the viscosity of alginate increased therefore avoid ovalbumin release from the matrix and slower the rate of release. From the results, this delivery system may be potential as protein or vaccine delivery system.

REFERENCES

- *. Ciofani, G., Raffa, V., Menciasci, A., Micera, S. and Dario, P., 2007. A Drug Delivery System Based On Alginate Microspheres: Mass-Transport Test And In Vitro Validation. Springer Science Business Media. Vol.9, p. 395-403
- *. Dubey, R., Shami, T.C., Brasker-Rao, K.U., 2009. Microencapsulation technology and application. Defence Sci. J., 59 (1), p. 82-95.
- *. Gombotz, W.R., Siow Fong Wee, 1998. Protein Release From Alginate Matrices. Advanced Drug Delivery Reviews 31, p. 267-285.
- *. Jin, M., Yanping Zheng, Qiaohong Hu., 2009. Preparation and characterization of bovine serum albumin alginate/chitosan microspheres for oral administration. Asian Journal of Pharmaceutical Sciences, p. 215-220.
- *. Joshi, S., Patel, P., Lin, S. and Madan, P.L., 2012. Development of cross-linked alginate spheres by ionotropic gelation technique for controlled release of naproxen orally. Asian Journal of Pharmaceutical Science, p. 134-142.
- *. Lanza, R., Langer, R. and Vacanti, J., 2007. Principles Of Tissue Engineering 3th ed. Elsevier Inc.
- *. Manjanna K. M., Shivakumar, B. and Kumar T. M. P., 2009. Formulation Of Oral Sustained Release Aceclofenac Sodium Microbeads. International Journal of PharmTech Research. Vol. 1 p. 940-952
- *. Maria, M.S., Scher, Herbert, Jeoh, Tina., 2012. Microencapsulation of bioactives in cross-linked alginate matrix. Journal of Microencapsulation, p. 286-295.
- *. Mishra, D. N. and Gilhotra, R. M. 2008. Design and characterization of bioadhesive in-situ gelling ocular inserts of gatifloxacin sesquihydrate. DARU Journal of Pharmaceutical Sciences. Vol. 16.
- *. Mowat, A. M. 1985. The Role Of Antigen Recognition And Suppressor Cells In Mice With Oral Tolerance To Ovalbumin. Immunology. Vol. 56 p. 253
- *. O'Neill, M. J., Patricia E. Heckelman, Cherie B. Koch, Kristin J. Roman, Catherine M. Kenny, Maryann R. D'Arececca. 2001. The Merck Index: An Encyclopedia Of Chemical Drug And Biological. 13th Ed., New Jersey: Merck & Co., inc.
- *. Singh, I. and Kumar, P., 2012. Formulation And Optimization Of Tramadol Loaded Alginate Beads Using Response Surface Methodology. Journal Of Pharmaceutical Sciences. Vol. 25 p 741-749
- *. Yeo, Y., Beck, N. and Park, K., 2001. Microencapsulation Methods For Delivery Of Protein Drugs. Biotechnol Bioprocess Eng. Vol. 6, p. 213-230



MUCOADHESIVE TABLET OF ETHANOLIC EXTRACT OF SAMBILOTO (*Andrographis paniculata*) AS ANTIDIABETIC USING CHITOSAN

Dhadhang Wahyu Kurniawan, Department of Pharmacy, Faculty of Medicines and Health Sciences, Universitas Jenderal Soedirman, Purwokerto, dhadhang.wk@gmail.com, Hening Pratiwi, Department of Pharmacy, Faculty of Medicines and Health Sciences, Universitas Jenderal Soedirman, Purwokerto, Lingga Ikaditya, Department of Pharmacy, Faculty of Medicines and Health Sciences, Universitas Jenderal Soedirman, Purwokerto

INTRODUCTION

Diabetes mellitus (DM) is a metabolic disease with chronic hyperglycemia that occurs due to abnormal insulin secretion, insulin damage, or a combination of both (Dipiro et al., 2009). Based on data from the Ministry of Health, diabetes prevalence rate in Indonesia, 2008, reached 5.7% of Indonesia's population or about 12 million people. In Central Java, the prevalence of type 2 diabetes has increased from 2006 to 2008, 0.83% in 2006, 0.96% in 2007, and 1.25% in 2008 (Anonymous, 2008). The increasing prevalence of diabetes same with increasing risk factors, like obesity (overweight), lack of physical activity, lack of fiber consumption, smoking, hypercholesterolemia, hyperglycemia, and others.

Treatment of diabetes mellitus use traditional medicine is mostly done by developing countries such as Indonesia. Traditional medicine has no side effects compared to synthetic drugs. Traditional drug therapy for diabetics can be obtained from various medicinal plants, which one is sambiloto (*Andrographis paniculata*).

Antidiabetic effects of sambiloto have been shown in rabbits and diabetics. In testing using the glucose tolerance test, the non-polar components of sambiloto has no activity to decrease blood sugar. Decreases blood sugar's activity found in the polar components, namely ethanol extract (Soetarno et al., 1999).

The use of sambiloto liquid extract's for the treatment of diabetes mellitus less attractive to consumers / patients because sambiloto has a bitter taste and is used repeatedly in a day. One way to make effective preparation

of sambiloto in diabetes mellitus treatment is make it become Mucoadhesive dosage in tablet form so it is not too bitter and can used once a day. Mucoadhesive drug delivery systems purpose to extend the residence time of the preparation at the site of application or extend the time of absorption and facilitate contacts between preparations with strong absorption surface so that it can fix and / or improve the performance of drug therapy (Agoes, 2008). Preparation of Mucoadhesive tablets requires a polymer bioadhesive. One type of polymer is chitosan bioadhesive (Bernkop-Schnurch, 2002).

Chitosan is obtained from chitin deacetylation leaving a free amino group that can make polycationic nature (Khan et al., 2002). Chitosan has been shown to have Mucoadhesive properties due to the electrostatic interaction between the positively charged chitosan and negatively charged mucosal surfaces. Chitosan has one primary amino group and two free hydroxyl groups for each monomer. Free amino groups in chitosan carries a positive charge then reacts with the surface/negatively charged mucus (Bernkop-Schnurch et al., 2004).

Based on that description, it is necessary to make a research on the formulation of the ethanol extract of sambiloto in Mucoadhesive tablet form so it can prolong the contact time of the drug with the intestinal mucosa, and improving the absorption of the drug. Drug absorption has important influence on the therapeutic effects of the drug in the body.



METHODS

Materials and Equipments

The materials of this study include: simplicia of sambiloto (*Andrographis paniculata*) purchased in the Wage Market Purwokerto, chitosan, 70% ethanol, lactose, magnesium stearate, talc, potassium dihydrogen phosphate (KH₂PO₄), disodium hydrogen phosphate (Na₂HPO₄), hydrochloride acid (HCl), sodium hydroxide (NaOH), aquadest, NaCl, fresh cow intestines.

The equipments of this study include: analytical balance, blender, water bath, stirrer, filter, spatulas, bowls vaporizer, stopwatch, calipers, evaporators, oven, sieve mesh (5, 14, and 16), single punch tablet machine, mucoadhesive tester (rotating cylinder), friabilator, dissolution tester from Erweka DT600, filter paper, glass apparatus.

Experimental Procedure

Preparation of ethanol extract of sambiloto

1. Preparation of simplisia
 - To make simplisia of sambiloto's powder, we used a blender and sieved with a 5 mesh sieve until we get granules to be easy for the extraction of sambiloto leaf.
2. Preparation of Ethanol Extract Sambiloto
 - The simplisia are macerated using 70% ethanol with ratio 1:4 in a closed container, then stirred and allowed to stand for 24 hours.
 - a) Every day after 24 hours, squeezed and filtered with filter paper and a Buchner funnel. Then squeezed again with 70% ethanol for 3 days.
 - b) Liquid maceration and pulp results mixed together.
 - c) The results of the extraction solvent was evaporated to help separate and extract condensed
 - d) The evaporated allowed for one day and concentrated on a water bath until a constant volume.
3. Preparation of Tablets

a. Tablet formulation

Preparation of ethanol extract of sambiloto granules made using wet granulation method by varying the amount of chitosan. The number of active substances used in the formulation is determined based on the dose that has been studied by Nugroho et al. (2012), which is 150 mg.

Table 1. Formula of tablets Ethanol Extract of sambiloto leaf

Materials	Formula			
	1	2	3	4
Ethanol extract of sambiloto (mg)	150	150	150	150
Chitosan (%)	20	40	60	80
Laktose (%)	77	77	77	77
Talk (%)	1	1	1	1
Mg-stearat (%)	2	2	2	2

b. Preparation of granules (granulation)

The phases of making granules were:

- 1) Ethanol extract of sambiloto, chitosan, lactose, talc, and Mg-stearate was weighed.
 - 2) The ethanol extract was mixed with partially lactose, and then added to the chitosan. The materials are mixed and stir until homogeneous, then added residual lactose.
 - 3) The result sieved using a 14 mesh sieve.
 - 4) After become granules, spread out on a sheet of aluminum foil on a flat tray and dried in an oven at a temperature of 40 - 60°C.
 - 5) The dried granules were sieved with a 16 mesh sieve.
 - 6) Then magnesium stearate and talc as the outer phase is added to the granules, mixed until homogeneous.
 - 7) Granules were prepared felted mass.
- ### c. Examination of Flowing Properties of granules
- Examinations of the flowing proer



ty of granules were observed by stationary angle and flowing time methods.

1) Angle of repose Method

Angle of repose measurement is carried out by weighing 100 g of granules, the granules inserted into the funnel flow time test standing at a height H above the graph paper in the horizontal plane. Cover is opened so that the granules out and placed on a flat surface (Carstensen, 1977). Measurements replicated three times. Angle of repose can be calculated by the formula:

$$\text{Tan } \alpha = \frac{H}{R} \text{ atau } \alpha = \text{arc tan } \frac{H}{R}$$

Description: = stationary angle

H = height

R = radius or $\frac{1}{2} d$

2) Flowing time

The flow time measurement method is done by weighing 100 g of granules, the granules then inserted into the funnel that closed. Cover is opened and the granules allowed to flow until the end. Calculated flow time granule. The granules have good flow properties when it has a flow time of no more than 10 seconds (Fudholi, 1983). Measurement of flow time was replicated three times.

d. Tablet compression

Compression tablets using a single punch tablet machine to adjust the size and weight of the tablet mass. When the tool has finished setting, granules were prepared and then inserted through the hopper and the machine starts (Voigt, 1994).

e. Evaluation of Tablets

1) Physical Characteristic

Tests of physical characteristic de

scriptively include testing for uniformity of color, presence or absence of odor, surface shape, consistency, and presence or absence of physical defects (damage).

2) Uniformity of size

Each formula is taken 20 tablets, then the tablet's diameter and tablet's thickness was measured using calipers and analyzed with the standard of uniformity in the size of the tablet edition of Indonesian Pharmacopoeia III (Anonymous, 1979).

3) Weight uniformity

Each formula is taken 20 tablets, and tablets that free from dust, weighed and the average weight was calculated, and then matched with a table percentage weight deviation allowed in the third edition of the Indonesian Pharmacopoeia (Anonymous, 1979).

4) Hardness test

Each formula is taken 10 tablets, then one by one tablet is placed in the middle to the hardness tester, first scale on the zero position, and then the tool rotated slowly until the tablet breaks. Read scale achieved when broken or crushed tablets (Voigt, 1994). Hardness is expressed in kilograms. The tablet has a hardness between 4 kg to 10 kg (Parrott, 1971).

5) Friability (fragility)

According Agoes (2006), 20 tablets of each formula that free from dust, placed in friabilator. Friabilator run 4 minutes or 100 times a round. Tablets were taken and cleaned of particles attached, by weight, calculated the percentage in weight. The total weight of the tested tablets should not be reduced by more than 1 % of the initial weight of the test. Testing was replicated three times.

Friability test results can be calculated using the following equation:

$$F\% = \frac{(W_0 - W_t)}{W_0} \times 100\%$$

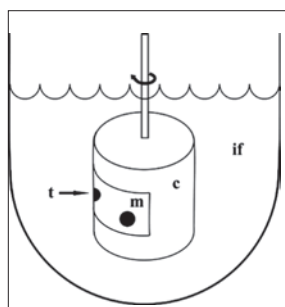
Description:

W₀ = initial weight of the tablet before intervened friabilator

W_t = weight of tablet after intervened friabilator

- f. In vitro evaluation of mucoadhesive properties by the rotating cylinder method

Tablet attached to the pressure of 500 Pa in the intestinal mucosa of cow, which was attached to a stainless steel cylinder (diameter 4.4 cm, height 5.1 cm, the 4-cylinder, USP XXVI) using cyanoacrylate adhesive. The cylinder is placed in the dissolution apparatus according to USP, entirely immersed in the dissolution medium of 100 mM phosphate buffer pH 6.8, at a temperature of 37°C and stirred at 100 rpm. Testing tools can be seen in picture 1. Tablet test apart, disintegrated and/or eroded observed for a period of 10 hours (Bernkop-Schnurch, 2002).



Picture 1. Testing system scheme which is used to evaluate the properties of mucoadhesive tablets based on various polymers. c: cylinder, if: in intestinal fluid, m: bovine intestinal mucosa, t: tablets (Bernkop-Schnurch, 2002).

- g. Data analysis

Data results of testing the physical properties of granules and tablets compared to physical evaluation requirements of tablets according to the third edition of the Pharmacopoeia of Indonesia (1979), Indonesia Pharmacopoeia IV edition (1995), and related literature.

RESULTS AND DISCUSSION

Results of determination of plant stated that the plant is *Sambilito* with the scientific name of *Andrographis paniculata* (Burm f.) Nees. Dry powder of *sambilito* was 1788 mg, obtained after the extraction process as much as 153 mg of extract thick, mean yield of extract of dried powder is 8.56%. Viscous extract obtained was then conducted organoleptic test. The results of the ethanol extract of *sambilito* organoleptic test are shown in Table 2.

Table 2. The results of organoleptic test ethanol extract of *sambilito*

No.	Organoleptic parameters	Description
1.	Color	Black greenish
2.	Odor	typical
3.	Taste	bitter
4.	consistency	condensed

Ethanol extract of *sambilito* granules that made by wet granulation subsequent physical characteristic test, including flowing properties of granules and granule moisture content. Data of flowing properties of granules are presented in Table 3.

Table 3. Test results of flowing properties of ethanol extract of *sambilito*

Formula	Flowing time (seconds)	Stationary angle (x°)	Specification
F1	4,33 ± 0,08	26,14 ± 1,06	Eligible
F2	3,77 ± 0,10	25,24 ± 1,66	Eligible
F3	4,77 ± 0,12	24,10 ± 0,48	Eligible
F4	4,64 ± 0,08	23,57 ± 0,77	Eligible



The character-istic	Formula		
	F1	F2	F3
Color	Black greenish (thick)	Black greenish	Black greenish (young)
Odor	Typical	Typical	Typical
Surface	Smooth and compact	Smooth and compact	Smooth and compact
Physical disabilities	None	None	None

* replicated 3 times.

Based on Table 3 , known that all formulas have the flowing time and repose angle qualified because 100 grams of ethanol extract of sambiloto granules flowing less than 10 seconds and repose angle less than or equal to 30°. Repose angle measurement shown that the higher amount of chitosan added, the smaller repose angle got. It means that the addition of chitosan effect on repose angle of granules.

Test of flowing time and repose angle describe the flowing properties of granules. Good flowing properties of the granules is essential to ensure efficient mixing and uniformity of weight (Siregar and Wikarsa, 2005).

Flowing properties are affected by particle size, particle shape, moisture granules, gravity and friction forces

Formula	Initial weight (gram)	Final Weight (gram)	Moisture content (%)
1	5,00 ± 0,00	4,86 ± 0,00	2,92 ± 0,08
2	5,00 ± 0,00	4,85 ± 0,00	3,16 ± 0,09
3	5,00 ± 0,00	4,84 ± 0,00	3,31 ± 0,08
4	5,00 ± 0,00	4,83 ± 0,00	3,53 ± 0,09

Based on Table 3 , known that all formulas have the flowing time and repose angle qualified because 100 grams of ethanol extract of sambiloto granules flowing less than 10 seconds and repose angle less than or equal to 30°. Repose angle measurement shown that the higher amount of chitosan added, the smaller repose angle got. It means that the addition of chitosan effect on repose angle of granules.

Test of flowing time and repose angle describe the flowing properties of granules. Good flowing properties of the granules is essential to ensure efficient mixing and uniformity of weight (Siregar and Wikarsa, 2005).

Flowing properties are affected by particle size, particle shape, moisture granules, gravity and friction forces

between particles. If a large particle size and spherical shape as well as gravity and friction forces small, it will be faster and easier flowing. The more flat cone generated, then the smaller the tilt angle and the better of the flowing properties. Based on the results of the study, increased of chitosan will accelerate the flowing time. This is due to the formula with the higher chitosan concentration resulted in large granules, granules that are large will have little friction so the flowing time is small (Lachman et al., 1994; Voigt, 1995).

The results of the determination of moisture content of the ethanol extract of sambiloto granules can be seen in Table 4 .

Table 4. The results of the determination of moisture content of ethanol extract of sambiloto granules.

* replicated 3 times

Based on the data in Table 4, shows that the granules of all formulas qualify moisture contents, because the content is in the range 2-4% moisture. According to Lachman et al., (1994) that the good moisture content of the granules is 2-4%.

The test results of physical characteristic ethanol extract of sambiloto tablet can be seen in Table 5. Physical characteristic showed that



tablets produced relatively good. Greenish black color tablet, the younger of the formula 1 to formula 4, it is caused by increasing of chitosan. The more chitosan used in this study resulted in younger creamy white colored tablet produced.

Uniformity test results measure the ethanol extract of sambiloto tablets are presented in Table 6 .

Table 5. The results of testing the physical characteristic of tablets

Table 6. Test results of tablet size uniformity ethanol extract of sambiloto

Formula	Thick of tablet (mm)	Diameter of tablet (mm)	Spesification
F1	0,33 ± 0,00	1,31 ± 0,00	Eligible
F2	0,33 ± 0,00	1,31 ± 0,00	Eligible
F3	0,33 ± 0,00	1,31 ± 0,00	Eligible
F4	0,33 ± 0,00	1,31 ± 0,00	Eligible

Based on the data in Table 6, it is seen that all the tablets eligible with requirements of uniformity of size . Thus, the ethanol extract of sambiloto tablet can be declared to have good size uniformity. One good indicator is expressed tablet is a tablet that has a good size uniformity.

Tablet weight uniformity test results of ethanol extract of sambiloto can be seen in Table 7.

Table 7. The results of uniformity test of ethanol extract of sambiloto tablet

Formula	Weight (mg)	Coefficient of Variation (CV)	Spesification
F1	498,3 ± 6,59	1,32%	Eligible
F2	502,15 ± 7,34	1,46%	Eligible
F3	498,5 ± 6,46	1,30%	Eligible
F4	505,55 ± 6,75	1,33%	Eligible

Based on the data in Table 7, it is seen that all

formula eligible weight uniformity, because none of the tablets deviated 5% and 10% of the average weight of the tablet and has a CV less than 5%. Tablets with a good weight uniformity can be assumed that the levels of active ingredient in the tablet as well uniform so that the therapeutic effect produced identical (Anonymous, 1979; Voigt, 1995).

The results of hardness test of the ethanol extract of sambiloto tablets are presented in Table 8.

Table 8. The results of hardness test of ethanol extract of sambiloto tablets

Formula	Hardness (kg)	Specification
F1	4,15 ± 0,24	Eligible
F2	4,05 ± 0,16	Eligible
F3	3,85 ± 0,24	Eligible
F4	3,65 ± 0,34	Eligible

Based on the data in Table 8, it is seen that all formulas eligible with tablet hardness scale between 4-10 kg (Anonymous, 1979). Hardness of formula 1 to formula 4 is getting smaller. Formula 1 with the highest levels of chitosan has the greatest hardness is 4.15 kg. Supposedly greater levels of chitosan will increase the bond between chitosan with other ingredients to produce a stronger bond and tablets are formed more compact and hard. But the results showed different results, this was caused by the size of the chitosan used larger than it should be. The size of chitosan amorphous powder/powder causes compactibility less than the maximum.

The results of ethanol extract of sambiloto tablet friability test can be seen in Table 9.

Table 9. The results of friability test of ethanol extract of sambiloto tablets

Formula	Friability (%)	Specification
F1	0,62 ± 0,20	Eligible
F2	0,55 ± 0,08	Eligible
F3	0,60 ± 0,28	Eligible
F4	2,10 ± 2,25	None eligible

*replicated 3 times



Based on the data in Table 9, shows that the friability test of formula 1 to formula 3 were eligible, because of losses weight were not more than 1% (Banker and Anderson , 1994). Friability formula 4 wasn't eligible, because the amount of chitosan used was more than it should, where the size of chitosan was large, so tablet compactibility and hardness wasn't good. Compactibility and hardness of tablets are good enough to make the tablets brittle. Tablet which has a high hardness means have strong bond between particles, so it is not easily damaged by shocks.

Friability is a parameter to assess the resilience of the tablet to a variety of things that can cause damage to the surface of the tablet (Ansel, 1989). According to Voigt (1995) friability is expressed as the mass of the entire particle released from the tablet due to mechanical load testers . Friability expressed as a percent of friability which refers to the mass of the initial tablet before testing.

Friability test is very important because tablet that easily crushed into powder, flakey, and cracked in handling will loses its aesthetic value so the consumer won't accept it, it also can caused contamination at the site of the transport and packaging, and also caused variations in tablet weight and content uniformity (Banker and Anderson, 1994).

At the time of the tablet contacted with a solution of phosphate buffer pH 6.8, all formulas tablet looked swell and form a hydrogel, and stick/attached firmly to the intestinal mucosa. Adhesion of tablets on the intestinal mucosa can be seen in Picture 2 .



Picture 2. Adhesion to the intestinal mucosa tablet

Hydrophilic chitosan can undergo hydration contact with water and form a hydrogel that expands into a tablet formula (Varshosaz et al., 2006). Hydrogels are three- dimensional cross linked polymer chains that have the ability to hold water in the porous structure. This hydrogel is formed by the presence of hydrophilic functional groups, such as hydroxyl, amino, and carboxyl. In the chitosan structure, there is a hydroxyl group that can form a chitosan hydrogel (Mythri et al., 2011).

Tablet expands slowly because chitosan has the ability controlled hydration (Jain et al., 2008). Hydration is controlled to prevent the occurrence of excessive hydration. Excessive hydration would reduce the flexibility of the polymer chains due to the formation of cross linked polymer chains thereby limiting excessive interpenetration of polymer chains into the mucus and eventually will reduce mucoadhesive strength (Mythri et al., 2011).

In theory, this mucoadhesive phenomenon takes place in two steps. The first step is a contact between the polymer bioadhesive (chitosan) and mucus due to wetting and development of bioadhesive materials (chitosan). The second phase is consolidation, a process where bioadhesive polymer penetrate into crevices and surface mucus occurring chemical bonds between the polymer and mucin bioadhesive (Carvalho et al., 2010). Mucoadhesive properties test results in vitro are presented in Table 10 .

Table 10. The results of in vitro testing mucoadhesive properties tablets ethanol extract of sambiloto

Formula	Mucoadhesive properties
1	4,33 minute 25,67 seconds ± 0,58
2	8 minute 20 seconds ± 2,00
3	17,33 minute 18,33 seconds ± 2,52
4	23 minute 16,33 seconds ± 2,00

*replicated 3 times



on Table 10, it is seen that of formula 1 to formula 4 with the increasing of chitosan resulted in an increase in mucoadhesive properties. Formula 4 with the highest levels of chitosan having the greatest mucoadhesive properties that can be attached for 23 minutes 16.33 seconds, while the lowest adhesion owned by Formula 1 with the lowest levels of chitosan which can be attached for 4.33 minutes 25.67 seconds. This is due to the higher levels of chitosan used; the ability of bonding with mucin is stronger. Chitosan has hydroxyl groups that are responsible for adhesion. Mucoadhesive properties possibly caused by the formation of hydrogen bonds between the hydroxyl groups of the chitosan with mucus components and ionic bonds between atoms N in chitosan with the S atom of cysteine contained in the mucus layer (Majithiya et al., 2008; Sreenivas and Pai, 2008). Hydrogen bonds are the bond between the H atoms in the molecule which attracted by the highly electronegative atom, in example F, O, or N from adjacent molecules. While the ionic bond is a bond that is formed due to the difference in charge between the two components, between chitosan and mucin (Petrucci, 1985). The higher levels of chitosan used, the stronger bond produced, so the mucoadhesive properties will be stronger (Majithiya et al., 2008).

CONCLUSION

Ethanol extract formula of sambiloto tablets made by using chitosan as a carrier qualify physical characteristic of tablets (physical appearance, uniformity of size, weight uniformity, hardness, and friability). Increased levels of chitosan on the ethanol extract of sambiloto tablets can improve mucoadhesive properties. Formula 4 with the highest levels of chitosan have the strongest mucoadhesive properties which can be attached for 23 minutes 16.33 seconds, while the lowest power possessed by the formula 1 with the lowest levels of chitosan which can be attached for 4.33 minutes 25.67 seconds.

REFERENCES

1. Agoes, G., 2008, Sistem Penghantaran Obat Pelepasan Terkendali, ITB, Bandung, 33-34, 231-244.
2. Agoes, G. 2006. Pengembangan Sediaan Farmasi. ITB, Bandung.
3. Anonymous, 1979, Farmakope Indonesia edisi III, Departemen Kesehatan Republik Indonesia, Jakarta
4. Anonymous, 2008, Profil Kesehatan Provinsi Jawa Tengah, Health Department of Central Java.
5. Banker, G.S., and Anderson, N.R., 1994, Tablet, dalam Lacman, L., Lieberman, H.A., dan Kanig, J.L., Tablet In The Theory and Practice of Industrial Pharmacy, Ed III, translate by Siti Suryatmi, Indonesia University, Jakarta, 648, 653, 662,684, 692-707.
6. Bernkop-Schnurch, A., Guggi, D., dan Pinter, Y., 2004, Thiolated Chitosans: Development and In Vitro Evaluation of a Mucoadhesive, Permeation Enhancing Oral Drug Delivery System, Journal of Controlled Release 94, 177-186.
7. Bernkop-Schnurch, A., 2002, Mucoadhesive Polymers in Polymeric Biomaterials, Severian Dumitriu (Editor), Marcell Dekker Inc., New York, p. 147-162.
8. Dipiro, J.T., Talbert, R.L., Yee, G.C., Matzke, G.R., Wells, B.G., dan Posey, L.M., 2009, Pharmacotherapy: A Pathophysiologic Approach 7th Edition. United States: The McGraw-Hill Companies, Inc.
9. Khan, T.A., Peh, K.K., dan Ch'ng, H.S., 2002, Reporting degree of deacetylation values of chitosan: the influence of analytical methods, J Pharm Pharmaceut Sci 5(3):205-212.
10. Nugroho, A.E., Andrie, M., Warditiani, N.K., Siswanto, E., Pramono, S., and Lukitaningsih, E., 2012, Antidiabetic and antihiperlipidemic effect of *Andrographis paniculata* (Burm. f.) Nees and Andrographolide in high-fructose-fat-fed rats, In



ICPPS 2014

Proceeding
The 1st International Conference
on Pharmaceutics & Pharmaceutical Sciences

dian Journal of Pharmacology, vol. 44 issue 3, 377-382.

11. Soetarno, S., Sukandar, E.Y., Sukrasno, and Yuwono, A., 1999, Aktivitas Hipoglisemik Ekstrak Herba Sambiloto (*Andrographis paniculata* Nees, Acanthaceae), J.M.S., 4:2, 62-69.
12. Voight, R., 1995, Pelajaran Teknologi Farmasi, Translated by Soendani Noerono Soewandhi, 5th edition, Gadjah Mada Press, Yogyakarta, 166, 215-218, 223, 570-571, 651.



PHYSICAL INTERACTION STUDY OF IBUPROFEN-STEARIC ACID BINARY MIXTURE

Diajeng Putri Paramita, Faculty of Pharmacy Airlangga University, Address, dputriparamita@gmail.com, +6285815586492; Dwi Setyawan, Faculty of Pharmacy Airlangga University; Dewi Isadiartuti, Faculty of Pharmacy Airlangga University.

INTRODUCTION

Ibuprofen is a non steroid anti-inflammatory drug (NSAID) derived from propionic acid [3]. It has low aqueous solubility but high permeability so it is classified into BCS (Biopharmaceutical Classification System) Class II [6]. High cohesivity and adhesivity cause ibuprofen has bad powder flow and also contributes to its high tendency for sticking to the punch. Granulation step is necessary in ibuprofen tableted dosage form manufacturing due bad compaction behaviour [9]. Thus, addition of appropriate excipients is hardly avoidable in order to improve powder properties in ibuprofen tableted dosage form formulation.

Pharmaceutical dosage form manufacturing always involves heat and mechanical energy during the process [10]. This energy could induce interaction between drug and excipient molecules [10] as well as eutectic formation. Eutectics are intimate crystalline mixture of one compound in another and it has unique property in its lower melting temperature than that pure compound. Generally, eutectic interaction does not impact the pharmacological activity, but may contribute in alteration of the pharmaceutical properties. Unintentional eutectic formation in tableted dosage form development have been reported to lead to unwanted changes in the physical and/or chemical characteristics of the tablets [2].

Ibuprofen is a kind of drug that forms eutectic with some kind of excipients as reported in many studies [7, 11, 1]. It has been identified by DSC analysis that ibuprofen forms eutectic with stearic acid [7], one of most frequently used lubricant [4]. Therefore, further physical characterization was conducted in this study for better understanding of eutectic formation in ibuprofen-stearic acid binary system.

MATERIALS AND METHODS

Materials

Ibuprofen was purchased from Shasun Chemicals and Drugs Ltd., India. Stearic acid was obtained from Hense Chemicals Manufacture Ltd., China.

Binary mixture was prepared by weighing each compound separately and mixing them gently in a mortar at ambient temperature. Weight ratio of 4:6 of ibuprofen and stearic respectively was used for each binary system. Eutectic formation of binary mixture was induced by heating the prepared binary mixture upon water-bath at temperature about 70°C.

Methods

Hot Stage Microscopy

Hot stage microscopy was performed under polarizing microscope observation equipped with heating apparatus. The higher melting compound, which is ibuprofen, was melted first on a microscope slide to occupy about half the area under cover slip. After the first compound had cooled and solidified, the second compound, stearic acid with lower melting temperature, was placed at very edge of cover slip, near the first compound. The sample was heated until stearic acid completely melted to contact with solidified ibuprofen. Then, the sample was allowed to cool. After the sample had solidified, the contact area of two compounds was observed whilst the temperature was gradually raised.

X-ray Powder Diffraction

X-ray powder diffraction data were obtained using a Phillips Xpert X-ray diffractometer, Netherland, with CuK α radiation (1,54Å), at 40 kV and 30 mA, and passing through a nickel filter with divergence slit (0,25°). Samples were scanned over 2 θ range of 5-50° with



step size of 0,017 μ m.

Scanning Electron Microscopy

Scanning electron-micrographs of crystal of pure compounds and binary mixture were collected by a Hitachi TM3000, Japan. Observation was conducted by magnification of 1000. Samples were fixed on aluminium stub with conductive double-sided adhesive tape and coated with gold in a low vacuum atmosphere.

Fourier Transform Infrared Spectroscopy

Fourier transform infrared spectra were obtained using a Shimadzu 8400s FTIR spectrometer, Japan. Samples of ~ 2 mg were mixed with 300 mg potassium bromide and then compressed in a hydraulic press to form transparent disc. Each sample was analysed from 4000 to 400 cm^{-1} .

RESULTS AND DISCUSSION

Hot stage microscopy was performed to identify the type of physical interaction between two compounds. It is a simple technique to understand phase behaviour in binary system upon heating. Under polarizing microscope, only crystalline phases will be visible because they direct the polarized light and, in other hand, liquid phases allow the light to pass through unchanged so no light reaches microscope [5]. Crystalline phases will be seen full of colours with different intensity which is affected by fragment orientation, thickness, and polarized light absorbed or pass through crystalline fragment [13]. When crystalline phases melt to form liquid phases, it will be quickly seen and recognized as a black line or region [5].

Figure 1 shows the behaviour of ibuprofen and stearic acid under hot stage microscopy observation. Area of A.1 and B.1 is re-crystallized phase of ibuprofen, A.2 and B.2 is re-crystallized phase of stearic acid, A.3 and B.3 is contact area of two compounds. It's clearly seen that contact area of two compounds is melted first than the pure compound when temperature increases (Figure 1 B), leaving single blank line between crystalline phases. This single eutectic formation indicates conglomerate crystallization [5].

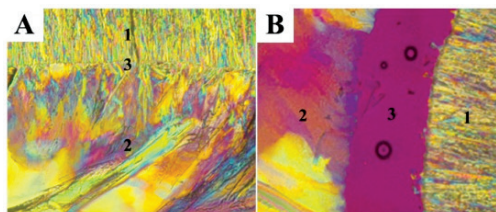


Figure 1 The mixed fusion behavior of ibuprofen and stearic acid, A. Contact area is formed, and B. Contact area is melted first.

Eutectic formation between two compounds also shown thermal analysis study we conducted (result not shown). Diagram phase obtained from DTA analysis of various weight ratio binary mixture in our study shows similarity pattern compared to previous study by Lerdkanchanaporn et al. (2001).

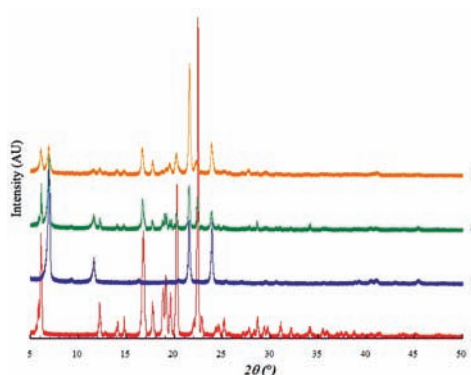


Figure 2 X-ray diffractograms of A. Ibuprofen, B. Stearic acid, C. Binary mixture in 4:6 weight ratio, and D. Eutectic-formed binary mixture in 4:6 weight ratio.

The crystalline nature of binary mixture of ibuprofen and stearic acid was examined by X-ray powder diffraction of binary mixture and eutectic-formed binary mixture as well as each pure compound.

Ibuprofen showed numerous strong diffraction peaks in 2θ of 6.07 $^\circ$, 12.18 $^\circ$, 16.71 $^\circ$, 17.71 $^\circ$, 18.83 $^\circ$, 19.59 $^\circ$, 20.32 $^\circ$, 22.45 $^\circ$. Stearic acid showed few strong diffraction peaks in 2θ of 6.94 $^\circ$, 11.62 $^\circ$, 21.49 $^\circ$, and 23.91 $^\circ$. These pure compound peaks superimpose each other as it

shown in X-ray diffractogram of binary mixture in 4:6 weight ratio (Figure 2 C). Eutectic-formed binary mixture showed similar X-ray diffraction pattern with binary mixture and it also shown superimposition diffraction peaks of the pure compound. This phenomenon indicates eutectic formation between ibuprofen and stearic acid do not result new crystalline phase but conglomeration two crystalline in solid state. Difference of peak intensity showed shifting on degree of crystallinity [13].

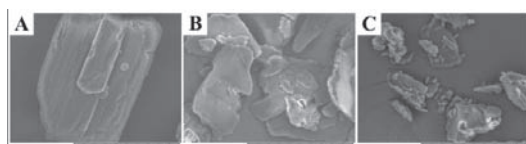


Figure 3 SEM photographs of A. Ibuprofen crystals, B. Stearic acid crystals, and C. Eutectic-formed binary mixture in 4:6 weight ratio.

The outer appearance of pure compound crystal can be distinguished each other as it can be seen in Figure 3. The typical outer appearance of ibuprofen no longer can be seen in photograph of eutectic-formed binary mixture whilst the layered-outer appearance of stearic acid still exists. Stearic acid is well-known to be a “boundary” type lubricant [12], so it may form thin film on ibuprofen crystal surface. Therefore, this stearic acid behavior may takes role in disappearance of ibuprofen crystal on eutectic-formed binary mixture photograph. Hydrogen bonding interaction of ibuprofen and stearic acid in their binary mixture and eutectic-formed binary mixture shown by FTIR spectra (Figure 4). It is characterized by shifting of carbonyl and hydroxyl functional groups vibration which can form hydrogen bond amongst themselves [8]. From this hydrogen bonding interaction, we can conclude that ibuprofen interacts physically with stearic acid to form conglomerate mixture.

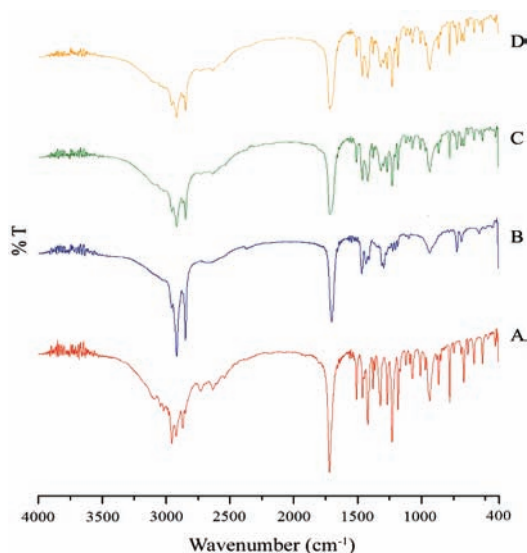


Figure 4 FTIR spectra of A. Ibuprofen, B. Stearic acid, C. Binary mixture in 4:6 weight ratio, and D. Eutectic-formed binary mixture in 4:6 weight ratio.

CONCLUSION

Identification of physical interaction with hot stage microscopy showed eutectic formation of ibuprofen and stearic acid leads to conglomerate crystallization. It is supported by X-ray powder diffraction that is diffraction peak superimposition characterizes conglomeration phenomena. Eutectic formation also leads to disappearance of ibuprofen crystal amongst stearic acid existence. Moreover, hydrogen bonding interaction is present in eutectic formation of two compounds. The study presented here allows a better understanding of the drug/excipient phase behavior in binary system.

REFERENCES

1. Ali, W., Williams, A.C., and Rawlinson, C.F. 2010. Stoichiometrically governed molecular interactions in drug: Poloxamer solid dispersion. *Int. J. Pharm.*, 391, pp. 162-8.
2. Bi, M., Hwang Sung-Joo, and Morris K.R. 2003. Mechanism of eutectic formation



- upon compaction and its effect on tablet properties. *Thermochim. Acta*, 404, pp. 213-26.
3. Brunton, L.L., Lazo, J.S., Parker, K.L. 2006. Goodman & Gilman's The Pharmacological Basis of Therapeutics 11th Edition. New York: McGraw-Hill.
 4. Corvis, Y., Négrier, P., and Espeau, P. 2011. Physicochemical Stability of Solid Dispersions of Enantiomeric or Racemic Ibuprofen in Stearic Acid. *J. Pharm. Sci.*, Vol. 100, No. 12: 5235-43.
 5. Davis, R.E., Lorimer, K.A., Wilkowski, M.A., Rivers, J.H., Wheeler, K.A., and Bowers J. 2004. Studies of phase relationships in cocrystal systems. *ACA Transactions*, 39, pp 41-61.
 6. Kawabata, Y., Wada, K., Nakatani, M., Yamada, S., and Onoue, S. 2011. Formula design for poorly water-soluble drugs based on biopharmaceutics classification system: Basic approaches and practical applications. *Int. J. Pharm.*, 420, pp. 1-10.
 7. Lerdkanchanaporn, S., Dollimore, D., and Evans, J. 2001. Phase diagram for the mixtures of ibuprofen and stearic acid. *Thermochim. Acta*, 367-368, pp. 1-8.
 8. Putra, O.D., Nugrahani, I., Ibrahim, S., dan Uekusa, H. 2012. Pembentukan Pa
datan Semi Kristalin dan Ko-kristal Para setamol. *JMS*, Vol. 17, No. 2: 83-8.
 9. Rasenack, N. and Muller B. W. 2002. Crystal habit and tableting behavior. *Int. J. Pharm.*, 244, pp. 45-57.
 10. Setyawan, D., Sumirtapura, Y.C., Soewandhi, S.N., Hadi, D. 2012. Characterization of physical properties and dissolution rate of binary systems erythromycin stearate-microcrystalline cellulose and spray dried lactose due to compression forces. *Int J Pharm Pharm Sci*, Vol 4, Suppl1, pp 652-7.
 11. Stott, P.W., Williams, A.C., Barry, B.W. 1998. Transdermal delivery from eutectics systems: enhanced permeation of model drug, ibuprofen. *Journal of Controlled Release*, 50, pp. 297-308.
 12. Wang, J., Davidovich, M., Desai, D., Bu, D., Hussain, M., and Morris, K. 2010. Solid-State Interaction of a Drug Substance and Excipients and Their Impact on Tablet Dissolution: A Thermal-Mechanical Facilitated Process-Induced Transformation or PIT. *J. Pharm. Sci.*, Vol. 99, No. 9: 3849-62.
 13. Zaini, E., Halim, A., Soewandhi, S.N., Setyawan, D. 2011. Peningkatan Laju Pelarutan Trimetoprim Melalui Metode Ko-kristalisasi dengan Nikotinamida. *JFI*, Vol. 5 No. 4 Juli 2011: 205-12.



MOLECULAR MODELING AND SYNTHESIS OF 1-(3,4-DICHLOROBENZOYL)-1,3-DIMETHYLUREA

Dian Agung Pangaribowo, Faculty of Pharmacy University of Jember, Jl. Kalimantan 1/2 Kampus Tegalboto Jember, agung.pangaribowo@gmail.com, +62 81553861546; **Siswando**, Faculty of Pharmacy Airlangga University, Jl. Dharmawangsa Dalam Surabaya 60286, siswando@unair.ac.id, +62 8123206328; **Bambang Tri Purwanto**, Faculty of Pharmacy Airlangga University, Jl. Dharmawangsa Dalam Surabaya 60286, bbg_tony@yahoo.com, +62 8123536513

INTRODUCTION

Cancer is a top killer of human beings. There is an urgency to develop highly efficacious and minimally toxic treatments for cancer. Most of the current cancer drugs usually exhibit high toxicity and are severely resisted by tumor cells in the clinic. This dilemma is particularly true for DNA-damaging agents, the mainstay of cancer treatment (Tao et al, 2007). Following DNA damage, normal cells arrest and attempt to repair at the cell cycle checkpoints G1 and S phases through tumor suppressor p53, and at G2 and S phases through checkpoint 1 kinase (Chk1) (Zhao et al, 2010). Checkpoint Kinase-1 (Chk1, CHK1, CHEK1) is a Ser/Thr protein kinase that mediates the cellular response to DNA-damage. Upon DNA-damage, Chk1 is activated by ATM and ATR kinases, which phosphorylate residues Ser-317 and/or Ser-345. Chk1 mediated signaling ultimately leads to S-phase or G2/M cell cycle arrest primarily driven by Cdk inhibition. Consequently Chk1 inhibition would abrogate this arrest, and therefore permit a cell with damaged DNA to continue through the cell cycle, ultimately resulting in mitotic catastrophe and/or apoptosis (Oza et al, 2006). Thus, selective inhibitors of Chk1 may be of great therapeutic value in cancer treatment (Li et al, 2006).

Several studies have been developed on urea derivatives as Chk1 inhibitors. As a part of our research for novel anticancer agents, we designed and synthesized 1-(3,4-dichlorobenzoyl)-1,3-dimethylurea.

Docking simulation was performed using Molegro Virtual Docker of the Chk1 in complex with an inhibitor to explore the binding modes of this compound at the active site.

MATERIAL AND METHODS

Materials and Measurements

All chemicals and reagents used in current study were analytical grade. The IR spectra was recorded on FT-IR Perkin Elmer Spectrum One. The ¹H-NMR and ¹³C-NMR spectra were recorded on BRUKER BioSpin Avance III NMR Spectrometer in Chloroform-d₆ and chemical shift was reported in ppm (δ).

General Procedure for Synthesis of 1-(3,4-Dichlorobenzoyl)-1,3-Dimethylurea

To a stirred solution of 1,3-dimethylurea (0,08 mol) and triethylamine (0,08 mol) in THF (30 mL) was added 3,4-dichlorobenzoyl chloride (0,04 mol) in THF (15 mL) and the reaction mixture was reflux for 4 hour. The product was washed carefully with water and extracted with ethyl acetate; the resulting 1-(3,4-dichlorobenzoyl)-1,3-dimethylurea was purified by crystallization from EtOH (Figure 1).

Molecular Modeling

To assess the anti-cancer behavior of 1-(3,4-dichlorobenzoyl)-1,3-dimethylurea on structural basis, automated docking studies were carried out using Molegro Virtual Docker program, the scoring functions and hydrogen bonds formed with the surrounding amino acids are used to predict their binding modes, their binding affinities and orientation of this compound at the active site of the Chk-1 enzyme. The protein-ligand complex was constructed based on the X-ray structure of Chk-1 (2YWP.pdb downloaded from the pdb).

RESULT AND DISCUSSION

Chemistry



In our study, 1,3-dimethylurea and 3,4-dichlorobenzoyl chloride were dissolved in a mixture of TEA and THF, then refluxed for 4 h at 80°C, and white needle crystal of 1-(3,4-dichlorobenzoyl)-1,3-dimethylurea was obtained with yields of 75% and melting point 110°C. The synthetic compound gave satisfactory analytical and spectroscopic data, which was in full accordance with their depicted structures.



Figure 1. Synthetic scheme for 1-(3,4-dichlorobenzoyl)-1,3-dimethylurea

The IR spectrum of the synthesized urea was recorded (Figure 2) and it gives an absorption band 3316 cm⁻¹ representing the presence of -NH group. The absorption band at 1696 and 1652 cm⁻¹ confirms the imide group, and the absorption band at 1534 cm⁻¹ confirms the aromatic -C=C- group

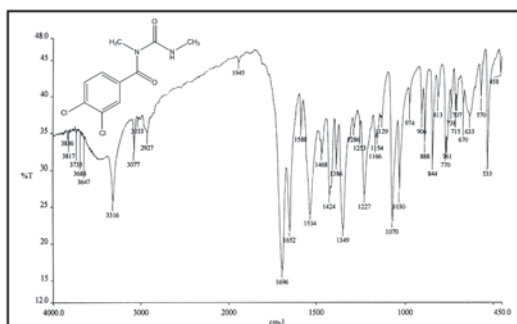


Figure 2. IR spectra of 1-(3,4-dichlorobenzoyl)-1,3-dimethylurea in KBr

The ¹H-NMR spectra (Figure 3) of synthesized urea give ¹H-NMR (400 MHz, Chloroform-d₆, δ ppm): 2.89 (d, 3H), 3.15 (s, 3H), 7.21-7.52 (m, 3H), 8.83 (s, 1H). The ¹³C-NMR spectra (Figure 4) of synthesized urea give ¹³C-NMR (400 MHz, Chloroform-d₆, δ ppm): 27.22 (-CH₃), 35.75 (-CH₃), 125.93-135.74 (-Ph), 155.79 (-C=O), 173.53 (-C=O).

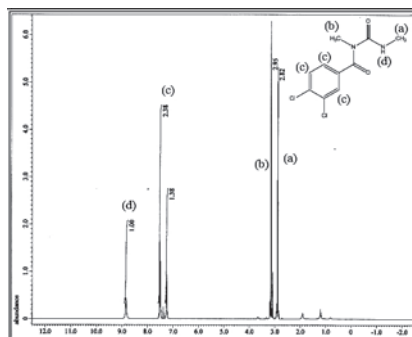


Figure 3. ¹H-NMR spectra of 1-(3,4-dichlorobenzoyl)-1,3-dimethylurea in Chloroform-d₆

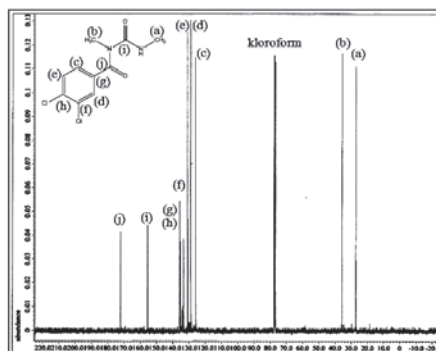


Figure 4. ¹³C-NMR spectra of 1-(3,4-dichlorobenzoyl)-1,3-dimethylurea in Chloroform-d₆

Molecular Modeling

In order to gain more understanding of the activity observed at the Chk1, molecular docking of 1-(3,4-dichlorobenzoyl)-1,3-dimethylurea into ATP binding site of Chk1 was performed on the binding model based on the Chk1 complex structure (2YWP.pdb). The binding model of this compound and Chk1 is depicted in Figure 5. 1-(3,4-dichlorobenzoyl)-1,3-dimethylurea shows Rerank Score of -68,1456 and form one hydrogen bond between carbonyl moiety and Cys 87.

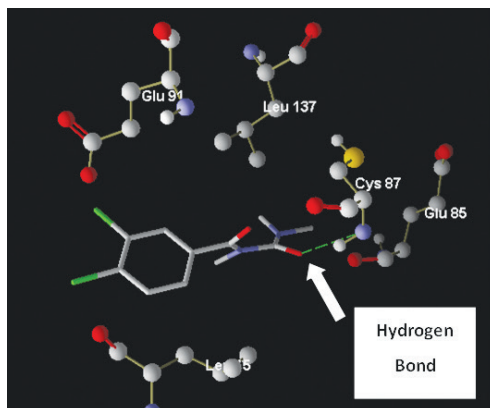


Figure 5. Docking of 1-(3,4-dichlorobenzoyl)-1,3-dimethylurea with Chk 1 shows intramolecular hydrogen bonds with Cys 87

CONCLUSION

A novel 1-benzoyl-1,3-dimethylurea has been designed and synthesized. The white needle crystal of 1-(3,4-dichlorobenzoyl)-1,3-dimethylurea was obtained with yields of 75% and melting point 110°C. The synthetic compound gave satisfactory analytical and spectroscopic data, which was in full accordance with their depicted structures. Docking simulation was performed to position the compound into the Chk1 active site to determine the probable binding model. 1-(3,4-dichlorobenzoyl)-1,3-dimethylurea shows Rerank Score of -68,1456 and form one hydrogen bond between carbonyl moiety and Cys 87.

REFERENCES

- *. Li, G., Hasvold, L.A., Tao, Z., Wang, G.T., et al. (2006). Synthesis and biological evaluation of 1-(2,4,5-trisubstitutedphenyl)-3-(5-cyanopyrazin-2-yl)ureas as potent Chk1 kinase inhibitors. *Bioorg Med Chem Lett.* 16: 2293–2299
- *. Oza, V., Ashwell, S., Brassil, P., Breed, J., et al. (2010). Discovery of a novel class of triazolones as Checkpoint Kinase inhibitors—Hit to lead exploration. *Bioorg Med Chem Lett.* 20: 5133–5138
- *. Tao, Z., Li, G., Tong, Y., Stewart, K., et al. (2007). Discovery of 4'-(1,4-dihydro-indeno[1,2-c]pyrazol-3-yl) benzonitriles and 4'-(1,4-dihydro-indeno[1,2-c]pyrazol-3-yl) pyridine-2'-carbonitriles as potent checkpoint kinase 1 (Chk1) inhibitors. *Bioorg Med Chem Lett.* 17: 5944–5951
- *. Zhao, L., Zhang, Y., Dai, C., Guzi, T., et al. (2010). Design, synthesis and SAR of thiopyridines as potent CHK1 inhibitors. *Bioorg Med Chem Lett.* 20: 7216–7221



EXPRESSION OF RECOMBINANT HUMAN GRANULOCYTE-COLONY STIMULATING FACTOR WITHIN PERIPLASMIC COMPARTMENT OF *Escherichia coli* USING PelB LEADER PEPTIDE

Dian Fitria Agustiyanti, Research Center for Biotechnology, Indonesian Institute of Sciences, Jl. Raya Bogor km 46, Cibinong, Bogor; Asrul Muhamad Fuad, Research Center for Biotechnology, Indonesian Institute of Sciences, Jl. Raya Bogor km 46, Cibinong, Bogor, asrul.m.fuad@gmail.com.

INTRODUCTION

G-CSF is a single polypeptide chain that consist of 174 amino acids, five cysteines that form two intra-molecular disulfide bridges (Cys36-Cys42 and Cys64-Cys74) and one free cysteine at residue 17 (Nagata et. al., 1986 and Lu et al, 1989). Overexpression of G-CSF generally results in partitioning of the expressed protein as insoluble material into inclusion bodies (IBs) (Vans et al., 2008). Protein in IBs form requires solubilization and renaturation steps to be biologically active. Disulfide bond formation in recombinant protein is important for their folding, stability, and function (Jalalirad, 2013). Incorrect disulfide bond formation can be solved by directing the recombinant proteins into the periplasm of *E. coli* (Yoon et al., 2010). Fusion of PelB leader peptide to mature protein sequences, had been well known to assist and facilitate the protein translocation into periplasmic compartment (Jin et al, 2011, Yoon et al, 2010).

However, some studies have also reported that the use of signal sequences such as pelB and ompA did not assist the secretion of mature proteins in *E. coli* (Sooryanarayana and Visweswadah, 1996; Chung et al, 1998). It appears that the secretion of heterologous proteins in *E. coli* is greatly influenced by the properties of the proteins themselves (Chung et al, 1998). In this study, a gene encoding hG-CSF was constructed by fusing with S-tag as well as poly-His tag at its N-terminal region in order to increase protein solubility. The S-tag sequence corresponds to the first 15 amino acid residues of the ribonuclease A. It is believed that the peptide with its abundance of charges

and polar residues could improve solubility of proteins that attached to (Raines et al, 2000).

MATERIAL AND METHODS

Bacterial strains, vectors and growth media
Two *E. coli* strains were used in the experiments, DH5 α for subcloning and plasmid amplification, and BL21(DE3) for protein expression. The pJ414 vector (DNA2.0) was linearized with XhoI and NcoI enzymes (Fermentas). The CSF3syn synthetic gene encoding hG-CSF has been previously constructed by PCR method (Fuad et al, 2013). Luria-Bertani broth (LB) and agar (LBA) media containing 50 μ g/ml of ampicillin (LBamp) were used for growing recombinant *E. coli* and protein p reduction.

Protein expression

Induction. A single colony of *E. coli* BL21(DE3) harboring pJ414-GCSF plasmid was inoculated into LB amp and incubated with 150 rpm at 37°C overnight (18-20 h). Five percent (v/v) of this overnight culture was inoculated into fresh LBamp broth and incubated with 150 rpm at 37°C until OD600 0.6-0.8 was reached. Protein expression was induced by addition of 0.4 mM IPTG (Isopropil- β -D-1-Thiogalactopyranoside). Cells were harvested 3 hours after induction by cold centrifugation at 4500 \times g for 15 min.
Autoinduction. Protein expression was also carried out using autoinduction media, which contains ZY (1% N-Z amine AS, 0.5% Yeast Extract), 1 M MgSO₄, 1000x metals mix (50 μ M Fe, 20 μ M Ca, 10 μ M Mn, 10 μ M Zn, 2 μ M Co, 2 μ M Cu, 2 μ M Ni, 2 μ M Mo, 2 μ M Se, 2 μ M H₃BO₃, 50x 5052 (0.5 % glycerol, 0.05% glucose, 0.2% α -lactose), 20x NPS (100 mM PO₄, 25 mM SO₄, 50 mM NH₄, 100 mM Na, 50 mM

K). One percent (v/v) of overnight culture was inoculated into fresh autoinduction media, then incubation was continued overnight at 22°C with agitation at 150 rpm.

Cell Fractionation

Osmotic shock. Cell pellets harvested from fermentation culture were resuspended in five percent of osmotic shock solution comprising 20 mM Tris-HCl buffer pH 8.0, supplemented with 2.5 mM EDTA and 20% sucrose. After a static incubation on ice for 30 min, the cells were harvested by centrifugation (15800 x g, 10 min) and the supernatants were immediately frozen at -20°C.

Freeze Thaw. Wet cell pellets were washed by phosphate buffer pH 7.4 (20 mM sodium phosphate and 0.5 M NaCl) and recovered by cold centrifugation at 4500 x g for 10 min. The cells were resuspended in lysis buffer (50 mM Tris HCl pH 7.4, 3 mM etilen diamin tetra acetate (EDTA), 1 mM phenil metil sulfonil florida (PMSF)) with ratio of 8 ml lysis buffer per gram pellet. The cell suspension was frozen at -20°C for 15 min, and then thawed at room temperature for 30 min, this freeze-thaw process was repeated 10 times. The crude cell lysate was recovered by cold centrifugation at 9600 x g for 10 min at 4°C.

RESULT AND DISCUSSION

With the aim of secretion of hG-CSF in *E. coli*, a PCR product containing S-tag and a gene encoding G-CSF (CSF3syn) was inserted into pJ414 at NcoI and XhoI sites, and fused in-frame with pelB signal sequence. The G-CSF fragment was cloned into linearized pJ414 previously digested with XhoI and NcoI. The recombinant pJ414-GCSF plasmid was transformed into *E. coli* BL21(DE3) strain. PCR amplification of transformed colonies using CSF-NcoF (forward) and CSF-XhoR (reverse) primers, showed a DNA band at 750 bp (Figure 1). The positive clone was named pJ414-GCSF. Eleven colonies out of 22 gave positive results. Confirmation of DNA integration into plasmid was conducted by restriction analysis using XhoI and NcoI (Figure 2). Correct

DNA integration into plasmid was verified by DNA sequencing using T7 primer.

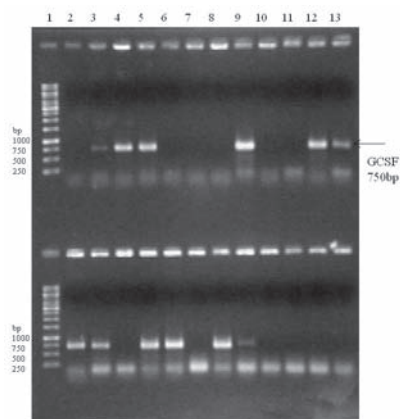


Figure 1. Electrophoregram of colonies PCR. Upper gel : 1. DNA ladder, 2. Negative control, 3. Positive control, 4–13 transformant colonies #1–#10. Lower gel : 1. DNA ladder, 2–13 transformant colonies #11–#22

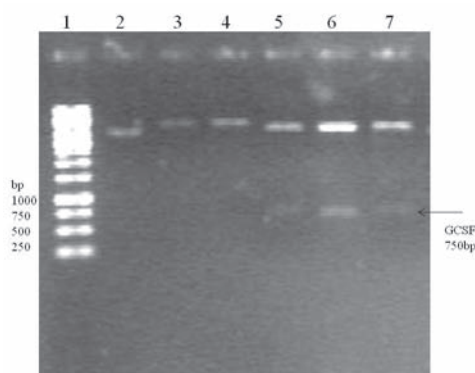


Fig 2. Electrophoregram of recombinant plasmids restriction. 1. DNA ladder, 2. pJ414-GCSF-01 uncut, 3. pJ414-GCSF-01 cut w/ XhoI, 4. pJ414-GCSF-01 cut w/ NcoI, 5. pJ414-GCSF 01 cut w/ XhoI+NcoI, 6. pJ414-GCSF-02 cut w/ XhoI+NcoI, 7. pJ414-GCSF-06 cut w/ XhoI+NcoI

G-CSF protein expression was conducted with induction and autoinduction methods. Culture samples were centrifuged at 4500xg and 4°C for 3 min. After removal of the supernatant, cell pellets were stored until further analysis. Preparation of cell extracts and determination of soluble and insoluble product fractions were performed by osmotic shock



and freeze thaw method. Sodium dodecyl sulfate polyacrylamide gel electrophoresis (SDS-PAGE) analysis of total cell protein and soluble and insoluble protein fractions was performed (Figure 4).

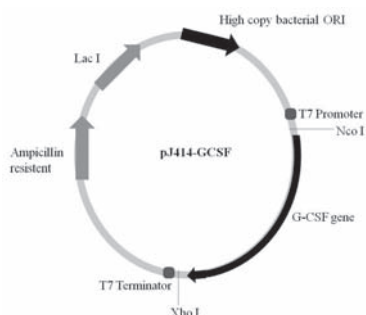


Figure 3. Plasmid construction

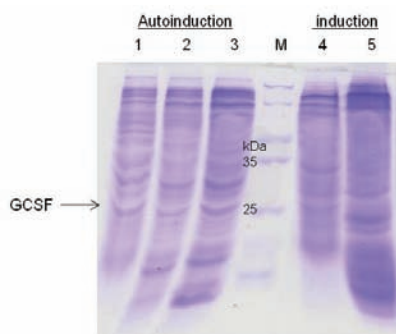


Figure 4. Protein extraction profiles from two different expression methods: autoinduction (lanes 1-3) and IPTG-induction (lanes 4-5). 1. Periplasmic fraction, 2. Cytoplasmic fraction (after periplasmic extraction), 3. Cytoplasmic fraction (without periplasmic extraction), M: protein marker, 4. Periplasmic fraction (induced w/ IPTG), 5. Cytoplasmic fraction (induced w/ IPTG).

Protein expression profiles analyzed by SDS-PAGE showed several protein bands, including protein bands in around 25 kDa, which is the suggested size of the recombinant G-CSF fusion protein. The band size corresponds to theoretical size of fusion protein of G-CSF with S-tag and 6xHis-tag. This periplasmic-derived

recombinant G-CSF has not been isolated or purified yet. However, western blot analysis that has been carried out confirmed this finding. Figure 5 shows the result of western blot analyses of both periplasmic and cytosolic protein extracts using either anti-His (Fig 5A) or anti-GCSF primary antibodies (Fig 5B). From Both western method, the periplasmic and cytosolic-derived recombinant G-CSF were detected. The periplasmic-derived G-CSF has a smaller molecular size compared to the cytosolic-derived one, which is accordance to the assumption that the PelB leader peptide was processed and cleaved. The cytoplasmic-derived G-CSF was higher than that from periplasmic space, indicating that the signal peptide was not processed and remained attached with target protein.

Protein expression using T7 lac promoter requires induction of T7-RNA polymerase followed by the release of lac repressor from its binding site at the T7 lac promoter. In BL21(DE3), protein expression is triggered by the release of lac repressor, which is generally induced by IPTG or auto-induced by the presence of lactose in the medium. The combination of expressing T7-RNA polymerase in the BL21(DE3) chromosome and the target gene from the T7 lac promoter in a multi-copy plasmid provides enough control that auto-induction of target protein production is feasible (Studier, 2005). Carbon substrate mixtures of glucose, glycerol, and lactose were used, where glucose as the preferred carbon substrate was utilized first, followed by glycerol then lactose which also acts as the inducer of lac operon-controlled protein production (Blommel et al, 2007). Auto-induction expression depends on bacteria mechanism to regulate the use of carbon and energy sources which present in the medium. If glucose is present, catabolite repression and inducer exclusion prevent the uptake of lactose by lactose permease, the product of lacY, thought to be the only means of lactose uptake in wild-type cells (Saiet et al, 1996 and Kimata et al, 1997)

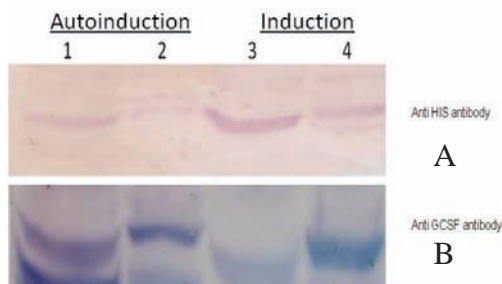


Figure 5. Western blot analyses of periplasmic and cytosolic-derived protein extracts using anti-His (A) and anti-GCSF (B) primary antibodies. 1. periplasmic extract from autoinduction, 2. G-CSF in cytoplasm, 3. G-CSF in periplasm, 4. G-CSF in cytoplasm

Generally, proteins found in the outer membrane or periplasmic spaces are synthesized in the cytoplasm as premature proteins. These premature proteins contain a short (15–30) specific amino acid sequence (called as signal sequence) that allows proteins to be exported outside the cytoplasm. A number of signal sequences have been used for efficient secretory production of recombinant proteins in *E. coli*, including PelB, OmpA, PhoA, endoxylanase-SP, and StII (Choi and Lee, 2004). In general, signal sequences are rich in hydrophobic amino acids, such as alanine, valine, and leucine, a feature essential for secretion of the proteins into the periplasm of *E. coli* (Pugsley 1993).

Some studies have shown that the use of pelB signal sequence did not result immature protein secretion. Expression of recombinant hG-CSF in *E. coli* periplasm has been reported using pYHM plasmid and expressed in BL21(DE3). There was no secretion of hG-CSF and no processing of signal peptide from the fusion protein have been detected (Chung et al., 1998). Although the same signal peptide (PelB) has been used to direct secretion of hG-CSF in *E. coli*, Chung et al (1998) has not succeed to express the recombinant hG-CSF into periplasm. However, the recombinant hG-CSF was highly expressed as IBs or insoluble pro-

tein within the cytosol of *E. coli*. The main difference of this study with our work is the addition of S-tag and 6xHis-tag sequences at the N-terminus of G-CSF. S-tag fusion is expected to convey the protein target more hydrophilic. Therefore, addition of S-tag as fusion partner in N-terminal of G-CSF would help the protein expression and translocation into periplasmic compartment of *E. coli*. S-tag peptide is composed of 7 charged polar, 3 uncharged polar and 5 non polar residues. This composition makes the S-tag peptide very soluble (Terpe, 2013). It provides an excessively soluble peptide with small structure and net charge in neutral pH. Fusion with S-tag as the carrier would not interfere the proper folding or function of a fused target protein (Kim and Raines, 1993).

CONCLUSION

Expression of G-CSF into periplasmic compartment of *E. coli* using pelB leader peptide was successfully performed. Addition of S-tag fusion protein in N-terminal of G-CSF as well as fusion with PelB were suggested to assists the delivery of the recombinant hG-CSF into periplasmic space of *E. coli*.

REFERENCES

- *. Bong Hyun Chung, Mi-Jin Sohn, Su Wan Oh, Ui Sun Park, Haryoung Poo, Beom Soo Kim, Mi Jin Yu, and Young Ik Lee, 1996, Overproduction of Human Granulocyte-Colony Stimulating Factor Fused to the PelB Signal Peptide in *Escherichia coli*, *Jurnal of Fermentation and Bioengineering*, vol 85, No. 44, 446 – 448.
- *. Blommel PG, Becker KJ, Duvnjak P, Fox BG (2007) Enhanced bacterial protein expression during auto-induction obtained by alteration of lac repressor dosage and medium composition. *Biotechnol Prog* 23:585–598.



- *. Chung B.H., Sohn M.J., Oh S.W., Park U.S., Poo H., Kim B.S., Yu M.J., and Lee J., (1998), Overexpression of human granulocyte-colony stimulating factor fused to the pelB signal peptide in *Escherichia coli*. *Journal of Fermentation Bioengineering*, 85, 443-446.
- *. Choi, J.H. and S. Y. Lee, 2004, Secretory and extracellular production of recombinant proteins using *Escherichia coli*, *Applied Microbiol Biotechnology* vol 64, 625-635.
- *. Fuad, AM, Yuliawati, Agustiyanti, DF. 2013. Design and Construction of CSF3 Synthetic Gene (CSF3syn) with Preference Codon of *Escherichia coli* using PCR Technique. *Prosiding Seminar Nasional Kimia XXII: "Kimia Dalam Industri dan Lingkungan"*. Yogyakarta, 21 November 2013.
- *. Jalalirad, Reza, (2013), Production of an antibody fragment (Fab) throughout *Escherichia coli* fed-batch fermentation process : Changes in titre, location and form of product, *Electronic Journal of Biotechnology*, vol 16, no 3.
- *. Kimata, K., H. Takahashi, T. Inada, P. Postma, H. Aiba, 1997, cAMP receptor protein-cAMP plays a crucial role in glucose-lactose diauxie by activating the major glucose transporter gene in *Escherichia coli*, *Proc. Natl. Acad. Sci. USA* 94, 12914-12919.
- *. Kim, J.S. and Raines, R.T. 1993. Ribonuclease S-peptide as a carrier in fusion proteins. *Protein Sciences* 2(3):348-356.
- *. Lu, S., Boone, T., Souza, L., Lai, P., 1989, Disulfide and secondary structure of recombinant human granulocyte colony-stimulating factor., *Arch. Biochem. Biophys.*, 1, 81-92.
- *. Saier, M.H.Jr., T.M. Ramseier, J. Reizer, 1996, Regulation of carbon utilization, in: F.C. Neidhardt (Ed.), *Escherichia coli and Salmonella typhimurium: Cellular and Molecular Biology*, 2nd ed. (Chapter 85), American Society for Microbiology, Washington DC.
- *. Nagata, S., Tsuchiya, M., Asano, S., Yamamoto, O., Hirata, Y., Kubota, N., Oheda, M., Nomura, H., dan Yamazaki, T., (1986) : The Chromosomal gene structure and two mRNA for human granulocyte colony stimulating factor. *European Molecular Biology Organization Journal*, 5 (3) : 575-581.
- *. Pugsley AP (1993) The complete general secretory pathway in gram-negative bacteria, *Microbiological Review* vol 57, 50-108.
- *. Raines, Ronald T., Mark McCormick, Thomas R. Van Oosbree, and Robert C. Mierendorf, (2000), The S-Tag Fusion System for Protein Purification. *Methods in Enzymology*, Vol. 326, 362-367
- *. Sooryanarayana, P.R. A. and Visweswadah, S. S. (1996), Hyperexpression of chicken riboflavin carrier protein: antibodies to the recombinant protein curtail pregnancy in rodents. *Protein Expression Purification*, 7, 147-154
- *. Studier, F. William, (2005), Protein production by auto-induction in high-density shaking cultures *Protein Expression and Purification*, 41, 207-234
- *. Terpe, K., (2003), Overview of tag protein fusions: from molecular and biochemical fundamentals to commercial systems, *Applied Microbiology and Biotechnology*, vol 60, 523-533.



- *. Vanz, Ana L.S., G. Renard, M.S. Palma, J.M. Chies, S.L. Dalmora, L.A. Basso, D.S. Santos, (2008), Human granulocyte colony stimulating factor (hG-CSF): cloning, overexpression, purification and characterization., *Microbial Cell Factories* vol 7, 13.
- *. Yoon, S.H.; Kim, S.K. and Kim, J.F. (2010). Secretory production of recombinant proteins in *Escherichia coli*. *Recent Patents on Biotechnology*, vol. 4, no. 1, p. 23-29.
- *. Jin, H., G.T. Cantin, S. Maki, L.C. Chew, S.M. Resnick, J. Ngai, (2011), Soluble periplasmic production of human granulocyte colony-stimulating factor (G-CSF) in *Pseudomonas fluorescens*. *Protein Expression Purification*, 78, pp. 69–77.



EVALUATION OF ANTIHYPERURICEMIC ACTIVITY FROM BULBS OF BAWANG TIWAI (*Eleutherine Palmifolia* (L.) MERR.) BY IN VITRO AND IN VIVO STUDIES

Dian Ratih Laksmiawati, Faculty of Pharmacy Pancasila University, Srengseng Sawah, Jagakarsa, Jakarta 12640, dianratih.ffup@gmail.com; **Rininta Firdaus**, Faculty of Pharmacy Pancasila University, Srengseng Sawah, Jagakarsa, Jakarta 12640, rininta.firdaus@gmail.com; **Yulinda**, Faculty of Pharmacy Pancasila University, Srengseng Sawah, Jagakarsa, Jakarta 12640, lindsayulinda93@yahoo.com; **Mediana Astika**, Faculty of Pharmacy Pancasila University, Srengseng Sawah, Jagakarsa, Jakarta 12640, mediana.astika@yahoo.com.

INTRODUCTION

Bawang tiwai (*Eleutherine palmifolia* (L.) Merr.) is a bulbous plant that numerous grows in Kalimantan. People in Kalimantan consume use the bulbs as an alternative medicine to treat constipation, also as diuretic and vomiting agent. The leaves are also consumed to stimulate breast-milk production from a breastfeeding mother. Bawang tiwai shows differences from red onion (*Allium cepa* L.) and garlic (*Allium sativum* L.). It has less odor and distinct flavour compared to the other bulbous plants. Moreover, it shows a stronger red pigment than the red onion.

Bawang tiwai contains flavonoid, alkaloid, glycoside, polyphenol, tannin, and steroid. It also contains eleutherin, eleutherol, and isoeleutherin which have been reported to show antifungal activity and improve the coronary bloodstream. At least 25 different flavonols have been characterized from onion cultivars. Quercetin derivatives are the most important showing a strong inhibition to activity of xanthine-oxidase (IC₅₀ = 7.23 μM)(Chang et al. 1993), IC₅₀ to bovine milk xanthin oxidase = 0,12 ppm (Hanaee et al. 2004).

Xanthine oxidase is an enzyme that catalyzes the oxydation of xanthine to uric acid in human body. The excess of uric acid (hyperuricemia) gives rise to arthritis gout, an inflammatory joints caused by deposition of the crystals. Although its risk of mortality is relatively low, the disease affects the productivity of the patients. Allopurinol, a drug used primarily to treat hyperuricemia and gout, inhibits the activity of xanthin oxidase to produce

uric acid. Until now, Indonesia still imports this substance from foreign countries. The dependency of imported drugs tends to rise the medication price in Indonesia. We performed this study to observe our local resources with potential anti-hyperuricemia activity. Thus, it would become the alternatives of allopurinol to treat the disease.

This study consisted of in vitro and in vivo studies. We performed the in vitro assay to investigate the inhibition of xanthine oxidase acitivity from ethanol extracts of bawang tiwai. Then, we performed the in vivo assay to study the antihyperuricemic effect on mice.

MATERIALS AND METHODS

Materials

Fresh bulbs of bawang tiwai were obtained directly from Kalimantan. The bulbs were determined by Herbarium Bogoriense-LIPI Bogor as *Eleutherine palmifolia* (L) Merr. Chemical solvent used to extract the bulbs was ethanol 70%. Allopurinol tablets 100 mg were used as control positive. Other chemical substances were xanthine oxidase (SIGMA 4376), xanthine (SIGMA 4002), and phosphate buffer (pH 7.5).

For the in vivo assay, thirty six of two-month old male ddY mice with body weight 20-30 gram were given daily standard-lab diet. We used fermipan yeast 15 mg/kg body weight to induce the level of uric acid in the blood serum, and potassium oxonate (SIGMA 156124), to inhibit the uricase in mice. The levels of uric acid were measured using spectrophotometer with dichlorohydroxybenzen sulfonate (DHBS) (BIOLABO) as reagent.



Methods

Preparation of Extract

Four hundred grams of dried bulbs of *Eleutherina palmifolia* (L.) Merr. were extracted with ethanol 70% by maceration process for 24 hours. The suspension was filtrated, and the precipitate was re-macerated twice subsequently. The resultant extract was concentrated using rotary evaporator at 50-60°C to obtain the dense ethanol-extract of *E. palmifolia*. (Extract of Bawang Tiwai /EBT)

In Vitro Assay of Xanthine Oxidase Inhibitory Activity

The in vitro assay to investigate the inhibitory activity of EBT was done by indirect methods measuring absorbance of remain xanthine at 265 nm. A half millilitre of extract solution with concentrations of 1, 5, 10, 20, 50, and 100 ppm were added with 1.45 mL of phosphate buffer 50 mM, pH 7.5. Then, 1 mL of 0.2 mM xanthine (Sigma X4002) in phosphate buffer was added to the previous mixture. The tubes were incubated at 25°C for 15 minutes.

incubation, 0.05 mL of 0.3 U/mL xanthine oxidase (Sigma X4376) was added to the tube and incubated for 45 minutes. The reaction was stopped by adding 0.5 mL HCl 1N. The absorbance of xanthine residue was measured using spectrophotometer at 265 nm. Allopurinol, as control positive, was measured with the same procedure. The standard curve was made using the absorbance of xanthine with known concentrations. The absorbance of the mixture of substrate and enzyme was used as blank, and the absorbance of substrate was used as negative control. The percentages of inhibitions were calculated using this equation:

$$\% \text{ inhibition} = \frac{(\text{Activity of xanthine oxidase without extract} - \text{activity of xanthin oksidase with extract})}{\text{Activity of xanthine oxidase without extract}} \times 100$$

In Vivo Assay of Antihyperuricemic Activity

Thirty six of male ddY mice were divided into six groups: a normal, negative control, positive control (allopurinol), experimental groups given low dose (84 mg/kg) of ethanol extracts

from bulbs of bawang tiwai (EBTL), experimental groups given middle dose (126 mg/kg) of the extract (EBTM), and experimental groups given high dose (186 mg/kg) of the extract (EBTH). Normal group was given standard lab diet, while other five groups were each given high-purine diet from 50% yeast, 15 mg/kg body weight for 7 days. Then one hour after feeding the yeast, mice from EBTL, EBTM, and EBTH were given the extract with referred dose. On day 7, one hour after feeding the yeast and extracts, the mice were given potassium oxonate 250 mg/kg body weight intraperitoneally. Three hours after the induction, all mice (except normal) were anesthetized with ether and the blood was collected intracardially. Plasma was separated from blood cells by centrifugation at 3000 rpm for 10 minutes. Uric acid levels were measured by DCHBS (dichloro-hydroxybenzene sulfonate) method using Biolabo kit and spectrophotometer (RD-60 Semi Auto Biochemistry) at 520 nm.

RESULTS

The extract yield obtained from the maseration process with ethanol 70% was 17.2%. The result of the assay of the xanthine oxidase inhibitory activity was presented in Table 1. The ethanol extract of bawang tiwai at 600 ppm showed 73.52% inhibition to the enzyme's activity. While allopurinol showed 73.74% inhibition only at 2 ppm concentration.

The result of the in vivo assay of antihyperuricemic activity was shown Figure 1. EBTM gave a significant lower uric acid level compared to negative control. Even mice from EBTH had similar uric acid level (2.52 mg/dL) to the normal group (2.16 mg/dL).

tubes were incubated at 25°C for 15 minutes.



Sample	Concentration (ppm)	Mean of percent inhibition (n=3)	±SD
Ethanol Extract of Bawang Tiwai	1	13.24	0
	5	42.44	0.52
	10	30.88	2.08
	20	37.13	1.56
	50	63.97	6.24
	100	73.52	1.04
Allopurinol	0.1	34.67	5.85
	0.25	41.74	6.54
	0.5	44.47	6.63
	1	67.16	3.86
	2	73.74	10.79
	5	85.78	1.48

Table 4. Percent inhibition of xanthine oxidase from the ethanol extract of bawang tiwai and allopurinol.

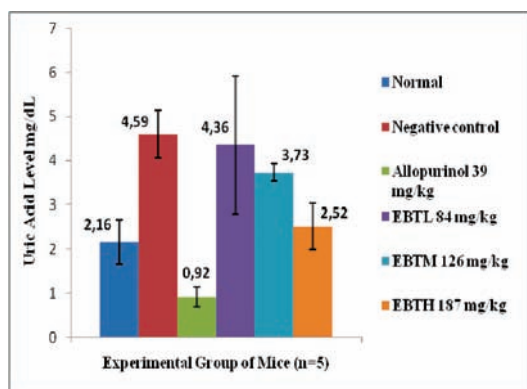


Figure 1. Effect of the ethanol extracts of bawang tiwai on uric acid level in mice serum (mean ± SD, n = 6).

DISCUSSION

We studied the ethanol extract of bawang tiwai (*Eleutherine palmifolia* (L.) Merr) in order to screen potential plants which are able to reduce the uric acid level; while each year gout and hyperuricemia increased rapidly.

In previous report, flavonoid showed inhibition to xanthine oxidase activity. Cos et al, in his in vitro study, approved that flavonoid including isorhamnetin, baicalein, kaempferol,

and morin had inhibition to the enzyme's activity with IC50 2.51, 2.79, 1.06, dan 10.1 μM respectively (Cos et al. 1998). While Mo et al performed in vivo assays of flavonoid including quercetin, morin, myricetin, kaempferol and puerarin which significantly reduced the uric acid level in mice in the amount of 26.94%, 28.99 %, 30.59%, 35.39%, 31.28%, respectively (Mo et al. 2007).

Bulbous plants are cultivars that contain flavonoid especially kaempferol and quercetin. We suspected bawang tiwai to possess these flavonoids as the other bulbous plants. Still, we could not find reports about flavonoid in bawang tiwai.

The amount of quercetin in bawang tiwai still have not been reported, thus we suggest a further research investigating the qualitative and quantitative study of flavonoids contained in bawang tiwai.

Different from the in vitro test, the in vivo assay gave an expected result. Least significant different, a statistical test, showed that EBTM (126 mg/kg body weight) had a significant lower uric acid level than negative control. EBTH also had lower uric acid, even the uric acid levels were similar to normal. The reduction effectiveness of EBTL (84 mg/kg body weight), EBTM (126 mg/kg body weight), and EBTH (187 mg/kg body weight) were 18,74 %, 45,09 %, 79,96 % respectively.

SUMMARY

In summary, the ethanol extracts of bawang tiwai (*Eleutherine palmifolia* (L.) Merr) were potential to reduce uric acid level at 186 mg/kg body weight, but possibly without inhibition of xanthine oxidase.

ACKNOWLEDGEMENT

The authors would like to thank Faculty of Pharmacy, Pancasila University to support this research through incentive funding in 2013.



REFERENCES

1. Chang, W. S., Y. J. Lee, F. J. Lu, and H. C. Chiang. (1993). Inhibitory Effects of Flavonoids on Xanthine Oxidase. *Anticancer Research* 13 (6 A): 2165–70.
2. Cos, Paul, Li Ying, Mario Calomme, Jia P. Hu, Kanyanga Cimanga, Bart Van Poel, Luc Pieters, Arnold J. Vlietinck, and Dirk Vanden Berghe. (1998). Structure-Activity Relationship and Classification of Flavonoids as Inhibitors of Xanthine Oxidase and Superoxide Scavengers. *Journal of Natural Products* 61 (1): 71–76.
3. Hanaee, Jalal, Mohammad-reza Rashidi, Abbas Delazar, and Saeed Piroozpanah. (2004). Onion, a Potent Inhibitor of Xanthine Oxidase, no. May: 243–47.
4. Mo, Shi-Fu, Feng Zhou, Yao-Zhong Lv, Qing-Hua Hu, Dong-Mei Zhang, and Ling-Dong Kong. (2007). Hypouricemic Action of Selected Flavonoids in Mice: Structure-Activity Relationships. *Biological & Pharmaceutical Bulletin* 30 (8): 1551–56.



**ANTIOXIDANT ACTIVITY OF 96% ETHANOL EXTRACT OF
COMBINATION OF STRAWBERRY FRUIT
(*Fragaria x ananassa* Duch.)
AND STARFRUIT (*Averrhoa carambola* L.)
USING ABTS FREE RADICAL SCAVENGING METHOD**

Diana Serlahwaty, Pancasila University, Srengseng Sawah Jagakarsa South Jakarta ,dianas_ffup@yahoo.co.id, 081808904001; **Indira Natalia Timang**, Pancasila University, Srengseng Sawah Jagakarsa South Jakarta, indirana-talia.timang@gmail.com, +6289630996686;

ABSTRACT

Strawberry and star fruit are fruit that have an antioxidant activity. Strawberry contains flavonoids, fenolic acid, and tannins while starfruit contains vitamin C, alkaloid, and tannins. This study aimed to determine the antioxidant activity of the extract using ABTS free radical Scavenging method (2,2'-azinobis[3-etilbenziazolin-6-sulfonat]) using visible light spectrophotometer. The tested samples were single and combination extracts of strawberry and star fruit using the ratio : 1: 1; 1: 3; 3: 1 in which vitamin C serves as a positive control. Strawberry and star fruit were extracted by maceration using 96% ethanol as a solvent. Phytochemical screening was carried out on both fruits and the extracts. The results of phytochemical screening showed the presence of flavonoids compound. Antioxidant activity of the strawberry extract is stronger than the starfruit extract in which IC50 value of the strawberry and starfruit extract are 20.76 and 131.99 ppm, respectively. In contrast, both activities are lower than vitamin C with IC50 value of 1.22 ppm, whereas the IC50 value of the combination extract with ratio of 1:1; 1:3; and 3:1 are 48.83; 79.88; 44.15 ppm, respectively. The highest antioxidant activity was found in the combination extract with ratio of 3:1 with IC50 value of 44.15 ppm. The analysis of statistical tests using one way ANOVA showed significant differences in antioxidant activity of combination extracts in all ratio.

Keywords: antioxidant, ABTS, strawberry, starfruit

INTRODUCTION

The growth in industrial sector causes pollution enhancement. That can change life style including food consumption alteration. According to National Social Economic Survey in 2012, the percentage of Indonesian population's expense for instant food and drink products was 24,90% which was the highest. Consumption of instant food and drink products continuously, such as instant noodle and canned products.

Pollution enhancement and life style alteration induce free radical production in the body. It induces oxidative stress that make cell damage and perceive as harm for the health (atherosclerosis, coronary heart, stroke, cancer)

Antioxidant is a compound to reduce free

radical. Fruits are the examples of antioxidant sources, especially strawberry and starfruit

In this research, antioxidant activity of combination of 96% ethanol extract of starfruit and strawberry was tested with free radical scavenging method ABTS. Sample absorption was measured by a visible light spectrophotometer and vitamin C serves as positive control .

INSTRUMENTS

The instruments in this research area UV-VIS spectrophotometer Shimadzu UV-1800, mixers, an analytic balance , glass beakers, Erlenmeyer, a vacuum rotavapor, a stir bar, filter papers, waterbath, vaporizer cups, dark bottles, Pasteur pipettes, aluminium foil, micropipettes, measuring glasses, and Moisturemeter Karl Fischer.

MATERIALS

1. Fresh strawberry and starfruit.
2. Chemical reagents: ABTS, 96% ethanol, aquadest, Magnesium plates, concentrated HCl, amilalcohol, ethanol pro analysis, and vitamin C.

RESEARCH PRINCIPAL

Strawberry and starfruit plants were determination, fruit drying exsiccate, extract water content, and phytochemical screening for both was obtained fresh fruit and extracts. Thick extract was using 96% ethanol by color changes. Macerate from each extract was concentrated until thick extract. Thick extract was combined = 1:0, 0:1, 1:1, 1:3, and 3:1. Then, all combination were tested by ABTS free radical method with visible light spectrophotometer at 412 nm

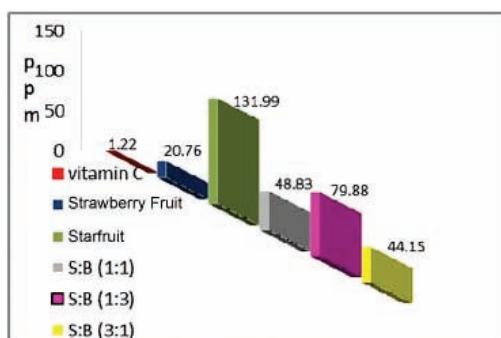


Figure 1. Result of antioxidant activity test (IC50) with ABTS method

RESULT AND DISCUSSION

According to antioxidant activity assay with ABTS method, we knew that strawberry thick extract had 20,76 ppm antioxidant activity. This result showed that IC50 value of strawberry was less than 50 ppm and it categorized as very strong antioxidant because strawberry had high vitamin C (about 58,8 mg in 100 gram fresh fruit) and flavonoid (4). Thick extract starfruit had 131,99 ppm antioxidant activity. It showed that IC50 value of which was about 100-150 ppm and categorized as medium antioxidant. It due to the strongest antioxidant

was flavonoid, eventhough starfruit content of had high vitamin C, but contributed in small part as antioxidant (5).

This result was compared to combination extracts. The extract combination (1:1) IC50 value of 48,83 ppm and was categorized as very strong antioxidant because strawberry was categorized as very strong antioxidant and could improve antioxidant activity of starfruit which was categorized as medium antioxidant.

The extract combination 1:3 showed 79,88 ppm and was categorized as strong antioxidant because IC50 in the range of value was 50-100 ppm. It due to amount of starfruit was more that of strawberry. Hence starfruit antioxidant activity shares more effect. The extract combination 3:1 test got result 44,15 ppm. This result was as not far as 1:1 composition which had very strong antioxidant activity. We assumed it because amount of strawberry was more than amount of starfruit. Hence, the antioxidant activity could raise. IC50 value of the combination in the ratio of was lower than that of 3:1 composition. It because the amount of strawberry used.

CONCLUSION

Antioxidant activity of strawberry extract was stronger than starfruit extract with IC50 value of 20,76 ppm and 131,99 ppm, but was lower than vitamin C as positive control with IC50 of 1,22 ppm. Antioxidant activity of combination extract with composition of strawberry and starfruit in the ratio 1:1, 1:3, and 3:1 had IC50 for each composition were 48,83 ppm, 79,88 ppm, 44,15 ppm and showed that the highest antioxidant activity was 1:3 composition.

REFERENCES

1. Francesca Giampieri, et al. The strawberry: composition, nutritional quality, and impact of human health. Nutrition. 2012;28(1):9-19.



2. Geeta Arya, Sunita Mishra. Effects of junk food and beverages on adolescent's health-a review article. IOSR-NHJS.2013;1(6):26-32.
3. RE Roberta, et al. Antioxidant Activity Applying An Improved ABTS Radical Cation Decolorization Assay. Journal of Biology and Medicine. London: Vol 26;1999. p.1231-7.
4. Tim Redaksi Pusat Data dan Sistem Informasi Pertanian. Pola konsumsi masyarakat. Buletin konsumsi pangan. 2013;4(2):5-6.
5. Winarsi Hery. Antioksidan Alami dan Rangkal Bebas. Yogyakarta: Penerbit Kanisius; 2007, h.77-82.



ENHANCEMENT OF SOLUBILITY AND DISSOLUTION ATORVASTATIN BY MICROCRYSTALLIZATION METHOD

Dolih Gozali, Pharmacy Faculty Universitas Padjadjaran Jl. Raya Bandung-Sumedang Km.21 Jatinangor, Sumedang 45363 West Java Indonesia Telp/Fax: +62 22 7796200. Website : <http://farmasi.unpad.ac.id>, dolihg@yahoo.com;
Yoga Windu Wardhana, Pharmacy Faculty Universitas Padjadjaran Jl. Raya Bandung-Sumedang Km.21 Jatinangor, Sumedang 45363 West Java Indonesia Telp/Fax: +62 22 7796200. Website : <http://farmasi.unpad.ac.id>;
Ronny Tandel, Pharmacy Faculty Universitas Padjadjaran Jl. Raya Bandung-Sumedang Km.21 Jatinangor, Sumedang 45363 West Java Indonesia Telp/Fax: +62 22 7796200. Website : <http://farmasi.unpad.ac.id>

INTRODUCTION

Low drug solubility in water is an important factor affecting the bioavailability of the drug. The solubility of drugs is one factor that determines the speed of absorption of the drug (Varshosaz J., et al, 2008). Atorvastatin including a group of drugs called statins are used to treat dyslipidemia and prevent coronary heart disease. Atorvastatin has a bioavailability of 12% (Parke-Davis, 1997). Small bioavailability can be used as an indication that the drug has a low dissolution rate. A drug that has a low dissolution rate can lead to a decrease in absorption power. Increased bioavailability of drugs that have low solubility, is one of the challenges in drug formulation development aspects. One way to improve the dissolution rate is to reduce the particle size, which will increase the total surface area, so it will easily dissolve drugs (Varshosaz J., et al, 2008).

One technique that can be used to reduce the particle size is mikrokristalisasi (Varshosaz J., et al, 2008). Mikrokristalisasi is a suitable method to produce micron-sized particles. The resulting particle size more uniform than the method of grinding (milling) (Soewandhi, 2006). Micronization using milling (milling) is very inefficient because it requires great energy. On the other hand, disorder in the crystal lattice can cause instability of physics and chemistry, because the irregularity in shape will result in products that are thermodynamically unstable. Changes in surface energy may also affect processing such as powder flow properties. Micronization powder with high surface ener-

gy indicates poor flow properties (Varshosaz J., et al, 2008).

In this study, the technique mikrokristalisasi performed using a ultra-high speed homogenizer (13,500 rpm and 24000 rpm) to obtain small crystals. After stabilization of the particles was carried out using a polymer material. Generally stabilization of the particles is not easy because of the tendency of the particles to grow, to see the ability of the polymer material as the stabilizing agent is then conducted two treatments with the addition of stabilizing agents and without the addition of stabilizing agent.

Crystals will be characterized using X-ray Diffraction (XRD), Infrared Spectroscopy and Scanning Electron Microscopy (SEM) to evaluate the crystal habit and size of the particles formed. Then the characterization results compared with before treatment. The dissolution test is then performed using UV-Vis spectrophotometer with a wavelength of 242 nm and a visible absorbance maximum of each treatment.

METHODOLOGY

The tools used in this study is the Ultra-homogenizer (IKA T25, Germany), freeze dryer (Vacuubrand, Germany), UV-Vis spectrophotometer (SPECORD 200, UK), means of X-Ray Diffractometer (Philips PW 1710 Diffractometer, Japan), Scanning Electron Microscopy (JEOL JSM-5310LV), analytical balance (Acculab VI, UK), stopwatch, oven glassware and tools commonly used in the laboratory.



The materials used in this study consisted of atorvastatin (DSM Anti-Infectives India), carboxymethylcellulose (Daichi, Japan), distilled water, methanol (Brataco), ethanol (Brataco), sodium hidoksida (Merck), potassium dihydrogen phosphate (Merck), sodium acetate (Merck), glacial acetic acid (Merck), klorida acid (Merck), and potassium chloride (Merck).

Examination of Raw Materials

The examination was conducted to identify atorvastatin. Inspection procedures in accordance with the fourth edition of the Pharmacopoeia Indonesia and other literature or by attaching a certificate of analysis of these substances. Examination includes: defining a, solubility, and chemical identification of the organoleptic and qualitative.

Preparation of microcrystals

Preparation of microcrystals with a stabilizing agent atorvastatin 5% using a ultra-homogenizer and freeze dryer

Make a solution of atorvastatin with atorvastatin by dissolving 0.5 grams in 30ml of methanol. In a separate container made the development of CMC CMC by dissolving 0.05 g in 70 ml of distilled water. Mixed with CMC rapidly to a solution of atorvastatin were accompanied stirring using ultra-homogenizer at a certain speed (13500 rpm and 24000 rpm) for \pm 15 minutes. After it was put into ice bath with stirring tool ultra-homogenizer at a speed of 3200 rpm for \pm 15 minutes, microcrystals will form spontaneously. Furthermore, the solution was put into an oven at 50 ° C for 3 hours to draw an organic solvent to obtain a solution of atorvastatin in water. Transfer the solution into a special container for frozen freeze dry. Once frozen, the samples are ready to freeze dry.

Preparation of microcrystals atorvastatin without stabilizing agents using a ultra-homogenizer and freeze dryer

Make a solution of atorvastatin with atorvastatin by dissolving 0.5 grams in 30ml of metha-

anol. Then added to 70 mL of distilled water to a solution of atorvastatin were accompanied stirring using a ultra-homogenizer at a certain speed (13500 rpm and 24000 rpm) for \pm 15 minutes. After it was put into ice bath with stirring tool ultra-homogenizer at a speed of 3200 rpm for \pm 15 minutes, microcrystals will form spontaneously. Furthermore, the solution was put into an oven at 50 ° C for 3 hours to draw an organic solvent to obtain a solution of atorvastatin in water. Transfer the solution into a special container for frozen freeze dry. Once frozen, the samples are ready to freeze dry.

Preparation of calibration curve of atorvastatin

Weighed 20 mg of atorvastatin standard, then diluted with phosphate buffer pH 6.8 in a 100 mL volumetric flask. Whisk until dissolved. Further dilution to obtain concentrations of 8, 10, 12, 15, and 20 ppm. Uptake of each solution was measured using UV-Vis spectrophotometer at a wavelength of 240nm. Then made a calibration curve in the equation $y = ax + b$.

Characterization of microcrystals crystal morphology

To microscopic examination by means of scanning electron microscopy (SEM) (JSM-5310LV EOL) to see the shape and size of the particles. A number of samples (standards and microcrystals atorvastatin) is placed on the holder which has been coated conductors. Subsequently incorporated into the vacuum device and wait until the coating is complete. Then examined the morphology of crystals.

X-ray diffraction

The samples were characterized using X-ray diffractometer (Philips PW 1710 Diffractometer, Japan). At first, the sample is placed in a holder made of aluminum. Then flattened parallel to the surface of the sample holder surface. Holder containing the sample is inserted in the goniometer then measured by means of



X-ray diffractometer.

Infrared Spectroscopy

Analysis of crystals was also performed using infrared spectroscopy. For infrared spectroscopy, 1 mg of sample was mixed with 200 mg KBr, and then made pellets. Measurement using infrared spectroscopy, and performed with the wave number range 4000 - 400cm⁻¹.

Solubility test

Solubility test conducted in accordance with the method of Higuchi and Connor. Solubility testing is done by adding an excess amount of a substance into the medium ethanol until the solution is saturated. Then do the shuffle using a shaker for 48 hours at a temperature of 25 ° C and constant speed. Further filtering performed using filter paper. The filtrate was measured using a UV-Vis spectrophotometer (SPECORD 200, UK). Each sample triplo.

Dissolution Test

Weighed amount of standard \pm 20 mg atorvastatin, \pm 20 mg atorvastatin with ultra-homogenizer processes and \pm 20 mg of atorvastatin containing 5% CMC with ultra-homogenizer processes. Then put in 900 mL dissolution medium HCl buffer pH 1.2, acetate buffer pH 4.5, and phosphate buffer pH 6.8 and dissolution testing using dissolution apparatus type II at a speed of 50 rpm and a temperature of \pm 37 ° C. The Decision samples were taken at 5, 10, 15, 30, and 45 minutes as much as 5 ml. Every time sampling, the addition of 5 ml of dissolution medium to maintain the volume remains. The absorbance of samples was measured using a UV-Vis spectrophotometer (SPECORD 200, UK) at a wavelength of 240 nm.

RESULTS

Preparation of microcrystals

Making microcrystals aims to improve the dissolution rate of atorvastatin which is based on the BCS (Biopharmaceutical Classification System) has a low solubility. One way to increase the solubility of the particle size shrink.

This method was chosen because it has several advantages, one of which is the active substance contained greater than with other methods, such as the method of solid dispersions using excipients that are usually larger than the active substance (Varshosaz J., et al, 2008). Therefore, by increasing the solubility of atorvastatin, is expected to increase the bioavailability of atorvastatin. In this study, a method for particle size reduction using a ultra-homogenizer.

In the ultra-homogenizer tool, mikrokristalisasi made using methanol solvent with rotary speed optimization ultra-homogenizer. Optimization is done on a rotational speed of 13,500 rpm and 24,000 rpm for 15 min \pm , after it was put into the glass beaker ice bath with stirring at a speed of 3200 rpm. After optimization of rotational speed, turns microcrystals produced at speeds of 24,000 rpm has a greater solubility than the speed of 13,500 rpm. Then do the process of withdrawal of an organic solvent, ie methanol were carried out using an oven at 50 ° C for 3 h. Temperature used in the oven is under the boiling point of methanol is 63.5 ° C.

The addition of the stabilizing agent CMC (carboxymethylcellulose) aims to inhibit the rate of crystal growth and crystal form that can later affect the solubility. CMC addition of 5% of the amount of solution is expected to produce crystals with micro size and have a stable form (uniformity of crystal form).

The results from the manufacture of microcrystals are as follows:

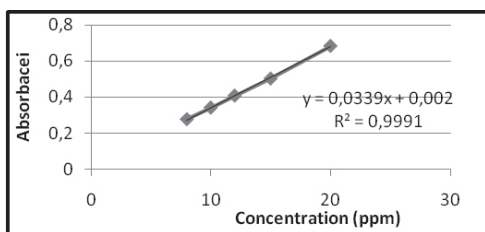
Table 1: Results of the manufacture of ultra-crystals using a homogenizer

Type	Initial Mass (mg)	Final Mass (mg)	Yield percentrage (%)
F1	510	452	88,62745098
F2	508	456	89,76377953
F3	505	440	87,12871287
F4	502	443	88,24701195



Calibration Curve

Here is a calibration curve was made (Figure 1) with 0.9991 linearity and line equation $y = 0.002 + 0,0339x$



Characterization of microcrystals Microcrystal Characterization

The morphology of microcrystals

Microcrystals on morphological observation using Scanning Electron Microscopy (SEM) is to look at the shape of the resulting microcrystals and crystals of raw itself. In these observations it appears that the form of raw blocks and atorvastatin have not distributed perfectly. While the microcrystals formed and distributed beam has the shape better. It is also seen that there is a stabilizing agent that coats the lining microcrystals formed.

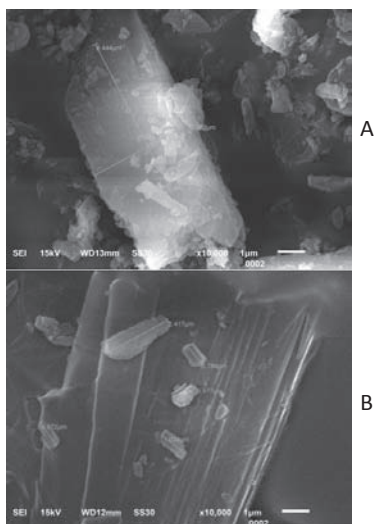


Figure 2. Micrograph of SEM a) Pure atorvastatin b) Atorvastatin microcrystal with stabilizing agent

X-Ray Diffraction (XRD)

In testing using XRD, it appears that the characteristics of a particular polymorph of the peaks seen in the diffractogram (Figure 3). In raw diffractogram atorvastatin and equally atorvastatin microcrystals showed the same peaks. This shows that there is a change in polymorph of microcrystals formed.

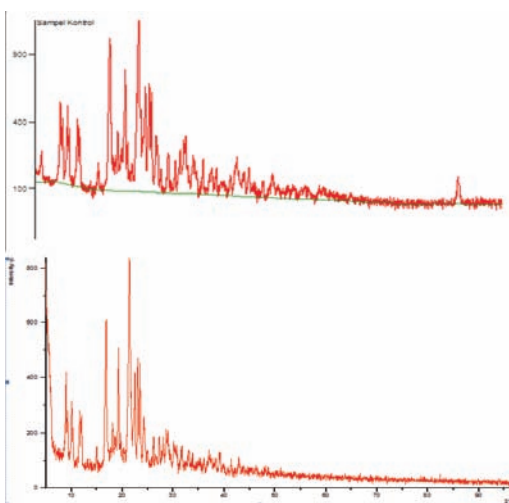


Figure 3. Diffractogram of a) Pure atorvastatin b) Atorvastatin microcrystal with stabilizing agent 5%

The difference of each diffractogram is high (intensity) of the peak generated. This shows that there has been a change in the crystal habit. May also indicate a change in the size of the crystals formed. According to the Bragg equation, if the X-ray beam was dropped on the sample crystal, then the crystal field will refract X-rays which have a wavelength equal to the distance between the lattice in the crystal. Refracted rays will be captured by the detector is then translated as the diffraction peaks. The decrease in the intensity of this sample is the result of a reduction in the field of crystal lattice or atorvastatin after experiencing micronization. Each peak that appears in the XRD pattern representing a lattice or fields that have specific orientation in three-dimensional axis, so that more and more areas of the crystal lattice or contained in a sample, the more powerful the resulting intensitas.

Infrared Spectroscopy

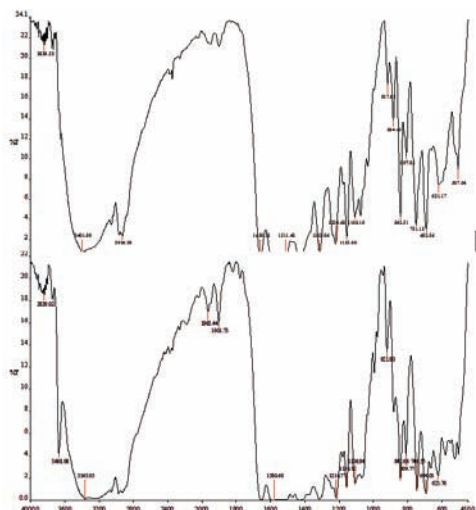


Figure 4. Infrared spectrum of (a) pure Atorvastatin (b) microcrystals with a stabilizing agent atorvastatin 5%

In infrared spectroscopy results (Figure 4), visible infrared spectrum of the substance and the microcrystals formed atorvastatin showed identical characteristics to the peak of 3403 cm^{-1} (NH stretching), 3059 cm^{-1} (C-HO stretching alcohol group), 2966, 15 cm^{-1} (CH-stretching), 1656 cm^{-1} (C = C bending), 1564 cm^{-1} (C = O stretching amide groups) 1313.56 cm^{-1} (CN -stretching), 1104 cm^{-1} (OH bending), 751 cm^{-1} and 695.08 cm^{-1} (CF stretching). This indicates the absence of a functional group changes microcrystals made and the lack of interaction between the stabilizing agent with microcrystals. The intensity of the microcrystals formed visible atorvastatin decreased compared with standard atorvastatin. This shows that there has been a change in the crystal habit and particle size reduction occurs in microcrystals (Varshosaz J., et al, 2008).

Solubility test

Testing the solubility of atorvastatin and microcrystals conducted by Higuchi and Connor. Testing is done by adding the number of

samples in ethanol and stirring until saturated with a shaker for 48 hours. And obtained the results as in Table 2.

Table 2: Results of solubility test in ethanol

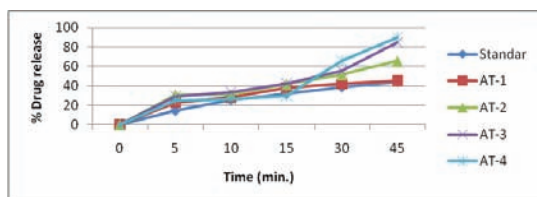
Type	Solubility in Ethanol (mg/ml)
Unprocessed drug	0,493
AT-1	0,513
AT-2	0,53
AT-3	0,591
AT-4	0,612

From Table 2 it can be concluded that the F4 has the greatest solubility. It also shows that the solubility of the microcrystals are formed due to the increased cross-sectional area of the enlarged substances.

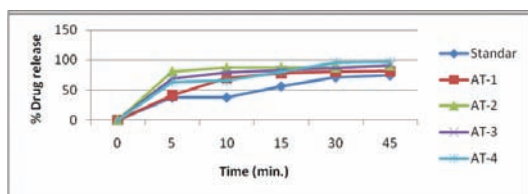
Dissolution Test comparative

In this research, dissolution testing compared atorvastatin crystalline powder. Basically dissolution rate was measured from the amount of active substance dissolved in a liquid medium tertbutyl in a known volume and a relatively constant temperature. The purpose of microcrystalline powder dissolution profile testing is to determine how much powder crystals dissolved at a given time.

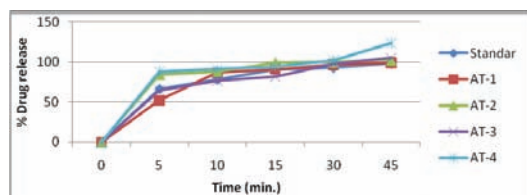
Dissolution test conducted in the medium of 900 mL HCl buffer pH 1.2, Acetate buffer pH 4.5 and phosphate buffer pH 6.8 and stirring with type II dissolution apparatus at 50 rpm at a temperature of 37 ° C \pm . Sampling interval was performed at 5, 10, 15, 30 and 45 minutes by taking a sample of 5mL and with the addition of medium with the same volume so that the volume of dissolution medium remains.



A



B



C

Figure 5: Dissolution profile of each treatment on (a) Media HCl pH 1.2 (b) Media Acetate buffer pH 4.5 (c) Media phosphate buffer pH 6.8

The results of dissolution testing in Figure 5 shows that the microcrystals are generated from mikrokristalisasi process can increase the solubility of atorvastatin. The number of pure atorvastatin (%) who terdissolusi after 45 minutes on medium HCl buffer, acetate buffer, and phosphate buffer was 44.12%, 74.42% and 98.17%. While microcrystals atorvastatin-CMC 5% through the homogenizer speed 24,000 rpm ultra results showed 90.16%, 97.07% and 123%. The difference in dissolution rate is often related to the crystal surface area, particle distribution and purity of the crystal.

CONCLUSION

Based on the research that has been conducted, an increase of dissolution of the active compound can be done with the process and the results of testing mikrokristalisasi showed that at pH 1.2 HCl solution increased about 2 times, in acetate buffer pH 4.5 an increase of 1.3 times and in phosphate buffer pH 6.8 an increase of 1.25 times.

REFERENCES

- Andrajati, R. dkk. (2008). ISO Farmakoterapi. Jakarta : ISFI.
- Al-Zoubi.N., Kachirimanis.K & Malamataris.S .(2002). Effects of harvesting and cooling on crystallization and transformation of orthombic paracetamol in ethanolic solution. European Journal of Pharmaceutical Sciences.13-21.
- Aryani, Yessi. (2009). Pengaruh Ultrasonik terhadap Pembentukan Kristal Glibenklamid. Departemen Farmasi FMIPA UI. Depok.
- Bernasconi, G., Gerster, Hauser, Stauble, H. & Schneiter, E. (1995). Teknologi Kimia II . Jakarta: PT. Pradnya Paramita. 192-201.
- British Comission Secretariat. (2007). British Pharmacopeia. London: British Comission Secretariat.
- Departemen Kesehatan RI. (1995). Farmakope Indonesia IV. Jakarta.
- Dhirendra K. Et al., (2009). Solid Dispersion : A Review. J. Pharm. Sci., Vol. 22. No. 2, pp. 234-246.
- Faroongsang, Sunthornpit.A. (2000). Thermal Behaviour of a Pharmaceutical Solid Acetaminophen Doped. AAPS Pharm.SciTech.



Florence, Atwood. (1988). Physicochemical Principles of Pharmacy Second Edition. Mac-Millan Press, London: 21,24.

Kebamoto, Sartono. (2006). Scanning Electron Microscopy. FMIPA UI, Depok: 1-2.

Martin, A. James S. And Cammaranta, A. 1993. Farmasi Fisik, Dasar-Dasar Kimia Fisik Dalam Ilmu Farmasetik. Vol 1. Jakarta: UI Press.

Nursanti, 2008. Eksplorasi Berbagai Kristal Ibuprofen dan Karakterisasinya. Departemen Farmasi FMIPA UI. Depok. 20-23.

Paryanto, Imam. (2009). Pengaruh Penambahan Garam Halus pada Proses Kristalisasi Garam Farmasetis. Jurnal Sains dan Teknologi Indonesia, Vol. 2.

Rajesh A, et.al (2010). Formulation and Physical Characterization of Microcrystals for Dissolution Rate Enhancement of Tolbutamide, International Journal Pharmaceutical Science. Vol 1.

Sachan, et. al. (2009). Biopharmaceutical classification system: A strategic tools for oral drug delivery technology. Asian Journal of Pharmaceutics. (<http://www.asian-pharmaceutics.info>).

Soewandhi, Sundani N. 2012. Kristalografi Farmasi II. ITB. Bandung: 5-8.

Swarbick, J. 2007. Encyclopedia of Pharmaceutical Technology 3rd ed vol6. USA.

Varshosaz J., et al, 2008. Dissolution enhancement of gliclazide using in situ micronization by solvent change method. Powder Tech. 187: 222-300.



IN VITRO ANTIMALARIAL ACTIVITY OF DICHLOROMETHANE SUB-FRACTION OF *Eucalyptus globulus* L. STEM AGAINST *Plasmodium falciparum*

Elis Suwarni, Akademi Farmasi Saraswati, Denpasar, Bali; **Achmad Fuad Hafid**, Department of Pharmacognosy and Phytochemistry, Faculty of Pharmacy, Universitas Airlangga, Surabaya 60286; Institute of Tropical Disease Universitas Airlangga, Campus C Unair Mulyorejo Surabaya 60115; **Aty Widwaruyanti**, Department of Pharmacognosy and Phytochemistry, Faculty of Pharmacy, Universitas Airlangga, Surabaya 60286; Institute of Tropical Disease Universitas Airlangga, Campus C Unair Mulyorejo Surabaya 60115, aty-w@ff.unair.ac.id

INTRODUCTION

Malaria is a serious infectious disease caused by protozoan parasites in tropical and subtropical regions. In 2010, malaria was endemic in about 104 countries worldwide and approximately 219 million cases of malaria caused 660.000 deaths. Approximately 90 % of malaria deaths occur in Africa (WHO, 2012). Global spread of multiple drug-resistant malaria has become a major health problem and efforts to search for new antimalarial are needed.

Eucalyptus globulus is a plant of the Myrtaceae family that in Indonesia commonly known as kayu putih and empirically used as an antipyretic (Backer, 1968). In Brazil, *E. globulus* is used as an antimalarial plants (Nagpal et al., 2010). In Cameroon, *E. globulus*, *Carica papaya* and *Psidium guajava* leaves are mixed and boiled as a decoction that is drunk for the treatment of malaria (Titanji et al., 2008). In Venezuela, *E. globulus* leaves is boiled as decoction for the treatment of malaria (Carballo et al., 2004).

Our preliminary study showed that the 80% ethanol extract and dichloromethane fraction were very active as an antimalarial with IC₅₀ of 0.090 µg/mL and 0.022 µg/mL, respectively. This study aims to separate the dichloromethane fraction and to test antimalarial activity of its subfractions.

MATERIAL AND METHODS

Plant Material

Eucalyptus globulus stem was obtained from

Cangar Forest at Malang, East Java on April 2010. Sample was authenticated by the authority of Purwodadi Botanical Garden, Pasuruan, East Java.

Separation Method

Vacuum liquid chromatography (VLC) of dichloromethane fraction of *E. globulus* stem was performed using hexane-CHCl₃ (25% gradient) to CHCl₃-MeOH (98:2, 96:4, 94:6, 90:10, 85:15 and 80:20).

Thin Layer Chromatography (TLC) Method

Sub-fractions obtained from Vacuum liquid chromatography (VLC) of dichloromethane fraction were monitored by TLC using silica gel F254 as stationary phase and chloroform-methanol (98:2) as mobile phase. The separated spots were visualized under ultra-violet light of two different wavelengths (UV254 nm and UV365 nm) and visible light before and after sprayed with 10% H₂SO₄ and heated at 105°C for 5 minutes.

In Vitro Antimalarial Activity Test

Antimalarial activity of sub-fractions was assessed against *Plasmodium falciparum* strain 3D7 which is sensitive to chloroquine. This strain was maintained in continuous culture in flask according to the methodology described by Tragger and Jensen (1976).

Percentage inhibition was calculated using formula:

$$\left[\frac{(\% \text{ parasitaemia in control wells} - \% \text{ parasitaemia of test wells})}{(\% \text{ parasitaemia of the control wells})} \right] \times 100$$

control]] x 100 (Ngemanya et al., 2006). IC50 values refers to the concentration required to inhibit 50% of parasite's growth (Mustofa et al., 2007).

RESULTS AND DISCUSSION

Vacuum liquid chromatography of dichloromethane fraction produced 8 sub-fractions (D.1 - D.8 sub-fractions). TLC chromatogram of dichloromethane sub-fractions was shown in figure 1.

Antimalarial activity test showed that IC50 value of each dichloromethane sub-fractions was 10.284 µg/mL, 16.387 µg/mL, 0.053 µg/mL, 1.059 µg/mL, 0.318 µg/ml, 0.387 µg/mL, 0.150 µg/mL and 0.040 µg/mL. D.8 sub-fraction has the lowest IC50 value of 0.040 µg/L. This activity was analysed in accordance with the norm of plants antimalarial activity of Rasoanaivo et al. (1992). According to this norm, an extract is very active if IC50 < 5 µg/mL, active 5 µg/mL < IC50 < 50 µg/mL, weakly active 50 µg/mL < IC50 < 100 µg/mL and inactive IC50 > 100 µg/mL. Based on this classification, result from this study of D.8 sub-fraction of *E. globulus* stem with IC50 of 0.040 µg/mL is said to have very active antimalarial activity. The result of antimalarial activity test of dichloromethane sub-fractions (D.1 - D.8 sub-fractions) can be seen in Table 1.

TLC test of sub-fractions indicated the presence of the most dominant spot (spot D) on D.8 sub-fraction with Rf values of 0.40 which gave a red purple colour after sprayed with 10% H2SO4 and heated at 105 oC for 5 minutes. Spot D began to appear on D.6 sub-fraction which has the IC50 value of 0.387 µg/L. Colour intensity of spot D increased on D.7 and D.8 sub-fractions which have the IC50 values lower than that of D.6 sub-fraction (0.387 µg/mL). From these data can be seen that the higher concentration of spot D, the lower IC50 value of sub-fractions. Therefore, it can be presumed that spot D on D.8 sub-fraction is a substance that is responsible for activity of D.8 sub-fraction.

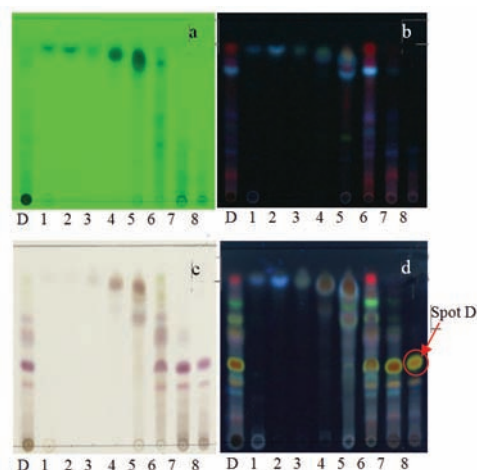


Figure 1. TLC chromatogram of dichloromethane sub-fraction using silica gel F254 as stationary phase and chloroform-methanol (98:2) as mobile phase, viewed under UV light : (a) 254 nm; (b) 366 nm; (c) after sprayed with 10% H2SO4 and heated at 105oC for 5 minutes. (d) 366 nm after sprayed with 10% H2SO4 and heated at 105oC for 5 minutes; D = dichloromethane fraction, D.1-D.8 = sub-fraction.

Table 1. IC50 values of dichloromethane sub-fractions of *E. globulus* L. stem against *P. falciparum*

Sam ple	Percent of average inhibitions at various doses (µg/mL)					IC ₅₀ (µg/mL)
	100	10	1	0.1	0.01	
D.1	73.46	40.42	31.63	21.42	16.32	10.284
D.2	63.27	46.95	29.77	10.38	1.63	16.387
D.3	89.83	79.10	69.52	51.22	41.12	0.053
D.4	87.40	54.41	44.55	39.60	21.58	1.059
D.5	92.41	75.86	52.80	43.27	24.13	0.318
D.6	90.20	70.94	55.43	36.34	27.30	0.387
D.7	89.50	73.96	58.95	45.41	36.15	0.150
D.8	92.24	80.80	72.99	53.92	41.85	0.040

CONCLUSION

D.8 sub-fraction of *E. globulus* possesses a very active antimalarial activity and might be a good candidate for antimalarial. Further work



is suggested to isolate, identify and characterize the active principles from this substance.

ACKNOWLEDGEMENTS

The authors acknowledge Satreps Lab-Natural Product Medicine Research Development Division, Institute of Tropical Disease Universitas Airlangga for supporting this research.

REFERENCES

1. Backer CA, van den Brink B. (1968). Flora of Java. vol 2, Noodhoff NV, Groningen, Nederlands, hal. 195, 203, 478.
2. Bloland PB, (2001). Drug Resistance in Malaria. WHO, Switzerland.
3. Caraballo A, Caraballo B, Acosta AR. (2004). Preliminary assessment of medicinal plants used as antimalarials in the southeastern Venezuelan Amazon. *Revista da Sociedade Brasileira de Medicina Tropical* 37(2) : 186-188.
4. Mustofa J, Sholikhah EN, Wahyuono S. (2007). In vitro and in vivo antiplasmodial activity and cytotoxicity of extracts of *Phyllanthus niruri* L. herbs traditionally used to treat malaria in Indonesia, *South east Asian Journal of Tropical Medicine and Public Health*, 38(4): 609-615.
5. Nagpal N, Shah G, Arora NM, et al. (2010). Phytochemical and Pharmacological Aspects of *Eucalyptus* Genus. *IJPSR* 1(12): 28-36.
6. Ngemenya MN, Akam TM, Yong JN, et al. (2006) Antiplasmodial activities of some products from *Turraethus africanus* (Meliaceae), *African Journal of Health Sciences*, 13: 33 - 39.
7. Rasoanaivo P, Ratsimamanga-Urverg S, Ramanitrhasimbola D, et al. (1992). Criblage d'extraits de plantes de Madagascar pour recherche d'activité antipaludique et d'effet potentialisateur de la chloroquine. *J Ethnopharmacol* 64:117-126.
8. Titanji VPK., Zofou D, Ngemenya MN. (2008). The Antimalarial Potential of Medicinal Plants Used for The Treatment of Malaria in Cameroonian Folk Medicine. *Afr. J. Trad. Cam* : 5(3) : 302 – 321.
9. Trager W, Jensen WB. (1976). Human Malaria Parasites in Continuous Culture. *In : Science* 193:673-675.
10. WHO. (2012),. World Malaria Report 2012, http://www.who.int/malaria/publications/world_malaria_report_2012/en/index.htm.



Arcangelisia flava INCREASES RATS' LEUKOCYTES BUT HAS BIPHASIC EFFECT ON RATS' LYMPHOCYTE

Endah Puspitasari, Faculty of Pharmacy University of Jember, Jl. Kalimantan 37 Jember, Indonesia, e.puspitasari@unej.ac.id; Evi Umayah Ulfa, Faculty of Pharmacy University of Jember, Jl. Kalimantan 37 Jember, Indonesia; Vita Ariati, Faculty of Pharmacy University of Jember, Jl. Kalimantan 37 Jember, Indonesia; Mohammad Sulthon Habibi, Faculty of Pharmacy University of Jember, Jl. Kalimantan 37 Jember, Indonesia.

INTRODUCTION

As a country rich of natural resources, especially in medicinal plant, Indonesia has many opportunities to develop medicinal sources originated from plants. One of the potential medicinal plant used for cancer chemoprevention agent is *Arcangelisia flava*. This plant was shown to have antioxidant and cytotoxic activity against breast cancer cell line, MCF-7. These ability were considered to be corresponding to the alkaloid content, especially berberine (Keawpradub et al., 2005). As this plant is easily to be found in Meru Betiri National Park situated in Jember (Koran Jakarta, 2012), we are eager to explore further about this plant.

To be developed as medicine, we have to know its safety. The sub-chronic toxicity assay was chosen to study the safety of ethanolic extract of *A. flava* leaves (EEAfL) use. This research was done to determine the EEAfL effect on leukocytes and lymphocytes cell count of rats receiving sub chronic EEAfL.

OBJECTIVES

This research was done to determine the EEAfL effect on immune response, especially on leukocytes and lymphocytes cell count of rats receiving sub chronic EEAfL.

MATERIAL AND METHODS

Plant materials and extraction

The *A. flava* leaves were collected from Meru Betiri National Park, Jember, Indonesia. They were selected for their freshness, old age, and healthy ones. The leaves were washed

thoroughly with water, then, were air dried followed by oven drying at 50 °C. The dried leaves were grounded and sieved. The ethanolic extract were prepared using 500 g of leaves powder according to the previous study with a slight modification (Keawpradub et al., 2005). The ground-dried leaves was sequentially extracted with n-hexane, chloroform, and ethanol. The extraction was repeated three times for each solvent. The ethanol extract was evaporated under reduced pressure (Heidolph, Laborota) resulting EEAfL. EEAfL was then suspended in CMC Na 1% before being administered to the animal.

Animals

Male Wistar rats (weighing 100-150 g) were housed at a constant temperature and light-dark cycle. Rats were fed with standard feed and water ad libitum. The rats were acclimatized and quarantined for at least 10 days prior to the experiment. The animal handling protocols of this study were in accordance with the guidelines of the animal care of University of Jember.

Experimental design

Fifteen rats were divided into three groups. Group I as control, received CMC Na 1 %. Group II received EEAfL 500 mg/kg BW. Group III received EEAfL 1,500 mg/kg BW. The treatment was done orally for 11 days. At the 12th day, the blood sample was collected and analyzed further for leukocytes and lymphocytes cell count.

Statistical analysis

All data were presented as mean + the stan-



dard error of the mean (SEM). Kruskal Wallis assay followed by Mann Whitney test were used to know the significance difference between groups, since the data could not meet the requirement for Anova analysis ($p < 0,05$).

RESULTS AND DISCUSSION

Leukocytes cell count

The leukocytes cell count (Figure 1) of rats receiving EEAfL were increased significantly than that of the control group, either at the dose of 500 or 1,500 mg/kg BW.

Lymphocytes cell count

The lymphocytes cell count of rats receiving 500 mg/kg BW EEAfL was increasing significantly, but the rats treated with EEAfL at the dose of 1,500 mg/kg BW had decreased lymphocytes (Figure 2).

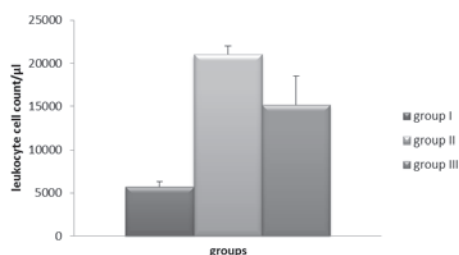


Figure 1. Leukocytes cell count of rats. Data represented as mean + SEM ($n = 5$). Different letter notation expressed significant difference according to Mann Whitney test ($p < 0,05$).

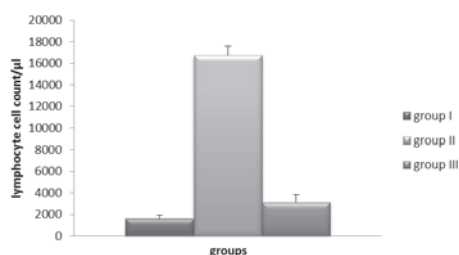


Figure 2. Lymphocytes cell count of rats. Data represented as mean + SEM ($n = 5$). Different letter notation expressed significant difference according to Mann Whitney test ($p < 0,05$).

Discussion

EEAFL seems to increase the immune system of normal rats, as it was expressed by leukocytes cell count. But it had biphasic effect on lymphocytes, as the higher the dose lowered the lymphocytes cell count. We could say that high dose of EEAfL decreased specific immune system as it decreased the lymphocytes cell count.

EEAFL contained berberine (Puspitasari and Ulfa, 2013). The higher the dose, the higher the berberine content. Berberine itself is an immunosuppressive agent. It inhibits the activation and proliferation of T cells, but no cytotoxic effect known (Xu et al., 2005). EEAfL might increase the non-specific immune system. Leukocytes consist of neutrophils, lymphocytes, monocytes, eosinophils, and basophils. Lymphocytes plays role in specific immune response, while others play in non-specific immune response.

Leukocytes cells count that was increasing while the lymphocytes cell count that was decreasing after treated with high dose of EEAfL suggested that the other kinds of leukocytes involving in non-specific immune response were higher. Water extract of *A. flava* increases macrophage activity (Florentina, 2013). Thus, EEAfL might also increase the macrophage activity. Still, we need to examined further for these hypothesis.

CONCLUSION

Based on the results, we can conclude that EEAfL increased the immune response on rats, but it had biphasic effect on lymphocytes suggesting that high dose of EEAfL might increased non-specific immune response instead of the specific one.

REFERENCES

1. Florentina, D. (2013). Pengaruh Ekstrak Larut Air Kayu Kuning (*Arcangelisia flava* (L.) Merr.) terhadap Fagositosis Makrofag secara In Vitro pada Tikus Galur



- Wistar. Yogyakarta: Skripsi Universitas Gadjah Mada. Hal. 39.
2. Keawpradub, N., Dej-adisai, A., and Yue nyongsawad, S. (2005). Antioxidant and Cytotoxic Activities of Thai Medicinal Plants Named Khaminkhruea: *Arcangelia flava*, *Coscinium blumeianum* and *Fibraurea tinctoria*. *The Songklanakarin Journal of Science and Technology*. 27(2). 455–427.
 3. Koran Jakarta (2012). Peneliti Temukan Obat Antikanker di Meru Betiri, Koran Jakarta Digital Edition, <http://koran-jakarta.com/index.php/detail/view01/93445>, diakses 14 Maret 2013
 4. Puspitasari, E. and Ulfa, E.U. (2013). Pengembangan Ekstrak Etanol *Arcangelia flava* Terstandar sebagai Agen Pendamping Kemoterapi Doxorubicin untuk Pengobatan Kanker, Laporan Tahunan Penelitian, Lembaga Penelitian Universitas Jember.
 5. Xu, L., Liu, Y., and He, X. (2005). Inhibitory Effects of Berberine on The Action and Cell Cycle Progression of Human Peripheral Lymphocytes. *Cellular and Molecular Immunology*. 2(4). 295–300.



IN VITRO ANTIMALARIAL ACTIVITY OF CHLOROFORM SUBFRACTION OF SALAM BADAK LEAVES (*Acmena acuminatissima*)

Erna Cahyaningsih, Akademi Farmasi Saraswati, Denpasar, Bali; **Achmad Fuad Hafid**, Department of Pharmacognosy and Phytochemistry, Faculty of Pharmacy, Universitas Airlangga, Surabaya 60826, Institute of Tropical Disease, Universitas Airlangga, Surabaya 60115; **Aty Widawaruyanti**, Department of Pharmacognosy and Phytochemistry, Faculty of Pharmacy, Universitas Airlangga, Surabaya 60826, Institute of Tropical Disease, Universitas Airlangga, Surabaya 60115, aty-w@ff.unair.ac.id

INTRODUCTION

Malaria is still an endemic disease in more than 90 countries, mainly in developing countries (Sanchez et al., 2004). Patients infected with malaria have doubled in the last two decades. This occurred mainly due to the emergence of resistant strains of *Plasmodium falciparum* malaria to the chloroquine and its derivatives (Trape et al., 2002). Perez et al. (1997) stated that the global spread of malaria parasites that are resistant to current antimalarial drug is a major health problem. Therefore, it is need to find new antimalarial substances to replace current drugs that are not sensitive anymore. One attempt to discover new antimalarial substances is through active exploration of the natural sources.

It is known that some species of the family Myrtaceae has an antimalarial activity. Previous studies shown that ethanol extract and chloroform fraction of *A. acuminatissima* leaves (Myrtaceae) were exhibited antimalarial activity with IC₅₀ value of 0.040 µg/ml and 0.006 µg/ml, respectively. Therefore, the separation of the chloroform fraction was done to determine the antimalarial activity substances of *A. acuminatissima*.

MATERIALS AND METHODS

Plant materials

A. acuminatissima leaves was obtained from Purwodadi Botanical Garden on December 2012. Sample was authenticated by the authority of Purwodadi Botanical Garden, Pasuruan, East Java.

Fractionation

Chloroform fractions which obtained from the fractionation of ethanol extract of *A. acuminatissima* leaves was separated by vacuum liquid chromatography (VLC) using hexane, chloroform, and ethanol at gradient condition. This separation was produced six subfractions, then evaporated using a vacuum evaporator and dried. These six subfractions was then analyzed by TLC and tested for antimalarial activity.

In vitro antimalarial activity test

Antimalarial in vitro test was performed based on Budimulya et al. (1997). Sample prepared in serial dilution at concentration of 0.01; 0.1; 1; 10 and 100 µg/ml in microwells. Each microwell was added with 500 µl parasite culture (1% parasitemia, 5% haematocrit) and incubated for 48 hours in 37°C. After incubation, thin blood smears were made and stained using 20% giemsa dye. Percentage of parasitemia was determined by counting infected erythrocytes per 1000 total erythrocytes under microscope.

RESULTS AND DISCUSSION

The separation results of *A. acuminatissima* leaves chloroform fraction was produced six subfractions (A-F). Each subfraction was tested for in vitro antimalarial activity against *P. falciparum* (3D7). According to Rasoanaivo et al. (2004), an extract is very active if IC₅₀ < 5 µg/mL, active 5 µg/mL < IC₅₀ < 50 µg/mL, weakly active 50 µg/mL < IC₅₀ < 100 µg/mL and inactive IC₅₀ > 100 µg/mL. The test re-

sults showed that all chloroform subfractions classified as very active and subfraction E was the most active with IC₅₀ value of 0.007 µg/mL. The result of antimalarial activity test of chloroform subfractions (A-F) can be seen in Table 1.

Identification of chloroform subfraction was performed by TLC method using silica gel GF254 as stationary phase and chloroform:methanol (98:2) as a mobile phase. Then observed under UV light in wavelength of 254 nm, 366 nm and sprayed with H₂SO₄ 10%. TLC chromatogram profile showed that all subfractions contain purple spot (Fig.1). According to Sharifa et al. (2012), terpenoid compounds will form a pink to purple or violet after being sprayed with 10% H₂SO₄. It can be considered that all subfractions were containing terpenoids.

Sub fraction	% Inhibition at a concentration of (µg/ml)					IC ₅₀ (µg/ml)
	100	10	1	0.1	0.01	
A	100	100	75.32	65.18	56.19	0.012
B	100	83.39	63.95	47.69	24.32	0.158
C	86.41	83.94	41.38	35.17	20.40	1.469
D	96.90	92.48	64.83	36.5	26.40	0.172
E	100	85.70	70.42	69.84	56.75	0.007
F	97.19	91.41	68.41	59.81	54.61	0.014

Table 1. IC₅₀ values of Chloroform subfractions against *P. falciparum* 3D7

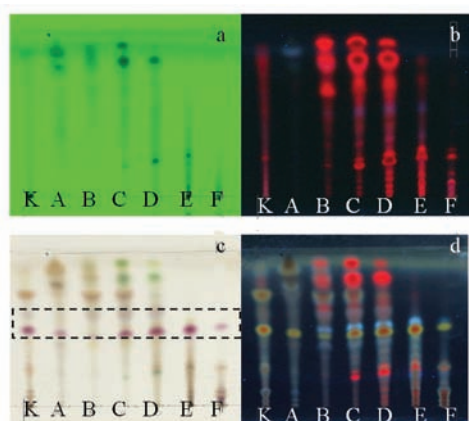


Figure 1. TLC chromatogram of chloroform subfraction using silica gel F254 as stationary phase and chloroform-methanol (98:2) as mobile phase, viewed under UV light : (a) 254 nm; (b) 366 nm; (c) after sprayed with 10% H₂SO₄ and heated at 105°C for 5 minutes. (d) 366 nm after sprayed with 10% H₂SO₄ and heated at 105°C for 5 minutes; K = chloroform fraction, A-F = subfraction.

[] = considered to contain terpenoids.

Subfraction A-F were exhibited antimalarial activity (IC₅₀ value of 0.007-1.469 µg/ml) and containing terpenoids substances. Based on that result, it is possible to conclude that antimalarial activity of subfractions was derived from terpenoids substances.

CONCLUSION

Subfraction E of *A. acuminatissima* leaves was the most active as antimalarial with IC₅₀ value of 0.007 µg/ml. The antimalarial activity was possible derived from terpenoids substances. Further study needed to isolate and identify the active compounds from *A. acuminatissima*

ACKNOWLEDGEMENT

The authors acknowledge Satreps Lab-Natural Product Medicine Research Development Division, Institute of Tropical Diseases Universitas Airlangga for supporting this research.

REFERENCES

1. Budimulya, AS., Syafruddin, Tapchaisri, P., et al. 1997. The sensitivity of *Plasmodium* protein synthesis to prokaryotic ribosomal inhibitors. *Mol Biochem Parasitol* 84:137-141
2. Perez, H., Diaz, F., Medina, JD., 1997. Chemical investigation and in vitro antimalarial activity of *Taebuina ochracea* ssp. *neochrysantha*. *International Journal of Pharmacognosy* 35(4) : 227-231.
3. Rasoanaivo, P., Dehar, OE., Ratsimaman



ICPPS 2014

Proceeding
The 1st International Conference
on Pharmaceutics & Pharmaceutical Sciences

- ga, U., et al. 2004. Guidelines for The Nonclinical Evaluation of The Efficacy of Traditional Antimalarials. In : Traditional Medicinal Plants and Antimalaria. CRC Press. USA 256-268.
4. Sanchez, BAM., Mota, MM., Sultan, AA., et al. 2004. Plasmodium berghei parasite transformed with green fluorescent protein for screening blood schizontocidal agents. Int. J. of Parasitology 34 : 485-490.
 5. Sharifa, AA., Jamaludin, J., Kiong, LS., et al. 2012. Anti-Urolithiatic Terpenoid Compound from Plantago major Linn. (Ekor Anjing). Sains Malaysiana, Vol. 41(1): 33-39.
 6. Trape. JF., Pison, G., Speigel, A., et al. 2002. Combating malaria in Africa. Trends in Parasitology 18 : 224-230.



CHARACTERIZATION OF DOSAGE FORM AND PENETRATION DICLOFENAC SODIUM WITH MICROEMULSION SYSTEM IN HPMC 4000 GEL BASE (Microemulsion W/O with ratio use of surfactant Span 80 – Tween 80 : Cosurfactant Ethanol 96% = 6:1)

Esti Hendradi, Pharmaceutics Department of Faculty of Pharmacy Universitas Airlangga, Surabaya, Indonesia esti_hendradi@yahoo.com; Tutiek Purwanti, Pharmaceutics Department of Faculty of Pharmacy Universitas Airlangga, Surabaya, Indonesia; Karina Wahyu Irawati, Pharmaceutics Department of Faculty of Pharmacy Universitas Airlangga, Surabaya, Indonesia

INTRODUCTION

Diclofenac is NSAID that has activated as anti-inflammation, analgesic and antipyretics (Schuelert, 2011). Diclofenac sodium has partition coefficient of 13.4 (Hasan et.al.2005) which means diclofenac sodium has a partition in oil a higher amount than in the water. By usage two phases to diclofenac sodium like emulsion, diclofenac sodium can dispersed in the initial phase oil and water. But emulsion has thermodynamically unstable (Allen, 1997). So that, needed a system more stable for dispersion of diclofenac sodium to produce a more effective preparation, namely microemulsion system.

The characteristics of microemulsion are stable in thermodynamics, transparent, low viscosity, and have high solubilisation so that it can increase bioavailability drugs in the body (Santos et al., 2008). To overcome the low viscosity of microemulsion by adding hydroxy propyl methyl cellulose (HPMC). The aim of this study was to observe characterization dosage form and penetration of diclofenac sodium in microemulsion system which contained ratio surfactant Span 80-Tween 80 an cosurfactant ethanol= 6:1.

METHODS

Material

Diclofenac sodium (PT. KIMIA FARMA), soybean oil (Sime Draby Edible Product Limited), Span 80 and Tween 80 (Croda), ethanol 96% (Merck), HPMC 4000 (Cosmetic Grade) (Dow Chemical Pacific), aquadem (PT Widatra Bhak-

ti), propyleneglycol (BASF SE, Germany).

Preparation of Microemulsion and emulsion
 The composition of microemulsion and emulsion system in table 1.

Preparation of Emulsion

Emulsion was made by mixing Span 80 and soybean oil as oil phase. As water phase was aquadem and Tween 80. Diclofenac sodium was added in the water phase and oil phase was 2% and 3%, respectively. Mixed the system using magnetic stirrer 500 rpm for 30 minutes.

Preparation of Microemulsion

Span 80, Tween 80, soybean oil, surfactant and cosurfaktant were mixed using magnetic stirrer 100 rpm for 15 minutes. Added aquadem and mixed 100 rpm, 15 minutes. Then, added diclofenac sodium into the system mixed at 150 rpm for 60 minutes.

Table 1. Formula of microemulsion and emulsion W/O type of diclofenac sodium

Material	Concentration (%) (b/b)	
	Microemulsion	Emulsion
Diclofenac sodium	5.00	5.00
Span 80	38.00	7.70
Tween 80	12.83	2.86
Etanol 96%	8.47	-
Soybean oil	33.74	64.41
Aquadem	1.95	20.03



Material	Concentration (%) (b/b)
HPMC 4000	1.5
Propyleneglycol	5
Aquadem	93.5

Table 2. Componen HPMC 4000 gel

Preparation of Microemulsion and emulsion diclofenac sodium in HPMC gel

The concentration of diclofenac sodium of Microemulsion and emulsion in HPMC gel was made 1%. Weigh the microemulsion or emulsion that contained 1% diclofenac and added in to HPMC gel and mixed.

Evaluation

Organoleptic Evaluation

Organoleptic evaluation carried out visually includes examining the color, odor, and consistency. The evaluations performed on microemulsion and emulsion of diclofenac sodium.

Determination of Droplet Size Distribution

Examination of the size and distribution of the microemulsion droplet size was performed with a submicron Delsa™ Nano Particle Size and Zeta Potential Dynamic Light Scattering. The droplet of emulsion of diclofenac sodium was determined using microscope.

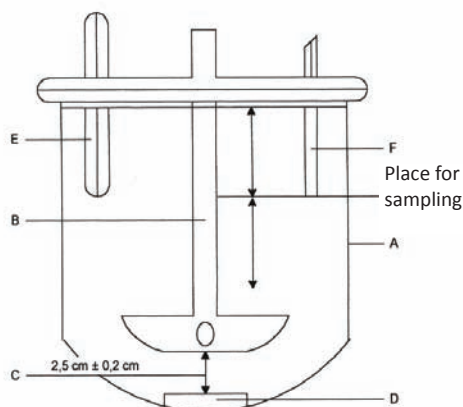
Determination of conductivity

Determination of conductivity was measured using conductometer to microemulsion and emulsion preparation.

Penetration of diclofenac sodium from the preparation

The penetration of diclofenac sodium from microemulsion gel through Wistar rat skin membrane was determined by dissolution test for 8 h. The gel microemulsions of diclofenac sodium (in cell diffusion) were placed respective in the dissolution chamber (Figure 1). All in vitro penetration were performed at 100 rpm, with each medium of dissolution (phosphate buffer saline pH 7.4 ± 0.05 at temperature 37 ± 0.5°C) was 500 mL. The samples withdrawn at different time intervals were analyzed for drug con-

tent using Spectrophotometer Double Beam UV-VIS Recording UV 160 A (Shimadzu). The result was analyzed by statistic programmed of using Independent sample t-Test with degree of confident 95% (α = 0.05).



- A :Diffusion chamber contain PBS pH 7.4
- C: Distance from paddle to diffusion membrane
- D: Diffusion cell
- E: Thermometer
- F: Sample holder

Figure 1. Apparatus 5-paddle Over Disk (TheUnited States Pharmacopeia Convention, 2002)

Penetration of diclofenac sodium was calculated using equation 1

$$J = \frac{dM}{S \cdot dt} \quad (1)$$

Where

J : flux

M : mass of compound (gram)

S : surface area of barrier/membrane (cm²)

t : time (minute/hour)

RESULTS AND DISCUSSION

The appearance system of microemulsion and emulsion shown in Figure 2 and Table 3. In this figure showed that microemulsion was clear and the emulsion was not clear.

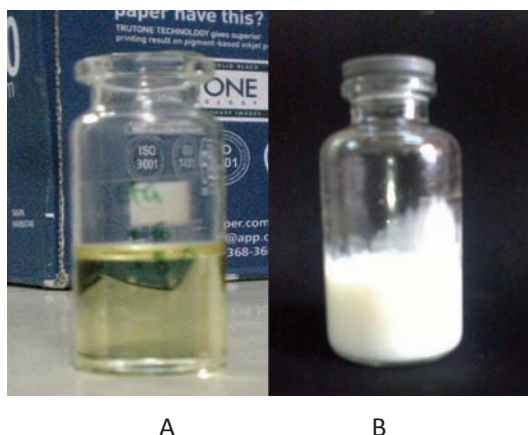


Figure 2. The appearance of microemulsion (A) and emulsion (B)

Table 3. The organoleptics, droplet size and conductivity microemulsion and emulsion of diclofenac.

Observation	Microemulsion of diclofenac sodium	Emulsion of diklofenac sodium
Organoleptics		
Consistency	Transparent fluid	Viscous liquid
Color	Yellow	White
Smell	No smell	No smell
Droplet size	117.2617 nm	1.04 μ m
Conductivity	0.40 \pm 0.01 μ S	0.92 \pm 0.01 μ S

The droplet size of microemulsion smaller compared with the droplet of emulsion of diclofenac. The results of conductivity test showed both of microemulsion and emulsion of diclofenac 0,40 \pm 0,01 μ S and 0,92 \pm 0,01 μ S, respectively. It means both the emulsion type were W/O.

Table 4. The spread diameter and pH of microemulsion and emulsion of diclofenac.

Observation	Microemulsion of diclofenac sodium	Emulsion of diklofenac sodium
Spread diameter	7.7 \pm 0.2 cm	12.73 \pm 0.2 cm
pH	6.33 \pm 0.02	6.33 \pm 0.02

Each data represents the mean \pm S.D. of 3 determinations

The data of spread diameter of microemulsion of diclofenac was lower than emulsion of diclofenac but the pH of two preparations were same. In this research the penetration of diclofenac from emulsion preparation was not done because the stability of emulsion of diclofenac only 2 hours. The flux of diclofenac from microemulsion preparation shown in table 5.

Table 5. Flux of diclofenac from microemulsion preparation

Replication	Flux of diclofenac sodium (μ g/cm ² /minutes)
1	0.24
2	0.18
3	0.24
Mean \pm SD	0.22 \pm 0.03
% KV	16.25 %

The permeability of rat skin to diclofenac shown in table 6.

Table 6. The permeability of rat skin to diclofenac sodium

Replications	Permeability of rat skin to diclofenac sodium (cm/minute)
1	2.18 \times 10 ⁵
2	1.63 \times 10 ⁵
3	2.21 \times 10 ⁵
Mean \pm SD	2.01 \times 10 ⁵ \pm 3.27 \times 10 ⁶
% KV	16.25 %



CONCLUSION

1. Characteristics of microemulsion system in gel base HPMC 4000 showed thicker consistency than emulsion system in gel base HPMC 4000. Different system gave no effect on pH but gave effect on spread diameter of zero load.
2. Penetration flux in microemulsion system in gel base HPMC 4000 was 0.22 ± 0.03 $\mu\text{g}/\text{cm}^2/\text{minute}$ and permeability of membrane was $2.01 \times 10^{-5} \pm 3.27 \times 10^{-6}$ cm/minute .

REFERENCES

Allen, L. V., Jr., 1997. The art and Technology of Pharmaceutical Compounding, Washington DC: American Pharmaceutical Association, p.173-185, 209.

Hasan, S. M., Ahmed, Tasneem., Talib, Nasira., Hasan, Fouzia., 2005. Pharmacokinetic Of Diclofenac Sodium In Normal Man, Pakistan Journal of Pharmaceutical Sciences Vol. 18, No.1, January 2005.

Santos, A.C. Watkinson, J Hadgraft, dan M.E. Lane. 2008. Application of Microemulsions in Dermal and Transdermal Drug Delivery . Journal Skin Pharmacol Physiology 2008; 21: 246-259.

Schuelert, Niklas., Russell, Fiona A., McDougall, Jason. 2011. Topical Diclofenac In The Treatment Of Osteoarthritis Of The Knee. Journal Orthopedic Research and reviews 2011:3., p.1-8

CONSTRUCTION AND VALIDATION OF THE STRUCTURE-BASED VIRTUAL SCREENING PROTOCOLS WITH PDB CODE OF 3LN1 TO DISCOVER CYCLOOXYGENASE-2 INHIBITORS

Mumpuni E, Faculty of Pharmacy Pancasila University Jakarta, esti_mumpuni@yahoo.com, 08151663201; **Nur-rochmad A**, Faculty of Pharmacy Gadjah Mada University Yogyakarta; **Pranowo HD**, Gadjah Mada University Yogyakarta; **Jenie UA**, Faculty of Pharmacy Gadjah Mada University Yogyakarta; **Istvastono EP**, Faculty of Pharmacy Sanata Dharma University Yogyakarta

ABSTRACT

Recently, a need to develop more potent COX-2 inhibitors is very important and one of the method that has been proven the effectivity and efficiency for new drugs research is in silico. Structure-based virtual screening (SBVS) protocols were developed to find cyclooxygenase-2 (COX-2) inhibitors using the Protein-Ligand ANT System (PLANTS) docking software, SPORES, BKChem and Open Babel. The directory of useful decoys (DUD) dataset for COX-2 was used to validate the protocols retrospectively; the DUD consist of 426 known COX-2 inhibitors and 13289 decoys. Based on the criteria value of EF20% and EFmax, the default validated protocol EE_COX2_v.1.0 showed very good results, with enrichment factor 20% (EF20%) value of 4,0 and maximum enrichment factor (EFmax) value of ~

Keywords: protocols, virtual screening, inhibitor, COX-2

INTRODUCTION

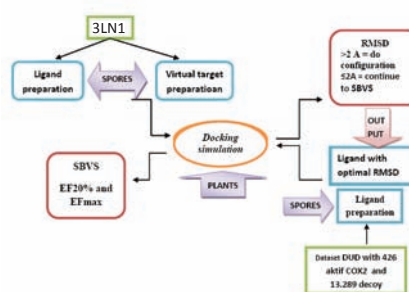
Non-steroidal anti inflammatory drugs (NSAID) as COX-2 inhibitor have been written by more than 70 milion prescriptions everyday and reach 30 bilion USD income each year (Roman B, 2011). The structure-based virtual screening protocols research can reduce costs and make the research of new drugs become more efficient.

Structure-based virtual screening (SBVS) protocols were developed to find cyclooxygenase-2 (COX-2) inhibitors using the new crystals structure COX-2 had been founded with agreat revolution with code PDB 3LN1. Based on the criteria value of EF20% and EFmax used in the article Huang et al (2006) and Yuniarti et al (2011).

METHOD

Instruments: Hardware: A set of computer with Intel (R) Core™ i3-2350 CPU M @ 2.30Ghz, 4 GB of RAM, 64bit operating system.

Software: Linux Ubuntu 10.04 LTS Operating System, SPORES, PLANTS, PyMOL, Open Babel and statistics R i386 3.0.1



RESULT AND DISCUSSION

Validated SBVS

The default validated protocol EE_COX2_v.1.0 showed very good results, with enrichment factor 20% (EF20%) value of 4,0 and maximum enrichment factor (EFmax) value of ~



```
#!/bin/sh
rm -rf penapisan
mkdir penapisan
cd penapisan

cp ../config.txt .
cp ../protein.mol2 .
cp ../ZINC03814547.mol2 .

export PLANTS='/home/esti/PLANTS'

bkchem uji.mol

babel --gen3d -p 7.4 --title uji
-imol uji.mol -omol2 uji.mol2
obconformer 10 1000 uji.mol2 > min_
uji.mol2
$PLANTS/SPORES --mode settypes min_
uji.mol2 uji.mol2
cat ZINC03814604.mol2 uji.mol2 > li-
gand_input.mol2
$PLANTS/PLANTS1.2 --mode screen con-
fig.txt

rm config.txt protein.mol2
ZINC03814547.mol2
grep -Ev TOTAL results/bestranking.
csv | awk -F, '{print $1" "$2}' >
hasil.tmp
sed "s/_entry_00001_conf_01//g" ha-
sil.tmp > hasil.tmp2
sed "s/_entry_00002_conf_01//g" ha-
sil.tmp2 > hasil.txt
more hasil.txt
rm hasil.tmp*
cd ..
echo ""
echo "bagaimana prediksi senyawa uji
anda?"
```

Figure 1. Protocol SBVS EE_COX2_v1.0; Enrichment factor 20% (EF20%) = 4,0; maximum Enrichment factor (EFmax) - ~

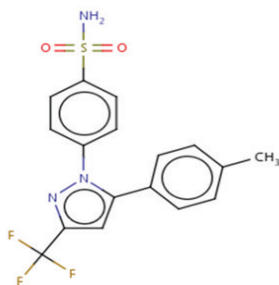


Figure 3. Reference ligand ZINC03814547 (IUPAC: 1-(4-fluorophenyl)-2-methyl-5-(4-methylsulfonylphenyl)-3-(trifluoromethylsulfonyl) pyrrole) as basic to build software

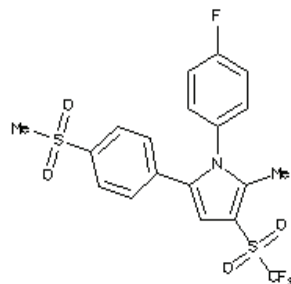


Figure 2. Ligand co-crystal protocol SBVS EE_COX2_V.1.0; IUPAC:4-[5-(4-Methylphenyl)-3-(Trifluoromethyl)-1H-Pyrazol-1-YL]Benzenesulfonamide

Compound (4,5)	Score	Reference Score	Prediction
Curcumin	-374,99	-380,86	Inactive
Demetoxicurcumin	-381,85	-380,86	Active
Bisdemetokxicurcumin	-363,87	-380,85	Inactive
Hexagamavunon	-302,21	-380,86	Inactive
Pentagamavunon	-252,10	-380,88	Inactive
Gamavuton 0	-346,77	-380,86	Inactive
Celecoxib	-396,07	-380,88	Active
EHP	-364,87	-380,86	Inactive

Table 1. Based on score ChemPLP from simulation docking with EE_COX2_V.1.0, the compound that have potential as anti-inflammation and anti-cancer with the mechanism of action as inhibitor COX-2 is Demetoxicurcumin with 3 active amino acid residue

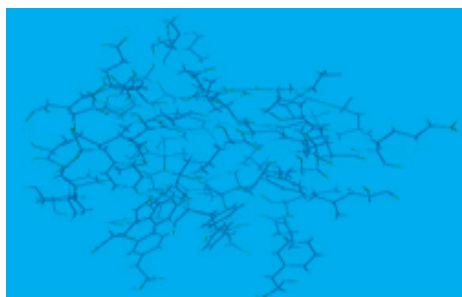
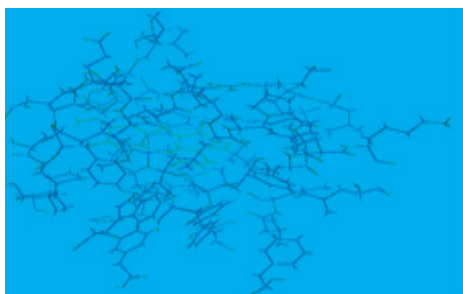


Figure 4. (A) 3D Pose Demetoxicurcumin compounds in bindingsite_fixed.mol2 active protein (B) amino acids 3LN1 with a 3D Pose

CONCLUSION

Based on criteria value of EF20% and EFmax used in the article Huang et al (2006) and Yuniarti et al (2011), the default validated protocol EE_COX2_v.1.0 showed very good results, with enrichment factor 20% (EF20%) value of 4,0 and maximum enrichment factor (EFmax) value of ~

The SBVS protocol with PDB code of 3LN1 (SOFTWARE EE_COX2_v1.0) to discover cyclooxygenase-2 inhibitors was successfully applied to identify COX-2 inhibitor in Curcuminoid.

REFERENCES

- *. Roman B.(2011). Anti-inflamasi nonsteroid Obat (OAINS):<http://www.phend.co.za/health/Nsaid.htm>,
- *. Yuniarti N., Zullies I., Istyastono E.P. (2011). The Importance Of ARG513 as a Hydrogen Bond Anchor to Discover COX-2 Inhibitors In a Virtual Screening Campaign www.bioinformatics.net.

- *. Huang N, Shoichet BK, Irwin JJ. (2006). Benchmarking sets for molecular docking. *J Med Chem*.Nov 16;49(23):6789-801.
- *. Esti Mumpuni, Indriana P, Evi L, Enjang R. (2010). Sintesis dan uji antioksidan senyawa 1,5-bis(3'-etoksi-4'-hidroksifenil)-1,4-pentadien-3-on (EHP) *Jurnal Ilmu Kefarmasian Indonesia*, Vol 8, No.2 Sept.
- *. Sardjiman. (2000). Synthesis of some new series of curcumin analogues, anti oxidative activity and Structure Activity Relationship (dissertation). Yogyakarta: Gadjah Mada University.



VALIDATED UV SPECTROPHOTOMETRIC METHOD FOR THE DETERMINATION OF ASPIRIN IN RABBIT PLASMA : APPLICATION TO BIOAVAILABILITY STUDY OF ASPIRIN MICROCAPSULE IN RABBIT

Faizatun, Faculty of pharmacy University of Pancasila, fazarum@yahoo.com; **Novi yantih**, Faculty of pharmacy University of Pancasila, novi_yantih@yahoo.com; **Teguh Iman Saputra**, Faculty of pharmacy University of Pancasila,

INTRODUCTION

Aspirin is non-steroidal anti-inflammatory (NSAID), acidic and has a greater cohesiveness than the adhesive properties making it hard contact with water. Aspirin has a rapid absorption and practically complete, especially in the first part of the duodenum. Lower bioavailability due to hydrolysis during absorption. At low doses of aspirin can inhibit platelet aggregation and used in the treatment of infarct myocardial and stroke. Aspirin acetylated cyclooxygenase enzyme and inhibits the formation of cyclic endoperoxides. Aspirin also inhibits the synthesis of thromboxane A₂ (TXA-2) in platelets, so that ultimately inhibits platelet aggregation. Onset of effect after 30 minutes and lasts 3-6 hours, $t_{1/2}$ 2-3 hours. Aspirin usually given orally but there are problems associated with side effects that can cause bleeding in the gastrointestinal tract.

Aspirin 80 mg is still the main choice as anti-thrombotic. Here is needed to bioavailability test of 80 mg aspirin as quality control efforts to protect consumers from 80 mg aspirin dosage that does not meet the standards, so that consumers get the precision of the dose of aspirin 80 mg dosage.

For the determination of plasma levels of aspirin are needed method of selective and sensitive analysis. Visible light spectrophotometry provide benefits fast, simple and selective. Aspirin was hydrolyzed to salicylic acid and acetic acid under alkaline conditions, then neutralized with acid, salicylic acid formed complexed with iron (III) nitrate will react with the phenol group of salicylic acid and produces a purple complex. Once validated analytical method, then this method will be applied to test the

bioavailability of microencapsulated aspirin 80 mg in rabbits.

MATERIALS AND METHODS

MATERIALS. Asetosal BPF (POM), aspirin raw materials (Yixing city, China), rabbit, heparin, ethanol, nitric acid, sodium hydroxide, iron (III) nitrate, distilled water.

INSTRUMENTATION. UV-Vis spectrophotometry (Shimadzu-1800), Microcentrifuge, vortex, micropipette.

METHODS. Fresh blood (from rabbit) was added anticoagulant (heparin) and centrifuged 3500 rpm for 10 minutes, the blood plasma of rabbits used for analytical method validation process aspirin in plasma. Visible light spectrophotometer optimization done by setting the maximum wave and a steady uptake of aspirin. Rabbit blood plasma was added a solution of a certain concentration asetosal then ethanol, and centrifuged divorteks back at 3500 rpm for 10 min, the supernatant obtained was added nitric acid, sodium hydroxide and iron (III) nitrate, was measured with a spectrophotometer absorbance of visible light at a wavelength of 525 nm maximum. Validation parameters tested were linearity, LLOQ determination, precision, accuracy, and recovery. The solution was prepared at a concentration asetosal low, medium and high absorbance measured at the maximum wavelength, using the solvent as a blank. Accuracy was calculated as the percent error, precision as coefficient of variation and recovery as the recovery value. For testing LLOQ can be obtained by dilution of the concentration LOQ obtained from calibration curves to one-half

or one-quarter and absorbance was measured 5 times with each concentration of visible light spectrophotometry. Data obtained calculated value percent error and relative standard deviation. LLOQ shows the accuracy shown by the percent error average value does not deviate from the $\pm 15\%$ and -15% except LLOQ levels of $\pm 20\%$ and -20% , and the precision indicated by the coefficient of variation of less than 15% except LLOQ levels of less than 20%.

RESULT

Linearity show that the relationship between the absorbance with concentration has linearity in accordance with the equation of the line and the price coefficient of variation is close to 1, as shown in Figure 1.

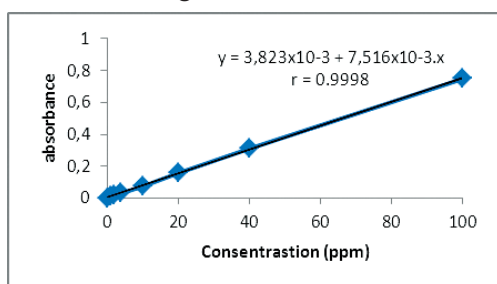


Figure 1. Calibration curve of aspirin in plasma at λ 525 nm

LLOQ

LLOQ measured by conducting experiments on concentration $\frac{1}{2}$ fold and $\frac{1}{4}$ fold of the LOQ, LOQ obtained from the linearity test is at a concentration of 1 ppm. Based on these experiments, it can be concluded that the level of LLOQ was 0.5 ppm, due to the accuracy of 0.5 ppm still meet the requirements of the FDA LLOQ ie% error $\leq + 20\%$ and -20% , while the accuracy at 0, 25 ppm does not meet the requirements of the LLOQ, and the recovery at 0.5 ppm is still said to be good because it is in the range of 80-120%.

Precision

Precision describes the closeness between the test results to one another, carried out using a minimum of 5 replicates for each concentration. The average value does not deviate from

the 15% except LLOQ levels of less than 20%. Precision test results can be seen in Table V.4. precision of the test results at LLOQ level (0.5 ppm); 2 ppm and 40 ppm, it is known that all levels of precision to meet the requirements of the FDA.

Table 1. Precision results show repeatability

Concentration claim (ppm)		Absorbance (A)	Concentration measured (ppm)	CV (%)
LLOQ (0,5)	1.	0,007	0,423	15,29
	2.	0,007	0,423	
	3.	0,008	0,556	
	4.	0,007	0,423	
	5.	0,008	0,556	
2	1.	0,018	1,886	3,97
	2.	0,017	1,753	
	3.	0,017	1,753	
	4.	0,018	1,886	
	5.	0,018	1,886	
40	1.	0,312	41,003	1,08
	2.	0,318	41,801	
	3.	0,315	41,402	
	4.	0,310	40,737	
	5.	0,317	41,668	

ACURACY

Accuracy describes the closeness of the test results with the actual levels in order to obtain the deviation of the actual values used to calculate the percent error. Performed by using a minimum of 5 replicates for each concentration. The average value does not stray from the $+ 15\%$ and -15% except LLOQ levels $+ 20\%$ and -20% . Accuracy of the test results can be seen in Table V.5. precision of the test results at LLOQ level (0.5 ppm); 2 ppm and 40 ppm, it is known that all the levels of accuracy to meet the requirements of the FDA.

Table 2. Acuracy readings of aspirin

Concentration claim(ppm)		Absorbance (A)	Concentration measured (ppm)	(%) Diff
LLOQ (0,5)	1.	0,007	0,423	-13,72
	2.	0,007	0,423	
	3.	0,008	0,556	
	4.	0,007	0,423	
	5.	0,008	0,556	
2	1.	0,018	1,886	-8,36
	2.	0,017	1,753	
	3.	0,017	1,753	
	4.	0,018	1,886	
	5.	0,018	1,886	
40	1.	0,312	41,003	3,31
	2.	0,318	41,801	
	3.	0,315	41,402	
	4.	0,310	40,737	
	5.	0,317	41,668	



Recovery

Recovery of the detector response ratio of analyte extracted from a biological sample detector response versus actual levels of pure standards. Extraction efficiency of the analytical method and measured at three different levels (high, medium, low), the recovery does not need a 100% recovery is important to be consistent, and reproducible pesis. Recovery test results can be seen in Table V.6. the acquisition of the test results back to the LLOQ level (0.5 ppm); 2 ppm and 40 ppm, it is known that all levels to meet the requirements of the FDA's recovery.

Table 3. % recovery

Concentration (ppm)		Absorbance (A)	% Recovery	CV (%)
LLOQ (0,5)	1.	0,007	84,60	15,30
	2.	0,007	84,60	
	3.	0,008	111,20	
	4.	0,007	84,60	
	5.	0,008	111,20	
2	1.	0,018	94,30	3,97
	2.	0,017	87,65	
	3.	0,017	87,65	
	4.	0,018	94,30	
	5.	0,018	94,30	
40	1.	0,312	102,51	1,08
	2.	0,318	104,50	
	3.	0,315	103,51	
	4.	0,310	101,84	
	5.	0,317	104,17	

CONCLUSION

Methods of analysis of aspirin by spectrophotometric methods are valid and can be used for the determination of bioavailability test of aspirin microcapsul in rabbits

REFERENCES

- *. Takka, S, F Acarturk. Calcium Alginate Microparticles for Oral Administration: I. Effect Effect of Sodium Alginate Type on Drug Release and Drug Entrappment Efficiency, *J. Miroencapsulation*, vol. 16, No. 3, 275-290. 1991
- *. U.S.Department of Health and Human Services. Food and Drug Administrations. Guidance for Industry. Bioanalytical Method Validation. 2001
- *. Moffat Anthony C, Osselton M David, Widdop Brian, Galichet Laurent Y. Clarke's Analysis of Drug & Poisons. Third edition. London-Chicago: Pharmaceutical Press. 2004

EFFECT OF COMPARISON OF SURFACTANT AND COSURFACTANT W/O MICROEMULSION OVALBUMIN WITH SOYBEAN OIL TO PHYSICOCHEMICAL CHARACTERIZATION

(w/o Microemulsion with Surfactant Span 80- Tween 80 : Cosurfactant Ethanol 96% = 5:1; 6:1 and 7:1)

Farida Mutiara Sari, Faculty of Pharmacy, Universitas Airlangga, Surabaya, Indonesia; **Riesta Primaharinastiti**, Faculty of Pharmacy, Universitas Airlangga, Surabaya, Indonesia; **Esti Hendradi**, Faculty of Pharmacy, Universitas Airlangga, Surabaya, Indonesia, esti_hendradi@yahoo.com

INTRODUCTION

Microemulsions are macroscopically isotropic mixtures of at least a hydrophilic, a hydrophobic and an amphiphilic component. Their thermodynamic stability and their nanostructure are two important characteristics that distinguish them from ordinary emulsions which are thermodynamically unstable¹). Microemulsions can protect drug from degradation²). Ovalbumin is protein carrier that used as adjuvant for vaccine. Mean while, many topical vaccines developed to induced imune function response³). Microemulsion expected to protect ovalbumin from degradation. In this study, microemulsions made from ovalbumin, aquabidestillata Span 80, Tween 80 as surfactant and ethanol as cosurfactant (surfactant : cosurfactant = 5:1; 6:1 and 7:1). The aim of this study was to know the influence of curfactant and cosurfactant comparison to microemulsion characteristics. Evaluation of this study included organoleptic, pH, surface tention, particle size distribution and drug entrapment.

MATERIALS AND METHODS

Material used in this study are ovalbumin pharmaceutical grade (Sigma-Aldrich), soy bean oil food grade (Moi Foods), Span 80 cosmetic grade (Croda), Tween 80 cosmetic grade (Croda), ethanol pro analysis (MERCK) dan aquabidestilata (PT. Widatra Bakti), Coomassie Brilliant Blue (Sigma-Aldrich).
 Microemulsion Preparation

Soy bean oil, Span 80, Tween 80 and ethanol 96% mixed in beaker glass with magnetic stirrer at 1000 rpm for 15 minutes then aquabidestilata added and stired at 1500 rpm for 15 minutes. Ovalbumin dissolved in microemulsion and stired at 1500 rpm for 60 minutes.

Evaluation of Microemulsion

Organoleptic

Organoleptic evaluation determined visually including color, odor, and consistension.

pH

pH evaluation determined by Eutech Instrument pH700 pH/ mV/ °C/ °F meter. All measurements were carried out in triplicate

Table 5. Formula of the microemulsion.

Material	Concentration (% b/b)		
	Formula I	Formula II	Formula III
Ovalbumin	1	1	1
Soy bean oil	31	31	31
Span 80	37.38	38.45	39.25
Tween 80	12.62	12.98	13.25
Ethanol 96%	10	8.57	7.5
Aquabidestilata	8	8	8



Surface Tension

Surface tension evaluation determined by Du Noüy tensiometer.

Droplet Size Distribution

Droplet size distribution evaluation determined by Delsa™ Nano Submicron Particle size and Zeta Potential Dynamic Light Scattering. Sample observed in 165° angle and temperature 25°C.

Drug Entrapment

The loaded microemulsion centrifuged in 2500 rpm for 15 minutes. 50 µl filtrate added with aquabidestillata up to 50,0 ml in volumetric flask. 50 µl aliquotes added with 2,5 ml Coomassie Brilliant Blue. Absorbance checked in wave length 620 nm. Ovalbumin absorbance was absorbance difference between loaded microemulsion and unloaded microemulsion.

Statistics

All of the results were analyzed by statistic using one way analysis of variance with degree of believed 95% ($\alpha = 0,05$) and followed by HSD (Honestly Significant Difference). Independent sample t-test used to know the difference between loaded and unloaded microemulsion.

RESULTS AND DISCUSSION

The results of organoleptics evaluation showed that microemulsions have transparent yellow colour and high fluidity for all formulas.

The data showed the mean of pH for unloaded and loaded of formula I were $6.89 \pm 5.77 \times 10^{-3}$ and 6.95 ± 0.036 , formula II were 6.87 ± 0.010 and $6.90 \pm 5.77 \times 10^{-3}$ and formula III were 6.76 ± 0.026 and $6,89 \pm 5.77 \times 10^{-3}$. This showed there was no significant difference between formulas but there is difference between loaded and unloaded microemulsions.

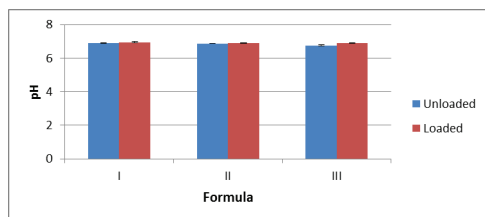


Figure 1. Histogram of microemulsions pH

The results of surface tension studies showed that the mean for unloaded and loaded of formula I were 0.3705 ± 0.0000 and 0.3297 ± 0.0051 Nm⁻², formula II were 0.3562 ± 0.0045 and 0.3397 ± 0.0015 Nm⁻² and formula III were $0,3900 \pm 0,0000$ and 0.3377 ± 0.00351 Nm⁻². This result showed there is difference between formulas for loaded and unloaded microemulsion. Surface tension value decreased after microemulsion loaded with ovalbumin this can be caused ovalbumin had a function as emulsifying agent at the interface of the microemulsion4).

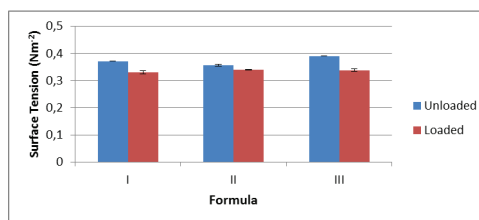


Figure 2. Histogram of microemulsion surface tension

The droplet size distribution for unloaded and loaded of formula I were 30.7 ± 4.01 and 0.26 ± 0.10 mn, formula II were 27.6 ± 2.97 and $23.8 \pm 0,26$ nm and formula III were 27.1 ± 1.70 and 25.0 ± 1.14 nm. This result showed that there was no significant difference between unloaded microemulsion and there was difference between loaded microemulsion. The loaded and unloaded microemulsion had no significant difference result.

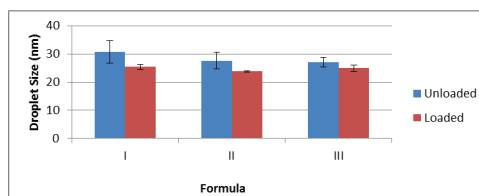


Figure 3. Histogram of microemulsion droplet size



Drug entrapment study showed the mean value of formula I was 25.77 ± 10.12 %, formula II was 46.01 ± 10.12 % and formula III was 29.14 ± 5.84 %. This result showed there was no significant difference between formulas made.

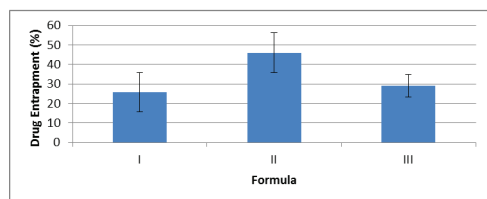


Figure 4 Histogram of microemulsion drug entrapment

CONCLUSION

The best formula can not define because in comparison of surfactant and cosurfactant in microemulsion showed no significant difference in physicochemical characteristic of microemulsion.

REFERENCES

1. Moghimipour E, Salimi A, Eftekhari S (2013). Design and Characterization of Microemulsion Systems for Naproxen. *Advanced Pharmaceutical Bulletin* 3(1), p. 63-71
2. Pathan M, Zikriya A, Quazi A, (2012). Microemulsion: As Excellent Drug Delivery System. *IJPRS V-1, I-3*, p. 199-210
3. Gupta PN, Singh P, Mirsha V, Jain S, Dubey PK, Vyas SP (2004). Topical Immunization: Mechanistic Insight and Novel Delivery Systems. *Indian Biotechnol* (3), January 2004, pp. 9-21
4. Kantarci G, Ozguney I, Karasulu HY, Arzik S and Guneri T (2007). Comparison of Different Water/Oil Microemulsions Containing Diclofenac Sodium: Preparation, Characterization, Release Rate, and Skin Irritation Studies. *AAPS PharmSci Tech.*, 8 (4) Article 91



pH INFLUENCE IN DESALTING PROCESS OF CRUDE PERTUSSIS TOXIN (PT) AND FILAMENTOUS HEMAGGLUTININ (FHA) PURIFICATION FROM *Bordetella pertussis* BY SEPHADEX G-25 COLUMN CHROMATOGRAPHY

Faris Adrianto, Airlangga University Department of Pharmaceutical chemistry, farisadrianto@gmail.com; **Esti Hendradi**, Airlangga University Department of Pharmaceutical sciences; **Neni Nurainy**, Biofarma; **Isnaeni**, Airlangga University Department of Pharmaceutical chemistry

INTRODUCTION

Preventing human infection by vaccination had been done by more than two centuries. Pertussis, commonly called whooping cough—is a highly contagious bacterial disease caused by *Bordetella pertussis*. In some countries, this disease is called the 100 days' cough or cough of 100 days. Symptoms are initially mild, and then develop into severe coughing fits, which produce the namesake high-pitched “whoop” sound in infected babies and children when they inhale air after coughing. The coughing stage lasts approximately six weeks before subsiding (Mahon et al., 2001).

The best way to prevent pertussis is to get vaccinated. Two different types of pertussis vaccine have been used in infant immunization programs. The whole-cell pertussis vaccine (Pw) consists of heat- and formalin-inactivated virulent whole bacteria, whereas the acellular pertussis vaccine (Pa) is composed of purified components of the bacteria, typically including inactivated pertussis toxin (PT) and Filamentous Hemagglutinin. Immunization with Pw has a high degree of efficacy and is associated with the induction of antigen-specific Th1 cells (Noble et al., 1987).

Purification of Acellular pertussis components has been done by many researchers before. This research was means to study the effect of pH in desalting, a step of purification of pertussis toxin (PT) and Filamentous Hemagglutinin (FHA) from *Bordetella pertussis*

MATERIALS AND METHODS

Equipments:

GE ÄKTApurifier UPC 900, Column GE XK 16, Resin Hydroxy Apatite (HA) Ultrogel®, Column

GE HiTrap® Desalting 5 mL, Sample Collector Frac-950, Column Sepharose, Vertical electrophoresis Mini-Protean®3 Cell BIO-RAD, Waterbath 95 oC, Varimix, Polystyrene microtitres plate, ELISA reader, Nanodrop 2000 spectrophotometer

Materials:

Bordetella pertussis Tahoma strain isolate (isolated by PT. BioFarma), NaOH 0.5 M ,WFI, Phosphate Buffer (PB) 50 mM pH 6, 7, and 8. Ethanol 20%, SDS PAGE kits, *B. pertussis* PT anti serum (sheep), antibody FHA anti serum (sheep), standard antigen FHA (JN1H-4), anti FHA monoclonal (JN1H-11), washing buffer (0.05% Tween 80 in aquadest), dilution buffer (0.1% protifar and 0.05% Tween 80 in PBS pH 7.2), blocking buffer (Protifar 0.05 gram in 50 mL PBS), standard Purified PT JN1H-5, anti-PT S1 subunit monoclonal antibody 10D6, Anti PT JN1H-12, anti mouse peroxidase conjugate, substrat TMB (Sodium acetate buffer pH 5.5 +in ethanol 96% + H2O2 7.5 mL buffer asetat + 125 uL TMB/Etanol 96% + 1.5 uL H2O2, 2M H2SO4

Methods:

1. Capturing PT dan FHA

Capturing was done for PT and FHA in the previous research. The sample obtained were used for this research.

2. Desalting PT and FHA

XK 16 Column packed with Sephadex G-25 medium 25 ml was attached to ÄK TApurifier UPC 900 system. WFI 4 CV was flows through the column with flowrate 0.5 mL/min. For the column stabilization,

phosphate Buffer (PB) 50 mM with suitable pH (6, 7, or 8) was flows with flow rate 1 mL/min. Sampel crude PT-FHA were injected and eluated with phosphate Buffer (PB) 50 mM pH 6.0 flowrate 1 mL/min. Fraction which produces peak were collected, and protein concentration were calculated for each fraction.

3. Protein quantitation

Protein quantitation was done using Nanodrop 2000 spectrophotometer with 280 nm wavelength.

4. SDS PAGE

SDS PAGE fpr the protein fraction was done using Vertical elektrophoresis Mini-Protean®3 Cell BIO-RAD with standard SDS PAGE kit

5. ELISA

ELISA was done using suitable ELISA kits for PT and FHA

RESULT AND DISCUSSION

1. Capturing PT dan FHA

Capturing was done in the previously re search and the protein concentration resulted was shown in the next table.

Sample ID	Protein Conc.	Unit	A280
161111-A4	1077	µg/ml	1,077
161111-A4	1090	µg/ml	1,090

Table 1. Protein concentration for the desalting process

After the protein concentration was obtained, ELISA was done to specify the PT and FHA in the sample. The ELISA resulted for PT titre in crude PT-FHA was 5,5 µg/mL and the FHA titre was 32,8 µg/mL. SDS PAGE was done to confirm which as the fractions obtained contain PT and FHA.

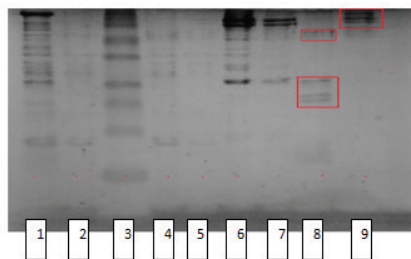
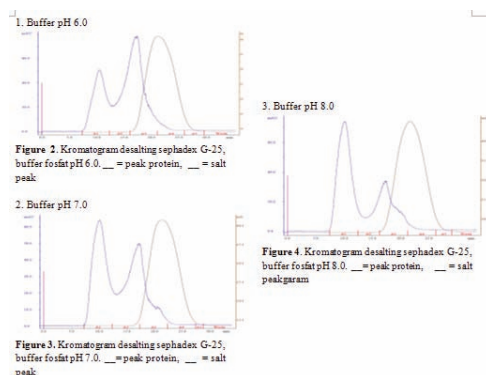


Figure 1. SDS PAGE for PT and FHA (6-7 were the samples, 8 are standard FHA, 9 are standard PT)

2. Desalting of PT and FHA

Desalting of PT and FHA were done using previously methods and the chromatogram resulted was shown in the next figure.



This result shown that the protein and the salt were not completely separated. But sample can be obtained by isolate the peak that were completely separated. After the chromatogram was obtained, the sample protein recoveries were calculated . The result was shown in the next table

Buffer pH	Protein recoveries
6.0	46.04%
7.0	74.23%
8.0	55.23%

Table 2. Protein recoveries in the desalting process



ACKNOWLEDGEMENTS

We thank PT. Biofarma Bandung for giving full supports for this research including materials and equipments

CONCLUSION

Elution pH influences the recovery percentage of the sample protein. The optimum recovery percentage resulted from the use of phosphate buffer pH 7.0 with 74,23 + 3,07 % recoveries percentage

REFERENCES

- *. Erkan O., Kamer K., Ozlem B., Ayfer G., (2003). Rapid purification of pertussis toxin (PT) and filamentous hemagglutinin (FHA) by cation-exchange chromatography. *Vaccine* 22: 1570-1575
- *. Hagel L. and Janson J.C., (2002). Size-exclusion chromatography, in Heftmann, E (ed), *Chromatography*, 5th edition. Amsterdam: Elsevier pp. A267-AA307.
- *. Hagel L., 1999. Gel Filtration in J.-C. Janson and L. Rydén (ed), *Protein Purification. Principles, High Resolution Methods and Applications*. New York: VCH Publisher Inc. p. 63–106.
- *. Mahon B.P., Darren P.J., Cassidy P., (2001). Acellular pertussis vaccine protects against exacerbation of allergic asthma due to *Bordetella pertussis* in a murine model. *Clin. Diagn. Lab. Immunol.* 12(3): 409-417
- *. Noble G.R., Bernier R.H., Esber E.C., Hardegree C., Hinman A.R., Klein D, Saah A. (1987). Acellular and whole cell pertussis vaccine in Japan. Report of a visit by US scientist. *J. Am. Med. Assoc.* 257: 1351-1356
- *. Sato Y., Cowell JI., Sato H. Burstin D.G., Manclark C.R., (1993). Separation and purification of the hemagglutinin from *Bordetella pertussis*. *Infect Immun* 41(1): 313-20

SEPARATION OF COSMETIC PRESERVATIVES USING SILICA-BASED MONOLITHIC COLUMN

Febri Annuryanti, Department of Pharmaceutical Chemistry, Faculty of Pharmacy, Airlangga University, Surabaya, febriannuryanti@yahoo.com; **Riesta Primaharinastiti**, Department of Pharmaceutical Chemistry, Faculty of Pharmacy, Airlangga University, Surabaya; **Moch. Yuwono**, Department of Pharmaceutical Chemistry, Faculty of Pharmacy, Airlangga University, Surabaya

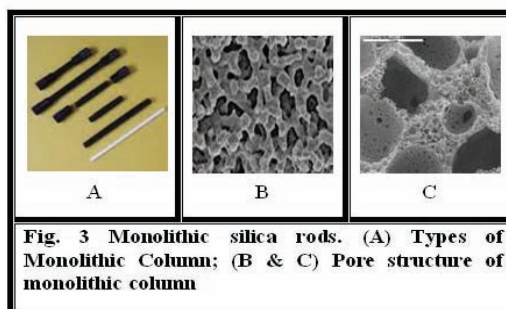
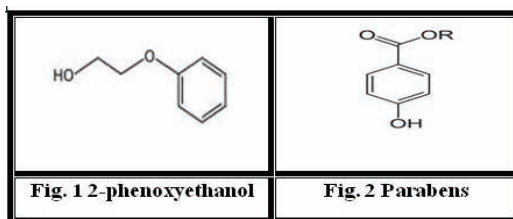
INTRODUCTION

Cosmetic products are particularly susceptible to microbial growth due to the nature of their ingredients. To prevent them from decay, preservatives such as 2-phenoxy ethanol and parabens have been commonly used as additives. Although the preservatives are frequently used in various cosmetic products, they are harmful at higher than permitted safety levels. Phenoxyethanol (1-hydroxy-2-phenoxyethanol) (Figure 1) is an organic chemical compound, a glycol ether, often used in dermatological products such as skin creams and sunscreen. It is a colorless oily liquid, a bactericide, usually used in conjunction with quaternary ammonium compounds, and often used in place of sodium azide in biological buffers as 2-phenoxyethanol which is less toxic and non-reactive with copper and lead. It is also used as a fixative for perfumes, an insect repellent, a topical antiseptic, a solvent for cellulose acetate, same dyes, inks, resins, preservatives pharmaceuticals, and in organic synthesis. It is moderately soluble in water. It is used as an anesthetic in the aquaculture of some fish. [1,2]. In Japan its usage level in cosmetic products is regulated. [3]

Parabens (Figure 2) are a class of chemicals widely used as preservatives in the cosmetic and pharmaceutical industries. Parabens are effective preservatives in many types of formulas. These compounds, and their salts, are used primarily for their bacteriocidal and fungicidal properties. Parabens can be found in shampoos, commercial moisturizers, shaving gels, personal lubricants, cosmetics, topical/parenteral pharmaceuticals, spray tanning solution and toothpaste. They are also used as

food additives. [4]

The most common analytical technique used for separation and determination of preservatives in cosmetics products is HPLC using RP-18 column. The method demonstrates a good sensitivity, however, the peaks are not good resolved and a longer analysis time needed. Monolithic HPLC columns consist of highly porous silica with a bimodal pore structure, which gives greatly improved chromatographic performance in terms of separation performance and column back pressure (Fig. 3) [5,6]



MATERIALS AND METHODS

Materials

Phenoxyethanol, methyl-, ethyl-, propyl-, and butylparaben standard were obtained from PT. Malidas Sterilindo, Buduran, Sidoarjo; HPLC Agilent LC-1100, Chromolith RP-18 (100 x 4.6)



MATERIALS AND METHODS

Materials

Phenoxyethanol, methyl-, ethyl-, propyl-, and butylparaben standard were obtained from PT. Malidas Sterilindo, Buduran, Sidoarjo; HPLC Agilent LC-1100, Chromolith RP-18 (100 x 4.6) mm stationary phase was obtained from Merck (Darmstadt, Germany); μ Bondapak C18 (300 x 3.9) mm column (Waters) was also used for this study. Methanol (J.T Baker, USA) and acetonitrile (Lichrosolv, Merck, Darmstadt, Germany) of HPLC grade and distilled water (PT. Otsuka Indonesia) were used as mobile phase. Whatman 0.2 μ m membrane filter was purchased from commercial suppliers; phosphate buffer pH 3 was freshly prepared in our laboratory.

Method

Two kinds of mobile phase systems (the mixture of acetonitrile and phosphate buffer pH 3; the mixture of methanol and water) and two columns (μ -Bondapak and Chromolith column) were used to find the optimum condition for separation of preservatives in cosmetics. Each mobile phase system with gradient flow was used in each column to find the optimum condition for peak separation. (CDER, 1994). The standard of phenoxyethanol, methylparaben, ethylparaben, propylparaben, and butylparaben were injected to the HPLC system. The wavelength was set at 254 nm.

RESULTS AND DISCUSSION

Two different columns have been used to separate preservatives in cosmetics. Some condition of experiment were used to achieve a good separation of cosmetics preservatives contains phenoxyethanol, methylparaben, ethylparaben, propylparaben, and butylparaben. The mixture of standard was injected to HPLC system.

The optimum condition for separating preservatives using μ Bondapak C18 column was obtained when phosphate buffer pH 3 and

acetonitrile were used as mobile phase with flow 1 mL/min and gradient system (Table 1). The retention time was 20 minutes (Figure 4). When the mixture standard of preservatives passed through Chromolith column, a good separation was obtained by using methanol and water as mobile phase with flow rate 3 mL/min and a gradient system (Table 2). The HPLC separation time for cosmetic preservatives using Chromolith Column is less than 6 minutes (Figure 5).

Time	Mobile Phase	
	Phosphate Buffer pH 3	Acetonitrile
0-12	80	20
13-15	20	80
15-20	80	20

Table 1. Gradient flow system for μ Bondapak C₁₈ column

Time	Mobile Phase	
	Methanol	Water
0-1	10	90
1-4	35	65
4-6	10	90

Table 2. Gradient flow system for Chromolith column

CONCLUSION

From the result, it showed that Chromolith column with mobile phase system methanol : water, flow rate 3 mL/min and a gradient flow system gives a minimum retention time compared with μ Bondapak column when it is used to separate cosmetics preservatives containing phenoxy-ethanol, methyl-, ethyl-, propyl- and butylparaben. The method can be used to determine the concentration of preservatives in cosmetics.

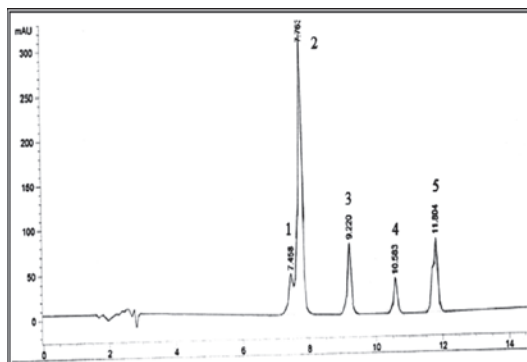


Figure 4. Chromatogram of preservatives separation using Bondapak column (1) 2-phenoxyethanol; (2) methyl-; (3) ethyl-; (4) propyl-; and (5) butylparaben

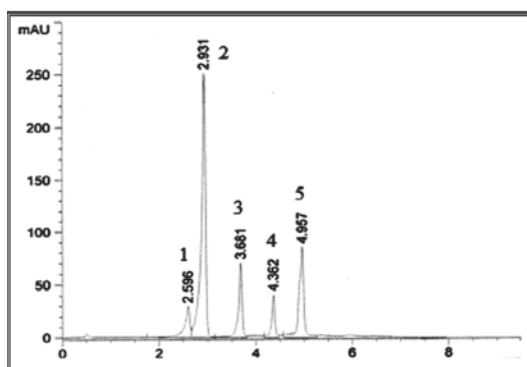


Figure 5. Chromatogram of preservatives separation using Chromolith column (1) 2-phenoxyethanol; (2) methyl-; (3) ethyl-; (4) propyl-; and (5) butylparaben

REFERENCES

1. Tsantilasa H., Galatosa A.D., Athanassopoulou F., Prassinosa N.N., and Kousoulaki K., 2006, Efficacy of 2-phenoxyethanol as an anaesthetic for two size classes of white sea bream, *Diplodus sargus* L., and sharp snout sea bream, *Diplodus puntazzo* C., *Aquaculture*, Vol. 253, 1-4, p. 64-70
2. Mylonas C., Cardilanetti G., Sigelaki I., Polzonetti-Magni A., 2005, Comparative efficacy of clove oil and 2-phenoxyethanol as anesthetics in the aquaculture of european sea bass (*Dicentrarchus labrax*)

and gilthead sea bream (*Sparus aurata*) at different temperatures. *Aquaculture*, vol. 246, 1-4, pp. 467-481

3. Tokunaga H., Takeuchi, O., Ko R., Uchino T., Ando M., 2003, "Studies for analyzing phenoxyethanol and parabens in commercial lotions", *Kokuritsu Iyakuhin Shokuhin Eisei Kenkyujo hokoku = Bulletin of National Institute of Health Sciences* (121): 25-9. ISSN 1343-4292. PMID 14740401
4. Polati S., Gosetti F., and Gennaro M.C., 2007, *Preservatives in Cosmetics. Regulatory Aspects and Analytical Methods, Analysis of cosmetics Products*, Elsevier BV, UK, p. 211-241
5. Mellwick R., 1994, *Monolithic silica columns : Benefits and applications of Chromolith® HPLC columns*
6. Cabrera K., Lubda D., Eggenweiler HM., Minakuchi H., Nakanishi K., 2000, A new monolithic-type HPLC column for fast separations, *Journal of High Resolution Chromatography*, Volume 23, Issue 1, pages 93-99.
7. Center for Drug Evaluation and Research (CDER), 1994, *Reviewer Guidance : Validation of Chromatographic Methods*, p. 2



PREPARATION AND CHARACTERIZATION OF TELMISARTAN-CITRIC ACID CO-CRYSTAL

Fikri Alatas, Faculty of Pharmacy, University of Jenderal Achmad Yani, Cimahi, fikrifaza@yahoo.co.id; Hestiary Ratih, Faculty of Pharmacy, University of Jenderal Achmad Yani, Cimahi; Sundani Nurono Soewandhie, School of Pharmacy, Institut Teknologi Bandung, Jl. Ganesha, No. 10, Bandung

ABSTRACT

Telmisartan (TMS) is an antihypertension that has a very low solubility in water. The aim of this study is to prepare and characterize co-crystal formation between TMS and citric acid (CIT). TMS-CIT co-crystal was prepared by solvent-drop grinding methods using methanol as solvent. The characterization of co-crystal was conducted by powder X-ray diffraction (PXRD), Fourier transform infrared (FTIR), and polarized microscope. The solubility and in vitro dissolution tests were performed to know changed in physical properties. The PXRD pattern, FTIR spectra, and photomicroscope of co-crystal were different from its starting components. TMS and CIT can form co-crystal that can increase the solubility and dissolution rate of TMS.

Keywords: telmisartan, citric acid, co-crystal, solubility, dissolution.

INTRODUCTION

Telmisartan (TMS) is an angiotensin II receptor blocker was used to treat hypertension. TMS has a very low solubility in water, so its dissolution rate is low. Co-crystals appeared as a solid form that promises to change the solubility, dissolution, and other physicochemical properties of the drug substance (McNamara et al., 2006). Pharmaceutical co-crystals provide an alternative to chemical modification of the drug substance as well as established salt, amorphous, solvate, and polymorphic drug forms that all have limitations in their utility (God and Rodriguez-Hornedo, 2009). The purpose of the study was to prepare a new co-crystal of TMS having better solubility by forming a co-crystal with citric acid.

MATERIALS AND METHODS

Materials

Telmisartan (TMS) commercial material with purity of >99% was obtained from Glenmark Pharmaceutical Limited, Mumbai, India. Citric acid monohydrate (CIT), methanol and other reagents were obtained from Merck Chemicals Indonesia without any purification.

Preparation of Co-crystal TMS-CIT by Solvent-drop Grinding

Equimolar quantities of TMS and CIT were combined in a mortar, and the material was ground together with the addition of three drops of methanol for five min. After grinding, the product was dried and stored at ambient temperature.

Characterization by PXRD

Experiments were performed on a Philips PW1710 X-ray diffraction system, using Cu K α radiation ($\lambda = 1.54180 \text{ \AA}$), 40 kV/40 mA. Data collected at room temperature in the scan range of $2\theta = 3^\circ$ to 45° .

Characterization by Fourier Transform Infrared (FT-IR)

Infrared spectra were recorded by using an FT-IR Affinity-1 spectrophotometer (DRS-8000) Shimadzu, Japan. The pure TMS, CIT, and co-crystal sample were previously ground and mixed thoroughly with KBr.

Characterization by Polarized Microscope

The physical mixture TMS-CIT (1:1) was placed on object glass. A drop of methanol was added to the physical mixture until dissolved and allowed to recrystallize. Recrystallization process was observed under a polarizing microscope and compared to the recrystallization of its pure components. The microscopic images were recorded with Optilab Advance camera

attached to the Olympus BX-53 polarized microscope.

Solubility Determinations

The solubility of TMS in water from TMS-CIT co-crystal and pure TMS were tested at room temperature using an orbital shaker. Excess amounts of compound were added to 10 mL of water, mix it continuously and then filtered after 24 h of equilibration. The bulk solutions were measured spectrophotometrically.

In Vitro Dissolution Test

Dissolution test of TMS from TMS-CIT co-crystal and pure TMS were carried out in pH 7.5 phosphate buffer solution (900 ml, $37 \pm 0.5^\circ\text{C}$, 75 rpm) for 60 min using the USP XXIII paddle apparatus (ZRS-6G, Tianjin, China). At predetermined time intervals, 10 ml samples were withdrawn and spectrophotometrically assayed for drug concentration at 295 nm.

RESULTS AND DISCUSSION

Preparation of Co-crystal TMS-CIT by Solvent-drop Grinding

Solvent-drop grinding involves the grinding of two materials together and a small quantity of solvent. This method only uses less solvent, so the method is more cost-effective and environmentally friendly than solution method (Trask et al., 2004). The presence of a small amount of the liquid phase can improve the rate of co-crystal formation (Shan et al., 2002).

Characterized of TMS-CIT Co-crystal formation
The co-crystal formation is mainly characterized by powder X-ray diffractometer (PXRD). If the resulting PXRD pattern of the solid product after milling pure solid compounds (drug and cofomer) is different from the reactants, it can be concluded that the new solid phase was formed (Shanpui et al., 2011). Fig. 1a shows the diffractogram of the product after solvent-drop grinding was different from its starting components. It was indicated TMS-CIT co-crystal formation. The TMS-CIT co-crystal have characterized peaks at about 6,3; 8,9; 10,0; 11,1; 15,7; 17,5; 20,1; 22,4; dan $27,5^\circ$.

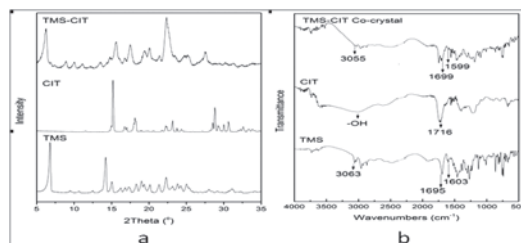


Figure 1. PXRD patterns (a) and FT-IR spectra (b) of TMS-CIT co-crystal compared to its starting components.

Infrared spectroscopy can be a very powerful tool in detecting co-crystal formation (Schultheiss and Newman, 2009). In the Fig. 1b, the shift of the -OH group and the imine group (C=N) of TMS from 3063 and 1603 cm^{-1} to 3028 and 1646 cm^{-1} , respectively after grinding process indicated the formation of co-crystal TMS-CIT. The disappeared of broad peak of OH group (3000-3300 cm^{-1}) from water molecule in the citric acid monohydrate showed co-crystal containing no water hydrate.

The TMS-CIT co-crystal formation can be observed under the polarized microscope after addition of a few drops of methanol. Fig. 2 shows the difference in crystal habit after a physical mixture of TMS-CIT recrystallized in methanol with TMS and CIT crystal habits. This indicates the formation of TMS-CIT co-crystal after the addition of methanol.

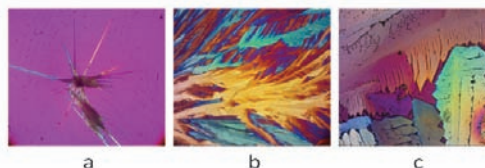


Figure 2. polarized microscope photo of TMS (a), CIT (b), and TMS-CIT co-crystal after recrystallized in methanol.

Solubility and in Vitro Dissolution Test

Solubility experiments showed that solubility of TMS in water increased in the TMS-CIT co-crystal. The solubility of TMS from pure TMS and TMS-CIT co-crystal were 3.9 ± 0.2 and 10.5 ± 0.1 $\mu\text{g/mL}$, respectively. The dissolution profiles of TMS from both pure TMS and TMS-



CIT co-crystal in pH 7.5 of phosphate buffer solution were shown in Fig 3. The percentage of TMS dissolved after 60 min or dissolution percentage (DP60min) from TMS-CIT co-crystal was higher than from pure TMS.

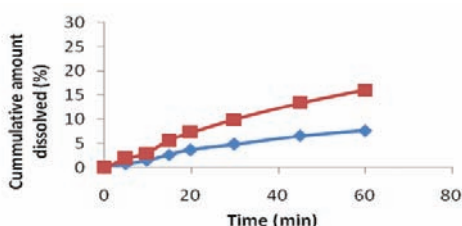


Figure 3. Dissolution profiles of TMS from pure TMS (—♦—) and TMS-CIT co-crystal (—■—)

CONCLUSION

The characterization by PXRD, FTIR, and polarized microscope methods showed that TMS and CIT formed co-crystal after solvent-drop grinding using methanol as solvent. The solubility and dissolution rate of TMS from TMS-CIT co-crystal higher than from pure TMS.

ACKNOWLEDGEMENT

We thanks to Directorate General of Higher Education of the Ministry of Education and Culture Indonesia for research grant.

REFERENCES

1. Jones W, Motherwell WDS, and Trask AV. (2006). Pharmaceutical cocrystals: an emerging approach to physical property enhancement. *MRS Bulletin*, 31:875-79.
2. Schultheiss N and Newman A. (2009).

Pharmaceutical cocrystals and their physicochemical properties. *Cryst Growth Des*, 9(6):2950-67.

3. McNamara D, Childs SL, Giordano J, Iarriccio A, Cassidy J, Shet MS, Mannion R, O'Donnell E, and Park A. (2006). Use of a glutaric acid cocrystal to improve oral bioavailability of a low solubility API. *Pharm Res*, 23, 1888-97.
4. Shanpui P, Goud NR, Khandavilli UBR, and Nangia A. (2011). Fast Dissolving Curcumin Cocrystals. *Cryst Growth Des*, 11, 4135-145.
5. Trask AV, Motherwell WDS, Jones W. (2004). Solvent-drop grinding: Green poly-morph control of cocrystallisation. *Chem Comm*, 890-91.
6. Good DJ, Rodriguez-Hornedo N. (2009). Solubility advantage of pharmaceutical cocrystals. *Cryst Growth Des*, 9, 2252-64.
7. Shan N, Toda F, and Jones W. (2002): Mechanochemistry and co-crystal formation: Effect of solvent on reaction kinetics. *Chem Comm*, 2372-73.



PATIENTS' AND CAREGIVERS' LIQUID MEDICATION ADMINISTRATION ERRORS

Gusti Noorrizka Veronika Achmad, MSc., Apt., Department of Pharmacy Practice Faculty of Pharmacy Universitas Airlangga, Dharmawangsa Dalam, Surabaya 60286, gustirizka@yahoo.com, +62315033710; **Gesnita Nugraheni**, MSc., Apt., Department of Pharmacy Practice Faculty of Pharmacy Universitas Airlangga, Dharmawangsa Dalam, Surabaya 60286, gesnita@gmail.com, +62315033710

INTRODUCTION

Medication error is defined as “any preventable event that may cause or lead to inappropriate medication use or patient harm while the medication is in the control of the health care professional, patient, or consumer. Such events may be related to professional practice, health care products, procedures, and systems, including prescribing; order communication; product labeling, packaging, and nomenclature; compounding; dispensing; distribution; administration; education; monitoring; and use” (US Food and Drug Administration, 2014).

Medication errors related to dispensing of medication at a pharmacy can occur because of several factors starting from pharmacists' heavy workloads, disturbance or distraction during dispensing the medication, working environment for example inadequate lighting, similar name of medications, the provision of inadequate drug information and others (Leedock, 2011).

Oral liquid medications are widely used either with or without prescription (self-medication), especially for pediatric and adult patients who have difficulty swallowing tablets or capsules. There is potential medication errors in administered oral liquid medications related to imprecise dose of the drug. The study in Minnesota found that a household teaspoon was the most frequently devices used for measuring liquid medication (J Madlon-Kay et al, 2000). According to the AAP Committee on Drugs, the volume of household teaspoons can range from 2 to 10 ml, on the other hand the volume of one teaspoon in liquid medication referred

to 5 ml.

However, although in other countries the information about the current use of oral liquid medication and its devices were easily found, there is limited information regarding to the administration of oral liquid medications by patients and caregivers in Indonesia.

METHODS

The interview was conducted in three community pharmacies in Surabaya, Indonesia. This study was a convenience sample of adult patients and caregivers who visited the pharmacy to purchase non-prescription oral liquid medication or receive liquid medication prescribed by a doctor during September 2014 to October 2014.

The interview consisted of several parts. First, we collected demographic information. Second, participants were shown the following liquid dosing devices: dosing spoon, printed dosing cup, and dropper. Furthermore, they were shown a household teaspoon and table-spoon. They were asked which of the dosing devices they usually use for dispensing oral liquid medications. Third, the participants were asked to demonstrate how they would measure the oral liquid medications. The volume was later measured by graduated cylinder glass.

We adapted the classification of liquid medication error rates from Gyeong Suk Ryu et al who classified liquid medication error into 4 groups, which are less than 5%, 6% to 10%, 11% to 20%, and more than 20%. The targeted volume was the volume instructed in the brochure, label or the medicine packaging box depends.



RESULTS AND DISCUSSION

Participant characteristic and dose errors are shown in Figure 1. During the study period, 80 participants agreed to participate. The majority of the participants were caregivers (73.8%, n=80) and 58.8% (n=80) were female, which is consistent with results obtained in previous study (J Madlon-Kay et al, 2000 and Yin et al 2014). Mother has the main role in the family as a caregiver. Therefore, female is more likely administering the medication for the patient compare to male. Seventy one participants (88.7%) were younger than age 47 and 73.7%

(n=80) participants were high school graduate or higher. At least 40% (n=59) of the participants whose high school degree or higher degree were practicing large dose errors.

The figure 1 reveals that more than fifty percent (51.3%) of the participants have large dose errors in measuring oral liquid medication, both female and male participants shares almost equal number. Of the 29 participants who chose tablespoon and teaspoon as their common measuring devices, 20 (71.4%) experienced large dose errors. In spite of using the correct calibrated measuring devices, 40%

PARTICIPANT CHARACTERISTIC		% (n)	No or Small Dose Errors		Large Dose Errors	
			≤5%	6%-10%	11%-20%	>20%
Gender	Male	41.2 (33)	36.4 (12)	18.2 (6)	6.1 (2)	39.4 (13)
	Female	58.8 (47)	29.8 (14)	14.9 (7)	19.1 (9)	36.1 (17)
Age (in years)	17-26	25.0 (20)	20.0 (4)	25.0 (5)	30.0 (6)	30.0 (6)
	27-36	36.3 (29)	34.5 (10)	6.9 (2)	13.8 (4)	41.4 (12)
	37-46	27.5 (22)	36.4 (8)	22.7 (5)	4.6 (1)	63.6 (14)
	>47	11.3 (9)	44.4 (4)	11.1 (1)	0.0 (0)	44.4 (4)
Status	Caregiver	73.8 (59)	35.6 (21)	16.9 (10)	13.6 (8)	33.9 (20)
	Patient	26.2 (21)	23.8 (5)	14.3 (3)	14.3 (3)	47.6 (10)
Education	Elementary school graduate	6.2 (5)	40.0 (2)	40.0 (2)	0.0 (0)	20.0 (1)
	Middle school graduate	16.3 (13)	38.5 (5)	15.4 (2)	15.4 (2)	30.8 (4)
	High school graduate	47.5 (38)	36.8 (14)	13.2 (5)	13.2 (5)	36.8 (14)
	College graduate or higher	26.2 (21)	23.8 (5)	14.3 (3)	19.0 (4)	42.9 (9)
	Others	3.8 (3)	0.0 (0)	33.3 (1)	0.0 (0)	66.7 (2)
Medication Measuring devices	Tablespoon	35.0 (28)	13.6 (3)	22.2 (6)	14.8 (4)	55.6 (15)
	Teaspoon	1.3 (1)	0.0 (0)	0.0 (0)	0.0 (0)	1.3 (1)
	Dosing spoon	53.8 (43)	41.9 (18)	16.3 (7)	11.6 (5)	30.2 (13)
	Printed dosing cup	6.3 (5)	80.0 (4)	0.0 (0)	20.0 (1)	0.0 (0)
	Dropper	1.3 (1)	0.0 (0)	0.0 (0)	0.0 (0)	100.0 (1)
	Changing over time	2.5 (2)	50.0 (1)	0.0 (0)	50.0 (1)	0.0 (0)



(n=49) of the participants still experienced large dose errors in measuring their liquid medication.

More than 90% (91.3%, n=80) participants purchased their medicine without prescription (self-medication). Of the 80 oral liquid medications purchased by participants, 30 were not equipped with any dosing devices. Furthermore 60% (18) of these participants choose household tablespoon and teaspoon for measuring their medication. As illustrated in Figure 1, dosing spoon (53.8%, n=80) and tablespoon (35.0%, n=79) were the most common devices used for measuring liquid oral medication. This finding is similar to previous studies (J Madlon-Kay et al, 2000 and Yin et al, 2007). Data obtained in previous studies indicated that regardless the recommendation from American Academy of Pediatrics (AAP) against use of unstandardized dosing instrument; patient and caregiver continue to use household tablespoon and teaspoon for administering their liquid oral medicine (J Madlon-Kay et al, 2000)

The most frequently oral liquid medication purchased was product for cough, cold and flu, both single component and multi-components (66.0%, n=80) as demonstrated by Figure 2. According to Berardi et al, there were seven conditions commonly treated with nonprescription drugs, such as pain, cough/flu/cold/sore throat, allergy/sinus problem, heartburn/indigestion, constipation/diarrhea/gas, minor infections, and skin problem.

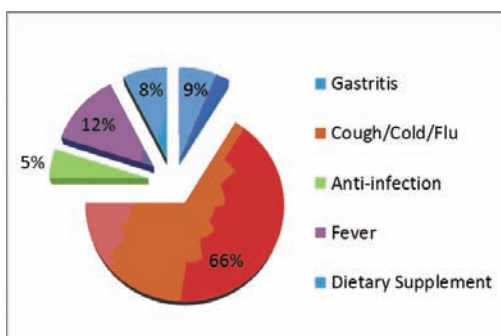


Figure 2: Type of Oral Liquid Medication Purchased

As can be seen in Figure 3, there are 8 age groups namely 0 to 1 years (infant), 1 to 3 years (toddler), 4 to 12 years (children), 13 to 18 years (adolescent), 19 to 25 years (late adolescent), 26 to 45 years (adult), 46 to 59 years (middle age), and 60 years old and above (elderly). More than 80% (n=59) patient supervised by caregiver were toddler and children.

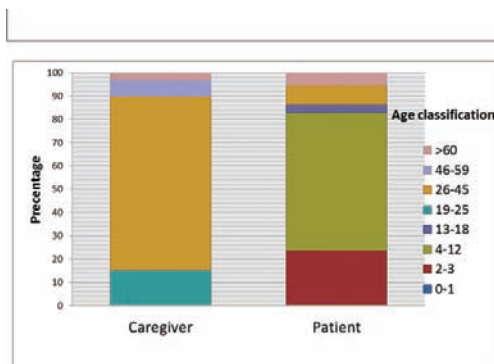


Figure 3: Age classification caregiver and their patient

It is alarming that almost 50% (28) of the caregivers had experienced large dose errors which may lead to overdosing. A systematic review on incidence and nature of dosing errors in pediatric revealed that eleven of the 16 studies found that dosing errors are the most common type of medication error (Wong et al, 2004).

CONCLUSION

Our study revealed that more than fifty percent of the participants have large dose errors in measuring oral liquid medication, both female and male participants shares almost equal number. Dosing spoon and tablespoon were the most frequently used dosing devices in administering oral liquid medication. Despite the correct choosing of dosing devices, the large dosing errors were found.



REFERENCES

- *. Berardi, Rosemary R. (2009). Hand book of Nonprescription Drugs 16th Edition:4.
- *. Gong Suk Ryu, Yu Jeung Lee (2012). Analysis of Liquid Medication Dose Errors Made by Patients and Caregivers Using Alternative Measuring Devices. *Journal of Managed Care Pharmacy*, July/August;18(6):439-445.
- *. J. Madlon-Kay, Diane, Mosch, Frederick S. (2000). Liquid Medication Dosing Errors. *The Journal of Family Practice*, August;49(08).
- *. US Food and Drug Administration, Medication Error. <http://www.fda.gov/drugs/drugsafety/medicationerrors/> Accessed November 7, 2014.
- *. Wong IC, Ghaleb MA, Franklin BD, Barber N., Incidence and Nature of Dosing Errors in Paediatric Medications: A Systematic Review. <http://www.ncbi.nlm.nih.gov/pubmed/15230647> Accessed November 12, 2014
- *. Yin, H. Shoona, Dreyer, Benard P. (2014). Liquid Medication Dosing Errors in Children: Role of Provider Counseling Strategies. *Academic Pediatrics*, May-June; 14(3):262-270.

THE POTENCY OF CANARIUM OIL (*Canarium indicum*) AS A MATERIAL FOR STRUCTURED LIPID PRODUCTION

Hamidah Rahman, Public Health Department, Muhammadiyah University of North Maluku, KH Ahmad Dahlan Street Ternate 97719 Indonesia, hamidahr42@gmail.com, +6281220480009; **Johner P Sitompul**, Chemical Engineering Department, Faculty of Industrial Technology Institute of Technology Bandung, Ganesha 10 Street Bandung 40132 Indonesia, sitompul@che.itb.ac.id, +628122167413; **Kusnandar Anggadiredja**, School of Pharmacy Institute of Technology Bandung, Ganesha 10 Street Bandung 40132 Indonesia, +6281513955364; **Tutus Gusdinar**, School of Pharmacy Institute of Technology Bandung, Ganesha 10 Street Bandung 40132 Indonesia, gusdinar@fa.ac.id, +62811237125

INTRODUCTION

The exploration to find the sources of fatty acids, especially essential fatty acids for humans and beneficial to health is still ongoing. This is due to the results of studies showing that unsaturated fatty acids (omega 3, omega 6 and omega 9) could be used to prevent and treatment several diseases, such as atherosclerosis, Alzheimer's, arthritis and inflammation (Kuhnt, et al. 2012). This paper studies the potency of canarium oil that used in manufacturing of structured lipid. Structured lipid is a triglyceride that has been modified by changing the composition or distribution of fatty acids position on the glycerol backbone through chemical conversions, enzymatic reactions and or genetic engineering. Structured lipids could be applied to nutritional, pharmaceutical, or medical applications (Osborn and Akoh. 2002).

METHODS

In particular, this research have extracted and characterized the composition of fatty acids in canarium oil, followed by the synthesis of 2-monoacylglycerols (2-MAGs) using 1,3 specific lipase against canarium oil as a substrat. Product of 2-MAGs will then be used for the synthesis of a structured lipid by incorporating medium chain fatty acid in position sn-1 and sn-3 of 2-MAGs compound in the next work. Oil extraction was performed by mechanical pressing with consideration that oil content in canarium seeds large enough and without using organic solvents. Analysis of

fatty acids composition was carried out by gas chromatography-mass spectroscopy (GC-MS) and high performance liquid chromatography (HPLC). Enzymatic reaction for synthesis of 2-MAG was conducted in an orbital shaker waterbath and followed purification by solvent extraction based on procedure by Esteban et al .

The characterization of products using thin layer chromatography and analysis of fatty acids composition by HPLC.

RESULT AND DISCUSSIONS

The result of the hydraulic-pressure extraction obtained the yield of oil was 70 % with the highest fatty acid composition respectively were oleic acid (47.0 %), palmitic acid (30.0%), stearic acid (15.3 %), and linoleic acid (7.3 %).





Figure 1. Characterization of reaction products (MAGs, DAGs, TAGs and EE) by thin layer chromatography using chloroform/acetone/methanol (95/4.5/0.5) as mobile phase, spots were visualized by iodine vapor. Hydroethanolic phase is coded by A and hexanic phase is coded by B. Comparison with spots using 2-oleoyl glycerol (C).

The characterization of 2-MAGs by thin layer chromatography using a standard 2-oleoylglycerol (Figure 1), purification by solvent extraction and followed by isolation to determine the fatty acids composition by preparative thin layer chromatography. After incubation

for 6 hours in an orbital shaker waterbath, temperature 35 °C with a shaking speed of 248 rpm to 750 mg of canarium oil and 3 grams of dry ethanol (1: 4 w/w) and 375 mg of the enzyme (10% of total substrate) was obtained 2-MAGs yield by 74% in the phase of EtOH/H₂O (90:10 v/v). The highest composition of fatty acids on the 2-MAGs were unsaturated fatty acids, namely oleic acid (939.8 ppm) and linoleic acid (445.5 ppm) that analyzed by high performance liquid chromatography (Figure 2), therefore it could be used for the next stage of the synthesis of structured lipid.

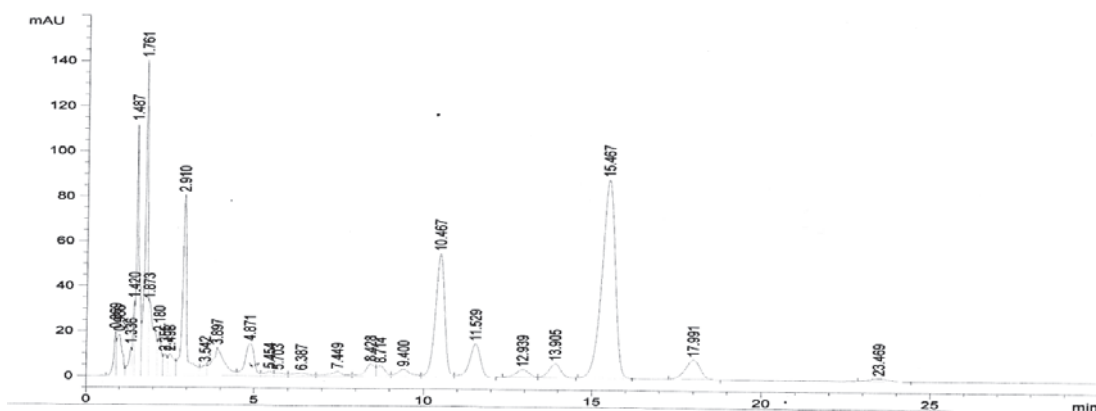


Figure 2. Fatty acids composition of 2-MAGs were analyzed by HPLC

CONCLUSION

Synthesis of 2-MAGs could be performed by ethanolysis reaction between canarium oil and dry ethanol in an orbital shaker waterbath incubator. Characterization of 2-MAG carried out by preparative thin layer chromatography using the standard 2-oleoylglycerol and obtained 2-MAG yield of 74% after purification by solvent extraction. Analysis of the fatty acids composition between canarium oil and 2-MAG using high performance liquid chromatography showed a similar composition. The highest composition of fatty acids of 2-MAGs were unsaturated fatty acids, namely oleic acid (18:1n-9) and linoleic acid (18:2n-6) that

could be used for production of structured lipids.

Acknowledgements

Thanks to the Food, Health and Medicine Research Center, Institute of Technology Bandung that has funded this research. The authors also gratefully acknowledge the funding from the Government of Korea through KRIBB (Korea Research Institute of Bioscience and Biotechnology).



REFERENCES

- *. Esteban L, Munio MM, Robles A, Hita E, Jimenez MJ, Gonzales PA, Camacho B, Molina E. (2009). Synthesis of 2-monoacylglycerols (2-MAG) by enzymatic alcoholysis of fish oils using different reactor types. *Biochem. Eng. J.* 44: 271-9.
- *. Kuhnt K, Degen C, Jaudszus A, Jahreis G. (2012). Searching for health beneficial n-3 and n-6 fatty acids in plant seeds. *Eur. J. Lipid Sci. Technol.* 114:153-60.
- *. Osborn HT, Akoh CC. (2002). Structured lipids-novel fats with medical, nutraceutical, and food applications. *Comprehensive Reviews in Food Science and Food Safety.* 3: 110-20.



EFFECT OF TREHALOSE ON THERMAL PROPERTIES OF PHOSPHOLIPID- DDA AND TPGS MIXTURES

Helmy Yusuf, Department of Pharmaceutics, Airlangga University. Jl. Dharmawangsa DAlam, Surabaya 60286, Indonesia. helmy-yusuf@ff.unair.ac.id

INTRODUCTION

The freeze-dried liposome as immunological adjuvant/vaccine delivery systems is one of recent particular interest in the area. DDA is one of the particular interests in immunological adjuvant materials. DDA is a quarterammonium compound with long chain alkyl groups that contribute to its lipophilic properties. It also comprises dimethylammonium head-group (positively charged) that is attached to the two carbon alkyl chains and contributes to its hydrophilic properties. Both properties of DDA make it suitable for such application in the preparation of cationic liposomes [1-3]. However, DDA liposomes have some drawbacks such as physical instability, as they are easily aggregate in presence of small amounts of salt or even in pure water [7, 8]. As water has been considered as an ideal dispersion medium, then improving DDA formulations is still challenging. This project focuses on the development of potential new formulations of lyophilized liposomes as immunological adjuvant in vaccine delivery system and investigations based on their physicochemical characteristics. Lyoprotectant, i.e. trehalose and membrane stabilizer, i.e. TPGS (D-alpha tocopherol polyethylene glycol 1000 succinate) were used in the freeze-dried liposomes formulations.

EXPERIMENTAL METHODS

Materials

TPGS, DDA and BSA were purchased from Sigma (UK), soyphosphatidylcholines (SPC) was purchased from Lipoid (Germany) and trehalose was purchased from Ferro Pfanstiehl (USA).

Sample Preparation of Phospholipid-DDA-

TPGS mixture

SPC, DDA and TPGS were dissolved and mixed in chloroform/methanol (9:1) solvent system. After solvent was removed, the resulted lipid film was then hydrated with pre-heated (60°C) 10 mM tris buffer (pH 7.4). Trehalose solution at concentration 0.02 M in this buffer were also used as hydration solutions. The ratio of DDA and SPC (1:1) was chosen for practical reason, regarding that these two lipids have same length of acyl chains. Samples were stirred for 30 min (at 60°C) and then sonicated for 2 min (probe sonicator, Fisher Scientific, USA) with pulsative mode. Single lipid components were also prepared in the same way with concentration 50 mg/ml. All samples were then freeze-dried (Advantage, VirTis, USA) for 36 h to obtain solid cakes.

Dry Product Characterization

Water Content. Water content in freeze dried cakes was measured by using thermogravimetric analysis (TGA) at 10°C/min to 200°C. **Differential Scanning Calorimetry (DSC).** DSC instrument (Q-100, TA Instruments, New Castle, DE USA) was used to determine the phase transition temperature (T_m) of the dried samples. T_m was measured as endothermic peak minimum for the lipid gel-to-liquid crystalline phase transition during the heating scan. Samples were scanned from -20°C to 200°C at 10°C/min. Annealing technique was applied with heating rate 10°C/min in range of 60° - 150°C for further investigation. All samples were measured in three replicates using aluminum hermetic. An empty pan was used as reference. Data were analyzed using Universal Analysis Software.

RESULTS AND DISCUSSIONS

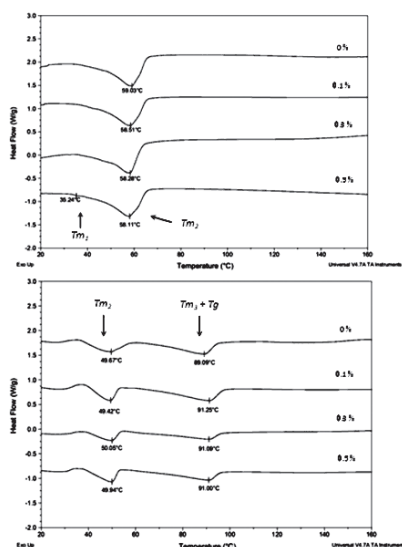


Figure 1. DSC thermograms of freeze-dried DDA-SPC (1:1 molar ratio) mixtures containing different concentration of TPGS as indicated; (A) without trehalose, and (B) with 0.02 M trehalose.

A small concentration of trehalose (0.02 M) was applied to the lipid mixture to make 1:4 molar ratios of sugar towards total lipid concentration of 0.08 M (Table 2.6.). In this particular experiment, the effect of trehalose was examined in the lipid mixtures with TPGS concentration of 0; 0.1; 0.3 and 0.5 mol %. The results showed that trehalose decreased the T_m of the lipid mixtures by approximately 10°C from 58° or 60°C to 49°C, regardless of the concentration of TPGS (Figure 1 and Table 1). The explanation of T_m depression by addition of trehalose can be attributed to the capability of trehalose to restrict or prevent lipid contraction during dehydration processes that would occur in the absence of trehalose (Ohtake, Schebor et al. 2005). This restriction that is achieved by the direct interaction of trehalose with phospholipids has also been reported in another study (Pereira, Lins et al. 2004). It has been proposed previously that the T_m depression of lipid by the presence of trehalose occurs through a ‘water replacement’ theory (Crowe, Crowe et al. 1985).

Phospholipid	TPGS (mol %)	Trehalose (M)	T_m (°C)		ΔH (KJ/mol) [#]		Water Content (%)
			1	2	1	2	
DDA – SPC 1 : 1	0	0	-	60.2 ± 1.2	-	39.1 ± 4.0	3.9 ± 0.2
	0.1		-	58.6 ± 0.2	-	34.9 ± 1.0	3.0 ± 0.4
	0.3		-	58.7 ± 0.4	-	34.1 ± 6.2	3.1 ± 0.6
	0.5		36.3 ± 1.2	59.7 ± 1.5	0.35 ± 0.3	31.9 ± 1.7	3.1 ± 0.7
DDA – SPC 1 : 1	0	0.02	-	49.2 ± 0.2	-	8.1 ± 1.2**	2.1 ± 0.1
	0.1		-	49.1 ± 1.5	-	8.0 ± 2.3*	2.2 ± 1.1
	0.3		-	48.7 ± 1.2	-	8.1 ± 1.8*	2.8 ± 0.6
	0.5		-	50.2 ± 0.9	-	9.0 ± 0.9	2.3 ± 0.7

* $p < 0.05$, ** $p < 0.01$ as compared to the corresponding lipid mixture without trehalose. #the enthalpy values (ΔH of T_m2) of lipid mixtures are presented in units of KJ/mol where the mol was calculated as total of mol fraction of every component in the mixtures.

Table 1. Transition temperature and the melting enthalpy of freeze-dried lipid mixture with and without the presence of trehalose 0.02 M ($n = 3 \pm$ represents SD).



CONCLUSION

Trehalose as a lyoprotectant interacts well with the phospholipid-DDA-TPGS mixture through water replacement mechanism is indicated by the decreased T_m of the lipid mixtures in the presence of 0.02 M trehalose.

REFERENCES

1. P.C.A. Barreleiro, R.P. May, B. Lindman, Mechanism of formation of DNA-cationic vesicle complexes, *Fara day Discuss.* 122 (2003) 191-201.
2. G.F. Shi, W.J. Guo, S.M. Stephenson, R.J. Lee, Efficient intracellular drug and gene delivery using folate receptor-targeted pH-sensitive liposomes composed of cationic/anionic lipid combinations, *J. Controlled Release* 80 (2002) 309-319.
3. K. Lappalainen, A. Urtti, E. Soderling, I. Jaaskelainen, K. Syrjanen, S. Syrjanen, Cationic Liposomes Improve Stability and Intracellular Delivery of Antisense Oligonucleotides Into Caski Cells, *Biochimica Et Biophysica Acta-Biomembranes* 1196 (1994) 201-208.
4. Ohtake, S., Schebor, C., Palecek, S.P. And De Pablo, J.J., 2005. Phase behavior of freeze-dried phospholipid-cholesterol mixtures stabilized with trehalose. *Biochimica et Biophysica Acta-Biomembranes*, 1713(1), pp. 57-64.
5. Pereira, C.S., Lins, R.D., Chandrasekhar, I., Freitas, L.C.G. And Hunenberger, P.H., 2004. Interaction of the disaccharide trehalose with a phospholipid bilayer: A molecular dynamics study. *Biophysical journal*, 86(4), pp. 2273-2285.
6. Crowe, L.M., Crowe, J.H., Rudolph, A., Womersley, C. And Appel, L., 1985. Preservation of freeze-dried liposomes by trehalose. *Archives of Biochemistry and Biophysics*, 242(1), pp. 240-247.

PREPARATION AND CHARACTERIZATION OF FLUKONAZOLE- β -CYCLODEXTRIN INCLUSION COMPLEXES

Hestiary Ratih, Department of Pharmacy, University of Jenderal Achmad Yani, Cimahi, hestiary_ratih@yahoo.co.id; **Erin Karlina**, Department of Pharmacy, University of Jenderal Achmad Yani, Cimahi; **Erin Karlina**, Department of Pharmacy, University of Jenderal Achmad Yani, Cimahi.

INTRODUCTION

Fluconazole is a triazole antifungal drug used in the treatment and prevention of superficial and systemic fungal infections. In a bulk powder form, it appears as a white crystalline powder, and it is very slightly soluble in water and soluble in alcohol³.

Cyclodextrins (CDs) are cyclic oligosaccharides containing six (α -CD), seven (β -CD) or eight (γ -CD) α -1,4-linked glycopyranose units, with a hydrophilic hydroxyl group on their outer surface and a hydrophobic cavity in the center. In previous years cyclodextrins (CDs) have been recognized as an important constituents of pharmaceutical excipients. CDs are capable of forming inclusion complexes with many drugs by including a whole drug molecule, or only some non-polar part of it, inside their cavity.

The aim of this study was to improve the solubility of fluconazole by the formation of fluconazole- β -cyclodextrin (β -CD) inclusion complex.

MATERIALS AND METHOD

Materials fluconazole from Chemo-Switzerland, β -cyclodextrin, hydroxypropyl methylcellulosa (HPMC), sodium chlorida, hydrochloric acid, sodium phosphat monobase, sodium hidroksida, sodium citric, citric acid, distilled water.

For preparation of complexes by slurry method, the fluconazole- β -CD in 1:1, 2:1, 4:1 and 8:1 molar ratio. The β -CD were suspended in 60% water with 0.5% hydroxypropyl methylcellulose (HPMC) to obtain a homogeneous paste. Fluconazole was then added slowly while grinding. The mixtures were heated and

stirred in a water bath at 40o-75oC for 1 hours . The pastes were dried in an oven at 80°C. The dried complexes were pulverized and then sieved through 60 #.

RESULT AND DISCUSSION

Phase Solubility Studies

The phase solubility diagram fluconazole- β -CD system in water can be characterized as AL type phase solubility curve. Results of the phase solubility studies are shown in Figure 1 that presents the solubility profiles of fluconazole as a function of increasing concentrations of β -CD in aqueous solution. This linear fluconazole- β -CD correlation, with a slope of less than 1, suggests the formation of a 1:1 (mol/mol) fluconazole- β -CD inclusion complex. The calculated stability constant values was 113,57 M⁻¹. Fluconazole indicating that fluconazole- β -CD complexes (1:1 molar ratio) are sufficiently stable. In fact, values of obtained stability constants are always within the range of 100 to 1000 M⁻¹, which is believed to fluconazole an ideal value.

Result of the inclusion complex solubility fluconazole- β -CD can increase the solubility of fluconazole in distilled water compared to pure fluconazole. Inclusion complex of fluconazole- β -CD 1: 1 has the highest solubility in distilled water compared to pure fluconazole and other complex, ie 8.98 mg / mL.

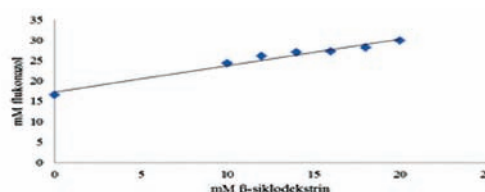


Figure 1. Phase solubility diagram of Fluconazole- β -CD



FT-IR Studies

The FT-IR spectrum of fluconazole showed peak at 1516,05 cm⁻¹, corresponding to the -NH stretch. A decrease in the -NH stretch frequency of fluconazole from 1516,05 cm⁻¹ to 1508,33 cm⁻¹. This shift indicates the weakness of the bond energy between β -CD and water, so the water out of the cavity when fluconazole into the cavity of β -CD which was followed by the formation of hydrogen bond with fluconazole- β -CD. A broad band at 1680 cm⁻¹ characterizes the spectrum for β -CD, which is due to the glycoside linkages. The cyclodextrin glycoside peak is unchanged in the presence of fluconazole on inclusion complex fluconazole- β CD. Disappearance most of the peaks and the shift of the wave number fluconazole, suggesting an interaction between fluconazole with β -CD, which means there in an inclusion complex between fluconazole- β -CD prepared by slurry method.

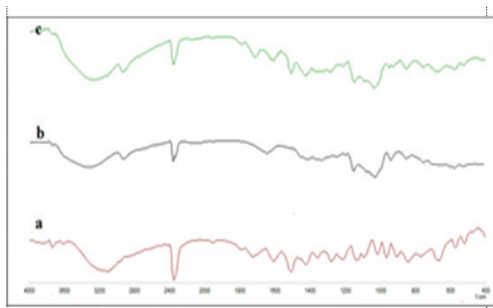


Figure 2. FT-IR spectrum of (a) Fluconazole, (b) β -CD, (c) Fluconazole- β -CD 1:1 inclusion complex

Powder X-Ray Diffraction (PXRD) Studies

Diffractogram on inclusion complex showed a sharp decrease in the intensity of fluconazole to approach the diffractogram profile β -CD. This suggests that the molecular fluconazole has entered into the structure of β -CD cavity so that it looks only diffractogram β -CD.

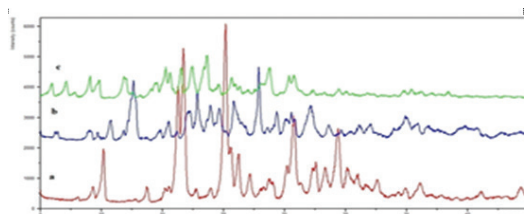


Figure 3. PXRD patterns of (a) Fluconazole (b) β -CD, (c) Fluconazole- β -CD 1:1 inclusion complex

In Vitro Dissolution Studies

Dissolution studies of fluconazole in powder form, and complexes with β -CD were performed to evaluate drug release profile. Dissolution studies were performed on USP dissolution apparatus type II with 900 ml dissolution medium pH 1.2 hydrochloric acid buffer, citrate buffer pH 4.5 and pH 6.8 phosphate buffer at 37 $0C \pm 0.5$ $0C$ at 50 rpm for 30 min. Inclusion complex capable of increase the rate of dissolution in hydrochloric acid buffer of pH 1.2, citrate buffer pH 4.5 and pH 6.8 phosphate buffer compared to pure fluconazole.

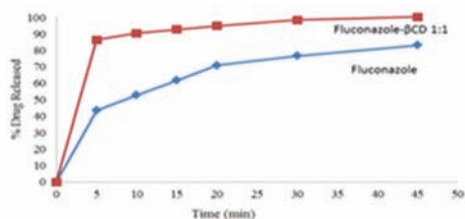


Figure 4. Dissolution profiles of fluconazole- β -CD 1:1 inclusion complex in pH 1.2 hydrochloric acid buffer

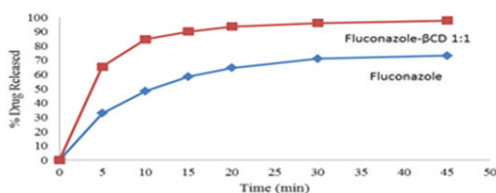


Figure 5. Dissolution profiles of fluconazole - β -CD 1:1 inclusion complex in citrate buffer pH 4.

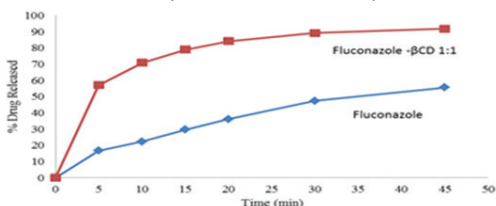


Figure 6. Dissolution profiles of fluconazole- β -CD 1:1 inclusion complex in pH 6.8 phosphate buffer



Conclusion

Results obtained during this study showed that β -CD is able to improve fluconazole dissolution properties. Inclusion complex of fluconazole β -CD 1: 1 with an equilibrium constant value of 113.57 M⁻¹ provides the best solubility than the complex fluconazole- β -CD 2: 1, 4: 1 and 8: 1.

REFERENCES

- *. Joyce, Nirmala, M., Srinivas, Allanki., Amitava, Mukherjee., N, Chandrasekaran. (2013). Enhancing the solubility of fluconazole using a new essential oil based microemulsion system. In International Journal of Pharmacy & Pharmaceutical Sciences, Vol 5 (3): 697-699.
- *. Loftsoon, T, M. E. Brewster. (1996). Pharmaceutical application of cyclodextrins. Journal of Pharmaceutical Sciences, 85 : 1022.
- *. Mukesh Chandra Sharma, Smita Sharma. (2011). Preparation, physicochemical characterization, dissolution, formulation and spectroscopic studies of β -cyclodextrins inclusion complex. International Journal of ChemTech Research. Jan ; 3(1): 104-111.
- *. Ramnik Singh, et al. (2010). Characterization of cyclodextrin inclusion complexes : a review. Journal of Pharmaceutical Science and Technology. Vol. 2 (3): 171-183.



ISOLATION AND IDENTIFICATION OF ANTIOXIDANT COMPOUND BY BIOPRODUCTION OF ENDOPHYTIC FUNGI OF TURMERIC (*Curcuma longa* L.) ISOLATE CL.SMI.RF11

Hindra Rahmawati, Faculty of Pharmacy Pancasila University, Jl. Srengseng Sawah, Jagakarsa, Jakarta 12640, Indonesia. Email: hindra_rahardjo@yahoo.com ; **Bustanussalam**, Research Centre for Biotechnology - Indonesian Institute of Sciences (LIPI), Jl. Raya Bogor Km 46 Cibinong 16911, Indonesia. Email: boest77@yahoo.com ; **Parto-muan Simanjuntak**, Faculty of Pharmacy Pancasila University; Research Centre for Biotechnology - Indonesian Institute of Sciences (LIPI), Email: partomsimanjtk@yahoo.com

INTRODUCTION

One of the problem concerning with human health is the presence of free radicals in the human body. The most effective way to prevent the deleterious effects of free radicals is the use of antioxidants. There is a preference for antioxidants coming from natural sources rather than from synthetic sources (Molyneux, 2003). One of the natural sources of antioxidant is turmeric (*Curcuma longa* L.). Virtually every higher plant is host to one or more endophytic fungi. These microbes may have established one of several kinds of biological relationship with the plant, varying from symbiotic to parasitic. The microbe may mimic the plant and make the same secondary compounds as its host that may also have pharmaceutical applications (Strobel, 1996). The aim of this research was to examine the bioproduction of endophytic fungi isolate CL.SMI.RF11 and to isolate and identify a compound produced by this isolate that was expected to have antioxidant activity.

METHODS

Material

One of endophytic fungi, CL.SMI.RF11, was isolated from turmeric tuber (*Curcuma longa* L.) which cultivated in Sukabumi, West Java. This isolate is a collection of Natural Product Laboratory, Research Centre for Biotechnology, Indonesian Institute of Sciences (LIPI), Cibinong.

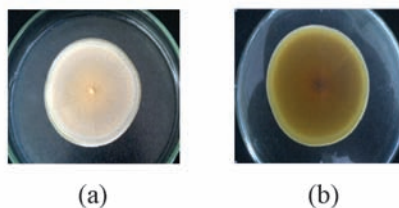


Fig. 1. Endophytic fungi of CL.SMI.RF 11. top side (a); bottom side (b)

Bioproduction

The endophytic fungi isolate CL.SMI.RF11 was inoculated in Potato Dextrose Agar (PDA) medium in Petri dish and incubated for seven days at room temperature (Jia-yao Li et al, 1996). The culture was then being transferred into Potato Dextrose Broth (PDB) medium and fermented for 12 to 14 days while being shaken using the rotary shaker at room temperature.

Extraction Procedure

The filtrate, which had higher antioxidant activity than the biomass, was extracted using ethyl acetate as solvent and evaporated under reduced pressure using rotary evaporator.

Antioxidant Activity Test

Series of concentration of the extract were made and each solution was added with one mL of 1,1-diphenyl-2-picrylhydrazyl (DPPH) solution (0.4 mM in methanol) and diluted until 5 mL with methanol. After being homogenized, the solutions were incubated for 30 minutes at 37°C. The absorptions were measured spectrometrically at 517 nm. The ascorbic acid was used as standard.



Fractionation and Purification

Fractionation procedure using column chromatography was carried out three times, and followed by preparative TLC to get pure substance(s).

First column chromatography: silica gel 60; gradient solvent system of n-hexane-ethyl acetate 10:1 to 4:1 followed by chloroform-methanol 15:1 to 1:1. TLC monitoring: silica gel GF254 plate developed in n-hexane-ethyl acetate 5:1 and chloroform-methanol 5:1; spray reagent cerium sulphate solution (1% in 10% sulphuric acid), heated electrically until the spots were appeared.

Second column chromatography: silica gel 60; gradient solvent system of chloroform-methanol 15:1 to 1:1. TLC monitoring: silica gel GF254, mobile phase: chloroform-methanol 3:1, the spots were examined by UV light 254 nm and spray reagent DPPH solution. The spot which performed yellow in colour was predicted containing antioxidant compound.

Third column chromatography: silica gel 60; n-hexane-ethyl acetate 5:1 followed by chloroform-methanol 10:1 to 1:1. TLC monitoring: silica gel GF254, mobile phase: chloroform-methanol 9:1, the spots were examined by UV light 254 nm and spray reagent DPPH solution. The most intensive yellow spot was predicted containing the most active antioxidant compound and selected for further purification.

Preparative TLC: silica gel GF254, mobile phase chloroform-methanol 9:1. Each of the bands was extracted with solvent mixture of chloroform-methanol 1:1. After filtering, the extract(s) were evaporated until the pure substances were obtained.

Two-dimension TLC

Two-dimension TLC was performed to confirm that the substance was pure enough to be identified. The mobile phase for first dimension TLC was chloroform-methanol 2:1, and the second was chloroform-methanol 1:1. The isolate was examined by means of spectroscopic method.

RESULT AND DISCUSSION

Seven fractions eluted from the first column chromatography were analysed for their antioxidant activities using free radical scavenger method, and Fraction V was found the most active fraction with IC₅₀ of 10.01 ppm, compared to ascorbic acid which has IC₅₀ of 3.13 ppm. Fraction V was further separated with the second column chromatography yielded six fractions. Examining with DPPH spray reagent on TLC plate indicated that Fraction V.2 revealed the most intensive yellow colour, indicating it to contain antioxidant compound(s). Fractionation of Fraction V.2 with third column chromatography eluted three fractions, and fraction V.2.2 was the most active one, therefore it was further purified by preparative TLC. Spectroscopic Analyses

The compound obtained from preparative TLC was identified spectroscopically (UV-VIS spectrophotometry, FTIR, ¹H-NMR, and ¹³C-NMR).

UV-VIS Spectrophotometry spectrum of the isolate in the range of 190-700 nm revealed the maximum wavelength at 324.0 and 208.0 nm, meaning that the compound has an aromatic group and saturated ketone. The FTIR spectrum indicated that the isolate has stretching vibration of C-H bonding (3059.86 cm⁻¹), hydroxyl group at 3611.46 cm⁻¹, and carbonyl group which appears at 1727 cm⁻¹. The NMR spectrum of proton at δH 6.66-7.28 revealed some protons of double bond carbons (δH 6.66 ppm, d, 1H; δH 6.82 ppm, dd, 1H; δH 7.28 ppm, d, 1H). This data indicated that the compound has a three-substituted aromatic group. The ¹³C-NMR and its DEPT spectra indicated that the compound consists of eight carbon atoms. Six resonances appeared at δC 116.93, 117.76, 119.08, 122.14, 150.01, and 155.83 ppm, showed the aromatic group as it is also stated by NMR-proton spectrum. The rest two carbon atoms resonance appeared at δC 177.06 ppm (carbonyl



carbon) and 30.59 ppm (methylene carbon) as indicated by DEPT spectrum.

CONCLUSION

Based on spectroscopic data, the compound that has antioxidant activity produced by bio-production of endophytic fungi isolate CL.SMI.RF11 was predicted as 3-hydroxy-bicyclo[4.2.0]octa-1,3,5-trien-7-one.

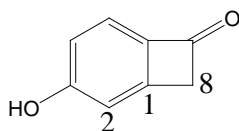


Fig.2. Structure of the compound 3-hydroxy-bicyclo [4.2.0]octa-1,3,5-trien-7-one) isolated from endophytic fungi isolate CL.SMI.RF11

Fig.2. Structure of the compound 3-hydroxy-bicyclo [4.2.0]octa-1,3,5-trien-7-one) isolated from endophytic fungi isolate CL.SMI.RF11

ACKNOWLEDGEMENTS

The authors wish to thank Mr. Eddy Wijaya for his assistance, Ms. Harmastini and her group who provided the endophytic fungi isolate CL.SMI.RF11, and Research Centre for Biotechnology - Indonesian Institute of Sciences (LIPI) for financial support and laboratory facility.

REFERENCES

1. Molyneux P (2004). The use of the stable free radical diphenylpicrylhydrazyl (DPPH) for estimating anti oxidant activity. *Songklanakarinn J.Sci. Technol*, Mar-Apr; (26)2:212-219.
2. Strobel G (1996). Endophytic fungi: New sources for old and new pharmaceuticals. *Pharmaceutical News* (3)6:7-9.
3. Li Jia-yao(1996). Endophytic taxol-producing fungi from bald cypress, *Taxodium distichum*. *Microbiology*;142:2223-2226.



MODIFICATION PROCESS OF NATURAL CASSAVA STARCH : THE STUDY OF CHARACTERISTICS AND PHYSICAL PROPERTIES

Prasetia, Jemmy A., C.I.S. Arisanti, N.P.P.A. Dewi, G.A.R. Astuti, N.W.N Yulianingsih, I M.A.G. Wirasuta

Department of Pharmacy, Pharmaceutical Technology, Faculty of Mathematics and Natural Science, Udayana University - Bali, ngurah_jemmy@yahoo.com, +628179373361.

INTRODUCTION

Natural cassava starch (Cass) has poor physical properties. Through modification, it can be increased. Fully pregelatinized is a physical modification by addition of water with heating above the gelatination temperature that causes rupture of entire starch granules. It will entangle amylose that was one of the component in starch. Co-processing method is a technique by combining existing excipients in order to obtain a new excipient with improved properties (Gohel, 2005). Additional excipient that commonly use is Acacia Gum (AG). There are two types of co-processing Cass with AG which are Partially Pregelatinized (Co-PPCass) and Full Pregelatinized (Co-FPCass). According to all of that, the aims of this study was to know the effect of modifications to the characteristic and physical properties of Cass.

METHODS

Materials

The material used were natural cassava (*Manihot esculenta* Crantz) and acacia gum (PT. Bratachem).

Methods

Preparation of cass

Cass was cutted into tiny size and then added amount distilled water to 2:1 w/v. Strain it with flannel cloth. After 24 hours, separate the supernatant from the precipitate. Then washed it with distilled water. After that, dried it at 50°C for 24 hours until it forming a slab of starch. Sieved it to obtain a starch powder (Soebagio et al, 2009).

Preparation of modified cass

1. Fully pregelatinized cass (FPCass)
Cass suspended in distilled water (1:1). The suspension was then heated over water bath at 80°C and stirred it for 10 minutes. The suspension was dried at 50°C for 48 hours. The dry starch then sieved through no 20 mesh sieve (Ohwoavworhwa and Osinowo, 2010).
2. Co-processed cass (Co-PPCass and Co-FPCass)
Co-processed was prepared by mixing Cass and AG (92,5:7,5). The required amount of Cass was dispersed in distilled water to get 40% w/w solid content. In the same way, a number of AG was also dispersed in distilled water (2:3 w/v). AG suspension was mixed into Cass suspension with stirring for 10 minutes. The CassAG suspension was heated on a water-bath in different temperature to obtain different types of co-processing Cass. Co-PPCass was obtained by heating it at 55°C. Meanwhile, if the temperature was increased into 80°C, the result is Co-FPCass. Furthermore, each type were dried at 60°C for 48 hours. The granule was powdered by no 20 mesh sieve (Ohwoavworhwa and Osinowo, 2010).

Characteristics of starch

Organoleptics

Weigh 1 gram of Cass and then observe the



color, smell and taste of it. Cass has a characteristic which are white color, odorless and tasteless.

Identification of cass

The suspension of Cass produced by weight 1 gram of Cass and mixed it in 50 mL of distilled water. 1 mL of Cass solution mixed with 0,05 mL of 0,005 M iodine.

Microscopics

Weigh 100 mg of Cass and placed on a glass object. Added 2 drops of distilled water and then observed the hilum and lamellae under a microscope.

Physical properties of starch

Determination of particle size

A 100 grams of Cass. Further, stratified it by sieving with mesh number 20, 40, 60, 80 and 100.

Amylose content

A 100 mg starch dissolved with 1 mL of 95% ethanol and 9 mL of 1 N NaOH. The solution was heated for 10 minutes on water bath at 100°C. After the solution was cooled, added 100 mL of distilled water (A). Take 5 mL of A and put it into 100 mL volumetric flask. Then, added 1 mL of CH₃COOH, 2 ml of iodine solution and distilled water until 100 mL (B). Shake B for 20 minutes and measure the absorbance by UV-VIS spectrophotometry at wavelength 620 nm (Adedokun and Itiola, 2009). Amylose content was calculated by the equation:

% Amylose levels = 3,06* x Absorbance x 20
..... Eq. (1)

*Conversion factor of amylose

RESULTS AND DISCUSSION

According to table 1, organoleptics and identification test obtained that overall starch produce a same result. In identification test, starch will form a dark blue-purple color caused by the formation of amylose binding with iodine. In other side, amylopectin binding with iodine and produces bluish violet color.

Evaluation	Results			
	Cass	FPCass	Co-PPCass	Co-FPCas
Organoleptics	White, odorless and tasteless			
Identification of starch	It formed a dark blue-purple and bluish violet color			
Microscopic	Hilum located in the middle of the straight line and form a three-pronged with unclear lamellae			

Table 1 Characteristic results of Cass and Cass modification

In microscopic test, hilum located in the middle point of the straight line and form a three-pronged. Lamellae is unclear. This result can be seen in figure 1. From this results concluded that Cass modification does not give the change of the characteristics of Cass.

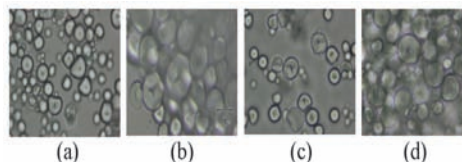


Figure 1. Microscopic test of Cass (a), FPCass (b), Co-PPCass (c) and Co-FPCass (d)

In figure 2 shows that Cass modification have a number of fines less than Cass. This is because of the increase in particle size of Cass modification through the process of unification of the starch particles are small in gelatination process so that the amount of fines can be reduced The number of small fines causes a better flowability and compressibility (Anastasiades, et al, 2002; Ansel, 2005). Modified Cass has good flow properties better than Cass.

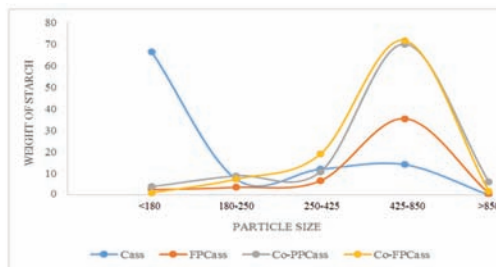


Figure 2. The particle size distribution of Cass and Cass modification

Figure 3 shows about amylose content in Cass and Cass modification. Amylose content in Cass is the biggest ones and the lowest content is in Co-FPCass. The reduction of amylose content from Cass into Cass modification is because of the gelatination during the heating process. When starch is heated at gelatination temperature, the thermal energy causes the hydrogen bonds in the starch is become weaken. This facilitate the water to enter into the granules and cause slight dissolution. It also induce the exchange of amylose molecules into the water (Lowenthal, 1972). Decreased levels of amylose can cause a decrease ability of starch as a disintegration ingredient that can inhibit dissolution of the tablet

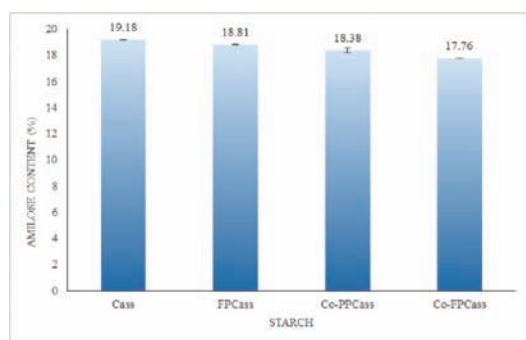


Figure 3 The correlation of Cass modification to amylose content

Conclusion

The results obtained based on this research is Cass modifications do not cause a changes of the characteristics but it leads to a change in particle size and amylose content in it.

The authors acknowledge technical support from Dewi, Astuti, and Yulianingsih (an undergraduate student) for assistance with the experimental work.

References

1. Adedokun, M. O. and O. A. Itiola. (2010). Material properties and compaction characteristics of natural and pregelatinized forms of four starch. *J. Carbohydrate Polymer*, 79:818-824
2. Anastasiades, A., Thanou, S., Louis, D., Stapatoris, A., and Karapanisios, T. D. (2002). Rheological and physical characterization of pre-gelatinized maize starches. *J. Food Eng.*, 52:57-66.
3. Ansel, H. C. (2005). Pengantar bentuk sediaan farmasi edisi keempat. UI-Press, 202-204, 259.
4. Carr, R.L. (1965). Classifying flow of solids. *J. Chemical Engineering*, 72:69-72.
5. Gohel, M. C. (2005). A review of co-processed directly compressible excipients. *J. Pharm Sci*, 8(1):76-93.
6. Lowenthal, W. (1972). Mechanism of action tablet disintegrant. *J. Pharm Sci.*, 61:455-459.
7. Ohwoavworhwa, F.O. and Osinowo, A. (2010). Preformulation studies and compaction properties of a new starch-based pharmaceutical aid. *Journal of Pharm Biol and Chem Sci*, 1(3):250-255.
8. Soebagio, B., N. Wathoni, and R.K. Meko. (2009). Profil aliran dispersi pati ubi jalar (*Ipomea batatas* (L)). *Farmaka*, 7(2):13-27.



DRUG USE PROFILE OF DIABETIC PATIENTS IN EAST SURABAYA PRIMARY HEALTH CARE

Nyoman Wijaya, Faculty of Pharmacy Airlangga University, nyoman_ffua@yahoo.com; **Azza Faturrohmah**, Faculty of Pharmacy Airlangga University; **Ana Yuda**, Faculty of Pharmacy Airlangga University; **Mufarrihah**, Faculty of Pharmacy Airlangga University; **Tesa Geovani Santoso**, Faculty of Pharmacy Airlangga University; **Dina Kartika**, Faculty of Pharmacy Airlangga University; **Hikmah Prasasti N.**, Faculty of Pharmacy Airlangga University; **Whanni Wido Agustin**, Faculty of Pharmacy Airlangga University

ABSTRACT

Diabetes mellitus is one of chronic metabolic disease. The number of patients are predicted to be increasing in the future. Hyperglycemia will occur if this disease isn't well handled. The aim of this study was to see the drug use profile of diabetic patients in Primary Health Care (PHC) in East Surabaya.

The sampling method of this study was non random sampling. Data was collected from May 1st to June 30th, 2014 by interviewing 138 patients in their homes. The variables of components of drug use profiles in this study were drugs amount, drugs pharmacological group, drugs type, drugs usage, and patient compliance.

The result showed that 29.71% of those patients used 4 different kinds of drugs. Vitamins-minerals (52.90%) were the most frequent drugs prescribed for the patients beside oral anti-diabetics drug. Most drugs (97.94%) were generic drugs. Most patients used glibenclamide (71.88%) and metformin (31.53%) once a day. Seventy three of 138 patients used glibenclamide prior to meal time, while 43 of 138 patients used metformin after meal.

Most patients used more than one kind of drugs in their therapies. Therefore, PHC pharmacists should increase their role to educate the patients about diabetes mellitus, give counseling about the patients' therapies, and monitor the patients' therapy outcomes.

Keywords: drug use profile, diabetes mellitus, East Surabaya Primary Health Care

BACKGROUND

Pharmacy services at this time has changed from the drug orientation paradigm to a patient orientation refers to pharmaceutical care. pharmaceutical care is a form of service and direct responsibility of the pharmacist profession of pharmacy work to improve the quality of life of patients (Kepmenkes, 2004). As a consequence of the change in orientation, the pharmacist is required to improve the knowledge, skills and behaviors to be able to carry out direct interaction with patients.

Diabetes mellitus (DM) is a group of chronic metabolic disorder due to abnormalities in the metabolism of carbohydrates, fats, and proteins are characterized by hyperglycemia resulting in microvascular complications, macrovascular, and neuropathic for the long term (DiPiro, et al., 2008). International Diabetes Federation (IDF) in 2005 stated that in the world there are 200 million (5.1%) of people with diabetes and is thought 20 years later

(2025) will increase to 333 million (6.3%) people.

DM is a long-term disease that requires long-term treatment as well. In this case the necessary education and motivation of health workers in health centers and support and supervision taking medication from the patient's family. Diabetes can lead to complications of acute and chronic (McPhee & Funk, 2006). Because of these complications, diabetic patients are also likely to use other drugs in addition to oral antidiabetic drugs. The use of many drugs at the same time is commonly known as polypharmacy (Saunders, 2007).

METHODS

This research was a descriptive and cross-sectional study were analyzed descriptively. The population in this study were DM patients of Menur, Mulyorejo, Mojo and Pucang Sewu Surabaya Health Center.

The sampling method of this study was non random sampling. Data was collected from



May 1st to June 30th, 2014 by interviewing 138 patients in their homes. The variables in this study include the amount of the drug, the pharmacological group of drugs, types of drugs, how to use drugs, and compliance.

RESULTS AND DISCUSSION

Table 1. Distribution of Patients by Sex

No	Sex	n	%
1	Male	44	31,88
2	Women	94	68,12
Total		138	100

Table 1 shows that the majority of diabetic patients (68.12%) were female. Women are more at risk of diabetes, because women have a history of pregnancy with birth weight > 4 kg, history of diabetes during pregnancy (gestational diabetes), obesity, use of oral contraceptives, and stress levels are quite high (DiPiro, et al., 2008) .

Table 2. Distribution of Patients by Age

No	Age (years)	n	%
1	<30	3	2,17
2	30-39	8	5,80
3	40-49	19	13,77
4	50-59	43	31,16
5	60-69	46	33,34
6	70-79	14	10,14
7	>80	5	3,62
Total		138	100

From the table 2, it can be seen that most patients were patients between the ages of 50-69 years (63.5%). This is consistent with the statement of the American Diabetes Association (ADA) (2014) that the age of 45 years and above a risk factor for diabetes. And as a result of the increasing age, a person is declining pancreatic beta cells and the progressive accumulation of amyloid in the vicinity. Pancreatic beta cells are left in general is still active, but less and less insulin secretion and sensitivity of receptors is also decreased (Tjay & Rahardja,2007).

Table 3. Distribusi Patients Based Jobs

No	Jobs	n	%
1	Private	41	29,7
2	Government employee	12	8,7
3	Retired	18	13,0
4	Housewife	67	48,6
Total		138	100

The majority (48.6%) patients with DM was housewife. Based on interviews, mostly Housewife just do their homework and have more free time at home. Lack of physical activity which the one risk factor for diabetes (Perkeni 2011). Lack of physical activity can lead to obesity and is one of the factors triggering the DM. The effects are large changes in metabolic and endocrine function that can stimulate the occurrence of obesity (Anisa, 2008).

Table 4. Distribution of Patients According to Level of Education

No	Level of Education	n	%
1	Uneducated	16	11,59
2	Elementary school	56	40,58
3	Junior high school	21	15,22
4	Senior High School	38	27,54
5	Higher Education	7	5,07
Total		138	100

From the table 4, it can be seen that most patients are patients with a elementary education or equivalent (40.6%). People who would normally be a high level of education has a lot of knowledge about health. With the knowledge that people will have in maintaining health awareness (Irawan, 2010). People with low education levels are usually less knowledgeable health especially so behave less healthy and susceptible to disease, and it will also affect the patient safety related to medication therapy. If the patient is unable to understand the information provided by health professionals, patients will be in a higher risk for medication errors (Beardsley, et al., 2012).



Table 5. Distribution of Patients According to the Old suffering DM

No	Old suffering DM (years)	n	%
1	<1	46	33,33
2	1-5	54	39,13
3	6-10	23	16,67
4	>10	15	10,87
Total		138	100

Long suffered diabetes mellitus patients <1 year to 5 years (72.46%) because patients are still relatively newly diagnosed diabetes mellitus, in general, very open and happy to be given the drug counseling, because the patient is still not well-informed about their disease and the treatment their suffered (Anisa, 2008). Patient became aware of their disease and their medicine so that patients have a great curiosity and want to recover so they diligently went to the primary health center. Meanwhile, long-suffering patients with diabetes mellitus > 5 years the percentage is small, it is because patients assume the disease is not harmful, or according to the results unsatisfactory experience during the treatment so that they no longer want to control to the clinic.

Table 6. Distribution of Patients by Type Used of OAD

No	Type of OAD	n	%
1	Glibenclamide	19	13,77
2	Metformin	41	29,71
3	Glibenclamide+Metformin	77	55,80
4	Glicazide	1	0,72
Total		131	100

Oral antidiabetic drugs in health centers, namely glibenclamide and metformin. The use of oral antidiabetic drugs in patients with diabetes is the thing to do when setting lifestyle (diet, exercise, and weight loss) showed no improvement in blood sugar levels (Tjay & Rahardja, 2007). DM corresponding treatment algorithm, patients with newly diagnosed diabetes should be given education on the pattern of life. If within one month there

was no improvement in blood sugar levels, the use of oral antidiabetic drugs is required. First-line oral antidiabetic drugs used is metformin, thiazolidinediones class, and the class of sulfonylureas. Half of the patients in the study received glibenclamide and metformin combination therapy, ie 55.8%. Combination therapy is commonly prescribed for patients who have no improvement in blood sugar levels within 3 months after the use of oral antidiabetic drugs. Glibenclamide and metformin combination therapy has a synergistic effect for both classes of drugs have an effect on the sensitivity of insulin receptors. Sulfonylureas (glibenclamide) will start to stimulate the secretion of the pancreas that allows biguanide compounds (metformin) to perform effectively (DiPiro, et al., 2008).

Table 7. Distribution of Patients According to Number of Drugs In Overall

No	Number of Drugs	n	%
1	1 drug	1	0,72
2	2 drugs	9	6,52
3	3 drugs	24	17,39
4	4 drugs	41	29,71
5	5 drugs	28	20,29
6	6 drugs	19	13,77
7	7 drugs	12	8,70
8	8 drugs	2	1,45
9	9 drugs	2	1,45
Total		138	100

From the number of drugs used in DM patients, as many as 104 of the 138 patients (75.36%) use more than three different drugs (polypharmacy). Polypharmacy may be unavoidable in patients with diabetes because it may be necessary to control blood sugar, medications are also needed to overcome the interference of blood pressure, dyslipidemia, and vascular complications and other disor-



ders (Kurniawan, 2010). Polypharmacy can lead to negative effects of a therapeutic drug for example the occurrence of side effects and reduced patient compliance in the use of the medicine (Viktil et al., 2006). The results showed that the more the number of drugs used, the patient will tend to forget and confused in using the medicine that will cause the drug therapy problem, one of which is non-compliance in the use of drugs.

Table 8. Distribution based on Group of Drug Pharmacology

No	Group of Drug Pharmacology	n	%
1	OAD	133	30,79
2	Vitamins+Minerals	73	16,90
3	NSAIDs	58	13,43
4	Antihyperlipidemia	38	8,80
5	Antihypertensi	60	13,90
6	Antigout	12	2,78
7	Antacids	10	2,31
8	Antibacterial	3	0,69
9	Diuretics	14	3,24
10	Antiemetics	2	0,46
11	Expectoransia	7	1,62
12	Antiallergi/Antihistamine	6	1,39
13	Corticosteroids	3	0,69
14	Oral Electrolyte Solution	1	0,23
15	Antidiarrheal	1	0,23
16	Analgesics + allergy + Antiasma	3	0,69
17	Antitusif	4	0,93
18	Antibiotics	2	0,46
19	Antianginal	2	0,46

From the table 8, it can be seen that vitamins and minerals (16.90%) and antihypertensive (13.90%) were the two groups of pharmacological drugs prescribed highly by health centers in addition to oral antidiabetic (30.79%). Types of vitamins and minerals that were prescribed vitamin B1 or thiamine. The use of vitamin B1

in patients with diabetes is essential, vitamin B1 used to treat neuropathic complications occur, the tingling and numbness, which is also known as neuralgia (Tjay&Rahardja,2007).

Table 9. Distribution of Drugs by Type of Drug

No	Jenis Obat	n	%
1	Generic drug	523	97,94
2	Trade name drug	11	2,06
Total		534	100%

Generic drugs most widely used by diabetic patients in East Surabaya primary health centers (97.94%). This is in line with the provisions of existing legislation, the doctor on duty at government health care facilities are required to prescribe generic drugs for all patients appropriate medical indication (Permenkes, 2010).

Table 10. Distribusi Patients Based on Frequency of Drug Use

No	Drug Name	Frequen cy (times)	n	%
1	Glibenclamide	0	2	2,08
		1	69	71,88
		2	22	22,92
		3	3	3,12
Total		96	100	
2	Metformin	0	5	4,50
		1	35	31,53
		2	31	27,93
		3	40	36,04
Total		534	100%	

From the results of the study, most patients using glibenclamide with a frequency of 1 time a day and metformin with a frequency of 3 times a day. Frequency of glibenclamide use is 1-2 times daily maximum 10 mg per day because the half-life of glibenclamide about 3-5 hours, but the last hipoglycemic effects



for 12-24 hours. Meanwhile, the frequency of metformin use is 1-3 times daily maximum of 3 grams per day (Tjay & Rahardja, 2007).

Table 11. Distribution of Patients Based on Time Drug Use

No	Drug Name	Time of Use	n	%
1	Glibenclamide	a.c	73	76,04
		p.c	12	12,50
		as remember	11	11,46
		Total	96	100
2	Metformin	a.c	18	16,22
		d.c	30	27,03
		p.c	43	38,74
		as remember	20	18,02
		Total	111	100

Some patients used glibenclamide before meals (76.04%) and metformin after meals (38.74%). Glibenclamide can cause hypoglycemia so that the gift must be before a meal (15-30 minutes). Side effect of metformin is can cause nausea, so it must use during meals or after meals (Perkeni,2011).

CONCLUSION

1. Diabetic patients generally used more than one drug.
2. Vitamins and minerals (16.90%), antihypertensives drugs (13.89%) and NSAIDs (13.42%) were the group of pharmacological drugs that mostly used in addition to oral antidiabetic.
3. Generic drugs (94%) were the type of drugs that were mostly used in PHC.
4. Patients generally used glibenclamide once a day and metformin more than once a day.
5. Patients used glibenclamide before meals (76.04%) and metformin after meals (38.74%).

REFERENCES

ADA (American Diabetes Association). 2014. Standards of Medical Care in Diabetes – 2014

in Diabetes Care, Volume 37, Supplement 1, January 2014. Alexandria: American Diabetes Association. p. 516.

Anisa, N. S. (2008). Factors Relating to the Status of Life Quality of Patients with Diabetes Mellitus. Surabaya: Airlangga University School of Public Health.

Beardsley, R. S., Kimberlin, C. L., Tindall, W. N. 2012. Communication Skills in Pharmacy Practice: A Practical Guide for Students and Practitioners. Philadelphia: Lippincot William & Wilkins. p. 172.

DiPiro, J. T., Talbert, R. L., Yee, G. C., Matzke, G. R., Wells, B. G., & Posey, L. M. 2008. Pharmacotherapy: A Pathophysiologic Approach 7th edition. USA: The McGraw-Hill Companies, Inc. p. 1205–1242.

Irawan, D. 2010. The prevalence and incidence of Risk Factors Type 2 Diabetes Mellitus in Urban Areas of Indonesia (Secondary Data Analysis Riskesdas 2007). Thesis. Jakarta: University of Indonesia.

Kepmenkes. 2004. The Minister of Health of the Republic of Indonesia No. 1027 / Menkes / SK / IX / 2004 on Standards of Pharmaceutical Services in Pharmacy. Jakarta: Department of Health. p. 3-7.

Kurniawan, I. 2010. Type 2 Diabetes Mellitus in the Elderly in the Indonesian. Medical Magazine Volume 60 Number 12 December 2010. Jakarta: Indonesian Medical Magazine Editors. p. 582.

McPhee, S. J. and Funk, J. L. 2006. Pathophysiology of Disease: An Introduction to Clinical Medicine 5th Edition. Connecticut: Appleton & Lange.

Perkeni (Society of Endocrinology Indonesia). 2011. Consensus Management and Prevention of Type 2 Diabetes Mellitus in Indonesia.



Jakarta: PB PERKENI. p. 6-7, 22, 43, 48.
Permenkes. 2010. Regulation of the Minister of Health of the Republic of Indonesia Number HK.02.02 / Menkes / 068 / I / 2010 on Liability Using Generic Drugs at public health facilities. Jakarta: Department of Health. p. 3-4.
Saunders. 2007. Dorland's Medical Dictionary for Health Consumers. Amsterdam: Elsevier, Inc.
Tjay, T. H. dan Rahardja, K. 2007. Obat-obat

Penting: Khasiat, Penggunaan, dan Efek-efek Sampingnya. Jakarta: Penerbit PT Elex Media Komputindo Kelompok Kompas-Gramedia. hlm. 747-749.

Viktil, K., Blix, H., Moger, T., and Reikvam, A. (2006). Polypharmacy as Commonly Defined is an Indicator of Limited Value in the Assessment of Drug-Related Problems, *British Journal of Clinical Pharmacology*, (63)2, pp. 187-192.



GLYCINE MAX DETAM II VARIETY AS PREVENTIVE AND CURATIVE ORGAN DAMAGE DUE TO EXPOSURE TO LEAD (Pb)

Rika Yulia, rika.y73@gmail.com; Sylvan Septian Ressandy, Sesz.92@gmail.com; Gusti Ayu Putu Puspikaryani, geikapuspika@gmail.com; I Putu Agus Yulyastrawan, agus.yulyastrawan@gmail.com; Dewa Ayu Kusuma Dewi, ayudewak@gmail.com
Faculty of Pharmacy University Surabaya

INTRODUCTION

Human life can not be separated from the objects that come from the metal. Metals are toxic to humans, which can be derived from consuming food, beverage or air inhalation, contaminated dust, skin contact, eye contact and parenteral. Metal that goes into the lungs through the respiratory events will be absorbed by the blood and binds to the lungs and then distributed to all tissues and organs⁶. The entry of the metal into the body of one of them can lead to the formation of a compound called free radicals. Free radical formed cause DNA base modification, increase lipid peroxidation and alter calcium homeostasis and sulfidril. Antioxidants provide protection against free radical-mediated attack by the metal^{3;5}. Flavonoids are antioxidants that are important for a high redox potential, which allows the flavonoids act as reducing agents, hydrogen donors, singlet oxygen and eliminate⁷. Isoflavone and anthocyanine are flavonoids that are widely available components in soy and dairy products¹. Consumption of soy and dairy product has been linked to reduced of various cancers and chronic inflammatory diseases. Health promotion activities associated with soy consumption was associated with the presence of isoflavone content. Soy is rich in phytochemical compounds that are essential to human life and therefore considered to nutraceutical functional food. In this study, the activity of soy isoflavones compared with the activity of vitamin C as an antioxidant. Vitamin C acts as a reducing agent for a variety of free radicals.

METHODS

Glycine max Detam II Variety extracted by kinetic maceration (Stirring Motor IKA Rw 20 N) with stirring speed 10rpm. Research carried out by using 25 mice strain BALB/C that were randomly divided into five groups of five mice including negative control, positive control treatment, reference and placebo. All groups except positive control were intoxicated with lead in a dose of 25 mg/kg body weight for the duration of seven days. 2.31 g/kg body weight of Glycine max detam II has been given to treatment and positive control⁴. Thereafter 64 mg/kg body weight of vitamin C has been given to the reference group. Measurement of lead concentration in mice blood and methanol extract Glycine max Detam II Variety used Atomic Absorption Spectrophotometry (AAS), for measurement of malondialdehyde was used Thiobarbituric acid Reactive Substance (TBARS) assay. Preparation of histology assay liver and renal mice by making incision (5mm), stained with haematoxylin-eosin (HE) and observed under the electron microscope^{2;8}.

RESULT

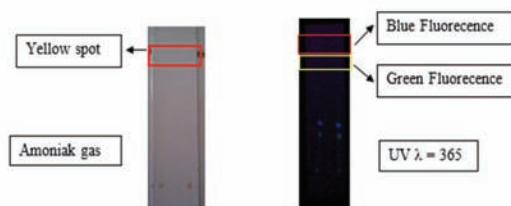


Figure 1. Identification results of Flavonoids in Extract Glycine max seed Varieties Detam II

No	Sample	Pb levels	unit
1.	Glycine max seed Varieties Detam II	0,04	ppm
2.	Glycine max extract Varieties Detam II	0,02	ppm

Table 1. Analysis lead levels in extract and Glycine max seed Varieties Detam II

Mice	Pb levels in the mice blood (ppm)				
	Placebo group	(-) Control group	(+) Control group	Tested group	Comparer group
1.	0,272	0,404	0,217	0,248	0,324
2.	0,288	0,38	0,324	0,314	0,382
3.	0,302	0,393	0,168	0,274	0,188
4.	0,318	0,234	0,192	0,262	0,278
5.	0,348	0,288	0,247	0,256	0,182
average	0,306	0,352	0,230	0,271	0,271
SD	0,029	0,056	0,060	0,026	0,087

Table 2. Analysis of Pb levels in mice blood

Mice	The percentage of kidney cell damage in mice (%)				
	Placebo group	(-) Control group	(+) Control group	Tested group	Comparer group
1	8,45	56,16	11,27	27,94	16,22
2	8,96	60,81	8,97	29,17	12,86
3	8,57	50,00	11,59	32,05	12,50
4	8,06	49,28	13,92	32,53	-
5	6,06	64,29	12,82	32,47	-
average	8,02	56,11	11,71	30,83	13,86
SD	1,14	6,58	1,86	2,13	2,05

Table 3. The percentage of kidney cell damage in mice

Mice	The percentage of liver cell damage in mice (%)				
	Placebo group	(-) Control group	(+) Control group	Tested group	Comparer group
1	6,25	51,43	11,27	27,94	9,86
2	3,9	46,91	8,97	29,17	13,16
3	6,41	42,11	11,59	32,05	9,72
4	3,7	44,05	13,92	32,53	-
5	5,19	51,47	12,82	32,47	-
average	5,09	47,19	11,72	30,83	10,91
SD	1,27	4,24	1,86	2,13	1,95

Table 4. The percentage of liver cell damage in mice

Mice	MDA levels (ppm)				
	Placebo group	(-) Control group	(+) Control group	Tested group	Comparer group
1.	28,418	58,305	23,785	53,543	18,980
2.	27,272	52,013	42,575	50,483	36,283
3.	23,699	28,418	18,98	15,834	33,137
4.	18,980	41,002	53,543	32,126	29,991
5.	23,785	33,924	34,71	58,132	25,272
average	24,431	42,732	34,719	42,024	28,733
SD	3,690	12,39	13,99	17,66	6,80

Table 5. MDA levels (ppm) of liver mice were given extract Glycine max Detam II Varieties

CONCLUSION

The result showed that Glycine max detam II varieties was significantly decrease the level of lead in mice's blood, not significantly decrease the level of malondialdehyde in mice's organ and also significantly decrease of damage organ.

REFERENCES

1. Cho KM, Ha TJ, Lee YB, Seo WD, Kim JY, Ryu HW, Jeong SH, Kang YM, Lee JH, 2013, Soluble Phenolics and Antioxidant Properties of Soybean (Glycine max L.) Cultivars with Varying Seed Coat Colors, Journal Of Functional Foods.
2. Janqueira, Luis Carlos, Carneiro, Jose, Kelley, Robert O, 1998, Basic Histology, 9th edition, Appleton & Lange, Stamford.
3. Khaki AA and Khaki A, 2010, Antioxidant Effect of Ginger to Prevents Lead-Induced Liver Tissue Apoptosis in Rat. Journal of Medicinal Plants Research Vol. 4(14), pp. 1492-1495.
4. Koswara, Sutrisno., 2006, Isoflavon, Senyawa Multi-Manfaat dalam Kedelai, Departemen Ilmu dan Teknologi Pangan, Fakultas Teknologi Pertanian, Institut Pertanian Bogor.
5. Sidik, 1997, Antioksidan Alami Asal Tumbuhan, Seminar Nasional Tumbuhan Obat XII, ITB, Bandung.
6. Palar H, 2004, Pencemaran dan Toksikologi Logam Berat, Rineka Cipta, Jakarta.
7. Ponnusha BS, Subramaniyam S, Pappasupathi P, Subramaniyam B, Virumandiyar R, 2011, Antioxidant and Antimicrobial Properties of Glycine Max-A review, International Journal of Current Biological and Medical Science. 1(2): 49 – 62
8. Subowo, 2009, Histologi Umum, edisi ke 2, Jakarta, CV Sagung Seto.

Researchers would like to say thank you to Dikti for giving grants in this study.



AN ACTIVITY TEST OF MATOA LEAVES EXTRACT AS HEART RATE FREQUENCY REDUCTION WITH ADRENALINE INDUCTION

Ika Purwidyaningrum, Setia Budi University, Jl. Letjend Sutoyo Surakarta, can_ika@yahoo.com, 085697489516; **Elin Yulinah Sukandar**, Institut Teknologi Bandung, Jl. Ganesa 10 Bandung, elin@fa.itb.ac.id, 081320552054; **Irda Fidrianny**, Institut Teknologi Bandung, Jl. Ganesa 10 Bandung, irda@fa.itb.ac.id

ABSTRACT

It is proven, empirically, that Matoa leaves have been used as an antihypertensive medicine by Pajang Surakarta people. Blood pressure is the result of cardiac output and peripheral resistance multiplication. Cardiac output influenced by pulse, contractility and filling pressure. Filling pressure influenced by blood volume and venous tone while peripheral resistance influenced by arterioles volume.

Heart rate frequency influence by contractility and will affect cardiac output and blood pressure. So, if the heart rate frequency increasing, the contractility, cardiac output and blood pressure will automatically increasing too.

The research used 6 groups of male Sparque Dawley's lab rats and it consists 5 lab rats for each group. 3 different groups had given 3 variants dose of 50mg/kg bw, 100mg/kg bw, and 150mg/ kg bw. Comparison groups are those with atenolol 9mg/kg bw, positive control and negative control. And data analyzed by using one way ANOVA.

The results showed that all groups have significantly different treatments especially the one with positive control. 50mg/kg bw dose is the most effective way to decrease heart rate frequency.

INTRODUCTION

Hypertension is one of the cardiovascular problems which happen to many people. It is commonly happen as they grow older. Hypertension (6,8%) is top 3 cause of death after Stroke (15,4%) and Tuberculosis (7,5%). Based on blood pressure measurement, it shows about 31,7% of Hypertension happen to Indonesian around 18 years old or more.

The highest rate of Hypertension in Indonesia

is in south Kalimantan about 39,6% of population and west Papua province is the lowest rate about 20,1% of population. 7,2% of health service Hypertension diagnosed and 7,6% of interviews, only 0,4% of the Hypertension patients who took medications.

So, this is why health service could only treated 24,0% out of 31,7% of Hypertension problems. It is like 76,0% of all Hypertension cases hasn't been treated (Depkes, 2008). WHO also explained that the percentage of Hypertension on adult (over 25 years old) men is quite larger than women. It is proven that 32,5% Hypertension happen on men and 29,3% on women (WHO, 2012).

There are some problems tend to happen in pharmacological Hypertension treatments. Hypertension treatments with antihypertensive medicine usually takes a lot of time to treat which cause some side effects.

And then, it is impossible to precisely predict the individual respond of each patients to certain antihypertensive medicines and many of the cases need more than 2 kinds of antihypertensive medicines to reach their blood pressure objective (Gilman, 2006). So, that's why in many Hypertension cases, a lot of patients got into therapy inconsistencies that cause them difficulties to reach their objectives.

Therefore, this is a huge opportunity to find a new, save, effective and high quality antihypertensive medicine. The best source to get a good antihypertensive medicine is from plants, the most natural source in every way. There are so many types of plant in Indonesia that have great effects to decrease blood pressure and one of them is a Matoa plant; which has been used by Pajang Surakarta people in a while.



Matoa is one of the plants that has not been research so much. On FV. Mohammad's research in 2010, titled; A new triterpenoid saponin from the stem bark of *Pometia pinnata*, shows that he succeed to isolate new compound of saponin and triterpenoid, and that is: pometin, 3-O-[beta-D-glukopiranosil-(1 → 2)-beta-D-glukopiranosil-(1 → 3)-beta-D-glukopiranosil acid-oleanolic, and FV. Mohammad in 2012 succeed to isolate kaemferol 3-O- α -L-rhamnopyranoside.

Next research had done by Suedee A in 2013, he succeed to isolate epikatekin, kaempferol-3-O-rhamnoside, quercetin-3-O-rhamnoside, glikolipid, 1-O-palmitoil-3-O-[α --galactopyranosyl-(1 → 6)- β -. -galactopyranosyl]-sn-glycerol, steroid glycosides, stigmasterol-3-O-glucoside, and triterpenoid saponin pentasiklik, 3-O- α --arabinofuranosyl-. (1 → 3) - [α --rhamnopyranosyl-(1 → 2)]- α --arabinopyranosyl hederagenin from Matoa leaves extract that has an activity as an anti HIV.

It is said that antihypertensive effect with an active compound haven't been researched before. Therefore, it is important to do a research to a Matoa plant as antihypertensive and find out how the activity mechanism to decrease blood pressure.

RESEARCH METHODOLOGY

Materials and tools

Research materials that have been used are Matoa leaves ethanol extract, atenolol, aquadest, 0,5% CMC, 70% alcohol, and adrenaline. Then, the tools that been used are 1 ml syringe, 5ml syringe, rat lab's oral sonde, and tail cuff.

The procedures

This research used 30 SD white male rat labs as sampling test and they divided into 6 groups. Sampling test was taking by a simple and random sampling. The samples took randomly simply because population has proven homogenous. Each group consist of 5 male lab rats. All lab rats adapted by a tail cuff test equipment about 2-3 times with the same foods and drinks for 14 days.

The procedures of the treatment explain as following:

a. The first group has given 50 mg/kg bw dose of Matoa leaves extract, 100mg/kg bw dose of Matoa leaves extract to the second group, 150mg/kg bw dose of Matoa leaves extract to the third group, 0,5% CMC to the control negative group and no treatment for the control positive. b. Comparison group has given atenolol 9mg/kg bw. C. All group except group with control negative have given 1,2μg/kg bw adrenaline. d. The heart rate frequency noted when;

T0 : the heart rate frequency before treatment

T1 : the heart rate frequency after treatment

T2 : the heart rate frequency after adrenaline induction And data analyzed statistically by using one way ANOVA.

RESEARCHS AND FINDINGS

Athenolol is an antihypertensive medicine and anti-tonsillitis which part of the beta blocker that worked based on heart rate decreases mechanism and Myocardia contractility so that the cardiac output will decrease. NE (nor epineprin) releases resistance through beta-2 receptor resistance; renin secretion resistance through beta-1 resistance receptor on kidney (Fatimah, 2012).

Adrenaline is always causes blood vessel arterial vasoconstriction, triggers pulse and cardiac contraction so the blood pressure increases rapidly and ends in a short term of time (Matsum 2008)

Group	T0	T1	T2
I (50mg/kg bw)	138,4±18,2	108,2±20,4	153,2±19,5
II (100mg/kg bw)	172,6±23,8	185,6±23	278,8±20,8
III (150mg/kg bw)	247,8±25,2	206,8±19,8	287,2±57
Atenolol 9mg/kg bw	127,4±12,1	123,2±29,9	145,6±24,3
Control+	113,8±14	128,6±27,4	288,6±57,7
Control-	171±40,4	168,6±43,1	179,6±22

Figure 1. Average heart rate frequency per-group/per-minute



Blood pressure happen because of cardiac output and the peripheral blood vessel resistance. Antihypertensive medicine is working through the peripheral resistance or cardiac output or even both. Cardiac output could decreasing by medicines that could clog myocardial contractility or decreasing the ventricular pressure charging.

The heart rate frequency related to heart contractility and cardiac output. If the heart rate frequency decreasing, cardiac output also will decreasing and then finally the blood pressure is automatically controllable

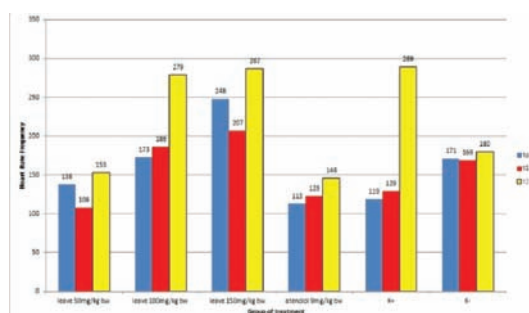


Figure 2. Average heart rate frequency graphic chart Based on the graphic on picture 1, it is shown that the heart rate frequency is rising after adrenaline induction (T2 yellow). However, 50 mg/kg bw dose of Mtoa leaves extract increasing insignificantly and equally like atenolol as a comparison.

CONCLUSION

1. Mtoa leaves extract proven decreasing heart rate frequency.
2. The effective dose from Mtoa leaves extract for decreasing heart rate is 50mg/kg bw.

REFERENCES

A. Suedee., et. al. 2013 Anti-HIV-1 integrase compound from *Pometia pinnata* leaves, Department of Pharmacognosy and Pharmaceutical Botany, Faculty of Pharmaceutical Sciences, Prince of Songkla University, Hat-Yai, Songkla 90112, Thailand

Departemen Kesehatan, 2008, Laporan Hasil Riset Kesehatan Dasar (Riskesdas) Indonesia Ta-

hun 2007, Jakarta: Balitbangkes-Depkes RI

Dipiro, J. T., et. al., 2008, *Pharmacotherapy A Pathophysiologic Approach*, 7th ed., McGraw Hill, New York, 705-759

FV.Mohammad., et. al., 2010 A new monodesmosidic triterpenoid saponin from the leaves of *Pometia pinnata*, H.E.J Research Institute of Chemistry, International Center for Chemical and Biological Sciences, University of Karachi, Karachi-75270, Pakistan.

FV.Mohammad., et. al., 2010 A new triterpenoid saponin from the stem bark of *Pometia pinnata*, H.E.J Research Institute of Chemistry, International Center for Chemical and Biological Sciences, University of Karachi, Karachi-75270, Pakistan.

Gilman, A. G., et. al., 2006, *Goodman and Gilman's The Pharmacological Basis of Therapeutics*, 11th Ed., The McGraw-Hill Companies, USA

JNC 7, 2003. The Seventh Report of the Joint National Committee on Prevention Detection, Evaluation, and Treatment of High Blood Pressure, National High Blood Pressure Education Program, available at <http://www.nhlbi.nih.gov/guidelines/hypertension/express.pdf>.

Katzung BG., 2002, *Farmakologi Dasar dan Klinik*, (penerjemah dan editor) Bagian Farmakologi Fakultas Kedokteran Universitas Airlangga, Salemba Medika, Surabaya.

Matsum, 2008, *Reaksi atropine dan adrenalin*, <http://matsum.blogspot.com/2008/05/reaksi-atropine-dan-adrenalin.html>

Radhi, Fatimah, 2012, *Atenolol*, <http://publichealthnote.blogspot.com/2012/03/atenolol.html>

Vogel, G. H. 2008, *Drug Discovery and Evaluation*, Pharmacological Assays, Edisi ke-2, Springer-verlag, Berlin

WHO, 2012, *World health statistics 2012*, Geneva: WHO Press, 111

EFFORT TO REDUCE COMPRESSIBILITY OF RAMIPRIL THROUGH CRYSTAL ENGINEERING

Indra, School of Pharmacy Institut Teknologi Bandung, Jl. Ganesha 10 Indonesia; indraf04@gmail.com; Sundani N Soewandhi, School of Pharmacy Institut Teknologi Bandung, Jl. Ganesha 10 Indonesia.

INTRODUCTION

In drug development process, one of the early decisions that must be made is determining crystalline forms or polymorphs of the drug. Physical properties of solid polymorphs can influence the quality, safety and efficacy of drug. Considering that the bond can affect the physical properties at the macroscopic level, the efforts to manipulate the physical properties by regulating the molecular re-arrangement in the solid state into a different crystal are things that can be importance in the pharmaceutical industry. Cocrystal has the physical properties, such as particle size and crystal habit that can influence the surface properties, suspended ability, dissolution rate, the behavior of powder compressibility and compactibility. Mechanical properties are those properties of a material under the influence of an applied stress. Compressibility, tabletability and compactibility are parameters to characterizing the mechanical properties whose are important to produce tablet dosage form. The aim of this study was to reduce the compressibility of ramipril due to formation of cocrystal.

MATERIALS AND METHODS

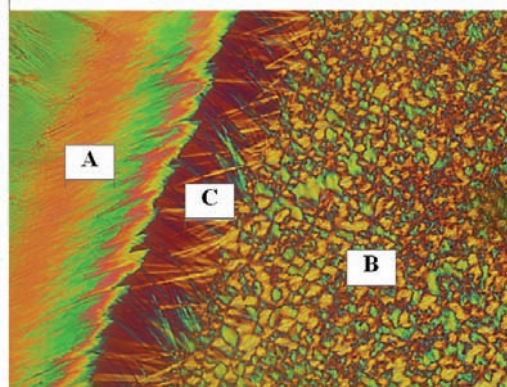
Ramipril (RA) was kindly obtained from PT Kimia Farma, Tbk, Indonesia. Vanilline (VA) and ethanol and other reagents were purchased from Merck Chemical without any purification. Hot Stages Method made to the RA and VA under the polarizing microscope equipped with an electric heater table (Hot Stage) crystal growth was observed in the contact zone (CZ) between RA and VA crystal. RA-VA binary mixtures prepared by physical mixing at various compositions based on the mole fraction. The physical properties of the binary system is characterized by DSC thermal analysis was

then made binary system phase diagram of RA and VA. Formation cocrystal RA-VA conducted by dissolving the molar ratio of 1: 1, then the samples were characterized by DSC and PXRD. Then cocrystal RA-VA sample tested compressibility.

The observation by polarizing microscopy, DSC and PXRD further processed and analyzed to identify and evaluate the RA-VA cocrystal formation, changes in compressibility.

RESULT AND DISCUSSION

Microscopic Analysis by Hot Stage Polarization and Electron Microscope



and VA. Formation cocrystal RA-VA conducted by dissolving the molar ratio of 1: 1, then the samples were characterized by DSC and PXRD. Then cocrystal RA-VA sample tested compressibility.

The observation by polarizing microscopy, DSC and PXRD further processed and analyzed to identify and evaluate the RA-VA cocrystal formation, changes in compressibility.

RESULT AND DISCUSSION

Microscopic Analysis by Hot Stage Polarization and Electron Microscope



This analysis provided a preliminary characterization of cocrystalline phase in binary mixture of RA-VA. Optical and electron microphoto was shown in Fig. 1 and 3. RA-VA cocrystal from solvent method was needle shaped habit and was obtained within two days. A sharp melting point at around 91.9 °C was observed for the RA-VA cocrystal (Fig 2).

Figure 1 Microphoto crystal habit A) VA, B) RA C) CZ

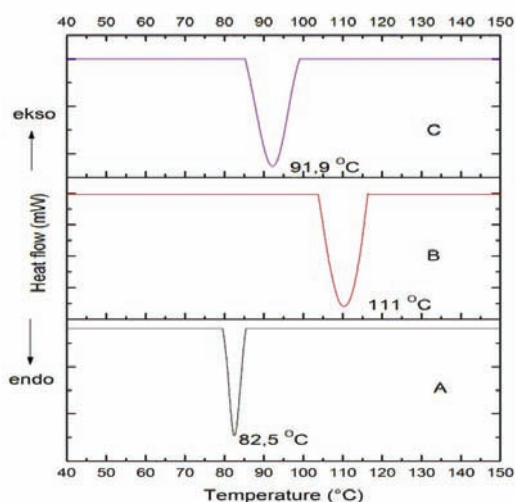


Figure 2 Thermogram DSC A) VA, B) RA C) RA-VA

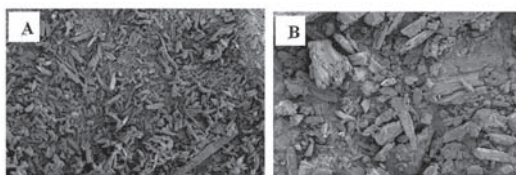


Figure 3 SEM Microphoto crystal habit a) RA, b) VA. Magnification 500x

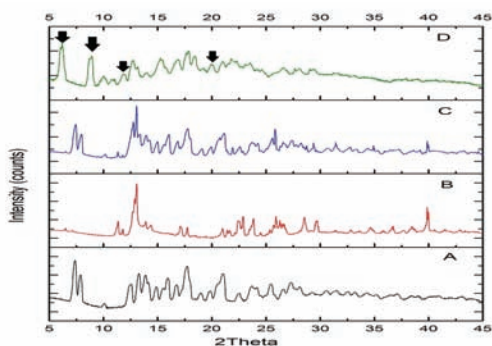


Figure 3 Powder Diffraction A) RA B) VA C) PM D) RA-VA

The diffraction pattern of cocrystal should be clearly distinct from that of the superimposition of each of the compound. If a true cocrystal has been formed between two solid phases. A different PXRD pattern for cocrystal of RA and VA (Fig. 3D) from those physical mixtures confirms the formation of a new cocrystal phase.

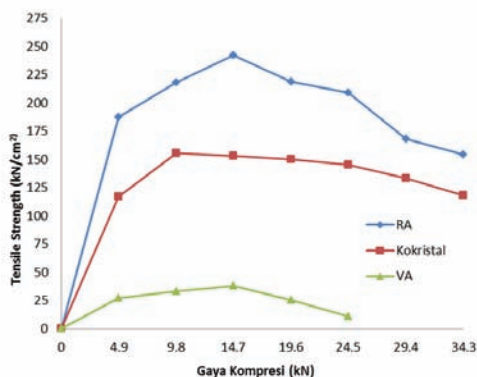


Figure 3 Compressibility Curve

Based on the above curves powder compressibility RA had the highest, while the lowest VA powder. The higher the compressibility curve of a material, the more easily the material to be compressed.

CONCLUSION

In the contact method, observed the formation of a new crystal habit elongated needle-shaped contact zone between ramipril (RA) and vanillin (VA), which has a different melting range from the melting point of the two components. X-ray diffraction pattern of the compound powder of the interaction of RA and VA showed different diffractogram of the two components which indicates the formation of cocrystal phase. The test results showed solubility of the sample results cocrystallization was higher than pure and recrystallization results. Characterization of compressibility shows that a decline in the compressibility of the powder RA after cocrystallization process with the VA. The results of dissolution test powders and tablets of various compression



cocrystal RA and RA-VA showed that kokristal RA-VA has a lower dissolution than RA either on medium 0.1N HCl (pH 1.2) and phosphate buffer pH 6.8.

REFERENCES

- *. Aher, S., Dhumal, R., Mahadik, R., Ketolainen, J., Paradkar, A., 2013, Effect of Cocrystallization Techniques on Compressional Properties of Caffeine/Oxalic Acid 2:1 Cocrystal, *Pharmaceutical Development and Technology*, 18(1), 55-60.
- *. Bhattacharya, A., Chattopadhyay, B., Chakraborty, S., Roy, B.N., Singh, G.P., Godbole, H, M., Rananaware, U., Mukherjee, A. K., 2012, Tris (hydroxymethyl) Aminomethane Salt of Ramipril: Synthesis, Structural Characterization from X-Ray Powder Diffraction and Stability Studies, *Journal of Pharmaceutical and Biomedical Analysis*, 70, 280-287.
- *. Morissette, S.L., Almarsson, O., Peterson, M.L., Remenar, J.F., Read, M.J., Lemmo, A.V., Ellis, S., Cima, M.J., Gardner, C.R, 2004, *High-Throughput Crystallization: Polymorph, Salts, Cocrystal and Solvates of Pharmaceutical Solids*, 125-181, Marcel Dekker, New York.



IN VITRO ALPHA-GLUCOSIDASE INHIBITORY ACTIVITY OF ETHANOLIC LEAF EXTRACT AND FRACTIONS OF *Rauvolfia serpentina* (L.) Benth. ex Kurz

Julie Anne D. Bolaños, Department of Chemistry, College of Science, Adamson University, 900 San Marcelino St., Ermita, 1000 Manila, juliea_bolanos@yahoo.com, +63935-1310959; **Ivan L. Lawag**, Department of Chemistry, College of Science, Adamson University, Ermita, Manila, Philippines, ivan.lawag@gmail.com, +63917-5045962

INTRODUCTION

Diabetes mellitus is a well-known metabolic disorder which is characterized by hyperglycemia resulting from the deficiency in the production of insulin by the pancreas or its action (Umar et al., 2010). According to International Diabetes Federation, this serious metabolic disease has been affecting 382 million (2013) of the population worldwide and this number is predicted to rise up to 592 million by the year 2035. Type 2 diabetes mellitus has more prevalent compared with Type 1 diabetes.

Alpha-glucosidase inhibition is one of the mechanisms involved in lowering blood glucose levels (BGLs). At present, synthetic alpha-glucosidase inhibitors have been made available as oral anti-hyperglycemic drugs, they have been found to cause negative hepatic and gastrointestinal side effects (Feng et al., 2009). The demand in using approaches to treat diabetes, such as plant-based medicines, has increased in countries which are industrially developed. Therefore, to search for new plant-based medicine to inhibit alpha-glucosidase activity and fight diabetes mellitus, this research was conducted.

Rauvolfia serpentina (L.) Benth. ex Kurz is a genus of the family Apocyanaceae (dogbane family) and occurs in nearly all habitable tropical and subtropical regions. This medicinal plant was therapeutically important because of the presence of indole alkaloids in the treatment of various diseases, which is in great demand of modern pharmaceutical industries (Nair et al., 2011). For α -glucosidase inhibitory activity, this medicinal plant has never been investigated.

MATERIALS AND METHODS

Chemicals

The chemical reagents used were analytical grade. Silica gel 60 HF254 was used for Vacuum Liquid Chromatography. Yeast α -glucosidase, p-nitrophenyl- α -D-glucopyranoside (p-NPG) and N-deoxynojirimycin were purchased from Sigma (Singapore).

Plant material

Sample of 3 kilos *Rauvolfia serpentina* leaves were collected from Tabang, Bulacan, Philippines last October 2013. Wilfredo F. Vendivil, Ph.D. identified and authenticated the plant with Herbarium Accession Number 777-01) at the Botany Division of National Museum, Manila, Philippines. The leaves were air-dried at room temperature for 20 days and oven dried at 40°C for 72 hours. The oven dried samples were ground using pulverized mill and were soaked with 80% ethanol for 3 times, 24 hours each time at room temperature. The ethanolic extracts were drained, filtered and concentrated in vacuo at 45°C using a rotary evaporator. *Rauvolfia serpentina* gave a 3.2% yield or 97.1 g of crude extract.

Fractionation of *Rauvolfia serpentina* crude extract and subfractions

The crude extract 97.1 g was subjected to Vacuum Liquid Chromatography (VLC). It was mixed with Silica gel in a reasonable amount. The extract-Silica gel mixture was placed on a top of a 9 cm height Silica gel 60 H254, 10 cm internal diameter VLC column, vacuum packed. Fractionation was done using solvents of increasing polarity and were concentrated in vacuo at 45°C. The same method was done on the DCM and ethyl acetate sub-



fractions. The crude extract as well as the four fractions were subjected to bioassay.

In Vitro Yeast α -Glucosidase Inhibitory Activity

The adopted method used for the yeast α -glucosidase enzyme inhibition assay was done by Lawag et al. The assay was done at Adamson University, Manila, Philippines.

A concentration of 0.017 units/mL of the enzyme and 0.7 mM of substrate were prepared and utilized for determination of the inhibitory activity of crude extract, fractions and subfractions. These were prepared in a 100 mM sodium phosphate buffer that was prepared in distilled water with the pH 6.8 which contains 50 mM NaCl. N-deoxynojirimycin was used as a positive control for the assay. Phytochemical screening of *Rauvolfia serpentina*

The phytochemical screening was performed on the crude extract and its fractions using different spray reagents: Potassium ferricyanide-ferric chloride was used for detection of phenols, tannins and flavonoids with a blue spots for positive result; Dragendorff's reagent was used for detection of alkaloids with a brown-orange visible spots immediately on spraying for positive result; Vanillin-sulfuric acid was used for detection of higher alcohols, phenols, steroids and essential oils with blue-violet spots for positive result of triterpenes and sterols while wide range of colors for essential oils; and α -Naphthol-sulfuric acid for detection of sugars with a blue spots for positive result.

RESULTS AND DISCUSSION

Sample	IC ₅₀ ($\mu\text{g/mL}^{-1}$)
<i>Rauvolfia serpentina</i> Crude extract	5.56 \pm 1.19
Hexane	4.47 \pm 1.08
Dichloromethane	1.40 \pm 1.24
Ethyl Acetate	1.06 \pm 1.04
Methanol	1.50 \pm 1.15
Dichloromethane subfractions	IC ₅₀ ($\mu\text{g/mL}^{-1}$)
Hexane	6.03 \pm 1.38
Hexane:Dichloromethane/75:25	4.06 \pm 1.34
Hexane:Dichloromethane/50:50	1.74 \pm 1.18
Hexane:Dichloromethane/25:75	5.54 \pm 1.53
Dichloromethane	4.07 \pm 1.26
Dichloromethane:Ethyl acetate	9.16 \pm 1.22
Ethyl acetate	3.86 \pm 1.25
Ethyl acetate:Methanol	5.35 \pm 1.46
Methanol	4.79 \pm 1.28
Ethyl acetate subfractions	IC ₅₀ ($\mu\text{g/mL}^{-1}$)
Hexane	36.77 \pm 1.32
Hexane:Dichloromethane	20.05 \pm 1.42
Dichloromethane	22.12 \pm 1.51
Ethyl acetate	21.40 \pm 1.66
Ethyl acetate:Methanol	19.17 \pm 1.67
N-deoxynojirimycin (Positive Control)	56.7 \pm 2.80

Table 1. α -Glucosidase inhibitory activity of *Rauvolfia serpentina* crude extract, fractions and subfractions

The ethanolic leaf extract of *Rauvolfia serpentina* was found to be a potential source of α -glucosidase inhibitor that has half maximal inhibitory concentration (IC₅₀) of 5.56 \pm 1.19 $\mu\text{g/mL}^{-1}$. Among the 4 fractions yielded from crude extract, the ethyl acetate fraction showed the highest enzyme inhibitory activity with IC₅₀ of 1.06 \pm 1.04 $\mu\text{g/mL}^{-1}$ followed by dichloromethane fraction with IC₅₀ at 1.40 \pm 1.24 $\mu\text{g/mL}^{-1}$, methanol fraction with IC₅₀ at 1.50 \pm 1.15 $\mu\text{g/mL}^{-1}$ and hexane fraction with IC₅₀ at 4.47 \pm 1.08 $\mu\text{g/mL}^{-1}$.

Further purification were done in dichloromethane and ethyl acetate fractions. In dichloromethane fraction, it obtained 9 subfractions. Among the 9 subfractions, hexane:dichloromethane/50:50 gave the highest enzyme inhibitory activity with IC₅₀ of 1.74 \pm 1.18 $\mu\text{g/mL}^{-1}$. In ethyl acetate fraction, it obtained 5 subfractions. In 5 subfractions, ethyl acetate:methanol/1:1 gave the highest enzyme inhibitory activity with IC₅₀ of 19.17 \pm 1.67



$\mu\text{g}/\text{mL}$ -1 against yeast α -glucosidase enzyme. *Rauvolfia serpentina* were screened for its phytochemical constituents. Alkaloids was present in ethyl acetate and methanol fraction. Tannins, flavonoids and phenols were present in dichloromethane fraction.

CONCLUSION

The result of the assay showed that *Rauvolfia serpentina* extract ($\text{IC}_{50}=5.56\pm 1.19 \mu\text{g}/\text{mL}$ -1) has a better enzyme inhibitory activity against N-deoxynojirimycin (positive control) ($\text{IC}_{50}=56.7\pm 2.80 \mu\text{g}/\text{mL}$ -1). Therefore, this leaves can be developed and lead to the formulation of new, affordable and effective anti-diabetic drugs as α -glucosidase inhibitors.

RECOMMENDATION

In future, specific inhibitor has to be isolated from the crude extract of *Rauvolfia serpentina* to characterized and therapeutically exploited. Subfractions were showed a good activity against the enzyme, further isolation and structure elucidation should be done to determine the compounds that are attributed to its α -glucosidase inhibitory activity.

ACKNOWLEDGEMENT

The author wish to express her sincere gratitude to the Center for Research Evaluation and Continuing Education (CRECE) of Adamson University, Manila, Philippines for financial assistance and Chemistry Laboratory of Adamson University for the facilities and equipment provided.

REFERENCES

1. Feng, J., Yang X., Wang, R., (2009). Bio-assay guided isolation and identification of α -glucosidase inhibitors from the leaves of *Aquilaria sinensis*. *Phytochemistry*, 242-247.
2. Lawag, I., (2014). Bio-assay Guided Isolation and Spectral Analysis of α -Glucosidase Inhibitors from the Leaves of *Antidesma bunius* Linn. Spreng, University of Sto. Thomas.
3. Lawag, I., Aguinaldo, A., Naheed, S., Mossihuzzaman, M., (2012). A-Glucosidase inhibitory activity of selected Philippine plants. *Journal of Ethnopharmacology*, 144(1).
4. Nair, V., Panneerselvam, R., Gopi, R., (2011). Studies on methanolic extract of *Rauvolfia* species from Southern Western Ghats of India- In vitro anti oxidant properties, characterization of nutrients and phytochemicals. *Industrial Crops and Products*, 17-25.
5. Umar, A., Ahmed, Q., Muhammad, B., Dogarai, B., Mat Soad, S., (2010). Anti-hyperglycemic activity of the leaves of *Tetracera scandens* Linn. Merr. (Dilleniaceae) in alloxan induced diabetic rats. *Journal of Ethnopharmacology*, 140-145.



PERIPLASMIC EXPRESSION OF GENE ENCODING ANTI-EGFRvIII SINGLE-CHAIN VARIABLE FRAGMENT ANTIBODY USING PeIB LEADER SEQUENCE IN *Escherichia Coli*

Kartika Sari Dewi, School of Pharmacy, Bandung Institute of Technology, Jalan Ganesa 10, Bandung; Research Center of Biotechnology, Indonesian Institute of Sciences (LIPI), Cibinong Science Center, Jalan Raya Bogor Km. 46, Cibinong, Bogor; **Debbie Sofie Retnoningrum**, School of Pharmacy, Bandung Institute of Technology, Jalan Ganesa 10, Bandung; **Catur Riani**, School of Pharmacy, Bandung Institute of Technology, Jalan Ganesa 10, Bandung; **Asrul Muhammad Fuad**, Research Center of Biotechnology, Indonesian Institute of Sciences (LIPI), Cibinong Science Center, Jalan Raya Bogor Km. 46, Cibinong, Bogor,
Corresponding author: asrul.m.fuad@gmail.com.

INTRODUCTION

Many growth factors and their receptors play important roles in modulating cell division, proliferation and differentiation. Overexpression of growth factor receptors has been implicated as an important factor in the proliferation of malignancies and has also been identified as a marker of poor prognosis (Kuan et al., 2001).

Epidermal growth factor receptor variant III (EGFRvIII) is a mutant variant of EGFR that commonly overexpressed in human malignant cells. EGFRvIII has in frame deletion of exons 2-7 that encodes extracellular domain, resulting in the formation of new Glycine residue. Although EGFRvIII is unable to bind EGF or other EGFR-binding ligands, it is constitutively phosphorylated and able to activate downstream signaling cascades, which end up with cell differentiation (Pedersen et al., 2001). The possibility of disrupting this process has led to the development of novel therapeutic agents for cancer treatment (Kuan et al., 2001).

EGFRvIII is commonly found in glioblastoma multiforme and has been reported also in breast, ovarian, prostate, lung, head and neck carcinomas, but did not found in normal cells (Huang et al., 1997; Batra et al., 1995; Sok et al., 2006). Lacks of 267 amino acids from extracellular domain of EGFRvIII has resulted in the formation of a new immunogenic epitope near the amino terminus. Therefore this receptor might be used as an ideal molecular target in immunology based cancer therapy

(Gupta et al., 2010). In such kind of targeted cancer therapy, antibody fragments were frequently used as targeting moiety.

Fv fragment is the smallest unit of antibody molecule that preserves its antigen-binding properties. Thus, it can facilitate a targeted drug delivery for a treatment that requires high specificity. Single-chain variable fragment (scFv) is an antibody fragment that consists of variable regions of heavy (VH) and light chains (VL), joined together by a flexible peptide linker. Thus, it can be easily expressed in *Escherichia coli* (Ahmad et al., 2012). However, an scFv molecule has at least two disulfide bonds in its structure which are required to be correctly formed in order to preserve its antigen-binding affinity. In *E. coli* expression system, periplasmic compartment is preferably used for recombinant protein production that needs a correct protein folding and disulfide bond formation (Kipriyanov et al., 1997).

Periplasmic production of recombinant proteins provides several advantages compared to cytosolic production. For example, the authentic N-terminal amino acid sequence without the Methionine extension can be obtained after cleavage by the signal peptidase. Also, there appears to be much less protease activity in the periplasmic space than in the cytoplasm. In addition, recombinant protein purification is simpler due to fewer contaminating proteins in the periplasm (Makrides, 1996; Choi et al., 2000)



In this study, we reported the periplasmic expression of an anti-EGFRVIII scFv in *E. coli* BL21(DE3) periplasm. Prior to periplasmic expression, the DNA fragment encoding anti-EGFRVIII scFv was subcloned into pJ414 expression vector containing pelB leader sequence, which is derived from *Erwinia carotovora* (Lei et al., 1987). This leader sequence consists of 22 amino acids residues, which directs the recombinant protein production fused with this leader sequence into periplasmic compartment in gram-negative bacteria, such as *E. coli* (Choi and Lee, 2004).

MATERIALS AND METHODS

Plasmid containing DNA fragment of anti-EGFRVIII scFv (pJ201_scFv) was obtained from previous research. Expression vector containing pelB leader sequence (pJ414_pelB), *E. coli* TOP10 and BL21(DE3) are available in our laboratory. Primers used in this study were: scFv1-forward primer containing NcoI site (5'-GGC-CATGGC TCAAGTTCAATTGGTTGAGTCAGG-3'), scFv1-reverse primer containing XhoI site (5'-CGCCATGGCTCGAGT GATTAACAATGATGATGGTGG-3'), and T7-promoter primer. All primers were purchased from IDT.

Construction of plasmid pJ414_pelB-scFv

DNA fragment encoding anti-EGFRVIII scFv was amplified from pJ201_scFv by PCR method. PCR was conducted as follows: initial denaturation at 95 °C for 1 m; 25 to 30 cycles of denaturation at 95 °C for 1 m, annealing at 60 °C for 30 s, and extension at 72 °C for 1 m, then final extension at 72 °C for 5 m. PCR products were analyzed with 1 % agarose gel electrophoresis. Purified PCR product and pJ414_pelB expression vector were double digested using NcoI and XhoI enzymes (3 IU /1 µg product), then incubated at 37 °C for 18 h. Digested products were examined with 1% agarose gel electrophoresis, subsequently isolated from an agarose gel using Gel/PCR DNA Fragments Extraction Kit (Geneaid).

Purified scFv gene and plasmid were ligated

using T4-DNA ligase (1 IU/50 ng plasmid), then transformed into *E. coli* TOP10 using transformation and stock solution (TSS) (Chung et al., 1989). Recombinant plasmids were isolated from *E. coli* transformants, then characterized by migration, restriction, and PCR analyses. It was subsequently sequenced to ensure no mutation presents within the gene sequence. Confirmed recombinant plasmid was then transformed into *E. coli* BL21(DE3).

Growth conditions for scFv expression

E. coli BL21(DE3) carrying pJ414_pelB_scFv were grown overnight in Luria Bertani medium with 100 µg/mL ampicilin (LBamp) at 37°C. This culture was diluted 1:50 with 20 mL LBamp medium, grown at 37°C in 100 mL shaking flask. When cultures reached OD600 = 0.8, IPTG was added and growth was continued at room temperature (20-23°C) for 18-20 h. Optimization of IPTG concentration was carried out by varying IPTG concentration from 0.1 to 1 mM.

Isolation of soluble periplasmic proteins

Cells were harvested by centrifugation at 5000 x g and 4°C for 15 m. Pelleted cells were resuspended with hypertonic solution consisting of 20% sucrose, 30 mM Tris-Cl, and 1 mM EDTA pH 8. After 1 h incubation on ice with occasional stirring, the spheroplasts were centrifuged at 11600 x g and 4 °C for 30 m, leaving the soluble periplasmic extract as the supernatant and spheroplasts plus the insoluble periplasmic material as the pellet (Kipriyanov et al., 1997). Supernatant containing periplasmic proteins were separated, and then analyzed by 10% SDS-PAGE.

Comparison of total proteins, soluble periplasmic and cytoplasmic proteins

As much as 100 mL culture was prepared by method previously described, induced by optimized IPTG concentration. Analysis of total proteins was done by adding 100 µL sample buffer into pellet cells from 1 mL culture. The remaining culture was pelleted, and then soluble periplasmic and cytoplasmic proteins were isolated.

Isolation of cytoplasmic proteins was performed by freeze thaw method. Spheroplasts from periplasmic extraction were resuspended with lysis buffer consisting of 50 mM Tris-Cl, 3 mM EDTA, and 1 mM PMSF. Spheroplast suspension was subjected to five freeze-thaw cycles by freezing at -20 °C for 15 m and thawing for 15 m in room temperature. After that, thawed spheroplasts suspension was centrifuged at 11600 x g and 4 °C for 30 m, leaving the soluble cytoplasmic extract as the supernatant (Johnson and Hecht, 1994; Shrestha et al., 2012). Total proteins, soluble cytoplasmic and periplasmic proteins were then analyzed by 10% SDS-PAGE.

RESULT AND DISCUSSION

The pJ201_scFv plasmid was used as template for the scFv gene amplification, resulting in 802 bp of PCR product. The amplification product contains poly-histidine tag at the downstream of scFv sequence, and also NcoI and XhoI restriction sites to facilitate the cloning step. This DNA fragment was subcloned into NcoI and XhoI sites of pJ414_pelB vector. The recombinant plasmid obtained was named pJ414_pelB_scFv. To confirm correct recombinant plasmids, some analyses were carried out including migration, restriction, PCR and DNA sequencing.

Recombinant plasmid (4852 bp) and control plasmid (5452 bp) were run on agarose gel electrophoresis. Migration rate of recombinant plasmid would be faster than the control plasmid due to their sizes. Figure 1A showed the band of recombinant plasmid compared to control plasmid. To determine the actual size of the plasmid and insert DNA, restriction analysis was carried out. Figure 1B showed restriction of recombinant plasmid using NcoI or XhoI, which showed a single DNA band of 4852 bp. Double restriction analysis using both (NcoI and XhoI) resulting DNA bands with size of 802 and 4050 bp which corresponded to the theoretical size of insert DNA and pJ414_pelB, respectively.

The PCR analysis was performed using T7-promoter and scFv1-reverse primers. These primers were used to determine the full-length construct of the gene within the pJ414_pelB plasmid. Thus, the PCR product would consist of T7 promoter, pelB leader sequence, scFv gene, and poly-histidine tag. Figure 1C showed a DNA band of approximately 900 bp, which corresponds to the theoretical size of desirable fragment. Based on DNA sequencing analysis (data not shown), there were no mutation in DNA encoding anti-EGFRvIII scFv gene. After all of analyses conducted, it could be concluded that the recombinant plasmid was successfully constructed.

E. coli is currently used as the host for producing antibody fragments. For disulfide-bonded proteins, good expression levels have been achieved via soluble production, secreting the proteins into the oxidizing environment of the bacterial periplasm where assembly and disulfide bond formation can occur. Periplasmic secretion is achieved by genetically fusing the leader sequence onto the N-terminus of the antibody sequence (Popplewell et al., 2005)

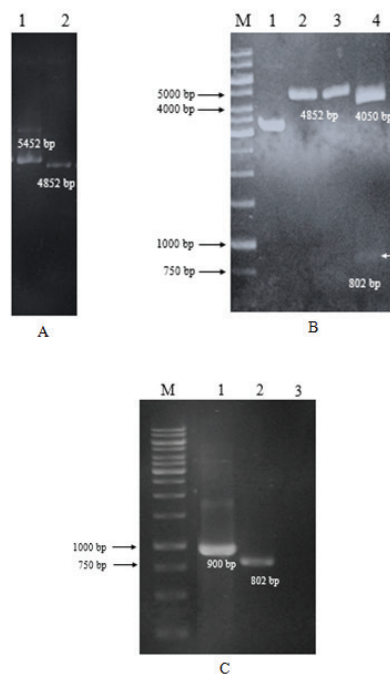




Figure 1. (A) Migration analysis of pJ414_pelB_scFv. Lane 1, comparator plasmid (5452 bp); lane 2, pJ414_pelB_scFv recombinant plasmid (4582 bp). (B) Restriction analysis of pJ414_pelB_scFv. Lane 1, pJ414_pelB_scFv uncut; lane 2, digested with NcoI restriction enzyme; lane 3, digested with XhoI restriction enzyme; lane 4, digested with NcoI and XhoI restriction enzyme. (C) PCR analysis of pJ414_pelB_scFv. Lane 1, using T7 promoter and reverse primers; lane 2, using forward and reverse primers; lane 3, negative control.

The oxidizing environment of periplasmic space, rich in proteins which are important for folding and catalyzing disulfide bond formation (PDI, DsbA and DsbC) or chaperones such as SKp (Fernandez, 2004; Bothmann and Pluckthun, 2000), is most suitable for proper folding of scFv fragment. Antibody fragments expressed in the periplasmic space have been shown to be correctly folded with excellent yield. Additionally, extraction of periplasmic-expressed proteins can easily be performed by a simple osmotic shock procedure (Tiwari et al., 2010)

The early stage in overproduction of scFv proteins was to optimize the optimal concentration of IPTG as inducer. Figure 2 lanes 3-6 showed total protein bands of induced E. coli culture using various IPTG concentrations. The scFv band is deduced to have approximate size of 28.76 kDa as it is shown on the SDS-PAGE analysis (Figure 2). The band size corresponds to the theoretical size of scFv proteins. Furthermore, total scFv proteins induced with 0.1 and 0.25 mM IPTG has a thicker band compared to those from 0.5 and 1 mM IPTG. However, such information was not enough to be used as a reference to determine the optimal concentration of IPTG in producing scFv proteins in periplasmic space. Therefore, analysis was continued to determine the effect of various IPTG concentration in the periplasmic protein expression.

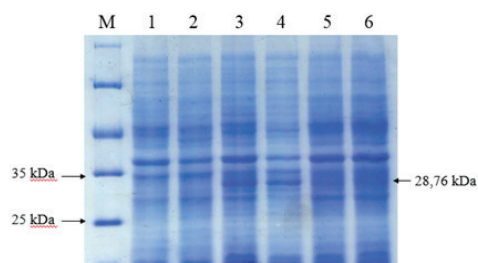


Figure 2. SDS-PAGE analysis of total proteins induced with various IPTG concentration. The scFv band is marked with an arrow (28.76 kDa). Lane 1, non transformant induced with 0.5 mM IPTG; lane 2, non induced transformant; lane 3, transformant induced with 0.1 mM IPTG; lane 4, transformant induced with 0.25 mM IPTG; lane 5, transformant induced with 0.5 mM IPTG; lane 6, transformant induced with 1 mM IPTG.

Figure 3 gives an overview of protein profiles extracted from the E. coli periplasm. Analysis was carried out to compare periplasmic protein profiles from induced and uninduced E. coli cultures. Based on the electrophoregram, it was observed that the bands of scFv protein clearly detected in periplasmic extract of transformant E. coli cultures induced with 0.1 and 0.25 mM IPTG. Considering these results, low concentration of IPTG was apparently optimum for periplasmic-proteins expression of this scFv.

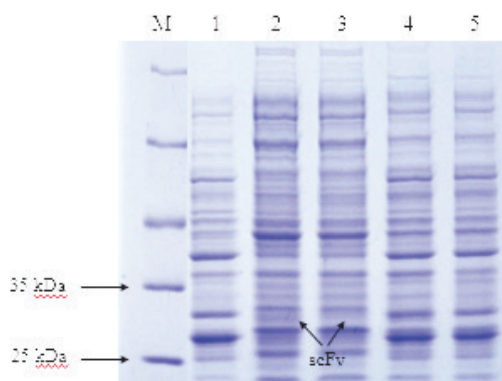


Figure 3. SDS-PAGE analysis of periplasmic proteins induced with various IPTG concentrations. The scFv bands are marked with arrows. Lane 1, non induced transformant; lane 2, transformant induced with 0.1 mM IPTG; lane 3, transformant induced with 0.25 mM IPTG; lane 4, transformant induced with 0.5 mM IPTG; lane 5, transformant induced with 1 mM IPTG.

To find out the protein profiles produced using this expression system, a comparative analysis of total proteins, periplasmic proteins, and cytoplasmic proteins was carried out. Cytoplasm has a much larger space than periplasm. However, Figure 4 lanes 5 and 6 showed that the soluble scFv protein in cytoplasmic space was much less than in periplasmic space. This result indicates that the majority of scFv proteins in the cytoplasm were in the form of inclusion bodies.

ScFv protein has a disulfide bond in each VH and VL domains, but the cytoplasmic space has a reductive environment (Snyder and Champness, 2003). Therefore, disulfide bonds are unlikely to be formed within the cytoplasm. Theoretically, it could be the cause of inclusion bodies formation within the cytoplasm.

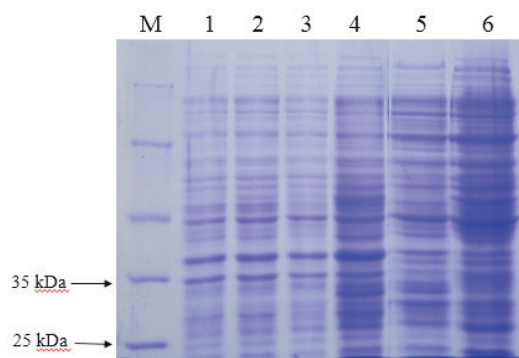


Figure 4. SDS-PAGE analysis of total proteins, soluble periplasmic and cytoplasmic proteins. The scFv band is marked with an arrow. Lane 1, total proteins of non induced non transformant; lane 2, total proteins of non transformant induced with 0.5 mM IPTG; lane 3, total proteins of non induced transformant; lane 4-6, total proteins, periplasmic and cytoplasmic proteins (respectively) of transformant cultures induced with 0.1 mM IPTG.

All of those analyses indicates a protein band of 28.76 kDa observed in protein profiles of periplasmic and cytoplasmic of induced culture extracts which is not present in uninduced culture extracts. These results suggest that the scFv protein has been successfully expressed and found in samples of total proteins, periplasmic and cytoplasmic fractions. Thus, it can be concluded that pJ414_pelB_scFv plasmid has successfully express scFv protein in the periplasmic space using PelB leader sequence.

CONCLUSION

The pJ414_pelB_scFv plasmid has been successfully constructed and its sequence has been confirmed. Protein expression analyses have confirmed that the scFv protein has successfully been expressed in periplasmic space using pelB leader sequence and showed molecular size of approximately 28.76 kDa.

REFERENCES

- Ahmad ZA, Yeap SW, Ali AM, et al. (2012). ScFv cliniantibody: principles and clinical application. *Clin Dev Immunol*, 2012:1-15.
- Batra SK, Shobha CP, Wikstrand CJ, et al. (1995). Epidermal growth factor ligand-independent, unregulated, cell-transforming potential of a naturally occurring human mutant EGFRVIII gene. *Cell Growth Differ*, Oct;6:1251-1259.
- Bothmann H, Pluckthun A. (2000). The periplasmic Escherichia coli peptidylprolyl cis,trans-isomerase FkpA. I. Increased functional expression of antibody fragments with and without cis-prolines. *J Biol Chem*, 275:17100-17105.
- Choi JH, Lee SY. (2004). Secretory and extracellular production of recombinant protein using Escherichia coli. *Appl Microbiol Biot*, 64:625-635.
- Fernandez LA. (2004). Prokaryotic expression of antibodies and affibodies. *Curr Opin Biotechnol*, 15:364-373.
- Gupta P, Han SY, Mitra SS, et al. (2010). Development of an EGFRVIII specific recombinant



antibody. *BMC Biotechnol*, Oct;10(72):1-13.
Huang HJS, Nagane M, Klingbeil CK, et al. (1997). The enhanced tumorigenic activity of a mutant epidermal growth factor receptor common in human cancers is mediated by threshold level of constitutive tyrosine phosphorylation and unattenuated signaling. *J Biol Activ*, 272:2927-2935.

Johnson BH, Hecht MH. (1994). Recombinant proteins can be isolated from *E. coli* cells by repeated cycles of freezing and thawing. *BIO/TECHNOLOGY*, 12:1357-1360.

Kipriyanov SM, Moldenhauer G, Little M. (1997). High level production of soluble single chain antibodies in small-scale *Escherichia coli* cultures. *J Immunol Methods*, 200:69-77.

Kuan CT, Wikstrand CJ, Bigner DD. (2001). EGF mutant receptor VIII as a molecular target in cancer therapy. *Endocrine-Related Cancer*, 8:83-96.

Lei SP, Lin HC, Wang SS, et al. (1987). Characterization of *Erwinia corotovor* pelB gene and its product pectate lyase. *J Bacteriol*, 169(9):4379-4383.

Makrides SC. (1996). Strategies for achieving high-level expression of genes in *Escherichia coli*. *Microbiol Rev* 60:512-538.

Pederson MW, Meltorn M, Damstrup L, Poulsen HS. (2001). The type III epidermal growth factor receptor mutation (biological significance and potential target for anti-cancer therapy). *Annals of Oncology*, 12:745-760.
Poplewell AG, Sehdev M, Spitali M, Weir ANC. (2005). Therapeutic proteins: methods and protocols. *Methods in molecular biology*, 308:17-30.

Shrestha P, Holland TM, Bundy BC. (2012). Streamlined extract preparation for *Escherichia coli*-based cell-free protein synthesis by sonication or bead vortex mixing. *Biotechnology*, Sep;53:163-174.

Snyder L, Champness W. (2003). Molecular genetics of bacteria. American Society for Microbiology Press. Washington D.C.

Sok CJ, Coppelli FM, Thomas SM, et al. (2006). Mutant epidermal growth factor receptor (EGFRVIII) contributes to head and neck cancer growth and resistance to EGFR targeting. *Clin Cancer Res*, 12(7):5064-5073.

Tiwari A, Sankhyan A, Khanna N, Sinha S. (2010). Enhanced periplasmic expression of high affinity humanized scFv against hepatitis B surface antigen by codon optimization. *Protein Express Purif*, Jun;74:272-279.

CHARACTERIZATION AND LD50 VALUE DETERMINATION OF 1,5-bis(3'-ethoxy-4'-hydroxyphenyl)-1,4-pentadiene-3-one (EHP)

Lestari Rahayu, tari2006@yahoo.com, 0817199415; Septian;
Esti Mumpuni, esti-_mumpuni@yahoo.com, 08151663201
Faculty of Pharmacy Pancasila University Jakarta

ABSTRACT

1,5-bis(3'-ethoxy-4'-hydroxyphenyl)-1,4-pentadiene-3-one (EHP) is a curcumin analogue which has been synthesized and proven to have antioxidant activities. The objectives of this research were to re-synthesis and characterize EHP compound and to determine its LD50 value. The synthesis was performed by reacting ethyl vanillin and acetone using hydrochloric acid as a catalyst. The product was then characterized by thin layer chromatography, ultraviolet-visible spectrophotometry, FT-IR spectrophotometry, high performance liquid chromatography, gas chromatography-mass spectrometry, densitometry and melting point while the acute toxicity test was performed by determining LD50 value of the compound with Weil C.S. method using male mice as experimental animals. The result showed that the yield of EHP was 48.12%. However, the end product was still founded a rest of ethyl vanillin mixed with EHP. The LD50 value of the synthesized EHP was 6,87 g/kg body weight with the criteria of mild toxic. Therefore, it is potential as a drug substance candidate.

Key word: characterization, EHP, LD50

INTRODUCTION

One of the curcumin analogue compounds is 1,5-bis (3'-methoxy-4'-hydroxyphenyl)-1,4-pentadien-3-one (abbreviated Gamavuton GVT-0). The chemical structure of GVT-0 was then modified by replacing two methoxy group on the aromatic ring with two ethoxy groups. It was obtained the 1,5-bis (3'-ethoxy-4'-hydroxyphenyl) -1,4-pentadien-3-on compound or EHP. This compound was proved to have an antioxidant activity more potent. (1;2). As anew drug substance candidate, needs to be determined its toxicity.

METHOD

Added acetone, ethyl vanillin (1:2) and chlorid acid, stirred in flat bottom-flask on cooling bath for ± 60 minutes. Then stirred in flat bottom-flask in room temperature ± 2 hours. Monitoring the reaction by TLC using stationary phase Silica Gel GF254 and mobile phase Chloroform-ethyl acetate (5:1). Synthesized end product EHP Washed with Glacial HOAc / Aquadest (1:1) ; Filtered with whatman no 1;

Washed with metabisulfit / aquadest (1:1). Purity test by TLC with stationary phase Silica Gel GF254 and mobile phase Chloroform-ethyl acetate (5:1) and melting point test. Identification and characterization by: FTIR; UV-Vis;GC-MS; HPLC and Densitometry. The acute toxicity assay was carried out by determining the LD50 value of the EHP with Weil C.S. method using male mice as an experimental animals

RESULT AND DISCUSSION

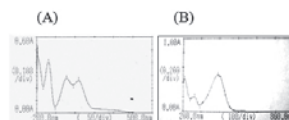


Figure 1. The characterization result by UV-VIS spectrometry ethyl vanillin (A) and EHP (B)

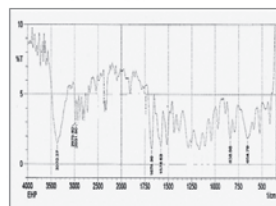


Figure 2. The characterization result by FTIR spectrophotometer

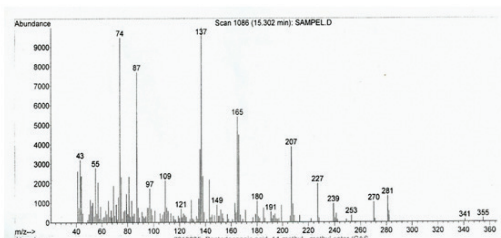


Figure 3. The characterization result by Gas Chromatography-Mass Spectrometry

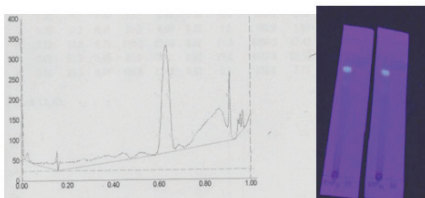


Figure 4. The characterization result TLC Densitometry

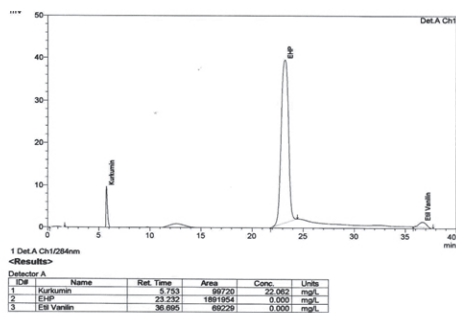


Figure 5. The characterization result by HPLC

Figure 5. The characterization result by HPLC Characterization of product synthesis was performed using organoleptic, the colours of product is yellow green, the odors is aromatic. It spot gave yellow fluorescence at TLC plate (UV 366) with average of Rf 0.65 at TLC chromatogram with eluent of ethyl acetat : chloroform(5:1).

The melting point of product synthesized is 161,7-163,6 °C and water concentration 0.043%.The UV spectrum (MeOH 1%) of product showed maximum absorbance at λ 390 nm and 267 nm. The IR spectrum (KBr) of product showed absorption bands at 3370 cm⁻¹ indicated the presence of OH group. Absorption bands at 2979 cm⁻¹ and 2931 cm⁻¹ indicated the presence of saturated C-H group. Absorp-

tion bands at 1578 cm⁻¹ , 838 cm⁻¹ and 654 cm⁻¹ indicated the presence of aromatic ring (C=C) and aromatic substitution (C-H). Characteristic absorption band at 1676 cm⁻¹ strongly correlated with C=O (carbonyl) group.Data of MS confirmed the existence of core EHP at m/z of 355.

The HPLC system results showed that the optimum separation was obtained with C18 stationary phase (octadecylsilane) Grace Column VP - ODS 4.6 x 250 mm ; 4.6 μm, by using methanol – water (30:70 v / v) as mobile phase with ultraviolet detection at 284 nm and 0.5 mL/min of flow rate.

Table 7. Based on the toxicity assay.

Group	Number of mice	Dose of samples (g/kg BB)	Amount of died mice
I	5	5,6760	0
II	5	6,7499	2
III	5	8,0269	5
IV	5	9,5456	5

Based on the table above and the biometric table from Weil C.S.; $f = 0,10000$; $\delta f = 0,24495$

$$\log LD_{50} = \log D + d(f+1)$$

$$LD_{50} = 6,87 \text{ g/kg BW}$$

$$\text{Lower limit } LD_{50} = \text{antilog} [\log LD_{50} - 2 \delta \log LD_{50}] \\ = 6,31 \text{ g/kg BW}$$

$$\text{Upper limit } LD_{50} = \text{antilog} [\log LD_{50} + 2 \delta \log LD_{50}] \\ = 7,47 \text{ g/kg BW}$$

Based on the toxicity assay it has the LD50 value of 6.87 g/kg body weight, it is belonged to the category of mild toxic substance, so that it is recommended as a safe drug substance candidate.

CONCLUSION

The 1,5-bis (3'-ethoxy-4-hydroxyphenyl) -1,4-pentadien-3-on (EHP) compound can be synthesized from ethyl vanillin and acetone by aldol condensation method using a hydrochloric acid as a catalyst. The EHP was successfully synthesized with yield of 48.12%

The EHP compound was characterized by us-



ing thin layer chromatography, ultraviolet-visible spectrophotometry, FT-IR spectrophotometry, high performance liquid chromatography, gas chromatography-mass spectrometry, densitometry, and melting point test

The LD50 value of the synthesized product (EHP compound) was 6.87 g/kg body weight, it is belonged to the category of mild toxic substance, so that it is potential as a drug substance candidate.

ACKNOWLEDGMENT

THE AUTHORS ARE GRATEFUL TO DITLITABMAS DITJEND DIKTI FOR HIBAH BERSAING RESEARCH FUNDING AS DIPA KOPERTIS WILAYAH III NUMBER 023.04.2.189705/2014 AND 191/K3/KM/2014

REFERENCES

1. Sardjiman., 2000, Synthesis of some new series of curcumin analogues, antioxydative activity and Structure Activity Relationship (dsertation). Yogyakarta: Gadjah Mada University
2. Esti Mumpuni, Indriana P, Evi L, Enjang R., 2010 Sintesis dan uji antioksidan senyawa 1,5-bis(3'-etoksi-4'-hidroksifenil)-1,4-pentadien-3-on. Jurnal Ilmu Kefarmasian Indonesia, Vol 8, No.2 Sept.
3. Weil C.S., 1952, Table for convenient calculation of median effective dose (LD50) and instruction in their use. Biometrics.
4. Lu FC. 1995., Toksikologi dasar asas, organ sasaran, dan penelitian resiko. Edisi 2. Diterjemahkan oleh Edi Nugroho. Jakarta : UI Press.



DEVELOPMENT OF MELOXICAM TRANSDERMAL MATRIX TYPE PATCH USING POLYVINYLPIRROLIDONE, HYDROXYPROPYL METHYLCELLULOSE, AND ETHYL CELLULOSE COMBINATION

Lidya Ameliana, Faculty of Pharmacy, Jember University, lidyaameliana@yahoo.co.id, 0331 324736; **Monica Iwud**, Faculty of Pharmacy, Jember University, miuwudh@gmail.com, 0331 324736; **Selly Rio**, Faculty of Pharmacy, Jember University, rio.selly@yahoo.co.id, 0331-324736

INTRODUCTION

Transdermal drug delivery system is an administration of a therapeutic agent in the form of patches or semisolids that deliver drugs through intact skin for systemic effect¹. The advantages of transdermal drug delivery systems are to avoid of hepatic first pass metabolism, ability to discontinue administration by removal of the system, to control drug delivery for a longer time than the usual gastrointestinal transit of oral dosage form³, to prevent irritation of the digestive tract⁸, improves patient compliance³. Transdermal drug delivery systems may prevent the drug from enzymatic reactions in the gastrointestinal tract walls⁵

Meloxicam is a nonsteroidal anti-inflammatory drug (NSAID) class enolate acid derivative oxicam⁶. Meloxicam inhibit the synthesis of cyclooxygenase-2 (COX-2) and prostaglandin². Meloxicam has a partition coefficient octanol / water (log P octanol / water) 3.43 and a molecular weight 351.4 Dalton⁴. The dose of Meloxicam is 7.5-15 mg / day⁷. Meloxicam was reported as a drug that can be applied to skin and mucosa because meloxicam has lower tissue toxicity than piroxicam, ketoprofen, indomethacin, diclofenac and ibuprofen⁶

The important component in the preparation of the patch is a polymer. The polymer used in this patch are hydrophilic and hydrophobic polymer. This research would be develop Meloxicam transdermal patch with some of hydrophilic and hydrophobic polymers, ethylcellulose (EC) -polivinilpirolidon (PVP), hydroxypropylmethylcellulose (HPMC) - EC, then compared the physical properties and the release of Meloxicam between the formulas.

MATERIALS AND METHODS

Meloxicam was obtained as a gift sample from PT. Deka Medica, HPMC, PVP K-30, Ethyl Cellulose N-22, Propylene glycol, Polyethylene glycol, Potassium Chloride, Potassium Phosphate Dibasic, Sodium Phosphate Dibasic, Sodium Chloride, Backing, Aquadest

Formulation of transdermal patches

Matrix type transdermal patches containing Meloxicam were prepared by solvent casting technique. HPMC or PVP K30 and EC-N22 solution was prepared using ethanol as solvent. Polymeric solutions were mixed thoroughly with the help of magnetic stirrer for 15 minutes. Meloxicam was added to propylene glycol and polyethyleneglycol and stirred for 30 minutes and then were poured into molds and dried at room temperature for 24 hours. The composition of transdermal patches is shown in Table 1.

Material	Formula (mg)					
	F1	F2	F3	F4	F5	F6
Meloxicam	7.5	7.5	7.5	7.5	7.5	7.5
PVP	57.75	38.5	19.25	-	-	-
HPMC	-	-	-	57.75	38.5	19.25
EC	134.75	154	173.25	134.75	154	173.25
Propylene glycol	150	150	150	150	150	150
Plasticizer	150	150	150	150	150	150
Total	500	500	500	500	500	500

Table 1. The Composition of Meloxicam Transdermal Patches

Evaluation Test

The prepared formulation were evaluated for different physiochemical characteristics such as color, odor, consistency, weight uniformity, thickness, moisture content, drug content, and in vitro release study.

RESULTS AND DISCUSSION

Formulation and Evaluation of Meloxicam Transdermal Patch

Transdermal drug delivery system containing Meloxicam was prepared by using different polymeric ratios of HPMC, PVP and hydrophobic polymer of EC in combination. The meloxicam patches can be seen in Fig.1. They all yellow, odorless, and dry. The results of various physico-chemical parameters were listed in Tables 2 The weight of the patches varied from 535.53 ± 0.67 to 574.53 ± 0.40 mg. The thickness of the patches varied from 0.224 ± 0.001 to 0.229 ± 0.001 mm

Meloxicam in methanol was scanned in the UV wavelength region of 200-400 nm for maximum absorption (λ max). The λ max was found to be at 364 nm. Linear relationship was observed between the concentration and absorbance value. (Slope=0.045, $r=0.998$). This regression equation was used to calculate the drug content of meloxicam patch.

The drug content of meloxicam patches were list in Table 3. They varied from 96.833 ± 0.673 to 98.200 ± 0.610 %. There were in accordance with the requirement of that the drug content was range 85% - 115% and the coefficient variation is less than 6 %.

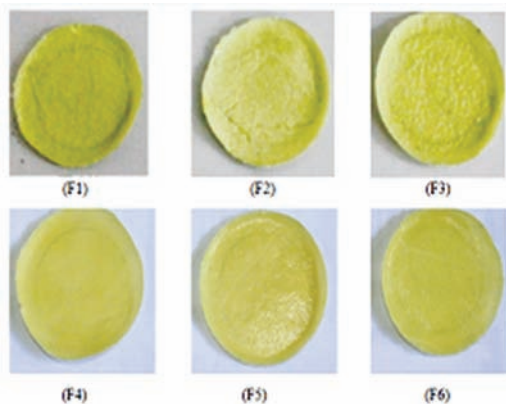


Fig.1 The Meloxicam Patch of Various Formulation

Fig.1 The Meloxicam Patch of Various Formulation

Formula	Appearance	Weight uniformity (mg) \pm SD	Thickness (mm) \pm SD
F1	Less smooth, less flexible	548.43 ± 0.71	0.226 ± 0.002
F2	Less smooth, less flexible	558.46 ± 0.70	0.227 ± 0.001
F3	Less smooth, less flexible	563.80 ± 0.60	0.224 ± 0.002
F4	Smooth, flexible	574.53 ± 0.40	0.227 ± 0.007
F5	Smooth, flexible	535.53 ± 0.67	0.224 ± 0.002
F6	Smooth, flexible	556.40 ± 0.72	0.229 ± 0.001

Table 2: Physicochemical Properties of Meloxicam patches

The moisture content in the formulations ranged from 3.528 ± 0.024 to 7.530 ± 0.023 %. The highest percentage of moisture content was found in F1 7.530 ± 0.023 % respectively which may be due to the hygroscopicity of nature of PVP. The highest percentage of moisture content of HPMC patches was found in F4 because it was the highest concentration of HPMC in patch. The results of patch's drug content and moisture content were listed in Table 3.

The In vitro drug release studies were carried out using cellophane membrane. The cellophane was mounted on the diffusion cell which acted as a donor compartment. 500 ml of phosphate buffer saline pH 7.4 as a diffusion medium was taken in the dissolution chamber which acted as the receptor compartment to maintain the sink condition. The donor compartment was kept in contact with receptor compartment and receptor compartment was stirred with paddle during the study. Sample 5 ml was withdrawn and replaced with 5 ml of PBS pH 7.4 at different time intervals. The samples were analyzed using UV spectrophotometer at 364 nm to estimate Meloxicam. Meloxicam in PBS was scanned in the UV wavelength at 364 nm. Linear relationship was observed between the concentration and absorbance value. (Slope=0.0293, $r=0.9933$). This regression equation was used to calculate the drug content on in vitro release study of



meloxicam patch. Flux of Meloxicam release study from patches can be seen in Fig.2.

Formula	Drug content (%) ± CV	Moisture content (%)
F1	97.833 ± 0.461	7.530 ± 0.023
F2	97.167 ± 0.079	5.383 ± 0.006
F3	96.833 ± 0.673	3.553 ± 0.030
F4	98.200 ± 0.610	5.332 ± 0.030
F5	97.266 ± 0.566	3.964 ± 0.024
F6	97.166 ± 0.875	3.528 ± 0.024

Table 3. Drug Content and Moisture Content Properties of Meloxicam patches

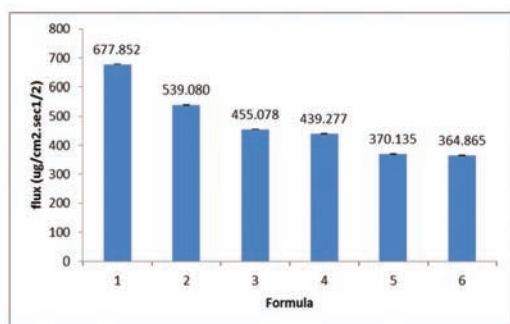


Fig 2. Flux of Meloxicam release study from patches

The flux ranged from 364,865 to 677,851 µg/cm².second^{1/2}. The highest flux was found in formulation F1 677,851 µg/cm².second^{1/2}, respectively which may be due to the nature of PVP (Fig.2).

CONCLUSION

Meloxicam patch in PVP-EC had moisture content and Meloxicam flux release higher than Meloxicam patch in HPMC-EC polymers. The highest flux and moisture content was on the highest PVP in Meloxicam patch formula.

REFERENCES

- *. Aulton. M.E.(2002). Pharmaceutics, The science of Dosage form Design, Churchill Livingstone, Elsevier. 499-533
- *. Jayaprakash S., Ramkanth S., Anitha P., Alagusundaram M., Saleem M., Chetty M.C. (2011). Design and evaluation of monolithic drug in adhesive transdermal patches of meloxicam. Malaysian Journal Of Pharmaceutical Sciences. Vol. 8 (2): 25-43.
- *. Modamio, P., Lastra, C. F. and Marin, E. L. (2000) A comparative in vitro study of percutaneous penetration of beta-blockers in human skin, International Journal of Pharmaceutics, 194: 249–259
- *. Moffat, A. C., Osselton, M. D., Widdop, B., dan Galichet, L. Y. (2005). Clarke’s Analysis of Drugs and Poisons, Third Edition. UK: Pharmaceutical Press
- *. Ranade, V. V., and Hollinger, M. A. (2004). Drug Delivery Systems. Second Edition. CRC Press LLC.
- *. Stei, P., Kruss, B., Wiegleb, J. & Trach, V. (1996). Local Tissue Tolerability of Meloxicam, a New NSAID: Indications for Parental, Dermal and Mucosal Administration, British Journal of Rheumatology, 35(Suppl. 1): 44–50.
- *. Sweetman, S. C., Paul, S. B., Alison, B., Julie, M. M., Gail, C. N., dan Anne, V. P. (2009) Martindale: The Complete Drug Reference, Thirtieth edition. London:Pharmaceutical Press.
- *. Zadeh, B. S. M., and Hansani, M. H. 2010. The Effect of Chemical and Physical Enhancers on Trolamine Salicylate Permeation through Rat Skin. Trop J Pharm Res. Vol. 9 (6): 541-548.



ANTIHEPATITIS C VIRUS ACTIVITY SCREENING ON *Harpullia arborea* EXTRACTS AND ISOLATED COMPOUND

Lidya Tumewu, Evhy Apryani, Institute of Tropical Disease Universitas Airlangga, Campus C Unair Mulyorejo Surabaya 60115; Mei Ria Santi, Department of Microbiology, Faculty of Medicine, University of Indonesia, Jakarta 10430; Tutik Sri Wahyuni, Department of Pharmacognosy and Phytochemistry, Faculty of Pharmacy, Universitas Airlangga, Surabaya 60286; Adita Ayu Permanasari, Myrna Adianti, Institute of Tropical Disease Universitas Airlangga, Campus C Unair Mulyorejo Surabaya 60115; Chie Aoki, Division of Microbiology, Kobe University Graduate School of Medicine, Kobe 650-0017, Japan; Aty Widawaruyanti, Achmad Fuad Hafid, Department of Pharmacognosy and Phytochemistry, Faculty of Pharmacy, Universitas Airlangga, Surabaya 60286; Institute of Tropical Disease Universitas Airlangga, Campus C Unair Mulyorejo Surabaya 60115, aty-w@ff.unair.ac.id; Maria Inge Lusida, Soetjipto, Department of Microbiology, Faculty of Medicine, Universitas Airlangga, Surabaya; Institute of Tropical Disease Universitas Airlangga, Campus C Unair Mulyorejo Surabaya 60115; Hak Hotta, Division of Microbiology, Kobe University Graduate School of medicine, Kobe 650-0017, Japan.

INTRODUCTION

Hepatitis C is a major healthcare problem worldwide. Available therapy for hepatitis C treatment is very expensive and probably not be accessible for all patients. Regarding to this reason, the development of safe and inexpensive antiviral drugs is required. Natural products as a source of new drugs are potential to study. Some antiHCV substances from plants were obtained (Wahyuni, 2013; Adianti, 2014; Aoki, 2014).

Harpullia arborea (tulip wood tree) is a member of Sapindaceae family commonly known as kayu pacat in Indonesia (Basuni, 1997). Traditionally, watery exudates from barks and fruits is used as leech repellent, oil extracted from seeds is a source of antirheumatics (Singh, 2011). *H. arborea* seeds extract also shown antibacterial activities against various strains of bacteria. *H. arborea* seeds contain glycosides, steroids, saponins and resins (Gowri, 2009). A norhopane triterpenoid also isolated from the leaves of *H. arborea* (Poovapathanachart, 2008).

This study was conducted to determine anti-HCV activity of *H. arborea* extracts and isolated compound.

MATERIALS AND METHOD

Plant material

Harpullia arborea was obtained from Alas Purwo National Park at Banyuwangi, East Java. Sample was authenticated by the authority of

Purwodadi Botanical Garden, Pasuruan, East Java.

Extraction dan fractionation

H. arborea was extracted by ultrasonic assisted extraction method using 80% ethanol as a solvent. Liquid fractionation was conducted using dichloromethane, ethyl acetate and buthanol respectively.

AntiHCV activity test

Extract was examined for antiHCV activity against JFH1a and J6/JFH1 in a cell culture system using Huh7 cells at a multiplicity of infection (MOI) of 0.1.

RESULTS DAN DISCUSSION

Anti-Hepatitis C Virus (anti-HCV) activity screening of *H. arborea* leaves and stem extract revealed that leaves extract exhibited anti-HCV with IC50 value of 17.5 µg/ml and 12.4 µg/ml against HCV JFH1a and J6/JFH1 respectively, meanwhile stem extract was found to be not active against both HCV type.

Fractionation of leaves extract resulted in 4 fractions which were dichloromethane, ethyl acetate, buthanol and aqueous fraction. Anti-HCV activity screening at a concentration of 30 µg/ml revealed that buthanol fraction inhibited HCV JFH1a growth by 54% in which other fractions only inhibited by 15-30%. Buthanol fraction contains yellow spot on TLC profile as a major compound. Further separation of buthanol fraction using sephadex LH-20 and



methanol 90% as a solvent was obtained 7 fractions (B1-B7). Fraction B5 contain yellow precipitate and by recrystallization process obtained a yellow crystal as a glycosylated flavonoid compound which identified as Kaempferitrin (3,7-di- α -L-rhamnopyranosyl kaempferol). Structure determination of compound was done by nuclear magnetic resonance spectroscopy and data were compared with references (Ouyang Ming-An, 2003; De Souza Menezes, 2007). Kaempferitrin was further tested against JFH1a. Anti-HCV activity test shown that kaempferitrin was not exhibited anti-HCV. It is possible to explain that anti-HCV activity of extract and buthanol fraction was produced by other compounds in the extract and buthanol fraction instead of kaempferitrin or the activity was created by synergism effect of many compounds. Previous studies were reported some activity of kaempferitrin. Like many flavonols, it has antimicrobial, antioxidant and antiinflammatory activities. It is also mimics insulin in stimulating glucose uptake in diabetic rats, but inhibits insulin-stimulated glucose uptake in 3T3-L1 cells (Jorge, 2004; Prasad, 2009). But no report about antiviral activity of kaempferitrin was found. Further study need to be done to investigate the anti-HCV compounds of *H.arborea*.

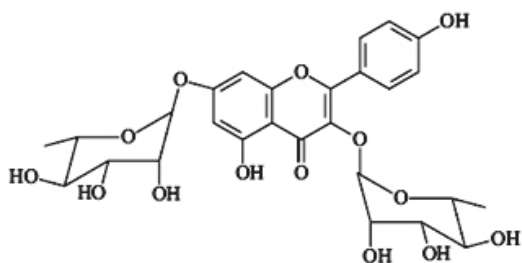


Figure 1. Kaempferitrin
(3,7-di- α -L-rhamnopyranosyl kaempferol)

CONCLUSION

In this study, we concluded that *H.arborea* leaves extract and buthanol fraction were exhibited anti-HCV activity against JFH1a virus,

while the isolated compound, kaempferitrin was not.

ACKNOWLEDGEMENT

This study was supported by Science and Technology Research Partnership for Sustainable Development (SATREPS) from Japan Science and Technology Agency (JST), Japan International Cooperation Agency (JICA) and Universitas Airlangga Indonesia.

REFERENCES

1. Adianti M, Aoki C, Komoto M, et al. (2014). Anti-hepatitis C virus compounds obtained from *Glycyrrhiza uralensis* and other *Glycyrrhiza* species. *Microbiol Immunol*, 58(3): 180-187.
2. Aoki C, Hartati S, Santi MR, et al. (2014). Isolation and identification of substances with anti-hepatitis C virus activities from *Kalanchoe pinnata*. *Int J Pharm Pharmaceut Sci*, Vol 6, Issue 2.
3. Basuni S, Haidir. (1997). Studi pola penyebaran, potensi dan habitat kayu pacat (*Harpullia arborea*) dalam rangka pembangunan bank plasma nutfah in situ di Taman Nasional Kerinci Seblat. *Media Konservasi* Vol V, 2: 85-88.
4. De Souza Menezes F, Minto ABM, Ruela HS, et al. (2007). Hypoglycemic activity of two Brazilian *Bauhinia* species: *Bauhinia forficata* L and *Bauhinia monandra* Kurtz. *Brazilian Journal of Pharmacognosy* 17(1): 08-13.
5. Gowri SS, Vasantha K. (2009). Solventbased effectiveness of anti bacterial and phytochemical derivatized from the seeds of *Harpullia arborea* (Blanco) Radlk (Sapindaceae). *J Appl Sci Environ Manage*, Vol 13,(4):99-101.
6. Jorge AP, Horst H, de Sausa E, et al. (2004). Insulinomimetic ef



- fect of kaempferitrin on glycaemia and on ¹⁴C-glucose uptake in rat soleus muscle. *Chem Biol Interact* 149, 89-96.
7. Ouyang Ming-An. (2003). Studies on lignans and flavonoid glycosides of *Ligustrum sinense*. *Chinese Traditional and Herbal drugs* 34, 196.
 8. Poovapathanachari R, Thanakijcharoenpath W. (2008). A New norhomo-epigallocatechin gallate from *Harpullia arborea*. *Fitoterapia* vol 79, issues 7-8, 498-500.
 9. Prasad CNV, Mohan SS, Banerji A, et al. (2009). Kaempferitrin inhibits GLUT4 translocation and glucose uptake in 3T3-L1 adipocytes. *Biochem Biophys Res Commun* 380, 39-43.
 10. Singh B, Singh VN, Sinha BK, et al. (2011). *Harpullia arborea* (Blanco) Radlk A New record to Meghalaya, *Journal of Non-Timber Forest products*, Vol 18(3), 237-238.
 11. Wahyuni TS, Tumewu L, Permanasari AA, et al. (2013). Antiviral activities of Indonesian medicinal plants in the East Java region against hepatitis C virus. *Virology Journal* 10:259.



HPLC METHOD PRECISION TO ASSAY OF α -Mangostin IN MANGOSTEEN (Garcinia mangostana L.) FRUIT RIND EXTRACT FORMULATED IN ORAL SOLUTION

Liliek Nurhidayati, liliek_nurhidayati@yahoo.com, 08129602984; **Siti Sofiah**, ssofiah19@gmail.com, 02170244949; **Ros Sumarny**, rosaries15@yahoo.com, 081318463091; **Kevin Caesar**, akevincaesar@hotmail.com, 081808153131
Faculty of Pharmacy, Pancasila University, Jakarta, Indonesia

INTRODUCTION

One of the compound from *Garcinia mangostana* rind extract that has antioxidant activity is α -mangostin. Oral solution formulation of *Garcinia mangostana* rind extract has been done using cosolvency method. Based on α -mangostin solubility the best choice of cosolvent was PEG 400 and glycerin of 40% (Sofiah et al., 2013). In the oral solution there are *Garcinia mangostana* rind extract and very complex excipient. To analyse the α -mangostin in oral solution, it need such a specific and sensitive method. Such as high performance liquid chromatography (HPLC). The optimum condition for HPLC was reached using octadecylsilane (C18) as stationary phase with methanol-water (90:10) as mobile phase, flow rate of 1.0 mL/min, and UV detector at 316 nm (Nurhidayati et al., 2014). Before its application to assay the α -mangostin in oral solution this methods should be validated. In this research, the precision of HPLC was evaluated.

MATERIAL AND METHODS

α -Mangostin standard compound was purchased from Chengdu Biopurify Phytochemicals Ltd. Oral solution of mangosteen (*Garcinia mangostana* L.) fruit rind extract was prepared using cosolvency methods (Sofiah et al, 2013). This assay was conducted using Shimadzu LC-20AD, with octadecylsilane (C18) Shim-pack VP-ODS 94.6 x 250 mm; 4.6 μ m at the temperature of 40oC.

System Suitability test

3.0 mL of oral solution was diluted until 10 mL with mobile phase. Shake and filter the solution. 20 μ L the solution was sonicated for 3-4

minute and injected to HPLC with optimum condition and the area was measured. The procedure was repeated for five times.

Precision test of HPLC methods for α -mangostin in oral solution determination.

Calibration curve

Preparation of calibration curve was performed by measuring the area of α -mangostin working standard solution (1 ; 2 ; 3 ; 4 ; 5 ; 6 and 7 ppm).

Assay of a-mangostin content

1.0 ml of the oral solution was diluted with methanol-water (90:10) until 10 mL, shake and filter the solution. 20 μ L of the solution was sonicated for 3-4 minutes and injected at optimum condition. α -Mangostin content was calculated using calibration curve equation. The procedure was repeated for six times.

RESULTS AND DISCUSSION

Chromatogram of α - mangostin standard solution and α - mangostin in the oral solution using mobile phase of methanol-water (90:10) with a flow rate of 1.0 mL / minute could be seen in Figure 1 and 2.

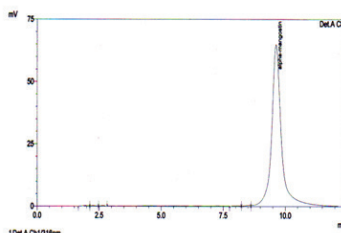


Figure 1. Chromatogram of α -mangostin standard solution

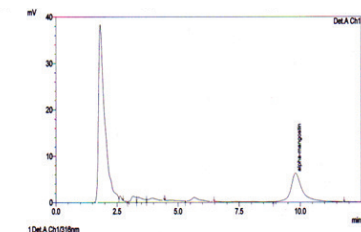


Figure 2. Chromatogram of α -mangostin in the oral solution

Calibration curve of α -mangostin that was performed using seven different concentrations of α -mangostin showed that the equation of regression line was $y = -14555,5124 + 72726,5024 x$ with correlation coefficient of 0.9993 in the range concentration of 1.12 ppm until 6.96 ppm. This equation was used to calculate α -mangostin content which was conducted six times to evaluate the precision of the methods. The results was showed in Table 1.

Extract weight in 100 mL of oral solution (mg)	Area	α -Mangostin content in oral solution ($\mu\text{g/mL}$)
17.04	315327	45.36
	313170	45.06
	316609	45.54
	312803	45.01
	314571	45.26
	324443	46.61
	Average	45.47
	SD	0.59
	RSD (%)	1.30

Table 1. The results of α -mangostin content determination

Determination results with six replication showed that the oral solution of mangosteen (*Garcinia mangostana* L.) fruit rind extract has α -mangostin content of 45.67 $\mu\text{g/mL}$ with RSD of 1.30%. RSD is not allowed if more than 2.0% (USP, 2012) or based on the analyte content not more than 11.31% (Harmita, 2004). The precision of this methods fulfill both re-

quirement. It is also showed that α -mangostin was homogeneous dispersed in the oral solution.

CONCLUSION

The HPLC methods with octadecylsilane as stationary phase (C18), mobile phase of methanol-water (90:10) with flow rate of 1.0 mL / minute fulfill the precision requirement.

ACKNOWLEDGMENT

The Authors are Grateful to thank to Ditlitabmas Ditjend Dikti for Hibah Bersaing research funding as DIPA Kopertis Wilayah III No. 023.04.189705/2014.

REFERENCES

1. Harmita. Petunjuk pelaksanaan validasi metode dan cara perhitungannya.(2004). Majalah Ilmu Kefarmasian. 1(3):117-20.
2. Nurhidayati L, Sofiah S, Sumarny R, Caesar K.(2014). HPLC Method Optimization of α -Mangostin Assay in Mangosteen (*Garcinia mangostana* L.) Fruit Rind Extract Formulated in Oral Solution. Jakarta International Symposium on Medicinal Plant and Traditional Medicine, Tawangmangu, Central Java, Indonesia, June 4th-6th 2014
3. Rohman A. (2009). Kromatografi untuk analisis obat. Yogyakarta: Graha Ilmu; p. 111-6,217-30.
4. Sofiah S, Sumarny R, Nurhidayati L. (2013). Teknologi Kosolvensi pada Formulasi Sediaan Larutan Oral Ekstrak Kulit Buah Manggis (*Garcinia mangostana* L) sebagai Antioksidan. Laporan Penelitian. Fakultas Farmasi Universitas Pancasila. Jakarta.
5. United States Pharmacopeial Convention. (2012). The United States Pharmacopeia 35-The National Formulary 30. Rockville: United States Pharmacopeial Convention. p. 877-81.



PREPARATION AND CHARACTERIZATION OF NARINGENIN-LOADED CHITOSAN NANOPARTICLES FOR CHEMOPREVENTION

Lina Winarti, Faculty of Pharmacy, University of Jember, Indonesia, lhinna_w@yahoo.com; Lusia Oktora Ruma Kumala Sari, Faculty of Pharmacy, University of Jember, Indonesia, oktorarks@gmail.com

INTRODUCTION

Naringenin (4', 5, 7-trihydroxy flavonone) is one of the naturally occurring flavonoids which exert a wide variety of activities such as anti-inflammatory, anti-mutagenic, anti-atherogenic and anti-cancer effects [1,2,7]. However, the therapeutic efficacy of naringenin is limited due to its poor oral bioavailability, which has been attributed to its poor aqueous solubility and extensive first-pass metabolism. Recently, nanochemoprevention, have received increased much attention for their ability to deliver anti-cancer drugs due to their small size, prolonged circulation time and sustained drug release profile [5]. Among all the recent materials used for polymeric nanoparticles synthesis, chitosan has gained considerable interest. Chitosan has promising biological implications such as nontoxic, biocompatible, biodegradable, bacteriostatic, and fungistatic [4,6]. The main aim of the present study was to develop naringenin-loaded chitosan nanoparticles for chemoprevention.

MATERIAL AND METHOD

Material

Low viscous chitosan [2-amino-2-deoxy-(1→4)-β-D glucopyranan] p.a, Pentasodium tripolyphosphate (TPP) p.a, and Naringenin ≥95% p.a were obtained from Sigma, Germany. Tween-80, Ethanol, acetic acid, and double distilled water were purchased from Brataco Chemica.

Methods

Preparation of naringenin-loaded chitosan nanoparticles

Chitosan nanoparticles were prepared via ionic gelation method developed by Calvo et al [3] with some modification. Chitosan solutions

0.08% w/v was prepared by dissolving chitosan in acetic acid (0.15% v/v). TPP solution (0.1% w/v) was prepared by dissolving it in double distilled water. For association of drug with chitosan nanoparticles, the pure naringenin powder was dissolved into 96% ethanol to produce 0.2% w/v naringenin solution. Afterward, the naringenin solution was mixed with chitosan solutions under magnetic stirring. Then, 1,5 mL of TPP solution (0.1% w/v) and 1,075 mL of Tween-80 solution (0.01% v/v) were added dropwise into mixtures under magnetic stirring at 1000 rpm, and naringenin loaded chitosan nanoparticles were simultaneously obtained.

Morphology of Nanoparticles

Drops of 10 mL freshly prepared nanoparticle solution were placed on pioloform coated grids and air dried for 15 min. The redundant fluid was removed while the dried nanoparticles remained on the grids. These grids were dried and examined by transmission electron microscope (JOEL-JEM 1400, Japan) with an in-column energy filter (EFTEM). Thus, nanoparticles were analyzed 120kV energy loss, depending on their density.

Particle Size and zeta (ζ) Potential

The resulting of cross-linked chitosan nanoparticles were analyzed for mean particles size, particle size distributon and zeta potential by DelsaTM Nano Submicron Particle size.

Fourier Transform Infrared Spectroscopy (FTIR) Analysis

FTIR spectra were taken in the wavelength region 4000 to 400 cm⁻¹ at room temperature using potassium bromide pellets (Merck, IR grade) for chitosan, TPP, naringenin, and nar-

ingenin loaded chitosan nanoparticles. The samples were allowed to form pellets at pressure of 10.3 x 104 Pa.

Differential Scanning Calorimetry (DSC)

The thermal behavior of the naringenin and naringenin loaded chitosan nanoparticles was characterized by DSC (Mettler Toledo DSC). The nanoparticles were heated from 30 to 3600C at a heating rate of 100 C/min per cycle. Inert atmosphere was maintained by purging nitrogen at the flow rate of 20 cc/min.

Evaluation of Encapsulation Efficiency (EE)

EE of naringenin was determined by measuring the ultraviolet (U.V) absorption of the respective supernatans of naringenin loaded chitosan nanoparticles obtained after ultracentrifugation. Naringenin was measured at 290 nm (λ_{max}). EE of naringenin was calculated according to the following formula:

$$EE (\%) = \left(\frac{W_t - W_f}{W_t} \right) \times 100 \dots\dots\dots(1)$$

Wt is the total initial amount of naringenin and Wf is the amount of free naringenin in the supernatant after ultracentrifugation (15.000 rpm, 80 minutes).

RESULTS AND DISCUSSION

Naringenin-loaded chitosan nanoparticles

In this preliminary experiment, formulation optimization of naringenin-loaded chitosan nanoparticle was run by mixing chitosan solution to naringenin solution. This formula was stored for 3 days at room temperature to observe the formation of sediment. Nanoparticles with chitosan concentration of 0.08 % were stable until 3 days.

Morphology of Nanoparticles

Morphology of naringenin-loaded chitosan nanoparticles was investigated by using a TEM. Result (Figure 1) generally showed that the shape of the nanoparticles is fairly spherical.

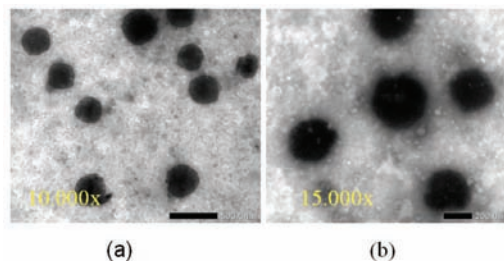


Figure 1. TEM images of nanoparticles

Characterization using Particle Size Analyzer and Zeta Sizer

The respective average diameters, measured by Zetasizer of naringenin-loaded chitosan nanoparticles were approximately 750 nm. Zeta potential of naringenin-loaded chitosan nanoparticles can greatly influence their stability in suspensions by means of electrostatic repulsion between the particles. The measurement demonstrated respective zeta potential of naringenin-loaded chitosan nanoparticles 35.72±0.64 mV.

FT-IR Analysis

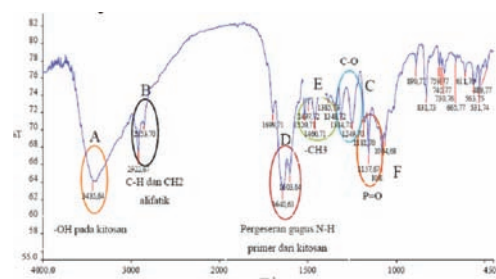


Figure 2. FT-IR of naringenin-loaded chitosan nanoparticle

In nanoparticles the peaks for N-H bending vibration of amine I at 1650 cm⁻¹ shifted and split to 1640 cm⁻¹ and 1603cm⁻¹. The cross-linked chitosan also show a P=O peak at 1157 cm⁻¹. These results have been attributed to the linkage between phosphoric and ammonium ion, these indicate that the tripolyphosphoric groups of TPP are linked with ammonium groups of chitosan.



Differential Scanning Calorimetry (DSC) Analysis

DSC spectrum of naringenin-loaded chitosan nanoparticle does not exhibit the sharp peak of naringenin from that conclusion was drawn that in the naringenin-loaded chitosan nanoparticle, drug was in partial crystalline state in naringenin-loaded chitosan nanoparticle and there is no interaction between drug and polymer.

Encapsulation Efficiency (EE) of Naringenin-loaded chitosan nanoparticles

Measurement demonstrated 64.45 ± 0.028 % of EE.

CONCLUSION

Chitosan nanoparticles-TPP conjugates have the capability to encapsulate naringenin.

REFERENCES

1. Ali, G., Hawa, Z., E., J., Asmah, R., (2010), Synthesis of Phenolics and Flavonoids in Ginger (*Zingiber officinale* Roscoe) and Their Effects on Photosynthesis Rate. *Int. J. Mol. Sci.*, 11, 4539–4555.
2. Chen, H., J., Baskaran, S., I., Chen, B., H., (2012), Determination of Phenolic Acids and Flavonoids in *Taraxacum formosa* num Kitam by Liquid Chromatography-Tandem Mass Spectrometry Coupled with a Post-Column Derivatization Technique. *Int. J. Mol. Sci.*, 13, 260–285.
3. Calvo, P., Remuñán-López, C., Vila-Jato, J., L., Alonso, M., J., (1997), Novel hydrophilic chitosan-polyethylene oxide nanoparticles as protein carriers, *Journal of Applied Polymer Science*, vol. 63, no. 1, pp. 125–132.
4. Hejazi, R., Amiji, M., (2003), Chitosan-based gastrointestinal delivery systems, *Journal of Controlled Release*, vol. 89, no. 2, pp. 151–165.
5. Hu, B., Ting, Y., Yang, X., Tang, W., Zeng, X., Huang, Q., (2012), Nanochemoprevention by Encapsulation of (-)-epigallocatechin-3-gallate with Bioactive Peptides/Chitosan Nanoparticles for Enhancement of its Bioavailability, *Int. J. Mol. Sci.*, 13, 14251-14261
6. Huanbutta, K., Luangtana-anan, M., Sri amornsak, P., Limmatvapi rat, S., Puttipipatkachorn, S., Nunthanid, J., (2008), Factor affecting preparations of chitosan microcapsules for colonic drug delivery, *Journal of Metals, Materials and Minerals*, vol. 18, pp. 79–83.
7. Raja, N., Z., R., A., R., Iffah, I., Z., Abu, B., S., Mahiran, B., (2012), Enzymatic Properties and Mutational Studies of Chalcone Synthase from *Physcomitrella patens*. *Int. J. Mol. Sci.*, 13, 9673–9691



RELATIONSHIP OF KNOWLEDGE AND PATIENT BEHAVIOR ON SELF MEDICATION PIROXICAM (Studies of Pharmacy in Sukun District , Malang City)

Liza Pristiany* , Reshtia Eriana Putri** , Hidayah Rachmawati**

*Faculty of Pharmacy, Airlangga University

**Prodi Pharmacy School of Public Health, University of Muhammadiyah Malang

Liza_ffua@yahoo.com

INTRODUCTION

Self medication more done by individuals to relieve health complaints. Efforts are made by using drugs on their own without any guidance from medical. Despite the fact that there are many actions self medication done in the community, but not many people are aware the rational treatment of self medication. Therefore, efforts to build the rational behavior in self medication be essential. The rational self medication is selecting and using appropriate medications correctly include medication, right dose, right duration of treatment , and the right way of life alert side effects. Based on data from the Central Bureau of Statistics 2011, there were 70.66% of women aged 15-49 years in Indonesia, if people feel the symptoms of pain then choose self medication. Results of research on self-medication profiles of consumers pharmacies in Surabaya in 2012 reported the incidence of self-medication of pain, rheumatism and toothache by 24% (liza, 2012). The results of the study in Chile on the pattern of self-medication pharmacy clients in mind that most clients use the drug without proper knowledge about the benefits of drug use, how to use drugs and duration of treatment (Katherin, 2008)

Self medication action describe the behavior in the community formed through the process and interaction between individuals and their environment. Drugs widely used in the community self medication is piroxicam are include drugs known as anti-inflammatory non-steroidal that may be submitted by the pharmacist directly to the clients. The drug is indicated to treat symptoms of rheumatoid ar-

thritis , osteoarthritis, acute gout, menstrual pain, migraines and headaches . The main side effects are more felt by clients with the use of piroxicam oral are the gastrointestinal tract as nausea ,vomiting ,diarrhea ,stomach bleeding and dyspepsia . Despite the fact that there are many acts of self medication in the community, but not many people who know the correct treatment of self-medication. Therefore, in this study wanted to know the relationship between the level of knowledge and behavior of the client in self medication piroxicam drug in the sub-district community Sukun, Malang City. The hypothesis of this study is a significant relationship between the level of knowledge and behavior of the client in self medication Piroxicam.

METHOD

This study was an observational analytic study with a questionnaire instrument. According to the time is the cross-sectional study, conducted in June 2013. The sample size of 100 people, sampling is done with accidental sampling method that is to the clients who buy drugs for his own use of piroxicam tablets. Sampling is done in several pharmacy district Sukun of Malang city. Clients were given a questionnaire on knowledge and behavior of the client in self medication piroxicam. The data were analyzed by the method of Spearman crosstab and correlation using SPSS.

RESULTS

Demographic characteristics

In this study obtained data from 100 respondents who are clients of several pharmacies



in the district Sukun of Malang City. From the data collected to analyze the characteristics of the respondents included: age, gender, education and employment. The survey results revealed, the highest percentage age distribution of respondents was 43-53 years by 33%. Picture of the distribution of respondents by sex unknown female respondents 62%. The highest education level is high school known by 38%. The results can be seen in Table 1

Demography	Category	Freq	Percent(%)
Age (years)	21-31	8	8
	32-42	23	23
	43-53	33	33
	54-64	25	25
	65-75	11	11
Gender	male	38	38
	female	62	62
Education	Elementary school	6	6
	Junior high school	19	19
	High school	38	38
	university	37	37
Type of work	housewife	41	41
	private	27	27
	Civil sevant	25	25
	retired	7	7

The data from the client questionnaire calculating the level of knowledge score of the correct amount, further categorized by the following criteria: good, quite good, less good, not good. The survey results revealed that the highest level of client knowledge on the criteria good enough (53%). It shows that most clients who do self medication piroxicam, have a good enough knowledge about the use of piroxicam, how to wear and why the use of piroxicam. The results can be seen in Table 2.

Table 2. Category Level of Knowledge

Criteria	Freq	Percent (%)
good	37	37
quite good	53	53
Less good	10	10
Not good	0	0

Remarks:

- Good: The value of 76-100%
- quite good: the value of 56-75%
- Less good: the value of 55-40%
- Not good: the value of <40%

Against the behavioral questionnaires perform calculations using values of T scores, further categorized by the criteria of positive and negative behaviors, the results can be seen in Table 3. From Table 3 note that clients who do self medication piroxicam 47% showed positive behavior and 53% showed negative behavior.

Table 3. Categories of client behavior self-medication piroxicam

Behavior	Freq	Percent (%)
Positive	47	47
Negative	53	53

Remark :

Positives: scores -T ≥ average T group

Negatives: scores -T ≤ average T group

DATA ANALYSIS

Crosstabs analysis

Furthermore, from the data level of knowledge and behavior analysis with crosstabs method to describe the percentage of each group of levels of knowledge on behavior. Crosstabs analysis results can be seen in Table 4.

Table 4. Level of Knowledge and Behavior Crosstab clients in self medication Piroxicam

Knowledge		Behavior		Total
		Positive	negative	
Good	count	37	0	37
	% of Total	37%	0%	37%
quite Good	count	10	43	53
	% of Total	10%	43%	53%
Less good	count	1	10	10
	% of Total	1%	10%	10%
Not good	count	0	0	0
	% of Total	0%	0%	0%
Total	count	47	53	100
	% of Total	47%	53%	100%

From Table 4 it can be seen that a client with a good level of knowledge, all of the respondents (37%) positive behavior, while clients



with a level of knowledge is quite good for 53%, only 10% of positive behavior while 43% of negative behavior. While clients with the level of knowledge is not good (10%), behave entirely negative and no clients with a level of knowledge is not good. While clients with the level of knowledge about behaving entirely negative or no positive client behavior. And no clients with a level of knowledge is not good.

Spearman Correlation Test

To prove a significant relationship between the level of knowledge and behavior of clients who do self medication piroxicam with the Spearman correlation test. The test results show the value of r_s count is $0.08 > r_s$ table 0.199 ($df = 98, \alpha = 0.05$) and the significance value $0.000 < 0.050$, these results indicate that H_0 rejected and H_1 accepted, which means there is a significant relationship between the level of knowledge and client behavior in self medication piroxicam. The results can be seen in Table 5.

Table 5. Analysis of Results of Spearman Relationship between Knowledge and Behavior Clients in a self-medication piroxicam

r_s count	sig	r_s table ($df=98, \alpha=0.05$)	Decision
0,800	0,000	0,199	H_0 rejected

DISCUSSION

Based on the analysis of crosstabs known clients with the level of knowledge of good, behave entirely positive, otherwise the client with the level of knowledge of less well behaved entirely negative. client with a pretty good level of knowledge, 10% were positive behavior, while 37% of the negative behavior. This indicates that the level of sufficient knowledge of self medication piroxicam can not guarantee that the client's positive behavior. To achieve positive behavior of the client, then it should be a good level of knowledge. From the Spearman correlation analysis it is

known that a significant relationship between the level of knowledge and behavior of the client in self medication piroxicam.

CONCLUSION

1. The level of knowledge of clients who do self medication piroxicam 37% had a good level of knowledge, 53% had a fairly good level of knowledge, 10% had less good of knowledge and no clients with the level of knowledge is not good
2. The behavior of client self medication piroxicam 47% positive behavior, and 53% negative behavior.
3. There is a significant correlation between the level of knowledge and behavior of the client in self medication piroxicam at some pharmacies Sukun district in Malang city with a count value of r_s ($0.08 > r_s$ tables ($df = 98, \alpha = 0.05$) (0.199))

REFERENCE

- Hartwig, MS Wilson LM, (2006) Pathophysiology: Clinical Concepts Disease Process 6th ed, vol 2, Jakarta EGC
- Cunningham G, Dodd TR, Grant DJ, McMurdo ME, Richards RM. 1997, Drug-related problems in Elderly Patients admitted to Tayside hospitals, methods for prevention and subsequent reassessment of Anti-Inflammatory Agents, Non-Steroidal / Adverse Effects of Drug, Pub Med.gov US National Library Of Medicine in September; 26 (5): 375-82
- Liza P, et al. 2012. Study of Consumer Behavior Swamedikasi Pharmacies in Surabaya area (study for adult patients and pediatric patients), Research Grant FFUA
- Katherine FA, Lorenzo VZ 2008 Analysis and quantification of self-medication patterns, of customers in community pharmacies in southern Chile, Pharm World Sci (2008) 30: 863-868, DOI 10.1007 / s11096-008-9241
- Rossi S, editor. Australian Medicines Handbook 2006. Adelaide: Australian Medicines Handbook; 2006



EFFECT OF CHRONIC USE OF ENERGY DRINK ON KIDNEY

Mahardian Rahmadi, Zamrotul Izzah, Mareta Rindang A., Aniek Setya B., Suharjo

Department of Clinical Pharmacy, Faculty of Pharmacy Universitas Airlangga,
Campus B Unair Jl. Dharawangsa Dalam Surabaya. mahardianr@yahoo.com

INTRODUCTION

Increasing in chronic kidney disease in USA was mainly caused nephrolithiasis. The prevalence in men was 10,6% and women 7,1% (Ferraro et al., 2013). The use of energy drinks has been widely used in the community and been a part of their lifestyle. Changes in lifestyle such as lack of drinking water and highly consumed energy drinks often lead to chronic kidney disease (Shoham et al., 2008). Some cases in hospitals showed an association between renal dysfunction and the use of energy drinks previously. A main content of energy drinks, caffeine was correlated with diuretics and the electrolyte balance. Caffeine also stimulates glomerular filtration and inhibition of sodium reabsorption. Caffeine also increases the excretion of water and ions (Carrillo, 2000). This study was aimed to determine the effect of chronic uses of energy drink on renal function based on the parameters of hematology, urinalysis and renal histopathology.

MATERIAL METHOD

Animal and other materials

Animal that used in this research were male, wistar rat and about 150-200 g of weight in the starting time of experiment. Animal were housed in animal cage which had constant temperature set at 23 ± 0.5 °C. Light was set so the time of dark and bright for each 12 h. Animals were acclimatized for at least 7 days before used.

Three (3) major brands of energy drinks in Indonesia were used, two in solution dosage form and one in effervescent powder dosage form. Other materials that used in this research were propofol, diethyl-ether, paraffin, phosphate buffer, formalin buffer, aquadest, NaCl 0.9%, dan hematoksilin-eosin.

Dose and Administration

All of energy drinks were administered orally twice a day for 30 days using animal sonde. The dose of energy drinks was calculated based on caffeine concentration of each energy drink. Each dose of energy drinks equivalent to 12.5 mg/kg caffeine. Volume of administration of each energy drink was 6.75 ml/kg of rat. Water was administered as a control. The powder dosage form of energy drink was dissolved in water before administration.

Urinalysis and Hematological Analysis

Twenty-four hours after last administration of energy drink

or water, 24h urine sampling was done by collect animal urine using standard metabolic cage for rat.

Albumin and creatinine level in urine were analyzed using standard enzymatic analysis for albumin and creatinine.

For hematological analysis, from each animal 2 ml of blood was collected via cardiac puncture method. The hematological analysis for serum creatinine, blood urea nitrogen and electrolyte were evaluated using standard hematological analyzer.

Histopathological Analysis

Animal was anesthetized using intravenous 20 mg/kg propofol and sacrificed. Left kidney was collected and fixed with 10% formalin buffer for at least 7 days. After dehydrated by alcohol sample was put in toluene for dealcoholization. Embed the kidney in paraffin for 4 h and sliced with the thickness of 5 µm. Sliced sample next putted on object glass for Hematoxylin-eosin staining.

Statistical Analysis

All statistical analysis that used in this research was performed using Graphpad® Prism 6.0. The difference between control and energy

drink groups in urinalysis and hematological analysis were analyzed using one-way ANOVA followed with Dunnet post-hoc analysis.

RESULTS

Effects of energy drink on urinalysis and hematological analysis can be seen at figure 1 and 2, respectively.

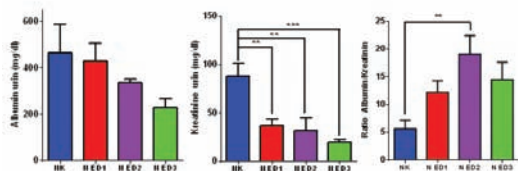


Figure 1. Profile of urinalysis parameter on control (NK) and energy drink groups (NED1, NED2 and NED3) after 30 days

administration of energy drink or water. Left: Albumin; Middle: creatinine; Right: Ratio of Albumin/creatinine. Post hoc analysis of one-way anova showed significant difference between control vs. ED1, ED2 ($p < 0,01$) dan control vs. ED3 ($p < 0,001$).

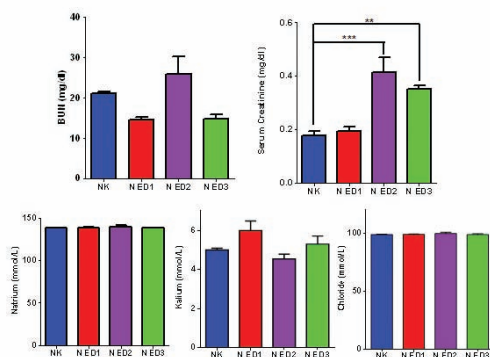


Figure 2. Profile of hematological analysis parameter on control (NK) and energy drink groups (NED1, NED2 and NED3) after 30 days administration of energy drink or water. Above-left: BUN; Above-right: creatinine serum; Lower-left: natrium serum; Lower-middle : kalium serum, Lower-right: chloride serum, Post hoc analysis of one-way anova showed significance different vs control group $**p < 0,01$; $***p < 0,001$.

The histopathological analysis data of kidney medulla of treated animal can be seen at figure 3.

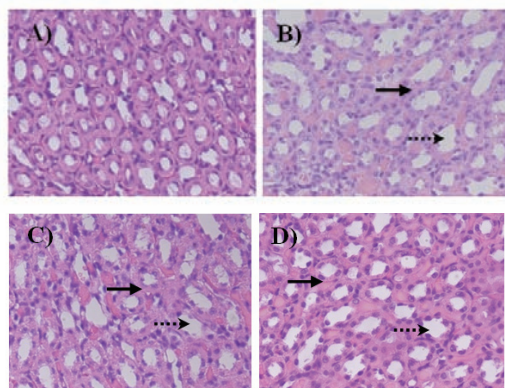


Figure 3. Representative histopathological analysis of the kidney medulla of rats which were 30 days treated half dose of with water (A) or energy drinks 1, 2 and 3 (B, C and D). Sliced sample were stained with haematoxylin-eosin, 400x magnification, showed thickening of medulla wall (line arrow) and dilatation of medulla lumen (dashed arrow).

DISCUSSION

Chronic administration of energy drinks for 30 days significantly change the urinalysis parameters especially on creatinine urine but not albumin urine, furthermore the ratio of albumin/creatinine also significantly increased on energy drinks administration groups. Decrease on 24 h creatinine urine concentration indicates decreased in the filtration rate of kidney glomerulus. While unchanged on albumin excretion in urine indicates that the level of kidney abnormality still on mild to middle stage of kidney diseases (Joy et al., 2008).

Hematological analysis data of kidney function indicates positive correlation with urinalysis data. None of serum electrolyte (Natrium, Kalium an Chloride) level were changed after chronic treatment with energy drinks. Even blood urea nitrogen (BUN) did not change, 30 days chronic administration of energy drinks significantly increased the level of creatinine serum (Saldana et al., 2007).

To investigate the abnormality in the kidney tissue, histopathological examination by hae-



matoxylin-eosin stained kidney sample were obtained. Half dose of energy drinks did not induces any abnormality in the glomerulus of kidney cortex (data not shown). In contrast, abnormalities were shown in medulla area of the kidney. Thickening of medulla wall and vasodilatation of medulla lumen at least in part contribute to the energy drinks-induced abnormalities on kidney function.

CONCLUSION

All urinalysis, hematological analysis and histopathological data proved that chronic administration of energy drink for 30 days could induce negative effect for the kidney.

REFERENCES

- *. Carrillo, J.A., Benitez, J., 2000. Clinically Significant Pharmacokinetic Interactions between Dietary Caffeine and Medications. In: *Clin Pharmacokinet*, 39: 127-153.
- *. Ferraro PM, Taylor EN, Gambaro G and Curhan GC, 2013. Soda and Other Beverages and the Risk of Kidney Stone. In: *Clin J Am Soc Nephrol* 8: 1-7.
- *. Joy, M.S., Kshirsagar, A., and Franceschini, N., 2008. Chronic Kidney Disease: Progression-Modifying Therapies. In: *Pharmacotherapy A Pathophysiologic Approach* 7th edition. The McGraw-Hill Companies Inc. p. 745-750.
- *. Saldana TM, Basso O, Darden R, and Sandler, 2007. Carbonated Beverages and Chronic Kidney Disease. *Epidemiology*.18(4): 501-506
- *. Shoham DA, Durazo-Arvizu R, Kramer H, Luke A, Vupputuri S, Kshirsagar A, Cooper RS. 2008. Sugary Soda Consumption and Albuminuria: Results from the National Health and Nutrition Examination Survey, 1999-2004. In: *PloS One*.Vol 3/ Issue 10/e 3431.

SCREENING OF SURFACE MODIFIERS TO PRODUCE STABLE NANOSUSPENSION : A GENERAL GUIDANCE

Maria Lucia Ardhani Dwi Lestari, Faculty of Pharmacy Airlangga University, Dharmawangsa Dalam Surabaya 60286 Indonesia, email : maria-lestari@ff.unair.ac.id

INTRODUCTION

Nanosuspension consists of two components: active pharmaceutical ingredient (API) and surface modifier or widely known as surfactant/stabilizer. In the nanosuspension system, the role of surface modifier is important to prevent nanoparticles from aggregation and agglomeration. Up to this date, the selection of surface modifier for the formulation of nanosuspension is most likely based on the experience of the formulators. Additionally, this process is time consuming, less effective and only limited information available in the literature on how to perform the screening of surface modifier. To overcome this problem, this work was performed to study the influence of physico-chemical properties of API on the stabilization system of nanosuspension and to provide a general guidance to select proper surface modifier in order to produce stable nanosuspensions.

MATERIALS

Amphotericin B (AmB) (Alpharma, Copenhagen, Denmark), curcumin (CUR) (Phytochemindo Reksa, Bogor, Indonesia), hesperetin (HES) (Exquim, S.A., Barcelona, Spain), ibuprofen (IBU) (BASF, Ludwigshafen Germany), resveratrol (RES) (E.Denk Feinchemie, Germany), rutoside trihydrate (RUT) (Exquim, S.A., Barcelona, Spain).

As surfactant and stabilizers the following excipients have been used: sodium dodecyl sulphate (SDS), sodium docusate, sodium cholate, Tween[®] 80 (Sigma Aldrich, Steinheim, Germany), dehyquart A-CA (Cognis, Düsseldorf, Germany), poloxamer 188 (Molekula, Dorset, UK), tocopheryl polyethylene glycol succinate (TPGS) (Eastman, Anglesey, UK), polyvinyl alcohol (PVA) molecular weight

80.000 (Serva Feinbiochemical , Heidelberg, Germany), hydroxypropyl methylcellulose E5 (HPMC E5) (Colorcon Ltd, Kent, UK).

METHODS

0.5g API was dispersed into vial containing 9.5g of surfactant/stabilizer solution and 5 mL of milling beads. Three concentrations of surface modifier were applied : 5x lower than its CMC value (low), at its CMC value (mid) and 5x higher than its CMC value (high). This mixture was then being stirred up to 72h and samples withdrawn every 24h, 48h and 72h. The nanosuspension formed was then characterized by photon correlation spectroscopy (PCS, Zetasizer Nano ZS (Malvern Instruments, UK)), laser diffractometry (LD, Mastersizer 2000 (Malvern Instruments, UK)), and light microscopy (Leitz Orthoplan, Germany)

RESULTS AND DISCUSSION

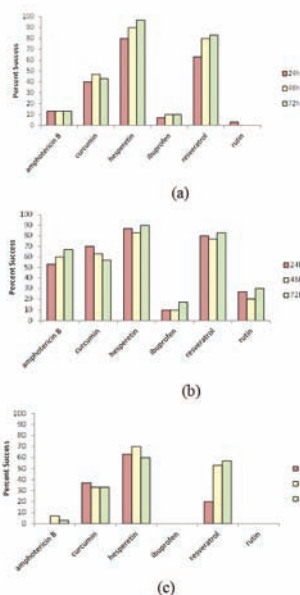




Figure 1. Percent success of each API during milling, from 24h to 72h based on : (a) z-average; (b) D50% value; (c) D90% value.

Based on the API applied, hesperetin was the API with highest millability to be nanosized whilst rutoside trihydrate was found to have the lowest millability as observed with its low percent of success to be nanosized. No correlations were found between the millability of the APIs with their physico-chemical properties such as molecular weight, log P value that represents lipophilicity, pKa and also melting point.

One important consideration for the surface modifier is the applied concentration. Screening results have shown that for anionic surfactant, concentrations higher than the CMC are beneficial to produce nanosuspensions with particle size <250nm.

Based on the screening result, the capability of anionic surfactants to produce stable nanosuspensions with particle size <250 nm can be ranked as follows: sodium cholate>SDS>sodium docusate. Furthermore, higher CMC value of anionic surfactant leads to better stabilization.

CONCLUSIONS

No general trend was found with regard to the physico-chemical properties of APIs and their millability. The API can be classified into compounds with good, medium or bad millability. Moreover, particle size obtained and particle size stability of the nanosuspensions depend on the stabilization principle and concentration of the surface modifiers. There are some surface modifiers that can be used to produce stable nanosuspensions independent from the API applied. These surface modifiers can be considered as "general surface modifiers"

ACKNOWLEDGMENTS

The author would like to thank :

1. Deutscher Akademischer Austauschdienst (DAAD) for the financial support.
2. Prof. Dr. R.H and Dr. J.P Möschwitzer (Freie Universität Berlin) for the laboratory support, guidance and advices in this study.

REFERENCES

- Eerdenbrugh BV, Vermant J, Martens JA, Froyen L, Humbeeck JV, Augustijns P, Mooter GVD. 2009. A Screening study of surface stabilization during the production of drug nanocrystals. *J Pharm Sci* 98:2091-2103.
- Lestari, M.L.A.D, Müller, R.H, Möschwitzer, J.P. 2014. Systematic screening of the different surface modifiers for the production of physically stable nanosuspensions. *J.Pharm.Sci.* accepted.

DEVELOPMENT OF SIMPLE POLYPHENOL SENSOR BASED ON SODIUM META PERIODATE AND 3-Methyl-2-Benzothiazolinone Hydrazone FOR COFFEE SAMPLES

Moch. Amrun Hidayat, Faculty of Pharmacy, University of Jember, Kalimantan 1/2 Kampus Tegal Boto Jember 68121, amrun.farmasi@unej.ac.id; **Nindya Puspitaningtyas**, Faculty of Pharmacy, University of Jember; **Agus Abdul Gani**, Faculty of Teacher Training and Education, University of Jember, Kalimantan 37 Kampus Tegal Boto Jember 68121; **Bambang Kuswandi**, Faculty of Pharmacy, University of Jember, b_kuswandi.farmasi@unej.ac.id;

INTRODUCTION

Based on various studies, it is well known that coffee has positive effect on human health as it consumed regularly as beverage¹. Coffee exhibited various pharmacological effects, such as reducing risk of diabetes, parkinson's diseases, and increasing cognition and mood². The polyphenolic compounds found in coffee are known responsible for their health effects, and their aromatic properties of coffee³.

Chromatographic (HPLC)^{4,5} and spectrophotometric (UV-Vis)⁶ method were used widely for polyphenol determination in coffee. Nevertheless, chromatographic and spectrometric methods suffer from tedious length procedure and the use of expensive and complicated instrumentation. Therefore, the development of alternative methods for polyphenol determination which simplify the analysis is needed.

One alternative method is using chemical sensor or biosensor for polyphenol determination, as these technologies are applicable for this field. This research was aimed to develop simple sensor for determination of total polyphenol content in coffee by immobilization of sodium meta periodate (NaIO_4) and 3-methyl-2-benzothiazolinone hydrazone (MBTH) reagents onto filter paper. NaIO_4 can oxidize the ortho-diphenols (in polyphenol's chemical structure) into their related ortho-diquinones, mimicking the natural polyphenol oxidase enzyme⁷. MBTH is chromogenic reagent for ortho-diquinones detection which in turn, resulting red color on the surface of the polyphenol sensor⁸.

EXPERIMENTAL DETAILS

Reagents

All reagents were used as purchased without further purification. NaIO_4 were obtained from BDH-Merck (UK). MBTH were obtained from Fluka (UK). Chlorogenic Acid (CA) were obtained from Aldrich (UK). For immobilization, a phosphate buffer solution (PBS) with pH 7.0 was prepared by adjusting amounts of NaCl, KCl, Na_2HPO_4 and KH_2PO_4 buffer systems; in all cases, the mixture were 0.2 M in each constituent. Whatman filter paper (CAT No.1095.093) for sensor host were obtained from Merck (UK).

Reagent Immobilization

Fresh solution containing 8 mM NaIO_4 dan 48 mM MBTH at equal volume was prepared for sensor reagent. The reagent was pipetted (4 μl) and dipped onto 0.5 x 0.5 cm² filter paper, and dried for 30 minutes at ambient temperature to make colorimetric sensor membrane. Afterward, the sensor membrane was placed gently onto plastic film to construct polyphenol sensor as it given in Fig. 1.



Figure 1. Sensor design and its application on samples.



Color Change Measurement

Since, the proposed sensor was intended to be used in visual mode, so that the color changes during polyphenol detection can be easily viewed by the naked eye. For quantification of color measurements of the sensor, a simple method using a flatbed scanner (CanoScan Lide110, Canon, Japan) was used. The color change of the sensor from colorless to red was used as the measurable response of the sensor toward polyphenol, after the sensor (as a dip stick test) was dipped into a sample solution for 5 seconds (Fig. 1). The color change of the sensor was quantified using ImageJ program^{9,10}, as previously scanned to determine the mean RGB value of the sensor color.

Optimization of Sensor

Since CA is known as major compound found in coffee as polyphenols, thus it can be used to represent polyphenol profile in coffee. Hence, CA (25-250 $\mu\text{g/mL}$) was used for optimization of the proposed sensor, and calibration curves were made for polyphenol determination. Here, polyphenol contents were expressed as mg/L chlorogenic acid equivalent (CAE).

Preparation of Coffee Samples

Coffee (Robusta and Arabica) samples were purchased from PT. Perkebunan Nusantara X, Jember-East Java, Indonesia. Coffee beverages were made by brewing dried powder of coffee bean with boiling water at 1% w/v. The coffee suspension were decanted and filtered through filter paper to obtain sample solutions. Afterward, sample solutions were cooled at ambient temperature for polyphenol analysis.

RESULTS AND DISCUSSION

Analytical Properties of the Sensor

The proposed sensors were used for the visual determination of total polyphenol content. The calibration curves are presented in Figure 2. Here, the sensor has a linear response in the range of 25-250 $\mu\text{g/mL}$ CAE (i.e., the intensity of red color increases) with a correlation coefficient (r) of 0.999. The limit of detection of

the sensor was 11,067 $\mu\text{g/mL}$ CAE, while limit of quantitation was found in the 36,888 $\mu\text{g/mL}$ CAE.

Response Time

The response time of the sensor was found as a time needed to change the color after the sensor reacted with polyphenol solution. A solution of 150 $\mu\text{g/mL}$ CA was used to determine response time. The response time was found to be 15 minutes, in which after this time, the sensor response was constant (Figure 3).

Reproducibility

In order to determine the reproducibility, the sensor response was tested toward 1% of coffee solution samples as given in Figure 4. The sensor response shows good reproducibility for both of Robusta (R.S.D. = 0.53%) and Arabica (R.S.D. = 0.87%) coffees. This reproducibility is higher compared to other reported polyphenol biosensors⁸.

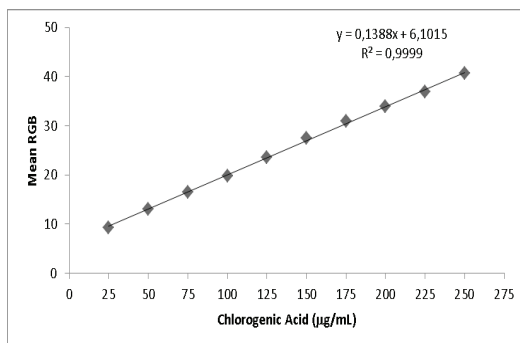


Figure 2. Calibration curve of CA for total polyphenol quantification.

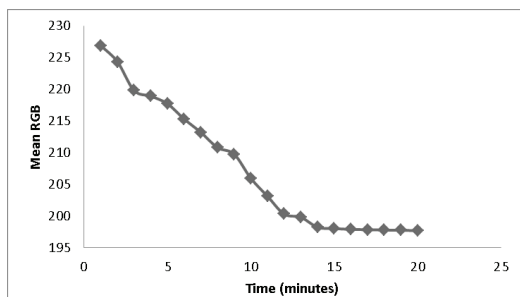


Figure 3. Response time of NaIO₄/MBTH-sensor toward CA.

Figure 3. Response time of NaIO₄/MBTH sensor toward CA.

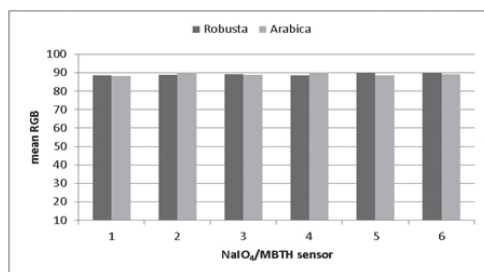


Figure 4. Reproducibility NaIO₄/MBTH sensor toward coffee samples.

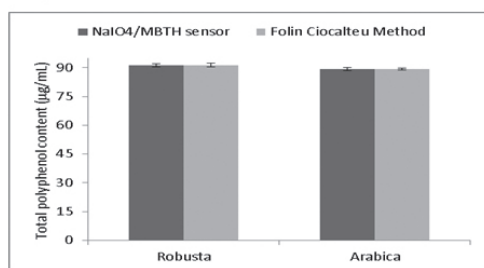


Figure 5. Comparison of polyphenol content in coffee samples determined by NaIO₄/MBTH sensor and standard folin method (n=3).

Determination of Polyphenol Content in Coffee Samples

The proposed sensor was used to determine polyphenol content in coffee beverages. The standard Folin-Cioalceu method was used to validate total polyphenol content obtained by the developed sensor. No significant different results ($p = 0.05$) were found compared with the Folin-Cioalceu method as it can be seen at Figure 5. Thus, the proposed sensor can be used as an alternative tool for determination of total polyphenol content in coffee beverage samples.

CONCLUSION

The proposed chemical sensor based on NaIO₄/MBTH reagents offers simplicity, rapid and cost effective in determination of total polyphenol content in coffee samples. Thus, the proposed sensor can be used as alternative method for polyphenol determination in coffee beverage samples.

Acknowledgment. The authors gratefully thank the DP2M, Higher Education, Ministry of Culture & Education, Republic of Indone-

sia, for supporting this work via the Higher Education Superior Research Project (Penelitian Unggulan Perguruan Tinggi, No. 306/UN25.3.1/LT6/2014).

REFERENCES

1. Coughlin JR. (2006). Coffee and health: The holistic approach. In Proceedings of the 21st ASIC colloquium, Montpellier, France, pp. 29-35.
2. Bisht S, Sisodia S. (2010). Coffea arabica: A wonder gift to medical science. J. Natural Pharmaceuticals. 1:58-65.
3. Farah A., Donangelo CM. (2006). Phenolic compounds in coffee. Braz. J. Plant Physiol., Vol. 18 (1): 23-36.
4. Farah A., Paulis TD, Moreira DP, et al. (2006). Chlorogenic acids and lactones in regular and water-decaffeinated Arabica coffees. J. Agric. Food Chem. 54: 374-381.
5. Ayelign A., Sabally K. (2013). Determination of chlorogenic acids (CGA) in coffee beans using HPLC. American Journal of Research Communication, 1(2): 78-91.
6. Belay A., Gholap AV. (2009). Characterization and determination of chlorogenic acids (CGA) in coffee beans by UV-Vis spectroscopy. African Journal of Pure and Applied Chemistry. 3 (11): 234-240.
7. Munoz JL, Molina FG, Varon R, et al. (2006). Calculating Molar Absorptivities for Quinones: Application to the Measurement of Tyrosinase Activity. Anal. Biochem. 35:128-138.
8. Oktem HA., Senyurt O, Eyidogan F, et al. (2012). Development of a Laccase Based Paper Biosensor for the Detection of Phenolic Compounds. J. Food. Agric. Env. 10 (2): 1030-1034.
9. Girish V, Vijayalakshmi A, (2004). Affordable image analysis using NIH Image/ImageJ. Indian J. Cancer, 41: 47.
10. Collins TJ. (2007) ImageJ for microscopy. BioTechniques. 43: 25-30.



VALIDATION OF AN HPLC ANALYTICAL METHOD FOR DETERMINATION OF LEVOFLOXACIN IN OPHTHALMIC PREPARATIONS

Mochamad Yuwono, Airlangga University, yuwono05@yahoo.com ; Riesta Primaharinastiti, Airlangga University, r.nastiti@gmail.com ; Ageng Teguh Wardoyo, Airlangga University, wardoyoageng@gmail.com , +628563004855

INTRODUCTION

Levofloxacin is the active L-isomer of ofloxacin, a fourth-generation fluoroquinolone derivative (Figure 1). The presence of unwanted or in certain cases unknown chemicals, even in small amounts, may influence not only the therapeutic efficacy but also the safety of the pharmaceutical products [04]. As per the requirements of various regulatory authorities [01,02,03], the impurity profile study of drug substances especially for impurity C ((S)-Ethyl-9-fluoro-2,3-dihydro-3-methyl-10-(4-methyl-1-piperazinyl)-7-oxo-7H-pyrido[1,2,3-de]-1,4-benzoxazine-6-carboxylate) has to be carried out using a suitable analytical method in the final product.

The research studied that the optimum chromatographic separation for levofloxacin and degradation products takes place when an aqueous solution containing 0.025 M phosphate buffer pH 6.0±0.05 and acetonitrile (88:12 v/v) are used as the mobile phase at a flow rate of 1.5 mL min⁻¹, and PDA detection at 294 nm [05].

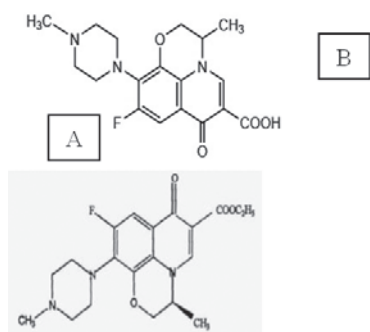


Figure 1. Structure of levofloxacin (A) and impurity C (B)

MATERIALS AND METHOD

Materials

Levofloxacin Hemihydrate ex. DR. REDDY'S/INDIA Batch No.ABBH001535, Volox Eye Drop Placebo pH 6.4, Volox Eye Drop Recovery (70%, 100%, 130%) (PT. Interbat Sidoarjo), Acetonitrile gradient grade for Liquid Chromatography, KH₂PO₄, TEA, HCl, NaOH, H₂O₂, H₃PO₄, C₂H₅OH analytical grade (Merck), highly pure HPLC grade Milli-Q water (Millipore).

Instrument

UHPLC Nexera L20154908961 Shimadzu, UFLC Shimadzu LC-20AD Prominence, Column Phenomenex Luna 5u C18(2) 100A 150 mm x 4.6 mm, Milli-Q water purification with Millipak-40 filter 0.22 µm, Analytical scales Mettler Toledo XP205, pH meter Mettler Toledo Seven Multi.

Chromatographic conditions:

The mobile phase consisted of a mixture of 0.025 M phosphate buffer pH 6.0±0.05 and acetonitrile (88:12), delivered at a constant flow rate of 1.5 mL/min, PDA detection at 294 nm, and the injection volume was 10 µL. Column temperature was fixed at 35°C. All mobile phases were filtered through a 0.22 µm Millipore filter.

Sample Preparations:

Standard solution:

Accurately weighed 50.0 mg levofloxacin hemihydrate is transferred to 25.0 mL volumetric flask, added 15 mL of mobile phase & sonicated to dissolve, diluted up to volume

with mobile phase. Pipetted 1.0 mL of solution, put in a 10.0 mL volumetric flask, diluted with mobile phase up to the mark, shake homogeneous. Obtained levofloxacin 200 ppm standard solution.

Impurity C solution [06]:

Accurately weighed 50.0 mg levofloxacin hemihydrate is transferred to 50.0 mL volumetric flask, added 40 mL of ethanol & sonicated to dissolve, diluted up to volume with ethanol. Added 1.0 mL of concentrated hydrochloric acid, shake homogeneous. Then the solution was heated in a water bath at 60°C for 3 hours.

RESULT AND DISCUSSIONS

Analytical Method development:

As results of these studies, using Phenomenex Luna 5u C18(2) 100A 150 mm x 4.6 mm column and a mobile phase consisted of a mixture of buffer phosphate pH 6.0±0.05 and acetonitrile (88:12 v/v) at a flow rate of 1.5 mL min⁻¹, and PDA detection at 294 nm was found appropriate to obtain an adequate separation of all the related impurities and degradation products of the levofloxacin.

Method validation study:

Selectivity:

The observation was made from the chromatogram of interference of diluent, placebo and impurities that no peak was found at the retention time of levofloxacin peak (Figure 2). Resolution between levofloxacin and impurity C was found more than 2.0. The peak purity angle was less than peak purity threshold, which indicated that the concern peak is spectrally homogeneous.



Figure 2. Chromatogram of levofloxacin and impurity C

Linearity:

The standard solution of levofloxacin hemihydrate at levels 140, 170, 200, 230, 260 ppm was injected. Parameter values obtained linearity of levofloxacin that $r=0.9994$. From these data it can be concluded that there is a linear relationship between the concentration of levofloxacin in the area over a range of concentrations (Figure 3).

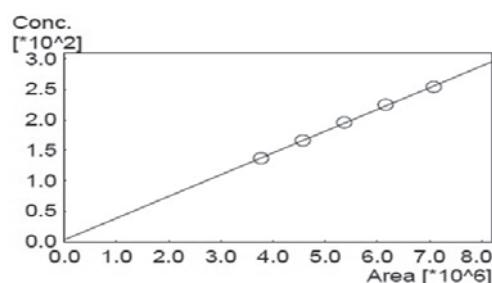


Figure 3. Linearity curve of levofloxacin

Accuracy:

The % recovery for three sets of accuracy sample preparation at each accuracy level was found within the acceptance criteria with acceptable limit (98%-102%).

Stressed Study:

The standard solutions are prepared to get the degradation at least in one condition and subjected to various stress condition as mentioned below (Table 1).

Acid Stress conditions		Alkali Stress conditions	
Concentration of acid	0.5 N HCl	Concentration of base	0.5 N NaOH
Time	1 hour	Time	1 hour
Temperature	60°C	Temperature	60°C
Oxidative Stress conditions		Temperature Stress conditions	
Concentration of Hydrogen peroxide	10% w/w H ₂ O ₂	Time	2 weeks
Time	1 hour	Temperature	60°C
Temperature	60°C	White Light Exposure conditions	
		Time	2 weeks

Table 1. Stress study conditions



Intermediate Precision:

Intermediate precision was evaluated by carrying out six independent assays at standard solution of levofloxacin on different tools by different analysts. Samples were analyzed by 6 times replication (Table 2).

	Condition I	Condition II
Analyst	Ageng	Maria
Instrument	UHPLC Nexera 2	UFLC Shimadzu 20AD
Column	Phenomenex Luna C18(2) 5u 150 x 4.6 mm	
SN Column	668873-12	676844-1
Replication	X _A	X _B
1	102,49	100,39
2	102,14	100,14
3	101,11	100,22
4	102,16	100,59
5	101,78	100,08
6	102,07	100,83
Total	611,75	602,25
Average	101,96	100,38
SD	0,4733	0,2897
RSD precision	0,4643	0,2887
RSD int.precision	0,8971	

Table 2. Data of Intermediate Precision

Intermediate Precision:

Intermediate precision was evaluated by carrying out six independent assays at standard solution of levofloxacin on different tools by different analysts. Samples were analyzed by 6 times replication (Table 2).

Robustness:

The determination was observed with small but deliberate changes in the parameters (column temperature (+5oC) and flow rate (+2)). Resolution between levofloxacin and impurity C, theoretical plates, tailing, %RSD were observed and found good with all the different altered conditions.

CONCLUSION

An HPLC method was proposed for the determination of levofloxacin in ophthalmic preparations and validated for selectivity, linearity, accuracy, stress study, intermediate precision and robustness.

REFERENCES

- *. ICH Guideline Q3A (R2), Impurities in New Drug Substances, October 25, 2006.
- *. ICH Guideline Q7A, Good Manufacturing Practice Guide for Active pharmaceutical Ingredients, November 2005.
- *. United States Pharmacopeia Medicines Compendium. 2013. USP Medicines Compendium - Levofloxacin Ophthalmic Solution. Rockville, USA: United States Pharmacopeial Medicines Compendium. Retrieved from <https://mc.usp.org>
- *. Vyas, N., Pancholi, Y., Patel, V., Kshatri, N., dan Mehta, J., 2010. Development and Validation of a Sensitive Stability Indicating Method for Quantification of Levofloxacin Related Substances and Degradation Products in Pharmaceutical Dosage Form. International Journal of PharmTech Research Vol. 2 No.3, pp. 1932-1942
- *. United States Pharmacopeial Convention. 2008. The United States Pharmacopeia 32 -National Formulary 27 (USP32-NF27). Rockville USA: The United States Pharmacopeial Convention Inc.
- *. Sultana, N., Arayne, M.S., Rizvi, S.B.S., Mesaik, M.A., 2009. Synthesis, Characterization and Biological Evaluation of a Series of Levofloxacin Carboxamide Analogues. Bull. Korean Chemical. Soc. Vol. 30, No.10, pp. 2294-2298

VALIDATION OF SPECTROPHOTOMETRIC METHOD FOR ESTIMATION OF EPERISONE HYDROCHLORIDE IN TABLET DOSAGE FORM

Nia Kristiningrum, Faculty of Pharmacy, University of Jember, Kalimantan I/2 Jember, neeya_k@yahoo.co.uk, +628123074417; **Diah Yuli Pangesti**, Faculty of Pharmacy, University of Jember, Kalimantan I/2 Jember

INTRODUCTION

Eperisone (EPE) is chemically 4'-ethyl-3-methyl-3-piperidinopropiophenone (Figure 1), is antispasmodic drug (Paresh, et al., 2012). It is used in the treatment of different pathological conditions like acute and chronic muscle spasm, electroconvulsive therapy, neurological conditions, orthopedic manipulation, myelopathy, encephalomyelitis, spondylosis, spondylarthrosis, cervical and lumbar syndrome, arthrosis of the large joints obliterating arthrosclerosis of the extremity vessels, diabetical anghthromboangitis obliterans and Reynaud's syndrome (Maske and Nagras, 2013). Literature survey revealed that EPE is estimated by HPLC (Din, et al., 2004) and AUC method of UV spectrophotometry (Maske and Nagras, 2013) in single component formulation. In this presentation we report a simple and rapid assay for the quantitation of EPE using UV spectrophotometry method.

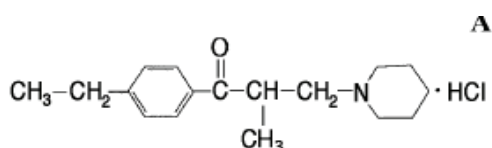


Figure 1 Chemical structures of eperisone

MATERIAL AND REAGENT

Working standard of pharmaceutical grade Eperisone Hydrochloride from PT Eisai Indonesia, (Wuhan Grand Pharmaceutical Group Co., Ltd.), methanol, commercial tablets contain EPE.

EXPERIMENTAL

Preparation of Standard Solutions and Pharmaceutical Samples

Stock standard solution was always freshly prepared by dissolving 25 mg of Eperisone Hy-

drochloride in 100 ml methanol (stock standard solution I) and 30 mg of Eperisone Hydrochloride in 50 ml methanol (stock standard solution II). Working standard solutions were prepared by dilution of stock solution with methanol to get solutions in concentration range of 1-18 µg/ml. For sample preparation, twenty tablets was weighed; average weight was determined and finely powdered. An accurately weighed quantity of tablet powder equivalent to 10 mg of Eperisone Hydrochloride was transferred to 100 ml volumetric flask and dissolved by sonication with methanol, volume was made up to mark. The solution was then filtered through filter membrane 0.45 µm. A 1.0 ml of the filtrate was further diluted with methanol in a 10 ml volumetric flask up to mark (10 µg/ml) on label claim basis.

Determination of λ max

A 10 µg/ml solution of Eperisone Hydrochloride was prepared and scanned in UV range of 200-400 nm and spectrum was obtained. The spectrum of Eperisone Hydrochloride as shown in figure 2.

Method Validation

The developed method was validated with the following parameters.

Specificity

The Specificity of this method was determined by analyzing standard and sample. Specificity was showed by scanning at 200nm – 400 nm and analyzed the spectrum of standard and sample.

Linearity

The evaluation of the calibration curve's lin



earity was done based on the absorbance of the standard solutions that were prepared in methanol at the concentrations 1-18 µg/ml. The calibration curve was plotted as concentration versus absorbance.

Limit of Detection and Quantification

Limit of detection (LOD) and Limit of Quantification (LOQ) were determined by preparing the standard solutions in methanol at the concentrations 1-18 µg/ml.

Precision

The precision of this method was performed by repeatability and intermediate precision studies. Repeatability studies was performed by analyzing one concentration of the drug for six times on the same day. The intermediate precision was checked by repeating studies on three different days.

Accuracy

The accuracy of this method was evaluated through recovery experiments by adding three different amounts of Eperisone Hydrochloride standards i.e. 30, 45 and 60% of the concentration samples. Each concentration were replicated (n=3)

Analysis of Marketed formulations

The Samples that is contain of Eperisone Hydrochloride (brand A and brand B) were prepared as sample preparation method. Each of samples were replicated (n=3). The analysis was done in the same way as described earlier.

RESULTS AND DISCUSSION

A validated, simple and accurate UV-Spectrophotometric methods has been developed for determination of Eperisone Hydrochloride in tablet dosage forms. Eperisone hydrochloride showed maximum absorbance at 255.5 nm. From UV-spectrophotometric, showed that the absorbance of analyte in sample were same as standard (figure 2).

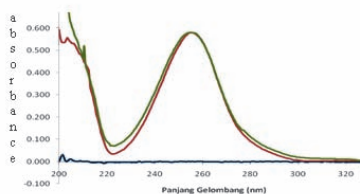


Figure 2 Spectra of, Wavelength (nm) and sample

Linearity was observed in concentration range 1-18 µg/ml and gave the equation $Y = 0,05493X - 0,00315$ with correlation coefficient value 0.9999 (figure 3).

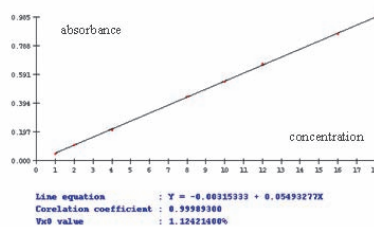


Figure 3 calibration curve of Eperisone in methanol

The LOD and LOQ were found to be 0.485 µg/ml and 1.373 µg/ml. The values of relative standard deviation (RSD) were found to be 1.13%; 0.16% and 0.74% in the different day. The three measurement were performed within one laboratory by same analyst in different days. The accuracy of the proposed method were $100.94\% \pm 0.81$.

Analysis of Marketed formulations

The proposed method has been applied to the determination of Eperisone Hydrochloride in commercial tablet formulations and the recovery of label claim were $98.84\% \pm 0.32$ µg/ml for brand A and $99.74\% \pm 0.47$ µg/ml for brand B. The result of the analysis of marketed formulations indicate that the concentrations of Eperisone hydrochloride in tablet is within the requirements (USP) 95-105% .

CONCLUSION

A new UV-spectrophotometry method has been developed for the quantification of Eperisone hydrochloride in tablet dosage forms. The method was found to be simple, rapid, specific, precise and accurate for esti-



mation and can be employed for the routine quality control analysis Eperisone hydrochloride in tablet.

REFERENCES

1. Ding L, Wei X, Zhang S, et al. (2004). Rapid and sensitive liquid chromatography-electrospray ionization-mass spectrometry method for determination of eperisone in human plasma : method and clinical applications. *Journal of Chromatographic Science*, May/June:42:254-258.
2. International conference on harmonization (ICH). (1995). Text on validation of analytical procedures: definitions and terminology, US FDA federal register, 60.
3. Maske PB, Nagras MA. (2013). Development and validation of spectrophotometric method for estimation of eperisone hydrochloride in bulk and tablet dosage form by using area under curve method. *International Journal of Chem Tech Research*, July-Sept: 5(5): 2210-2215.
4. Pares P, Sejal P, Umang P. (2012). Spectrophotometric method for simultaneous estimation of eperisone hydrochloride and diclofenac sodium in synthetic mixture. *IRJP*, Sept : 3(9):203-206.
5. The United State Pharmacopoeia 30-National Formulary 25. (2007). Asia Edition. Rockville: United State Pharmacopoeial Convention.



ANTIOSTEOPOROTIC ACTIVITY OF 96% ETHANOLIC EXTRACTS OF *Abelmoschus Manihot* L. Medik LEAVES AND EXERCISE ON INCREASING BONE DENSITY OF FEMALE MICE'S FEMORAL TRABECULAR

Niliestria Ayu Faramitha Sholikhah

Airlangga University, e-mail :niliestriaayufs@gmail.com, 085646415899

INTRODUCTION

Osteoporosis is a disease characterized by decrease in BMD (Bone Mineral Density) and degeneration of bone microarchitecture, thereby increasing the risk of fracture (Noor et al, 2011).

Osteoporosis influences the health of more than 200 million people around the world in recent years (Jia et al, 2012). Prevalence of osteoporosis in women is higher than men. This is due to women 50 years of ages, women going through menopause (Rao et al, 2008). Menopause is the permanent cessation of menstruation due to the ovaries fail to produce estrogen (Goodman et al, 2011). the decrease in production can increase bone resorption process thus increasing the occurrence of osteoporosis (O'connell et al, 2008). In a previous study, powder of leave's gedi red bulbs (*Abelmoschus manihot* (L.) Medik) have shown that the ability to prevent bone loss in rats that had their ovaries removed. Gedi 's leaf consumption can increase the BMC (Bone Mineral Content) on the femur as a whole in these mice, because it increases the BMC at the femur metaphysis and diaphysis (Puel et al, 2005).

Based on the above research, it is necessary to study to determine the activity of 96% ethanol extract of the leaves of red gedi (*Abelmoschus manihot* (L.) Medik) increasing trabecular bone density of the femur. In this study, the activity of the extract to be tested using animal research subjects mice female who has osteoporosis.

MATERIALS AND METHODS

PLANT MATERIAL

Leaves of red gedi (*Abelmoschus manihot* (L.) Medik) were used in this study was obtained from the area Buha village, Mapanget, Manado, North Sulawesi, the 90-day-old taken on January 20, 2014.

CHEMICALS

Dexamethasone, Ethanol 96% technical, Alendronate, CMC Nat, Dyes HE (Hematoxylin eosin)

TOOLS

Mice cages, maseras tool set, Rotary Evaporator Buchi R-200, Laminar air flow cabinet, Tool - glassware, animal scales, Sonde, Mortar and Stamper, Microscope Boeco, computer and software Nikon Image, Means treadmill for mice

ANIMAL TRIAL

Animals used in this study were adult female mice aged 70-80 days with a healthy body condition on visual observations, has a weight between 20-30 grams. In this study required 36 mices, all the mice with dexamethasone induced osteoporosis were divided into 6 groups with each group containing 6 mices.

RESEARCH DESIGN

1. Preparation of materials

Leaves were elected cleaned under running water until clean and then drained. After it leaves aerated in open to dry. After becoming simplicia dried, then ground to obtain a fine powder.



2. Extraction of materials

Gedi red's leaves powder 356 grams of macerated with ethanol using 96% as much as 9 L. Furthermore allowed to stand for 24 hours and stirring regularly. Then filtered with a Buchner funnel connected to a vacuum pump to obtain the filtrate. The filtrate obtained was concentrated using a rotary evaporator at 50 ° C until a viscous extract.

3. Test antiosteoporosis activity

Determination of the activity test antioateoporosis 96% ethanol extract of the leaves of red gedi (*Abelmoschus manihot* (L.) Medik) in increasing bone density performed using female mices study subjects. Mices were induced with dexamethasone for 4 weeks, then continued with the different treatment regarding to the division of the group. Effect of increased bone density in this study was determined by measuring the thickness of the trabecular bone of the femur in microscopy and by computer. The thickness of the trabecular bone is comparison of trabecular bone area to total area of prepat.

• positive control group

After induced osteoporosis, alendronate was given the suspension as much as 0.4 ml / 20 g mice / day orally for 4 weeks.

• The negative control

After induced osteoporosis, given the 0.5% Na CMC suspension as much as 0.4 ml / 20 g mice / day orally for 4 weeks.

• Group 1 test

After induced osteoporosis, given the suspension of 96% ethanol extract of leaves of red gedi (*Abelmoschus manihot* (L) .Medik) at a dose of 24.89 mg / 20 g of as much as 0.4 ml / 20 g mice / day orally for 4 weeks.

• Test Group 2

After induced osteoporosis, given the suspension of 96% ethanol extract of the leaves of red gedi (*Abelmoschus manihot* (L) .Medik) at a dose of 24.89 mg / 20 g of as much as 0.4 ml / 20 g mice / day orally along with physical exercise 3 times a week for 4 weeks.

Physical exercise in mice conducted in this

study is an exercise run by means of a treadmill. Physical exercise performed starting from a low initial velocity which is 10m / min with a duration of 5 minutes and then will be increased according to the ability of mice.

• Group 3 test

After the suspension-induced osteoporosis given 96% ethanol extract of the leaves gedi (*Abelmoschus manihot* (L.) Medik) at a dose of 49.78 mg / 20 g of as much as 0.4 ml / 20 g mouse / day orally for 4 weeks.

Group exercise

After physical exercise induced osteoporosis done for 4 weeks, the walking exercise using a treadmill means. Physical exercise is started from the speed of 10m / min with a duration of 5 minutes, kemudian increased gradually according to the ability of mice.

RESULTS

The occurrence of osteoporosis with a decrease in bone density as a result of dexamethasone induction is characterized by the formation of a bump on the vertebrae that is shown in Figure 1. After administration of dexamethasone daily for 4 weeks, all female mice visually osteoporosis.

96% leaf Red Gedi in increasing bone density obtained from the average value histomorfometri trabecular bone density of the femur. In the negative control group, ie, in a state of widespread osteoporosis bone trabekularnya lowest when compared with the group given ethanol extract after experiencing

The observation of the ethanol extract activity test

REFERENCES

1. Goodman, N. F., Cobin, R., & Ginzburg, S. B., 2011. American Association of Clinical Endocrinologists Medical Guidelines for Clinical Practices for The Diagnosis and Treatment of Menopause. AACE .
2. Jia, M.,Nie,Yan., Cao , Da-Peng.,Xue, Yun-Yun., Wang, Jie Si., Rahman ,Kha



- lid ., Zhang, Qiao Yan., Qin, Lu-Ping., 2012. Potential Antiosteoporotic Agents from Plants: A comprehensive review. Second Military Medical University,
3. Noor, Z., Sumitro, S. B., Hidayat, M., Rahim, A. H., & Taufiq, A., 2011. Assessment of Microarchitecture and Crystal Structure of Hydroxyapatite in Osteoporosis. *Univ Med* ,p. 29-35.
 4. O'connell, M. B., & Vondracek, S. F., 2008. Osteoporosis and Other Metabolic Bone Disease. In J. T. Dipiro, R. L. Talbert, & G. C. Yee, *Pharmacotherapy a Pathophysiologic Approach seventh ed.* (p. 1484). New York : The Mc Graw Hill Companies.
 5. Puel, C., Mathey, J., & Lebecque, P., 2005. Preventive Effect of *Abelmoschus manihot* L.Medik on Bone Loss in the Ovariectomised Rats . *Journal of Ethno-Pharmacology* , p.55-60.
 6. Rao, S. S., Singh, M., Parkar, M., & Sugumaran, R., 2008. Health Maintenance for Postmenopausal Women . *American Academy of Family Physicians* , p(593).

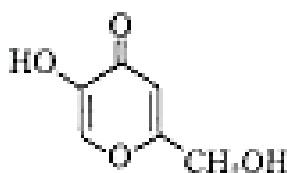
EFFECT OF β -Cyclodextrin ON SPF VALUE AND INHIBITION OF KOJIC ACID TYROSINASE ACTIVITY IN VANISHING CREAM BASE FORMULATION (ON SUNSCREEN PRODUCT CONTAINED OXYBENZONE)

Noorma Rosita, Pharmaceutics Department, Faculty of Pharmacy Airlangga University, itanr@yahoo.com or noorma-r@ff.unair.ac.id, +6281331031346; **Diana**, Pharmaceutics Department, Faculty of Pharmacy Airlangga University, **Diana Winarita**, Pharmaceutics Department, Faculty of Pharmacy Airlangga University, **Tristiana Erawati**, Pharmaceutics Department, Faculty of Pharmacy Airlangga University, **Widji Soeratri**, Pharmaceutics Department, Faculty of Pharmacy Airlangga University

INTRODUCTION

Newly, we found many cosmetics combined of sunscreen substance and lightening agent in their ingredients.

Kojic acid is a skin lightening agent which has very small molecular size, so easily absorbed up through the basal membrane. Because of its small molecule, kojic acid hardly absorbed through the lipid membrane of its target sites, the melanocytes (Manosroi et al, 2005) and can penetrate into the systemic (Nakayama et al., 2005). It is likely absorbed through voids between cells on the skin. Kojic acid is produced mainly by microbial fermentation using *aspergillus* and *penicillium* spp. In vivo test, cream containing kojic acid compounds have been reported as effective in preventing pigmentation changes in human skin due to exposure to UVA and UVB. This inhibition has been shown to be due to chelation of Cu, a prosthetic group in tyrosinase (Barel et al, 2001). Cream contained 1 % of kojic acid showed steady but slow whitening effect. ¹⁴C-labeled kojic acid cream was observed to be quickly absorbed from the skin to the liver, intestines, and kidneys in mice.



MW: 142.1
MP: 153-154°C
pKa: 7.90-8.
Log P (octanol-water): -0,64

Fig 1. Properties of Kojic Acid
5-hidroksi-2-hidroksimetil-4-pyron

When the absorption was thus quick, the depigmentation agent did not stay at the epidermis where it had its target organ, melanocytes, for a long enough time to inhibit melanogenesis. Therefore, kojic acid was mixed with β -cyclodextrin to slow the absorption into the dermis (Elsner and Maibach, 2005). Losses due to kojic acid to the systemic is not able to work effectively inhibits melanin formation took place in the basal membrane of skin that results are not optimal lightening effect. Addition of β -cyclodextrin reported can decrease penetration of kojic acid (Nakayama et al., 2005).

Cyclodextrins are cyclic oligosaccharides with a hydrophilic outer surface and a somewhat hydrophobic central cavity. Cyclodextrins are able to form inclusion complexes with many drugs by taking up the drug molecule, or a lipophilic moiety of the molecule, into the cavity (Loftsson and O'Fee, 2003).

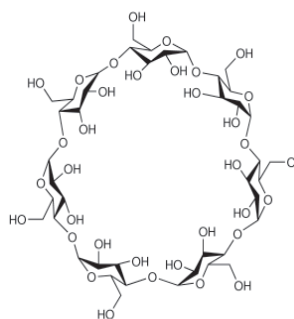


Fig 2. β -cyclodextrin (Sweetman, 2007)



Sunscreen agents, such as: oxybenzone and octyl dimethyl PABA, are commonly present in whitening products to compensate for the photosensitivity effect caused by the whitening agent. This combination is more efficient but may have a profound effect on the efficacy of the sunscreen agent.

Therefore, this study was aimed to investigate the SPF value of sunscreen product contained oxybenzone and octyl dimethyl PABA (3:7) with the addition of kojic acid 1% w/w as whitening agent and their complex with β -cyclodextrin in 1:1 molar equivalent. In this research, we also studied the effect of β -Cyclodextrin (BCD) on penetration of Kojic Acid, as lightening substance In Vanishing Cream Base Formulation (on Sunscreen Product Contained Oxybenzone), by determination of tyrosinase activity inhibition.

MATERIAL AND METHODE

Material

Oxybenzone, Octyldimethyl PABA and Kojic Acid were from Surya Dermato, β -cyclodextrin p.a (Sigma Aldrich), Stearic Acid, cetyl alcohol, span 80, tween 80), Methyl paraben Propyl paraben, sorbitol 70%, Isopropanol p.a., (Brataco Chemicals). All of the active ingredients used here were in a pharmaceutical grade except for the chemical reagent isopropanol and β - cyclodextrin which were in pro analytical grade. While material for inhibition of tyrosinase activity test is the Mushroom tyrosinase, L-Tyrosine, NaH₂PO₄. 2H₂O (p.a) and Na₂HPO₄ (p.a).

The SPF assay were carried out by using a Double Beam Spectrophotometer UV- Vis Perkin Elmer Lambda EZ 201, Ultrasonic Branson 3510, Hettich zentrifugen EBA 20, Mettler Toledo AL 204 analytical balance. Digital pH meter Schott CG 842 and spreading capacity measurer are also used for the organoleptic analysis.

Method

The sunscreen product contained oxybenzone and octyl dimethyl PABA (3:7) with the addition of kojic acid 1% w/w as whitening agent and their complex with β -cyclodextrin in 1:1 molar equivalent. Vanishing cream as base was made with inversion technique.

The characteristics of the finished product evaluated were emulsion type, pH, spreading-ability, and organoleptic such as colors, odors.

Table 1. Formula composition

Component	Percentage		
	F1	F2	F3
Kojic acid	1	1	1
β cyclodextrin	4	-	4
oxybenzone	-	3	3
Octyl dimethyl PABA	-	7	7
Vanishing cream base	Ad 100	Ad 100	Ad 100

Determination of SPF value

The SPF value was determined by Petro correlation for in vitro method. 2 mg/cm² or 2 μ L/ cm² sunscreen agent for in vivo test was equivalent with 10 ppm sunscreen agent dissolved in isopropanol. An UV spectrum of this solution was then measured at 290-400 nm by using Double Beam UV-Vis Spectrophotometer Perkin Elmer Lambda EZ 201 at an interval of 2 nm which has absorbance for 0.05 or more. According to Petro, the absorbance was then converted into the absorbance for 10 ppm solution concentration for each wavelength. Then it was proceed in this following equation:

$$AUC_{\lambda_{p-\alpha}}^{\lambda_p} = \frac{A_{p-\alpha} + A_p}{2} (\lambda_p - \lambda_{p-\alpha})$$

Whereas:

AUC = Area under curve

A_p = Absorption on p wavelength

A_{p- α} = Absorption on p- α wavelength



The total AUC were obtained by totaling each AUC between 2 wavelengths in series from 290 nm till 400 nm which has an absorbance value above 0.050 and the SPF value of a formula were obtained by inserting the total AUC into the equation below:

$$\text{Log SPF} = \frac{\text{Total area}}{\lambda_n - \lambda_1} \times 2$$

Whereas:

λ_n = longest wavelength above 290 nm that has an absorbance higher than 0.050

λ_1 = shortest wavelength 290 nm

Determination of tyrosinase activity inhibition:

A. Preparation of a solution of the reaction components. The solution should be prepared for the implementation of this study was 0.1 M phosphate buffer pH 6.5, solution of tyrosinase (5370 units / mg solid in 0.1 M phosphate buffer pH 6.5 to 100.0 ml volume), a solution of 5.52 mM L-tyrosine, and 30% TCA.

B. Preparation of test sample solution. The cream (around 3 grams) was put in the diffusion cell then covers with the Millipore membrane which was impregnated with isopropyl-myristate as modified lipid membrane. Then the preparation of cream in diffusion cell was put into the penetration chamber contain 500 ml of phosphate buffer pH 6.5 \pm 0.05 at 37 \pm 0.5°C as diffusion medium, and then the paddle was stirred 100 rpm. The sample solution around 3 ml was collected at 6 hours after it penetrated.

Determination of the dopakrom maximum wavelength. L-tyrosine solution of 5.52 mM has taken a number of prepared and then added 0.5 ml 3 ml of buffer solution pH 6.5 \pm 0.05. Then the mixture add with 1.0 ml of tyrosinase and oxygenated for 5 minutes. The mixture was incubated for 15 minutes at 26 \pm

0.5 °C then added 0.5 ml of 30% TCA. The solution is then inserted into cuvet and placed on the sample position in the spectrophotometer. Used as a blank solution 0.1 M phosphate buffer pH 6.5. Then do the reading of absorbance values from a wavelength of 400 nm to 500 nm, and the selected wavelength that gives the greatest absorption.

Inhibition Tyrosinase Activity Determination L-tyrosine solution 5.52 mM added with 0.5 ml 3 ml of sample solution. Then the mixture added with 1.0 ml of tyrosinase and oxygenated for 5 minutes. The mixture was incubated for 15 minutes at 26 \pm 0.5 °C. Then add 0.5 ml of TCA 30% and observed the absorbance at dopacrom maximum wavelength. Inhibition tyrosinase activity is the percent inhibition values obtained from the later absorbance value calculated by the equation:

$$A \times 100$$

$$\% \text{ Inhibition} = 100 -$$

B

A = Absorbance at the maximum with the skin lightening

B = Absorbance at maximum λ without the skin lightening

RESULT AND DISCUSSION

All the formulas had either pH in skins pH range or similar spreadability.

The SPF value increased in formula 3. The complex formation of the sunscreen agent with BCD was suspected to be responsible for this phenomenon. It might be caused by complex formation of the sunscreen agent with β - cyclodextrin increased sunscreen agent solubility.

Based on one way ANOVA test, known that the addition of BCD decreased inhibition percent compared to the control constraints. Nevertheless the addition of sunscreen does not affect the inhibition percent of tyrosinase activity. Addition of BCD on combination kojic acid-sunscreen preparations showed the



same phenomena such as decreased its inhibition percent of tyrosinase activity. Decreasing of inhibition percent of tyrosinase activity after addition of BCD or combination BCD-sunscreen was might be caused by decreasing of kojic acid penetration. It was probably caused by some of the things that the release process of kojic acid from base and in the process of penetration through the membrane. Before reach basal membrane where the kojic acid site of action, kojic acid molecule should released from base further more penetrate through the skin. Increasing viscosity will decrease the molecules mobility of active ingredient that caused barriers against the release of kojic acid.

Table 2. Average of pH

FORMULA	pH ± SD
1	4,51 ± 0,08
2	4,29 ± 0,03
3	4,04 ± 0,03

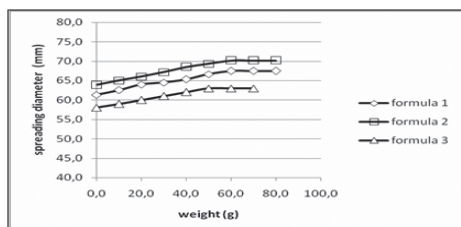


Figure 3. Profile of Spreading-ability

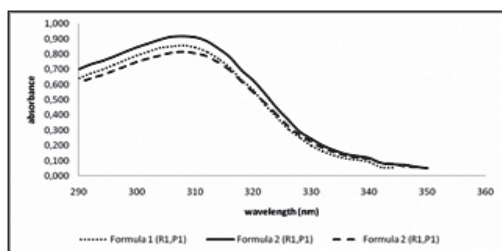


Figure 4. Profile of sunscreens absorbance measurement

Table 3. Average of SPF

Formula	SPF (average)
1	10,607 ± 0,432
2	11,741 ± 0,479
3	19,113 ± 0,295

Table 5. Average percent of tyrosinase inhibition

Formula	% tyrosinase activity inhibition
1	28,39 ± 0,51
2	60,50 ± 0,98
3	23,69 ± 0,61

CONCLUSION

1. The complex formation of the sunscreen agent with BCD decreased the SPF value of sunscreen product.
2. BCD decrease penetration kojic acid based on inhibition of tyrosinase enzyme activity in invitro.
3. The existence of BCD and combination sunscreen oxybenzone and octyl dimethyl PABA (3:7)% w/w decrease penetration kojic acid based on inhibition of tyrosinase enzyme activity in invitro.

REFERENCE

- Barel, A.O., Paye, M., Maibach, H.I., 2001. Handbook of Cosmetic Science and Technology. New York: Marcel Dekker Inc.
- Elsner, P., Maibach, H.I., 2005. Cosmeceuticals and Active Cosmetics: Drug Versus Cosmetics, 2nded, Boca Raton: Taylor and Francis Group.
- Loftsson, T., O'Fee, R., 2003. Cyclodextrins in Solid Dosage Forms. Business Briefing Pharmatech.
- Manosroi., Wongtrakul., Midorikawa., Hanyu., Yuasa., Sugawara., Sakai., Abe, 2005. The Entrapment of kojic oleate in bilayer vesicles, International Journal of Pharmaceutics.
- Nakayama, H., Ebihara, T., Satoh, N., dan Jinnai, T., 2000. Depigmentation Agents. In: Elsner, P., dan Maibach, H.I. (eds.). Cosmeceuticals and Active Cosmetics: Drug vs Cosmetics, Boca Raton: Taylor & Francis, p. 185-204.
- Petro, A.J., 1981. Correlation of Spectrophotometric Data with Sunscreen Protection Factors. International Journal of Cosmetic Science, Vol. 3, p. 185-196.



ANTIMICROBIAL ACTIVITY OF LACTOBACILLI PROBIOTIC MILK AND GUAVA LEAF ETHANOLIC EXTRACT (*Psidium guajava*) COMBINATION AGAINST BACTERIAL CAUSE OF DIARRHEA

Nur Putri Ranti, Department of Pharmaceutical Chemistry, Airlangga University, nurputriranti@gmail.com; Isnaeni, Department of Pharmaceutical Chemistry, Airlangga University, isnaeni_yudi13@yahoo.com; Juniar Moechtar, Department of Pharmaceutical Chemistry, Airlangga University; Febri Annuryanti, Department of Pharmaceutical Chemistry, Airlangga University.

INTRODUCTION

Probiotics is live microorganisms which, when administered in adequate amounts, confer a health benefit on the host. Probiotics are live microbes that can be formulated into many different types of products, including foods, drugs, and dietary supplements. Species of *Lactobacillus* and *Bifidobacterium* are most commonly used as probiotics. The treatment of diarrhea can be done by using probiotics. The use of probiotics has been developed and is essential for maintaining the balance of microflora in the digestive tract (WGO, 2008).

In addition to the use of probiotics, diarrhea treatment can be done with the use of medicinal plants. Based on research, the medicinal plants is *Psidium guajava* L. leaves. *Psidium guajava* L. leaves contain tannins, essential oils, flavonoids, carotenoids, sirtaresin, also avicularin and guajaverin. Quercetin is thought to contribute to the anti diarrhea effect of guava, it is able to relax intestinal smooth muscle and inhibit bowel contractions. (Joseph et.al, 2010).

Antibacterial effect of combination of *Lactobacilli* probiotic milk and guava leaf ethanolic extract is not yet investigated. The purpose of this study is to determine the antimicrobial activity of combination of *Lactobacilli* probiotic milk and guava leaf ethanolic extract. *Lactobacillus acidophilus*, *Lactobacillus casei*, and *Lactobacillus plantarum* were used for making probiotic milk, while *Escherichia coli*, *Salmonella typhimurium*, and *Vibrio cholerae* were used as pathogenic microbes. Based on the content of compounds in guava leaf ethanolic

extract and probiotic microbes from milk, it is expected that the antibacterial power combination probiotic milk and guava leaf extract in ethanol increases, so will obtain a better antibacterial activity than antibacterial potency of each component.

MATERIALS AND METHODS

Samples used : simplicia guava leaves, skim milk, microbial growth media: media Nutrient Agar (NA), MRS (de Man ROGOSA and Sharpe) broth and MRS agar, isolates of lactic acid bacteria (*Lactobacillus acidophilus*, *Lactobacillus casei*, *Lactobacillus plantarum*) and bacterial isolates pathogens (*Escherichia coli*, *Salmonella typhimurium*, *Vibrio cholerae*).

Source of samples : Isolates of lactic acid bacteria and pathogenic bacteria derived from pure isolates were obtained from the Institute of Tropical Disease, Airlangga University, Surabaya. SImplicia guava leaves originating from Materia Medika.

Preparation Media : Nutrient agar as much as 18.0 grams dissolved in 1 liter of distilled water and stirred until homogeneous. The solution is heated by heating slowly to the boil for a minute or two. That has a homogenous solution was poured into a container and sterilized at 121 ° C for 15 minutes. MRS broth as much as 52.0 grams dissolved in 1 liter of distilled water and stirred until homogeneous and MRS agar as much as 56.0 grams of medium MRS agar dissolved in 1 liter of distilled water and stirred until homogeneous.

Preparation of Guava Leaf Extract : Prepara



tion of extracts made by maceration, extraction bulbs using 40 grams of simplicia guava leaves in 400 ml of 70% ethanol at room temperature for 24 hours. Results maceration filtered and concentrated by rotary vacuum evaporator at a temperature less than 50°C to evaporate the solvent depleted. Furthermore, extracts prepared in a concentration of 20% by weighing 20 grams of the extract, dissolved in 100 ml of distilled water.

Probiotic Milk Preparation : 200 ml of skim milk 15% (w / v) heated by means of reconstituting skim milk 15 grams in 100 ml of distilled water at a temperature of 80-85° C for 15 min, cooled to a temperature of 45 ° C and then added 20ml starter probiotics, were incubated at 37 ° C for 24 hours.

Test Antibacterial Activity Guava Leaf Ethanol Extract and Probiotic Milk : Ethanol extract of guava leaves 20% in water mixed with a probiotic milk in the ratio 1: 9, 2: 8, 3: 7, 4: 6, 5: 5, 6: 4, 7: 3, 8: 2, and 9: 1. Test antibacterial power of probiotic milk and guava leaf extract performed using Nutrient Agar media was planted pathogenic bacteria test is then perforated, the available hole shed 100 mL probiotic milk has been added guava leaf extract with various comparisons. Samples were incubated for 24 hours at 37°C, then observed and measured the resulting inhibition zone diameter in millimeters. Tests performed on the activity of pathogenic bacteria to replicate as much as three times.

RESULTS AND DISCUSSION

Activity against pathogenic bacteria in milk containing the probiotic *Lactobacillus* occurs through multiple mechanisms function, is protective function by its ability to inhibit pathogens in the gastrointestinal tract. The formation of the colonization of probiotics in the digestive tract. The growth of probiotics will also produce a variety of anti-bacterial components (organic acids, hydrogen peroxide, and bacteriocins were able to suppress the growth

of pathogens); the function of the immune system, with an increase in the body's immune system (Collado et al, 2009). While the guava leaf extract, there are four antibacterial compounds discovered from the results of the isolation and effective against pathogens that two flavonoid glycosides, morin-3-O- α -L-lyxopyranoside and morin-3-O- α -L-arabopyranoside, and two flavonoids, quercetin and guaijavarin (Arima and Danno, 2002).

The use of a combination of *Lactobacillus acidophilus*, *Lactobacillus casei* and *Lactobacillus plantarum* based on that each type of probiotic bacteria bacteriocins have different kinds of compounds. In *Lactobacillus acidophilus* known to produce bacteriocins named lactacin B and acidocin A (Barefoot and Kleinhamer, 1984; Kanatani et al., 1995), *Lactobacillus casei* produce bacteriocins bernamacaseicin (Olasupo et al., 1995), whereas bacteriocins plantaricin is produced by *Lactobacillus plantarum* (Son et al., 2009). The presence of bacteriocins produced more than one type of bacteria that can help protect the producer from the effects of antimicrobial compounds produced guava leaf extract and inhibition of pathogenic bacteria stronger.

Antibacterial activity test was carried out by combining the ethanol extract of guava leaf in water and 20% probiotic milk with varying ratios (1: 9.2: 8, 3: 7, 4: 6, 5: 5, 6: 4, 7: 3, 8: 2, 9: 1). Tests performed on the activity of pathogenic bacteria with the replication of three times. Activity test was also performed on a single probiotic milk, a single guava leaf ethanol extract, positive control and a negative control. Positive control used was antibiotic Ciprofloxacin and negative control used was milk skim. From the results of the antibacterial activity of a combination of *Lactobacilli* probiotic milk and guava leaf ethanol extracts against diarrhea-causing bacteria, inhibition zone diameter data obtained. Combination dosage that produces the greatest inhibition of bacterial third test is the ratio of 9: 1 as shown in Table 1, and in combination with a



ratio of 9: 1 was chosen as a component in the formulation of probiotic preparations. Inhibition zone on a combination of probiotic milk plus ethanol guava leaf extract at a concentration of 20% has inhibitory effect on bacterial pathogens test. In combination preparations, the ratio of 9: 1 has the largest clear zone between the ratio of the combination of the other preparations. In the test preparation combined inhibition against *Escherichia coli*, *Salmonella typhimurium*, and *Vibrio cholerae* inhibition zone values obtained by an average of 14.10 mm, 15.50 mm and 15.17 mm.

Extract:Probiotic	Diameter of Inhibition Zone (mm) Against Bacteria		
	<i>E.coli</i>	<i>S.typhi</i>	<i>V.cholerae</i>
1 : 9	11,50 ± 0,43	10,63 ± 0,21	13,30 ± 0,70
2 : 8	11,38 ± 0,77	11,30 ± 0,36	13,56 ± 0,90
3 : 7	11,70 ± 0,17	11,27 ± 0,47	12,23 ± 0,55
4 : 6	12,22 ± 0,47	10,70 ± 0,43	12,23 ± 0,42
5 : 5	12,40 ± 0,43	13,03 ± 1,10	11,60 ± 0,10
6 : 4	12,00 ± 0,53	13,43 ± 0,50	12,57 ± 0,35
7 : 3	13,13 ± 0,74	14,50 ± 0,61	13,80 ± 0,50
8 : 2	13,23 ± 0,47	15,17 ± 0,87	14,67 ± 0,28
9 : 1	14,10 ± 0,58	15,50 ± 0,56	15,17 ± 0,38
Probiotic Milk	11,90 ± 0,26	11,50 ± 0,17	12,10 ± 0,70
Guava Leaf Ethanol Extract	15,36 ± 0,93	17,67 ± 0,72	15,83 ± 0,60
Positive Control (Ciprofloxacin)	16,60 ± 0,00	18,20 ± 0,00	18,10 ± 0,00
Negative Control	-	-	-

Table 8. Diameter of Inhibition Zone of Guava Leaf Ethanol Extract and Probiotic Milk bacteria test against *Escherichia coli*, *Salmonella typhimurium*, *Vibrio cholerae*

CONCLUSION

The antibacterial activity combination of *Lactobacilli* probiotic milk and guava leaf ethanol extract against *Escherichia coli*, *Salmonella typhimurium* and *Vibrio cholerae* has the largest inhibition zone ratio of 9: 1. Average inhibitory combination preparations *Lactobacilli* probiotic milk and guava leaf ethanol extract against

Escherichia coli, *Salmonella typhimurium* and *Vibrio cholerae* are 14.10 mm, 15.50 mm and 15.17 mm.

REFERENCES

1. Arima, H.; Danno, G. 2002. Isolation of antimicrobial compounds from guava (*Psidium guajava* L.) and their structural elucidation. *Bioscience, Biotechnology and Biochemistry*. Vol. 66 (8), pp.1727-1730.
2. Collado, M.C., Isolauri, E. Salmien, S. and Sanz, Y. 2009. The impact of probiotic on gut health. *Curr Drug Metab*. Vol. 10, no.1, pp. 68-78.
3. Joseph, B. 2011. Review on nutritional, medicinal and pharmacological properties of guava (*Psidium Guajava* Linn.). *International Journal of Pharma and Bio Sciences*. Vol.2, Issue 1, pp. 53-69.
4. World Gastroenterology Organization. 2008. Probiotics and Prebiotics. *World Gastroenterology Organization*.
5. Son VM., Chang CC., Wu MC., Guu YK., Chiu CH., Cheng W. 2009. Dietary administration of the probiotic, *Lactobacillus plantarum*, enhanced the growth, innate immune responses, and disease resistance of the grouper *Epinephelus coioides*. *Fish Shellfish Immunol*. Vol. 26, no. 5, pp. 691-698



THE INFLUENCES OF PARTICLE SIZE AND SHAPE ON ZETA POTENTIAL OF COENZYME Q10 NANOSUSPENSION

Nuttakorn Baisaeng, University of Phayao, School of Pharmaceutical Sciences,
19 M. 2 Maeka, Muang, Phayao 56000 Thailand, patchateeya@yahoo.com

INTRODUCTION

Coenzyme Q10 (CoQ10) nanosuspension, which is colloidal dispersion of nanosized CoQ10 particle stabilized by surfactants, was produced to enhance its solubility by cold high-pressure homogenization technique in this study. A decrease in size of CoQ10 is not only enhancing its solubility, but also its stability [1]. Zeta potential or surface charge, which directly measures the electrophoretic mobility of dispersed particles, can predict a long term stability of nanosuspension. According to Henry's equation, zeta potential increases with increasing the electrophoretic mobility that is a proportion of the drift velocity of dispersed particles and the applied electric field strength [2]. Therefore, the particle size and shape of dispersed particles attribute to get the drift velocity resulting in the differences of the obtained zeta potential. To prove the above equation, this present investigation aimed at studying the influence of particle size and shape on zeta potential of CoQ10 nanosuspension.

MATERIALS AND METHODS

Materials

CoQ10 was obtained from Cognis (Germany). Polyoxyethylene (20) sorbitan monooleate (Tween[®] 80) was purchased from Uniqema Ltd. (Belgium). Milli-Q water was produced by a Milli-Q Plus system, Millipore (Germany).

Methods

Production of CoQ10 nanosuspension

5% CoQ10 was dissolved in 1% Tween[®] 80 solution at an ambient temperature. A pre-homogenization was homogenized 2 cycles at each pressure of 200, 500 and 1000 bar by using a Micron Lab 40 high pressure homogenizer (APV Gaulin GmbH, Germany). Then it was

homogenized by applying a pressure of 1500 bar for up to 20 cycles at 4°C.

Characterization of CoQ10 nanosuspension

The particle size, polydispersity index and zeta potential of CoQ10 nanosuspension were characterized by using a Malvern Zetasizer ZS (Malvern Instruments, UK). In order to detect the larger particles, Laser diffraction (LD) were performed with a measuring range of particle up to 2000 μm by static light scattering (SLS) by using a Mastersizer 2000 (Malvern Instrument, UK) [3]. In addition, the morphology of CoQ10 nanosuspension was analyzed by using light microscope (Leitz, Wetzlar, Germany) equipped with a CMEX-1 digital camera (Euromex microscopes, Arnhem, Netherlands) connected to Image Focus software version 1.3.1.4. (Euromex microscope, Arnhem, Netherlands). The magnification of the analyzed material was possible with the equipment by 100x10-fold.

RESULTS AND DISCUSSION

A decrease in particle size of CoQ10 nanosuspension from 914 to 258 nm with a uniform particle size distribution ($\text{PI} < 0.4$) was achieved by cold high-pressure homogenization at 1500 bar and 20 cycles, and a significant difference between an electrostatic potential surface or zeta potential of pre-homogenization and CoQ10 nanosuspension is shown in Table 1. More negative charge of CoQ10 nanosuspension was found with increasing the number of homogenization cycle for up to 20 cycles. This assumed that decreasing particle size leads to increasing the drift velocity resulted in more negative zeta potential. Owing to a zeta potential more negative than 30 mV, CoQ10 nanosuspension will have a good physical stability for long-term storage.

Samples	Size (nm)	Polydispersity Index (PI)	Zeta potential (mV)
Pre-homogenization	914 ± 106	0.61 ± 0.15	-45.5 ± 0.9
1500 bar x 1 cycle	766 ± 71	0.64 ± 0.06	-45.6 ± 0.7
1500 bar x 5 cycles	670 ± 55	0.40 ± 0.10	-47.9 ± 1.2
1500 bar x 10 cycles	369 ± 31	0.32 ± 0.12	-50.6 ± 2.8
1500 bar x 15 cycles	288 ± 19	0.30 ± 0.08	-52.8 ± 1.3
1500 bar x 20 cycles	258 ± 8	0.34 ± 0.07	-54.1 ± 2.9

Table 9. Size, polydispersity index and zeta potential of CoQ10 nanosuspension by a Malvern Zetasizer ZS.

the limitation of particle size measurement from Zetasizer ZS (0.6 nm – 6.0 μm); the larger particles than 6 μm were detected in CoQ10 nanosuspension by laser diffraction as shown in Figure 1. These particles might effect to a size distribution of CoQ10 nanosuspension.

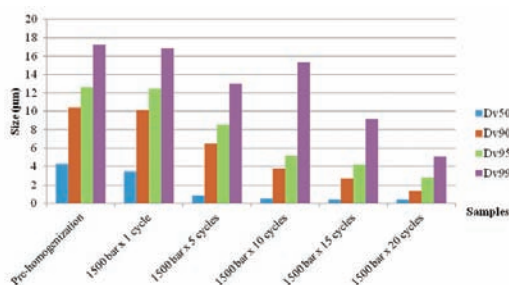


Figure 1. Size distribution of CoQ10 nanosuspension by laser diffraction.

In addition, light microscopy was used to get more valuable information about the particle size and shape of CoQ10 nanosuspension. Figure 2 shows a big morphological difference between a pre-homogenization of CoQ10 and CoQ10 nanosuspension at 1500 homogenization bar and 20 cycles. The big crystals with non-spherical and some small spherical CoQ10 particles are shown in a pre-homogenization image on the left, and the mixture of smaller non-spherical and spherical particles

are pronounced in CoQ10 nanosuspension image on the right. These results can be explained how the differences of zeta potential of CoQ10 nanosuspension were obtained. According to Henry's equation, more negative zeta potential causes by increasing electrophoretic mobility and the smaller particles with more spherical shape of dispersed particles attribute to a higher electrophoretic mobility. Therefore, more negative zeta potential of CoQ10 nanosuspension was obtained by decreasing particle size with more spherical shape of CoQ10.

CONCLUSION

CoQ10 nanosuspension was successfully produced by cold high-pressure homogenization technique. It was proven that more negative zeta potential was obtained with increasing the number of homogenization cycles, and the smaller particles with more uniform spherical shape influenced on zeta potential of CoQ10 nanosuspension according to Henry's equation.

ACKNOWLEDGEMENTS

This research was supported by University of Phayao, Phayao, Thailand. The author wishes to gratefully thank Prof. Dr. Müller from Free University of Berlin, Berlin Germany and Prof. Dr. Keck from University of Applied Sciences Kaiserslautern, Pirmasens, Germany for supporting laboratory equipment and a useful advice.



REFERENCES

- *. Müller RH, Jacobs C, Kayser O. (2000). Nanosuspensions for the Formulation of Poorly Soluble Drugs, in: Pharmaceutical Emulsions and Suspensions (Nielloud, F. and Marti-Mestres, G., eds.), Marcel Dekker, 383-407.
- *. Hunter RJ. (1988). Zeta Potential in Colloid Science: Principles and Applications; Academic Press: London, U.K.
- *. Mauludin R, Keck CM. (2008). Production of lyophilised coenzyme Q10 nanocrystals. 10th European Workshop on Particulate Systems, 30-31 May, Berlin/German.

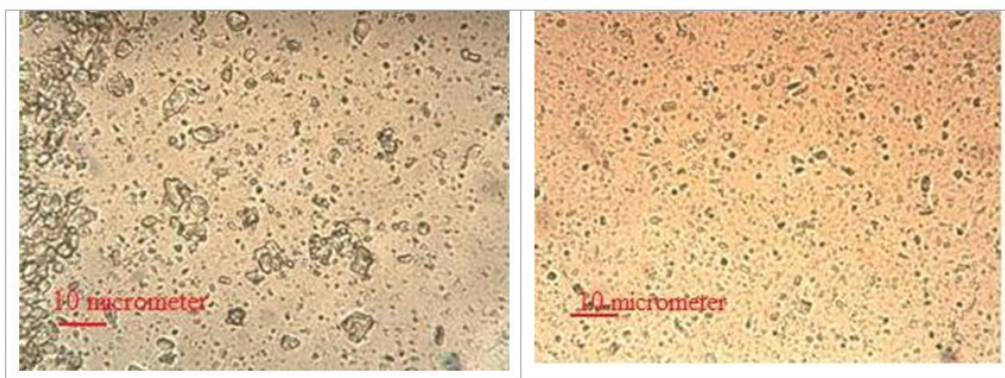


Figure 2. CoQ₁₀ nanosuspension: Pre-homogenization (left) and CoQ₁₀ nanosuspension at 1500 bar 20 cycles (right).

SYNTHESIS, MOLECULAR DOCKING, AND ANTITUMOR ACTIVITY OF N,N'-Dibenzoyl-N,N'-Dimethylurea AGAINST HUMAN BREAST CANCER CELL LINE (MCF-7)

Nuzul Wahyuning Diyah

Department of Pharmaceutical Chemistry-Faculty of Pharmacy Airlangga University
Jl. Dharmawangsa Dalam Surabaya 60286, e-mail: nuzul_wd@yahoo.com

INTRODUCTION

Some urea derivatives have been used as anti-cancer drug, such as hydroxyurea (HU) which act by inhibiting the enzyme ribonucleotide reductase/RR (1). Benzoylureas (BU) has been reported as potential antitumor agents (2). The research has been continued to improve their antitumor activity by attaching two aromatic ring and methyl groups on both N atom of urea. The objectives were to synthesize N,N'-dibenzoyl-N,N'-dimethylurea (DBDM), investigate its antitumor activity against human breast cancer lines, and explore in silico molecular interaction between tested compound and target molecule, RR (pdb id. 3HNC) (3).

MATERIALS AND METHODS

Materials

All reagents were purchased from standard commercial suppliers. The N,N'-dibenzoyl-N,N'-dimethyl urea (DBDM) was synthesized by reacting benzoyl chloride with N,N'-dimethylurea using tetrahydrofuran (THF) as solvent in the presence of pyridine (Figure 1).

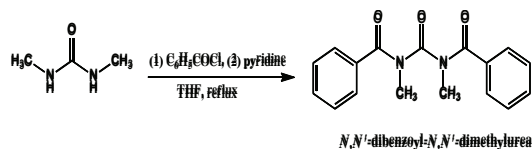


Figure 1. Scheme of synthesis reaction of compound DBDM

Melting point was measured by a Fischer-Johns melting point apparatus without correction. TLC was carried out on aluminium plates coated with silica gel using UV lamp 254 nm to spot detection. The molecular structure of compound was confirmed by IR, ¹H-NMR, ¹³C-

NMR, and Mass spectroscopy. IR spectrum was recorded on Jasco FT-IR 5300, ¹H-NMR and ¹³C-NMR spectra were taken at JEOL ECS-400 spectrometer using internal standard Me₄Si. Mass spectrum was measured by Agilent 6890N spectrometer using EI methods.

Synthesis procedure

To N,N'-dimethylurea in THF and a few drops of pyridine, an equimolar of benzoyl chloride was added at ice bath while stirring. Then the temperature was raised and the mixture was refluxed for 24 hours at room temperature. The THF was evaporated and the solid was washed with water and saturated sodium bicarbonate respectively. The resulting solid was recrystallised from hot ethanol-water (1:1).

Antitumor Activity

In vitro antitumor activity was tested against MCF-7 cancer cell lines and expressed in IC₅₀ (4). Cancer cell lines at a density of 5x10³ cells/well in 96-well plates were exposed to the test compounds in DMSO. After 48 hours incubated in a 5% CO₂ incubator at 37°C, cell survival was determined using the MTT reagent where the absorbances were observed at 595 nm on ELISA-reader. The survival ratio of living cells were expressed in percentages with respect to untreated cells. Hydroxyurea (HU) was used as the reference drug. The IC₅₀ value of tested compounds were shown in Table 1.

Molecular Docking

The structure of human RR (pdb. 3HNC, at 2.50 resolution) was obtained from the Pro



tein Data Bank (www.pdb.org). 3D structure of compounds were built using CS ChemBioDraw Ultra 11.0 (Cambridge Soft) and their geometry were optimized by the MMFF94 method and then saved as Sybyl Mol2 format. Molegro Virtual Docker ver 5.0 (CLC Bio) was the docking program used. The tested compounds were placed into binding site of 3HNC (cavity-3) by aligning to the reference ligand, TTP (5). The binding affinity between ligand and enzyme was evaluated using MolDock Score, which is the total of ligand-protein interaction energies including hydrogen bonds. The highest-scoring pose (lowest energy) represent the best-found binding mode of ligand-protein. The docking procedure was validated by redocking TTP into cavity-3. Docking score of test compounds were listed in Table 1.

RESULTS AND DISCUSSION

Synthesis product

N,N'-dibenzoyl-*N,N'*-dimethylurea (DBDM) can be synthesized from *N,N'*-dimethylurea in one step. The compounds is white solid and water insoluble substances. The structure of the synthesized compounds were confirmed by IR, ¹H-NMR, ¹³C-NMR, and MS spectroscopy as follows:

N,N'-carbonylbis(*N*-methylbenzamide)=*N,N'*-dibenzoyl-*N,N'*-dimethylurea: Yield 50% as white crystal, m.p. 143 OC. UV (ethanol, λ_{max}, nm): 234.0. ¹H-NMR (CDCl₃, 400 MHz, δ ppm): 7.5 (=CH benzene, 2H, m); 7.4 (=CH benzene, 8H, m); 3.0 ppm (CH₃, 6H, m). ¹³C-NMR (CDCl₃, 400 MHz, δ ppm): 171.18 (Ar-(C=O)-N); 158.94 (N-(C=O)-N); 135.21 (ar =C-C=); 132.26 (ar =C-C=); 128.21 (ar =C-C=); 127.81 (ar =C-C=); 34.3 (CH₃). IR (KBr, λ_{max}, cm⁻¹): 3059 (Csp²-H), 2977 (Csp³-H), 1713, 1676 (-C=O amide), 1600 (C=C). MS m/z EI : 296(M⁺).

The *N,N'*-dibenzoyl-*N,N'*-dimethylureas were produced from acylation of *N,N'*-dimethylurea by benzoyl chloride. The structural change of *N,N'*-dimethylurea to *N,N'*-dibenzoyl-*N,N'*-dimethylureas was characterized by the con-

version of -NH- moiety of dimethylurea to -N=C=O(Ar). As there are two symmetric -NH-, the new compounds bear two symmetric benzoyl moieties, each attached on their N atom. It could be observed in ¹H-NMR spectrum which didn't showed proton peak at -NH region, supported by IR spectrum without N-H bands.

Compound	IC ₅₀ (μg/mL)	MolDock Score
DBDM	170.4	-101.296
BU	266.1	-71.071
HU	411.2	-33.746

Table 1. IC₅₀ of tested compounds against MCF-7 cell lines and their docking score to RR binding site

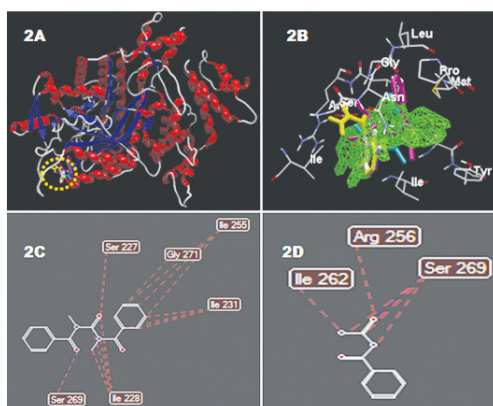


Figure 2. 3D-view of three molecules (yellow dashed-line) in secondary structure of ribonucleotida reductase (2A), in its binding site (2B). 2D-view show H-bond (blue dashed-line) and hydrophobic interaction (red dashed-line) of DBDM (2C) and BU (2D) with amino acid residue Serin 269. There was no H-bond interaction for HU.

In table 1 the new compound, DBDM, shows IC₅₀ lower than BU and anticancer drug, HU, indicating that DBDM is more active than BU and HU. Its highest docking score among BU and HU which indicating high ligand-protein binding affinity support its higher antitumor activity. Molecular interaction between tested

compounds with amino acids in the RR binding site are displayed in Figure 2 and Figure 3.

From Figure 2 and 3 it could be explained that the aromatic ring and methyl groups on both N atom urea contributed to stronger binding of DBDM to the protein enzyme as DBDM could formed two H-bonds whereas BU only formed one H-bond.

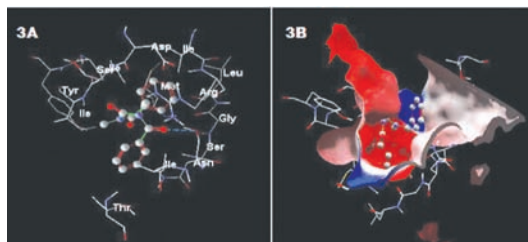


Figure 3.3D-view show H-bond interaction (blue dashed-line) of DBDM with Serin 269 (3A) and molecule in electrostatic surrounding of cavity-3, 3HNC binding site (3B).

CONCLUSION

This study concluded that N,N'-dibenzoyl-N,N'-dimethyl urea which has been synthesized from reaction of N,N'-dimethylurea and benzoyl chloride showed antitumor activity against human breast cancer cell line (MCF-7) three-fold higher than hydroxyurea. The antitumor activity was enhanced by methyl and aromatic rings attached to both N atom which could strengthen the binding affinity of compound to target molecule, 3HNC.

Acknowledgement

The research was supported by Airlangga University Research Grant BOPTN 2013. The molecular docking was supported by licenced MVD ver 5.0 with permission from Prof. Dr. Siswandono, MS., Apt.

References

- (1) Saban, N. Bujak, M. 2009. Hydroxyurea and Hydroxamic Acid Derivatives as Antitumor Drugs. *Cancer Chemother Pharmacol.* 64: 213 – 221
- (2) Diyah, N.W., Siswandono, Hardjono, S., Purwanto, B.T. 2013. Molecular Modeling And QSAR Of Ring-Substituted Benzoylurea Derivatives as Antitumor, *Pharmaceutical Chemistry Bulletin Vol 2, No 2:* 20-27.
- (3) Fairman, J.W., S.R. Wijerathna, M.F. Ahmad, H. Xu, R. Nakano, S. Jha, J. Prendergast, R.M. Welin, S. Flodin, A. Roos, P. Nordlund, Z. Li, T. Walz, C.G. Dealwis, 2011. Structural Basis for Allosteric Regulation of Human Ribonucleotide Reductase by Nucleotide-induced Oligomerization. *Nat. Struct. Mol. Biol.* 18: 316-322
- (4) Jin, C., Liang, Y-J., He, H., Fu, L., 2011. Synthesis and antitumor activity of ureas containing pyrimidinyl group. *European Journal of Medicinal Chemistry* 46: 429-432



EXPRESSION OF ANTI-EGFRVIII SINGLE CHAIN FRAGMENT ANTIBODY (scFv) ON THE SURFACE OF *Pichia pastoris*

Pratika Viogenta, Department of Biotechnology Post Graduate School-Bogor Agricultural University, Gd. PAU, Jalan Kamper IPB Dramaga Bogor, West Java 16680, pratikaviogenta@gmail.com, 085658848800; **Asrul Muhamad Fuad**, Reasearch Center for Biotechnology, Indonesian Institute of Sciences, Cibinong Science Center, Jalan Raya Bogor Km 46, Cibinong, 16911, Indonesia, asrul.m.fuad@gmail.com, 081295813111; **Suharsono**, Department of Biotechnology Post Graduate School-Bogor Agricultural University, Gd. PAU, Jalan Kamper IPB Dramaga Bogor, West Java 16680, sony.suharsono@yahoo.com, 08128812239

INTRODUCTION

Epidermal growth factor receptor variant III (EGFRvIII) is the most common variant of the EGF- receptor (EGFR). This mutant variant of EGFR is expressed in some cancer such as glioblastoma multiforme (GBM) (50-60%) [5], breast cancer (67,8%) [6], non-small cell lung cancer (30-76,39%) [11], and head and neck squamous cell carcinoma (42%) [13]. However, this mutant is not observed in normal tissue. Expression of EGFRvIII in cells leads to unregulated growth and cells proliferation. This variant receptor was formed due to in-frame deletion of exons -2 through exon-7 of the native EGFR. This causes a deletion of a large portion of the extracellular domain and the generation of a novel glycine at the fusion junction between exon-1 and exon-8. EGFRvIII becomes a spesific target for cancer therapy because of the juxtaposition of exon-1 and -8 plus the novel glycine that creates a highly immunogenic tumor specific antigen at its N-terminal domain [4].

Single chain variable fragment (scFv) antibody is an engineered antibody fragment that contains a complete antigen-binding site of an antibody. This antibody fragment should have the same monomeric binding affinity as the parental monoclonal antibody [14]. Yeast surface display system is engineering techniques that express any heterologous protein on the surfaces of yeast's cell wall [9]. This system becomes an increasingly popular tool for protein engineering and offers many applications, such as application for selection and screening of antibody library [12]. Most of proteins

that have been engineered by yeast display are monomeric proteins or single chain oligomers [2, 8].

In the present study, cell surface expression of a fusion protein of an anti-EGFRvIII scFv and TagRFP in *Pichia pastoris* was attempted using glycosylphosphatidylinositol (GPI)-anchored α agglutinin protein (AG α), derived from *Saccharomyces cerevisiae*. This α - agglutinin functions as a covalently anchoring system of the displayed molecules to the cell wall by fusing it to a cell wall bound protein [1]. The methy-totropic yeast *P. pastoris* has advantages as a recombinant protein expression system, such as high-level

Expression and post-translation modifications processing. Unlike *S. cerevisiae*, hyper-glycosylation was not observed in *P. pastoris* during post-translation likes modification [10]. The aim of this research is to express and display an anti-EGFRvIII scFv using α -agglutinin as the ligand and TagRFP as a reporter protein on cell surface of *P. pastoris*.

MATERIAL AND METHODS

Strain and Media

Escherichia coli TOP10F' was used as the host for transformation of recombinant plasmids. Cells were cultivated at 37°C in Low Salt Luria-Bertani (LSLB) medium with 25 μ g/mL zeocin when necessary. *P. pastoris* SMD1168H was used as the host for protein expression. *P. pastoris* was grown in yeast peptone dextrose (YPD) medium or buffered minimal glycerol yeast (BMGY) medium. Heterologous protein expression was induced in buffered minimal

methanol yeast (BMMY) medium that had the same BMGY formulation except that 0.5% (v/v) methanol was substituted with glycerol.

Construction of Plasmids and Transformation
The anti EGFRvIII-scFv coding region (scFv) was amplified from the pJ201-scFv plasmid (DNA 2.0) by PCR method. Primers used were as follows: VH101-Sall forward (5'-CGTC-GACCAAGTTCAATTGGTTGAGTCA G-3') and VL101-Sall reverse (5'-CGGTCGACTCT AGAATC-GATAGAACCAC-3'). Two Sall sites were added at two terminals of scFv fragment during

amplification. The amplified product was digested by Sall and inserted into the cassette vector pJ912-AG α at the Sall site. The scFv gene in the recombinant vector was analyzed by colony-PCR using primers: VH101-Sall forward and VL101-Sall reverse. Gene orientation was analysis using primers: AOX1 forward (5'-GACTGGTTCCAATTGAC AAGC-3') and VH101 reverse (5'-AGACGACACTGTTCACAGCGT-3'). The vector was also and analyzed by restriction digest using Sall. The final construct of recombinant scFv plasmids was named as pJ912-AG α -scFv.

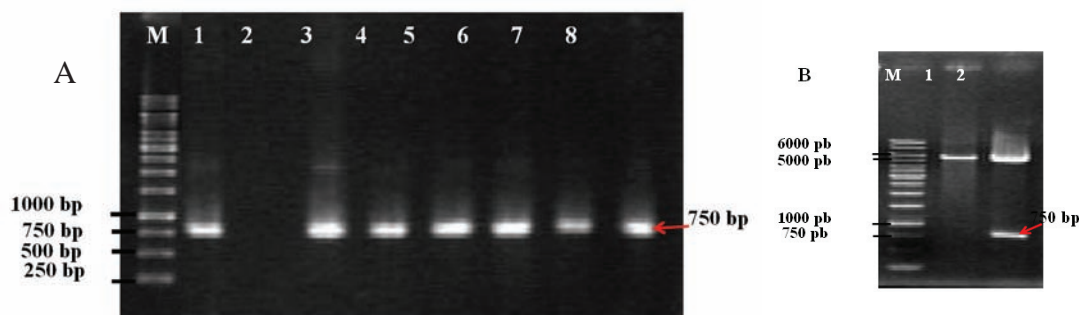


Figure 1. A. PCR colony analysis of *E. coli* TOP10F' transformant. Positive clone of *E. coli* transformant for scFv genes were indicated by a 750 bp DNA band. Lane M = 1 kb DNA marker. Lane 1: positive control (pJ201-scFv). Lane 2: negative control (pJ912-Ag α). Lane 3-8: positive clone containing scFv gene. B. Restriction analysis of a recombinant plasmid with Sall. The recombinant plasmid releases the insert scFv genes (750 bp) after Sall restriction. Lane M: 1kb DNA marker. Lane 1: negative plasmid (pJ912-Ag α). Lane 2: recombinant plasmid (pJ912-Ag α -scFv).

Introduction of the Recombinant Plasmid into *P.pastoris*

Both plasmids, pJ912-AG α and pJ912-AG α ::scFv, were linearized (0,5 μ g each) by SacI and introduced into the *P. pastoris* SMD1168H by electroporation method (Gene Pulser Xcell Electroporation System, Bio-Rad) [7]. The *Pichia* transformants were spread on YPDS agar plates containing 100 μ g/mL zeocin. To obtain high stability and multi-copies gene integration clones, the *Pichia* clones that grew on zeocin selection plates were recultured in fresh YPD-zeocin agar plates with multilevel concentration of zeocin (0-1000 μ g/mL). To confirm the integration of scFv gene in the

yeast genome, transformant clones were amplified by colony PCR using the VH101 forward and VL101 reverse primers.

Expression Analysis of the Fusion Protein
Some colonies of recombinant *P. pastoris* were cultured in YPD containing zeocin (100 μ g/mL) and incubated at room temperature (30°C) for 48 hours. Next, the cultures were transferred into a fresh BMGY medium and incubated at (30°C) for 24 hours. The cells culture BMGY were harvested by centrifugation and supernatant was removed. BMMY was added to the cell pellet at an OD600 = 1. Next, methanol was added into the culture to give 0.5% (v/v)



every 12 h of culture for 72 h to induce protein expression. Fluorescence microscopy was employed to observe directly the expression of active reporter protein (TagRFP) that should be displayed on the cell surface of *P. pastoris*. The induced cultures of *P. pastoris* were spotted on microscope slides. Fluorescence was detected with Leica DM1000 fluorescence microscope using N2.1 filter cube (excitation at 515-560 nm, emission > 590 nm).

RESULT AND DISCUSSION

Vector Construction for Yeast Surface Display
The antiEGFRvIII-scFv gene was fused in-frame with α factor signal peptide at 5' -end and TaqRFP::AG α gene at 3' -end under control of inducible AOX1 promotor. The open reading frame (ORF) of antiEGFRvIII-scFv gene was fused C-terminally to the ORF of TaqRFP gene. Taq RFP is a red fluorescence protein that would facilitate observation of the target protein expression from the host cells. To display antiEGFRvIII-scFv and Taq RFP protein on the cell surface of *P.pastoris*, the 3'-half of the AG α 1 gene of *S. cerevisiae* was fused N-terminally to the TaqRFP gene. This construct was cloned into Sall site in pJ912-AG α . To screen *E. coli* transformant having recombinant plasmids with scFv insert, colony-PCR method was carried out. Figure 1 shows screening of *E.coli* transformant having the recombinant plasmids. Positive clones having scFv gene showed a DNA band at 750 bp. These positive clones were further analyzed

for the gene orientation. Nearly all of those clone showed a correct orientation (data not showed). Furthermore, several plasmids with correct construction was verified by DNA sequencing (data not shown).

Screening *P.pastoris* Transformant

Vectors with and without scFv gene were transformed into *P. pastoris* SMD1168H as described above giving the novel strain of *P.pastoris* pJ912-AG α and *P. pastoris* pJ912-AG α -scFv. Genomic DNA analysis showed that the scFv gene had been integrated into the chromosomal DNA of *P. pastoris* pJ912-AG α -scFv (Fig. 2).

Selection of transformants on zeocin medium needs to be done to have genetically stable transformants and potentially to have multicopy gene integrant. The level of antibiotic resistance will reflect the number of the recombinant gene dosage that has been incorporated into the yeast genome. *P. pastoris* expression vector carry *Sh ble* gene which encodes a protein conferring resistance towards zeocin. An increased number of inserted sequence (plasmids) can indeed enhance expression of the heterologous protein. In this study, selection on varying antibiotic concentrations was applied with zeocin concentration of 0, 100, 200, 500 and 1000 $\mu\text{g}/\text{mL}$. All of transformants of *P. pastoris* pJ912-AG α and *P. pastoris* pJ912-AG α -scFv could grow on zeocin medium up to 1000 $\mu\text{g}/\text{mL}$ whereas non transformant strain of *P. pastoris* SMD1168H could not grow on zeocin medium.

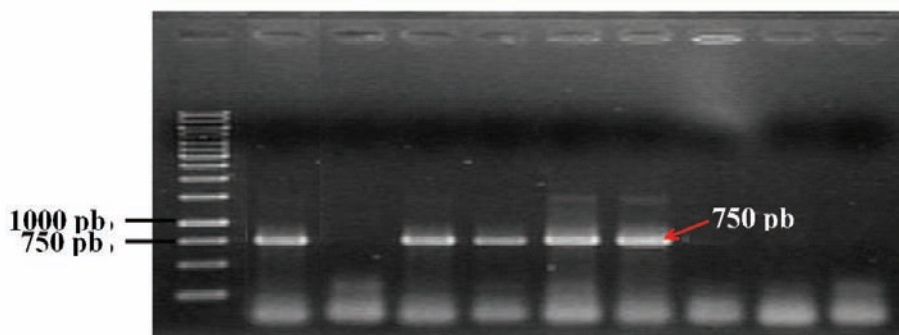


Figure 2. PCR colony analysis of *P. pastoris* transformant and non transformant clones. *P. pastoris* pJ912-AG α -scFv positive clones showed by a DNA band at 750 bp. Lane M= 1 kb DNA marker. Lane 1: positive control (pJ912-AG α -scFv). Lane 2: negative control (*P. pastoris* SMD1168H non transformant). Lane 3-6: *P. pastoris* pJ912-AG α -scFv positive clones containing scFv gene. Lane 7-9: *P. pastoris* pJ912-AG α transformant clones without scFv gene.

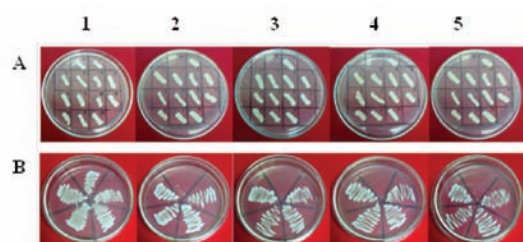


Figure 2. PCR colony analysis of *P. pastoris* transformant and non transformant clones. *P. pastoris* pJ912-AG α -scFv positive clones showed by a DNA band at 750 bp. Lane M= 1 kb DNA marker. Lane 1: positive control (pJ912-AG α -scFv). Lane 2: negative control (*P. pastoris* SMD1168H non transformant). Lane 3-6: *P. pastoris* pJ912-AG α -scFv positive clones containing scFv gene. Lane 7-9: *P. pastoris* pJ912-AG α transformant clones without scFv gene.

Expression of Fusion Protein on Surface of *Pichia pastoris*

To verify the expression efficiency of fusion protein on the cell surface, pJ912-AG α plasmid was designed in fusion with TagRFP that is used as a reporter protein. The successful display of Tag RFP on the cell surface of *P. pastoris* was confirmed by fluorescence microscopy. After induction of gene expression using methanol, both *P. pastoris* transformants (*P. pastoris* pJ912-AG α and *P. pastoris* pJ912-AG α -scFv) have been observed to successfully expressed TagRFP under fluorescence microscope observation. On the other hand, non-transformant strain of *P. pastoris* SMD1168H showed no fluorescence at all (Fig. 4). These results strongly suggest that the recombinant fusion anti-EGFRvIII scFv protein including TagRFP had been successfully expressed on the cell surface of *P. pastoris*. Fusion with a fluorescence protein has been a popular choice for recombinant protein expression since the expressed recombinant protein is easily observed by visual

means using a microscope fluorescent. Protein fusion with a fluorescence protein could also be applied to study other than protein expression, such as protein localization, protein translocation, interaction between proteins or degradation of the fusion protein in the cell. Fluorescent protein monomers such as TagRFP is generally able to function properly even after fusion with other proteins [3]. A GPI anchor attachment domain located in the 3'-half region of α -agglutinin functioned to binds and localizes this fusion protein into the cell wall structure. Binding of the GPI-anchor domain was facilitated by covalent binding to the carbohydrate moieties of the yeast cell wall structure, resulting a very stable protein attachment on the cell surface. The reporter system on the cell surface developed in this work will have a much more powerful ability to detect molecular events inside or outside living cells than the system in which the reporters were expressed inside the cells. This yeast display system is very useful for the development an antibody screening method, in which a cDNA library of any antibody could be expressed on the surface of yeast cell and the gene of this antibody could be retrieved back from the yeast genome.

CONCLUSION

The recombinant vector pJ912-AG α -scFv has been constructed and successfully transformed into *P. pastoris* SMD1168H. This recombinant vector was stably integrated into the genome of *P. pastoris* SMD1168H through homologous recombination. Stable transformed yeast has been obtained through selection on zeocin medium. Observation using fluorescence microscopy has demonstrated that the transformant cells successfully emit



ted red fluorescence light derived from functionally expressed TagRFP, which is actually part of the fusion molecules. It suggests that

the recombinant fusion antibody protein has also been expressed on the yeast cell surface with a correct folding.

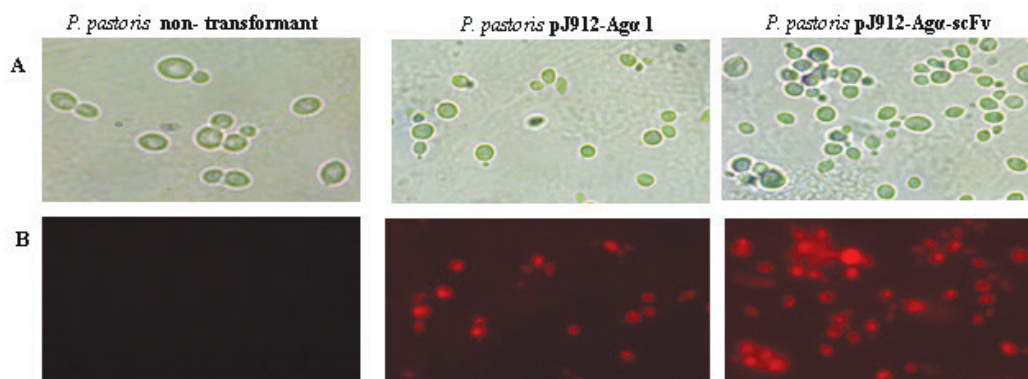


Figure 4. Microscopic observation of *P. pastoris* transformant and non transformant cells under fluorescence microscope. A. Phase contras. B. Phase fluorescent. 1. *P. pastoris* SMD 1168H non-transformant. 2. *P. pastoris* pJ912-AG α induced with methanol. 3. *P. pastoris* pJ912-AG α -scFv induced with methanol

REFERENCES

- *. Chen MH, Shen ZM, Bobin S, Kahni PC, Lipke PN. 1995. Structure of *Saccharomyces cerevisiae* α -Agglutinin. *The J. of Biol Chemis.* 270 (44) : 26168-26177
- *. Cho BK, Kieke MC, Boder ET, Wittrup KD, Kranz DM. 1998. A yeast surface display system for the discovery of ligands that trigger cell activation. *J Immunol Methods.* 220:179–188.
- *. Chudakov DM, Matz MV, Lukyanov S, Lukyanov KA. 2010. Fluorescent proteins and their applications in imaging living cells and tissues. *Physiol Rev.* 90: 1103–1163.
- *. Gupta P, Han SY, Madruga MH, Mitra SS, Li G, Nitta RT1, Wong AJ. 2010. Development of an EGFRvIII specific recombinant antibody. *BMC Biotechnol.* 10:72.
- *. Heimberger AB, Suki D, Yang D, Shi W, Aldape K. 2005. The natural history of EGFR and EGFRvIII in glioblastoma patients. *J Transl Med.* 3:38.
- *. Hong GE, Xiaoqi G, Careen KT. 2002. Evidence of high incidence of EGFRvIII expression and coexpression with EGFR in human invasive breast cancer by laser capture microdissection and immunohistochemical analysis. *Int. J. Cancer.* 98:357–361..
- *. [Invitrogen]. 2008. pPICZ α A,B, and C *Pichia* expression vectors for selection on zeocin and purification of secreted recombinant protein. Version F.
- *. Lim KH, Madabhushi SR, Mann J, Nee lamegham S, Park S. 2010. Disulfide trapping of protein complexes on the yeast surface. *Biotechnol and Bioengi.* 106(1): 27-41.
- *. Lim KH, Hwang I, Park S. 2011. Biotin-assisted folding of streptavidin on the yeast surface. *Biotechnol Prog.* 28:276-283.



- *. Muharsini S, Vuoclo T. 2000. Expression in yeast (*Pichia pastoris*) of recombinant Cb-perotrophan-42 and Cb-perotrophin-48 isolated from *Chrysomya bezziana* (the old world screw worm fly). *Jurnal ilmu Ternak dan Veteriner*, 5(3):177-184.
- *. Okamoto I, Kenyon LC, Emlet DR, Mori T, Sasaki J, Hirosako S, Ichikawa Y, Kishi H, Godwin AK, Yoshioka M, Suga M, Matsumoto M. 2003. Expression of constitutively activated EGFRvIII in Non-Small Cell Lung Cancer. *Cancer Sci.* 94(1):50-56.
- *. Pepper LR, Cho YK, Boder ET, Shusta EV. 2008. A decade of yeast surface display technology Where are we now?. *Com Chem High Throughput Screen.* 11(2): 127-134.
- *. Sok JC, Coppelli FM, Thomas SM, Lango MN, Xi S, Hunt JL, Freilino ML, Graner MW. 2006. Mutant epidermal growth factor receptor (EGFRvIII) contributes to head and neck cancer growth and resistance to EGFR targeting. *Clin Cancer Res.* 12(17):5064-73.
- *. Wörn A, Plückthun A. 2001. Stability Engineering of Antibody Single-chain Fv Fragments. *J Mol Biol.* 305: 989-1010.



SUBCLONING OF *csf3syn* (COLONY STIMULATING FACTOR-3) GENE INTO pGAPZ α AND TRANSFORMATION OF RECOMBINANT VECTOR INTO *PICHA PASTORIS*

Prety Ihda Arfia, Department of Biology, Faculty of Mathematics and Natural Sciences, University of Indonesia, Depok; Research Center for Biotechnology, Indonesian Institute of Sciences-Cibinong Science Center, Jalan Raya Bogor Km 46, Cibinong 16911, Indonesia; **Asrul Muhamad Fuad**, Research Center for Biotechnology, Indonesian Institute of Sciences-Cibinong Science Center, Jalan Raya Bogor Km 46, Cibinong 16911, Indonesia, corresponding author: asrul.m.fuad@gmail.com

INTRODUCTION

Granulocyte Colony-Stimulating Factor (G-CSF) is a protein that stimulates the formation and maturation white blood cells, especially neutrophils (Leischke, 1994). The protein consists of 174 or 177 amino acid with molecular weight of 19.6 kDa. G-CSF also has an O-glycosylation site to protect the protein from coagulation without affecting binding to its receptor. G-CSF is important for the formation and maturation of neutrophils and is widely used by patients with neutropenia. Therefore, this protein G-CSF had been used for more than 2 decades as therapeutic produced by recombinant way (Lieschke, 1994).

G-CSF is encoded by *csf3* gene located on chromosome no. 17 loci q21 - q22 (Nagata et al., 1986; Hill et al., 1993). Lasnik (2001) and Bahrami (2007), have been successfully subclone *csf3* gene into pPIC9 and expressed in *Pichia pastoris* GS-115. However, they used c-DNA-derived *csf3* gene to produce recombinant G-CSF. In this study, we reported subcloning of *csf3syn* synthetic gene in pGAPZ α expression vector and transformation of the recombinant vector into *P. pastoris*. The gene had been synthesized previously by a PCR-based method and cloned in a cloning vector pTZ57R/T (Fuad et.al, 2009). The *csf3syn* gene has been codon optimized for efficient expression in *P. pastoris*.

MATERIALS AND METHODS

Construction of pGAPZ α -CSF3ye-I (Type I Recombinant Vector)

Synthetic gene *csf3syn* had been cloned previously in the cloning vector pTZ57R/T. The gene was separated from the vector by digestion with enzyme XhoI. Expression plasmid pGAPZ α [Invitrogen] was digested with enzyme XhoI. Furthermore, the gene was ligated with pGAPZ α using T4 DNA ligase [Fermentas]. The recombinant vector was transformed into *E. coli* XL1-Blue. Transformation was carried out using Transform Aid™ Bacterial Transformation Kit [Fermentas]. Transformants were grown in Low Salt Luria Bertani agar medium (LS--LB) containing zeocin 25 μ g/ml [Invitrogen] and pH 7.5. LS--LB agar medium consists of 1% trypton, 0,5% yeast extract, 0,5% NaCl, and 1,7% agar. Transformants were verified using PCR, plasmid restriction, and DNA sequencing. Positive clones were PCR-verified using pGAP forward and AOX1 reverse primers and recombinant vectors were purified prior to DNA sequencing analysis. Figure 1 (A) shows the construct of pGAPZ α -CSFye-I (named as type I recombinant vector).

Construction of pGAPZ α -CSF3ye-II (Type II Recombinant Vector)

pGAPZ α -CSF3ye-II (named as Type II recombinant vector) was obtained by digesting type I recombinant vector with Sall restriction enzyme [Fermentas]. In this process DNA fragment located between 2 site of Sall on type I recombinant vector were removed so that the 3'-end of *csf3syn* gene was directly fused with 6xHis Tag. Furthermore, the recombinant vector was religated using T4 DNA ligase [Fermentas] and transformed into *E. coli* XL1-Blue.

Transformants were verified by plasmid restriction method. First, transformant plasmids were digested with XhoI that cut the plasmid once and makes linear vector from the correct vectors. Second, transformant plasmids were digested with EcoRI that do not from the correct recombinant vector. Figure 1 (B) shows the construc of type II recombinant vector (pGAPZ α -CSF3ye-II).

Transformation of Type II Recombinant vector (pGAPZ α -CSF3ye-II) into *Pichia pastoris* PGAPZ α -CSF3ye-II vector was digested BspHI, so the plasmid become linier. Linear plasmid would facilitate integration of the vector into *P. pastoris* genome. The *P. pastoris* competent cell was prepared according to the method of invitrogen (2008:17). Transformation of recombinant vector into *P. pastoris* was carried out using electroporation method (Invitrogen 2008:18). Transformants were grown in YPDS agar plates (yeast extract, peptone, dextrose, agar, sorbitol) containing zeocin (100 μ g/ml) [Invitrogen]. The plates was incubated at 30 $^{\circ}$ C for 2-3 days until colonies formed. Transformants colonies that grew on YPD agar plates (yeast extract, peptone, dextrose) containing zeocin at 200 μ g/ml and 1000 μ g/ml.

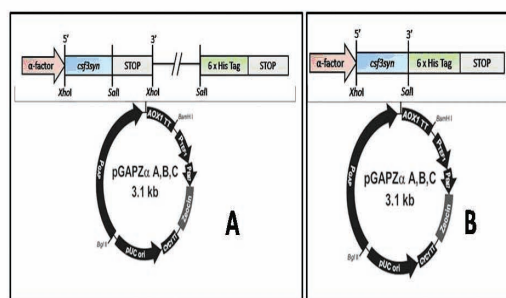


Figure 1. Construct of pGAPZ α -CSF3ye-I (type I) vector (A) and pGAPZ α -CSF3ye-II (type II) vector (B).

RESULT AND DISCUSSION

Construction of Type I Recombinant vector (pGAPZ α -CSF3ye-I)

The csf3syn gene used in this research was PCR amplified from pTZ57R_CSF3ye_PR3_005 clone. The gene was ligated with pGAPZ α linier using T4 DNA ligase. Insert DNA and plasmid used in ligation reaction were 1 : 2. The ligation reaction was transformed into *E.coli* XL1-Blue. A number of 30 transformant colonies were obtained LS--LB agar medium containing zeocin 25 μ g/ml.

Verification of the target gene in recombinant vectors was carried out using PCR method. Transformants were grown in LS--LB liquid medium containing zeocin (25 μ g/ml) for plasmid isolation. The clones were PCR-amplified with AF_1 forward and PR3_CSFye reverse primers. Positive clones showed PCR product (around 567 bp). Figure 2 shows PCR results of several clones that were amplified gene specific primers. A number of 10 positive clones were obtained out of 15 clones. The positive recombinant vectors show a DNA band because they have the target gene (csf3syn) that are recognized by AF_1 forward and PR3_CSF3ye reverse primers. Both primers are specific to csf3syn gene.

Gene orientation in recombinant vectors were also verified using PCR method. Proper orientation was achieved when the 5'-end of csf3syn gene fused with α -factor secretion signal and the 3'-end fused with restriction sites. Positive clones that were previously obtained were amplified with AF_1 forward and AOX1 reverse primers. AF_1 forward attached to the 5'-end of csf3syn gene and AOX1 reverse primer attached to the termination sequence (AOX1-TT) as part of pGAPZ α backbone. Inserted gene with correct orientation would produce a 825 bp of DNA fragment using those pair of primers. Figure 3 shows 4 positive clones out of 8 that were succesfully obtained.

Verification of recombinant vectors were also carried out by plasmid digestion method. Clones that have been verified with PCR



method were digested with XhoI. This enzyme was used because the XhoI restriction site were found in both the 5'-end and the 3'-end of *csf3syn* gene. Those clones showed that the gene (*csf3syn*) of 567 bp was cleaved out after digestion. Figure 4 shows 4 positive clones out of 4 gave a DNA band after digestion with XhoI.

Three positive vectors have been choosed and sequenced. DNA sequencing analysis confirmed that the sequence of *csf3syn* gene in recombinant vectors was similiar with sequence of *csf3syn* gene that has been constructed previously (Fuad et al., 2009). It also showed that the 5'-end of *csf3syn* gene has been correctly fused with α -factor signal (Figure 5A), whereas the 3'-end of the gene contain Sall site and stop codon (Figure 5B). The gene sequence was not fused with 6xHis Tag in this pGAPZ α -CSF3ye-I vector. This recombinant vector was used for the construction of pGAPZ α -CSF3ye-II (type II) vector.

method were digested with XhoI. This enzyme was used because the XhoI restriction site were found in both the 5'-end and the 3'-end of *csf3syn* gene. Those clones showed that the gene (*csf3syn*) of 567 bp was cleaved out after digestion. Figure 4 shows 4 positive clones out of 4 gave a DNA band after digestion with XhoI.

Three positive vectors have been choosed and sequenced. DNA sequencing analysis confirmed that the sequence of *csf3syn* gene in recombinant vectors was similiar with sequence of *csf3syn* gene that has been constructed previously (Fuad et al., 2009). It also showed that the 5'-end of *csf3syn* gene has been correctly fused with α -factor signal (Figure 5A), whereas the 3'-end of the gene contain Sall site and stop codon (Figure 5B). The gene sequence was not fused with 6xHis Tag in this pGAPZ α -CSF3ye-I vector. This recombinant vector was used for the construction of pGAPZ α -CSF3ye-II (type II) vector.

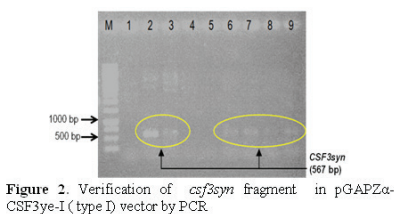


Figure 2. Verification of *csf3syn* fragment in pGAPZ α -CSF3ye-I (type I) vector by PCR

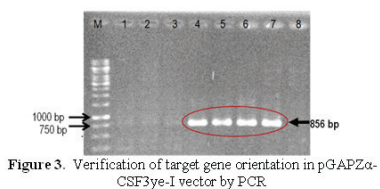


Figure 3. Verification of target gene orientation in pGAPZ α -CSF3ye-I vector by PCR

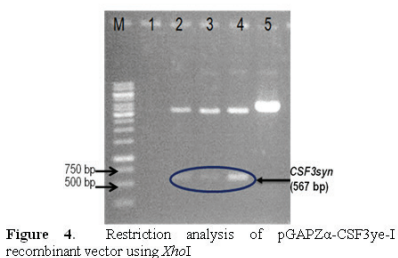


Figure 4. Restriction analysis of pGAPZ α -CSF3ye-I recombinant vector using XhoI

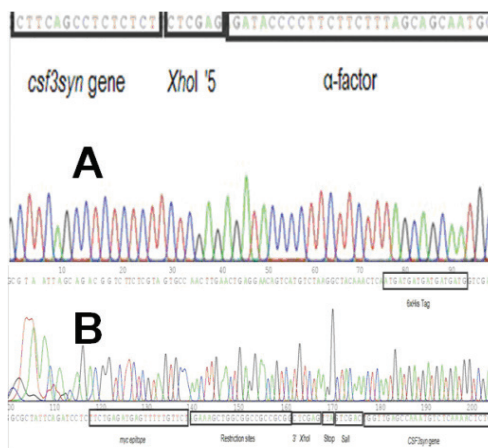


Figure 5. Sequence analysis of pGAPZ α -CSF3ye-I (type I) vector at the 5'-end (A) and the 3'-end (B)

Construction of Type I Recombinant vector (pGAPZ α -CSF3ye-I)
pGAPZ α -CSF3ye-II recombinant vector is a vector in which the 3'-end of *csf3syn* gene was fused with 6xHis Tag. This type II recombinant

vector was made by digesting previously construct type I recombinant vector with Sall. The plasmid that have been digested and purified was religated using T4 DNA ligase and then transformed into *E. coli* XL1-Blue. Transformation into *E. coli* produce a number of 190 colonies that were grown in LS-LB agar medium containing zeocin (25 µg/ml).

pGAPZα-CSF3ye-II recombinant construct were verified by restriction analysis. Plasmid restriction was performed in 2 different reactions, the first reaction using XhoI and the second reaction using EcoRI. Positive construct of type II recombinant vector would produce a single DNA band 3,530 bp (Figure 6 A) after digestion with XhoI and no restriction occurred with EcoRI (Figure 6B). Figure 6A shows 9 positive vectors out of 10 were obtained. The type II recombinant vector has one XhoI site left in the plasmid backbone. Therefore, restriction with XhoI will produce a linear plasmid.

Type II recombinant vector was derived from type I vector constructed after plasmid restriction with Sall. This process led to removal of some restriction site including EcoRI. The correct type II plasmids are not affected by restriction with EcoRI. Therefore, the type II recombinant vector would show as indigested plasmid pattern when digested with EcoRI (Figure 6B). The result shows 9 positive clones out of 10 were obtained. Figure 6B (Lane 2) shows pGAPZα plasmid that was digested with EcoRI. Plasmid pGAPZα has one unique EcoRI restriction site (Invitrogen, 2008).

Two positive recombinant vector were choose and sequenced. The result of DNA sequencing analysis showed that sequence of csf3syn gen was correct and no mutation was observed. The sequencing analysis showed that the 5'-end of csf3syn has been fused in-frame with α-factor signal (Figure 7A) and the 3'-end of csf3syn gene also fused in-frame with 6xHis Tag (Figure 7B)

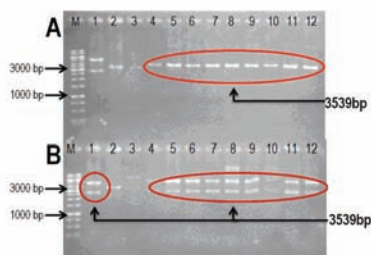


Figure 6. Verification of type II recombinant vectors by restriction analysis. The recombinant vectors were digested with XhoI (A). The recombinant vectors were digested with EcoRI (B)

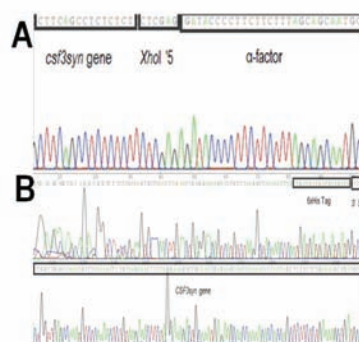


Figure 7. Sequence analysis of pGAPZα-CSF3ye-II (type II) vector at the 5'-end (A) and the 3'-end (B).

Transformation of Type II Recombinant Vector (pGAPZα-CSF3ye-II) into *P. pastoris*

Type II recombinant vector (pGAPZα-CSF3ye-II) was transformed into *P. pastoris* in order to express recombinant G-SCF an eukaryot expression system. *P. pastoris* was used in this research for its ability to produce complex protein and high yield protein. Yeast system is also known to enable post-translational modification process, such as protein folding, glycosylation and disulphide bond formation (Glick & Pasternak, 2003).

The recombinant plasmid pGAPZα-CSF3ye-II was digested with BspHI to form linear plasmid before transformation. The BspHI was



used in this purpose since it cut once within the promotor region of pGAP in the recombinant vector, so the vector become linear (Invitrogen, 2008). Linearisation of the plasmid aims to facilitate the integration of recombinant vector into *P. pastoris* genome. According to Glick & Pasternak (2003), plasmid can be integrated into the host genome, if those plasmids have any sequence that complemented with the host genome. The recombinant pGAPZ α -CSF3ye-II plasmid was designed to be integrated into GAP promoter sequence of the *P.pastoris* genome. The GAP promoter is a promoter that drive glyceraldehyde-3-phosphate-dehydrogenase (GAP) gene (Gellisen, 2005).

Plasmid was transformed into *P. pastoris* using electroporation method (Invitrogen, 2008). The method is used because it doesn't destroy the host cell or limit the cell damage. Electroporation technique uses an electric shock to open the pores of the cell membrane. Electric shock caused the gap in membrane cell which permit the DNA can go through to the cell membrane and the gap in the cell membrane will be closed again (Wong, 1997). Figure 8A shows competent cells as control that grew well on the YPDS agar medium after electroporation. This result indicates that cell has a good quality after electric shock. Figure 8B shows transformant colonies that grew well on YPDS medium containing zeocin (100 $\mu\text{g/ml}$). Transformation efficiency obtained was 4.9×10^3 cfu/ μg plasmid DNA. This transformation efficiency is fair enough if compared to the protocol given by invitrogen, which mentioned that tranformation efficiency could reach 103 to 104 cfu/ μg plasmid DNA using this plasmid system.

Transformant colonies were grown on YPD agar plates containing higher zeocin concentration (200 $\mu\text{g/ml}$ and 1,000 $\mu\text{g/ml}$). This was carried out to assay the stability of transformant colonies well as to screen colonies having multiple

gene integration. It was observed that 85.5% of transformant colonies grew well on YPD agar medium containing 200 $\mu\text{g/ml}$ zeocin (Table 1). It means that 85.5% of those colonies were stable transformants. When the screening was continued using medium containing 1,000 $\mu\text{g/ml}$ zeocin, it showed that 96% of the transformant colonies that grew well on YPD agar medium containing 1,000 $\mu\text{g/ml}$ zeocin (Table 1). This result indicates that transformant colonies have high stability against antibiotic zeocin and allegedly had multicopy gene. Recombinant clones that have been obtained would be used as prodecer strain for expression of csf3syn gene in *P. pastoris*.

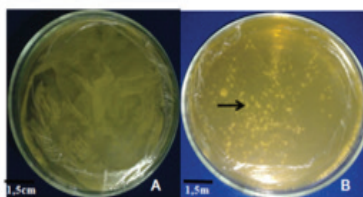


Figure 8. Transformation of *P.pastoris* GS-115 with pGAPZ α -CSF3ye-II vector. Competent cell *P. pastoris* as control (A) and transformant colonies (B).

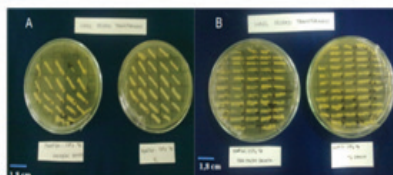


Figure 9. Stability assay of *P.pastoris* transformant colonies on medium containing higher zeocin concentration. Transformant colonies on YPD agar medium containing 200 $\mu\text{g/ml}$ (A) and 1,000 $\mu\text{g/ml}$ (B) zeocin

Concentration of zeocin	Number of tested colonies	Number of growing colonies	Presentase (%)
200 $\mu\text{g/ml}$	90	77	85.5%
1000 $\mu\text{g/ml}$	49	47	96%

Table 1. Stability assay of *P. pastoris* transformant colonies on medium containing higher zeocin concentration



CONCLUSION

The csf3syn gene was successfully subcloned into pGAPZ α and produce two versions of recombinant vector, pGAPZ α -CSF3ye-I (no fusion with 6xHis Tag) and pGAPZ α -CSF3ye-II (fusion with 6xHis Tag). The pGAPZ α -CSF3ye-II has been successfully transformed into *P. pastoris* with transformation efficiency of 4.9x10³ cfu/ μ g plasmid DNA.

REFERENCES

1. Bahrami, A., Shojaosadati, S. A., Khalilzadeh, R., Saeedinia, A. R., Farahani, E.V. , & Mosaabadi, J.M. (2007). Production of recombinant human granulocyte-colony stimulating factor by pichia pastoris. Iranian Journal of Biotechnology. 5(3): 162--163.
2. Fermentas.(2008). TransformAid™Bacterial Transformation Kit. from www.fermentas.com.
3. Fuad, A.M., Agustiyanti, D.F., Yuliawati & Santoso, A.(2009). Konstruksi gen CSF3 sintetik penyandi granulocyte-colony stimulating factor (G-CSF) manusia dengan teknik PCR. Journal of Applied And Industrial Biotechnology in Tropical Region, 2(2): 1--10.
4. Gellissen, G.(2005). Production of recombinant protein: Novel microbial and eukaryotic expression systems. Weinheim: Wiley-VCH Verlag GmbH & Co.
5. Glick, B.R & Pasternak, J. J.(2003) Molecular biotechnology. Washington: ASM Press.
6. Hill, C.P., Osslund, T.D. & Eisenberg, D.(1993). The structure of granulocyte-colony-stimulating factor and its relationship to other growth factors. Proc. Natl. Acad. Sci. USA, 90: 5167--5171.
7. Invitrogen. 2001. EasySelect™ pichia expression kit: A manual of methods for expression of recombinant proteins using pPICZ and pPICZ α in pichia pastoris. California: Invitrogen Corp.
8. Lasnik, M.A., Porekar, V.G. & Stalc, A.(2001). Human granulocyte colony stimulating factor (hG-CSF) expressed by methylotrophic yeast pichia pastoris. Springer Verlag, (442): 184-186.
9. Lieschke, G.J.(1994). Granulocyte colony stimulating factor (G-CSF). from www.australianprescriber.com.
10. Nagata, S., Tsuchiya, M., Asano, S., Yamamoto, O. , Hirata, Y., Kubota, N., Oheda, M., Nomura, H., & Yamazaki, T. (1986). The chromosomal gene structure and two mRNAs for human granulocyte colony-stimulating factor. European Molecular Biology Organization Journal, 5(3): 575--581.
11. Wong, D.W.S. (1997). The ABC of gene cloning. New York:International Thomson Publishing.



THE USE OF PERICARP MANGOSTEEN (*Garcinia mangostana* L.) EXTRACT IN FORMULATION OF CREAM-TYPE O / W

Rahmah Elfiyani, Faculty of Pharmacy and Sains, University of Muhammadiyah Prof. DR. Hamka, Jakarta-Indonesia, rahmaelfiyani@yahoo.com; **Naniek Setiadi Radjab**, Faculty of Pharmacy and Sains, University of Muhammadiyah Prof. DR. Hamka, Jakarta-Indonesia; **Mia Sagita Sofyan**, Faculty of Pharmacy and Sains, University of Muhammadiyah Prof. DR. Hamka, Jakarta-Indonesia

INTRODUCTION

The pericarp of the mangosteen fruit (*Garcinia mangostana* L.) containing xanthone which has many benefits, one of them as an antioxidant (Subroto 2008). Based on previous studies showed that 5% viscous extract of pericarp of mangosteen (*Garcinia mangostana* L.) as a potent antioxidant (Trifena 2012). Viscous extract of pericarp of mangosteen formulated in a cream-type oil in water (O / W). To stabilize the cream-type O / W required the addition of an emulsifier, more easily by using a combination of hydrophilic surfactant and lipophilic surfactant (Lachman et al., 1994).

In this study, the viscous extract of pericarp mangosteen made into a cream dosage form by using a combination of Tween 80 and Span 80 as emulsifier with different concentrations in each formula. This study aims to determine the concentration of combination between Tween 80 and Span 80 as an emulsifier in a cream formula of the viscous extract of pericarp mangosteen which fulfill physical stability.

MATERIALS AND METHOD

Materials

Dry extract of pericarp mangosteen (PT. Borobudur Semarang), H₂SO₄ (pa), FeCl₃, ethanol 70%, cetyl alcohol (Cognis), paraffin oil, white petroleum (Merkur), methyl paraben, propyl paraben (Gujarat), butyl hydroxy toluene (BHT) (SPP Chemical), Tween 80 (Kao Co.), Span 80, propylene glycol (Dow Chemical Co.) and aquadest.

Preparation and Evaluation of the Viscous Extract of Pericarp Mangosteen

The powder dry extract of pericarp mangosteen macerated using 70% ethanol. Then

maserat thickened by using a rotary evaporator at a temperature of 60°C to obtain a viscous extract. Characteristic evaluation to viscous extract of pericarp mangosteen (VEPM) include organoleptic test, loss on drying, viscosity and flavonoid.

Preparation of Cream

Preparation of oil phase : cetyl alcohol, white petroleum, paraffin oil, span 80, propyl paraben, and BHT melted at water bath until the temperature reaches above 70°- 72°C. Then the manufacturing of water phase : methyl paraben, Tween 80, and propylene glycol diluted with distilled water and heated until the temperature reaches 70°C - 72°C. Furthermore phase of water mixed with the oil phase at a temperature of 70°C - 72°C then homogenized using a mixer until the homogenous creamy base obtained with 40°C temperature. To the base is added viscous extract of pericarp mangosteen, then homogenized again to form a homogenous cream dosage form. Evaluate the cream of viscous extract of pericarp mangosteen.

Text	F1 (%)	F2 (%)	F3 (%)	F4 (%)	F5 (%)
VEPM	5	5	5	5	5
Cetyl alcohol	8	8	8	8	8
White petroleum	20	20	20	20	20
Paraffin oil	16	16	16	16	16
Propyl paraben	0,02	0,02	0,02	0,02	0,02
Tween 80 & Span 80 (1:1)	2	4	6	8	10
Methyl paraben	0,18	0,18	0,18	0,18	0,18
BHT	0,1	0,1	0,1	0,1	0,1
Propylene glycol	10	10	10	10	10
Aquadest ad	100	100	100	100	100

Table 10. Cream Formulas of Viscous Extract of Pericarp Mangosteen.



Evaluation the Cream of Viscous Extract of Pericarp Mangosteen

Evaluation cream consists of organoleptic test, homogeneity, pH, viscosity, flow properties, emulsion type, and test phase separation with freeze-thaw and centrifugation method. Data analysis of the results of the pH and viscosity measurements using 2-way ANOVA to see any difference of each formula.

RESULTS AND DISCUSSION

Evaluation of the Viscous Extract of Pericarp Mangosteen

Characteristic of viscous extract of pericarp mangosteen were has dark brown color, loss on drying at 30.84%, viscosity at 9500 cps using spindle numbered 6 at 20 rpm and positive contain flavonoids.

Evaluation the Cream of Viscous Extract of Pericarp Mangosteen

Organoleptic and homogeneity test of the cream indicates that the storage of the cream for 6 weeks did not change the color, consistency, odor and remain homogeneous.

Results of pH measurements for 6 weeks showed that there were difference between the fifth creamy formula, but the difference was not significant by 2-way ANOVA statistical analysis that obtained sig 0.164 > α of 0.05, so it can be said that the fifth formula cream were stable. Values of pH were obtained from the fifth formula is within the normal pH of the skin is 4,5 to 6,5.

Test the cream-type performed by coloring method using methylene blue solution. Methylene blue is water soluble so that when methylene blue solution mixed in the cream with the type of O / W, it directly mixed with water and spread evenly on the cream. From the test results of the five formulas, the resulting type of cream is a cream-type O / W, because after adding methylene blue then blue color is uniformly dispersed in the cream. There were no change of the type of cream during storage time and an increase in the concentration of combination between Tween 80 and Span 80 (1: 1) does not affect the type of cream.

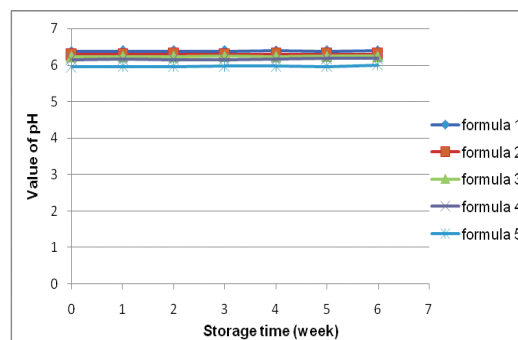


Figure 1. The Results of pH Measurement

Viscosity measurements for 6 weeks performed using Brookfield viscometer-type RVDVE with spindle number 6 at a speed of 10 rpm. Based on Figure 2 shows that there is an increasing viscosity on the fifth formulas with increasing storage time. Viscosity value is different in each formula. The higher of concentration of combination between Tween 80 and Span 80 (1: 1) used in the formula produces a more viscous cream and the higher of the viscosity value. The higher viscosity will decrease the rate of precipitation due to the climate of the movement of particles of a material tends to be difficult so that the tendency to join the dispersed phase becomes smaller and more stable emulsion. Stokes law shows that the rate of separation formation is inversely proportional to viscosity, generally increase the viscosity will minimize the occurrence of creaming or separation so as to improve the stability of the cream (Kim, 2004). Two-way ANOVA test results on viscosity data based on concentration (formula) and storage time showed the value of sig 0.000 < α 0.05, which indicates that the value of the viscosity on the fifth formulas and at storage time has significant differences. Tukey test results against concentration (formula) that there are significant differences in the viscosity of each formula, and the results of Tukey's test against the storage time is significantly different in each week of storage means storage time affects the viscosity value.

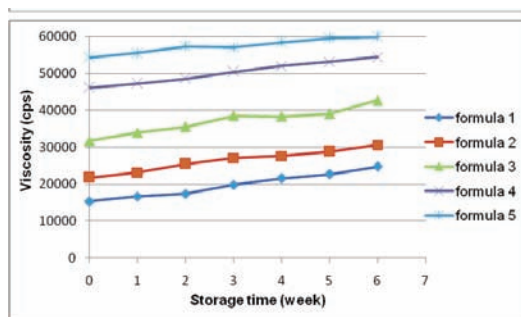


Figure 2. The Results of Viscosity Measurement

Rheology curve created using data between torque (dyne/cm²) and sliding speed (rpm) (Triantafillopoulos 1988), it can be concluded that the five-cream formula has thixotropic plastic flow properties. Determination of the nature of plastic flow because the curve does not start from the point (0,0) but cut the shearing stress axis, or be cut off if the straight part of the curve is extrapolated to the axis at a certain point, known as the yield value. The existence of a yield value due to the contact between adjacent particles that must be broken down first so that preparations flows (Martin et al., 1993).

The five creams also have thixotropic flow properties due to the curve looks curves down to the left of the curve up, it shows the cream has a lower viscosity at all shear rates on the curve down. This is due to the breakdown structure is not formed again immediately if the stress is removed or reduced (Martin et al., 1993). Flow properties of the fifth formula from week 0 to sixth week were unchanged.

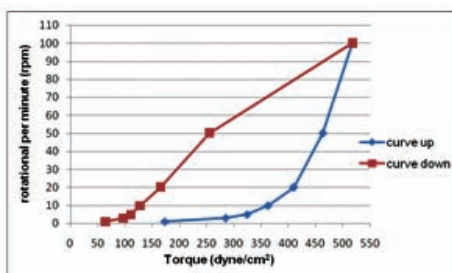


Figure 3. Rheology Curve of Formula 5 (t = week 0)

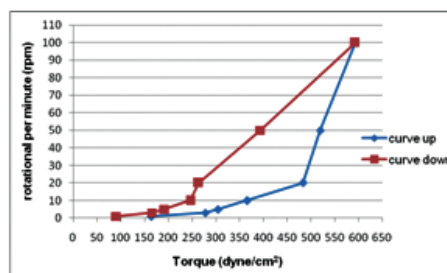


Figure 4. Rheology curve of formula 5 (t = sixth week)

	F1	F2	F3	F4	F5
High of separation (cm)	1,1	0,7	0,5	0,4	0,2

Table 2. Centrifugation Results of Cream of Viscous Extract of Pericarp Mangosteen.

Test phase separation with freeze-thaw method performed a total of 6 cycles (Lachman et al., 1994). Testing is done by storage at two different temperatures is 4°C and 45°C respectively for 48 hours. The results of these tests showed that there is a separation of Formula 1 at the time of cycle 4, and Formula 2 separation occurs during cycle 5. Separation that occurs is indicated by the formation of two layers of cream. This occurs due to temperature changes can alter the density of the particles. The larger the particle density difference between the two phases, the easier it is to join together the dispersed phase so that the larger the oil balls are formed and decreasing the viscosity of the external phase, so that the greater the rate of creaming (Martin et al., 1993). Meanwhile, Formula 3, Formula 4 and Formula 5 did not occur phase separation so that the cream can be said to be stable at cold and hot temperatures during storage. Separation that occurs can be influenced by the concentration of emulsifier. If a high enough concentration of emulsifier, emulsifier will form a rigid layer between the phases, which act as a barrier to the merger of the emulsion droplets (Lachman et al., 1994).

Test phase separation by centrifugation method, performed at a speed of 3750 rpm for 5 hours (Lachman et al., 1994). Based on Table 2



shows the fifth formula cream had separation but the high separation in each formula were different forms. The higher the concentration of combination between Tween 80 and Span 80 (1: 1) were used resulting in lower sedimentation. This happens because the higher concentration of emulsifier were used, the ability to form a film coating will be greater so as to minimize the occurrence of phase separation.

CONCLUSION

Increasing the concentration of combination between Tween 80 and Span 80 (1: 1) can increase the viscosity of the cream so as to minimize the occurrence of phase separation, thereby improving physical stability cream of viscous extract of pericarp mangosteen (*Garcinia mangostana* L.). Formula cream of viscous extract of pericarp mangosteen that fulfill the physical stability is a cream formula with a concentration of combination between Tween 80 and Span 80 (1: 1) by 10% of the concentration range 2-10%.

REFERENCES

- Subroto, A.M. 2008. Real Food True Health. Agro Media. Ciganjur. page 73-74
- Trifena. 2012. Analisis Uji In Vitro dan In Vivo Ekstrak Kombinasi Kulit Manggis (*Garcinia mangostana* L.) dan Pegagan (*Centella asiatica* L.) Sebagai Krim Antioksidan. Tesis. FMIPA UI, Depok. page. 41, 55, 66.
- Lachman, L., Lieberman, H.A, Kanig, J.L. 1994. Teori dan Praktek Farmasi Industri II Edisi ke-3, Terjemahan: Siti Suyatmi. UI Press, Jakarta. Hlm. 1030, 1055, 1061, 1076-1079, 1080-1081, 1087.
- Kim, Chong-ju. 2004. Advanced Pharmaceutics : Physicochemical Principles. CRC Press LLC, Florida. page 229 - 235
- Triantafillopoulos N. 1988. Measurement of Fluid Rheology and Interpretation of Rheograms Second Edition. Kaltec Scientific, Inc. USA. page. 4-5, 31.
- Martin, A., James, S., Arthur, C. 1993. Farmasi Fisik 2, Edisi Ketiga, Terjemahan : Yoshita. UI Press, Jakarta. page. 1077-1095, 1154-1161, 1164.



CHITOSAN BASED PARTICULATE CARRIER OF DITERPENE LACTON OF SAMBILOTO PREPARED BY IONIC GELATION-SPRAY DRYING :EFFECT OF STIRRING RATE AND NOZZLE DIAMETER

Retno Sari, Faculty of Pharmacy, Airlangga University, Surabaya, Indonesia, retnorhd@gmail. Com; **Titin Suhartanti**, Faculty of Pharmacy, Airlangga University, Surabaya, Indonesia; **Dwi Setyawan**, Faculty of Pharmacy, Airlangga University, Surabaya, Indonesia; **Esti Hendradi**, Faculty of Pharmacy, Airlangga University, Surabaya, Indonesia; **Widji Soeratri**, Faculty of Pharmacy, Airlangga University, Surabaya, Indonesia.

INTRODUCTION

Chitosan, a cationic polysaccharide has many advantages as carrier for drug delivery system such as biocompatible, biodegradable and non toxic. Chitosan has amino group that could be crosslinked with polyanion such as tripolyphosphate so that the active ingredient will be entrapped (Agnihotri, 2004, Sinha, 2004). Diterpene lactone fraction of sambiloto (*Andrographis paniculata*) has antimalarial activity but it has low solubility in water. Entrapped diterpene lactone into chitosan matrix could improve the bioavailability of the active substance.

The aim of this research is to investigate the effect of process parameter of chitosan carrier preparation : stirring rate (500 rpm and 1000 rpm) during ionic gelation and nozzle diameter (0.5 mm and 1.0 mm) of spray dryer on physical characteristics of diterpene lactone fraction-chitosan particles. Evaluation of morphology, thermal analysis and drug entrapment were conducted.

EXPERIMENTAL METHODS

Material and Methods

Material

Diterpene lactone fraction of sambiloto was obtained from Department of Pharmacognosy and Phytochemistry, Faculty of Pharmacy, Airlangga University, chitosan with deacetylation degree 85% was purchased from Biotech Surindo, Natrium tripolyphosphate, pro analysis grade from Nacalay Tesque. All other reagents used in this experiment were pro analysis grade.

Preparation of chitosan particles

Independent variable	Nozzle diameter	
Stirring speed	1.0 mm	0.5 mm
500 rpm	P1	P3
1000 rpm	P2	P4

Chitosan was dissolved in 0.15% acetic acid to make 0.1% chitosan solution. Preparation of diterpene lactone - chitosan particles was done by mixing chitosan solution and diterpene lactone fraction solution and then 0.1% tripolyphosphate solution was added while stirring with two stirring speed.. The mixture was continuously stirred with magnetic stirrer for 2 hours. Subsequently the mixture was dried with Labplant SD-Basic Spray Dryer at 100°C, flow rate 5 ml/min, pressure 2 bar with two different nozzle diameter. The ratio of drug-chitosan-TPP was 4:10:8.

Evaluation of nanoparticles morphology

The particles were evaluated by Scanning Electron Microscopy (SEM) FEI Inspect S50. Particles were dried and coated with gold palladium and then observed for its shape and surface morphology.

Thermal analysis

Thermal analysis for diterpene lactone fraction of sambiloto, chitosan and nanoparticles was performed with Differential Thermal Analyzer (DTA) Metler Toledo FP 85. Samples were scanned from 50 to 250°C at a rate of 10°C/min.

Entrapment efficiency (EE)

5 mg sample was dissolved in 10 ml of ethanol then filtered. Solution was analyzed by HPLC Agilent 1100 with mobile phase of methanol: phosphoric acid pH 3=50: 50 at wavelength of 228 nm. The assays were performed in triplicate. The entrapment efficiency (EE) of diterpenelactone in chitosan nanoparticles was calculated by this equation :

$$EE = (\text{actual drug} / \text{theoretically drug}) \times 100\%$$

RESULTS

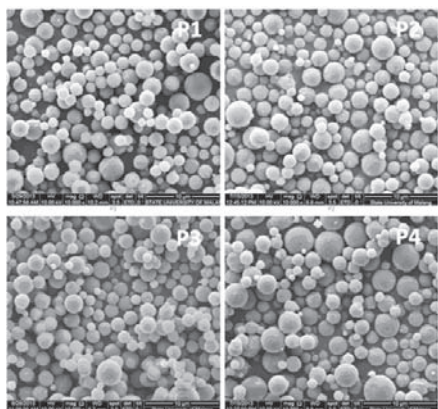


Figure 1 SEM micrographs of particles of diterpene lactone-chitosan prepared with different condition (mag 10.000x)

Sem photograph of particles diterpene lactone - chitosan (figure 1) showed that the particles have spherical shape and smooth surface with wide range particle size.

From DTA thermogram (Figure 2) it was indicated that endothermic peak of diterpene lactone appears at 222 °C and chitosan glass transition appears at 146.6 °C. Endothermic peak of diterpene lactone fraction was no longer exist in chitosan particulate system since it had been entrapped in chitosan matrix.

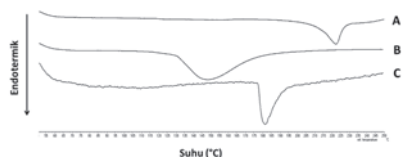


Figure 2. DTA thermogram of diterpene lactone (A), chitosan (B) and diterpene lactone-chitosan particles (C)

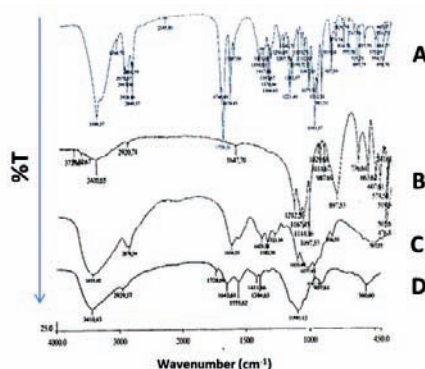


Figure 3. FTIR spectra of diterpene lactone (A), tripolyphosphate (B), chitosan (C), diterpene lactone-chitosan particles (D)

	Drug content ± SD (%)	EE ± SD (%)
P1	4.79 ± 0.04	26.36 ± 2.42
P2	3.84 ± 0.04	21.11 ± 2.04
P3	4.38 ± 0.02	24.12 ± 0.82
P4	3.82 ± 0.03	21.01 ± 1.69

Table 2. Drug content and Entrapment Efficiency (EE) of diterpene lactone- chitosan particles (n=3)

FTIR analysis was performed to confirm the crosslink interaction of chitosan and tripolyphosphate. Absorption band at 1643 cm⁻¹ attributed to amide bond of chitosan. New band at 1555 cm⁻¹ indicated hydrogen bond and 1643 cm⁻¹ band confirmed linkage between P3O5-5 of tripolyphosphate and NH3⁺ of chitosan (Figure 3).

From drug entrapment efficiency, it was known that as stirring speed increased from 500 rpm to 1000 rpm, the entrapment of drug become lower decrease from about 24-26% to 21% (Table 2). From statistical analysis of one way Anova with α 0.05, it was known that drug entrapment efficiency of particles prepared with different stirring rate was significantly difference since nozzle diameter didn't affect the entrapment efficiency.



CONCLUSION

The result showed that diterpen lactone – chitosan particles prepared by ionic gelation-spray drying with composition and condition in this study has spherical shape with wide range size from 400 nm to 4000 nm. Highest drug entrapment efficiency was obtained from particles prepared with 500 rpm stirring rate and 1,0 mm nozzle diameter.

REFERENCES

Agnihotri, S.A., Mallikarjuna, N.N., Aminabhavi, T.M., 2004. Recent advances on chitosan based micro-nanoparticles in drug delivery. *Journal of Controlled Release*, Vol. 100, p. 5-28

Amaro, M.I., Tajber, L., Corrigan, O.I., Healy, A.M., 2011. Optimisation of spray drying process conditions for sugar nanoporous microparticles (NPMPs) intended for inhalation. *International Journal Pharmaceutics*, Vol. 421 p. 99-109

Bhumkar, Devika R., Pokharkar, Varsha B.,

2006. Studies on effect of pH on cross-linking of chitosan with sodium tripolyphosphate: a technical note. *AAPS PharmSciTech*, Vol. 7, article 50.

Gupta, Vivek Kumar., Karar, P.K., 2011. Optimization of process variable for the preparation of chitosan/alginate nanoparticles. *International journal of pharmacy and pharmaceutical sciences*, Vol 3, Suppl 2, p. 78-80.

He, P., Davis, S.S., Illum, L., 1999. Chitosan microsphere prepared by spray drying. *International Journal of Pharmaceutics*, Vol. 187, p. 53-65.

Ko, J.A., Park, H.J., Hwang, S.J., Park, J.B., Lee, J.S., 2002. Preparation and characterization of chitosan microparticles intended for controlled drug delivery. *Int J Pharm*, Vol. 249, p. 165-174.

Sinha, V.R., A.K. Singla, S. Wadhawan, R. Kaushik, R. Kumria, K. Bansai, S. Dhawan. 2004. Chitosan Microspheres as a Potential Carrier for Drugs. *Int. J. Pharm.* Vol. 274, p. 1-33.



GAS CHROMATOGRAPHY-MASS SPECTROMETRY METHOD VALIDATION FOR PESTICIDES RESIDUES ANALYSIS IN FOOD USING QuEChERS KIT

Riesta Primaharinastiti, Pharmaceutical Chemistry, Faculty of Pharmacy Airlangga University, Surabaya, East Java, Indonesia, r.nastiti@gmail.com, Setyo Prihatiningtyas, Pharmaceutical Chemistry, Faculty of Pharmacy Airlangga University, Surabaya, East Java, Indonesia, Mochammad Yuwono, Pharmaceutical Chemistry, Faculty of Pharmacy Airlangga University, Surabaya, East Java, Indonesia

INTRODUCTION

The use of pesticides can leave residues that may cause pollution of the environment and human health problems¹. It is necessary to supervise the use of pesticides through the fulfillment of the MRL (Maximum Residue Limits). And so as to ensure food safety by limiting the levels of pesticide residues, including organophosphate and organochlorine, in food commodities.

Organophosphate is a toxic compound that affect the nervous system in a way disrupt enzyme that regulates acetylcholine, a neurotransmitter that is necessary for our nerves can work normally. In general, organophosphate pesticides are not persistent both in the environment and in living organisms, including plants. Consequently, to obtains the necessary level of effective pesticides, farmers spraying with increasing frequency. Organochlorine compounds are non-volatile, insoluble in water, except for lindane, easily soluble in organic solvents, persistent in the environment, while in plant tissues undergo biotransformation into metabolites that can be toxic.

Samples of food, such as vegetables and fruit, has a very complex matrices that requires optimal, accurate, economical, and efficient extraction procedure for routine analysis. Various extraction procedures organochlorine and organophosphates pesticides have been published in scientific articles and to achieves the level of very small concentration of the residue, chromatographic methods such as High Performance Liquid Chromatography (HPLC) or gas-chromatography (GC) is used. Several studies using GC/MS with different sample preparation techniques have been de-

veloped for the analysis of pesticides in food. Lehotay⁴ analyzed 22 samples of pesticides in apples, green beans and carrots by GC/MS-MS, sample preparation is done using solvent extraction with acetonitrile without clean-up process, and using GC/MS with supercritical extraction (Supercritical Fluid extraction/SFE)⁵, Saqib Hussain¹¹ examined the pesticide residues on fruits mango with GC-ECD method (Electron Capture Detector) using cyclohexane and ethyl acetate to solvent extraction and gel permeation chromatography (Gel Permeation Chromatography/GPC) for the clean-up stage, to eliminate the effect of the sample matrix Consuelo¹ added analyte protectant in the analysis of pesticides in soil, juice, and honey using GC/MS.

Pesticide analysis methods easily and quickly introduced by Steven J Lehotay^{6,7,8}, known by the method of "QuEChERS" (Quick, Easy, Cheap, Effective, Rugged, and Safe). The study was conducted to analyze 229 pesticides with samples of lettuce and citrus fruit. This method includes the step of solvent extraction with acetonitrile, liquid-liquid partition using MgSO₄ and NaCl, and clean up using a dispersive phase Solid Phase Extraction (SPE dispersive), whereas the analysis was conducted using GC/MS and LC/MS. This method was later refined to analyze pesticides that can not be detected in the previous method by adding acetate buffer for extraction pH 4-5. Other studies are still using GC/MS and LC/MS analysis of deltamethrin in plants by extracting acetone, petroleum ether, and dichloromethane and clean-up using GPC²; analysis of 446 pesticides in fruit and vegetable samples with three-cartridge SPE ex



traction using acetonitrile-toluene solvent10 and Yukiko13 using supercritical extraction. GC method used for the analysis of pesticide multiresidues has been done by Yanli12 with FPD detector and Nuria9 using ECD detector. The QuEChERS method has been adopted as the AOAC method in 2007.

In Indonesia, there was indication of an increase in the use of pesticides based on pesticide product registration data from 1557 products in 2006 to 2628 products in 2010. However, it is only few testing laboratories that have capability to perform pesticide residue analysis with adequate analytical methods. In this study, the validation of analytical method to determine the residue of pesticides on fruit and vegetable using GC-MS and QuEChERS kit is conducted to provide valid and ready to use analytical methods. Pesticides used in this study are organochlorine and organophosphates pesticides. GC is the chosen analytical method in thi study because it can achieve high sensitivity and also equipped with a highly selective detectors such as MS (Mass Spectrometry). Besides, GC does not require expensive HPLC solvent system.

METHODS

Materials

Fruits and vegetables are used as samples (cabbage, carrots, tomatoes, apples and green grapes), Organochlorine p.a (Sigma-Aldrich); Organophosphates (Sigma-Aldrich), acetonitrile pa (Merck); ethyl acetate p.a (Mallinckrodt), acetone pa (Merck); anhydrous Na₂SO₄ pa (Riedel-de Haen); NaCl pa (Merck), general purpose Agilent QueChERS AOAC kit.

Instrument

Agilent 6789 GC with Agilent Technologies 5973 inert Mass Selective Detector, Agilent capillary column HP-5 413 320 x 30.0 x 0.25 lm, QuEChERS AOAC kit (Agilent Bond Elut Buffered extraction kit and Bond Elut dispersive SPE kit for general vegetables and fruits), micro scales (Mettler Toledo Balance microgram AB204-S), micropipette (Thermo Scien-

tific FJ76476).

Sample Preparation

Fruits and vegetables are cut into pieces and then washed and drained for 15 minutes and blend until homogen.The sample then stored in the freezer for subsequent analysis. The samples are removed from the freezer and allowed to room temperature and then weighed again and ready to be used for analysis.

Extraction method

Extraction method used in this research is in accordance with the manual of Agilent QuEChERS AOAC kits, according the following chart.

Gas Chromatography conditions

Oven temperature: 180°C maintained 2 minutes increased 190°C (1°C/min), up 204°C (2°C/min), increased to 206°C (1°C/min) and then rose again to 290°C (2°C/min) was maintained for 2 minutes.

Validation Methods

Validation of test methods based on USP with parameters : specification/selectivity, linearity, range, limit detection, limit quantitation, accuracy, and precision.

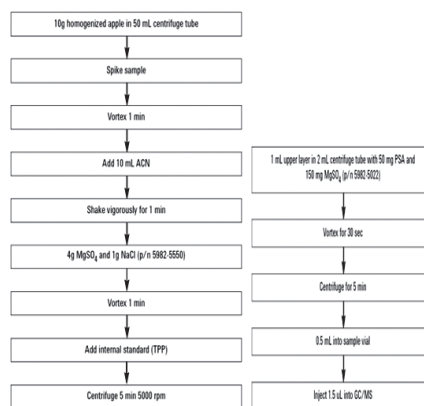


Figure 1. Flowchart of Extraction method according to QuEChERS AOAC kit procedures

Sample Preparation

Fruits and vegetables are cut into pieces and then washed and drained for 15 minutes and blend until homogen. The sample then stored in the freezer for subsequent analysis. The samples are removed from the freezer and allowed to room temperature and then weighed again and ready to be used for analysis.

Extraction method

Extraction method used in this research is in accordance with the manual of Agilent QuEChERS AOAC kits, according the following chart.

Gas Chromatography conditions

Oven temperature: 180°C maintained 2 minutes increased 190°C (1°C/min), up 204°C (2°C/min), increased to 206°C (1°C/min) and then rose again to 290°C (2°C/min) was maintained for 2 minutes.

Validation Methods

Validation of test methods based on USP with parameters : specification/selectivity, linearity, range, limit detection, limit quantitation, accuracy, and precision.

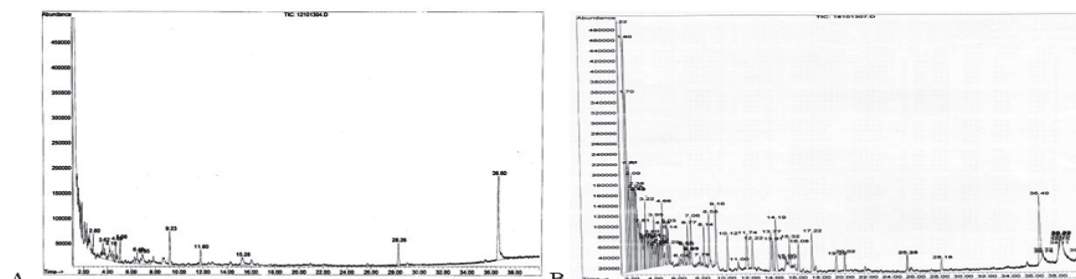


Figure 3. Chromatogram of A. green grape extract blank, B. spiked green grape extract. No interfere was found in both extracts.

Linearity, Limit Detection and Limit Quantitation

The linear calibration curve of each pesticide was 0.7 – 7 ppm, 6 concentrations according to AOAC procedures. The result shows that the regression equation of each pesticide has correlation coefficient $R^2 > 0.99$, giving a good

linearity on the concentration range. LOD-LOQ determination is done by measuring the slope of the standard deviation of the response calibration curve consisting of five low concentrations in the area LOD-LOQ. Data obtained regression equation in the concentration range 0.7-1.5 ppm. The data is shown in Table 1.

No	t_R (min)	Pesticide	Class	LOD (ppm)	LOQ (ppm)
1	3.213	Etophorphos	Organophosphate	0.22	0.66
2	3.921	α -Lindane	Organochlorine	0.21	0.63
3	4.537	β -Lindane	Organochlorine	0.21	0.62
4	4.643	γ -Lindane	Organochlorine	0.21	0.63
5	5.144	Disulfoton	Organophosphate	0.21	0.62
6	5.226	δ -Lindane	Organochlorine	0.21	0.62
7	6.531	Methyl parathion	Organophosphate	0.21	0.61
8	6.771	Heptachlor	Organochlorine	0.21	0.62
9	7.055	Ronnel	Organophosphate	0.21	0.62



10	8.144	Aldrin	Organochlorine	0.21	0.62
11	8.582	Chlorpyrifos	Organophosphate	0.21	0.62
12	10.123	Heptachlor epoxide	Organochlorine	0.21	0.62
13	12.198	Endosulfan I	Organochlorine	0.21	0.62
14	13.908	Dieldrin	Organochlorine	0.21	0.62
15	14.192	p',p'-DDE	Organochlorine	0.21	0.62
16	15.338	Endrin	Organochlorine	0.21	0.63
17	16.089	Endosulfan II	Organochlorine	0.21	0.64
18	17.24	p',p'-DDD	Organochlorine	0.22	0.66
19	19.113	Endosulfan sulphate	Organochlorine	0.24	0.74
20	20.044	o,p'-DDT	Organochlorine	0.21	0.63
21	25.286	Methoxychlor	Organochlorine	0.21	0.62

Table 11. Linearity of each pesticide

Accuracy and Precision

Accuracy and precision test are performed to measure the accuracy and repeatability of the analytical method. Accuracy is expressed in per cent recovery, using spiking of organochlorine and organophosphate standard mixture into the vegetables and fruits matrix, ie 0.02 mg/10 g samples for each analyte and 6 replications is performed (ICH, 2005).

Precision is expressed in coefficient variation (CV). Some pesticides are having relatively larger CV than the other due to the peak of the analyte compounds produced relatively smaller compared to others, so that the resulting error is also greater. Based on the value of the CV of all pesticides, then this method meets the acceptance criteria for precision, ie CV<20% for biological analysis (AOAC, 2002).

No	t _R (min)	Pesticide	Class	Recovery (%)	CV (%)
1	3.213	Etophorphos	Organophosphate	70.08	11.71
2	3.921	α-Lindane	Organochlorine	101.64	16.24
3	4.537	β-Lindane	Organochlorine	110.49	2.24
4	4.643	γ-Lindane	Organochlorine	74.08	17.91
5	5.144	Disulfoton	Organophosphate	71.28	6.40
6	5.226	δ-Lindane	Organochlorine	79.56	20.06
7	6.531	Methyl parathion	Organophosphate	77.55	20.20
8	6.771	Heptachlor	Organochlorine	74.03	3.76
9	7.055	Ronnel	Organophosphate	66.29	2.12
10	8.144	Aldrin	Organochlorine	101.75	15.38
11	8.582	Chlorpyrifos	Organophosphate	74.84	19.94
12	10.123	Heptachlor epoxide	Organochlorine	93.99	20.18
13	12.198	Endosulfan I	Organochlorine	100.82	20.88
14	13.908	Dieldrin	Organochlorine	-	-
15	14.192	p',p'-DDE	Organochlorine	108.55	15.85
16	15.338	Endrin	Organochlorine	111.60	20.02
17	16.089	Endosulfan II	Organochlorine	92.34	20.36
18	17.24	p',p'-DDD	Organochlorine	99.82	17.28
19	19.113	Endosulfan sulphate	Organochlorine	70.78	15.81
20	20.044	o,p'-DDT	Organochlorine	105.12	20.77
21	25.286	Methoxychlor	Organochlorine	102.95	18.24

Table 2. Accuracy and Precision of each pesticide



CONCLUSION

Based on the validation parameter values obtained in this study, it can be concluded that the gas chromatographic method for the analysis of organochlorine and organophosphate pesticide residues in fruit and vegetable samples with QuEChERS extraction method has met the requirements.

REFERENCES

1. Consuelo Sanches, Beatriz Albero, German Martin, Jose LT. (2005). *Analytical Sciences* 21 : 1291-1296
2. Dieter Zimmer, Christiane Philipowski. (2006). *Journal of AOAC International* 89(3) : 786-796
3. Horwitz, William. (2000). *Official Methods of Analysis of AOAC International*. 17th Ed, Vol. 2. Gaithersburg, Maryland: *Journal of AOAC International*, Chapter 10, p.11.
4. Lehotay, S.J. (2000). Analysis of Pesticide Residues in Mixed Fruit and Vegetable Extracts by Direct Sample Introduction/Gas Chromatography/Tandem Mass Spectrometry. *Journal of AOAC International* 83(3) : 680-697
5. Lehotay, S. J. (2002) Determination of pesticide residues in non-fatty foods by supercritical fluid extraction and gas chromatography/mass spectrometry: collaborative study. *Journal of AOAC International* 85(5) : 1148-1166
6. Lehotay, Steven J. (2005). *Journal of AOAC International* 88(2) : 595-614
7. Lehotay, Steven J, Katerina Mastovska, Alan R Lightfield. (2005). *Journal of AOAC International* 88(2) : 615-629
8. Lehotay, Steven J. (2007). *Journal of AOAC International* 90(2) : 485-520
9. Nuria Vela, Gabriel Perez, Gines Navarro, Simon N, 2007, *Journal of AOAC International* 90(2) : 544-549
10. Pang, Guo-Fang; Chun-Lin Fan, Yong-Ming Liu, Yan-Zhong Cao, Jin-Jie Zhang, Xue-Min Li, Zeng-Yin Li, Yan-Ping Wu, Tong-Tong Guo, 2006, *Journal of AOAC International*, 89(3) : 740-771
11. Saqib Hussain, Tariq Massud, Karam Ahad, 2002, *Pakistan Journal of Nutrition* 1(1) : 41-42
12. Yanli Xi, Huiru Dong, 2007, *Analytical Sciences* 23 : 295-297
13. Yukiko Ono, Takashi Yamagami, Takeshi Nishina, Toshiaki Tobino, 2006, *Analytical Sciences* 22 : 1473-1476



CHARACTERIZATION OF PARACETAMOL ORALLY DISINTEGRATING TABLET USING GELATIN 1% AND 2% AS BINDER AND POLYPLASDONE XL-10 10% AS DISINTEGRANT (Prepared by Freeze Drying Method)

Roisah Nawatila, Faculty of Pharmacy, Airlangga University, roisahnawatila90@yahoo.com; Dwi Setyawan, Department of Pharmaceutics, Airlangga University;
Bambang Widjaja, Department of Pharmaceutics, Airlangga University

INTRODUCTION

Paracetamol, a para-aminophenol derivative, is usually given per oral as antipyretic and analgesic for the treatment of fever¹. Pediatric patients may have difficulty in ingesting conventional tablets because of their underdeveloped muscular and nervous systems². The concept of Orally Disintegrating Tablets (ODT) emerged with an objective to improve patient's compliance. ODTs disintegrate and dissolve in the mouth in less than 1 minute without the need of water³. Various technologies used in the manufacture of ODT include freeze drying, moulding, direct compression, spray drying, sublimation, and mass extrusion. In the freeze drying method, drying is carried out at low temperature under conditions involving removal of water by sublimation. Here, the drug is physically entrapped in a water soluble matrix, which is then freeze dried to give a product that is highly porous and amorphous³. Freeze drying has some disadvantages such as the product obtained has poor mechanical stability and fragile⁴. Gelatin can inhibit the recrystallization process of amorphous paracetamol by cross-linking and hydrogen bonding between paracetamol and polymer. This interaction may increase the mechanical strength of ODT and keep the amorphous structure⁵. This study aims to determine the characterization of paracetamol ODT using gelatin as binder (1% and 2%)⁶, polyplasdone XL-10 as disintegrant (10%)⁷, and mannitol as filler which prepared by freeze drying method. Paracetamol ODT, physical mixture, and single compound of the material were characterized using Powder X-ray Diffractometry (PXRD), Dif-

ferential Thermal Analyzer (DTA), and Scanning Electron Microscope (SEM).

MATERIALS AND METHODS

Materials

Paracetamol (Hengshui Jiheng Pharmacy[®]), Mannitol (Cargill[®] Cpharm Mannidex 16700), Gelatin (Megasetia[®]), and Polyplasdone XL-10 (ISP Technologies, Inc.).

Methods

Formulation

There were 3 formulations of paracetamol ODT used in this study, each formula contained 120 mg paracetamol/tablet (Table 1).

Materials	F1	F2	F3
Paracetamol	120 mg	120 mg	120 mg
Mannitol	400 mg	400 mg	400 mg
Gelatin	-	1%	2%
Polyplasdone XL-10	10 %	10%	10 %
Weight*	577,78 mg	584,27 mg	590,91 mg

*The content of gelatin and polyplasdone XL-10 calculated from the total weight of the ODT

Table 12. Formulation of Paracetamol ODT

Preparation of Paracetamol ODT

Mix paracetamol, mannitol and Polyplasdone XL-10 carefully by geometric dilution. Gelatin solution was added to powder mixture until a good suspension obtained. The suspension

were then filled into blister by syringe. The blisters were placed in a deep freezer (-80oC) for 24 hours and then freeze dried (-4oC, 20 Pa) for 24 hours. Tablets obtained were stored at room temperature in a close container.

Characterization of Paracetamol ODT
PXRD (Philips X'pert, Netherland): radiation source Cu-K α filter Ni and scintillation counter detector. The condition of instrument was about 40kV, 30 mA, and the divergence-scatter slits 0,5o. Scattering intensity used to fixed-time step scanning around 5o-40o.

DTA (Melter Toledo FP 85 TA Cell, US): the experiment were conducted with temperature 50-250oC and heat flow 10oC/minute.

SEM (Jeol-JSM-6360LA, Japan) was performed on the surface and cross section of the tablet with 200x magnification.

RESULTS AND DISCUSSION

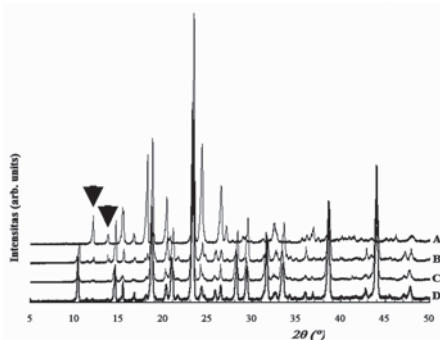


Figure 1. Diffractogram of Paracetamol (A), ODT F1 (B), ODT F2 (C), ODT F3 (D)

Figure 1 showed that single compound of paracetamol showed characteristic crystalline intensity peaks at 12,1o and 13,7o. These peaks showed the alteration of crystallization intensity between paracetamol single compound with paracetamol ODT. The diffractogram showed that F2 has the lowest intensity. However, the decreasing of paracetamol intensity of F2 and F3 was not very significant because of the differences in the amount of gelatin was very small.

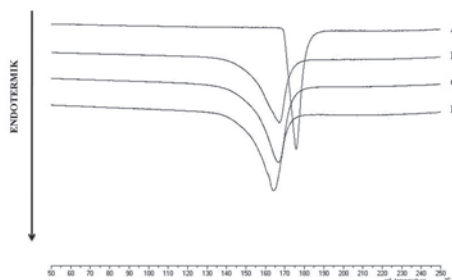


Figure 2. Termogram of Paracetamol (A), ODT F1 (B), ODT F2 (C), ODT F3 (D)

Figure 2 showed the melting point of paracetamol ODTs in each formulation compared to pure paracetamol. The melting point of paracetamol, mannitol, F1, F2, F3 were 171,8oC; 169,6oC; 163,6oC; 162,9oC; 161,2oC. The decreasing in melting point of F1, F2, F3 were due to the eutectic formation of paracetamol and other excipients Formula F3 (with 2% gelatin) showed the lowest melting point. DTA study showed that paracetamol enthalpy could not be determined because of the overlapping of endothermic peaks occurred between paracetamol and other excipients.

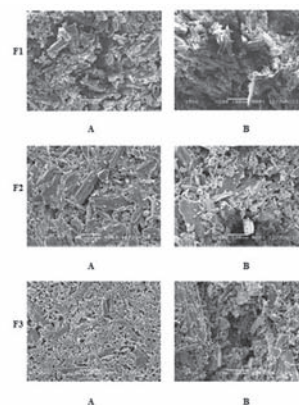


Figure 3. SEM photomicrograph of paracetamol ODT, tablet surface (A), tablet cross section (B)

Figure 3 showed the SEM photomicrograph of the paracetamol ODTs. F3 (gelatin 2%) showed the most subtle particles. This is due to the rigid nature of the gelatin. The characterization using SEM showed that paracetamol ODT prepared by freeze drying method was porous.



CONCLUSION

PXRD study demonstrated that there was significant decrease of paracetamol's intensity in the freeze dried ODTs compared to the single compound of paracetamol, but there was no significant decrease between F2 (gelatin 1%) and F3 (gelatin 2%). DTA study showed that paracetamol enthalpy cannot be determined because of the overlapping of endothermic peaks occurred between paracetamol and other excipients. The SEM photomicrograph showed that paracetamol ODTs prepared by freeze drying method were porous.

REFERENCES

1. McEvoy GK. (2002). AHFS Drug Information. Ed. 4th, Bethesda: American Society of Health-System Pharmacists, Inc., p. 2016-2020
2. Rovers JP, Currie JD, et al. (1998). A Practical Guide to Pharmaceutical Care. Ed. 1st, Washington DC: American Pharmaceutical Association., p. 227-229.
3. Kinchi MPr, Gupta MK, et al. (2010). Orally Disintegrating Tablets: A Future Prospectus. International Journal of Pharmaceutical Science and Biotechnology. Vol.1. No.2, p.71-79.
4. Shukla D, Chakraborty S, et al. (2009). Mouth Dissolving Tablets I: An Overview of Formulation Technology, Scientia Pharmaceutica.
5. Chandrasekhar R., Hassan Z, et al. (2008). The Role of Formulation Excipients in the Development of Lphlised Fast- Disintegrating Tablets. European Journal of Pharmaceutics and Biopharmaceutics, Vol. 72, p. 119-129.
6. Hamed E, Moe D, et al. (2005). Binders and Solvents. In: D.M., Parikh. Handbook of Pharmaceutical Granulation Technology, Ed. 2nd, Boca Raton: Taylor & Francis Group. LLC., p. 109-125.
7. Quadir A, and Kolter K. (2006). A Comparative Study of Current Super disintegrants, Pharmaceutical Technology, Advanstar Communication Inc.



ANTIOXIDANT STUDY OF COSOLVENT SOLUTION OF MANGOSTEEN (*Garcinia mangostana* L.) RIND EXTRACT IN RATS BY USING MDA PA- RAMETER

Ros Sumarny, Liliek Nurhidayati, Yati Sumiyati, Fransiska Diana Santi

Faculty of Pharmacy, Pancasila University, Jakarta, Indonesia

Email: rosaries15@yahoo.com

INTRODUCTION

Mangosteen (*Garcinia mangostana* L.) is a tropical fruit where utilization of mangosteen rind mostly for tanning leather, anti-rust and textile dyes. Research showed that mangosteen rind contains many compounds that are beneficial to health such as anthocyanins, tannins, polyphenols, epicatechin, and xanthone. More than 50 xanthone have been isolated from the rind including α -, β -, γ -mangostin in which α -mangostin is the largest component and is regarded as a marker for product quality control (1). Jung HA, et al showed α -mangostin has antioxidant potency with IC₅₀ of 1,0 ppm using the Mouse Mammary Organ Culture Assay (MMOC) (2).

Mangosteen rind extract were marketed in capsule dosage form meanwhile it is known that mangostin solubility in water is very low (1:>10.000). Enhancement of α -mangostin solubility and in vitro antioxidant effect has been studied by Fatimah who formulate oral solution mangosteen rind extract by using cosolvency technique. The formula include PEG 400, glycerol, sorbitol and 70% demineralized water as cosolvent. The results showed that cosolvent solution meet the requirements for organoleptic, pH, specific gravity and clarity and has antioxidant activity (3).

Thus, to determine in vivo antioxidant effect of cosolvent mangosteen rind solution a comparison study against mangosteen rind extracts suspension was conducted. There are two types of extracts: the same extracts of cosolvent solution (hereinafter referred to as

extract) and marketed extracts from capsule dosage form (hereinafter referred extract[®]). Levels of α -mangostin in cosolvent solution and extracts is equated, 33.1 mg/kg.

MATERIALS AND METHOD

Materials

Mangosteen rind extract solution with 8,94% α -mangostin; mangosteen rind extract capsule with 15,32% α -mangostin; vitamin C; chloroform-ethanol (3:5) solution; 0,01 M epinephrine; 70% and 90% alcohol; 0,0518 M carbonate buffer; ethylene diamine tetra acetate (EDTA); distilled water; 0,9% NaCl; 70% sorbitol; PEG 400; glycerol; aqua demineralization; 0,01 N HCl; MDA standards (SIGMA); carbon tetrachloride (CCl₄); olive oil; 20% trichloroacetic acid (TCA); 0,067% tiobarbiturat acid (TBA) (Merck).

Method

Cosolvent Solution and Extracts Suspension Preparation. Determination of mangosteen rind was performed at "Herbarium Bogoriense", Indonesian Institute of Sciences - Cibinong. 1 kg of mangosteen rind powder was extracted by maceration using 70% ethanol (1:4) for 3x24 hours with stirring. The filtrate is evaporated at 400C and 120 mBar, and evaporated on a water bath to obtain a viscous extract. Solution is made from the extract by cosolvency techniques. Extract and extract[®] suspension were suspended into CMC.

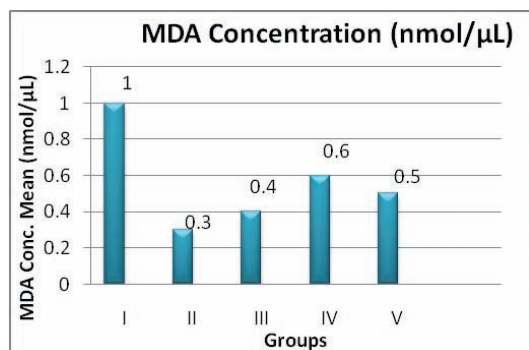
Animals. Twenty five of Sprague-Dawley strain rats were adapted to the laboratory environ-



ment for a week and divided into 5 groups: group I (negative control) were given cosolvent, group II (positive control) were given vitamin C, group III (cosolvent solution), group IV (extract suspension), group V (extract[®] suspension). Treatments were given for 14 days. CCl₄ (dose of 1 mL/kg bw) were induced on day 14, two hours after the last administration of preparation. Blood was collected on day 16. Measurement of MDA concentration. 200 μ L of EDTA plasma was added 1.0 mL of 20% TCA and 2 mL of 0,067% TBA. Mixed on a water bath for 10 minutes. Ambient solution is centrifuged at 3000 rpm for 10 minutes. Pink filtrate absorbance was measured by UV-Vis spectrophotometer at 532 nm wavelength. MDA levels were calculated by using MDA standard curve (4).

RESULT AND DISCUSSION

The average of MDA concentration on day 16 is ranged from 0,3 to 1,0 nmol/mL. Table 1 showed that there were significant differences between group I with group II, III, IV and V ($p < 0,05$) where the highest MDA levels found in group I. High levels of MDA was due to administration of CCl₄ which generated trichloromethyl radicals. This radicals can bind covalently to proteins and unsaturated lipids cause lipid peroxide while animal in group I has no protection.



Notes:

I: Negative control; II: Positive control; III: Cosolvent solution; IV: Extract suspension; V: ekstrak[®] suspension

Figure 1. Average MDA concentration after treatment

Group	Average MDA level (nmol/ μ L)
I (negative control)	1,0 \pm 0,19 ^a
II (positive control)	0,3 \pm 0,05 ^{bc}
III (cosolvent solution)	0,4 \pm 0,04 ^{bc}
IV (extract suspension)	0,6 \pm 0,04 ^{bd}
V (extract [®] suspension)	0,5 \pm 0,00 ^{be}

Note: different sign on the same column showed significant differences ($p < 0,05$)

Generally, a product of lipid peroxidation is determined by measuring the levels of MDA. Highest MDA products in group I related to lowest antioxidant status (5). Lower level of MDA in group II, III, IV and V mean the treatments was able to inhibit the formation of MDA. There was no significant difference ($p > 0,05$) between groups II and group III showed that cosolvent solution has the same capacity as positive control to inhibit MDA formation.

Administration of vitamin C as positive control impacted to the lowest MDA level compare to all groups. As known that vitamin C is an antioxidant which has electron donating groups that can inhibit lipid peroxidation process and stop a formation of new free radical. The same result performed by Ismiyati who found the administration of vitamin C can eliminate free radicals as indicated by the decrease in MDA levels (6).

MDA levels in groups III, IV and V are lower compare to group I, meaning cosolvent solution and extracts have the ability to prevent lipid peroxidation and MDA formation. The results in line with Arsana, et al. which showed that mangosteen rind extract can inhibit the formation of MDA in rats given maximum physical activity (5).

Potential inhibition of MDA formation against negative control in group II by 70% and group III by 60%, the ability of inhibition in both groups did not differ significantly ($p > 0,05$). Group IV



is able to inhibit the formation of MDA by 40% and group V by 50%, both lower than cosolvent solution. Difference ability to inhibit MDA formation between treatments occur due to the differences in the dosage form. Cosolvent solution was able to decrease MDA levels higher than extracts suspension, because the solubility of α -mangostin has been enhanced with cosolvency method. The results of this study indicate that the dosage form cosolvent solution has a higher antioxidant capacity than the extracts suspension dosage form. These results are supported by previous research by Fatima who showed solubility of α -mangostin enhancement with cosolvency techniques obtained IC50 value 2,4809 ppm (very active) by using 1,1-Difenil-2-picrylhydrazyl (DPPH) (3).

CONCLUSION

The results showed that cosolvent solution has higher antioxidant capacity to inhibit MDA level compare to extracts suspension. Potential inhibition of MDA formation of cosolvent solution is 60% while extracts suspension are 40% and 50%.

REFERENCES

1. Aisha AFA, Abu-Salah KM, Ismail Z, Majid AMSA. (2013). Determination of total xanthones in Garcinia mangostana fruit rind extracts by ultra violet (UV) spectrophotometri. *J Med Plants Res*;7(1):29.
2. Jung AH, Su BN, Keller, Mehta RG, Kinghorn AD. (2006). Antioxodant xanthones from the pericarps of *Garcinia mangostana* (Mangosteen). *J Agric Food Chem*;54:2077-82.
3. Fatimah. (2013). Formulasi larutan oral ekstrak kulit buah manggis (*Garcinia mangostana* L.) sebagai antioksidan dengan teknik kosolvensi (script). Jakarta: Fakultas Farmasi Universitas Pancasila;.24-32.
4. Panjaitan RGP, Handharyani E, Chairul, Masriani, Zakiah Z. (2007). Pengaruh pemberian karbon tetraklorida terhadap fungsi hati dan ginjal tikus. *Makara Kesehatan*;11(1):11-16.
5. Arsana IN, Adiputra, N, Pangkahila, JA, Putra-Manuaba, IB. (2013). *Garcinia mangostana* L. rind extract and physical training reduce oxidative stress in wistar rats during maximal physical activity. *J Bio Sci*;7(2):63-68.
6. Winarsi H. (2007). Antioksidan alami & radikal bebas: potensi dan aplikasinya dalam kesehatan. Yogyakarta: Kanisius;15,11-22,56-57,77-81,86-96,141.

ACKNOWLEDMENT:

The authors are grateful to Ditlitabmas Ditjend Dikti for Hibah Bersaing research funding as DIPA Kopertis Wilayah III No. 023.04.189705/2014.



SCREENING OF SELECTED PHILIPPINE ROOT CROPS FOR α -Glucosidase INHIBITION

Sarah Jane S. Almazora, Adamson University, 900 San Marcelino St., Ermita, Manila, Philippines, sarah_almazora@yahoo.com, +63907-722-5090 / +63927-481-7189

Ivan L. Lawag, Chemistry Department, College of Science, Adamson University, 900 San Marcelino St., Ermita, Manila, Philippines, ivan.lawag@gmail.com, +63917-504-5962

INTRODUCTION

A number of developing countries all around the world are still dependently using traditional herbal medicines in curing numerous illnesses since it is the only affordable sources of healthcare with fewer side effects (Odhav et al., 2010). Traditionally, diabetes is one of the common diseases that are used to be treated with herbal medicines. Diabetes is a chronic metabolic disorder of carbohydrates, fats and proteins that can affect a large number of populations in the world (Patel et al., 2012). It is generally attributed to the in unhealthy lifestyle and aging that is characterized by a high blood glucose level due to some abnormalities in pancreas that results to low insulin level (Patel et al., 2012 and Lawag et al., 2012).

According to Odhav et al., 2010, it is about 173 million of people suffer from diabetes worldwide and about 5% of those diabetic patients died. If this would not be prevented, the expected mortality would increase by 50% in the next 10 years. In the Philippines, over a million of Filipinos have been suffering from such chronic disease (Patel et al., 2012 and Lawag et al., 2012).

A number of different ways of treating such disease were established by many researchers. The α -glucosidase enzyme inhibition would be one of the responsible for the decrease of blood glucose level that is needed to breakdown the sugars which resulted to decrease in glucose levels (Odhav et al., 2010 and Lawag et al., 2012). These enzymes inhibitors only delays and prevents the absorption

of ingested carbohydrates that controls the elevated blood glucose level therefore treats diabetes and prevents other complications brought by the disease (Lawag et al., 2012). Plants are always been good provider of different medicine for different illness. Numerous of plants and its parts such as leaves, fruits, bark and roots have been investigated and reported to possessed anti-diabetic property that lowers blood glucose activity without side effects (Odhav et al., 2010).

Similar with the numerous edible plant species, root crops can also be identified for having a compound which can inhibit α -glucosidase enzyme (Kumari et al., 2012). Root crops are one of the most important staple foods and a substitute food worldwide. It is grown all over the world and usually has low commercial value for direct consumption (Champagne et al., 2011 and Wickramasinghe et al., 2009). Root crops are widely used as food and as major ingredients for the production of beverages, pasta, alcohol drink, and natural colorants (Xu et al., 2010). There are several root crops have been reported to treat various diseases such as diabetes. In this study, the selected Philippine root crops used (Fig.1) are *Dioscorea alata* L. and *Dioscorea* sp. (Dioscoreaceae), *Manihot esculenta* Crantz (Euphobiaceae), *Maranta arundinacea* L. (Marantaceae), *Xanthosoma sagittifolium* (L.) Schott (Araceae) and *Stenomeris dioscoreifolia* Planch (Dioscoreaceae). These root crops are widely used as folk medicine in treating diverse diseases and can be identified for having a compound which can inhibit α -glucosidase enzymes (Ku-

mari et al., 2012). In order to investigate the anti-diabetic property of selected Philippine root crops, the crude extract was screened for

α -glucosidase enzyme inhibitory activity and for phytochemical constituents.



Figure 1: Selected Philippine root crops (from left: *Dioscorea alata* L., *Manihot esculenta* Crantz, *Maranta arundinacea* L., *Xanthosoma sagittifolium* (L.) Schott and *Stenomeris dioscoreifolia* Planch)

METHODS

The root crops were washed, peeled, separated the peel from the flesh, oven-dried at 40°C, pulverized using laboratory mill and extracted using 90% ethanol. Crude extracts were obtained by using rotary evaporator under reduced pressure at 40-50°C. These crude extracts were screened for phytochemical constituents such as alkaloids, phenolic compounds, essential oils, triterpenes, steroids, sugars, and flavonoids using 20% H₂SO₄ in ethanol, vanillin-sulfuric acid, α -naphthol-sulfuric acid, potassium ferricyanide-ferric chloride and Dragendorff's reagent as spray reagents. The α -glucosidase enzyme inhibitory activity was screened using yeast α -glucosidase enzyme and analyzed using enzyme-linked immunosorbent assay (ELISA).

RESULTS AND DISCUSSION

Except for the *Stenomeris dioscoreifolia* Planch peel, with the highest inhibition activity, *Dioscorea* sp. peel, *Stenomeris dioscoreifolia* Planch flesh, *Dioscorea alata* L. peel and *Dioscorea alata* L. flesh with IC₅₀ value of 55.10±1.48 μ g/mL, 109.72±1.58 μ g/mL, 166.32±3.34 μ g/mL, 346.49±1.35 μ g/mL and 651.79±1.39 μ g/mL respectively; all other crude extracts shows no inhibition or has an IC₅₀ values that is greater than 1000 μ g/mL. The qualitative phytochemical analysis of ethanolic crude extract showed the presence

of alkaloids, flavanoids, triterpenes, phenols, tannins, steroids, sugars, and essential oils.

ROOT CROPS		IC ₅₀ RESULT
<i>Dioscorea alata</i> L.	Peel	346.49±1.35 μ g/mL
	Flesh	651.79±1.39 μ g/mL
<i>Dioscorea</i> sp.	Peel	109.72±1.58 μ g/mL
	Flesh	<1000 μ g/mL
<i>Manihot esculenta</i> Crantz	Peel	<1000 μ g/mL
	Flesh	<1000 μ g/mL
<i>Maranta arundinacea</i> L.	Peel	<1000 μ g/mL
	Flesh	<1000 μ g/mL
<i>Xanthosoma sagittifolium</i> (L.) Schott	Peel	<1000 μ g/mL
	Flesh	<1000 μ g/mL
<i>Stenomeris dioscoreifolia</i> Planch	Peel	55.10±1.48 μ g/mL
	Flesh	166.32±3.34 μ g/mL

Table 13: IC₅₀ values of selected Philippine root crops

Diabetes is one of the chronic diseases worldwide that is necessary to have immediate action for its prevention. A lot of herbal medicinal plants have been proven to be effective on preventing diabetes. The significance of this study was its contribution to the new information about the root crops which has α -glucosidase enzyme inhibitory activity that may help in controlling the blood glucose level. It also provides a new α -glucosidase inhibitor which is necessary in preventing diabetes. The effects of starchy foods, such as root crops which are rich in carbohydrates, on blood glu-



cose and insulin level may differ extensively because of the difference in carbohydrate, fat, protein and dietary fiber content that may be ingested (Bornet et al., 1989).

CONCLUSION

The crude extract of *Stenomeris dioscoreifolia* Planch peel and flesh, *Dioscorea* sp. Peel and *Dioscorea alata* L. peel and flesh showed a significant enzyme inhibitory activity. This indicated that the root crops can be identified as α -glucosidase enzyme inhibitor which may help in controlling the blood glucose level that may prevent diabetes.

This study contributes to the aim of the other researchers to give additional knowledge by providing adequate information about the capabilities of the selected root crops. Moreover, it could also be a reference of the medical practitioners specially the pharmacist and pharmacological laboratories in formulating a new drug that may help in preventing diabetes.

This is the first screening of the anti-diabetic property of the selected Philippine root crops, this study also gives awareness to the diabetic patients specially the local people that eating root crops as part of their diet may help prevent diabetes and may reduce the number of mortality of diabetic patients. Since this is the first screening of the anti-diabetic property of the selected Philippine root crops and further study must be done to determine the compound that is responsible for the α -glucosidase enzyme activity.

REFERENCES

1. Bornet F.R.J., Fontvieille AM., Rizkala S., Colonna P., Blayo A., Mercier C, & Slama G. (1989). Insulin and glycemic responses in healthy humans to native starches processed in different ways: correlation with in vitro α -amylase hydrolysis. *American Society for Clinical Nutrition, Am J Clin Nutr* 1989;50:315-23.
2. Kumari B., Sharma P. & Nath A.K. (2012). α -Amylase inhibitor in local Himalyan collections of *Colocasia*: Isolation, purification, characterization and selectivity towards α -amylases from various sources. *Pesticide Biochemistry and Physiology* 103, 49–55.
3. Lawag I.L., Aguinaldo A.M., Naheed S. & Mosihuzzaman M. (2012). α -Glucosidase inhibitory activity of selected Philippine plants. *Journal of Ethnopharmacology* 144, 217–219.
4. Odhav B., Kandasamy T., Khumalo N. & Baijnath H. (2010). Screening of African traditional vegetables for their α -amylase inhibitory effect. *Journal of Medicinal Plants Research* Vol. 4(14), pp. 1502-1507.
5. Patel DK, Kumar R, Laloo D & Hemalatha S (2012). Diabetes mellitus: An overview on its pharmacological aspects and reported medicinal plants having anti-diabetic activity. *Asian Pacific Journal of Tropical Biomedicine*, 411-420.



NIOSOME EMULGEL FORMULATION AND STABILITY TEST OF CINNAMON (*Cinnamomum burmanii* Nees & Th. Nees) BARK ETHANOLIC EXTRACT AS ANTIOXIDANT

Darijanto, Sasanti T., Faculty member of School of Pharmacy ITB, Ganesha 10, Bandung 40132, sasanti@fa.itb.ac.id. 022-7108158; Fidriani, Irda., Faculty member of School of Pharmacy ITB, Ganesha 10, Bandung 40132, irda@fa.itb.ac.id. 022-2504852 ; Widhita P.A.S., student assistent of School of Pharmacy ITB, Ganesha 10, Bandung 40132, widhita@live.com. 085623402920

INTRODUCTION

Exposure of UV radiation on earth is a serious threat for human skin because of its ability to increase the risk of photo oxidative damage which can lead to skin aging by the presence of free radical. Therefore, added of exogenous antioxidant may needed to prevent the damage caused by free radical. There was a study who claimed that cinnamon contains several compounds such as phenol, flavonoid, and tannin that have antioxidant activity and an emulgel formulation of cinnamon extract was also already developed. However, the emulgel formulation of cinnamon extract showed a decreasing antioxidant activity. This research aimed to make a niosome formula of cinnamon extract to increase its stability

MATERIALS AND INSTRUMENT

Materials

Cinammon bark, ethanol, sorbitan monostearic, cholesterol, water de ion, ascorbic acid, DPPH (2,2-difenil-1-pikrilhidrazil), Virgin coconut oil (VCO), glycerin, Sodium lauryl sulfic, cetostearyl alcohol, polyvinyl pirolidone (PVP). Instrument

Reflux apparatus, rotary evaporator , UV lamp (Desaga Starded Gruppe), vortex, spectrofotometer UV-Vis (Beckman coulter DU 720), particle size analyzer (Beckman Coulter®DelsaTM Nano C Particle Analyzer), probe sonicator (Ivymen Homogenaizer), vacuum desicator.

Simplisia preparation

Cinammon bark collected from Lembang , East Java, in January 2014. Plant determination was done in Herbarium Bandungense, SITH ITB. Cinammon bark cut and dried in oven at

40oC for 4 days, after that its grinding until a fix range of particle size

EXPERIMENT METHODE

Extraction and extracts characterization

Crude drug of cinnamon bark was extracted by reflux method using solvent ethanol 96%, monitoring was done using thin layer chromatography with toluene-ethyl acetate (93:7) as mobile phase and then determinate the spot appearance

Phyto chemistry screening

Identification chemistry group in extracts includes : alkaloid, flavonoid, saponin, , steroid /terpenoid, tannin and quinon. Completed with another test included: determined water content of simplisia , concentration of extracts that its soluble in water and soluble in ethanol and also extracts densities

Antioxidant activity test of extracts with DPPH as scavenging agent

Absorption determination of extracts
Cinammon bark after incubation the extracts methanol solution 1 : 1 (volume) with DPPH methanol solution for 30 minutes. The change of absorbance determined with spectrofotometri method, at maximum wave length 517 nm . As standard solution used 50 µg/ml ascorbic acid solution in methanol to compare the antioxidant activities.

Niosome preparation of ethanol extracts cinammon bark

Niosome was prepared using thin layer hydration method with various weight of cinnamon extract loaded and various molar ratio of surfactant and cholesterol. Sorbitan monostearic,



cholesterol and extracts dissolved in chloroform and then the solvent evaporated used rotary evaporator until its formed dry lipid thin layer in the evaporator vessel. After that lipid thin layer hydrated with water de ion, its formed vesicles with random particle sizes.

Reduced particle size of niosome

Reduced the vesicle size with probe sonicator for 5 minute in cool box, with 60 % amplitude and pulse mode 5 seconds ran and 5 seconds stop. These method to obtain vesicles with average size less than 300 nm

Evaluation and characterization of extracts cinnamon bark niosome

Determined the particle size and polydispersion index of niosome vesicle, activities antioxidant and scavenging activity of niosome, emulgel and emulgel niosome formulation of extracts ethanol cinnamon bark, performance evaluation of the dosage form, and accelerated stability test.

EXPERIMENT RESULTS

Table 1 Phytochemistry Screening

Chemistry groups	Simplisia	Extract
Saponin	-	-
Quinon	+	+
Flavonoid	+	+
Alcaloid	+	-
Tanin Chatechat	+	+
Tanin Galat	-	-
Steroid/Triterpenoid	+	+

Table 2 Characterization of Cinnamon Bark simplisia

Characterization (%)	Value
Water content	4,00
Concentration of extract soluble in ethanol	68,83
Concentration of extract soluble in water	18,83

Amount of extracts about 29,27% calculated from simplisia weight and density of 1% extract ethanol of cinnamon bark 0,8189 g/mL. Determined scavenging activity of DPPH as free radical, gave value of Ic50 extracts ethanol cinnamon bark provide DPPH scavenging activity, compared with ascorbic acid as a standard solution 50 ppm was 0.299 µg/ml and Ic50 value of ascorbic acid was 0.280 µg/ml .

Statistically, scavenging activity DPPH emulgel niosome of extracts ethanol cinnamon bark, there was no significant change of the scavenging activity DPPH ($p < 0,05$). In the other side decreased scavenging activity DPPH of extracts ethanol cinnamon bark significantly changed ($p < 0,05$).

.Table 3. Final Formula of emulgel and emulgel niosome of extracts ethanol cinnamon bark

Component	Emulgel Extract (w/w)	Emulgel Niosome (w/w)
VCO	20	20
Glycerin	10	10
SodiumLauril	0,7	0,7
Sulfic		
Cetostearil	6,3	6,3
Alcohol		
PVP	3	3
Metyl Paraben	0,18	0,18
Propyl Paraben	0,02	0,02
BHA	0,02	0,02
Extracts of cinnamon bark	0,05	0,05 (in 0,2 mmol niosome)
Water de ion	100	100

CONCLUSION

IC50 of extracts ethanol cinnamon bark was 0,299 ppm and IC50 of ascorbic acid was 0,280 ppm. From these result IC50 extracts ethanol of cinnamon bark compared with ascorbic acid most equal. Composition of niosome consist of 200 µmol surfactant and 20 µmol cholesterol and 10 mg extracts ethanol of cinnamon



bark have a good stability and could optimal entrapment. Based from characterization and stability test of the niosome, there was no differentiation of particle size $166,63 \pm 1,72$ nm, polydispersity index $0,296 \pm 0,02$ and activity antioxidant $80,44 \pm 1,58\%$. Formulation final emulgel exhibited good physical stability and for extracts and extracts niosome

REFERENCES

- Ahmad M., Pin Lim C., Akowuah G.A, Ismail N., Hashim M.A, Hor S.Y, Ang L.F, Yam M.F. 2013. Safety assessment of standardised methanol extract of *Cinnamomum burmannii*. *Phyto-medicine* 20, 1124-1130
- Azima, F., Muchtadi, D., Zakaria, F., & Priosoeryanto, B., 2004, Kandungan Fitokimiadan Aktivitas Antioksidan Ekstrak Cassia Vera (*Cinnamomum burmannii*), *Stigma* Volume XII, ISSN: 0853-3776, 233-234
- Bishnu, J., Sunil, L., Anuja, S., 2009. Antibacterial property of different medicinal plants: *Ocimum sanctum*, *Cinnamomum zeylanicum*, *Xanthoxylum armatum* and *Origanum majorana*. *Kathmandu University Journal of Science, Engineering and Technology* 5 (1), 143–150
- Lauer, A.C., Lieb, L.M., Ramachandran, C., Flynn, G.L., Weiner, N.D., 1995. Transfollicular drug delivery. *Pharm. Res.* 12, 179–186
- Sarker, S. D., Latif, Z., and Gray, A. I. (Eds.). 2005. *Natural Products Isolation* (2nd ed.), Humana Press Inc, New Jersey.



THEOPHYLLINE RELEASE FROM SUSTAINED RELEASE TABLET USING LACTOSA AND PVP K30 AS A CHANELLING AGENT

Sugiyartono, Faculty of Pharmacy Airlangga University, Darmawangsa Dalam Surabaya, sgytnff@yahoo.com ; 08155125474; **Retno Sari**, Faculty of Pharmacy Airlangga University, Darmawangsa Dalam Surabaya; **Agus Syamsur Rijal**, Faculty of Pharmacy Airlangga University, Darmawangsa Dalam Surabaya; **Tri Mulyani**, Faculty of Pharmacy Airlangga University, Darmawangsa Dalam Surabaya; **Agustina Maharani**, Faculty of Pharmacy Airlangga University, Darmawangsa Dalam Surabaya.

INTRODUCTION

Sustained release dosage form, in the last two decades, have made significant progress in term of clinical efficacy and patient compliance (Merkus, 1986). Sustained release preparation is a pharmaceutical preparation which releases the drug substance in the long term. The duration of this release is intended to minimize the release rate so that it can function as a decisive step to achieve the desired therapeutic effect like.

Various synthetic as well as natural polymer have been investigated and developed in sustained drug delivery application.

Non ionic cellulose ether, and most frequently hydroxypropyl methyl cellulose (HPMC) have been widely studied for their applications in oral slow drug released system, Sustained Released (SR) system. Among the polymers which can be used as an active ingredient elepasan controller, HPMC K100M has been widely studied. As a hydrophilic matrix, HPMC K100M has advantages such as: can release the active ingredient to 100%, thereby reducing the trapped material.

HPMC K100M is a high viscosity so that it can significantly slow down the release. To fix these adverse characteristics, HPMC K100M is often combined with other matrices having high solubility so as to increase the release of the active ingredient. B Polymers of this kind is referred to as channeling agent. Materials that can be used as a channeling agent include lactose and PVP K30.

The influence of commonly used channeling agent, lactose and PVP K30, on drug release from HPMC K100M

(Hydroxypropylmethylcellulose K100M) has been investigated.

HPMC K100M matrix tablet of theophylline using lactose and PVP K30M as a channeling agent were prepared by wet granulation.

A model formulation contained 60% w/w drug (theophylline), 30% w/w HPMC K100M, 0,5% w/w Magnesium Stearate, 4%, 6% and 8% PVP K30 and 10%, 15% and 20% Lactose.

METHODS

Table 1 A model HPMC and Channeling Agent formulation Used in This Study

FORMULA	THEO -HYLLINE (mg)	HPMC K100M (mg)	MgSTEA RATE (mg)	LACTOS E (%)	PVPK 30M (%)
FL0	200	100	1,5	-	
FL1	200	100	1,5	10%	
FL2	200	100	1,5	15%	
FL3	200	100	1.5	20%	
FP1	200	100			4%
FP2	200	100			6%
FP3	200	100			8%

Tablets containing 200 mg drug, were compressed using a Graseby Specac hydraulic press equipped with an 10,0 mm flat faced punch and die set. The compression force and compression time were 0,5 ton, 30 seconds respectively (FP1, FP2 and FP3) and 0,5 ton. 5 seconds (F, FL1, FL2 and FL3)

In vitro release studies of theophylline Drug release was determined by using dissolution tester USP XII. The dissolution tester were performed using 900 ml distilled water at 37°C ± 0,5°C and rpm was set at 50. Samples



of 5 ml were withdrawn from the dissolution medium at 5', 10', 20', 30', 60', 120', 180', 240', 300', 360', 420' and 480'. That amount was replaced with fresh medium to maintain the volume constant.

The absorbance of the sample, were measured at 272 nm using a Shimadzu UV-1201 UV/Vis doubled beam spectrophotometer (Shimadzu, Japan)

RESULT AND DISCUSSION

Kinetic modelling of drug release

Afer completing in vitro dissolution of all batches for eight hours, the data was treated with zero order, Higuchi and First order

1. $Mt = M_0 + k_0.t$
2. $\ln Mt = \ln M_0 + k_1.t$
3. $Mt = M_0 - kHt^{1/2}$

Table 2 : Release rate constant and R-squared values for different release kinetics

FORMULATION	% Release	Zero Order (R ²)	First Order (R ²)	Higuchi (R ²)
F	29,43±1,25	0,9796	0,9889	0,9945
FL 1	31,18±1,49	0,9780	0,9886	0,9957
FL2	31,32±0,72	0,9750	0,9862	0,9958
FL3	41,32±0,45	0,9734	0,9877	0,9916
FP1	29,13±0,82	0,9792	0,9888	0,9949
FP2	31,26±0,82	0,9508	0,9696	0,9935
FP3	28,12±1,26	0,9835	0,9906	0,9890

From the kinetic of drug release studying, the result showed that all of the formulation followed Higuchi's model.

The experimental was undertaken to observe the influence of channelling agent (lactose and PVP K30) on theophylline release from HPMC K100M.

Drug release of tablet containing channelling agent (lactose and PVP K30) and tablet without channelling agent (F) were evaluated . The result shows that channelling agent increase theophylline release, that is attributed mainly to the excipients solubility.

Table 3 : The criteria of theophylline release (states in USP XXIV) and Theophylline Release

T (hr)	% release	% Theophylline Release						
		F	FL1	FL2	FL3	FP1	FP2	FP3
1	3-15	7,38	7,96	7,84	12,52	7,54	7,47	6,66
2	20-40	12,67	13,60	13,65	15,87	12,79	15,55	12,29
4	50-75	18,97	20,32	20,63	27,77	18,19	22,01	16,94
6	65-100	24,49	27,29	27,89	36,98	23,66	27,00	23,06
8	>80	29,43	31,18	31,32	41,32	29,13	31,26	28,12

Table 3 : The criteria of theophylline release (states in USP XXIV) and Theophylline Release

All of the formulation didn't meet to the criteria of theophylline release from sustained release dosage form that stated in USP XXIV

CONCLUSION :

- 1.Theophlline release affected by channelling agent in this formulation. Lactose and PVP K30 increase drug release
- 2.All Formulation did not meet o the criteria of theophlline release from sustaned release dosage form that stated in USP XXIV

REFERENCES

1. Ansel, H.C., Popovich, N.G., Allen, L.V., Jr. 1995. Pharmaceutical Dosage Form and Drug Delivery System. 6th Ed. Philadelphia of Pharmacy 20thphia: Lea Febiger
2. Aulton : M.E., 2002. Pharmaceutics: The Science of Dosage Form Design. 2Ed.Ed. Churchill Livingstain, London p. 298
3. Gennaro, A.R., 2000. Remington : The Science and Practice of Pharmacy. 20th Ed., Volume 2., Philadelphia : Lippincott Williams & Wilkins
4. Kibbe, A.H., 2000, Handbook of Pharmaceutical Exipients, 3th Edition, American Pharmaceutical Associa



ICPPS 2014

Proceeding
The 1st International Conference
on Pharmaceutics & Pharmaceutical Sciences

- tion USA, p. 252-254, p. 305-307, p. 392-396 Bethesda, p. 1954-1956
5. McEvoy, G.K., 2002. AHFS Drug Information. American Society of Health System Pharmacist Inc.,
 6. Shargel, L., Wu-Pong, S. Dan Yu, A.B., 2005, Applied Biopharmaceutics and Pharmacokinetics, 5th Edition, USA: McGraw-Hill, p. 414, 422-424, 515-532
 7. Sweetman, S.C., 2009. Martindale : The Complete Drug Reference. 36th Edition. London: Pharmaceutical Press, p. 1766-1768
 8. The United States Pharmacopoeial Convention Inc., The Pharmacopoeia of The United States of America. 24th Revision. The United States Pharmacopoeia Pharmacopoeia Inc. Washington D.C.



EFFORTS TO PRODUCE 1-(BENZOYLOXY)UREA AS ANTICANCER DRUG CANDIDATE

Suko Hardjono, Faculty of Pharmacy, Airlangga University, Indonesia
e-mail : suko.hardjono@yahoo.com, phone : 0818311345

Backgrounds

Hydroxyurea is an antineoplastic compound which has activity to inhibit ribonucleotide reductase enzyme. The function of the enzyme is to inhibit DNA biosynthesis by converting ribonucleotides to deoxyribonucleotides. This activity is called cytotoxic or antineoplastic, which has special effects on S phase. (Salim, 2004).

Hydroxyurea is also useful in treatment of sickle cell anemia because it eases the pain of the patients, which has been attributed to its ability to generate nitric oxide, a potent vasodilator. Nitric oxide may also contribute to the antitumor effect of hydroxyurea, since it is known to inhibit ribonucleotide reductase probably because it contains an unpaired electron and therefore it is able to quench the tyrosine radical. (Avendano, 2008)

There are facts which show that with the substitution on the lead compound has the consequence which will change the lipophilic, electronic and steric effects (Korolkovas, 1988). To design new drugs, the physicochemical properties of the drug molecules should be predicted before they are synthesized and purified.

Molecular modeling and virtual screening have become an established method to lead discovery to enhance efficiency in activity optimization of lead compound. In silico test or molecular modeling is a term for experiment or test that has been done with computer simulation. (Istiyasto, 2007). Molecular interaction energy between receptor and ligand is observed with Rank Score. In silico test is done through docking the molecules of drug compound candidate with the chosen receptor. Docking is a means to harmonize ligand which is

small molecule into receptor which is a big protein molecule, with regard to their nature to one another (Jensen, 2007).

Ribonucleotide reductase was established as the principal target of anticancer compounds as hydroxyurea and its derivative 1-(benzoyloxy)urea. These compounds formed a complex with crystal structure of yeast ribonucleotide reductase I (2EUD).

Synthesis of 1-(benzoyloxy)urea was performed by reacting hydroxyurea with benzoyl chloride. The reaction mechanism is inclusion of the nucleophilic hydroxyl group of hydroxyurea to the carbonyl group of benzoyl chloride (Clayden et al., 2001; Zinner et al., 1969).

The objectives of this research are to synthesize the compound and determine anticancer activity.

Methods

The docking scores of hydroxyurea and 1-(benzoyloxy)urea which formed a complex with crystal structure of yeast ribonucleotide reductase I (2EUD) calculated by Molegro program.

Synthesis of 1-(benzoyloxy)urea was performed by reacting hydroxyurea with benzoyl chloride. The reaction mechanism is inclusion of the nucleophilic hydroxyl group of hydroxyurea to the carbonyl group of benzoyl chloride. The TLC and melting point test were indicated the purity of the compound. Structure identification was done based on FT-IR, and ¹H/¹³C-NMR spectrometry.

Results



a. Molecular modeling

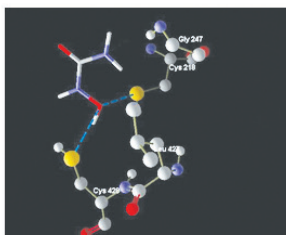


Figure 1: Interaction of hydroxyurea – 2EUD

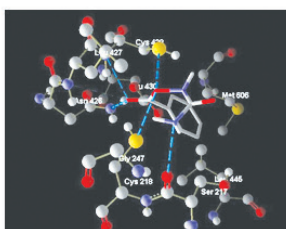


Figure 2: Interaction of 1-(benzoyloxy)urea – 2EUD

Compound	Amino acid
hydroxyurea	Cys 428, and Cys 218
1-(benzoyloxy)urea	Cys 428, Cys 218, Ser 217, Asn 426 and Leu 427

Table 1: Hydrogen bonding involved in interaction of the compounds with 2EUD

Table 2: Rerank Score of the compounds with 2EUD

b. Synthesis

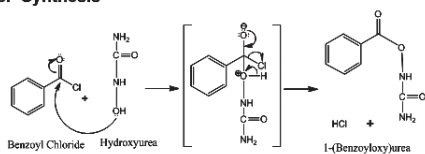


Figure 3 : The reaction mechanism of 1-(benzoyloxy)urea synthesis

Form	white powder
Melting point	128-129 °C
FT-IR	3131 and 3205 (-NH2); 3273 (-NH); 1747 (-C=O ester); 1671 (-C=O amide); 1581(-C-C-ar);1103(-C-O-);703 (-C-H ar)
¹ HNMR	9.77 (-NH); 7.63-7.99 (benzene ring); 6.56 (-NH2),
¹³ CNMR	164,9 (-CON-);159,2 (-COC-); 127.6 to 133.7 (6C ar).
MS	m/z135(C ₇ H ₆ NO ₂ ⁺);105(C ₇ H ₅ O ⁺);77(C ₆ H ₅ ⁺)

Table 3 : The result of 1-(benzoyloxy)urea synthesis data.

c. Anticancer activity test

Compound	IC ₅₀
hydroxyurea	430.21µg/ml.
1-(benzoyloxy)urea	76.38µg/ml

Table 4: Anticancer activity of the compounds

Discussions

Hydrogen bonding involved in interaction of 1-(benzoyl- oxy)urea with 2EUD are: Cys 428, Cys 218, Ser 217, Asn 426 and Leu 427. While hydroxyurea only interacted with Cys 428, and Cys 218.

The final Rerank Score (RS), which is the score of the last stage. Rerank score of the compounds with 2EUD by molegro showed that 1-(benzoyloxy)urea (-79.9432) has lower energy values than hydroxyurea (-43.3565) It means that the compounds are reasonable to be synthesized.

TLC results of only one spot and sharp melting point indicates that the pure powder. According to the FT-IR, ¹HNMR, ¹³CNMR and MS spectra, 1-(benzoyloxy)urea was successfully synthesized.

The result of anticancer activity test with HeLA cell showed tha 1-(benzoyloxy)urea (IC₅₀ 76,38 µg/ml) more active than hydroxyurea (IC₅₀ 430.21 µg/ml).

Conclusions

1. From the results of the in silico test can be predicted that 1-(benzoyloxy)ureahas anticancer activity better than hydroxyurea. It means that the compounds is reasonable to be synthesized.
2. From the results of the identification of the structure showed that 1-(benzoyloxy)urea has been successfully synthesized.
3. As anticancer drug candidate, 1-(benzoyloxy)urea was more active than hydroxyurea.

Acknowledgement

I would like to express my deepest gratitude to: Prof. Dr. Siswandono, MS., Apt., Airlangga University as promotor; Prof. Dr. Purwanto, Apt. and Prof. Drs. Win Darmanto, MSi.,PhD., Airlangga University as co-promotor; Prof. Dr. Toshio Honda, Hoshi University, Japan,



for mass spectroscopy; Prof. Supargiyono, DTM&H, SU, Sp.Par (K), Gajah Mada University, for the permission in anticancer activity determination test.

References

1. Avendano C & Menendes J.C, 2008, Medicinal Chemistry of Anticancer Drugs, p.13, Elsevier, Amsterdam.
2. Clayden, Greeves, Warren & Wothers, 2001, Organic Chemistry, Oxford University Press, New York : 279-303;
3. Istyastono E.P.,2007, (<http://www.komputasi.lipi.go.id>. 16/12/2007)
4. Jenzen. F.,2007, Introduction to Computational Chemistry, 2nd Ed, Odense, Denmark: 415-416.
5. Korolkovas Andrejus, 1988, Essentials of Medicinal Chemistry, Development of Drugs, pp.53-90;
6. Salim A.K et al, 2004, Genetics and Molecular Biology, Vol.27,no 1,Sau Paulo;
7. Silverstein R.M. et al, 2005, Spectroscopic Identification of Organic Compounds, John Wiley & Sons, Inc, 82;
8. Xu. H. et al, 2006, Structure of eucaryotic ribonucleotide reductase I efine gemcitabine diphosphate binding and subunit assembly, Proc.Nat. Acad.Sci.Use 103: 4026 – 4033;
9. Zinner G., Staffel R., 1969, Carbamylation of hydroxylamine. 36. Hydroxylamine derivatives, Arc Pharm Ber Ges, pp.438-447;



DEVELOPMENT OF PEGYLATED RAPAMYCIN LITHOCHOLIC ACID MICELLE FOR CANCER THERAPY

Aran Tapsiri, beth_kung_konnarak@hotmail.com; Kanokwan Jaiprasert, nokzy.rx.469@gmail.com; Rungtip Nooma, mai_mcd@hotmail.com; Awadsada Sukgasem, feeble_playgirl@hotmail.com; Supang Khondee, School of Pharmaceutical Sciences, University of Phayao, 19 M. 2 Maeka, Muaeng, Phayao 56000 Thailand, s.khondee@gmail.com.

INTRODUCTION

Rapamycin is an inexpensive but effective lipophilic macrolide antibiotic with anti-fungal, immunosuppressive, and anticancer characteristics. Rapamycin was formulated as an anti-rejection drug for kidney transplant, i.e. Rapamune®, and an anti-restenosis agent in drug-eluting coronary stents, e.g. Johnson and Johnson's Cypher® stent. In addition, recent studies reported that rapamycin can induce significant regression of colonic adenomas in CPC;Apc mice and could improve therapy of colorectal cancer. Rapamycin has poor water solubility (2.6 µg/mL at 25°C), and is difficult to formulate as an injectable solution without using a co-solvent. In addition, rapamycin is very unstable in PBS and HEPES buffer. Micelles are attractive drug delivery systems for hydrophobic drugs because of their solubilizing ability that can increase drug loading, extend drug release, and lengthen plasma half-life. Many of micellar platform are biocompatible and biodegradable. They also have been studied extensively for drug delivery. Deoxycholic acid and derivatives have been used to modify chitosan as nanocarriers for cancer treatment. In this study, hydrophobic lithocholic acid (LCA) was conjugated with hydrophilic polyethylene glycol (PEG) to prepare micelles for packaging rapamycin, a model lipophilic drug. This micelle was expected to increase rapamycin solubility, has good in vitro stability and long circulation half-life from a PEG sheath.

METHODS

Synthesis of micelle platform
PEG amine (3 kDa) was dissolved in ethanol and NaOH was added. LCA was dissolved in ethanol. EDC was added to LCA solution, following by adding NHS. PEG amine solution was

added to LCA after 10 min for activation. The reaction was allowed to stir overnight at RT. The solvent was partially removed under N₂ and the product was precipitated in cold diethyl ether, centrifuged, and vacuum dried.

Micelle preparation

Micelles were prepared by dissolving pegylated LCA in PBS. Conjugates were sonicated. Rapamycin stock solution was added to polymer solution. The solution was sonicated. The organic solvent was removed by purging with N₂. The micelle solution was centrifuged to remove insoluble material.

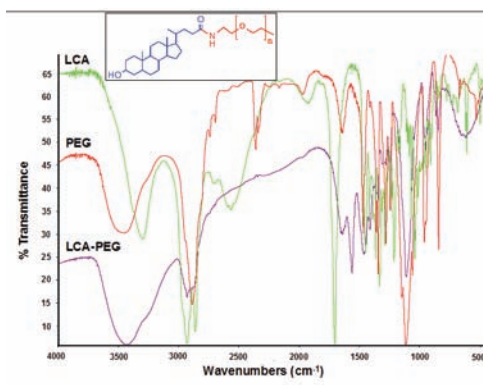


Figure 1. FTIR spectrum of LCA-PEG and parent compounds. Inset shows chemical structure of LCA (blue)-PEG (red) conjugate.

micelle solution was centrifuged to remove insoluble material.

Micelle characterization

Dynamic Light Scattering (DLS)

Hydrodynamic diameters and surface charges of micelles were determined on a Mavernanosizer.

Transmission Electron Microscopy (TEM)

Samples were prepared onto copper grids

with 1% uranyl acetate (negative staining). TEM images were obtained on a Philips CM-100 TEM.

Critical micelle concentration (CMC)

CMCs were determined by following changes in the fluorescence emission spectra of pyrene in the presence of different concentrations of micelles. Pyrene was dissolved in acetone and aliquots of stock solution were added to tubes

to provide final pyrene concentrations of 6 μ M. Acetone was evaporated and replaced with micelles prepared in serial dilution. Solutions were incubated at 55°C overnight. Excitation and emission wavelengths were set at 335, 371 and 383 nm, respectively.

Entrapment efficiency (EE)

The amount of rapamycin was determined by HPLC with C18 column. Detection was set at wavelength of 276 nm.

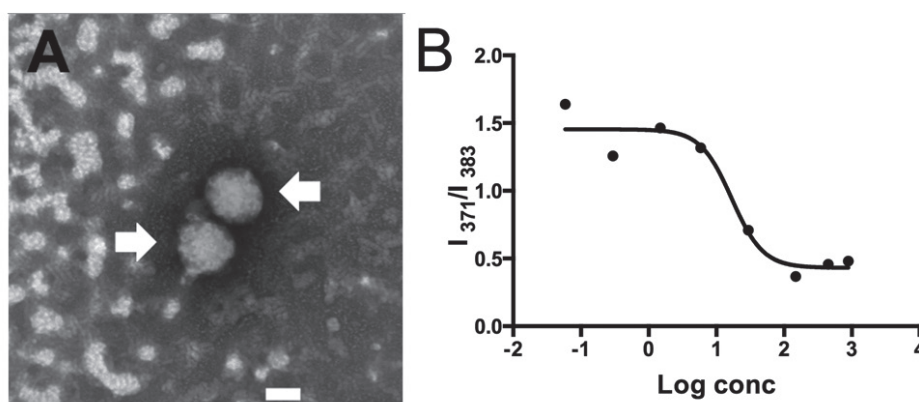


Figure 2: (A) TEM image shows morphology of LCA-PEG micelle, scale bar 100 nm. (B) Critical micelle concentration (CMC) of pegylated LCA micelle; I_1 = emission peak 1 intensity at 371 nm, I_3 = emission peak 3 intensity at 383 nm.

Mobile phase was methanol and 0.1% glacial acetic acid in water (85:15) at a flow rate of 1 mL/min.

Release study

Micelle solutions were prepared at 6.7 mM. Rapamycin was encapsulated ~9% (w/w) in micelles, and 6 mL of each solution was transferred into 12 kDa MWCO dialysis bag. Dialysis bags were placed in PBS (37°C). At fixed time points, aliquots were taken and drug concentrations were measured by HPLC.

RESULTS AND DISCUSSION

Synthesis of LCA-PEG had high yield (91.6 \pm 3.7%). The change in structure of resulting product was monitored using FTIR. LCA-PEG showed a combination of LCA and PEG characteristics (3200-3600 cm^{-1}) and had similar C-H stretching (2800-3000 cm^{-1}) compared to parent compounds (Fig. 1). On dynamic light scattering, the mean hydrody-

namic diameters of plain and rapamycin LCA-PEG micelles were 183.2 \pm 19.3, 234.6 \pm 4.5 nm, respectively, with slight negative surface charges. The micelle has polydispersity index (PDI) of ~0.1. This parameter provides an estimate of the size distribution, and shows that the micelles were relatively monodispersed. Micellar size observed on TEM was similar with that determined on DLS. The TEM observation revealed that the spherical micelles were formed by self-assembly of pegylated lithocholic acid, Fig. 2A. Fluorescence probe studies with pyrene on micelles revealed low critical micelle concentration (CMC), 17 μ M, Fig. 2B. CMC is the concentration at which micelles form spontaneously. Micelles that have low CMCs are good candidates for solubilization of hydrophobic substances in water. The entrapment efficiency (%EE) of rapamycin LCA-PEG micelle was 24.9 \pm 1.1 or 29% (w/w).



With pegylated LCA micelle, rapamycin solubility was improved (~86 fold). Rapamycin LCA-PEG micelles showed sustained release of rapamycin with a half-life of 9.5 hours.

CONCLUSION

The lack of suitable rapamycin formulations had hampered its progression into clinic. We have reported a formulation of rapamycin that does not require organic co-solvent or harsh surfactants to solubilize rapamycin. The sustained release and high rapamycin loading of this micelle may offer significant benefits in cancer treatment, and the nanoscale dimension may improve tumor delivery through the EPR effect. This approach may be generalized further to formulation of other large, lipophilic chemotherapy or imaging agents.

REFERENCES

- Forrest ML, Won C-Y, Malick AW, Kwon GS. In vitro release of the mTOR inhibitor rapamycin from poly (ethylene glycol)-b-poly (ϵ -caprolactone) micelles. *Journal of Controlled Release*. 2006;110(2):370-377.
- Kim K, Kwon S, Park JH, et al. Physicochemical characterizations of self-assembled nanoparticles of glycol chitosan-deoxycholic acid conjugates. *Biomacromolecules*. 2005;6(2):1154-1158.
- Miller SJ, Heist KA, Feng Y, et al. Multimodal imaging of growth and rapamycin-induced regression of colonic adenomas in apc mutation-dependent mouse. *Translational oncology*. 2012;5(5):313-320.



FEASIBILITY OF ORAL IMMUNIZATION AGAINST JAPANESE ENCEPHALITIS VIRUS USING CHITOSAN PARTICLES

Supavadee Boontha, School of Pharmaceutical Sciences, University of Phayao, Phayao, 56000, Thailand, e-mail address: supa0865@hotmail.com; **Worawan Boonyo**, Department of Technical Pharmacy Program, Sirindhorn Collage of Public Health Phitsanulok, Phitsanulok, 65130, Thailand ; **Hans E. Junginger; Tasana Pitaksuteepong; Neti Waranuch; Assadang Polnok**, Department of Pharmaceutical Technology, Faculty of Pharmaceutical Sciences, Naresuan University, Phitsanulok 65000, Thailand; **Narong Nitatpattana; Sutee Yoksan**, Center for Vaccine Development, Institute of Molecular Biosciences, Mahidol University, Salaya, Nakhonpathom 73170, Thailand.

INTRODUCTION

Japanese encephalitis virus (JEV) causes human encephalitis in several of Asian countries including Japan, South Korea, Taiwan and Thailand. There are estimated 35,000-50,000 annual cases and approximately 20%-30% of patients die (1). There is no effective treatment for encephalitis from JEV and the therapy only consists of palliative care and management of complication. Hence, vaccination presents the most efficient and cost-effective disease control tool to prevent JE encephalitis in humans. However, JE vaccine is administered only via subcutaneous (S.C.) or intramuscular (I.M.) routes, which may have a high risk of infection with blood-borne pathogens. Oral vaccinations are safe and a convenient alternative. It offers several advantages over parenteral immunization. Due to the needle-free, non-invasive nature, oral administered vaccines may reduce the risk of infection, and may also be more cost-effective because they enable large scale immunization without trained medical personnel. They also can increase vaccinee compliance. Particulate delivery systems are known to protect the associated antigen from degradation when in contact with the gastrointestinal (GI) fluids and to enhance absorption of antigens in the GI tract (2). To design these systems, chitosan was chosen as particulate carrier because it is biodegradable, biocompatible and safe for use in humans (3). In the pharmaceutical field, chitosan is used as excipient and drug carrier. Moreover, chitosan is able to reversibly open the tight junctions and possesses mucoadhesive properties

which enhance the absorption across mucosal epithelium as well as it is able to prolong the residence time of delivery systems at the absorption sites (4). Also, it has been reported that the molecular weight (MW) of chitosan influences the potency and duration of immune responses (5). Therefore, the aim of this study was to evaluate the feasibility of using chitosan particles for oral vaccination against JEV.

MATERIALS AND METHODS

Materials

Three types of chitosan having low (Chi-L), medium (Chi-M) and high (Chi-H) molecular weight (MW) were used. Chi-L (MW = 160 kDa, degree of deacetylation (DD) = 96%) and Chi-H (MW = 500 kDa, DD = 96%) were obtained from Aqua Premier (Chonburi, Thailand). Chi-M (MW = 270 kDa, DD = 93%) was received from Primex (Haugesund, Norway). Mouse brain-derived formalin inactivated JEV (Beijing-1 strain, lot JVJ51001) was a kind gift from the Thai Government Pharmaceutical Organization (GPO) (Bangkok, Thailand). Preparation of JEV-loaded chitosan particles JEV-loaded chitosan particles were prepared by ionic gelation with tripolyphosphate (TPP) as reported by Boontha et al. 2010 (6). For characterization of particles, size and surface charges of particles were determined by using a photon correlation spectroscopy (PCS) (Zeta-Plus, Brookhaven Instrument, UK). Loading efficiency (LE) was determined by using Micro bicinchoninic acid (Micro BCA) assay. Particles



morphology were determined with a scanning electron microscope (SEM) (LEO 1455VP, LEO Electron Microscopy Ltd, UK).

Immunization protocol

Five groups of 8 Swiss albino mice were immunized orally or subcutaneously (s.c.) on days 0, 7 and 30 with various formulations (Table 1). Blood samples were collected on days 37. JEV neutralizing antibody in mouse sera was measured using a virus plaque reduction neutralization test (PRNT) with a 50% plaque reduction endpoint (PRNT₅₀).

Oral immunization

Group 1: 10 µg protein content of JEV in sterile water for injection (SWFI)

Group 2: 10 µg protein content of JEV in Chi-L particle

Group 3: 10 µg protein content of JEV in Chi-M particle

Group 4: 10 µg protein content of JEV in Chi-H particle

Subcutaneous immunization

Group 5: 2 µg protein content of JEV in SWFI

Table 14. Immunized formulations.

RESULTS AND DISCUSSION

Characteristic of JEV-loaded chitosan particles

Particles	Size (µm)	Charge (mV)	LE (%)
Chi-L	2.18 ± 0.15	+12.3 ± 2.7	38 ± 3
Chi-M	2.30 ± 0.16	+9.9 ± 1.7	36 ± 1
Chi-H	2.52 ± 0.26	+14.9 ± 1.5	36 ± 1

Table 2. The characteristic of JEV-loaded particles.

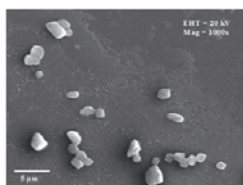


Figure 1. SEM image of JEV-loaded particles prepared from high MW chitosan (Chi-H) 1000x

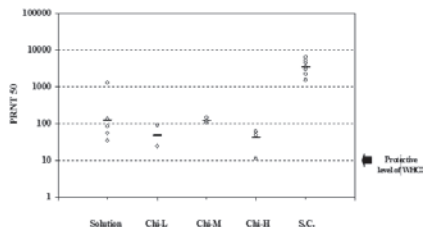


Figure 2. The PRNT₅₀ of JEV-neutralizing antibodies obtained in the sera of mice following oral immunization with JEV in different formulations.

The protective immunization titers of JEV-neutralizing antibodies were determined from all groups of mice as shown in Fig. 2. Immunization of JEV via s.c. route (Group 5) induced the highest level of JEV-neutralizing antibodies (GMT = 3366) when compared with immunization potential of free JEV and JEV-loaded chitosan particles via the oral route. JEV encapsulated in all types of chitosan particles could induce the JEV-neutralizing antibodies levels higher than the minimal requested level (>1:10) by the WHO following oral immunization. Using the different types of chitosan, Chi-M particles could induce the highest JEV neutralizing antibodies GMT level of 119 whereas Chi-L and Chi-H particles could generate the JEV antibodies GMT level of 46 and 40, respectively. However, the JEV neutralizing antibodies initiated by particles prepared using three types of chitosan were not significantly different. This may be due to the fact that the JEV-loaded chitosan particles have similar characteristics in terms of size, charge and loading contents, resulting in the similar results of the potential of carriers for provoking immune responses to JEV following oral administration. Also, comparison between mice administered with Free JEV (inducing JEV-neutralizing antibodies GMT of 120) and JEV encapsulated in chitosan particles through the oral route, resulted in no significant differences.

CONCLUSION

The results of this work demonstrate that chitosan particles as adjuvant have the feasibility for oral JEV immunization and the MW of chitosan appeared to have no effect on the ability to elicit protective neutralizing antibodies to JEV in Swiss albino mice after oral immunization. Interestingly, although the differences were not statistically significant, free JEV (i.e. JEV in SWFI) seemed to be better in the initiation of immune responses to JEV compared with particles-encapsulated JEV.



REFERENCES

1. Solomon T, Dung NM, Kneen R, Gainsborough M, Vaughn DW, Khanh VT. (2000). Japanese encephalitis. *J Neurol Neurosurg Psychiatry*, 68:405–15
2. Van der Lubben IM, Kersten G, Fretz MM, Beuvery C, Verhoef JC, Junginger HE. (2003). Chitosan microparticles for mucosal vaccination against diphtheria: oral and nasal efficacy studies in mice. *Vaccine*, 21:1400-8.
3. Illum L. (1998). Chitosan and its use as a pharmaceutical excipient. *Pharm Res*, 15:1326-31.
4. Kotzé AF, De Leeuw BJ, Lueßen HL, De Boer AG, Verhoef JC, Junginger HE. (1997). Chitosan for enhanced delivery of therapeutic peptides across intestinal epithelia: in vitro evaluation in Caco-2 cell monolayer. *Int J Pharm*, 159:243-53.
5. Boontha S, Junginger HE, Waranuch N, Polnok A, Pitaksuteepong T. (2010). Formation of particles prepared using chitosan and their trimethyl chitosan derivatives for oral vaccine delivery: Effect of molecular weight and degree of quaternization. *Songklanakarin J Sci Technol*, 32:363-71
6. Vila A, Sanchez A, Janes K. (2004). Low molecular weight chitosan nanoparticles as new carriers for nasal vaccine delivery in mice. *Eur J Pharm Biopharm*, 57:123-31.

ACKNOWLEDGEMENTS

The authors wish to acknowledge the National Center for Genetic Engineering and Biotechnology (BIOTEC) for the financial support of this study.



THE INFLUENCE OF HYDROXY GROUP AT ORTHO (o) AND PARA (p) POSITIONS ON METILBENZOAT AGAINST SYNTHESIS OF HIDROKSIBENZOHIDRAZIDA DERIVATIVES

Suzana, Departement of Pharmaceutical Chemistry, Faculty of Pharmacy Airlangga University, suzanarushadi@yahoo.com; **Adita R.**, Alumni Faculty of Pharmacy Airlangga University; **Melanny Ika .S.**, Departement of Pharmaceutical Chemistry, Faculty of Pharmacy Airlangga University; **Juni Ekowati**, Departement of Pharmaceutical Chemistry, Faculty of Pharmacy Airlangga University; **Marcellino Rudyanto**, Departement of Pharmaceutical Chemistry, Faculty of Pharmacy Airlangga University; **Hadi Poerwono**, Departement of Pharmaceutical Chemistry, Faculty of Pharmacy Airlangga University; **Tutuk Budiati**, Departement of Pharmaceutical Chemistry, Faculty of Pharmacy Airlangga University

ABSTRACT

This study aims to determine the effect of the hydroxy groups at ortho (o) and para (p) positions on methylbenzoate against synthesis 2-hydroxybenzohydrazide and 4-hydroxybenzohydrazide. Percentage of synthesized compounds were obtained, benzohydrazide 61% with melting point 109-111 oC, for compounds 2-hydroxybenzohydrazide obtained 75%, m.p 140-141 oC and 4-hydroxybenzohydrazide obtained percentage yield 79%, m.p 264-265 oC. Identification of compounds were used UV-Vis, Infrared and ¹H-NMR spectroscopies. Hydroxy groups at the ortho and para positions on methylbenzoate can increase the reactivity of the carbonyl C atom, so increasing of percent reaction yields.

Keyword : Synthesis, hydroxy group, hydroxybenzohydrazide derivatives

INTRODUCTION

Synthesis of drugs interest in the development of the pharmaceutical industry. Modifying of the structures can change to its biological activity. Hydrazide derivatives are often used because they have biological activities and diverse clinical applications such as anticancer, antimicrobial and anti-tuberculosis. Awathi et al (2007) have conducted research synthesis hydrazide derivative 2-hydroxybenzylidene and ((1H-indole-3-ilmetlen) hydrazide) using microwave irradiation, a mixture of ester and hydrazine hydrate (mole ratio 1:1), the results obtained about 85 -90%. In another study conducted Jain et al, 2007, the synthesis of 2-hydroxybenzohydrazide using microwave irradiation within 120 seconds, the synthesis results obtained 90%. In this research synthesis benzohydrazide, 2-hydroxybenzohydrazide and 4-hydroxybenzohydrazide. Synthesis is done by using the conventional method , without

the toxic solvents and more environmentally friendly methods. Reduced use of toxic solvents and energy savings in accordance with campaign green chemistry.

Based on the background above, the problems are formulated in this study : whether can be synthesized benzohydrazide, 2-hydroxybenzohydrazide and 4-hydroxybenzohydrazide compounds? Is there any effect of the hydroxy group at the ortho and para positions on the methylbenzoate of synthesized benzohydrazide derivatives? The benefits of research can yield new knowledge about the reaction method to synthesize of benzohydrazide, 2-hydroxybenzohydrazide and 4-hydroxybenzohydrazide compounds. The reaction is described as Figure 1.

MATERIALS AND METHODS

Materials

All chemicals were used in this study with a

degree of purity p.a unless otherwise stated. The chemical were methylben-zoate, methyl-salicylate, methyl-4-hydroxybenzoate, hydra-zine hydrate, ethanol 95%, chloroform, ethyl acetate, acetone, hexane, KBr, silica gel 60 GF254.

Instruments

Glasswares commonly used in the chemical synthesis laboratories ; Sanyo microwave EM-S 800 Watt, UV-Vis Spectrophotometer HEWLETT PACKARD 8452A; IR Spectrophotometer M 500 Buck Scientific; FT- NMR spectrometer JEOL ECS -400.

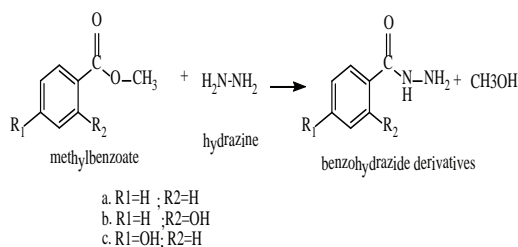


Figure 1. Reaction of benzohydrazide derivatives formation from methylbenzoate and hydrazine hydrate

Methods

Synthesis of benzohydrazide and hydroxybenzo-hydrazide derivatives (Qinrong et al , 2011) Methylbenzoate/derivatives (10 mmol) and hydrazine hydrate (20 mmol) were mixed enter in the reaction flask (25 ml). A mixture was stirred until homogeneous. The mixed solution was refluxed on a water bath for 2 h with stirring (perfection reaction was monitored by thin layer chromatography). The mixture was cooled to room temperature and then added to 20-30 ml of aquadest, washed with ethanol, filtered. Crystals were recrystallized with ethanol 95%. The purity tests use melting point and thin layer chromatography using three different eluent. Identification of compounds were performed using UV-VIS, FT-IR and 1H-NMR spectroscopies.

RESULTS AND DISCUSSION

Synthesis benzohydrazide derivatives were done with nucleophilic substitution reaction. Benzohydrazide is obtained as a white needles crystalline. Synthesized percentage is 61%. Purity test results with thin-layer chromatography shows a stain, with melting point 109-111 oC. Identification benzohydrazide with UV-Vis, FT-IR, and 1H-NMR spectroscopies can be seen in Table 1. 2-Hydroxybenzohydrazide is white needles crystalline. Synthesized percentage is 75%. Purity test results with thin-layer chromatography shows a stain, m.p 140-141 oC. Identification results of 2-hydroxybenzohydrazide with UV - Vis, Infrared, and 1H - NMR spectroscopies can be seen in Table 2.

Table 1. Identification of UV-Vis , Infrared, and 1H-NMR spectra of benzohydrazide

UV-Vis Spectrum: λ max (nm) in ethanol solvent	203 and 221
Infrared spectrum : ν (cm^{-1}) in the KBr pellet	1662 (-C=O amide), 3295 and 3194 (-NH ₂), 1609 (-C=C- aromatic ring), 1532(-NH), 1342 (C -N amide), 3006 (Csp ² -H)
¹ H- NMR Spectrum : δ (ppm) In the solvent DMSO - D ₆	10.00, singlet, 1H (NH), 7.41 -7.93, multiplet, 5 H (C ₆ H ₅ -)

Table 2. Identification of UV-Vis , Infrared, and 1H-NMR spectra of 2-hydroxybenzohydrazide

UV-Vis Spectrum: λ max (nm) In ethanol solvent	210, 236 and 300
Infrared spectrum : ν (cm^{-1}) in KBr pellet	1645 (-C=O amide), 3266 (-OH phenolic), 1590 (-C=C- aromatic ring), 1532(-NH), 1354 (C -N), 3053 (Csp ² -H), 750 (orto substitution), 3266 and 3319 (-NH ₂)
¹ H - NMR Spectrum : δ (ppm) in the solvent DMSO-D ₆	12.47, singlet, 1H (-OH), 12.07 singlet, 1H(-NH), 6.90, doublet, J=8.5 Hz, 1H (C ₆ H ₄ -), 6.85, triplet, J=8.1 Hz, 1H (C ₆ H ₄ -), 7.40 triplet, J=8.8 Hz, 1H (C ₆ H ₄ -), 7.80, doublet, J=9.1 Hz, 1H(C ₆ H ₄ -), 4.66, singlet (-NH ₂)



4-Hydroxybenzohydrazide is white needles crystalline. Synthesized percentage is 79%. Purity test results with thin-layer chromatography shows one stain, m.p 264-265 oC. Identification results of 4-hydroxybenzohydrazide with UV-Vis, Infrared, and ¹H-NMR spectroscopies can be seen in Table 3.

Shintthesized of 2-hydroxybenzohydrazide and 4-hydroxybenzohydrazide compounds are obtained respectively 75% and 79% greater than benzohydrazide (61%). The presence of hydroxy groups in positions ortho and para at methylsalicylate and methylparaben cause to the carbonyl C increase the reactivity. Hydroxy groups act as negative inductive (-I) that can increase the electron density on the aromatic rings (from methylsalicylate and methylparaben), so it becomes more electronegative. As a result, the carbonyl C atom becomes more electropositive. Thus C carbonyl of methyl-2-hydroxybenzoate (methylsalicylate) and methyl-4-hydroxybenzoate (methylparaben) are more easily attacked by nucleophiles (hydrazine). So that the hydroxy group at ortho and para positions can increase the yield of hydroxybenzohydrazide derivatives.

Table 3. Identification of UV-Vis, Infrared, and ¹H-NMR spectra of 4-hydroxybenzohydrazide

UV-Vis Spectrum: λ max (nm) in ethanol solvent	208 and 254
Infrared spectrum : ν (cm ⁻¹) in KBr pellet	1674 (-C=O amide), 3318 (-OH phenolik), 1590 (-C=C- aromatic ring), 1536 (-NH), 1326 (C-N amide), 3005 (Csp ² -H), 767 (orto substitution), 3197 (-NH-) and 3318 (-NH ₂)
¹ H-NMR Spectrum : δ ? (ppm) in the solvent DMSO-D ₆	9.89, singlet, 1H (-OH), 9.45, singlet, 1H (-NH-), 7.64, doublet, J=9.1 Hz, 2H (C ₆ H ₄ -), 7.73 doublet, J=9.1 Hz, 2H (C ₆ H ₄ -), 4.32, singlet (-NH ₂)

CONCLUSION

The compounds of benzohydrazide, 2-hydroxybenzohydrazide and 4-hydroxybenzohydrazide can be synthesized by react methylbenzoate derivatives and hydrazine hydrat

. The yield percentage were obtained 61% (benzohydrazide), 75% (2-hydroxybenzohydrazide) and 79% (4-hydroxybenzohydrazide). Hydroxy group at orto and para positions on methylbenzoate can increase yield percentage 2-hydroxybenzohydrazide and 4-hydroxybenzohydrazide.

REFERENCES

1. Ajani, OO, Obafemi C A, Ikpo CO, Ogunniran Ko and James OO, 2009. Comparative Study of microwave assisted and Conventional Synthesis of Noval 2-quinaxa. Journal of Physical Sciences Vol.4(4), pp.156-164,
2. Awathi S, Rishishwan P, Rao A.N, Ganesha K, Malhotra R.C, 2007. Synthesis Characterization and Spectral Studies of Various Never Long Chain Aliphatic acid (2-hydroxy benzylden and 1H-indol-3-ylmethylene) hydrazides as mosquito para-pheromon, Journl of The Korean Chemical Society Vol.51(6):pp. 506-512.
3. Furniss B.S., Hannaford A.J., Smith P.W.G., Tatchell A.R., 1989. Vogel's Text book of Practical Organic Chemistry, 5th edition, Longman, London, p.236.
4. Jain AK, Gupta PK, Ganesan K, Pande A, Malhotra RC, 2007, Rapid solvent free Synthesis of Aromatic Hydrazides under Microwave Irradiation, Defence Science Journal Vol.57(2) : 267-270.
5. McMurry, J. 2008. Organic Chemistry 7th Edition Thomson Learning Inc. USA pp. 877-884.



6. Rollas S.S., Kucukguzel G., 2007. Review Biological Activities of Hydrazone Derivatives, *Molecules*, 2007, (12), pp.1910-1939, (online), (www.mdpi.org/molecules/abstract/23-08-2011).
7. Qinrong W., Ying P., Jinzhi W., Qing P., Hongjun L., Jinghong Z., 2011. Synthesis and biological activities of substituted N'-benzoylhydrazone derivatives, *African Journal of Biotechnology*, Vol. 10(78), pp. 180



ANTIOXIDANT ACTIVITY TEST OF BEE PROPOLIS EXTRACT (*Apis mellifera* L.) USING DPPH (1,1-diphenyl-2-picrylhydrazyl) FREE RADICALS SCAVENGING ACTIVITY

Titiek Martati, Faculty Pharmacy Univ.of Pancasila, Srengseng Sawah Jagakarsa, South Jakarta, titiek_martati@yahoo.com, (021) 7864727; Shahyawidya, FFUP, Srengseng Sawah Jagakarsa, South Jakarta, 6281315377950

INTRODUCTION

Propolis or bee glue is a resin collected by honey bees from the sap flow sources such plants or sapling which is mixed with saliva and various enzymes that exist in honey bees(1). Propolis has antioxidant activity, contains a variety of compounds such as polyphenols (flavonoids aglycones, phenolic acids, alcohols and ketones), sesquiterpenes, coumarins, steroids, sour variety of trees. The chemical composition of propolis varies depend on the origin of the material collected by honeybees, different trees will produce different compositions. The most important is the composition of propolis flavonoids and phenolic acids (2). Test antioxidant activity using 1,1-diphenyl-2-picrylhydrazyl (DPPH) as a source of free radicals. DPPH in this test is reduced by antioxidants which releases hydrogen to form the reduced DPPH-H (3). The color changed from violet to yellow and followed by a decrease in the absorption wavelength of 517 nm, with a decrease in absorption, then the catcher radical antioxidant activity can be determined. (4) The antioxidant activity of propolis is affected by its chemical composition. In this study assessed the antioxidant activity of honey bee propolis originating from the three different types of kapok, rambutan and longan trees(4).

MATERIALS AND METHODS

MATERIALS. Pure propolis is derived from the kapok, longan and rambutan trees. Equipment used in this investigation were extraction unit, evaporation unit and one set of ascorbic acid (vitamin C) unit, DPPH radical scavenging activities were evaluated by using spectrophotometry.

METHODS. Isolation of propolis. Pure propolis from 3 trees was isolated by extraction. Approximately 10 g of propolis was maserated with 500 ml of ethanol for 6 hour at 40o C allowed to stand 24 h and partition with ethyl acetate:water (1:1) 3 times 100 ml. Solvent was then evaporated using vacuum rotary evaporator to obtain dry extract. The weight and yield of the dried extract were then calculated.(5) Analysis of free radical scavenging activity Phytochemical screening showed that ethanol and ethyl acetate extracts were contained flavonoids. The antioxidant activity was analyzed by 1,1-diphenyl-2-picrylhydrazyl (DPPH) 0.4 mM. IC50 (Inhibition Concentration) is the concentration of antioxidants (ppm) capable of inhibiting 50% of the activity of free radicals. The data were analyzed using the regression equation. IC50 obtained from the equation $y = a + bx$ where $y = 50$ and showed IC50 values of x . Data analysis. The data obtained were analyzed by two ways ANOVA ($p < 0.05$), followed by the Least Significant Difference Test (LSD).

RESULTS AND DISCUSSION

Yield of ethanol extract showed 89.93%, 79.96%, 81.83% and ethyl acetate extract 98.31%, 75.41%, 66.55% and all extracts positive for flavonoids. IC50 of the ethanol extract of propolis kapok tree is 10.04 ppm and ethyl acetate fraction of propolis kapok tree is 7.79 ppm. IC50 of the ethanol extract of propolis rambutan tree is 11.02 ppm and ethyl acetate fraction of propolis rambutan tree is 9.07 ppm. IC50 value of ethanol extract of propolis longan tree is 9.31 ppm and the ethyl acetate fraction of propolis longan tree is 6.35 ppm. The highest antioxidant activity of ethyl ac-

etate fraction of propolis longan tree because it has the smallest IC₅₀ among all the samples of propolis, it caused by vitamin C and quercetin contained as antioxidants. Beside longan leaves also contain flavonoids which are antioxidants. Longan and rambutan fruit both contain vitamin C 84 mg, 58 mg each in 100 g samples. The antioxidant activity of propolis extracts kapok tree is higher than the propolis extract rambutan tree, this is due to the presence of the polyphenol contained in kapok tree. Sugar or carbohydrates contained in the longan and rambutan tree act as antioxidants.

Statistical analysis ($\alpha = 0.05$) showed significant differences in the respective extracts of propolis and propolis samples of each treatment. Two-ways analysis of variance (ANOVA) was tested and showed significant differences result due to $F_{count} > F_{table}$ is $956.82 > 3.98$ for samples and $3364.91 > 4.84$ for treatment at $\alpha = 0.05$. The LSD showed significant differences as indicated by the difference in the values.

Conc. (ppm)	Blank absorb. (Ab)	Absorbans				Inhibition (%)	IC ₅₀ (µg/mL)
		AS ₁	AS ₂	AS ₃	AS ₄ (rata-rata)		
1	0,843	0,770	0,772	0,769	0,770	8.6200	3,07
1,5		0,617	0,618	0,615	0,617	26.8486	
2		0,563	0,563	0,562	0,563	33.2543	
2,5		0,516	0,516	0,517	0,516	38.7505	
3		0,386	0,385	0,386	0,386	54.2507	
3,5		0,336	0,336	0,337	0,336	60.1028	
4		0,294	0,295	0,295	0,295	65.0455	
4,5		0,229	0,228	0,234	0,232	72.4397	
5		0,171	0,172	0,171	0,171	79.6758	

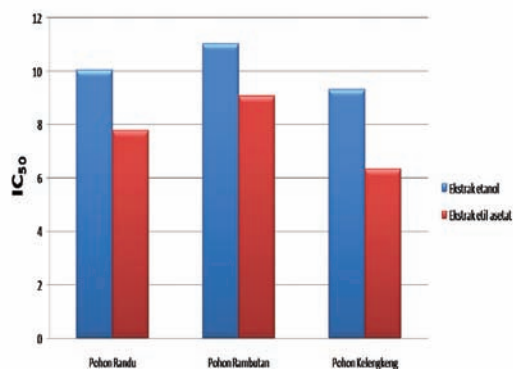
Table 1. Antioxidant activity of vitamin C

Ethanol extracts of propolis	IC ₅₀			
	IC ₅₀ (1)	IC ₅₀ (2)	IC ₅₀ (3)	IC ₅₀ (average)
Kapok tree	9,89	10,10	10,14	10,04
Rambutan tree	11,04	10,99	11,03	11,02
Longan tree	9,40	9,25	9,28	9,31

Table 2. IC₅₀ ethanol propolis extract

Ethyl acetate extract of propolis	IC ₅₀			
	IC ₅₀ (1)	IC ₅₀ (2)	IC ₅₀ (3)	IC ₅₀ (average)
Kapok tree	7,63	7,88	7,87	7,79
Rambutan tree	9,14	8,97	9,09	9,07
Longan tree	6,35	6,37	6,32	6,35

Table 2. IC₅₀ ethanol propolis extract



CONCLUSION

1. Each sample of propolis extract has antioxidant activity due to the IC₅₀ of less than 200 ppm.
2. The best antioxidant is ethyl acetate fraction of propolis longan tree because it has the smallest IC₅₀ value among all the samples and treatments (6.35 ppm).

REFERENCES

- Siripatrawan U, Vitcayakitti W, Sanguandeeukul R. (2012). .Antioxidant and antimicrobial properties of Thai propolis extracted using ethanol aqueous solution. International Journal of Food Science and Tchonology.;(48):22-27.
- Radiati L, Thohari I, Agustina N H.(2007). Kajian propolis, pollen, and royal jelly pada produk madu sebagai antioksidan alami. Jurnal Ilmu dan Teknologi Hasil Ternak.; 2(1):35-39.
- Kumar N, Ahmad M, Dang R, Husain A (2008).. Antioxidant and antimicrobial activity of propolis from Tamil Nadu zone. Journal of Medicinal Plants Research.;2(12):361-364
- <http://id.wikipedia.org/wiki/Lengkeng>, (2013). accessed December 2nd
- Departemen Kesehatan Republik Indonesia (2000). Buku panduan teknologi ekstrak. Jakarta: Direktorat Jenderal Pengawasan Obat dan Makanan; .6-16.



CAPSULE FORMULATION and EVALUATION COMBINATION OF AQUEOUS EXTRACT OF Phaleria's (Phaleria macrocarpa (Scheff Boerf)) FRUITS and LEAVES as ANTIHYPERTENSIVE AGENT

Titta H Sutarna, Program Studi Farmasi, Fakultas Farmasi UNJANI, air_titta@yahoo.com; **Sri Wahyuningsih**, Program Studi Farmasi, Fakultas Farmasi UNJANI; **Julia Ratnawati**, Program Studi Farmasi, Fakultas Farmasi UNJANI; **Fahrouk P**, Program Studi Farmasi, Fakultas Farmasi UNJANI; **Suci Nar Vikasar**, Program Studi Farmasi, Fakultas Farmasi UNJANI; **Ita Nur Anisa**, Program Studi Farmasi, Fakultas Farmasi UNJANI.

ABSTRACT

Some plants have traditionally been used as an antihypertensive, one of which is the fruit and leaves of Phaleria's (Phaleria macrocarpa (Scheff Boerf)). Aqueous ekstrak of phaleria's (Phaleria macrocarpa (Scheff Boerf)) has been studied and shown to have efficacy as an antihypertensive. Based on research conducted by Wahyuningsih S, a combination of 25 % aqueous extract of the fruit of the phaleria's (155 mg / kg body weight) and 75 % aqueous extracts of leaves phaleria's (75 mg / Kg body weight) is the best combination for antihypertensive dose to be able to use for human it was designed for pharmaceutical capsules of the extract combinations, dose aqueous extract of fruits and leaves of phaleria's is 1064 mg divided into 2 capsules size 0 with aerosil filler. Evaluations were conducted on combination leaf and fruit aqueous extract phaleria's capsules is disintegration time, weight uniformity, moisture content, aflatoxin contamination, and microbial contamination. Evaluation results capsule fruit and leaf extracts aqueous phaleria's is destroyed time 7 minutes 23 seconds, uniformity of weight 552 ± 14 mg, 4 % moisture content, aflatoxin contamination is negative, total plate count of 0 CFU / g, mold and yeast numbers 0 Colony Forming Units (CFU) / g, E. coli bacteria contamination 0 CFU / g, contamination of Salmonella sp 0 CFU / g, and the contamination of Pseudomonas aeruginosa 0 CFU / g. Evaluation results capsule combination of fruit and leaves extracts aqueous phaleria's indicates that the aqueous extract fruit capsules and leaves of phaleria's with a dose of 552 mg / capsule meets the requirements BPOM No. 12 of 2014 on Quality Requirements for Traditional Medicines.

Keyword : Aqueous extract of fruits and leaves of Phaleria's, antihypertensives, traditional medicines, capsules.

INTRODUCTION

Hypertension is a major risk factor for death from cardiovascular disorders that result in 20-50 % of all deaths. Control of hypertension is done with the goal of primary prevention and prevent complications. Hypertensive therapy can be done with pharmacological and non-pharmacological therapies. Treatment of hypertension in general require considerable time and thus the cost is quite expensive This encouraged many people are turning pick herbs

as alternative medicine(1). One plant that is often used by the public is the fruit Phaleria 's (Phaleria macrocarpa (Scheff Boerf)). Community Phaleria 's used to treat diabetes mellitus, cancer, gout, heart, liver, high blood pressure, rheumatism, kidney and others. This plant is native to Indonesian and the flora is very easily cultivated and very promising in terms of the economy so as to be readily accessible to the public. For that need to be made herbal medicine preparations. The preparation of herbal medicine is a form in capsule, because it is

easier to form capsules in the formulation and can mask the taste of the plant extracts .

METHOD

Preparation of aqueous extract of leaves and fruit of Phaleria carried by hot extraction which is done by boiling for 30 minutes repeated 3 times, the liquid extract is then concentrated then dried at 90°C to obtain dry extract.

After each dose was calculated from the aqueous extracts of fruit and leaves to be formulated into a hard shell capsule.

Evaluations were conducted on combination of leaves and fruit aqueous extract capsules is disintegration time, weight uniformity , moisture content , aflatoxin contamination, and microbial contamination.

RESULTS AND DISCUSSIONS

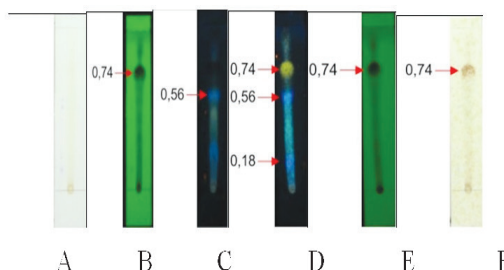
Formulation of aqueous extract of fruits and leaves Phaleria 's is a capsule dosage form . The preparation has been selected capsule that is easy and economical construction . In addition, the formulations into capsule form is intended to reduce taste and odor typical of the extract. Determination of aqueous content of the fruit and leaf extracts Phaleria 's each capsule is based on test results of the antihypertensive effect of aqueous extracts of fruit and leaves Phaleria 's on male Wistar rats . (Wahyuningsih, 2013) Capsule formulations aqueous extract of fruits and leaves Phaleria 's can be seen in Figure 1.



Picture 1. Capsule fruit and leaf aqueous extract Phaleria 's

Results of organoleptic examination showed preparations in powder form , distinctive smell , taste typical extract and brown.

Result of KLT from combination of Aqueous extract fruit and leaves phaleria's shown in picture 2.



Explanation :

Picture	Explanation	Result
A	Visual	It does not look spot on observations
B	254 nm	Pedaman visible spot at Rf 0.74
C	365 nm	There are several colors on TLC trajectory , but that form terlinhar spot at Rf 0.56
D	AlCl ₃ (365 nm)	Spots appear at Rf 0.74 fluoresensi yellow , blue spot at Rf 0.56 more visible color intensity , be gitu also by a blue spot at Rf 0.18 . Spot at Rf 0.74 can be identified as one band (ring B) on flavonoid
E	AlCl ₃ (254 nm)	Pedaman spot Rf 0.74 indicates the tape 2 (ring A) of flavonoids
F	FeCl ₃	Visually appear brown spots after spraying using FeCl ₃ indicating the presence of phenolic compounds on the spot

Table 1. Explanation table for the result of KLT Combination aqueous extract fruits and leaves.

Results of testing the disintegration time capsule aqueous extract of fruits and leaves Phaleria 's is 7 minutes 23 seconds so it can be said that the aqueous extract capsules fruit and leaf aqueous Phaleria 's meet the requirement that destroyed waktu requirements capsule is ≤ 30 minutes.

Results of testing uniformity of weight capsule aqueous extract of fruits and leaves Phaleria 's was 552 ± 14 mg , so it can be said that the capsule aqueous extract of fruits and leaves Phaleria 's meet the requirement that 20 capsules of no more than 2 capsules , each of which weighs it deviates from the bulk density average -rata greater than 10 % and not the weight of its contents kapsulpun that deviate from the average bulk density of greater than 25 %.



Results of testing the disintegration time capsule aqueous extract of fruits and leaves *Phaleria* 's is 7 minutes 23 seconds so it can be said that the aqueous extract capsules fruit and leaf aqueous *Phaleria* 's meet the requirement that destroyed waktu requirements capsule is ≤ 30 minutes.

Results of testing uniformity of weight capsule aqueous extract of fruits and leaves *Phaleria* 's was 552 ± 14 mg , so it can be said that the capsule aqueous extract of fruits and leaves *Phaleria* 's meet the requirement that 20 capsules of no more than 2 capsules , each of which weighs it deviates from the bulk density average -rata greater than 10 % and not the weight of its contents kapsulpun that deviate from the average bulk density of greater than

No.	Type Examination	Reference	Result
1.	Organoleptic	Materia Medika Indonesia	brown, weak odor, bitter taste
2.	The water content of the powder	Materia Medika Indonesia	4%
3.	Disintegration time capsule	Farmakope Indonesia IV	7 minute 23 seconds
4.	Capsule weight uniformity	Lampiran Kep. Menkes. RI No. 661/Menkes/SK/VII/1994	552 ± 14 mg
5.	aflatoxin contamination	Lampiran Kep. Menkes. RI No. 661/Menkes/SK/VII/1994	Negatif
6.	Microbial contamination : contamination of bacteria (total plate count), numbers of fungi and yeasts, <i>E. coli</i> <i>Salmonella</i> sp <i>Pseudomonas aeruginosa</i>	Farmakope Indonesia IV	0 CFU/g 0 CFU/g 0 CFU/g 0 CFU/g

Explanation : CFU = Colony Forming Unit

Table 1. Evaluation results capsule fruit and leaf aqueous extract *Phaleria* 's (*Phaleria macrocarpa* (Scheff Boerf)).

According to the requirements, the maximum moisture content is 10 %, while the result of the determination of the aqueous content of the fruit aqueous extract capsules and leaves *Phaleria* 's is 4 % so that it can be said that the aqueous extract fruit capsules and leaves *Phaleria* 's meet the requirements.

TLC results capsule fruit and leaf aqueous extract *Phaleria* 's showed that capsules containing aqueous extract of fruits and leaves *Phaleria* 's not contaminated with aflatoxin . Examination of aflatoxin contamination needs to be done especially when storage is not done properly extract . Aflatoxins are produced by *Aspergillus flavus* that may grow can cause liver damage and carcinogenic , especially if used

continuously (Kepmenkes , 1994).

The test results of bacterial contamination of the aqueous extract fruit capsules and leaves *Phaleria* 's is negative, this shown that the aqueous extract fruit capsules and leaves *Phaleria* 's meet the requirements.

The results of contamination testing molds and yeast extract capsules fruit and leaf aqueous *Phaleria* 's is negative, this shown that the leaf aqueous extract capsules *phaleria*'s meet the requirements.

The test results of microbial contamination (*E. coli*, *Salmonella* sp, and *Pseudomonas aeruginosa*) aqueous extract capsules *Phaleria* 's fruit and leaves are negative, so it mean that the aqueous extract combination of fruit and leaves *Phaleria* 's capsules meet the requirements.

CONCLUSION

The results of the evaluation of the combination of aqueous extract fruit capsules and leaves *Phaleria* 's grading 552 mg extract per capsule , has met the requirements BPOM No. 12 of 2014 on Quality Requirements for Traditional Medicines.

ACKNOWLEDGEMENT

The author thanks to Ministry of Higher Education Republik Indonesia for funding this research.

REFERENCES

1. Wahyuningsih S. dkk, 2013, Antihypertensive effect of Water extract of *Phaleria* Fruit (*Phaleria macrocarpa* Scheff Boerf) on Male Wistar Rats, Jurnal Farmasi klinik Indonesia, volume 2 , suplemen 2 , hal 64-67
2. Wahyuningsih S. dkk, 2014, Antihypertensive Activity Combination Of Water Extract Leaves And *Phaleria* Fruit (*Phaleria macrocarpa* Scheff Boerf) On Male Wistar Rats,
3. Ditjen POM, Menkes RI, 2014, Per



- aturan Kepala BPOM No. 12 tahun 2014 tentang Persyaratan Mutu Obat Tradisional.
4. Ditjen POM, Depkes RI, 1989, *Materia Medika* jilid VI, Jakarta, Hal 114-119, 321-325.
 5. Departemen Kesehatan Republik Indonesia, 2000, *Parameter Standar Umum Sekstrak Tumbuhan Obat*, Direktorat Jendral Pengawasan Obat dan Makanan, Dep. Kes.RI, Jakarta 2-19
 6. Winarto, W.P, 2003, *Mahkota Dewa Budidaya dan Permanfaatannya untuk Obat*, Penebar Swadaya, Jakarta. Hal 3-9.
 7. Fransworth, N.R., *Biological and Phytochemical Screening of Plants*. *J.pharm sci.*55 (33), Hal 243-268.
 8. Rowe, Raymond C, P.J., Sheskey, Sian C Owen. *Handbook of Pharmaceutical Excipients*. Fifth Edition. London, Chicago: Pharmaceutical Press, American Pharmaceutical Association; 2006.



MANUFACTURE AND CHARACTERIZATION OF SOLID DISPERSION GLIKLAZID- PVP K90

Titta H Sutarna, Program Studi Farmasi, Fakultas Farmasi UNJANI, air_titta@yahoo.com ; **Fikri Alatas**, Program Studi Farmasi, Fakultas Farmasi UNJANI; **Cicah Ayu Ningsih**, Program Studi Farmasi, Fakultas Farmasi UNJANI.

Abstract

Gliclazide is an active substance which has a solubility practically insoluble in water and into BCS class II, low solubility and high permeability. In order to increase the solubility of gliclazide performed various methods of increasing the solubility, one of which used the method of solid dispersion. Study begun by physical mixing gliklazid and PVP K - 90 solid dispersions then gliklazid with PVP K - 90 with a ratio of one (1 : 1 , 2 : 1 , 3 : 1 , 4 : 1) using the solvent methylene chloride. The results showed the highest solubility in solid dispersion gliklazid and PVP K - 90 as compared with the pure and mixed physical gliklazid gliklazid with PVP K - 90 in four media (water , pH 6.8 ; pH 4.5, and pH 1.2). Dissolution rate of gliclazide solid dispersion PVP K - 90 is higher than the pure and mixed physical gliklazid gliklazid with PVP K - 90. There were changes in the physical form of gliklazid seen from the results of X-ray powder diffraction showed a change in the physical form of gliclazide crystalline form into a form more amorphous

Keywords : gliclazide , PVP K - 90 , solid dispersion , dissolution rate

INTRODUCTION

Gliclazide are derivatives toluisulfonilurea second generation hypoglycemic drugs sulfonylurea group used to treat diabetes mellitus type 2. Long working six times more powerful with longer work more than 12 hours ($t_{1/2}$ was approximately 10 hours).(1) Class of first -generation sulfonylureas include (asetoheksamida , klorpropamida , tolazamide and tolbutamide) , while in group II generation sulfonylureas include (glibenclamide , glipizida , gliclazide , glimepirida and Gliquidone) . Gliclazide including active compounds belonging to the group II of the classification system biofarmasetika or Biopharmaceutical Classification System (BCS), which means that gliclazide has a low solubility in water but has a high permeability . Low solubility in water associated with a low dissolution rate , thus limiting absorption and result in low bioavailability(1).

Several experiments have been conducted to overcome formulation problems of drug solubility class II such as the use of surfactants , cyclodextrins , nanoparticles , solid dispersions , micronization , and use of lipid components focused on improving drug bioavailability poor solubility in water(2).

METHOD

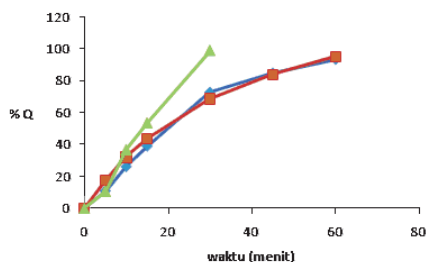
Making Solid dispersions by solvent method using methylene chloride solvent . Gliclazide and PVP K - 90 were weighed separately and carefully in accordance with the ratio of each (1 : 1 , 2 : 1 , 3 : 1 , 4 : 1) . PVP K - 90 was dissolved in methylene chloride until dissolved , then add gliclazide and shaken with a magnetic stirrer. The solution was put in a drying cabinet until the solvent evaporates , and then put in a desiccator . After a solid mass is obtained , the mass of crushed and then sieved with a sieve mesh 60. Once it was ready to do further testing.

RESULTS AND DISCUSSIONS

Ingredients	Solubility concentration (mg . ml ⁻¹) in a variety of media			
	Pure water	buffer solution HCl pH 1.2	Buffer Solution acetate pH 4.5	Buffer solution phosphate pH 6.8
Gliklazid	0.0424±0.01	0.3430±0.02	0.1389±0.01	0.6127±0.02
DP 1 1	0.4291±0.01	0.7262±0.04	0.1681±0.01	0.7785±0.01
DP 2 1	0.0513±0.01	0.3727±0.01	0.1587±0.01	0.5146±0.03
DP 3 1	0.1146±0.01	0.4535±0.03	0.1451±0.01	0.5366±0.06
DP 4 1	0.0939±0.01	0.4503±0.03	0.1412±0.01	0.5507±0.01
CF 1 1	0.0770±0.01	0.3452±0.02	0.1409±0.01	0.4695±0.02
CF 2 1	0.0624±0.01	0.3462±0.01	0.1655±0.01	0.4607±0.04
CF 3 1	0.0504±0.01	0.3407±0.01	0.1333±0.01	0.4550±0.03
CF 4 1	0.0484±0.01	0.3448±0.01	0.1288±0.01	0.4633±0.04

Explanation
DP Solid dispersion (Gliklazid-PVP K-90)
CF physical mixture (Gliklazid-PVP K-90)

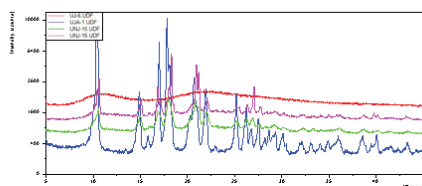
Table I. Solubility test results in four media namely phosphate buffer pH 6.8 ; hydrochloride buffer pH 1.2; acetate buffer pH 4.5 and water



Explanation

- ◆ Gliklazid
- Fisik 1:1
- ▲ Dispersi 1:1

Picture 1. The results of the dissolution rate of gliclazide solid dispersions -PVP K90, pure gliclazide and physical mixture of gliclazide and PVP K-90.

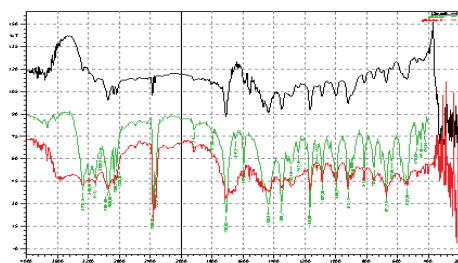


Gambar V.13 Hasil Difraktogram Sinar-X Serbuk

Keterangan:

- PVP K-90
- Campuran Fisik (Gliklazid-PVP K-90) 1:1
- Dispersi Padat (Gliklazid-PVP K-90) 1:1
- Gliklazid

Picture 2. The results of X-ray difraktogram



Gambar V.14 Hasil Spektrofotometer FTIR

Keterangan

- Campuran Fisik (gliklazid-PVP K-90) 1:1
- Gliklazid
- Dispersi Padat (gliklazid-PVP K-90) 1:1

Gambar V.14 The Result of IR spectrophotometry

CONCLUSION

Results of this study of manufacture and characterization of solid dispersions of gliclazide - PVP K90 showed that the manufacturing of solid dispersions with PVP K90 polymer can increase the solubility and dissolution rate of gliclazide . Deformed gliklazid seen from the results of X-ray powder diffraction showed a change in the physical form of gliclazide crystalline form into a form more amorphous.

REFERENCES

Tjay, Tan Hoan dan Kirana Rahardja. Obat-obat penting, Khasiat, Penggunaan, dan Efek-Efek Sampingnya. Edisi 5. Jakarta: Gramedia; 1991. hal 752-753

Dewi, Mega., S. 2011. Peningkatan laju disolusi gliklazid menggunakan sistem solid self emulsifying. Skripsi. Jakarta: Fakultas Farmasi UI. Hal: 1-2

European Pharmacopoeia 7th ed. 2010. EDQM. European Pharmacopoeia. Council of Europe, Strasbourg, France. Page : 2096-2097

Pandharinath, Moreshwar Patil1, Naresh Jandardan Gaikwad2. Characterization of gliclazide-polyethylene glycol solid dispersion and its effect on dissolution. Brazilian Journal of Pharmaceutical Sciences vol. 47, 2011.

Sweetman, S. C, Ed. 2009. Martindale: The Complete Drug Reference. 36th Edition, London : Pharmaceutical Press. Page : 440 – 441.

Rowe, Raymond C, P.J., Sheskey, Sian C Owen. Handbook of Pharmaceutical Excipients. Fifth Edition. London, Chicago: Pharmaceutical Press, American Pharmaceutical Association; 2006.

Leuner, C. and J. Dresman. Improving Drug Solubility for Oral Delivery Using Solid Dispersion., Europ. J. Pharmaceutics and Biopharmaceutics, 50 ;2000. hal 47-60.



ANTI-INFLAMMATORY ACTIVITY OF PARA METHOXY CINNAMIC ACID (PMCA) IN NANOEMULSION USING SOYBEAN OIL

Tristiana Erawati M., Pharmaceutics Department of Faculty of Pharmacy, Universitas Airlangga, Surabaya, era_ffua@yahoo.co.id, **Anneke Indraswari P.**, Pharmaceutics Department of Faculty of Pharmacy, Universitas Airlangga, Surabaya, **Nanda Ghernasih N.C.**, Pharmaceutics Department of Faculty of Pharmacy, Universitas Airlangga, Surabaya, **Noorma Rosita**, Pharmaceutics Department of Faculty of Pharmacy, Universitas Airlangga, Surabaya, **Suwaldi Martodihardjo**, Pharmaceutics Department of Faculty of Pharmacy, Universitas Gadjah Mada, Yogyakarta, **Widji Soeratri**, Pharmaceutics Department of Faculty of Pharmacy, Universitas Airlangga, Surabaya.

INTRODUCTION

Inflammation is a protective mechanism of the local microcirculation to tissue injuries caused by physical trauma, stimulation by hazardous chemicals, heat, antigen-antibody reaction and the effect of microbial.[2] It is known to be involved in the inflammatory reactions such as release of histamine, bradykinin, prostaglandins, fluid cell migration, extravasations, tissue break down and repair which are aimed at host defense and usually activated in most disease conditions. Para methoxy cinnamic acid (PMCA) known has topical anti-inflammatory effect but only 0.64 compare with Na-diclophenac.[4] Its cause PMCA is a poorly soluble drug substance (BCS II), the solubility in acetate buffer pH 4.2 ± 0.2 was 70.04 ± 0.66 mg/liter.[3] So in this study to increase the solubility PMCA loaded in nanoemulsion using soybean oil. And then the anti-inflammatory activity of PMCA in nanoemulsion was measured by the release rate, penetration rate through rat skin using Franz diffusion cell and histological test on mice's ear skin.

MATERIAL AND METHODS

Research Material:

Para methoxy cinnamic Acid (Sigma Aldrich), soybean oil (PT Kurniajaya), Tween 80 (Sigma Aldrich), Span 80 (Sigma Aldrich), ethanol 96 % (Merck), acetic acid (Merck), sodium acetate (Merck), NaCl (Merck), NaH₂PO₄ (Merck), Na₂HPO₄ (Merck), croton oil (Sigma) and aquademineralisata (PT Brataco)

Animals

Male Wistar rats (150 - 230 gm) and mince (20 - 30 gm) were taken from PUSVETMA Suraba-

ya. The animals were housed under standard conditions of temperature (25±2)°C, 12/12 hours light/dark cycles and fed with standard pellets. All animal experiments were conducted with the permission from Animal Care and Use Committee (ACUC) of Veterinary Faculty, Airlangga University, Indonesia. (Reference number; 378-KE).

Research Method

Nanoemulsion formula containing PMCA PMCA in nanoemulsion produced base on the formula presented in Table 1.

Materials	Concentration (%)
PMCA	0.2
Soybean oil	2.66
Span 80	1.92
Tween 80	18.66
Ethanol 96%	3.42
Acetate buffer solution pH 4.2 ± 0.2	ad 100

Table 1. PMCA Nanoemulsion Formula

Nanoemulsion formula used in this study is the result of a previous study by Erawati et.al, using a combination of surfactant Tween 80 and Span 80 with a ratio of 9:1 (having HLB 14), the ratio of surfactant and co surfactant 6:1, the ratio of oil phase (soybean oil) and water phase (acetate buffer solution pH 4.2 ± 0.2) is 27.5:1. [3]

Solubility test

PMCA solubility test; on the nanoemulsion



using soybean oil (as oil phase) added with 500 mg PMCA, then it was sonicated for 10 minutes and shaking with 150 rpm for 60 minutes. And then, the amount of PMCA dissolve in nanoemulsion was determined using spectrophotometer. After that the nanoemulsion PMCA characterized include; density, viscosity, pH, droplet morphology, droplet size and polydispersity index.

Release test

Membrane Preparation; the membrane used in the test release of PMCA in nanoemulsion system is a cellophane membrane. Membrane cut to size, then immersed in aqua-demineralization for ± 12 hours. A moment before use, the membrane is drained until no water is dripping, and then mounted on the surface of the receptor compartment of Franz diffusion cell.

Measurement the amount of the PMCA release from the nanoemulsion; receptor compartment of Franz diffusion cell filled with phosphate buffer pH 6.0 ± 0.2 up to full. Then, 2 ml of nanoemulsion PMCA inserted into the donor compartment. Experimental temperature is set and maintained at a temperature of $32 \pm 2^\circ\text{C}$. Magnetic stirrer rotated at a speed of 100 rpm. Samples of 1 ml were taken within a certain time interval, i.e. at 0, 5, 10, 15, 30, 45 minutes, and then 1, 1.5, 2, 3, 4, 6, 8, 10, 12, 24 hours. Immediately after sampling medium was replaced with phosphate buffer pH 6.0 ± 0.2 with a volume of samples taken. Subsequently, samples were taken observed with spectrophotometer. PMCA concentration in the sample was calculated using the regression equation of standard curve. Determination of PMCA cumulative amount released per unit membrane area (mg/cm^2) was calculated from the concentration obtained each time ($\mu\text{g}/\text{ml}$) which had been corrected with the Wurster's equation. Furthermore, multiplied by the number of medium and divided by the membrane surface area. The results obtained by the cumulative number of PMCA released per unit time. The release profile of PMCA, is

done by making a relations curve between the cumulative number of PMCA released (mg/cm^2) versus time (minutes). The release rate of (Flux release) PMCA was obtained from the slope of the regression equation in the steady state.

Penetration test

Membrane Preparation; skin male Wistar rats that had been shaved used as the membrane in the penetration test of PMCA in nanoemulsion system.

Measurement the amount of PMCA penetrate through rat skin; receptor compartment of Franz diffusion cell filled with phosphate buffer pH 7.0 ± 0.2 up to full. Then, 2 ml of nanoemulsion PMCA inserted into the donor compartment. Samples of 1 ml were taken within a certain time interval as in release test.

RESULT AND DISCUSSION

The PMCA solubility in nanoemulsion 3.07 ± 0.19 g/liter (presented in Table 2) increased than its solubility in acetate buffer pH 4.2 ± 0.2 is 70.04 ± 0.66 mg/liter. The characteristics of nanoemulsion containing PMCA presented in Table 3; the density value was 1.0263 ± 0.0002 is almost equal to the density of water; the viscosity was $5.58 \pm 0.05\text{cP}$; the pH value was 4.47 ± 0.006 it was in the range of human skin pH, so it will not cause irritation; the droplet size was 57.3 ± 7.6 nm and the polydispersity index was 0.548 ± 0.044 it was indicate a moderate particle size distribution.[1] The droplet morphology of empty nanoemulsion and nanoemulsion containing PMCA in saturated solubility by TEM.type JEM-1400 was resented in Figure 1.

Medium	The amount of PMCA dissolved
Nanoemulsion	3.07 ± 0.19 g/liter
Acetate buffer pH 4.2 ± 0.2	70.04 ± 0.66 mg/liter

Table 2. The solubility of PMCA in nanoemulsion and in acetate buffer pH 4.2 ± 0.2



The characteristics of nanoemulsion containing PMCA	
density	1.0263 ± 0.0002
viscosity	5.58 ± 0.05 cP
pH	4.47 ± 0.006
droplet size	57.3 ± 7.6 nm
polydispersity index	0.548 ± 0.044

Table 3. The characteristics of nanoemulsion containing PMCA

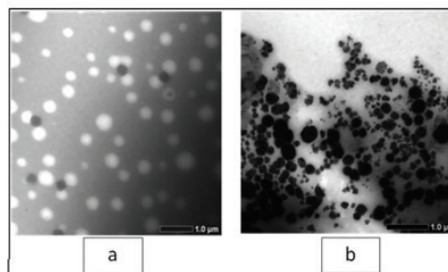


Figure 1. Droplet morphology of a) empty nanoemulsion and b) nanoemulsion containing PMCA in saturated solubility by TEM type JEM-1400

The release profile and the release rate of PMCA in acetate buffer pH 4.2 \pm 0.2 and in nanoemulsion were presented in figure 2 and figure 3. After investigate for 24 hours (1440 minutes) the result shows that the release rate of PMCA in nanoemulsion (0.4024 ± 0.0339 $\mu\text{g}/\text{cm}^2/\text{minute}$) increased compare with it in acetate buffer pH 4.2 \pm 0.2 is 0.0239 ± 0.0003 $\mu\text{g}/\text{cm}^2/\text{minute}$.

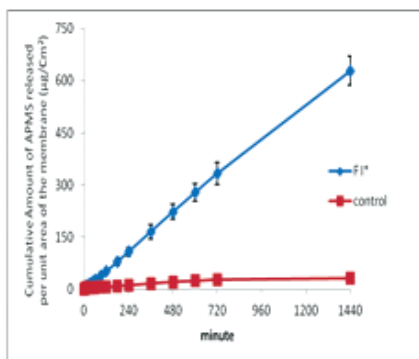


Figure 2. Release profile of PMCA in acetate buffer pH 4.2 \pm 0.2 (control) and in nanoemulsion (FI*)

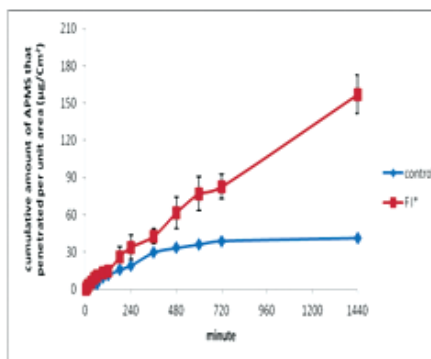


Figure 2. Penetration profile of PMCA in acetate buffer pH 4.2 \pm 0.2 (control) and in nanoemulsion (FI*)

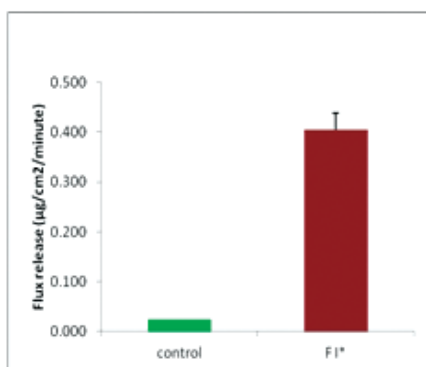


Figure 3. Histogram of release rate of PMCA in acetate buffer pH 4.2 \pm 0.2 (control) and in nanoemulsion (FI*)

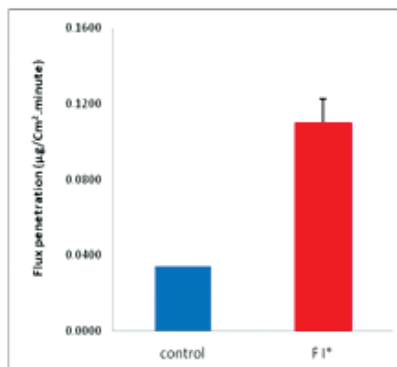


Figure 5. Histogram of penetration rate of PMCA in acetate buffer pH 4.2 \pm 0.2 (control) and in nanoemulsion (FI*)

Also the penetration rate of PMCA in nanoemulsion was increased too ($0.1513 \pm 0.0314 \mu\text{g}/\text{cm}^2/\text{minute}$) compare with the penetration rate of PMCA in acetate buffer pH 4.2 \pm 0.2 ($0.0341 \pm 0.0003 \mu\text{g}/\text{cm}^2/\text{minute}$) as presented in figure 4 and 5. The increased of penetration rate of PMCA in nanoemulsion caused by 1) the solubility of PMCA in nanoemulsion increased (more than 43x compare with the solubility of PMCA in acetate buffer pH 4.2 \pm 0.2) and 2) the surfactant and co surfactant in nanoemulsion formula can function as enhancers.

From figure 6 and table 4, known that the anti-inflammatory effect of PMCA in nanoemulsion (F I*) higher than the anti-inflammatory effect of PMCA in acetate buffer pH 4.2 \pm 0.2 (control). The result of statistical test using ANOVA-one way ($P = 95\%$), known there are no significant different between the ears mice skin thickness after treated with PMCA in nanoemulsion (F I*) with health skin (K-) but thinner than inflammation skin (K+) also with the ears mice skin after treated with PMCA in acetate buffer pH 4.2 \pm 0.2 (control).

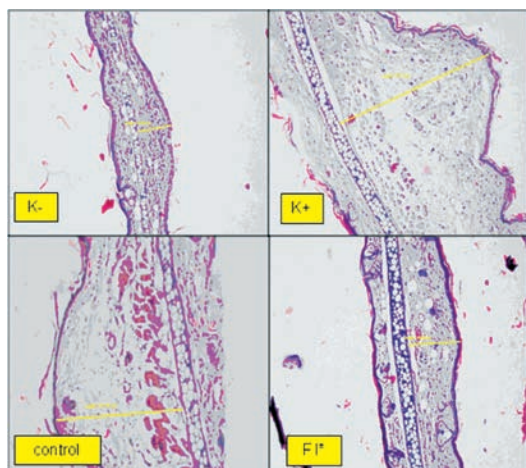


Figure 6. The histology profile of ears mice skin, health skin (K-), inflammation skin (K+), after treated with PMCA in acetate buffer pH 4.2 \pm 0.2 (control), and in nanoemulsion (F I*)

Sample	The Average Of Skin Thickness (μm)
K-	282.96 ± 36.80
K+	592.53 ± 59.81
Kontrol	541.69 ± 56.56
F I*	310.56 ± 30.76

Table 4. The average of ears mice skin after treated with PMCA in acetate buffer pH 4.2 \pm 0.2 (control), and in nanoemulsion (F I*) compare with health skin (K-) and inflammation skin (K+).

CONCLUSION

The nanoemulsion with soybean oil as drug delivery system can increase the anti-inflammatory activity of PMCA.

ACKNOWLEDGMENT

Thank to Indonesia Government (DIKTI) who give Research Fund through Rector of Universitas Airlangga (through LPPM-UA).

REFERENCES

1. Duan C.Y., Xia Z.Y., Gui B.S., Xue J. F., Ouyang J.M, 2013, Changes in urinary nanocrystallites in calcium oxalate stone formers before and after potassium citrate intake. International Journal of Nanomedicine, Vol. 8, p. 909-918.
2. Mahesh G, Ramkanth S, Saleem MTS. Anti-inflammatory drugs from medicinal plants A comprehensive review. International Journal of Review in Life Sciences 2011; 1(1): 1-10.



ICPPS 2014

Proceeding
The 1st International Conference
on Pharmaceutics & Pharmaceutical Sciences

3. Tristiana Erawati M, Esti Hendradi, Widji Soeratri, 2014, Praformulation Study Of p-Methoxycinnamic Acid (PMCA) Nanoemulsion Using Vegetable Oils (Soybean Oil, Corn Oil, VCO), Int J Pharm Pharm Sci, ISSN-0975-1491, Vol. 6, Issue 2, 2014, 99-101
4. Widji Soeratri, Tristiana Erawati M., Diny Rahmatika, Noorma Rosita, 2014, PMCA Dose as Topical Antiinflammation and Its Penetration Study Through Full-thick Rat Skin and Without Stratum Corneum, Indonesian Journal of Pharmacy and Pharmaceutical Science, ISSN- 2406-9388. Vol. 1, No. 1, June 2014 p. 28-30



PHYSICAL CHARACTERISTICS AND PENETRATION OF DICLOFENAC SODIUM NIOSOMAL SYSTEM USING SPAN 20 AND SPAN 60

Tutiek Purwanti, Department of Pharmaceutics, Faculty of Pharmacy, Airlangga University (UNAIR), Surabaya, 60282, Indonesia, tutiek_purwanti@yahoo.com; **Esti Hendradi**, Department of Pharmaceutics, Faculty of Pharmacy, Airlangga University (UNAIR), Surabaya, 60282, Indonesia; **Noverika A. Putri**, Department of Pharmaceutics, Faculty of Pharmacy, Airlangga University (UNAIR), Surabaya, 60282, Indonesia; **Nurtya J. Devi**, Department of Pharmaceutics, Faculty of Pharmacy, Airlangga University (UNAIR), Surabaya, 60282, Indonesia

INTRODUCTION

Vesicular system, both liposomes and niosomes are uni- or multi lamellar spheroidal structures composed of amphiphilic molecules assembled into bilayers. They are considered primitive cell models, cell-like bioreactors and matrices for bio encapsulation. In the recent years, nonionic surfactant vesicles known as niosomes received great attention as an alternative potential drug delivery system to conventional liposomes. Moreover, compared to phospholipid vesicles, niosomes offer higher chemical and physical stability (Vora et al., 1998) with lower cost and greater availability of surfactant classes (Manconi et al., 2006). Niosomes have been reported to enhance the residence time of drugs in the stratum corneum and epidermis, while reducing the systemic absorption of the drug and improve penetration of the trapped substances across the skin. In addition, these systems have been reported to decrease side effects and to give a considerable drug release (Schreier and Bouwstra, 1994). They are thought to improve the horny layer properties both by reducing trans epidermal water loss and by increasing smoothness via replenishing lost skin lipids (Junginger et al., 1991). Moreover, it has been reported in several studies that compared to conventional dosage forms, vesicular formulations exhibited an enhanced cutaneous drug bioavailability (Manconi et al., 2006; Mura et al., 2007).

Non-ionic surfactant in niosome system can affect the conformation and structure of skin lipid bilayer to facilitate penetration of the drug (Shahiwala, 2002). In addition, the niosome

system can be a depot of drug on hydrophobic layer (Tangri & Khurana, 2011) so that the service life of the drug becomes longer.

This research was to compare the penetration of diclofenac sodium in span 20 and span 60 niosomal system with molar ratio of diclofenac sodium – span – cholesterol was 1:6:6.

MATERIALS AND METHODS

Diclofenac sodium (Yung Zip Chemical Ind-Taiwan), Span 20 and span 60 (Sigma), cholesterol (Sigma), HPMC 4000 (Shin-Etsu Chemical Co. Ltd), chloroform (Biesterfeld Siemsgluss International GmbH), on pharmaceuticals grade. Sodium Chloride, Na₂HPO₄·2H₂O and KH₂PO₄ (E. Merck) on analytical grade

Identification and standardization of drug and other excipients were carried out as the official procedures mentioned in respective monographs.

Preparation of Niosomes

Niosomes containing diclofenac sodium were prepared by Reverse Phase Evaporation Technique using non ionic surfactant (span 20 and span 60) with a molar ratio of diclofenac sodium : span : cholesterol 1 : 6 : 6. Cholesterol and surfactant were dissolved in chloroform, add this mixture with a solution of diclofenac sodium in free carbon dioxide aqua and then sonicated them on 4 – 5 °C for 16 minutes. Pour into this mixture a solution of buffer phosphate saline with pH 7.4 and then sonicated again on 4-5 °C for 12 minutes. Evaporation process to remove chloroform at temperature 40 °C and pressure ± 200 mmHg. The evalua-



tion of niosome included organoleptics (odor, color and consistency), morphology and size of vesicle, entrapment efficiency, and in-vitro drug penetration across abdominal skin from male Wistar rat.

RESULT AND DISCUSSION

Organoleptics of Niosome

Table 1. Organoleptic Evaluation Niosome Span 20 and Span 60

Consistency	thick suspension
Colour	milky white
Odor	specific odor

The organoleptic of diclofenac niosome span 20 and span 60 was similary, but consistency of niosome span 60 is higher than niosome span 20.

Table 2. Entrapment efficiency of span 20

ΔA absorption	Concentration ($\mu\text{g/mL}$)	%EP	Mean \pm SD	%CV
0,022	39,369	68,43	65,50% \pm 1,21	5,49%
0,028	48,043	61,49		
0,021	41,847	66,58		

Table 3. Entrapment efficiency of span 60

ΔA bsorption	Concentration ($\mu\text{g/mL}$)	%EP	Mean \pm SD	%CV
0,0140	3,3173	44,05	43,33	2,79%
0,0140	3,4412	41,94	% \pm	
0,0140	3,3173	44,05	1,21	

Morphology of Niosome Span 20 and Span 60 Morphology of diclofenac sodium span 20 and span 60 were evaluated with Scanning Electron Microscopy (SEM) with a magnification of 2500 times. This result showed on figure 1 and 2.

The size of niosome diclofenac sodium span 60 (1.3 -14.00 μm) higher than niosom diclofenac sodium span 20 (0.1-3,75 μm).

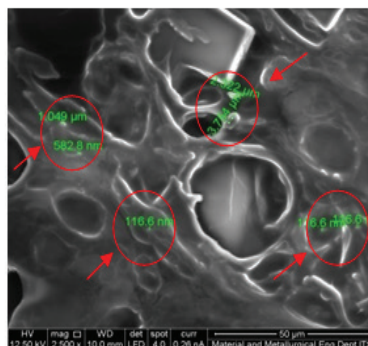


Figure 1 Morphology of niosome span 20 (0.1-3,75 μm)

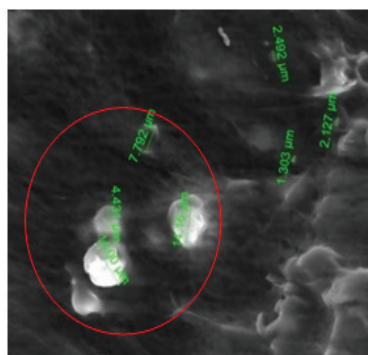


Figure 2 Morphology of niosome span 60 (1.3 - 14.00 μm)

Entrapment efficiency of Span 20 and Span 60 Span 60 (C=16) has a longer chain alkyl than span 20 (C=12), consequently the molecule of Span 60 is bigger and more hydrophobic. Whereas span 20 with HLB 8,6 (Rowe, 2009) is more hydrophilic. Diclofenac sodium has a partition coefficient value 13,4 (O'Neil, 2001), consequently, diclofenac sodium more hydrophobic. Because of this reason, span 60 more ability to trapped a diclofenac sodium than span 20, consequently the amount of diclofenac sodium which is trapped more than span 20, and the amount of diclofenac sodium which is trapped is bigger. In Niosom span 60, the entrapment efficiency value is 65%, whereas in niosome span 20 has an entrapment efficiency value 43%.

Table 4. pH value of niosome span 20 and span 60

Niosome	Replication	pH	Mean
Span 20	1	6,69	6,67 ± 0,02
	2	6,65	
	3	6,67	
Span 60	1	6,58	6,58 ± 0,01
	2	6,57	
	3	6,59	

The statistical test showed that different pH value of niosome span 20 and niosome span 60 is not significant, so influence pH on ionized / unionized drug in this research which may affect the penetration does not exist.

Penetration Test of Diclofenac Sodium
Penetration profile of diclofenac sodium span 20 and span 60 showed in figure 3 and 4.

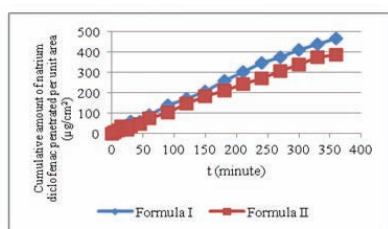


Figure 3 Penetration profile of diclofenac sodium span 20 niosome system and control

Figure 3 Penetration profile of diclofenac sodium span 20 niosome system and control

Table 5. Penetration Flux of Diclofenac Sodium Span 20

Formula	Replication	Flux (µg/cm ² /minute)	Mean ± SD	% CV
I	1	1,2386	1,3062 ± 0,0929	7,11%
	2	1,2678		
	3	1,4121		
II	1	0,9232	1,1010 ± 0,1553	14,11%
	2	1,2100		
	3	1,1699		

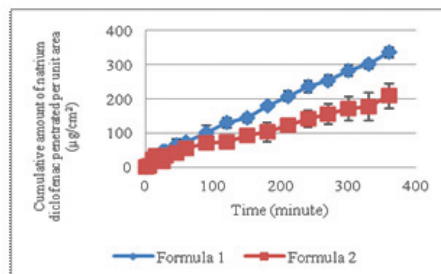


Figure 4. Penetration profile of diclofenac sodium span 60 niosome system and control

Table 7. Penetration Flux of Diclofenac Sodium Span 60

Formula	Replication	Flux (µg/cm ² /minute)	Mean	SD	% CV
1	1	0,9529	0,8627	0,1094	12,6748
	2	0,7411			
	3	0,8942			
2	1	0,5062	0,5003	0,0076	1,5226
	2	0,5030			
	3	0,4917			

Table 8. Membrane Permeability for Diclofenac Sodium Niosome Span 60

Formula	Replication	Permeability (cm/minute)	Mean	SD	% CV
1	1	6,0260.10 ⁻⁵	6,5533.10 ⁻⁵	7,8476.10 ⁻⁶	11,98
	2	6,1787.10 ⁻⁵			
	3	7,4551.10 ⁻⁵			
2	1	4,6635.10 ⁻⁵	4,3960.10 ⁻⁵	2,3663.10 ⁻⁶	5,38
	2	4,3107.10 ⁻⁵			
	3	4,2139.10 ⁻⁵			

Penetration test on this research used dissolution medium solution buffer phosphate saline pH 7,4 ± 0,05 at temperature 37 °C with the speed 100 rpm as long as 6 hours. In penetration test, it was used penetration flux and permeability of membrane to diclofenac sodium as a penetration parameter. Each niosome (niosome span 20 and niosome span 60) are performed three times replication and they were compared with a control where it was the same formula but wasn't made a niosome system. The result of penetration test of diclofenac sodium span 20 was obtained flux 1,3062 ± 0,0929 µg/cm²/minute and control 1,1010 ± 0,1553 µg/cm²/minute. Diclofenac sodium span 60 was obtained flux 0,8627 ± 0,1094 µg/cm²/minute and control 0,5003 ± 0,0076



$\mu\text{g}/\text{cm}^2/\text{minute}$.

Based on statistically analysis, It can be concluded that no significant differences of flux and membrane permeability between diclofenac sodium niosom span 20 and control was found, whereas there were significant differences on the diclofenac sodium niosom span 60. Flux of diclofenac sodium niosom span 20 was higher than diclofenac sodium span 60, this may be due to low entrapment efficiency of diclofenac sodium span 20 caused very few diclofenac sodium was unentrapped.

CONCLUSION

It can be conclude that unentrapped diclofenac sodium had been penetrated within 6 hours study, therefore it is recommended to have longer study period and also suggested to separate niosom and its medium.

REFERENCES

- Manconi, M., Sinico, C., Valenti, D., Loy, G., Fadda, A.M. 2002. Niosomes as carriers for tretinoin. I. preparation and properties. *Int. J. Pharm*, Vol. 234, p. 237–248 in Keservani, R.K., Sharma, A.K., Ayaz, Md. Kesharwani, R.K. 2011. Novel drug delivery system for the vesicular delivery of drug by the niosomes. *International Journal of Research in Controlled Release*, Vol. 1, p. 1-8
- Mura, S., Pirot, F., Manconi, M., Falson, F., Fadda, A.M., 2007. Liposomes and niosomes as potential carriers for dermal delivery of minoxidil. *J. Drug Target*, Vol. 15, p. 101–108 in Balakrishnan, P., Shanmugama, S., Lee, W.S., Lee, W.M., Jong Oh Kim, J.O., Oh, D.H., Kim, D., Kim, J.S., Yoo, B.K., Choi, H., Woo, J.S., Yong, C.S. 2009. Formulation and in vitro assessment of minoxidil niosomes forenhanced skin delivery. *International Journal of Pharmaceutics*, Vol. 377, p.1–8
- Schreier H. & Bouwstra JA. 1994. Liposomes and niosomes as topical drug carriers: dermal and transdermal drug delivery. *J. Con. Rel*, Vol. 30, p. 1-15 in Jigar, V., Puja, V., Krutika, S. 2011. Formulation and Evaluation of Topical Niosomal Gel of Erythromycin. *International Journal of Pharmacy and Pharmaceutical Sciences*, Vol. 3, p. 123-126
- Shahiwala A, Misra A. 2002. Studies in topical application of niosomally entrapped Nimesulide. *J Pharm Pharm Sci*, Vol. 5, p. 220-225 in Kumar, R. Design and Evaluation of Niosomal Gel Delivery Systems for Topical Application of Clotrimazole. M. Pharm Dissertation Protocol Submitted to the Rajiv Gandhi University of Health Sciences, Bangalore, India
- Tangri, P., and Khurana, S., 2011. Niosomes : formulation and evaluation. *International Journal of Biopharmaceutic*, Vol. 2 (1), p. 47-53
- Vora B, Khopade AJ, Jain NK. 1998. Proniosome based transdermal delivery of levonorgestrel for effective contraception. *J Control Release*, Vol. 54, p.149–65 in Jadon, P.S., Gajbhiye, V., Jadon, R.S., Gajbhiye, K.R., and Ganesh, N. 2009. Enhanced Oral Bioavailability of Griseofulvin via Niosomes. *AAPS PharmSciTech*, Vol. 10, No. 4, p. 1186-1192



FORMULATION AND CHARACTERIZATION OF JUICE OF LIME GEL USING CMC-NA BASE

Uswatun Chasanah, University of Muhammadiyah Malang, u.chasanah@yahoo.co.id, +6285755911904; **Esti Hendradi**, Airlangga University, esti_hendradi@yahoo.com, +6281330175672; **Inayah**, University of Muhammadiyah

INTRODUCTION

Lime (*Citrus aurantifolia*) is a plant that is efficacious and commonly used by the people. It is used for juice, dessert, pickle, medicinal purpose and cosmetic. In the field of beauty lime is used to whiten the skin, obesity and cellulite and has an astringent and toning action to clear oily skin and acne [1,2].

The content of lime is very much, such as carbohydrate, sugar, protein, minerals (Ca, Fe, Mg, P, K, Na, Zn), vitamins (ascorbic acid, thiamin, riboflavin, niacin, vitamin B6, folate, vitamin B12, vitamin A, vitamin E) [3] and volatile oil that most important flavoring oils, lemon essential oil are complex mixtures of chemical compounds like limonene, γ -terpinene, citral, linalool and β -caryophyllene [4]. The organic acid component of acid lime juice is primarily composed of citric acid [5]. Ascorbic acid and citric acid have antioxidant activity and one of the activities of antioxidant is to prevent premature aging [6], so the lime can be used as a sunscreen.

This study was to determine of physical and chemical characteristics of the juice of lime gel formulation with dosage levels of 10%, 20% and 30% in the CMC-Na base.

MATERIAL AND METHODS

The research material used is lime (*Citrus aurantifolia*) was obtained from Malang and was identified by Materia Medica Technical Service Unit.

PREPARATION GEL JUICE OF LIME

The composition of the gel lime juice with dosage levels of 10%, 20% and 30% seen in Table 1.

Material name	Quantity		
	F I	F II	F III
Juice of lime	20.0 g	40.0 g	60.0 g
CMC-Na	8.0 g	8.0 g	8.0 g
Propylene glycol	30.0 g	30.0 g	30.0 g
Nipagin	0.5 g	0.5 g	0.5 g
Aqua distilled ad	200.0 g	200 g	200 g

Table 15. The composition of the gel formulation of lime juice.

Method of preparation gel juice of lime as follows: Making gel of juicy lime begins by dispersing CMC-Na in aqua CO₂-free to make a gelling base. Juice of lime mixed into the gelling base, then nipagin dissolved in propylene glycol, which is then appended to the gelling base that contained the juice of lime slowly and mixed until homogeneous. Last added aqua distilled until the desired weight and stirred until homogeneous.

EVALUATION PREPARATION

Characterization of the gel formulation of lime juice

Characterization of the gel formulation of lime juice includes organoleptic, viscosity and pH.

Organoleptic examination

Organoleptic examination of the gel formulation of lime juice includes texture, color, and odor

Measurement of the viscosity

Measurement of the viscosity of the gel of lime juice using a cup and bob Viscometer (Visco Rion tester vT-04F).



Measurement of pH gel of lime juice
Measurement of pH gel of lime juice done by 20 + Basic pH meter.

Determination of the release of citric acid from lime juice gel formulation
Diffusion cells, which had been prepared, put into the glass beaker at test release tools contained CO₂-free distilled water. The experiments were performed at room temperature (27°C ± 0.5°C). Paddle rotated every 10 minutes, 10.0 ml of footage taken at minute 0, 60, 120, 180, 240 and 300, subsequently it's absorption observed with UV-Vis spectrophotometer at a wavelength of 512 NM. To account for the dilution of 10.0 ml of the release medium, the measured levels corrected with Wurster equation.

Determination of acceptability of lime juice gel preparation.
The test is performed using a 10 woman aged 19-24 years old with no distinguishable types of skin. Respondents using gel juice of lime on the forearm and then asked his opinion about the ease of smeared, sensation while in use and easy to clean.

RESULTS AND DISCUSSION From the results of the observation appears that the organoleptic of lime juice at a dosage level of 10%, 20% and 30% has a dense and creamy texture, but it possesses a different color and odor, the lime juice gel at a dosage of 10% is clear and odorless, the dosage of 20% is slightly yellowed and a bit smelly, whereas dosage of 30% is yellow with lemon smell sharper. Its suggest that elevated dosage of lime juice will increase the intensity of the color gel preparation and sharpen the lemon smell. For the viscosity of lime juice gel preparations at a dosage of 10 %, 20% are similar, and at dosage of 30% the viscosity of gel of lime juice is increasing (Table 2).

Formula	organoleptic	viscosity	pH
F I	clear, odorless	50.000cPs	4.64±0.50
F II	slightly yellowed, bit smelly	50.000cPs	4.39±0.15
F III	yellow, lemon smell sharper	60.000cPs	3.77±0.09

Table 2. Characteristic of lime juice gels at dosage of 10% (F1), 20% (F II) and 30% (F III) of lime juice.

Measurement of pH on the lime juice gel at a dosage of 10% and 20% are similar, where use the gel of lime juice at a dosage of 30% is higher than the other formula (Anova, α=0.05). This is caused by the pH of lime juice is 2.33, so that the addition of lime juice will lower the pH of the gel preparation (Table 2).

Based on the data obtained from the release of citric acid from lime juice gel preparation, calculated the area under the curve (AUC) to determine the release rate of citric acid from the gel of lime juice (*Citrus aurantifolia*). The result of AUC calculation can be seen in Figure 1.

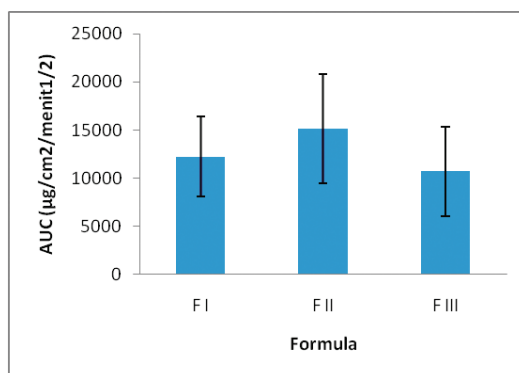


Figure 1: Histogram of AUC of citric acid release from the lime juice gel preparation at dosage of 10% (F I), 20% (F II) and 30% (F III) of lime juice.



It is showed that the AUC of the three formulas are not significantly different (Anova, $\alpha=0.05$). It can be concluded that elevated concentration of lime juice on the formula of this gel formulation does not increase the value of AUC on a test release of citric acid from lime juice gel preparation. These may be caused by the interaction between active ingredient with material and viscosity of preparation.

From the results of the test acceptability of gel lime juice preparation is known that the formula contained 30% of lime juice has a high percentage of ease smeared (softness) and cold sensation. For ease of cleared, gel content of 20% of lime juice has a higher percentage, this is due to its has lower viscosity than gels lime juice content of 30%, so that the formula of gel contained of 30% lime juice is the most acceptable (Table 3).

Formula	Parameters of acceptability (%)		
	Ease smeared	Cold sensation	Easy to clean
F I	66.70	70.00	63.33
F II	70.00	73.33	76.70
F III	73.33	83.33	66.47

Table 3. The results of acceptability test of lime juice gel content of lime fruit at dosage of 10% (F I), 20% (F II) and 30% (F III).

CONCLUSION

The results obtained in this study showed that the differences in the levels of the juice of lime (10%, 20% and 30%) on lime juice gel formula with CMC-Na base produces a characteristic and acceptability are different, but the results of the test release of citric acid from lemon juice gel is similar. Base in characteristic physical (organoleptic, pH and viscosity), acceptability and effectiveness of the lime juice gel formulations, the formula that content of 20% of lime juice is the best.

REFERENCES

1. P. P. Joy, J. Thomas, Samuel Mathew, Baby P. Skaria. (1998). Medicinal Plants. Aromatic and Medicinal Plants Research Station. pg:189.
2. C. P. Khare. (2007). Indian Medicinal Plants: An Illustrated Dictionary. Springer publication. pg:153-157.
3. United States Department of Agriculture. (2014). National Nutrient Database for Standard Reference Release 27. Basic Report 09160, Lime juice, raw.
4. Benvenuti F, Gironi F, Lamberti L. (2001). Supercritical deterpenation of lemon essential oil, experimental data and simulation of the semicontinuous extraction process. J of Supercritical Fluids, May;20(1):29-44.
5. R. K. Soost and J. W. Cameron. (1961). Fruit Characters in Young Trees of Long-Established Nucellar Lines. Proc. 2nd Conf. Intern. Org. Citrus Virol.: 8-14.
6. Murray JC, Burch JA, Streilein RD, et al.(2008). A topical antioxidant solution containing vitamins C and E stabilized by ferulic acid provides protection for human skin against damage caused by ultraviolet irradiation. J Am Acad Dermatol, Sep; 59(3):481-25.



HEPATOPROTECTIVE ACTIVITY OF *Bidens pilosa* L. IN CARBON TETRACHLORIDE INDUCED HEPATOTOXICITY IN RATS

Vina Alvionita Soesilo, Department of Pharmacy, Sanata Dharma University, vina.alvionita93@gmail.com, +62 962 440 2990; **Prof. Dr. C.J. Soegihardjo, Apt.**, Department of Pharmacy, Sanata Dharma University, constantinus_soegihardjo@yahoo.com

ABSTRACT

The aim of this study are to prove the influence of hepatoprotective time infusion of *Bidens pilosa* L. herb in acute and the most effective protection time of the Alanine Aminotransferase (ALT) and Aspartate Aminotransferase (AST) serum in rats that induced by carbon tetrachloride.

This study is a pure experimental with randomized complete direct sampling design. A total of 30 female Wistar rats, age 2-3 months, weighing \pm 150-250 g were divided into seven groups by five rats each. Rats in group I were orally administered 2 mL/kgBB olive oil, group II were intraperitoneal administered 2 mL/kgBB carbon tetrachloride 50% as hepatotoxin, group III were orally administered 2 mg/kgBB infusion of *Bidens pilosa* L. for 6 hours, group IV administered 1 mg/kgBB infusion of *Bidens pilosa* L. and was injected with 2 mL/kgBB carbon tetrachloride 50% after 1 hours, group V administered 1 mg/kgBB infusion of *Bidens pilosa* L. and was injected with 2 mL/kgBB carbon tetrachloride 50% after 4 hours, group VI administered 1 mg/kgBB infusion of *Bidens pilosa* L. and was injected with 2 mL/kgBB carbon tetrachloride 50% after 6 hours. Data of ALT-AST activity were analyzed by One Way ANOVA and continued to Post Hoc Scheffe test.

This study showed that infusion of *Bidens pilosa* L. herb in acute influence Alanine Aminotransferase (ALT) serum and Aspartate Aminotransferase (AST) serum in rats that induced by carbon tetrachloride. The most effective protection time to give influence of Alanine Aminotransferase (ALT) serum and Aspartate

Aminotransferase (AST) serum in rats that induced by carbon tetrachloride is 4 hours with % hepatoprotective ALT serum was 107.83 % and the % hepatoprotective AST serum was 102.34 %.

Key words : *Bidens pilosa* L., herb, infusion, acute, ALT, AST, carbon tetrachloride

INTRODUCTION

Liver is an important organ which regulating homeostasis in the body. It is involved in the detoxification and excretion of various endogenous and exogenous substances. It protects against the harmful effects of drugs and chemicals and thus frequently exposed to variety of toxicants resulting in liver diseases¹. The major functions of the liver are carbohydrate, pretein and fat metabolism, detoxification, secretion of bile and storage of vitamin. Thus, to maintain a healthy liver is a crucial factor for overall health and well being. But it's continuously and variedly exposed to environmental toxins, and drug abuse along with alcohol and prescribed & over-the-counter drug which can eventually lead to various liver ailment like hepatitis, cirrhosis, and alcoholic liver disease^{2,3}. Liver diseases, a leading cause of death in many countries, is a major concern throughout the world. The different medical, surgical, and therapeutic methods available at present for the treatment of liver diseases are inadequate with generally poor results⁴. Therefore, it is essential to search for newer drugs for the treatment of liver diseases. Liver injury due to chemicals (or) infections agents may lead to progressive liver fibrosis and ultimately cirrhosis and liver failure⁴.

However, no effective treatment that delays disease progression and complications has yet been found. Several recent studies suggest that traditional herbs and micronutrients such as carotenoids and selenium may be useful for this purpose^{5,6}.

Carbon tetrachloride CCl₄ is widely used for experimental induction of liver damage⁷. The principle cause of carbon tetrachloride (CCl₄) is induced hepatic damage in lipid peroxidation and decreased activities of antioxidant enzymes and generation of free radicals^{8,9}. Various medicinal plants have been used to treat for various diseases in all over the world. Nowadays, Indian medicinal plants are belonging to about 40 families were investigated as liver hepatoprotective drugs¹⁰.



Figure 1. *Bidens pilosa* L.

The *Bidens pilosa* L. has various chemical constituents like polyacetylenes, polyacetylenic glycosides, aurons, auron glycosides, p-coumeric acid derivatives, caffeoylquinic acid derivatives, pheophytins, diterpenes, tannins, phytosterols, ascorbic acid, carotene, essential oils, saponins, steroids and flavonoids and many others were recognized in this plant¹³.

MATERIAL AND METHODS

Procurement and Authentication of the Plant
The herbs of *Bidens pilosa* L. were collected from local area of village Jenengan, Maguwo-

harjo, Depok, Sleman, Yogyakarta and it was authenticated by Yohanes Dwiatmaka, M.Si., at Laboratory of Pharmacognosy and Phytochemistry, Faculty of Pharmacy Sanata Dharma. The herb was deposited at Department of Pharmacognosy and Phytochemistry, Faculty of Pharmacy Sanata Dharma.

Preparation of An Infusion of *Bidens pilosa* L.

The infusion was prepared with the dry powdered herbs 10,0 g in 100 mL of aquadest at temperature 90 °C for 15 minutes so obtained the concentrate of infusion 10%.

Animals

Female Wistar albino rats (120-200 g) used in studies, was procured from Laboratory of Imonology, Faculty of Pharmacy Sanata Dharma, Yogyakarta. The animals were fed with standard pellet diet (AD-2 pellet) and reverse osmosis (RO) water. All the animals were acclimatized for a week before use. Before and during the experiment, the rats were kept in a standard environmental conditions (temp. 25-28 °C and 12h light / dark cycle). The experimental protocols were approved by Medical and Health Research Ethics Committee (MHREC) after scrutinization. Animals were received the drug by oral administration. The laboratory conditions duly undertaken by registered veterinary practitioner.

Chemicals

All the chemicals and solvents were of analytical grade. Standard kits for SGOT and SGPT were obtained from PT. Kimia Farma, Indonesia.

Treatment schedule

Animals were divided into six groups of five animals each in all the sets of experiments. CCl₄ mixed with olive oil (1:1) was used as hepatotoxic agent. The drugs were administered in 1, 4, and 6 hours after CCl₄ administration.

Group I was olive oil control by giving as much as 2 mL/kgBW intraperitoneally; Group II was carbon tetrachloride hepatotoxin control dose 2 mL/kgBW intraperitoneally; Group III was control treatment given 2 g/kgBW infu



sion of *Bidens pilosa* L. herb orally; Group IV was treatment group for infusion of *Bidens pilosa* L. dose 1 g/kgBW and was injected with 2 mL/kgBW carbon tetrachloride after 1 hours; Group V was treatment group for infusion of *Bidens pilosa* L. dose 1 g/kgBW and was injected with 2 mL/kgBW carbon tetrachloride after 4 hours; Group VI was treatment group for infusion of *Bidens pilosa* L. dose 1 g/kgBW and was injected with 2 mL/kgBW carbon tetrachloride after 6 hours.

Assessment of hepatoprotective activity

After 24 hour of CCl4 administration, all groups had blood drawn at the orbital sinus region. Blood samples were allowed to clot for 10 min at room temperature. Serum was separated by centrifugation at 8000 rpm at 30 OC for 15 min and utilized for the estimation of various biochemical parameters including SGOT and SGPT13. After collection of blood samples, the animals were sacrificed under deep ether anesthesia.

The hepatoprotective activity, expressed as percentage hepatoprotection (H), was calculated using the following equation,

$$H = [1 - (T - V) / (C - V)] \times 100$$

Where, T = mean value of treatment group, C = mean value of CCl4 control group, and V = mean value of olive oil control group14.

Statistical analysis

The results of the biochemical estimations are reported as mean ± S.E. Statistical analysis was done by one-way analysis of variance (ANOVA) followed by Scheffe test by using 16th version of SPSS software. P values < 0.05 were considered as significant.

RESULTS AND DISCUSSION

The effect of exposure time of *Bidens pilosa* L. infusion on carbon tetrachloride induced hepatotoxicity in rats is presented in table no 1. The levels of SGOT and SGPT were markedly elevated. In hepatotoxin control group as compared to the olive oil control, indicating hepatocellular damage. The activities of biomarker

enzymes for liver such as SGOT and SGPT were elevated on administration of CCl4 to 409.6 ± 7.79 and 149.2 ± 1.39 U/L respectively in comparison to olive oil control values of 101.8 ± 2.08 and 57.2 ± 3.07 U/L respectively. Treatment of the rats with infusion of *Bidens pilosa* L., a standardized infusion of *Bidens pilosa* L. at dose levels 1 g/kgBW, prevented CCl4-induced elevation of SGOT and SGPT. The effect of exposure time of *Bidens pilosa* L. infusion on carbon tetrachloride induced hepatotoxicity in rats prevented the CCl4 induced hepatotoxicity as they decreased the levels of SGOT (106.4 ± 1.81; 94.6 ± 1.50; 234 ± 3.67 U/L) and SGPT (71.4 ± 3.14; 50 ± 3.08; 69 ± 3.00 U/L). % hepatoprotective SGPT and SGOT group IV are 84.57 and 98.51 %; group V are 107.83 and 102.34 %; group VI are 87.17 and 57.05%.

Table 16. The effect of exposure time of *Bidens pilosa* L. infusion on carbon tetrachloride induced hepatotoxicity in rats

Groups	SGOT (U/L)	SGPT (U/L)
I	409.6 ± 7.79	149.2 ± 1.39
II	101.8 ± 2.08**	57.2 ± 3.07**
III	105.6 ± 3.75**	57.4 ± 2.93**
IV	106.4 ± 1.81**	71.4 ± 3.14**
V	94.6 ± 1.50**	50 ± 3.08**
VI	234 ± 3.67**	69 ± 3.00**

Keys: Values are Mean ± S.E. (n = 5 animal per group); SGOT –Serum Glutamic Oxaloacetic Acid Transaminase; SGPT- Serum Glutamic Pyruvic Transaminase; P denotes statistical not significance P*>0.05 vs CCl4; significance P**<0.05 vs CCl4.

In the group III CCl4 induced animals were showed the level of marker enzymes significantly elevated (P<0.05) when compared to the group II (control) olive oil. But there was a sig



CONCLUSION

In the present study, administration of infusion of *Bidens pilosa* L. containing quercetin (flavonoids group) significantly protected against CCl₄ induced hepatotoxicity in rats. The best exposure time of *Bidens pilosa* L. infusion dose 1 g/kgBW in 4th hours after administered carbon tetrachloride, % hepatoprotective SGPT and SGOT are 107.83 and 102.34 %. Further studies are needed to evaluate the potential usefulness of this infusion in clinical conditions associated with liver damage.

ACKNOWLEDGEMENTS

The authors are thankful to the Head, Department of Pharmacy, Sanata Dharma University for providing necessary research facility. Our sincere thank to Prof. Dr. C.J. Soegihardjo, Apt., Department of Pharmacy, Sanata Dharma University for his valuable suggestion and constant encouragement.

REFERENCES

1. Meyer SA, and Kulkarni AP. (2001). Hepatotoxicity. In: Introduction to biochemical toxicology. New York: John Wiley & Sons: 3rd ed., pp. 487-518.
2. Sharma A, Chakraborti KK, Handa SS. (1991). Anti-hepatotoxic activity of some Indian herbal formulations as compared to silymarin. *Fitoterapia* 62: 229-235.
3. Subramonium A, Pushpangadan P. (1999). Development of Phytomedicines for liver diseases. *Indian J. Pharmacol*; 31: 166-175.
4. Anand BS. Cirrhosis of liver. (1999). *West L Med* 171: 110-115.
5. Hinds TS, Wesk WL, Knight EM. (1997). Carotenoids and retinoids: A review of research, clinical and public health applications. *Clin. Pharmacol.* 37: 551-8.
6. We YT, Liu DW, Ding LY, Liq, Xiao YH. (2004). Therapeutic effects and molecular mechanical of antifibrosis herbs and selection on rats with hepatic fibrosis. *World J. Gastroenterol.* 10: 703-6.
7. Parola M, Leonarduzz G, Biasi F, Albono M, Biocca G, Polic, Dianzani MU. (1992). Vitamin E dietary Supplementation. Protects against CCl₄ induced chronic liver damage and cirrhosis. *Hepatology* 16: 1014-1021.
8. Castro JA, De Ferreyra EC, De castro CR, Fenoos OM, Sasame H, Gillette JR. (1974). Prevention of carbon tetrachloride-induced necrosis by inhibitors of drug metabolism-further studies on their mechanism of action. *Biochem. Pharmacol.* 23: 295-302.
9. Poli G. (1993). Liver damage due to free radicals. *Br Med bull.* 49: 604-20.
10. Handa SS, Sharma A, Chakraborti KK. (1986). Natural products and plants as liver protecting drugs. *Fitoterapia.* 57: 307-351.
11. Davies DM. (1985). *Text Book of Adverse Drug Reactions.* Oxford University Press, New York, 3rd ed., pp. 2-669.
12. Bairwa K, Kumar R, Sharma RJ, Roy RK. (2010). An updated review on *Bidens pilosa* L. *Der Pharma Chemica*; 2(3): 325-337.
13. Reitman S, Frankel S. (1957). A colorimetric method for the determination of serum glutamic oxalacetic and glutamic pyruvic transaminases. *American Journal Clinical Pathology* 203: 1033-1037.
14. Wakchaure D, Jain D, Singhai AK, So mani R. (2013). Hepatoprotective Activity of *Symplocos racemosa* Bark on Tetrachloride-Induced Hepatic Damage in Rats. *Journal of Ayurveda*



- & Integrative Medicine 2 (3): 137-143.
15. Johnson DE, Kroening C. (1998). Mechanism of early carbon tetrachloride toxicity in cultured rat hepatocytes. *Pharmacol. Toxicol.* 83: 231-239
 16. Srivastava SP, Chen NO, Hotlzman Cl. (1990). The in-vitro NADPH dependant inhibition by CCl₄ of the ATP dependant calcium uptake of hepatic microsomes from malerats. Studies on the mechanism of inactivation of the hepatic microsomal calcium pump by CCl₃ radical. *J. Biol. Chem.* 265: 8392-8399.
 17. Timbrell JA. (2008). *Principles of Biochemical Toxicology*. New York: Informa Health Care: 4th ed., pp. 211-213, 308-311.
 18. Kosina P, Kren V, Gebhardt R, Grabal F, Ulrichova J, Walterova D. (2002). Antioxidant properties of silybin



CYTOTOXIC ACTIVITY ASSAY AGAINST HELA CELL LINES OF NOVEL ANTI-CANCER DRUG : N-(PHENYLCARBAMOYL) ISOBUTIRAMIDE

Wimzy Rizqy Prabhata: undergraduate student of Faculty of Pharmacy Airlangga University; Gubeng kertajaya XIII B/17, Surabaya; wr.prabhata@gmail.com ; +62 85869161800;

Tri Widiandani, Department of Chemical Pharmacy, Faculty of Pharmacy, Airlangga University; Jl. Darmo Permai Tmr.VIII / 42 Surabaya; triwidiandani@gmail.com ; +62 81803022660; **Siswando-no,** Department of Chemical Pharmacy, Faculty of Pharmacy, Airlangga University; Jl. Ketintang Timur PTT 5 Surabaya; sis_ffua@yahoo.com; +62 8123206328

INTRODUCTION

Cancer is still remains to be the most feared diseases in the modern world. In most of developed countries, cancer is the second biggest cause of death after cardiovascular disease. Judged from its development, the number of cancer cases in developing countries is less compared than in the developed countries, but mortality cases is greater [1]. Based on research conducted by Basic Medical Research, cancer ranks sixth in the various largest disease cause of death in Indonesia [2], which also one of developing countries. Based on the facts that rapid development of cancer and the failures of cancer therapy goal, the development of anticancer agent is needed to treat cancer, with the aim of obtaining drugs with higher cytotoxic activity, lower toxicity and more selective in the receptor binding. One example of an anticancer agent is urea. Various kinds of research have been conducted to confirm that urea derivatives also have anticancer cytotoxic activity, for example, thienopyridine urea working as anticancer agent by inhibiting KDR kinase [3], phenylurea and its derivative were developed as anticancer agent [4], hydroxyurea as an anticancer agent which has been used clinically as well. However, this urea derivative anticancer compounds need to be developed to improve its potency and lower its toxicity. To increase its activity, in our previous research we tried to develop a new urea derivative anticancer agent. Our previous research has confirmed that in silico

study of N-(phenylcarbamoil)isobutiramide gives higher anticancer activity than hydroxyurea by using 2YWP receptor. In silico study approach has become the earliest way to develop a new urea derivative anticancer agent. The results of in silico study is a proof that N-(phenylcarbamoil)isobutiramide deserves to be synthesized. N-(phenylcarbamoil)isobutiramide obtained from the synthesis of starting material phenylurea with isobutiril chloride through acylation reaction. With the aim to determine the potency of N-(phenylcarbamoil)isobutiramide as an anticancer agent, we conducted a research to assay cytotoxic activity of N-(phenylcarbamoil)isobutiramide by MTT assay method.

MATERIALS AND METHODS

Material

Our previous studies have managed to synthesize N-(fenilkarbamoil)isobutiramida from starting materials fenilurea and isobutiril chloride through acylation reaction. Synthesized compound was identified qualitatively to determine its purity by determining the melting range and thin layer chromatography. And the structure was confirmed by IR and ¹H-NMR. Cytotoxicactivity assay of N-(phenylcarbamoil)isobutiramide againsts HeLa cell lines In vitro antitumor activity against MCF- 7 cancer cell lines was assayed by MTT method and expressed in IC50, concentration of the compounds inducing a 50% inhibition of cell growth of treated cells compared to the growth



of control cells. Hydroxyurea (HU) was used as reference drug. RPMI was used as growing medium. Cancer cell lines were seeded at a density of 104 cells/well in 96-well microplates. After 24 hours, exponentially growing cells were exposed to the test compounds in DMSO at final concentration ranging from 62,5 to 4000 mg /mL. After 24 hours incubated in a 5 % CO₂ incubator at 37°C, cell survival was determined by the addition of MTT solution (100 µL of 10 % MTT solution in RPMI medium). Once formazan was formed, 100µL 10 % SDS in 0.1 N HCl was added and plates were incubated in the dark at 37°C overnight. The absorbance was observed at 595 nm on ELISA-reader and survival ratio of living cells were expressed in percentages with respect to untreated cells. Each experiment was performed at least three times. IC₅₀ value was determined by using log probit analysis [5].

RESULT AND DISCUSSION

Our previous study managed to synthesize N-(phenylcarbamoyle)isobutiramide from starting materials phenylurea and isobutiril chloride. Synthesized compound was identified qualitatively to determine its purity by determining the melting range and thin layer chromatography. And the structure was confirmed by IR and ¹H-NMR. Table 1 and 2 shows confirmation result by using IR and ¹H-NMR Table 1 Confirmation result by using IR spectrophotometry

Wavelength (cm ⁻¹)	Functional groups	Phenylurea	Synthesized material
3500-3100	R-NH ₂	+	-
	R ₂ -NH	+	+
2968	C-H Alkil	-	+

Table 2 Confirmation result by using ¹H-NMR spectrometry

δ (ppm)	Multiplicity	Relative intensity
1,02-1,09	Doublet (J=6,8 Hz)	6
2,45-2,59	Septet	1
6,95-6,99	Triplet	1
7,18-7,25	Triplet	2
7,55-7,57	Doublet	2
9,76	Singlet	1

With the aim to obtain new anticancer agents, we examined anticancer activity of N-(phenylcarbamoyle)isobutiramide that we already have synthesized before. In vitro anticancer activity assay conducted against cervical cancer cells (HeLa cells). The results of the absorbance of the test compound treatment can be seen in Table 3 and Table 4.

Table 3. Absorbances with hydroxyurea treatment

Compound	absorbances*							
	4000	2000	1000	500	250	125	62,5	
Hydroxyurea	Rep. 1	0,510	0,532	0,550	0,606	0,587	0,600	0,638
	Rep. 2	0,497	0,565	0,565	0,574	0,617	0,594	0,642
	Rep. 3	0,534	0,572	0,581	0,619	0,624	0,619	0,632
	average	0,514	0,556	0,565	0,600	0,609	0,604	0,637

(*) concentration expressed in µg/mL.

Compound		Absorbances *						
		2000	1600	1000	800	400	200	100
N-(phenylcarbamoyle)isobutiramide	Rep. 1	0,08	0,08	0,34	0,18	0,60	0,639	0,64
		7	5	1	9	4		4
	Rep. 2	0,09	0,18	0,40	0,52	0,60	0,646	0,65
		0	8	5	7	0		1
	Rep. 3	0,09	0,10	0,46	0,51	0,60	0,635	0,64
		1	5	9	3	0		1
	average	0,08	0,12	0,40	0,41	0,60	0,640	0,64
		9	6	5	0	1		5

(*) concentration expressed in µg/mL

After we got absorbance value, we subsequently converting this absorbance value into survival ratio. This survival ratio needed in probit analysis to calculate IC₅₀ value of tested compound.

Table.5 IC₅₀ value of in vitro cytotoxic activity assay of tested compounds againsts HeLa cell lines

Compounds	IC ₅₀ cytotoxic (µg/mL)
N-(phenylcarbamoyle)isobutiramide	706
Hidroksiurea	86012

Table 5 indicated that N-(phenylcarbamoyle)isobutiramide gives lower IC₅₀ values than those in hydroxyurea. So the activity of N-(phenylcarbamoyle)isobutiramide is higher than those in hydroxyurea. Lower IC₅₀ values prove that the ability of N-(phenylcarbamoyle)



isobutiramide to inhibit the growth of cancer cells is larger than those in hydroxyurea.

Table.6 Comparison between in vitro cytotoxic activity against HeLa cell lines and in silico study with 2YWP receptor of tested compounds.

Compounds	IC ₅₀ sitotoksik (µg/mL)	Rerank score
N-(phenylcarbamoil)isobutiramide	706	-66,8086
Hidroksiurea	86012	-32,8856

Table 6 Indicated that both of in silico and in vitro study proves that N-(fenilkarbamoi)isobutiramida gives higher activity than those in hydroxyurea.

Lower rerank score value indicated that N-(phenylcarbamoil)isobutiramide gives lower affinity bond with receptor 2YWP than those in hydroxyurea, thus N-(phenylcarbamoil)isobutiramide more stable in the drug-receptor binding. In silico study predicted correctly that N-(phenylcarbamoil)isobutiramide has higher activity than hydroxyurea. So that in silico study can be used as an initial approach to develop new anticancer agent.

CONCLUSION

This research concluded that N-(phenylcarbamoil)-isobutiramide gives higher anticancer activity than hydroxyurea. N-(phenylcarbamoil)isobutiramide gives IC₅₀ values lower than those in hydroxyurea. Lower IC₅₀ values indicated that the ability of N-(phenylcarbamoil)-isobutiramide to inhibit the growth of cancer cells is higher than those in hydroxyurea. This research also concluded that in silico study can be used as an initial approach to develop new anticancer agent. With in silico approach, we can reduce trial and error as well as time and costs consumed in the developing of new anticancer agents.

REFERENCES

1. International Agency for Research on Cancer. GLOBOCAN 2012 : Estimated Cancer Incidence, Mortality, and Prevalence Worldwide in 2012. World Health Organization.
2. Agency for Health Research and Development. Department of Health, Republic of Indonesia. 2008. Basic Health Research - National Report 2007. p. 322.
3. Heyman, H. Robin, Michael, L. Curtin, Robin, R. Frey, Niru, B. Soni, Patrick A. Marcotte, Lori, J. Pease, Keith, B. Glaser, Terrance, J. Magoc, Paul, T., Daniel, H., Albert, Donald, J. Osterling, Amanda, M., Olson, Jennifer, J., Bouska, Zhiwen, Guan, Lee C., Preusser, James, S., Polakowski, Kent, D. Stewart, Chris Tse, Steven, K. Davidsen, Michael, R. Michaelides. (2007). Thienopyridine Urea Inhibitors of KDR Kinase. *Bioorganic & Medicinal Chemistry Letters*, 17 1246–1249.
4. Song, Q. Dan, Du Na-na, Wang, Y. Ming, He, W. Ying, Jiang Z. En, Cheng shi-xiang, Wang Yan-Xiang, Li Ying-Hong, Wang Yu-Ping, Li Xin, Jiang Jian-Dong. (2009). Synthesis and activity evaluation of phenylurea derivatives as potent anti tumor agents. *Bioorganic & Medicinal Chemistry*, 17.p.3873–3878.
5. Nuzul, W.D., Juni, E., Siswandono. (2014). Synthesis and Antitumor Activity Evaluation of N,N'-dibenzoyl-N,N'-diethylurea Againsts Human Breast Cancer Cell Line (MCF-7). *International Journal of Pharmacy and Pharmaceutical Science.*, 6.p.315-318



SIMPLE STEPS PURIFICATION OF RECOMBINANT HUMAN ERYTHROPOIETIN PRODUCED IN CHINESE HAMSTER OVARY CELL CULTURE

Yana Rubiyana, Research Center for Biotechnology, Indonesian Institute of Science, Cibinong, Bogor 16911, Indonesia, rubiyana39@yahoo.co.id; **Endah Puji Septisetyani**, Research Center for Biotechnology, Indonesian Institute of Science, Cibinong, Bogor 16911, Indonesia; **Adi Santoso**, Research Center for Biotechnology, Indonesian Institute of Science, Cibinong, Bogor 16911, Indonesia

ABSTRACT

To have correct information of biological analysis, pure recombinant protein is required. Consequently a suitable and efficient techniques for protein purification was needed. In this study, simple two step chromatographic purification process was developed with relatively high yield and purity of rhEPO using blueseparose affinity chromatography combined with Q-sepharose ion exchange chromatography. A single protein zone with molecular mass of 47 kDa was appeared in SDS-PAGE analysis of the purified rhEPO. Final result showed that rhEPO protein exhibited at more than 90% purity.

Key words: blueseparose, erythropoietin, purification, ion exchange.

INTRODUCTION

Erythropoietin (EPO) is a glycoprotein hormone that controls red blood cell formation. Lacking of EPO in the body can cause anemia due to low process of erythropoiesis. rhEPO has been used for clinical treatment of patients with anemia caused by cancer, HIV infection, kidney failure, and bone marrow transplantation (Park et al. 2000). Therapy with recombinant EPO decreases the need for blood transfusion, thus reducing the risk of coming down with illness such as viral hepatitis or HIV AIDS [1].

Methods of EPO purification have been developed (Ben-Ghanem et al.,1994). Surabattula et al. (2011) described an improved purification of EPO from mammalian cell cultures. In this study, a two step chromatographic purification process that combines blue sepharose affinity chromatography with Q-sepharose ion exchange chromatography was examined.

MATERIALS AND METHODS

Cell Culture

CHO-K1 cells were cultured in Dulbecco's Modified Eagle's medium (DMEM) (Gibco) supplemented with 10% Fetal Bovine Serum

(FBS) (Gibco) and 1% Penicillin-Streptomycin (Gibco).

Clarification and Diafiltration

Supernatant was filtered through 0.45 µm membrane using a sterile syringe filter (Corning) to remove the remaining cells and debris. After the clarification, filtrate was concentrated by TFF (tangential flow filtration) system using a 10 kDa cut-off membrane (Millipore) to about 10 fold volume reductions.

Affinity Chromatography and Buffer Exchange

Glass column 10 mm internal diameter and 100 mm length) was packed with 1 ml of Blue sepharose 6 fast flow matrix (Amersham). Column was equilibrated with 3 column volumes of 20 mM phosphate buffer pH 8. Column was washed 10 column volumes with 20 mM phosphate buffer pH 8 after loading with concentrated supernatant. The protein was eluted with 20 mM phosphate buffer + 1.5 M NaCl, peak containing the active fractions was pooled and buffer exchanged against 20mM Tris pH 8 by Amicon 10 kDa cut off membrane (Millipore).

Ion-Exchange Chromatography

Prepack column Sartobind IEX 15 (Sartorius)



mounted on AKTA system (AKTA purifier 10, GE Healthcare). Column was equilibrated with buffer A containing 20 mM Tris (pH-8.0). After desalted blue sepharose elute was loaded on to the column. Column was washed with Buffer A. EPO protein was then eluted with gradient using buffer B containing 20 mM Tris, 1M NaCl (pH-8.0). Result of purification was detected by UV detector with wavelength 280 nm. Fraction containing EPO was sterilized by passing through a 0.22 µm pore size filter (Corning).

SDS-PAGE Analysis

SDS/PAGE and Western blot analysis were performed to detect each fraction of protein after purification. Following SDS/PAGE, protein inside the gel was transferred into Hybond nitrocellulose membrane (GE Healthcare) by using electroblotting. Immunodetection was achieved by using anti-hEPO antibody (Calbiochem) as primary antibody and anti-rabbit IgG peroxidase conjugate (Biorad) as secondary antibody.

Result and Discussions

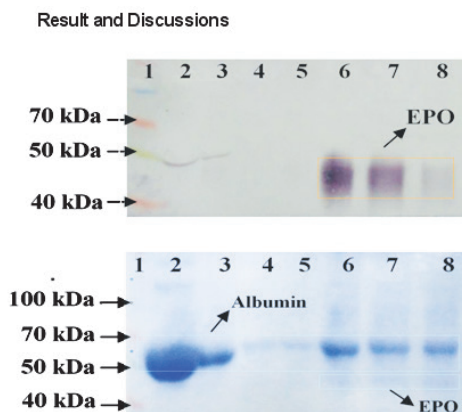


Figure 1. Purification using Blue Sepharose Western blotting and Commasie Brilliant analysis. Lane 1: Marker Protein, Lane 2: Flow Through, Lane 3: Washing, Lane 4: Washing, Lane 5: Washing 5, Lane 6-8: Elution 1-3

The cell culture supernatant was filtered through 0.45µm membrane filter and then directly loaded onto Blue sepharose column (1ml). To eliminate non-specific adsorption

caused by weak interactions, the column was washed properly with 20 mM Phosphate buffer. The band of interest band was seen in elution 1-3 which corresponds to EPO molecular weight on SDS-PAGE (Fig: 1). No EPO band was seen in flow through fraction or washing fraction, this result showed that the purification process was performed properly. In mammalian cell growth medium contains lots of albumin which is one of the contaminants that must be removed. Affinity purification is a helpful tool for cleaning up and removing albumin contamination from samples. One purification method which can be used to remove these contaminants is blue sepharose affinity chromatography. In This method, The dye of blue sepharose (Cibacron Blue) is capable of removing over 90% of albumin in the sample (Travis et al, 1976). In This result (Fig 1), blue sepharose can substantially remove albumin in the sample

However, some contaminant protein bands with high and low molecular weights were still present. The next stage is purification by ion-exchange chromatography in order to obtain a more pure rhEPO protein.

Purification used ionic exchange

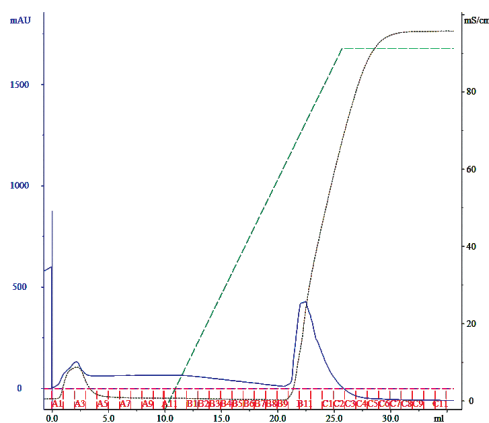


Figure 2. Graphic of ion exchange data from AKTA System.

Figure 2 shows two peaks which contained in the flow-through and elution fractions. The separation is expected to occur between the target protein and other impurities. For conformation, fractions were analyzed using Western blot protein and Commasie brilliant blue analyses.

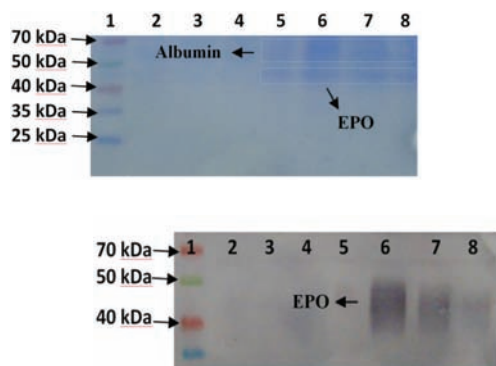


Figure 3. Western blotting and Commasie Brilliant analysis. Lane 1: Marker Protein, Lane 2: fraction A2, Lane 3: fraction A3, Lane 4: fraction A7, Lane 5: fraction B10, Lane 6: fraction B11, Lane 7: fraction B12, Lane 8: fraction C1.

EPO band was seen in fraction B11, B12 and C1, (Fig. 3). These bands correspond with the peak in the graph. This data showed that combination of two chromatography methods was able to purify the rhEPO from impurities that are present in the media. Signifies the purification process is well.

CONCLUSIONS

Simple two step chromatographic purification process was developed with relatively high yield and purity of EPO using bluesephare affinity chromatography combined with Q-sepharose ion exchange chromatography. Densitometric scanning of gels demonstrated that the final purity of the protein is more than 90%.

ACKNOWLEDGEMENT

This study was supported by the National Innovation Program (SiNas), Ministry of Research and Technology (Menristek) (grant No. RD 2013-096). The authors are grateful to Prof. Masashi Kawaichi for providing CHO-K1 cells.

REFERENCES

- Charlton A, Zachariou M. 2008. Immobilized metal ion affinity chromatography of histidine-tagged fusion proteins. Di dalam: Zachariou M, editor. *Methods in Molecular Biology*. Vol. 421: Affinity Chromatography: Methods and Protocols. Ed ke-2. Totowa: Humana Pr. hlm 137-140.
- Egrie J. 1990. The cloning and production of recombinant human erythropoietin. *Pharmacotherapy* 10:3s-8s.
- Park JH, Kim C, Kim WB, Kim YK, Lee SY, Yang JM. 2000. Efficiency of promoter and cell line in high-level expression of erythropoietin. *Biotechnol Appl Biochem* 32:162-172.
- Sytkowsky AJ. 2004. *Erythropoietin: Blood, Brain and Beyond*. Weinheim: Wiley-VCH.
- Yin H, Blanchard KL. 2000. DNA methylation represses the expression of the human erythropoietin gene by two different mechanisms. *Blood* 95:1-4.



KINETICS STUDY COCRYSTALS KETOCONAZOLE-SUCCINIC ACID PREPARED WITH SLURRY METHOD BASED ON POWDER X-RAY DIFFRACTION (PXRD)

Yuli Ainun Najih, Department of Pharmaceutics, Airlangga University, Surabaya-East Java Indonesia, yuli_aminareka@yahoo.com; Dwi Setyawan, Department of Pharmaceutics, Airlangga University, Surabaya-East Java Indonesia; Achmad Radjaram, Department of Pharmaceutics, Airlangga University, Surabaya-East Java Indonesia.

INTRODUCTION

The compounds with low solubility drugs can be a problem in the development of drugs for the pharmaceutical industry. Group of drugs that are included in the Biopharmaceutical Classification System (BCS) class II drugs can be a challenge for the preparations of pharmaceutical development because of low solubility drugs as well as the rate of dissolution. In this case to increase the solubility of drugs besides salts, pharmaceutical cocrystals opened a new dimension to search for solid forms such as solubility, dissolution rate, stability, and shelf life of active pharmaceutical ingredients (APIs) without affecting their inherent pharmacological properties¹.

Pharmaceutical co crystals are materials or crystalline materials consisting of at least two different components (multicomponent crystals or mixed crystals)²⁻³. Co crystal could be prepared by several methods, such as solvent evaporation, slurry, melt, and grinding. Co crystals formed between ketoconazole (KTZ) as an active pharmaceutical and succinic acid (SA) as a co crystal former (co-former)⁴ was increased dissolution rate of pure ketoconazole in equimolar ratio (1:1)¹. Physical characterization of co crystal was performed by physical mixture of binary system with molar ratio using different thermal analyzer (DTA) data from KTZ and SA. Besides that, physicochemical characterizations of cocrystal were performed by using PXRD and infrared spectroscopy (IR). Active solid materials in the manufacture of pharmaceutical preparation suffered in various thermic or mechanical processed such as grinding, milling, granulations (wet and

dry granulations), tabletasi, and storage at various temperature, so the materials can occur transformation polymorph or hidrat/solvat⁵. Kinetic study of cocrystal KTZ-SA prepared with slurry method at various solvent concentrations a follows 2%, 3%, 4%, 5% and 6% (w/w). Therefore, the aim of the present study was determined the kinetics of co crystals KTZ-SA prepared with slurry method by using Powder X-ray Diffraction (PXRD) data such as the research of co crystalline phase transformation of binary mixture of trimethoprim (TMP) and sulfamethoxazol (SMZ) by slurry technique⁵.

MATERIALS AND METHODS

Materials

Ketoconazole was purchased from Zhejiang East-Asia Pharmaceutical Co., Ltd, China, batch no. DC-0101H-1209001. Succinic acid was purchased from Merck KGaA, Germany, batch no. K43601782. Distilled water and ethanol p.a.

Methods

Preparation of Phase Diagram of Binary System

KTZ and SA were sifted and weighed to obtain particle size in similar range. The obtained physical mixtures were obtained by simply mixed KTZ with SA at different molar ratios as follows: (10:0), (9:1), (8:2), (7:3), (6:4), (5:5), (4:6), (3:7), (2:8), (1:9) and (0:10) respectively. The mixtures were gently mixed in mortar for 5 minutes. The melting point of physical mixtures of KTZ-SA was determined by DTA. Endothermic peak was plotted against molar



fraction of mixture to obtain the phase diagram of KTZ-SA.

Preparation of KTZ-SA Physical Mixture

KTZ and SA equimolar carefully weighed; 0.5314 grams and 0.1181 grams respectively. Both powders were mixed homogeneously in a mortar.

Preparation of Cocrystal Using Solvent Evaporation Method

KTZ and SA equimolar carefully weighed; 0.5314 grams and 0.1181 grams respectively. Each compound was dissolved in ethanol separately. KTZ was dissolved in approximately 30 mL of ethanol to form a clear solution. SA was dissolved in approximately 8 mL of ethanol to form a clear solution. The two solutions were mixed and stirred for a few minutes. The solvent evaporated at room temperature for 48 hours. Co crystal solids stored in a desiccators under vacuum.

Preparation of Cocrystal Using Slurry Method
KTZ and SA equimolar carefully weighed; 0.5314 grams and 0.1181 grams respectively. Both powder were mixed homogeneously with various solvent concentration added in mortar. Slurry method used water distilled as a solvent. Various solvent concentration added to the mixture mixed slurry samples formed as follows: 2%, 3%, 4%, 5% and 6% (w/w), it means waters added to the mixture mixed slurry samples formed as follows: 2 mL, 3 mL, 4 mL, 5 mL and 6 mL. The mixtures were gently mixed in mortar for 10 minutes. Co crystal formed was dried at room temperature for 48 hours. Co crystal solids stored in a desiccators under vacuum.

Physicochemical Characterization Co crystals
Differential Thermal Analyzer (DTA) was used to analyze the thermal properties. The DTA (Mettler Toledo FP 85, Switzerland) was calibrated with indium before analysis. Certain amount of samples i.e. 5-7 mg samples were placed in a sealed aluminum pan. The analysis was performed in a temperature range of 50-300°C with heating rate of 10°C per minute.
Characterization By Powder X-Ray Diffraction

Method

Powder X-Ray Diffraction (Philips X'Pert Diffractometer) analysis performed at room temperature. Condition of measurement was set as follows: Cu metal target, K α filter, voltage of 40 kV, 40 mA. Performed analysis on the range of 2 θ (theta) of 5-40°. Sample placed on the sample holder and lattes to prevent particle orientation during preparation. Characterization Using Fourier Transform Infrared Spectroscopy (FTIR)
Approximately 1% (w/w) dispersion of sample powder in potassium bromide (KBr) was prepared by mixing the sample powder with KBr. The infrared spectrum was obtained using infrared spectrophotometer (Spectrum One, Perkin Elmer) in wave length range 400-4000 cm⁻¹.

PXRD Calibration Curve

Prepared calibration curve of co crystal with mixed physical mixture KTZ-SA equimolar and co crystal KTZ-SA equimolar at various percentage comparison as follows: (0/100), (10/90), (30/70), (50/50), (70/30), (90/10) and (100/0). A value percentage of zero percent is a KTZ-SA physical mixture of binary system and a hundred percent is KTZ-SA co crystalline phase. Both of mixed powders characterized with PXRD, choose the unique interference peaks or different peaks among co crystal, physical mixture and pure each component material, and then choose a unique peak with the highest maximum intensity made calibration curve of co crystal and calculated kinetics of co crystal. The calibration curve of co crystal plotted the value of maximum intensity (intensity-background) against percentage of co crystal in binary mixture. We get a value of linear regression equation ($y = ax \pm b$), a value of x showed co crystal percentages.

Kinetics Study of Co crystal Prepared with Slurry Method Using PXRD

The results of characterization prepared with slurry method used PXRD at each various solvent concentration were calculated maximum



intensity respectively to linear regression equation from calibration curve of co crystal.

RESULT AND DISCUSSION

Phase Diagram of Binary System

The phase diagram of KTZ-SA mixture was made using different molar ratio (i.e. (10:0), (9:1), (8:2), (7:3), (6:4), (5:5), (4:6), (3:7), (2:8), (1:9) and (0:10)) respectively presented in figure 2 and the result of DTA thermogram respectively presented in figure 1. KTZ melted at 152.4oC and SA melted at 192.3oC. The result showed two eutectics (E1 and E2), it means that the type of phase diagram of binary mixture is a congruently melted point of molecular compound (co crystal). First eutectic (E1) at molar ratio (3:7) has a melting point temperature of 143,9oC $\Delta H = 68.7$ J/g and second eutectic (E2) at molar ratio (9:1) has a melting point temperature of 147,9oC $\Delta H = 56.0$ J/g. KTZ melted at 152.4oC was decreased until minimum melting point temperature of E1 when it was added in SA into the mixture and melting point of E1 increased because SA added in the mixture until maximum melting point temperature of 164.7oC $\Delta H = 20.0$ J/g, it was called congruently melting point of molecular compound⁷. Increasing the number of fraction mol of SA will further cause a decrease in melting point of binary mixture at minimum temperature of SA, it was called second eutectic (E2)

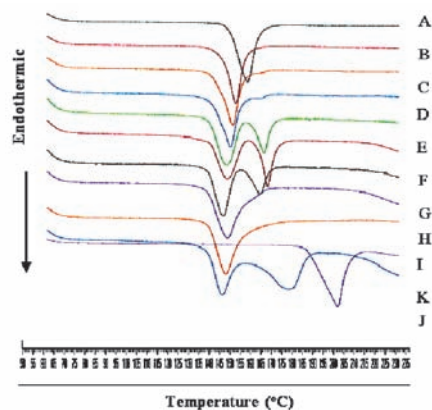


Figure 1: DTA thermogram KTZ (A), SA (K), KTZ-SA physical mixture (9:1) (B), (8:2) (C), (7:3) (D), (6:4) (E), (5:5) (F), (4:6) (G), (3:7) (H), (2:8) (I), (1:9) (J).

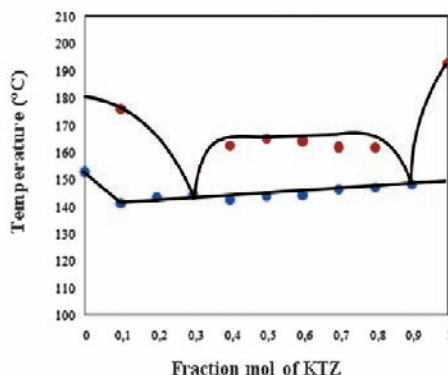


Figure 2: Phase diagram of binary system KTZ-SA with various compared of fraction mol.

DTA Analysis

DTA analysis was performed to characterize thermal behavior of KTZ-SA co crystal phase in relation to intact component and KTZ-SA physical mixture of binary system presented in figure 3. KTZ and SA showed a single endothermic peak at 152.4oC $\Delta H = 63.3$ J/g and 192.3oC $\Delta H = 199.0$ J/g respectively. KTZ-SA physical mixture showed two endothermic peaks at 143.5oC $\Delta H = 26.2$ J/g and 164.7oC $\Delta H = 20.0$ J/g . KTZ-SA co crystal showed only a single endothermic peak at 165oC indicated co crystalline phase formed between KTZ and SA⁵. It was occurred fusion of eutectic mixture in KTZ-SA physical mixture due to KTZ-SA co crystal phase⁵.

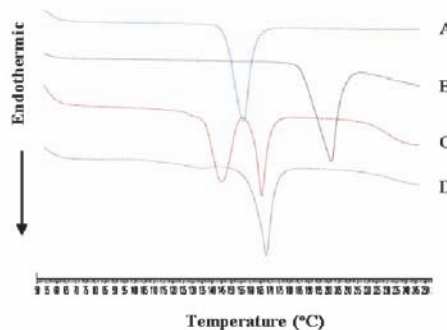


Figure 3: DTA Thermograms of KTZ (A), SA (B), KTZ-SA physical mixture (1:1) (C), KTZ-SA cocrystal (1:1) (D).

PXRD Analysis

PXRD analysis used to characterize a new crystalline phase formed in solid state and showed superposition of two materials, it means that there is an interaction between two materials, such as interactions between KTZ and SA in this case, the interactions may produce new diffraction peaks as compared the constituent materials⁶. In this case, PXRD analysis performed at the angle of $2\theta = 5-50^\circ$. PXRD diffractograms of KTZ, SA, KTZ-SA physical mixture (1:1) and KTZ-SA co crystal (1:1) solvent evaporation were showed at figure 4.

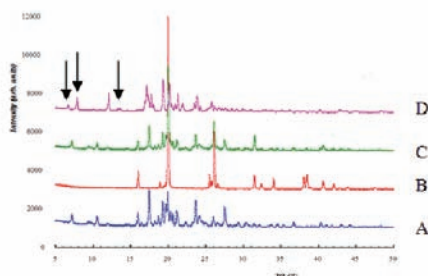


Figure 4: PXRD diffractograms of KTZ (A), SA(B), KTZ-SA physical mixture (1:1) (C) and KTZ-SA co crystal (1:1) (solvent evaporation) (D).

Based on these data, PXRD diffractogram of KTZ was showed at the angle of $2\theta = 5.3^\circ$, 7.1° , 9.4° , 10.4° , 11.9° , 14.3° , 15.9° , 16.4° and 17.4° . PXRD diffractogram of SA was showed at the angle of $2\theta = 15.8^\circ$, 16.0° , 18.0° , 18.8° and 19.9° . KTZ-SA physical mixture (1:1) diffractogram was specific angle of $2\theta = 5.4^\circ$, 6.7° , 7.2° , 7.8° , 9.4° , 10.5° , 12.0° , 13.5° , and 14.6° . KTZ-SA co crystal (1:1) (solvent evaporation) diffractogram was specific angle of $2\theta = 6.6^\circ$; 7.8° and 13.3° whereas no peaks were found in KTZ-SA physical mixture diffractograms,

FTIR Spectroscopy Analysis

FTIR spectroscopy analysis used to study the chemical and physical structure changed in the molecular structure of substance⁶. Infrared spectra of KTZ, SA, KTZ-SA physical mixture (1:1) and KTZ-SA cocrystal (1:1) solvent

evaporation were showed at C=O, O-H and N-H stretch bend (figure 5). KTZ has a C-H alkana stretch bends at 2883 cm^{-1} , C-H amine stretch bends at 1290 , 1244 , 1224 , and 1201 cm^{-1} , C-N stretch bends at 1546 and 1512 cm^{-1} , C=O stretch at 1755 and 1647 cm^{-1} , C=C aromatic stretch bends at 1647 , 1546 and 1512 cm^{-1} , C-Cl stretch bends at 815 cm^{-1} , O-H stretch at 3448 , 3176 , 3118 and 2883 cm^{-1} and N-H stretch at 3448 cm^{-1} . SA has a peak O-H stretch at bends 2931 cm^{-1} , C-H alkana stretch at 2931 cm^{-1} , C=O stretch at 1691 cm^{-1} , C-C stretch at 1203 , 1074 and 916 cm^{-1} . The interactions of KTZ-SA were showed at 1755 and 1647 cm^{-1} referred peaks of C=O stretch from KTZ and at 1691 cm^{-1} referred peak of C=O stretch from SA shifted peaks 1710 and 1691 cm^{-1} referred peaks of C=O stretch from KTZ-SA physical mixture of binary system and shifted peaks at 1787 and 1714 cm^{-1} referred C=O stretch from KTZ-SA co crystalline phase. Second, the interactions of KTZ-SA were showed peaks at 3448 , 3176 , 3118 and 2883 cm^{-1} referred peaks of O-H stretch from KTZ and at 2931 cm^{-1} referred peaks of O-H stretch from SA shifted at 3431 and 2885 cm^{-1} for KTZ-SA physical mixture of binary system and shifted at 3421 , 3271 and 2893 cm^{-1} for KTZ-SA co crystalline phase. The last, interactions of KTZ-SA were showed at 3442 cm^{-1} referred peak of N-H stretch, and there was no peak in SA, the peak of N-H stretch was appeared at 3431 cm^{-1} for KTZ-SA physical mixture of binary system and appeared at 3421 for KTZ-SA co crystalline phase⁸.

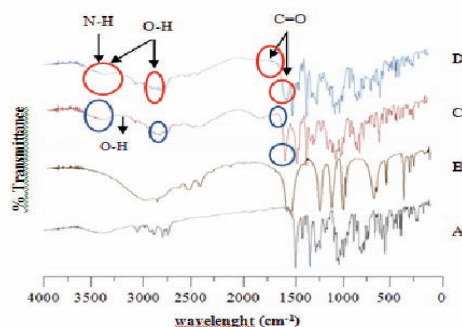




Figure 5: Infrared spectra of KTZ (A), SA (B), KTZ-SA cocrystal (1:1) (solvent evaporation) (C) and KTZ-SA physical mixture (1:1) (D).

PXRD Calibration Curve

Based on the data from PXRD diffractogram, KTZ-SA cocrystal (1:1) (solvent evaporation) diffractogram was specific angle of $2\theta = 6.6^\circ$; 7.8° and 13.3° whereas no peaks were found in KTZ-SA physical mixture diffractograms. Selected a unique interference peak from three specific peaks from the angle of $2\theta = 6.6^\circ$; 7.8° and 13.3° which have highest maximum intensity. The angle of $2\theta = 6.6^\circ$; 7.8° and 13.3° have maximum intensity at 213, 620 and 151 respectively. The angle of $2\theta = 7.8^\circ$ was selected for a unique peak for making calibration curve and reference calculated kinetic study cocrystal KTZ-SA prepared with slurry method used PXRD data.

Calibration curve of cocrystal prepared with mixed physical mixture KTZ-SA equimolar and cocrystal KTZ-SA equimolar at various percentage compare as follows: (0/100), (10/90), (30/70), (50/50), (70/30), (90/10) and (100/0). Zero percent as KTZ-SA physical mixture of binary system and a hundred percent as KTZ-SA co crystalline phase. The results of PXRD diffractogram at various percentage compare were showed at figure 6. After that, calculated maximum intensity (intensity - background) for each percent of cocrystal and then prepared the calibration curve with plotted percent of cocrystal against maximum intensity of characteristic interference peak showed at figure 7 and table 1. WinPLOTR (version march 2007) software was used to determine the maximum intensity (intensity - background) in PXRD diffractogram.

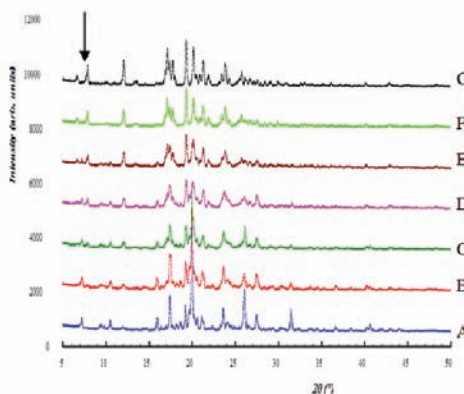


Figure 6: PXRD diffractograms of KTZ-SA mixed physical mixture of binary system and KTZ-SA co crystalline phase at various percentage of (0/100) (A), (10/90) (B), (30/70) (C), (50/50) (D), (70/30) (E), (90/10) (F) and (100/0) (G).

Table 17. Percent of maximum intensity cocrystal

% Cocrystal	0	10	30	50	70	90	100
Max. Int	0	75	146	275	362	468	620

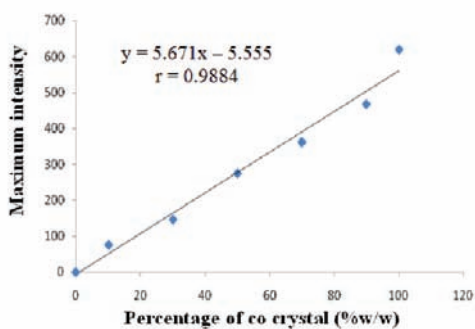


Figure 7: Calibration curve of percentage cocrystal in binary mixture against maximum intensity based on PXRD analysis data at the angle of ($2\theta = 7.8^\circ$).

Kinetics Study of Cocrystal Prepared with Slurry Method Using PXRD

Kinetics study of cocrystal prepared with slurry method using PXRD data from each various solvent concentration (i.e. 2%, 3%,



4%, 5% and 6% (w/w)) calculated with linear regression equation of maximum intensity calibration curve of percentage cocrystal, so we will get cocrystal percentage. PXRD diffractogram of slurry method was showed at figure 8. A good linear curve of percentage of solvent concentration prepared with slurry method obtained by plotting various solvent concentration against maximum intensity (figure 9 and table 2) and so do the curve of percentage cocrystal prepared with slurry method by plotting various solvent concentration against percentage of cocrystal (figure 10 and table 3). WinPLOTR (version march 2007) software was used to determine the maximum intensity (intensity - background) in PXRD diffractogram.

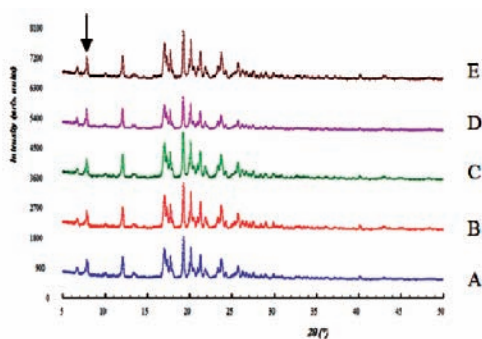


Figure 8: PXRD diffractograms of KTZ-SA slurry method with various solvent concentrations of 2% (A), 3% (B), 4% (C), 5% (D) and 6% (E).

Table 2. % Solvent concentration against maximum intensity.

% Solvent concent.	2	3	4	5	6
Max. Int	427	435	478	495	527

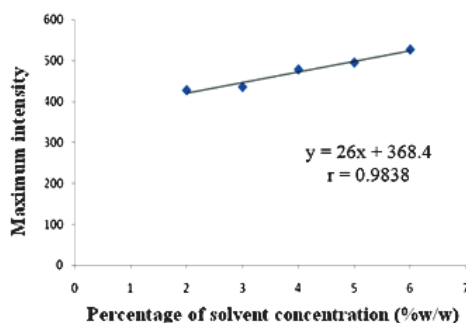


Figure 9: Curve of percentage solvent concentration (%w/w) prepared with slurry method against maximum intensity based on PXRD analysis data at the angle of ($2\theta = 7.8^\circ$).

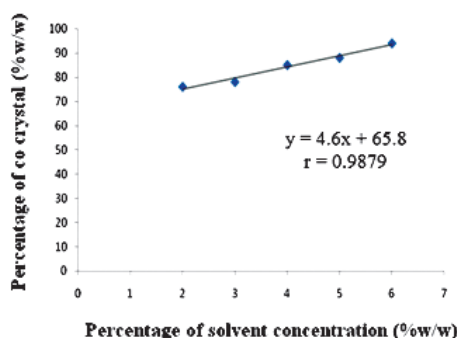


Figure 10: Curve of percentage solvent concentration (%w/w) prepared with slurry method against percentage of cocrystal (%w/w) based on PXRD analysis data at the angle of ($2\theta = 7.8^\circ$).

Table 3. Solvent concentration (%w/w) against cocrystal (%).

% Solvent	2	3	4	5	6
% cocrystal	427	435	478	495	527

Based on these data (figure 10 and table 3), the kinetics of cocrystals were determined based on PXRD analysis data. Cocrystal formed occur between contact of solvent activated with the molecular compounds of the energy added in the mixture during grinding both components (KTZ and SA) in mortar. So, increasing percentage solvent concentration was made contact activated with both molecular compounds increased so percentage cocrystal was produced faster. So that the number of cocrystal form were increased.



CONCLUSION

The kinetics study of cocrystals KTZ-SA prepared with slurry method were determined based on PXRD analysis data.

ACKNOWLEDGEMENT

The authors would like to thank for the advisors were given suggestion and support to finish this paper.

REFERENCES

1. Martin FA, Mihaela MP, Borodi G, et al. (2013). Ketoconazole salt and cocrystals with enhanced aqueous solubility. *Romania Crystal Growth, Des*;13(10):4295-4303.
2. Schultheiss N and Newman A. (2009). Reviews pharmaceutical cocrystal and their physicochemical properties. *Crystal Growth & Design*, 9(6): No. 2950-2967.
3. Vishweshwar P, McMahan JA, Bis JA, et al. (2006). Review pharmaceutical co-crystals. *Journal Of Pharmaceutical Sciences in Wiley InterSciences*, 95(3): 499-516.
4. Otte A, Boerrigter SXM, and Pinal R. (2012). Cocrystal of ketoconazole with dicarboxylic acids. *APPS Annual Meeting and Exposition*, Chicago.
5. Zaini E, Sumirtapura YC, Soewandhi SN, et al. (2010). Cocrystalline phase transformation of binary mixture of trimethoprim and sulfamethoxazole by slurry technique. *Asian Journal of Pharmaceutical and Clinical Research*, 3(4): 26-29.
6. Setyawan D, Sari R, Yusuf H, et al. (2013). Preparation and characterization of artesunate-nicotinamide cocrystal by solvent evaporation and slurry method. *Asian Journal of Pharmaceutical and Clinical Research*, 7(1): 62-65.
7. Davis, RE, Lorimer KA., Wilkowski MA., et al. (2004). Studies of Relationship in Cocrystal System. *ACA Transaction*, 39: 41-61.
8. Silverstein, RM, Francis XW, David JK. (2005). Spectrometric identification of organic compounds. *John Wiley & Sons, Inc.*, 7th Ed, p.75-107.



CONSTRUCTION OF RECOMBINANT IMMUNOTOXIN Anti-EGFRvIII scFv::HPR FUSION PROTEIN AND INDUCIBLE EXPRESSION IN *Pichia pastoris* AS A TARGETED DRUG CANDIDATE

Yuliawati, Research Center For Biotechnology - Indonesian Institute of Sciences (LIPI), Cibinong Science Center, Jalan Raya Bogor Km.46, Cibinong, Bogor 16911; Bogor Agricultural University, Department of Biotechnology Post Graduate School - Gd. PAU, Jalan Kamper IPB, Dramaga, Bogor; Asrul Muhammad Fuad, Research Center For Biotechnology - Indonesian Institute of Sciences (LIPI), Cibinong Science Center, Jalan Raya Bogor Km.46, Cibinong, Bogor 16911, asrul.m.fuad@gmail.com

INTRODUCTION

Single chain antibody fragment (scFv) is part of an antibody molecule comprising the variable light chain (VL) and variable heavy chain (VH), connected by a peptide linker. The scFv is much smaller in size (30 kDa) compared to the intact antibody molecule (eg. IgG 150 kDa). Because of its small size, scFv molecules can penetrate tissues and tumor cells easily (Sun et al. 2003). ScFv showed rapid pharmacokinetics, high specificity to target molecules and low immunogenicity in animal models. In addition, autoradiography studies showed that scFv can penetrate more extensive and homogeneous in tumor cells than intact antibody molecules or other greater antibody fragments (eg. Fab', Fab'2). This characteristic is important for radioimmunotherapy (Kuan et al. 2000, Ahmad et al. 2012).

EGFR (epidermal growth factor receptor) has been extensively studied in relation to cancer in the last few decades since this receptor protein was often found overexpressed on the surface of various cancer cells. It was suggested that this molecule plays a major role in the development of cancer cells. Therefore, this protein becomes a potential target molecule in cancer therapy (Mammoth & Rochlitz 2006). However, native EGFR is also present in normal tissue. Thus, targeting EGFR could cause serious side effects, immune damage, and be tolerant of this treatment. Studies have shown that EGFR mutates on cancer cells and many different EGFR mutant variants found in various types of cancer (Kuan et al., 2001,

Frederick et al. 2000).

EGFR variant III (EGFRvIII) is the most common mutant variant found in a number of solid tumors, including glioblastoma multiforme (GBM), breast, brain and cervical cancers. EGFRvIII is not present in normal tissues. This mutant receptor has deletion of exon-2 through exon-7 from native EGFR gene. A glycine residue is formed at the junction of fusion between exon-1 and exon-8. This fusion creates a new specific antigen. This mutant variant is known as EGFRvIII (Gupta et al. 2010).

An alternative strategy for development of targeted drug delivery is using basic immunotoxin. Immunotoxin is an a toxin molecule that is fused or conjugated to an antibody or antibody fragment (eg. scFv) . Researches on immunotoxin-based immunotherapy have been more developed. One example is an 'imunoR-Nase' (IR) that uses ribonuclease (RNase) as the active compound (toxin) (Lorenzo et al. 2004). One type of RNase that is used in this study is a human pancreatic RNase (HP-RNase or HPR). This RNase is not toxic outside the cell, however it becomes toxic when it enters the target cells. It may find a way to enter the cell through binding to surface epitopes that are recognized by the antibody moiety (Rybak & Newton 1999).

Pichia pastoris was chosen as the host for the chimeric protein production. It is a methylotrophic yeast that are able to grow at high cell densities in a simple media. The yeast has other advantages as the host such as high level protein production and secretion, and geneti-



cally stable transformant. Peterson (2006) has reported that scFv can be expressed in *P. pastoris* into correct structure. This yeast-based expression system provides a right protein folding of scFv molecules. It also offers a virus-free as well as endotoxin-free expression system that can be applied not only for drugs production, but also for other biotechnological applications (Joosten et al. 2003).

The aim of this research is to construct an immunotoxin conjugate comprising an anti-EGFRvIII scFv fused with HPR variant mutant, and expressed the chimeric protein in yeast *P. pastoris*.

MATERIALS AND METHODS

Microorganisms used were *Escherichia coli* TOP10F', *E. coli* DH5 α and *Pichia pastoris* SMD1168H (Invitrogen). *E. coli* TOP10F' and DH5 α were used for cloning purpose. Plasmids used were pPICZ α A (Invitrogen), pJ201-scFv (DNA 2.0), and pJ912-HPR (DNA2.0). All DNA primers used in this study were purchased from 1st Base. The anti-EGFRvIII scFv and HPRmut genes were ordered and made synthetically by DNA 2.0, cloned in pJ201-scFv and pJ912-HPR, respectively.

Construction of scFv::HPRmut fusion protein
Sub-cloning of scFv gene into pPICZ α A vector. The scFv gene encoding anti-EGFRvIII was made synthetically at DNA2.0 based on previously published sequence (Weber et al., 2009) and cloned in pJ201-scFv. The scFv gene was PCR-amplified by PCR method and was cloned into the pPICZ α vector at XhoI site right after α -factor secretion signal, resulted in the recombinant plasmid pPICZ α -scFv. The plasmid sequence was verified and the correct one was used for the next sub-cloning. The HPRmut gene was then subcloned into pPICZ α -scFv and fused at 3'-end of the scFv. The HPRmut gene (Leland et al., 2001) was PCR-amplified from pJ912-HPR in two steps. First, the gene was amplified using internal primers pair, then the gene was re-amplified using another pair of primers containing a short spacer (G4S) and XbaI sites. Both gene and plasmid were cut

with XbaI, isolated and purified. The gene was ligated and transformed into *E. coli* TOP10F' according to Ausubel (2002). *E. coli* transformants were selected on LS-LB agar medium (1% peptone, 0.05% NaCl, 0.5% yeast extract, 1.7% agar) containing zeocin (25 μ g/ml) and analyzed by colony PCR. Positive clones were further analyzed to determine gene orientation by PCR and sequence verified.

Expression of scFv::HPRmut fusion protein in *P. pastoris*

Transformation and selection of transformed cells.

The selected pPICZ α -scFv-HPR recombinant plasmid was linearized with SacI. Transformation of the plasmid into *P. pastoris* was carried out by electroporation according to the protocol suggested by Invitrogen and Biorad. Transformed colonies were grown and selected on YPDS zeocin medium (1% yeast extract, 2% peptone, 2% dextrose, 1 M sorbitol, 1.7% agar) containing 100 μ g/ml zeocin (Invitrogen). Selection of yeast transformants was carried out according to the procedure given by Invitrogen. All of transformant colonies that grew on the selection medium were transferred into a new fresh YPD zeocin medium containing 100 μ g/ml zeocin. The plates were incubated at 30°C for 2 to 4 days. Stable transformants that grew on this medium were further transferred into YPD zeocin agar medium containing higher concentrations of zeocin (200, 500, and 1000 μ g/ml) to acquire recombinant clones having multicopy gene integration.

Protein expression from transformed *P. pastoris*

A number of 10 individual transformant colonies were cultured to evaluate recombinant protein expression according to protocols of *Pichia* expression kit (Invitrogen). Cultures were incubated at 30°C and 250 rpm for 3 days and methanol was added at 0.5% (v/v) into the culture every 24 hours. Cultures were harvested by centrifugation (10,000

rpm, 15 min, 4°C). Cell biomass was stored at -20°C and the cell-free culture medium (supernatant) was stored at 4°C for further protein analysis. Recombinant protein (extracellular product) was analyzed using SDS-PAGE method. Proteins were precipitated from cell-free supernatant samples by TCA (trichloro acetic acid) solution (Sanchez, 2001). Protein purification using Pure Proteome Nickel magnetic beads (Merck) was performed for isolation and purification of the recombinant protein. Detection was carried out using Coomassie Blue (Biorad).

RESULT AND DISCUSSION

Construction of fusion protein scFv::HPR

Recombinant plasmid containing anti-EGFRvIII scFv gene (pPICZ α -scFv) has been previously constructed. The scFv gene was inserted at XhoI site next after mating secretion signal factor- α (MF- α) for secretion of recombinant proteins. The pPICZ α -scFv plasmid used in the construction of the fusion antibodies had been previously sequence-verified. This fusion scFv::HPR protein has a relatively small size which is expected to be effective in targeting tumor cells. The pPICZ α -scFv clone no. 41 has been confirmed both in size and gene orientation, as well as its sequence. This plasmid clone was further used in the next HPRmut subcloning.

The HPRmut gene was successfully inserted into pPICZ α -scFv at XbaI site. Selection of transformed colonies by PCR was performed from 100 E. coli colonies using HPR-F and HPR-R primers to detect the inserted HPRmut gene in the plasmid (Figure 1). Positive clones were indicated by the presence of a 400 bp DNA band. This PCR-colony analysis showed that 90 colonies out of 100 were positive clones.

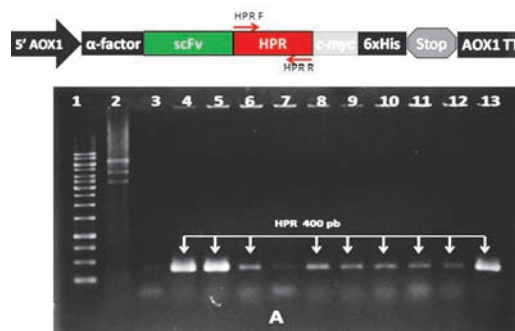


Figure 1. Electropherogram of colony PCR result for selection of pPICZ α -scFv-HPR recombinant plasmids in E. coli. 1: DNA marker; 2: negative control; 3-13: clones of E. coli transformants. Positive clones were indicated by the presence of 400 bp DNA band.

Further analysis was carried out to determine the gene orientation by PCR using HPR-F and AOX1-R primers. Clones containing gene insert in the correct orientation produces a DNA band around 650 bp. It was found that 42 clones out of 90 had allegedly correct HPRmut gene insertion (Figure 2A). Restriction analysis using XbaI resulted 8 positive clones in which the insert gene were completely restricted and released from the plasmid backbone (Figure 2B). Furthermore, three of the eight clones were analyzed for their nucleotide sequences. One clone with a correct nucleotide sequence has been obtained, which is the pPICZ α -scFv-HPR clone no. 44. Riccio et al. (2012), reported the same technique for constructing fusion of RNase and antibody fragment of anti-ErbB2 receptor, named as ERB-HP-RNase-DDADD. The construct was subcloned into pET22b+ vector and expressed in E. coli BL21(DE3). ImmunRNase molecule is reported to demonstrate biological activities of both the antibody domain and the RNase domain.

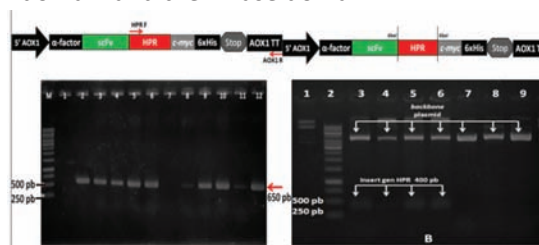




Figure 2 Electropherogram of colony PCR (A) and the plasmid digestion results (B) for the selection of recombinant plasmids containing the scFv:: HPR gene fusion. (A) Colony PCR analysis to confirm gene orientation using HPR-F and AOX-R primers. M: DNA marker; 1: negative control; 2-12: Positive clones of *E. coli* transformants. (B). Restriction analysis of recombinant plasmids using XbaI. 1: negative control; 2: DNA marker; 3-9: recombinant plasmids. Positive clones were indicated by a 400 bp DNA band.

HPRmut gene has been successfully fused at the 3'-end of scFv gene in pPICZ α -scFv. The 5'-end of scFv was fused to the secretion signal sequence factor- α . A peptide linker (L) was placed between the scFv and HPR, providing sufficient free space and minimize steric hindrance between the two domains. The scFv was preferred to be placed at the N-terminal rather than C-terminal of the HPR to provide better accessibility to the target antigen. The relative position of scFv and HPR is similar to the research conducted by Lorenzo et al. (2004), in which the anti-ErbB2 scFv was fused with HPR. Riccio et al. (2012) has also reported the construction of protein chimera comprising a fusion protein of an anti-ErbB2 scFv Erbicin and HPR.

The recombinant plasmid pPICZ α -scFv-HPR was linearized with SacI before it was transformed into *P. pastoris*. Transformation of this plasmid into the yeast has resulted in a small number of yeast transformants. We did have 27 independent clones only of *P. pastoris* transformants with a transformation efficiency of 0.54×10^2 cfu/ μ g DNA. This transformation efficiency rate is very low if compared to the level of efficiency that could be attained as high as 10^3 to 10^4 cfu/ μ g DNA as it is mentioned in some references (Invitrogen, 2010). Many factors may affect transformation process that lead to low level of transformation efficiency, such as low amount of DNA, DNA impurities, excess volume of DNA, poor integration process, imperfect competent cells

preparation (too low or too high cell concentration), unoptimal electroporation process (Hornstein 2012). In this experiment, the amount of DNA used for transformation was 500 ng, much smaller than the recommended amount, which was 1 to 5 μ g (Invitrogen, 2010).

Genetic stability analysis was performed by growing the transformant colonies from the selection medium into to a new fresh media containing zeocin (100 μ g/ml). It was found that all of transformant colonies could grow very well on this new medium, indicating that all of those transformed colonies were genetically stable.

Yeast transformants having potentially multi-copy gene integration could be screened using medium with higher zeocin concentration. Yeast transformants were grown and screened on YPD_{Azeo} medium containing 100, 200, 500, and 1000 μ g/ml of zeocin (Figure 3). Number of integrated plasmid of each transformed clones might be different one to another. Higher copy-number of integrated plasmid has a linear correlation to the resistency toward higher zeocin concentrations. All transformed colonies grew well on media control and media with zeocin 100 μ g/ml. In zeocin concentration of 200 and 500 μ g/ml several colonies began to look stunted, leaving approximately 93% of the clones that grew well. At zeocin concentration of 1000 μ g/ml, there was about 70% of transformed clones that grew well. Norden et al. (2011) suggested that resistency variation against antibiotic (zeocin) could be used to determine the gene copy number integrated into the genome, Assuming that Sh ble gene (zeocin resistance gene) has the same ratio as the target gene, one copy of Sh ble gene is the minimum requirement to be able to grow at zeocin concentrations of 100 μ g/ml, 4 copies of gene to grow at 500 μ g/ml and 9 copies of gene to grow at 1000 μ g/ml. Clones with as many as 17 copies of the Sh ble gene are able to grow on zeocin concentration of up to 2000 μ g/ml (Norden et al., 2011).

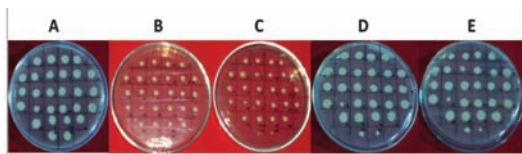


Figure 3 Genetic stability test and selection of multiple gene integration of yeast transformant colonies on YPDAzeo medium, with different zeocin concentrations: 0 µg/ml (A), 100 µg/ml (B), 200 µg/ml (C), 500 µg/ml (D), and 1000 µg/ml (E).

The pPICZα plasmid containing scFv::HPR fusion gene has been successfully integrated into the genome of *P. pastoris*. Analysis of the genomic DNA of yeast transformants were performed by PCR using two primer pairs (HPR-F / HPR-R and F-VH101 / VH10-R) to confirm the integration of each genes (HPRmut and scFv) within the *P. pastoris* genome. PCR results from 10 colonies of *P. pastoris* transformants showed that all clones gave a 400 bp (Figure 4A) and 750 bp DNA bands (Figure 4B), correspond to the size of HPRmut and scFv genes respectively. This result suggests that all yeast transformants contain both HPRmut and scFv genes in their genome.

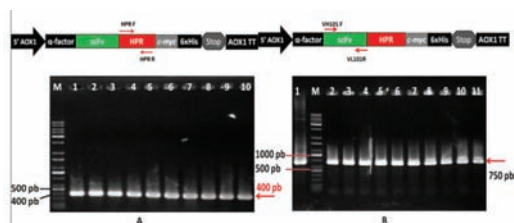


Figure 4 Electropherogram of colony PCR to confirm the insertion of scFv::HPR fusion gene in the genome of *P. pastoris* transformants. (A) Colony PCR using HPR-F and HPR-R primers. Positive clones having HPRmut gene give a 400 bp DNA band. M = DNA marker; 1= positive control; 2-10= clones of *P. pastoris* transformants. (B). Colony PCR using VH101-F and VL101-R primers. Positive clones having scFv gene give 750 bp DNA band. M= DNA marker; 1= positive control; 2-11= *P. pastoris* transformants.

This recombinant scFv::HPR fusion protein contains his-tag marker (6xHis) at its C-terminal to facilitate production, purification, and detection of the desired protein. Secreted protein produced by *P. pastoris* transformant was analyzed on SDS-PAGE analysis as shown in Figure 5A. There are few bands of extracellular protein observed from the sample preparation. To confirm the target protein band, the protein sample was purified through an affinity-based protein isolation. This recombinant fusion protein has been successfully isolated and purified using Pure Proteome Nickel magnetic beads (Merck) as shown in Figure 5B. From these results, it was suggested that the recombinant fusion scFv::HPR protein has a molecular size of around 50 kDa (Figure 5B).

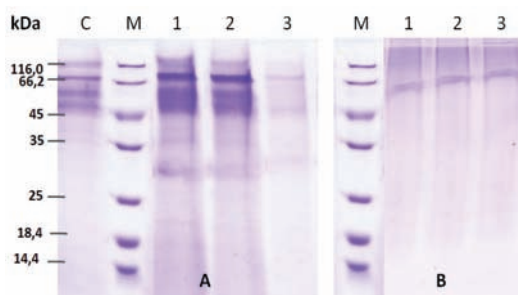


Figure 5 SDS-PAGE analysis of extracellularly expressed *P. pastoris*-derived scFv::HPR fusion protein from several yeast transformant clones. (A) Concentrated recombinant fusion protein. (B) Purified fusion scFv-HPR protein (mark by arrow). C= protein sample of untransformed clone; M= protein marker; 1, 2, 3= protein samples of transformed yeast clone no.3, 4, 5 respectively.

CONCLUSION

Gene fusion of anti-EGFRvIII scFv::HPR has been successfully constructed and transformed into *P. pastoris* SMD1168H with a transformation efficiency of 54 cfu/µg DNA. Approximately 93% of *P. pastoris* transformants were able to grow up to 500 µg/ml zeocin (~4 gene copies) and 70% up to 1000 µg/ml zeocin (~9 gene copies). The recombinant



fusion protein has been successfully expressed and secreted from *P. pastoris* as showed by SDS-PAGE analysis, showing a molecular size of around 50 kDa..

REFERENCES

1. Ahmad ZA, Yeap SK, Ali AM, et al. (2012). Review Article: scFv Antibodi: Principles and Clinical Application. *Clin & Devel oplmmunol* Volume 2012, doi:10.1155/2012/980250.
2. Ausubel FM, Brent R, Kingston RE, et al. (editors). (2002). *Short Protocol in Molecular Biology*. 5th Edition. John Wiley & Sons Inc.
3. Frederick L, Wang XY, Eley G, James CD. (2000). Diversity and Frequency of Epidermal Growth Factor Receptor Mutations in Human Glioblastomas. *Cancer Res* 60, p1383–1387.
4. Gupta P, Han S-Y, Madruga MH, Mitra SS, Nitta GLiRT, Wong AJ. (2010). Development of an EGFRvIII specific recombinant Antibodi. *BMC Biotechnol* 2010 10:72.
5. Invitrogen. 2010. EasySelect™ Pichia Expression Kit; For Expression of Recombinant Proteins Using pPICZ and pPICZα in *Pichia pastoris*. Cat. no. K1740-01. MAN0000042. Carlsbad, CA.
6. Joosten V, Lokman C, vd Hondel CAM JJ, Punt PJ. 2003. The Production of Antibody Fragments and Antibody Fusion Proteins by Yeasts and Filamentous Fungi. *BioMed Central Ltd*.
7. Kuan CT, Wikstrand CJ, Archer G, et al. (2000). Increased Binding Affinity Enhances Targeting of Glioma Xenografts by EGFRvIII-Specific scFv. *Int J Cancer*: 88, 962–969.
8. Kuan C-T, Wikstrand CJ, Bigner DD. (2001). EGF Mutant Receptor VIII as a Molecular Target In Cancer Therapy. *Endocr Relat Cancer* 8: 83–96.
9. Leland PA, Staniszewski KE, Kim B-M, Raines RT. (2001). Endowing Human Pancreatic Ribonuclease with Toxicity for Cancer Cells. *J Biol Chem* Vol. 276, No. 46, Issue of November 16, Pp. 43095–43102.
10. Lorenzo CD, Arciello A, Cozzolino R, Palmer DB, Laccetti P, Piccoli R, D'Alessio G. (2004). A Fully Human Antitumor Immunoreceptor Selective for ErbB-2-Positive Carcinomas. *Cancer Res* 64, 4870–4874.
11. Mamot C, Rochlitz C. (2006). Targeting the epidermal growth factor receptor (EGFR) – a new therapeutic option in oncology?. *Swiss Med Wkly* 136: 4 – 12.
12. Nordén K, Agemark M, Danielson JÅH, Alexandersson E, Kjellbom P, Johanson U. (2011). Increasing gene dosage greatly enhances recombinant expression of aquaporins in *Pichia pastoris*. *BMC Biotechnol*, 11:47.
13. Peterson E, Owens SM, Henry RL. (2006). Monoclonal Antibody Form and Function: Manufacturing the Right Antibodies for Treating Drug Abuse. *The AAPS Journal* 2006; 8 (2) Article 43.
14. Riccio G, D'Avino C, Raines RT, De Lorenzo C. (2012). A novel fully human antitumor Immunoreceptor resistant to the RNase inhibitor. *Protein Engineering, Design & Selection* 26(3): 243–248. DOI 10.1093/protein/gzs101.
15. Rybak SM, Newton DL. (1999). Immune Enzymes, in *Antibody Fusion Proteins* (Chamow, S. M. and Ashkenazi, A., eds.). Wiley, New York, pp. 53–110. 13.
16. Sanchez L. (2001). TCA protein precipitation protocol. www.its.caltech.edu. Downloaded on 1 May, 2012.
17. Sun C, Wirsching P, Janda KD. (2003). Enabling scFvs as Multi-Drug Carriers: A Dendritic Approach. *Bioorg & Med Chem*, 11 : 1761–1768.
18. Weber R, Feng X, Foord O, et al. (2009). Antibodies directed to deletion mutants of epidermal growth factor receptor and uses thereof. US Patent Application Publication No. US2009/0240038 A1.



ALTERED PHARMACOKINETIC OF LEVOFLOXACIN BY COADMINISTRATION OF ATTAPULGITE

Zamrotul Izzah, Department of Clinical Pharmacy Faculty of Pharmacy Airlangga University, Jl. Dharmawangsa Dalam Surabaya – Indonesia, zamrotulizzah@ff.unair.ac.id, phone +62 31 5033710 ext. 119; **Toetik Aryani**, Department of Clinical Pharmacy Faculty of Pharmacy Airlangga University, Jl. Dharmawangsa Dalam Surabaya – Indonesia; **Amalia Illiyin**, Undergraduate Student Faculty of Pharmacy Airlangga University, Jl. Dharmawangsa Dalam Surabaya – Indonesia; **Budi Suprapti**, Department of Clinical Pharmacy Faculty of Pharmacy Airlangga University, Jl. Dharmawangsa Dalam Surabaya – Indonesia

INTRODUCTION

Levofloxacin is a third-generation of fluoroquinolone which exhibits broad-spectrum in vitro bactericidal activities against gram-positive and gram-negative aerobes (Mc Evoy, 2002). It shows elevated activity against *Staphylococcus aureus*, *S. epidermidis*, and *Streptococcus* spp. Besides that, levofloxacin has lower incidence of resistance, higher concentration in bone, and longer half-life, so it can be administered once daily. The most common side effects of levofloxacin are nausea, vomiting, and heartburn (Lee et al., 1997).

Attapulgit, a hydrated magnesium aluminum silicate, has aluminum cations which can bind to the carboxylic acid and ketone groups at positions 3 and 4 on levofloxacin thus forming nonabsorbable chelate complexes. Adsorption nature of attapulgit may also inhibit the absorption of levofloxacin after oral administration. As a result, this drug-drug interaction may reduce levofloxacin bioavailability.

However, impact of this interaction on the pharmacokinetic of levofloxacin was unknown. The purpose of this study was to determine the effect of coadministration of attapulgit on the pharmacokinetics of a single orally-administered levofloxacin. (This study was presented at the 1st International Conference on Pharmaceutics and Pharmaceutical Sciences, Surabaya, Indonesia, 14-15 November 2014)

METHODS

Subjects and study design

The study was ethically approved by the Ani-

mal Care and Use Committee of Airlangga University. Six New Zealand white rabbits (3-6 months and 2.0-3.0 kg) received each of the following oral treatments in a randomized, two-way crossover sequence, separated by a 7-day washout period: (i) levofloxacin (23 mg/kgBW) alone; (ii) levofloxacin (23 mg/kgBW) given simultaneously with attapulgit (28 mg/kgBW). The rabbits were fasted overnight prior to treatments and given free access to water. Blood samples (1.0 mL) were collected from the marginal ear vein by direct venipuncture just prior to levofloxacin administration up to 240 min postdose (Fernandez et al., 1999).

Samples were collected into sterile vacuum tubes and centrifuged within 30 min of collection. Plasma was stored in a sterile microtube at -20°C until analyzed.

Drug assay

The plasma concentrations of levofloxacin were determined by a validated high-performance liquid chromatography assay and a modification of the method reported by USP (USP/NF, 2009). Briefly, 200.0 µL of spiked standards (levofloxacin 5.0 µg/mL) was added to 200.0 µL of plasma, and the mixture was vortexed for 60 s. Next, 200.0 µL of acetonitrile and 100.0 µL of H₃PO₄ 0.02 M (pH 3.0, adjusted with triethanolamine) were added to the mixture and then centrifuged at 4,000 rpm for 20 minutes. The supernatant was filtered by a 0.2 µL filter membrane and then 10.0 µL of solution was injected into the HPLC system. The chromatographic system was composed of a HPLC-DAD Agilent 1100 series, diode ar-



ray detector, and Licrospher ODS @ 100 RP-18 column. The detector wavelength was set to 280 nm. Mixtures of acetonitrile : H₃PO₄ 0,02 M (pH 3, adjusted with triethanolamine) (16:84, v/v) were used as the mobile phase at a flow rate of 1.5 mL/min. The retention time was 6.9 min. The calibration curve of levofloxacin was linier within range 0.50 to 13.0 µg/mL (r = 0.9997). Detection limit was 0.025 µg/mL and quantification limit was 0.084µg/mL. The within-day (n = 6) and day-to-day (n = 6) coefficient of variation was 1.93 ± 0.06 %. Recovery (%) was assessed from replicate analysis (n = 6) and shown 87.17 ± 2.34%.

Pharmacokinetics and statistical analysis
The maximum concentration (C_{max}) and the time of maximum concentration (T_{max}) of levofloxacin in plasma were obtained directly from the plasma concentration-time curve for each subject. The area under the plasma concentration-time curve from 0 to 240 min (AUC₀₋₂₄₀) was calculated by using the linear trapezoidal rule method.
Differences in the mean AUC₀₋₂₄₀min and the maximum levofloxacin concentrations among the treatment groups were analyzed for significance by a two-way ANOVA (analysis of variance) with an alpha value of 0.05.

Treatment	C _{max}		t _{max} (min)	AUC ₀₋₂₄₀	
	µg/mL	% of control		µg.min/mL	% of control
Levofloxacin alone (control)	7.99 ± 0.80	0	120 ± 0	1407.06 ± 155.01	0
Levofloxacin with Attapulgite 28 mg/kgBW	3.60 ± 0.56 ^b	54.65 ± 7.51	120 ^c ± 0	544.25 ± 55.59 ^b	59.83 ± 4.68

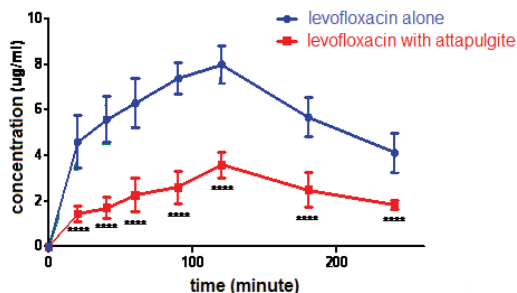
Table 1. Pharmacokinetic parameters of a single orally-administered levofloxacin and co-administered with attapulgite in rabbitsa

- a. Data are mean values (± standard deviations as appropriate) for six subjects
- b. Significantly different (p < 0.001) from control
- c. No significant difference (p > 0.05) from control

RESULTS

The concentration-versus-time profiles of a single orally-administered levofloxacin and co-administered with attapulgite in rabbits are shown in Figure 1. The pharmacokinetic parameters of levofloxacin are described in Table 1. As shown in Table 1, no significant difference in the time to reach maximum plasma concentration was observed (p>0.05). T_{max} was 120 min either in control or with attapulgite. In contrast, levofloxacin concentrations in plasma were decreased when levofloxacin was used concurrently with attapulgite. Concomitant administration of attapulgite significantly decreased the peak plasma concentration and oral bioavailability (AUC₀₋₂₄₀ min) of levofloxacin by around 55% and 60% (p<0.001)

respectively. C_{max} of levofloxacin decreased (7.99 ± 0.80 and 3.60 ± 0.56 µg/mL for control and with attapulgite, respectively), and AUC₀₋₂₄₀min of levofloxacin reduced (1407.06 ± 155.01 and 544.25 ± 55.59 µg.min/mL for control and with attapulgite, respectively).



**** significantly different (p<0.005)

Figure 1. Mean plasma levofloxacin concentration-versus-time profiles for levofloxacin 23 mg/kgBW alone and levofloxacin 23 mg/kgBW with attapulgite 28 mg/kgBW (Values are means \pm standard errors)

DISCUSSION

The absorption process plays an important role in achieving maximum concentrations and bioavailability of drugs in the systemic circulation. If there is an interaction during this phase, it will reduce the amount of drug that enters the body. Furthermore, reduced bioavailability of drug has an impact on decreasing the effectiveness of therapy (Garrelts et al, 1990; Stockley, 2008). The present study demonstrated that the bioavailability of levofloxacin was markedly reduced by concomitant ingestion of attapulgite. Attapulgite is not absorbed in the gastrointestinal tract and its adsorption nature may also inhibit the absorption of levofloxacin after oral administration.

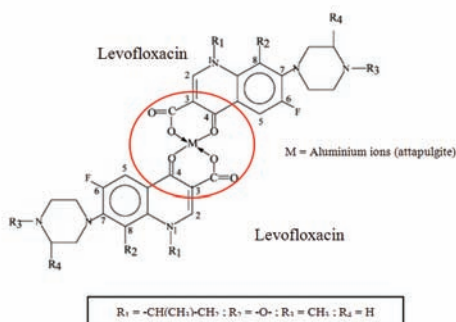


Figure 2. Chelate formation between attapulgite and levofloxacin

Furthermore, the most plausible explanation for levofloxacin-attapulgite interaction is the formation of levofloxacin-aluminium chelates during the absorption phase (Lautenbach et al, 2002). Attapulgite has aluminium ions which are available to form chelation complexes with levofloxacin, resulting in impaired absorption of levofloxacin. Chelation probably occurs between the cation and the 4-keto and 3-carboxyl groups of levofloxacin (Figure 2).

Some investigators have evaluated the effect of staggered dosing of fluoroquinolones and sucralfate on the extent of drug-drug interaction (Garrelts et al, 1990; Stockley, 2008). Sucralfate which also has aluminum cations appeared to reduce the bioavailability of ciprofloxacin by 88% (with 1 g of sucralfate administered four times on the day before the study and the fifth dose given with ciprofloxacin). However, when a 1 g dose of sucralfate was given 6 and 2 h before ciprofloxacin, only a 30% decrease in the bioavailability of ciprofloxacin was observed (Garrelts et al, 1990). Clearly, not only the time interval between administrations of these interacting drugs, but also the sequence in which they are given, is important when trying to prevent this potential interaction.

Levofloxacin should not be used together with attapulgite. Since levofloxacin is administered once daily, drug-drug interaction is easier to manage. The interaction, however, should be minimal if the interval separating the intake of both agents is lengthened. The maximum concentration of levofloxacin in plasma was achieved in 2 h, so it is reasonable to assume that levofloxacin should be given 2 h before attapulgite. The absorption process was completed before levofloxacin came into contact with released aluminum ions when levofloxacin given 2 h before attapulgite.

This present study does not investigate the impact of drug-drug interaction on decreasing the effectiveness of therapy. Nonetheless, further studies on assessing the clinical outcomes from the concomitant use of attapulgite and levofloxacin are needed to address this issue.

CONCLUSION

The oral bioavailability of levofloxacin was markedly reduced when coadministered with attapulgite. Therefore, it may not be advisable to concomitantly administer levofloxacin with attapulgite. The altered pharmacokinetic of levofloxacin might decrease its clinical efficacy and promote antimicrobial resistance.



ACKNOWLEDGEMENT

The authors declare no conflict of interest. This study was funded by the research grant of BOPTN Airlangga University. Sincere appreciations are intended to all staff of the Assessment Laboratory Unit of Universitas Airlangga and the Animal Care Laboratory, Faculty of Pharmacy Airlangga University.

REFERENCES

1. Fernandez, J., Barrett, J.F., Licata, L., AMaratungga, D., Frosco, M., (1999). Comparison of Efficacies of Oral Levofloxacin and Oral Ciprofloxacin in a Rabbit Model of a Staphylococcal Abscess. *Antimicrobial Agents and Chemotherapy*, No. 3, Vol. 43, p. 667-671.
2. Garrelts JC, Godley PJ, Peterie JD, Gerlach EH, Yakshe CC., (1990). Sucral fate significantly reduces ciprofloxacin concentrations in serum. *Antimicrobial Agents and Chemotherapy*, 34 (5): 931-933.
3. Lautenbach E, Fishman NO, Bilker WB, Castiglioni A, Metlay JP, Edelstein, PH, et al., (2002). Risk factors for fluoroquinolone resistance in nosocomial *Escherichia coli* and *Klebsiella pneumoniae* infections. *Archives of Internal Medicine*, 162: 2469 – 2477.
4. Lee, L.J., Hafkin, B., Lee, I.D., Hoh, J., and Dix, R., (1997). Effects of food and sucralfate on a single oral dose of 500 milligrams of levofloxacin in healthy subjects. *Antimicrobial Agents and Chemotherapy*, 10: 2196-2200.
5. McEvoy, G.K., (2002). AHFS Drug Information. American Society of Health-System Pharmacists.
6. The United State Pharmacopeia/ The National Formulary (USP/NF)., (2009). USP 32/NF 27. United States Pharmacopeia Convention, Inc.: Rockville.
7. Stockley IH, Sweetman SC., (2008). A source book of interactions, their mechanism, clinical importance and management 8th edition. The Pharmaceutical Press: London.